UNCLASSIFIED

AD NUMBER
AD387338
CLASSIFICATION CHANGES
TO: unclassified
FROM: confidential
LIMITATION CHANGES
TO: Approved for public release, distribution unlimited
FROM: Distribution: No Foreign
AUTHORITY
Group-4 DoDD 5200.10, 26 Jul 1962; AFRPL ltr., 22 Jan 1986

THIS PAGE IS UNCLASSIFIED

AD 382 338

AUTHORITY: AFRPL

ltr, 17 JAN 86

CONFIDENTIAL

Report AFRPL-TR-67-300

(Unclassified Title)

AD 387338

FEASIBILITY DEMONSTRATION OF A SINGLE-CHAMBER CONTROLLABLE SOLID ROCKET MOTOR

(19)

Final Report

Contract AF 04(611)-10820

Charles T. Levinsky
Gerald F. Kobalter

Aerojet-General Corporation
Sacramento, California

January 1968

In addition to security requirements which must be met, this document is subject to special export controls and each transmittal to foreign governments or foreign nationals may be made only with prior approval of AFRPL (RPPR/STINFO), Edwards, California 93523

0987

CONFIDENTIAL

Report AFRPL-TR-67-300

(Unclassified Title)

FEASIBILITY DEMONSTRATION OF A SINGLE-CHAMBER CONTROLLABLE SOLID ROCKET MOTOR

FINAL REPORT

CONTRACT AF 04(611)-10820

Charles T. Levinsky
Gerald F. Kobalter

In addition to security requirements which must be met, this document is subject to special export controls and each transmittal to foreign governments or foreign nationals may be made only with prior approval of AFRPL (RPPR/STINFO), Edwards, California 93523.

Air Force Rocket Propulsion Laboratory
United States Air Force
Edwards, California

FOREWORD

(U) This is the final report of Contract AF 04(611)-10820, covering the technical effort from 1 July 1965 through 1 August 1967. This report is submitted in partial fulfillment of the contract work statement, and reports the effort that was completed during the above-mentioned time period. The contract involves the exploratory development of a single-chamber controllable solid rocket motor. Work on this program was performed by the Research and Technology Operations of the Aerojet-General Corporation under the direction of the Air Force Rocket Propulsion Laboratory.

(U) This report contains information, data, and figures that are classified CONFIDENTIAL. The classified information falls under the Group 4 downgrading category, to be downgraded at 3-year intervals and unclassified after 12 years.

(U) This technical report has been reviewed and is approved.

Charles R. Cooke
Division Chief, Solid Rocket Division
Air Force Rocket Propulsion Laboratory

Report AFRPL-TR-67-300

UNCLASSIFIED ABSTRACT

(U) This report deals with the technical effort conducted during the total period of time covered by Contract AF 04(611)-10820, "Exploratory Development of a Single-Chamber Controllable Solid Rocket Motor." During the 24-month period covered by this contract, a preliminary design phase, a propellant development phase, a lightweight motor development phase, and a lightweight motor demonstration phase were conducted. Detailed discussions of the work performed in the first four phases and the first half of the fifth phase were reported in the first five quarterly reports, AFRPL-TR-65-204, AFRPL-TR-66-12, AFRPL-TR-66-99, AFRPL-TR-66-164, and AFRPL-TR-66-281. This report includes a general recap of the program as reported in the first five quarterly reports, and a detailed discussion of those portions of the program that have not been previously reported.

(U) In the preliminary design phase, a trade-off study was conducted to size the system and a preliminary lightweight motor design was prepared and analyzed. In the propellant development phase, a family of extinguishable propellants was investigated to improve extinguishability and tailored for variable thrust. In the subscale design and development phase, the basic material selections were test fired in a motor which was designed to simulate the fullscale CSRM. In the heavyweight motor development phase, a fullscale CSR motor was designed and fabricated, three units were processed, and four tests conducted -- two at sea level and two at altitude. In the lightweight motor development phase, the propellant was changed and the nozzle design was modified. Four sea level tests were conducted with varying degrees of success. In the demonstration phase, four motors were fired at Arnold Engineering Development Center, Tullahoma, Tennessee.

TABLE OF CONTENTS

TABLE OF CONTENTS (cont.)

TABLE LIST

FIGURE LIST

FIGURE LIST (cont.)

FIGURE LIST (cont.)

FIGURE LIST (cont.)

FIGURE LIST (cont.)

FIGURE LIST (cont.)

FIGURE LIST (cont.)

FIGURE LIST (cont.)

SECTION I

INTRODUCTION

(U) This report describes the objectives and summarizes the progress attained during the total effort funded under Contract AF 04(611)-10820. This program was monitored by the Air Force Rocket Propulsion Laboratory, and was conducted by the Research and Technology Operations of the Aerojet-General Corporation. The overall objective of this exploratory development program was to design, develop, and demonstrate a single-chamber controllable solid rocket motor. To accomplish this objective, the technical effort was subdivided into seven technical phases: Preliminary Design, Propellant Tailoring, Subscale Motor Design and Development, Heavyweight Motor Development, Lightweight Motor Development, and AEDC Demonstration Tests.

A. PRELIMINARY DESIGN

(U) The purpose of this phase was to establish a baseline for program definition. The major efforts in this phase consisted of (1) Review of current technology, (2) Preliminary trade-off study, (3) Cold-Flow Testing, and (4) Preliminary Motor Design.

B. PROPELLANT TAILORING

(C) The purpose of this phase was to tailor an existing propellant formulation to improve termination ability by L* and P-dot at all back pressures, increase the specific impulse to a design goal of 240 sec at standard conditions and to characterize the final propellant with respect to extinguishability, ballistics, ignitability, mechanical properties, safety, and processing behavior.

C. HEAVYWEIGHT MOTOR DEVELOPMENT

(U) The objective of this phase was to develop the critical motor components by design, analysis, fabrication, and testing of conservative designs to develop the technology necessary to design the lightweight motor. Included in this technical effort was a subscale motor design and test program, the purpose of which was to evaluate the various materials for restart use in a pintle nozzle design. Six subscale and three full-scale motors were planned for this effort.

D. LIGHTWEIGHT MOTOR DEVELOPMENT

(C) The objective of this phase was the development of a lightweight single-chamber controllable solid rocket motor. This motor had a design goal of a mass fraction of 0.80, must be capable of six thrusting periods with the length and dwell time between periods of thrusting fully controllable by the operator, must be capable of a minimum thrust variation of 3:1 and must be operable at any back pressure from sea level to hard vacuum. Eight fullscale motors were planned for this effort.

SECTION II

SUMMARY

(U) The results of the total technical effort conducted under Contract AF 04(611)-10820 are presented in this report. As shown on Figure II-1, the initiation of work on this contract occurred 1 July 1965 and continued for the eighteen month period through 31 December 1966. An extension of this effort was approved by the Air Force (AFRPL) to permit the inclusion of the demonstration test results in this report. Previous efforts on this program (from 1 July 1965 through 30 September 1966) were reported in the five quarterly reports issued under Contract AF 04(611)-10820. These reports are available under the following AFRPL report numbers: First Quarterly Report - AFRPL-TR-65-204, Second Quarterly Report - AFRPL-TR-66-12, Third Quarterly Report - AFRPL-TR-66-99, Fourth Quarterly Report - AFRPL-TR-66-164, and the Fifth Quarterly Report - AFRPL-TR-66-281.

A. PRELIMINARY DESIGN

(C) During this task, a comprehensive review of current technology was conducted. More than 55 documents were reviewed and abstracted for information pertinent to this program. A study was conducted to investigate the interrelated parameters of throat area change, thrust modulation capability, extinguishment capability, maximum and minimum chamber pressure and propellant burning rate exponent. Based on this study, a preliminary design was formulated. The baseline motor shown on Figure II-2 has the following characteristics: Thrust variation range of 5:1 from a maximum thrust of 8250 lb, pressure range from 660 - 50 psia, minimum pressure attainable for extinguishment of 15 psia, area change from 6.75 - 30.25 inches-squared, area change response of 10 cps, and propellant burning rate exponent of 0.60.

B. PROPELLANT TAILORING

(C) Working from a basic formulation originally derived under Contract AF 04(611)-9962, a propellant tailoring effort was initiated to modify the ballistic properties and extinguishability of this basic formulation to meet the requirements of the CSRM. Tailoring activities included the investigation of various oxidizers and oxidizer grinds to increase the burning rate exponent, additives to improve the extinguishability of the propellant, and modification of the solids content to improve the specific impulse to meet the 240 sec goal. Three formulations were used in this program: AAB-3216 for the subscale motor tests, AAB-3220 for the Heavyweight Motor Development, and AAP-3249 for the Lightweight Motor Development.

(C) The use of AAB-3216 in the subscale motors was predicted on the similarity of the exhaust gas by-products and thermal environment of this propellant with that expected in the final formulation. This propellant contained

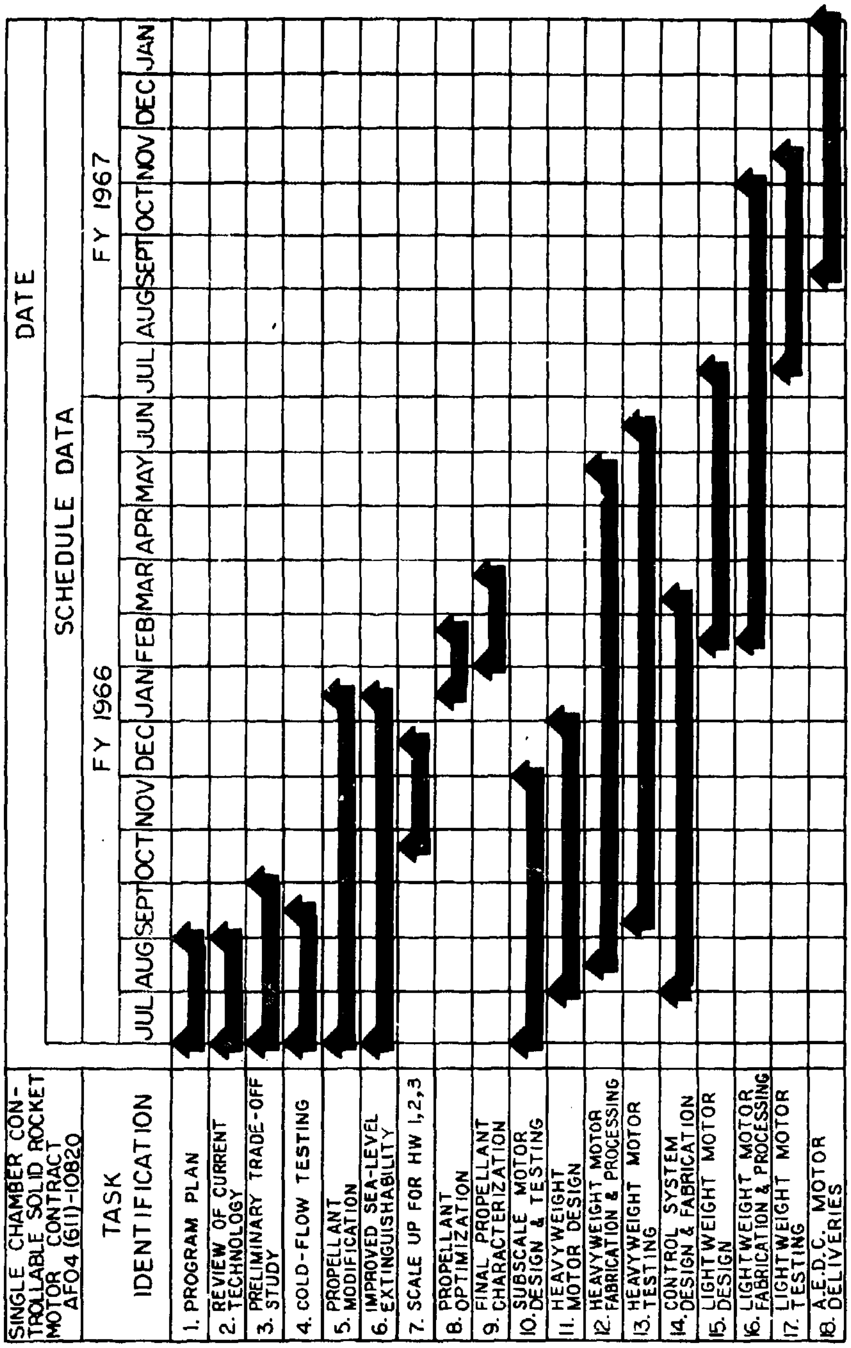

Cost Planning and Appraisal Chart

Figure II-1

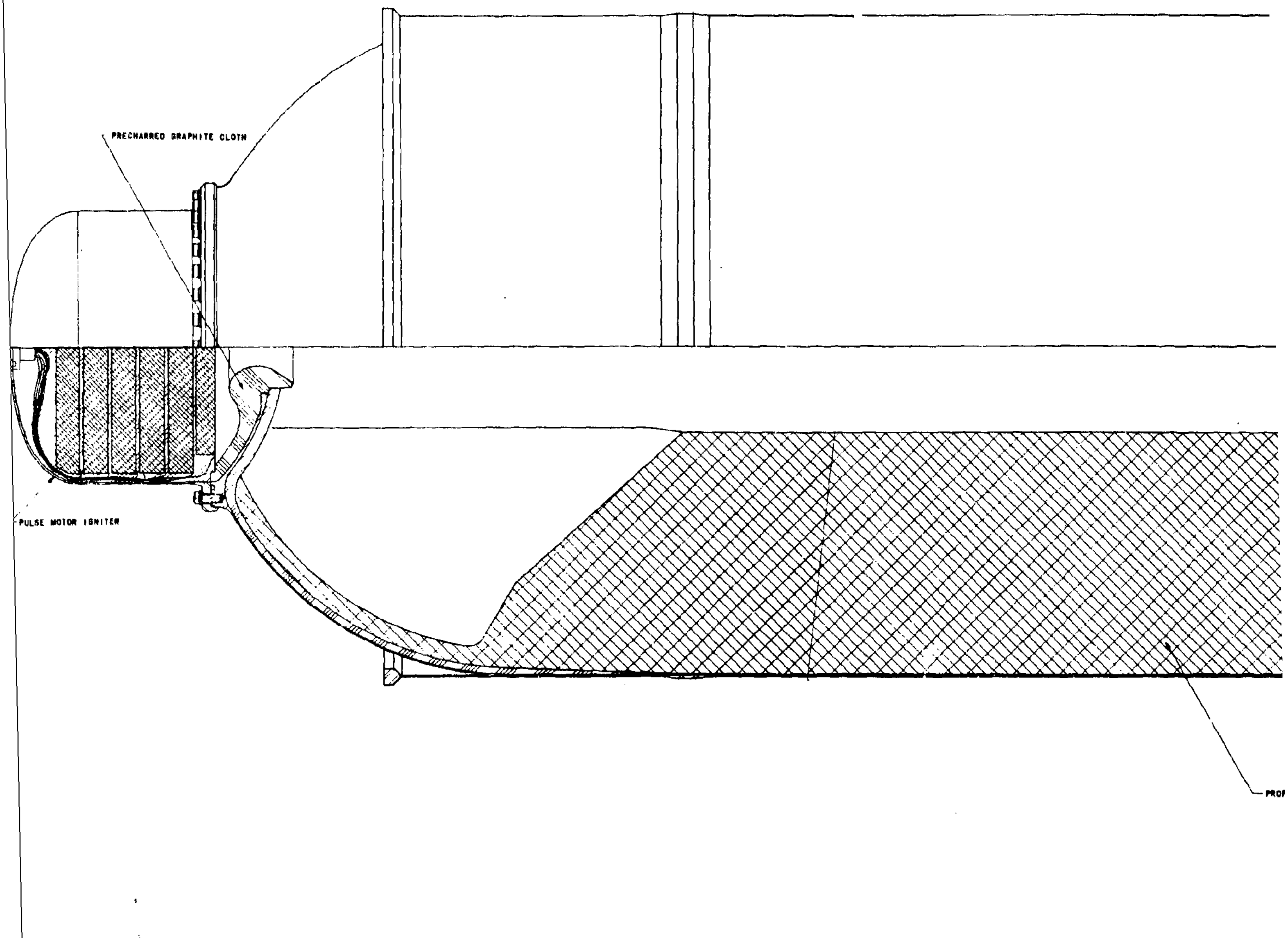
PRECHARRED GRAPHITE CLOTH
PULSE MOTOR IGNITER

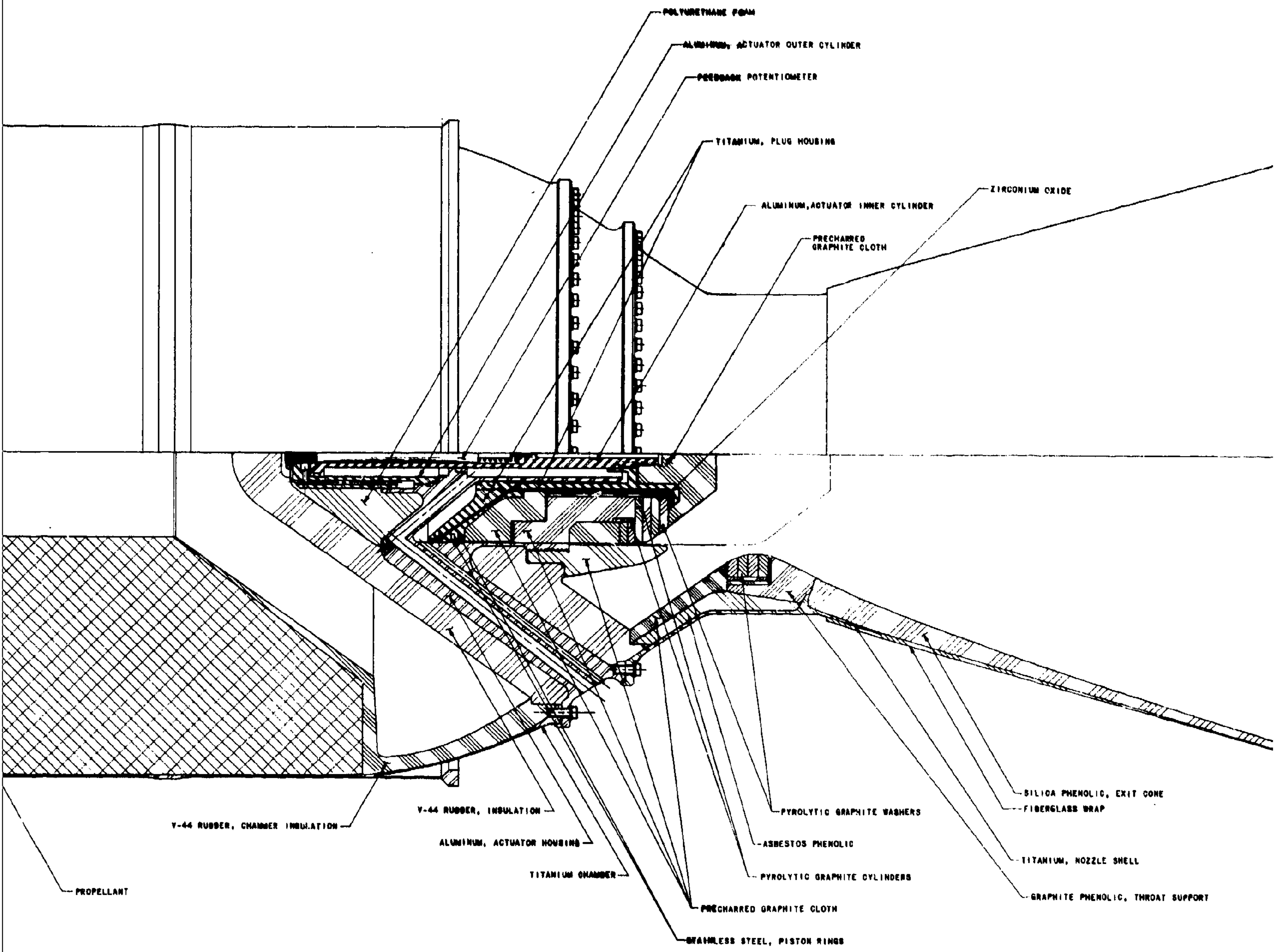

Preliminary Motor Design -

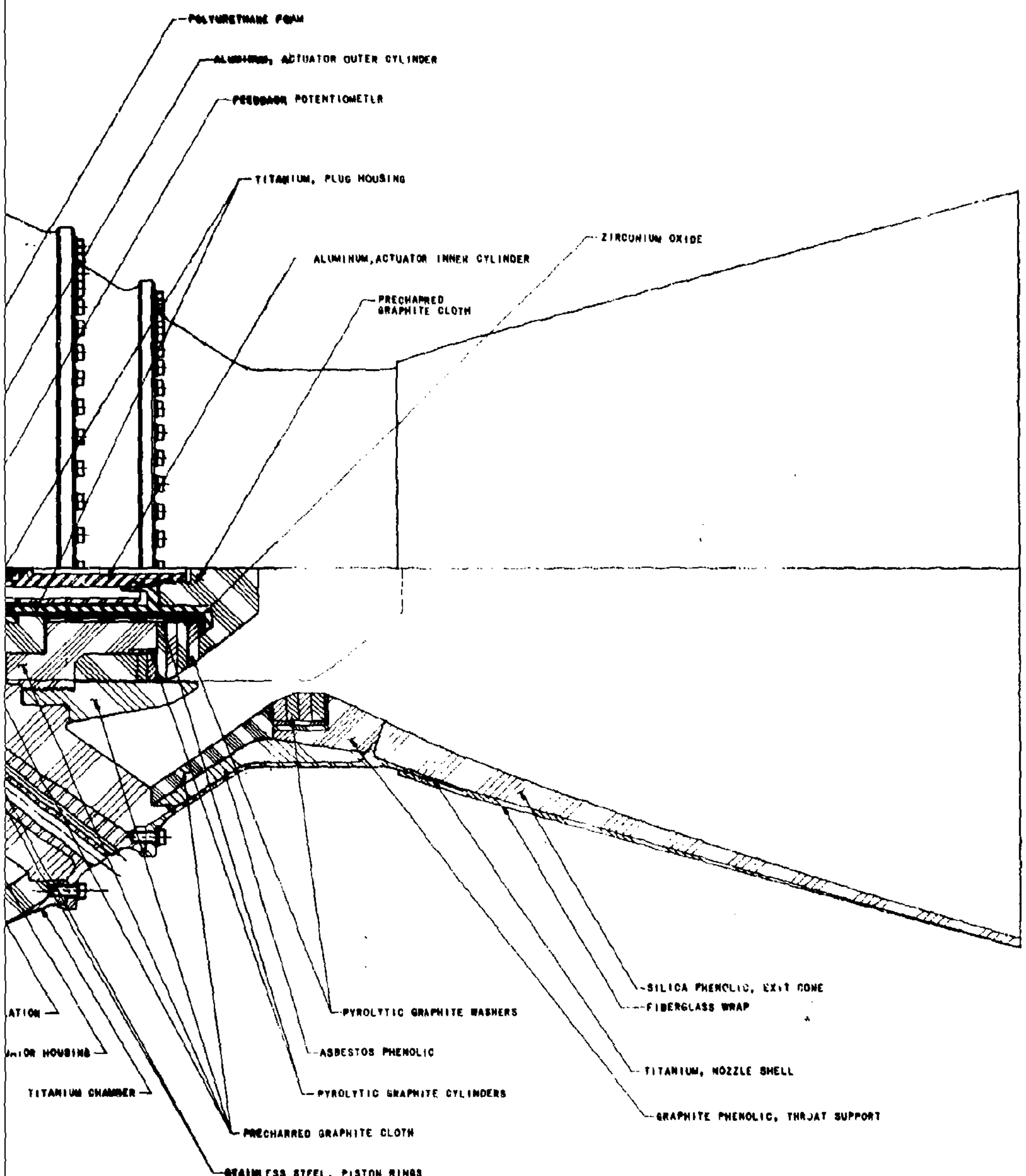

WEIGHTS

CASE	34.09
INTERNAL INSULATION	61.11
NOZZLE	40.34
PLUG AND HOUSING	37.06
IGNITER INERT	8.13
HYDRAPAC	9.50
TOTAL INERT	190.13
MAIN PROPELLANT	697.06
IGNITER PROPELLANT	12.76
TOTAL PROPELLANT	709.82
TOTAL MOTOR WEIGHT	900.25
MASS FRACTION	0.788

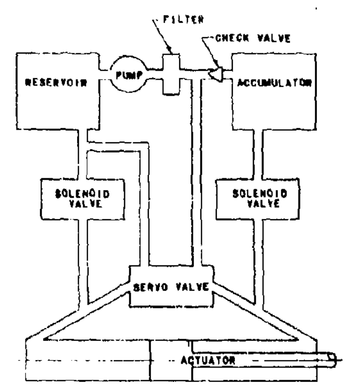

PLUG ACTUATION SYSTEM SCHEMATIC

Preliminary Motor Design - Controllable Solid Rocket Motor (u)

Figure II-2

CONFIDENTIAL

II, B, Propellant Tailoring (cont.)

61% NH_4ClO_4, 10% $KClO_4$, 15% Al, 2% NaCl, and 12% epoxy cured PBD. The formulation selected for the heavyweight motor was AAB-3220, an outgrowth of the subscale formulation that had better extinguishment properties. This formulation contained 50% NH_4ClO_4, 20% $KClO_4$, 16% Al, and 14% PBD. The expected specific impulse of this formulation was 238 plus sec, slightly less than the 240 sec goal.

(C) Due to burning rate difficulties at the low pressure end of the CSR operating region and the marginal characteristics of AAB-3220, the propellant formulation was changed for the lightweight motors to AAP-3249. This formulation contains 51% NH_4ClO_4, 15% NQ (nitroguanidine), 10% Al, 3% NaCl, and 21% NPPU. This propellant had a lower burning rate than AAB-3220 over the entire range of pressures and appeared to have better extinguishability properties based on subscale test data.

C. HEAVYWEIGHT MOTOR DEVELOPMENT

(U) During this effort, a total of six subscale motors, containing 100 pounds of AAB-3216 propellant each, were tested to verify the materials selections for the nozzle design, to establish the refire capability of pintle nozzles, and to establish the thermal environment due to radiation feedback from the nozzle after extinction had been accomplished. All of the above objectives were met during this effort, and the selection of the materials for the heavyweight motor nozzle design were verified by successful testing of this design in a subscale version. An alternate nozzle materials selection was eliminated by failure of that design in the subscale motor.

(C) A total of three heavyweight motors were fabricated and test fired in this effort. Each motor contained approximately 590 pounds of AAB-3220 propellant. The first motor, HW-1, was fired to establish the ballistics of the system, verify the design integrity, and check the materials' performance prior to varying the thrust or extinguishing the motor. Since this sea level test was completely successful, the second motor was fired for thrust variation and sea level extinguishment. Motor HW-2 fired successfully and achieved thrust variation from 8600 - 1250 pounds; however, the sea level extinguishment was aborted by reignition after approximately 1.2 seconds of extinction. Motor HW-3 was fired at a simulated altitude of 60,600 feet. This motor was successfully extinguished once after 5 seconds of burning. On refire of this motor, a malfunction of the special test equipment combined with an error in external insulation of the nozzle precluded achievement of extinction.

(U) A pressure feedback control system was designed and built to control the CSR motor based upon the multiple of chamber pressure and nozzle throat area signals being fed back from the motor. This system contains an analog computer that is capable of varying the system gains depending upon chamber pressure, and is fully capable of controlling any type of controllable solid

rocket motor by minor modifications of the inputs and initial set-point gains. The system can fire the motor a total of ten times, can vary thrust from an external program input or manually, and can effect shutdown by either P-dot or L*. To operate this system, only 115 vac and 28 vdc power inputs are required, all other power and checkout systems being self-contained.

D. LIGHTWEIGHT MOTOR DEVELOPMENT

(U) During this effort a total of eight lightweight motors were fabricated. The basic difference between the lightweight motor design and the heavyweight motor design was the propellant used and the nozzle pintle design used. Of these eight motors, four were test fired at Aerojet's Sacramento Test Facility and four were fired at Arnold Engineering Development Center, Tullahoma, Tennessee.

(C) Two of the four motors fired at Aerojet failed early in the test due to pintle insert malfunctions. Both malfunctions were traced to low physical properties of the materials used. The other two motors fired for over 40 seconds, exhibiting good control; however, LW-2 ejected its pintle at 43.5 seconds. Some oscillation was experienced in LW-2; however this was due to a servo valve stickage which was corrected in the test of LW-4. A design change from the use of silver infiltrated tungsten as a pintle insert to the use of pyrolytic graphite washers was verified by the test of LW-4.

(C) The first motor tested at AEDC, LW-5, was programmed to vary thrust and extinguish after approximately eight seconds. The thrust variation was subject to lags and some oscillations due to a bad component in the analog computer used to control the motor. Extinguishment was temporarily achieved; however, reignition occurred probably due to gas phase ignition at the nozzle surface with the pintle in the minimum throat position.

(C) The firing of LW-9, LW-10, and LW-11 at AEDC took place in July 1967. Motor LW-9 was fired a total of six times, demonstrated a thrust variation capability of approximately 6:1 (6500-1050 pounds). Each pulse was extinguished and the motor permitted to cool for a minimum of three hours between firings. Motor LW-10 was fired a total of six times and demonstrated a thrust variation of 6100-4000 pounds. This motor was also permitted to cool between pulses. Motor LW-11 was fired a total of five times: the first pulse was manually controlled from the throttle on the control console, the second and third pulses were fired remotely only two minutes apart, and the final two pulses were permitted to cool between firings. This motor demonstrated a controlled thrust variation from 6300-3500 pounds. On the last two motors, no effort was made to demonstrate the low end of the thrust capability as the first motor had experienced some inadvertent extinctions when asked to lower the thrust level to 1000 pounds.

(U) Although the pintle end insulation cap and some of the pyrolytic graphite in the pintle throat area were lost during the AEDC demonstration test series, the motor was demonstrated as required by the program work statement, surpassing the required thrust variability. Although some of the pintle flame liner material was lost, the control of the motor was excellent; the only change in the characteristics of control noted was the change in thrust level at which control occurred due to the physical change in the available nozzle throat area due to the loss of the components. This factor indicated that the system is apparently capable of completing a mission although some damage is sustained in the nozzle area so long as the hydraulic system and the control system are not damaged.

SECTION III

TECHNICAL DISCUSSION

A. PRELIMINARY DESIGN

1. Review of Current Technology

(U) A comprehensive literature search was conducted to accumulate a bibliography of published technical data applicable to variable thrust-stop-restart. The majority of these documents have been obtained, reviewed, and data applicable to this program abstracted. A list of the documents received and reviewed is included as the list of references.

(U) During the review of these documents, much information directly applicable to this program was obtained. Some of this more pertinent information is summarized in the following section.

Ref 1. Landers, L. C., Development of Extinguishable Solid Propellant (u), RPL-TR-65-147, Final Report for AF 04(611)-9889, 19 July 1965 (CONFIDENTIAL).

(C) The composite propellant developed on this program exhibited an extinguishability greatly improved over the conventional state-of-the-art propellants by its use of $KClO_4$ and NaCl; in motor tests, it extinguished at less than 5% of the depressurization rate required for extinguishment of a conventional propellant. The critical depressurization rate for extinguishment of this propellant in vacuum does not appear to be significantly affected by grain temperature in the region of -40 to 150°F.

(U) A theoretical study of propellant extinguishment was made on the basis of the development of an equation describing the instantaneous burning rate as a function of both pressure and rate of pressure change. From this the condition for extinguishment initiation is obtained by solving for the depressurization rate which causes the instantaneous burning rate to vanish. The transient burning rate equation was critically reviewed with regard to assumptions made in its derivation. Correction terms were derived for the heat release or absorption at the propellant surface, erosive burning, and the time lag in solid phase response to gas phase changes. Only the last factor is considered to be significant.

(U) A theoretical criterion of extinguishment permanence was derived using the approach that the condition for extinguishment permanence is met if after extinguishment initiation (burning rate becomes zero) the hot chamber gases vent to below the critical propellant ignition pressure in a time interval less than the ignition induction time. The chemical induction theory of solid propellant ignition was used in the derivation.

(U) A theoretical analysis was made of the problem of thrust transients or spikes resulting when a motor is rapidly vented by increasing the nozzle throat area. The analysis showed that the significant parameters affecting thrust spike were motor L* (free volume/throat area) and the rate of nozzle area increase; whereas, the burning rate and pressure exponent have negligible effects. Thus, a reduction in the critical depressurization rate required for propellant extinguishment is very desirable for reducing thrust spike.

(U) Firings in movable pintle nozzle motors of various configurations showed that extinguishment was little affected by motor geometry, but was significantly affected by the depressurization path and therefore the "level-off" pressure to which the nozzle is opened. In other words, extinguishment cannot be characterized by a simple depressurization rate at a certain initial chamber pressure as was done heretofore, but must be reviewed from the standpoint of the entire path during depressurization. This is a parameter which had not previously been taken into account; propellants have been characterized only by a critical depressurization rate determined in tests of essentially constant level-off pressure.

(U) An analysis of all firing results leads to the following conclusions:

(C) 1. In all cases where extinguishment occurred, the observed $\dot{p}$ exceeded the calculated $\dot{p}_{r=0}$, which is the instantaneous depressurization rate theoretically required to reduce the instantaneous burning rate to zero. Where permanent extinguishment did not occur, the observed $\dot{p}$ usually but not always failed to reach or exceed the theoretical requirement. This is consistent with the view that the transient burning rate equation can be used to define conditions for extinguishment initiation which are necessary but not always sufficient for permanent extinguishment, and that a no-reignition criterion must also be satisfied to achieve permanent extinguishment.

(C) 2. The extinguishment of a motor-propellant system may be initiated only after satisfying a critical combination of p and $\dot{p}$; i.e., the instantaneous depressurization rate and the corresponding instantaneous pressure must satisfy the initiation condition defined by the transient burning rate equation somewhere along the depressurization path (usually not initially). The parameters most commonly used heretofore, namely maximum $\dot{p}$ and initial chamber pressure (before depressurization), may define an extinguishment or no-extinguishment condition only after satisfying the qualifying conditions discussed below in Conclusion 4.

(C) 3. Even after the instantaneous $\dot{p}$-p meets the extinguishment initiation conditions so that the instantaneous burning rate is zero, permanent extinguishment can be realized only when reignition conditions do

not exist. In this respect the level-off pressure (corresponding to the final A_t) and the ambient back pressure are important considerations.

(U) 4. Earlier work in which extinguishment criteria were defined in terms of a $\dot{p}_{cr}$ corresponding to a given initial chamber pressure for a propellant motor system are subjected to the following qualifications:

a. The "depressurization path" must follow a fixed mathematical function of the initial chamber pressure, be it exponential, sine, linear, hyperbolic, or some other type. In other words, for fixed values of initial chamber pressure and $\dot{p}_{max}$ the rest of the p-t (and $\dot{p}$-p) curve is defined.

b. The level-off pressure must be either constant or low enough so that the reignition consideration is not significant.

c. The ambient back pressure must be either kept constant or low enough so that the reignition consideration is not significant.

(U) All $\dot{p}$ firing tests at Aerojet, as well as those of Ciepluch satisfied the above conditions in that (1) an essentially exponential depressurization path was followed, (2) the nozzle was opened to a relatively low level-off pressure and the effect of p-t and p-$\dot{p}$ history was clearly demonstrated in the pintle-nozzle motor firing in this work.

Ref 2. Sanders, J. W., Theoretical and Experimental Characterization of Technique for Extinguishment of Solid Propellant Rocket Motors (L*), preliminary draft final report for Contract AF 04(611)-9662, 16 June to 19 July 1965.

(C) The L* extinguishment characteristics of a polyurethane and a polybutadiene propellant were improved by incorporating $KClO_4$ and NaCl. These propellants that extinguished in a pressure range of 19 to 44 psia for an L* range of 100 to 250 in. in cylindrical-core configurations are of practical interest for stop-start and controllable-thrust motor applications. Experimental data indicated that it would be extremely difficult to increase the L* extinguishment pressure to over 100 psia for a conventional AP/Al composite system. Theoretical studies also indicate this, since the L* extinguishment initiation has been calculated to occur in the 50 to 100 psia range. However, the following propellant formulation variables were found to affect the L*-p_e relationship:

III, A, Preliminary Design (cont.)

(C) 1. The incorporation of 10% $KClO_4$ in place of NH_4ClO_4 and 3% NaCl in place of binder produced a marked improvement in extinguishment by L* techniques as well as by rapid depressurization.

(C) 2. The propellant binder significantly affected L* extinguishment characteristics. Polyurethane propellants extinguished easier (at a higher pressure for a given L* value) than polybutadiene propellants with the same solids loading. A nitroplastisol propellant also extinguished more easily than a polybutadiene and polyurethane propellant of the same I_{sp}.

(C) 3. Incorporation of nitroguanidine in place of NH_4ClO_4 made extinguishment pressure less sensitive to L*.

(C) 4. The effect of replacing aluminum with NH_4ClO_4 is dependent on the propellant binder and the total solids loading. The effect is small in a polybutadiene binder or at high solids loading.

(C) Variation in the propellant temperature from -40 to plus 150°F was found to have no significant effect on L* extinguishment behavior. This is an agreement with theoretical predictions.

(C) A unified theory of extinguishment by pressure perturbation was developed. The theory is applicable independent of the origin of the pressure perturbation; e.g., externally induced rapid depressurization or internally induced pressure fluctuation inherent in any motor firing. Extinguishment is initiated by the burning rate suppressing effect of a depressurization transient; whereas, the permanence of such initiated extinguishment is governed by the ignition process during the venting following initiation. The L* extinguishment phenomenon can be treated as a special case of the generalized theory.

(C) A theoretical study of propellant extinguishment initiation was made based on the transient burning rate equation which gives the instantaneous burning rate as a function of both pressure and rate of pressure change. From this equation the condition for extinguishment initiation is obtained by solving for the depressurization rate that causes the instantaneous burning rate to vanish. This criterion is applicable regardless of the source of pressure perturbation.

(C) The transient burning rate equation was critically reviewed with regard to assumptions made in its derivation. Correction terms were derived for the heat release or absorption at the propellant surface, erosive burning, and the time lag in solid phase response to gas phase changes. Only the last factor is considered to be significant.

III, A, Preliminary Design (cont.)

(C) A theoretical criterion of extinguishment permanence is met if after extinguishment initiation (burning rate becomes zero) the hot chamber gases vent to below the critical propellant ignition pressure in a time interval less than the chemical induction time for ignition. The chemical induction theory of solid propellant ignition was used in the derivation.

(C) To predict the extinguishment behavior of a motor-propellant system, the motor transient interior ballistic equations for describing the depressurization process of a motor-propellant system have been derived. When used in conjunction with the $\dot{p}$ required to completely suppress burning rate, these equations predict the point of extinguishment initiation. The equations are also unified in the calculation of venting time following extinguishment initiation for the prediction of extinguishment permanence.

(C) Theoretical predictions were checked against the experimental L* extinguishment data. The L* instability region defined by the L*-p_i (extinguishment initiation pressure) was consistent with experimental L*-p_e (extinguishment pressure) results, in that L*-p_e always falls within the calculated instability region. The theoretical L*-p_e relationship calculated based on the arc-image ignitability data using the extinguishment permanence criterion was found to agree well with the experimental results.

(U) The L* extinguishment characteristics of the polyurethane and PBD propellants developed on the program were studied in motors with movable pintle-nozzles. The following significant observations of the effects of grain size and configuration on L* extinguishment were made.

(C) 1. End-burning configurations were found to be much more difficult to extinguish than the internal-burning configurations; the extinguishment pressures of end-burning grains were less than 15 psia in all cases and shown to be less than 3 psia in several (L*-range 60 to 500 in.). Grains of the same OD, but with a cylindrical-core configuration extinguished in pintle-nozzle motors at pressures in the range of 19 to 44 psia.

(C) 2. L* extinguishment of grains with cylindrical cores were affected by the length of the grain. Short grains ($L_p \approx 8$ in.) extinguished at significantly lower pressures (closer to extinguishment characteristics of end-burning grains) than did longer grains ($L_p \approx 26.5$ in.).

(C) The results of tests in pintle-nozzle motors indicated a strong effect of motor configuration on L* extinguishment phenomena, which is in sharp contrast to the lack of a significant configuration effect on extinguishment by rapid depressurization. The results are reasonable since L* extinguishment is initiated and is dependent entirely on the internal system instability at low pressures. On the other hand, $\dot{p}$ extinguishment is caused by an externally applied pressure drop, and in this situation, the internal system instability plays only a relatively minor role.

III, A, Preliminary Design (cont.)

Ref 3. Development of an Intermittent Operating Variable Thrust Solid Propellant Rocket Motor, Contract AF 04(611)-8175, Amcel Propulsion Company, Asheville, N.C., July 1962.

QR-1, 16 April - 15 July 1962, APR-7, (C) July 1962

(C) The basic fuel-rich propellant PPO-4 contains approximately 43.5% of "Fluid Ball" powder Type B, 43.5% TEGDN, 1% Resorcinol and 12% polyethylene. Substitution of $KClO_4$ (5%) of RDX (7.5%) for part of the "Fluid Ball" powder increased n from 0.8 to 1.0. The oxidizer-rich propellant containing 90% AP/10% Kel-F burns when heated above 300°F in air or when hot (1600°F) fuel rich gases pass over it; burning rates of int-ext burning grains agree closely with those of pure AP pressed strands.

Ref 4. Development of an Intermittent Operating Variable Thrust Solid Propellant Rocket Motor, Contract AF 04(611)-8175, Amcel Propulsion Company, Asheville, N.C., July 1962.

QR-2, 16 July - 15 October 1962, APR-7-2, (C) October 1962

(C) Burning rate data of fuel-rich propellant PPO-4 containing 12% polyethylene from 6-in. motors differed greatly from 2-in. pipe motors; polyethylene appears to char and leave carbonaceous residue in 6-in. motor. Replacing polyethylene with nitroguanidine (PPO-13) eliminates both carbonaceous residue and discrepancy in burning rate data.

Ref 5. Development of an Intermittent Operating Variable Thrust Solid Propellant Rocket Motor, Contract AF 04(611)-8175, Amcel Propulsion Company, Asheville, N.C., July 1962.

(C) Combustion of fuel-rich propellant PPO-13 was terminated by increasing A_T by a factor of 4.3 (explosive bolts); dp/dt not given.

Ref 6. Controllable Solid Propellant Rocket Motor, Contract AF 04(611)-9067, Amcel Propulsion Company, Asheville, N. C., June 1963.

QR-1, 15 March 1963 - 15 June 1963, APR-21-1 (C) June 1963

III, A, Preliminary Design (cont.)

(C) A series of HMX/AP/PBAA-epoxy propellants were evaluated for effect of HMX/AP ratio and certain additives on burning rate vs pressure. As HMX/AP increased, n increased. Ten percent $KClO_4$ in place of AP lowered n. Two percent Fe_2O_3 increased n slightly.

(C) Five percent Al substituted for AP in the oxidizer-rich propellant 90/10:AP/Kel-F decreased the pressure deflagration limit (P_{DL}) from 900 to 400 psi.

(C) Castable propellants of 77 to 80% solids were made with a C_9 fluoromethacrylate.

Ref 7. Controllable Solid Propellant Rocket Motor, Contract AF 04(611)-9067, Amcel Propulsion Company, Asheville, N. C., June 1963.

QR-2, 16 June - 15 September 1963, APR-21-2 (C), September 1963

(C) One fullscale motor was stopped and restarted four times on command and thrust was modulated by a factor of approximately 3:1; dp/dt not given. The forward-propellant PPO-13, terminated by dp/dt, contained 43.5% Ball Powder B, 43.5% TEGDN, 1% Resorcinol and 12% nitroguanidine; the aft propellant OX-1 contained 90% AP and 10% Kel-F. No chuffing or reignition after extinguishment was encountered.

Ref 8. Controllable Solid Propellant Rocket Motor, Contract AF 04(611)-9067, Amcel Propulsion Company, Asheville, N. C., June 1963.

QR-3, 16 September - 15 December 1963, APR-21-3 (C), December 1963

(C) A noncombustible copolymer of C_9 fluoromethacrylate and C_5 fluoroacrylate was developed for bonding pressed grains of AP/Kel-F to the case. Propellants with binder of fluoroacrylates, fluoromethacrylates and carboxy-terminated fluorocarbons could not be loaded with more than 80% total solids. $LiClO_4$ propellants with acrylamide or acrylonitrile binders are too brittle.

(C) Forward-propellant PPO-61 can be terminated by rapid depressurization, but reignition occurs at sea level. A plot of critical dp/dt versus chamber pressure for forward-propellant PPO-13 was derived from over 20 firings. Aft-propellants OX-5 and OX-6 containing 10 and 15% aluminum, respectively, often reignited and burned with a series of explosions after the forward-propellant had extinguished; this phenomenon had not occurred with nonaluminized aft propellant OX-1.

III, A, Preliminary Design (cont.)

(U) The first attempts of providing a feedback control system are presented.

Ref 9. Controllable Solid Propellant Rocket Motor, Report Contract AF 04(611)-9067, Amcel Propulsion Company, Asheville, N. C., June 1963.

9067, Second Annual Report - Fiscal Year 1963, APR-21-4 (C) September 1964 (RPL-TRR-64-52)

(C) A fullscale motor operated through five on-off cycles at sea level. Motor conditions including dp/dt at 25% decay point are tabulated for subscale and fullscale extinguishment tests. Most extinguishment tests used a forward grain of nitroplastisol propellant PPO-13 (43.5% Ball Powder B, 43.5% TEGDN, 13% nitroguanidine and 1% Resorcinol) and pressed aft grains of AP and Kel-F with and without Al.

(C) Lab studies of PBAA-HMX-AP forward-propellants and castable aft-propellants with fluoroacrylate and methacrylate binders or $LiClO_4$-acrylamide solid solutions are described.

Ref 10. Dual chamber Controllable Solid Propellant Rocket Motor, Contract AF 04(611)-9067, Amcel Propulsion Company, Asheville, N. C.

QR-4, 10 February - 10 May 1964, APR-21-5 (C) May 1964

(C) In a nitroplastisol binder, ammonium oxide was incompatible, TAZ was slightly incompatible, and both $KClO_4$ and HMX increased n.

(C) A processable nonaluminized solid-solution propellant has been made containing 76% AP and 14% $LiClO_4$ in a polyacrylamide-ethylene glycol binder. The burning rate exponent was 0.75 to 0.77. This propellant extinguished reproducibly in subscale motors when forwarded propellant was terminated. Adding 10% Al and reducing $LiClO_4$ to 12% caused propellant to reignite after extinguishment at sea level.

(C) A series of insulation tests were run but no conclusions drawn as to which insulation was best for a CSR application.

Ref 11. Dual-Chamber Controllable Solid Propellant Rocket Motor, Contract AF 04(611)-9067, Amcel Propulsion Company, Asheville, N. C.

QR-5, 10 May - 9 August 1964, APR-21-6 (C) August 1964

III, A, Preliminary Design (cont.)

(U) This report presents the results of a reignition study that was conducted. This analysis showed that the most important parameter affecting the energy absorbed by the propellant's surface is the ratio of chamber free volume to propellant surface area. The analysis consisted of a heat balance on the propellant surface of an uninsulated pancake motor as a function of time, with time zero at termination. In this analysis the chamber residual gas temperature was assumed to be that resulting from an isentropic expansion from the termination to sea-level pressures from the propellant flash temperature. A series of tests to verify this analysis was conducted. In these tests the ratio of chamber free volume to propellant surface area was varied over a wide range. These tests show that the critical value of the free volume to surface area ratio above which complete extinguishment could not be achieved is a function of the termination chamber pressure. This is explained by, first, residual gas temperature being higher at the lower chamber pressures from an assumed isentropic expansion; therefore, for an equal free volume with a constant surface area, the internal energy of the residual gases is greater at low pressures. Secondly, the expression for the propellant preheat shows that the preheat is inversely proportional to chamber pressure to the nth power. Therefore, as the pressure decreases, the preheat increases. As the result of these factors, less heat transfer from the residual chamber gases is required to raise the propellant surface to auto-ignition temperature at the lower chamber pressures than at high chamber pressures.

(C) Also in this report, the design of a chamber purging system is provided. This chamber purge consists of supplying a small amount of nitrogen gas from a standard cylinder through a regulator to a purging accumulator and then into the motor. The amounts of nitrogen are varied to develop a general procedure for predicting the amount of coolant that will be required in the test motors.

(C) Addition of 5 and 10% oxamide to a nitroplastisol propellant system increased n; this formulation was extinguished in subscale motors using very high dp/dt, but was not tested with low dp/dt. Laboratory studies of aft-propellants based on $LiClO_4$-acrylamide solid-solutions containing AP or HMX continued.

Ref 12. Dual-Chamber Controllable Solid Propellant Rocket Motor, Contract AF 04(611)-9067, Amcel Propulsion Company, Asheville, N. C.

QR-6, August - 9 November 1964, APR-21-7 (C) November 1964

(C) Characterization of forward propellant PPO-90 containing 47% Ball Powder, 47% TEGDN, 1% Resorcinol and 5% Oxamide was completed, its extinguishment was studied only with relatively high dp/dt's.

III, A, Preliminary Design (cont.)

(C) A castable aft-propellant of 63% AP, 15% Al, and a C_7 fluoroacrylate binder was tested for extinguishment with forward propellant PPC-13. Reignition of the aft grain occurred when dp/dt in the forward chamber was relatively low; a nitrogen purge normally prevents reignition of the aft grain. HNF has been processed in 20 to 50-gram batches of the following systems: (1) $LiClO_4$-acrylamide solid-solution, failed to cure, (2) nitroplastisol and (3) siloxane, burned at 1 atm pressure, and (4) Viton.

(C) Fullscale motor tests showed pressure oscillations in the aft-chamber of 8 to 11 cps, typical of L* instability; average chamber pressures were in the range of 150 to 300 psia. Aft propellant OX-5 contained 80% AP, 10% Al and 10% Kel-F.

(C) Tests with the nitrogen purge system to prevent reignition of the forward chamber were conducted but the minimum amount of purge required to prevent reignition was not determined. Three insulation materials, V3021, V44, and 39322, manufactured by B. F. Goodrich were installed and tested. Tests were conducted for over 2 min and the motor disassembled, but there was no significant difference in the char characteristics of the three materials. Each formed a hard flaky char, but the ablative properties of V44 appeared slightly superior. Two demonstration tests were conducted at sea level. Permanent extinguishment was achieved on the first cycle but the motor reignited after termination of the second cycle in each case, in spite of increased amount of the nitrogen purge. It was considered that the cause of reignition was unrelated to the residual hot gas in the motor since most of the gas should have been expelled by the purge. It was considered more likely that reignition resulted from hot aluminum or aluminum oxide that remained on the surface of the aft grain after termination. A thin layer of aluminum was observed on the aft grain following the first cycle tests.

Ref 13. Dual Chamber Controllable Solid Propellant Rocket Motor, Contract AF 04(611)-9067, Amcel Propulsion Company, Asheville, N. C.

QR-7, 10 November 1964 - 10 February 1965, APR-21-8 (C) February 1965

(C) Efforts to develop a castable aft-grain propellant with n = 1 continued with the fluoroacrylate (C_7FA) system and MMM's fluorocarbon monomer FX-189. Low n and low elongation are major problems.

(C) In this report period three additional fullscale motors were tested. During the first test, reignition after the fourth pulse was observed in spite of the nitrogen purge. The remaining two tests were terminated successfully in every case without reignition. These tests apparently showed that the purge is necessary to prevent reignition of fullscale motors after

III, A, Preliminary Design (cont.)

termination at sea level. Also the amount of purge must be increased on successive terminations of the same motor since the free volume increases. A reignition that occurred on the first series of tests was attributed to the hot gases remaining in the chamber following termination. By increasing the amount of purge in the remaining tests, it was able to achieve successive termination without reignition.

Ref. 14. Bennett, H. L., Dual-Chamber Controllable Solid Propellant Rocket Motor, Quarterly Progress Report NOTS TP 3789 (C), May 1965.

(C) This report presents the results of progress made towards the development of a controllable solid propellant rocket motor at NOTS, China Lake. This report is principally propellant development effort and reports from the flow coefficient of the aft grain.

Ref 15. Bennett, H. L., Dual-Chamber Controllable Solid Propellant Rocket Motor, Quarterly Progress Report NOTS TP 3789, May 1965.

(C) This is a continuation of the previous report. Again, this report is principally propellant development and continues to show problems associated with injecting the gas from the forward chamber into the aft chamber.

Ref 17. An Investigation and Feasibility Demonstration of Nozzles for Restartable Solid Rocket Motors, Second Quarterly Technical Report, Philco C-2952 (C), RPL-TDR 64-158, 20 December 1964.

(U) Thermal analysis of various material stackups shows a considerable thermal advantage of using an annealed pyrolytic graphite as opposed to the as-deposited pyrolytic graphite. The difference apparently is the direct consequence of the increase in the thermal conductivity in the AB direction resulting from annealing. Because of this higher conductivity it is possible to run for a longer duration before the surface reaches 5000° and to refire after a shorter delay because it cools off faster.

(U) In the study of the application of various backup materials for throat insert insulation, a stackup consisting of a pyrolytic graphite shell backed with an asbestos phenolic was found to exceed all other material configurations investigated. This was attributed to the fact that the pyrolytic graphite backup provided additional heat capacity to the throat insert and also insulated the throat insert from the ablator causing the ablation to be delayed and to proceed at a slower rate. Asbestos phenolic was found to be superior to silica from a thermal standpoint.

III, A, Preliminary Design (cont.)

(U) Materials analysis show that pyrolytic graphite has very little strength after being subjected to high temperature, approximately 2800°C, for a short period of time approximately 15 sec under high axial loads. The material probably becomes very similar to fully annealed pyrolytic graphite which is very soft and weak.

(C) In the rocket motor tests with insulation materials as backup not exposed to the flame front, after three firing cycles both asbestos and Refrasil phenolic showed to be in very good structural condition. The Refrasil phenolic showed a relatively high char depth, almost twice as much as the asbestos phenolic, but had little or no structural deteriorations, indicating a high strength char.

(C) Summarizing the results of the five subscale tests indicates that pyrolytic graphite throated nozzles of the washer type offer a very good possibility in a restart application. Both asbestos and silica phenolic looked very good in the area of backup insulators which are not exposed to the flame. Molded asbestos phenolic appears to be the superior system of those that were examined. The attributes of the asbestos phenolic are its (1) lower char growth, which means longer service life, (2) relatively good structural integrity after cycling, (3) good insulating properties, (4) ease of machining, and (5) relatively low cost of fabrication.

(U) This report provided much valuable data of thermal analysis, structural analysis, and materials behavior. The thermal analysis consisted of continued discussion of an improvement of the convection heat-transfer problem, presented conduction calculations for various nozzle material combinations, predicted the effects of ablation of insulation materials on cooldown, and presented the effects of pulse operation on various heat-sink designs.

Ref 18. An Investigation and Feasibility Demonstration of Nozzles for Restartable Solid Rocket Motors, Third Quarterly Technical Report, Philco C-3023 (C), RPL TDR 65-53, 22 March 1965.

(U) This report provides a very versatile method for determining throat insert duty cycles using the thermal analysis. This method consists of developing heat content curves that specify the energy level of throat inserts during firing and cooldown. The maximum firing time with the number of short pulses given the firing time for each pulse to achieve the initiation of throat recession can be determined. The minimum length of the cooldown period can be found before a throat insert can be restarted for any continuous pulse motor firing.

(C) From the firings conducted it is apparent that the duty cycle limitations for tungsten nozzles are far more subtle than for pyrolytic graphite washer nozzles and are more dependent on the design limits than the limitations of the supporting nozzles materials. There does not appear to be any simple relationship between firing duration, cooldown period, and erosion rate such as applied to the other throat materials.

(C) Throughout all the tests conducted in this series, severe problems were encountered with the entrance section; more so than with the throat. The use of ATJ graphite in conic and cylindrical sections still produced severe erosion, gouging, and cracking. Substituting graphitite GX showed only a marginal improvement. On Test 12, carbon-cloth phenolic was substituted for graphite, and exhibited a marked improvement over graphite. While the regression rate was still relatively high, the erosion proceeded in a uniform rate and was not characterized by the gross cracking and failures that occurred at the graphite entrances. The material was a tape grade of a bias wrap of a 45° orientation normal to the gas stream. In subsequent tests, graphite cloth phenolic was substituted for the carbon cloth, and showed a performance the same as that of carbon cloth.

(U) The conclusions presented at the completion of the subscale program are extremely interesting and worth repeating. The overall areas of interest are broken down into the following basic sections and treated individually.

a. Limitations of Nozzle Throat Materials

(1) Polycrystalline Graphite

(C) Polycrystalline graphite is a throat material and is limited to short pulses with adequate cooldown between pulses and a maximum of eight to ten restarts. The higher density polycrystalline graphite such as graphitite GX extends these limits slightly but not sufficiently.

(2) Pyrolytic Graphite (Edge-Oriented Configuration)

(C) The use of an edge-oriented pyrolytic graphite throat is primarily a function of chemical corrosion. Indications are that annealing or partial annealing of pyrolytic graphite can extend the total allowable firing duration to a degree. The use of a maximum pulse length before adequate cooling effectively reduces the maximum allowable pulse length of subsequent cycles slightly due to washer gapping and creation of resultant sites for selective erosion. Design mechanics such as allowances for thermal expansion does not appear to be a limiting problem.

(3) Pyrolytic Graphite (Shell Configuration)

(C) The present state-of-the-art of fabrication of P.G. shells precludes its use in a restart application.

(4) Tungsten

(C) Although tungsten has exhibited excellent erosion resistance, it has some serious restart limitations when compared to polycrystalline graphite for short pulse or to edge-oriented pyrolytic graphite for long firing times. There is the possibility of fracture after a small number of pulses because of the property changes which occur during thermal cycling. Dimensional changes during long firings and carbon diffusion while hot can seriously limit its capabilities.

b. Limitations of Nozzle Insulation Material

(C) Of the materials examined, a molded asbestos phenolic or possibly a low resin content filled silica phenolic system appears to afford the most promise in the restart application. This conclusion is based on (1) low char growth, (2) relatively good structural integrity after cycling, (3) good insulating properties, (4) ease of machining, and (5) relatively low cost of fabrication.

c. Limitations of Nozzle Insulation Material

(1) Polycrystalline Graphite

(C) Neither of the two grades of polycrystalline graphite considered in the entrance section can be considered as adequate for restart application particularly where many multiple restarts are to be effected. In all tests the ATJ graphite or the graphitite GX entrance section cracked in either the first or second cycle. These cracks worsened on subsequent restarts and where the duty cycles were severe enough, the entrance section failed completely. This failure invariably occurred while the remainder of the nozzle was still in the condition acceptable for restart.

(2) Ablative Plastics

(C) The performance of carbon cloth phenolic and graphite cloth phenolic in the rocket motor engine section was comparable. Both showed superior performance for the polycrystalline graphite in terms of physical integrity. Although the erosion rates were comparable or slightly higher than the polycrystalline graphite, this erosion was a uniform regression free of catastrophical failures. As a result a more adequate protection of the throat was achieved.

III, A, Preliminary Design (cont.)

d. Limitations of Nozzle Exit Flame Front Materials

(C) No particular limitations appear to be critical for exit material for either graphite class or for the ablative plastics.

e. Effects of Alumina Deposition of Nozzle Performance

(C) The deposition of Al_2O_3 was encountered on the rocket motor tests.

Ref 19. Overall, R. E. and Sawyer, T. T., Design, Development and Demonstration of On-Off-On Device for Solid Propellant Rocket Motors, NAS 3-2563 (U), TCC R-40-64, Thiokol Chemical Corp., Huntsville, Ala., 4 December 1964.

(U) Dual pyrogen igniters were employed at the forward end of the motor, each mounted on a little block but they did not feed into a common manifold. Each had its own individual nozzle inside the chamber.

Ref 20. Elzufon, E. E., An Applied Research Program to Demonstrate the Feasibility of a Solid-Propellant Pulse Rocket, RPL TDE 64-66 (C), AF 04(611)-8531, Atlantic Research Corp., Alexandria, Va., January-September 1963.

(C) One significant conclusion applicable to this program: that Gen-Gard V-44 insulation offers an acceptable compromise between the optimum case insulator and the insulator which would radiate the least quantity of heat to the propellant during cooldown.

Ref 21. Study, Design, Analysis, Fabrication and Test of a Solid Propellant Pulse Rocket Motor, LPC 654-Q2 (C), AF 04(611)-9716, RPL TDE 64-102, Lockheed Propulsion Co., Redlands, Calif., 23 July 1964.

(C) This report contains excellent ignition reliability redundancy study applicable to the design of a pulse motor igniter for the CSR. For the first ten pulses, the ignition reliability of all ten wafers is 0.9963.

(C) A series of tests was conducted which provided enough information about recharred carbon cloth to establish its areas of usefulness and its limitations for pulsing operations for the nozzle. The high erosion rate (2.2 mil/sec at 500 psi) is too high for a throat material. However, the unique properties that are recharred cloth include relatively low thermal conductivity, and the char characteristics allow it to be used

III, A, Preliminary Design (cont.)

as a primary throat insert backup material. Its char characteristics are such that the surface supporting the throat insert will not deteriorate under repeat thermal cycling, thus providing a good structural support for the insert material even after a large number of cycles. Furthermore, this material has a low or relatively low thermal conductivity, can effectively be used as an insulator between throat insert and the nozzle supporting structure. An additional wrap of RPD 41 was applied over the exterior of the recharred carbon cloth to further ensure low temperature steel structures. The problem associated with delamination of the recharred carbon cloth was avoided by supporting the insert in such a fashion that axial tensile strength was not required.

Ref 22. Study, Design, Analysis, Fabrication and Test of a Solid Propellant Pulse Rocket Motor, LPC R-654-Q3 (C), RPL TR 64-153, Lockheed Propulsion Co., Redlands, Calif.

(C) Not much additional data in this report except confirming the fact the continuous long durations are more disastrous to the aft closure insulation than short pulses. Confirmation in the test program that precharred carbon cloth worked very well in the nozzle backup material.

Ref 23-27. Bureau of Naval Weapons, Supporting Research Program, Quarterly Report ABL QPR-49, 50, 51, 50 and ABL/X-134 (C), Hercules Powder Co., Cumberland, Md., 1 January - 31 March 1964.

(C) These reports represent the results of a program to develop a variable area nozzle using an isentropic plug nozzle. Significant results to date are the testing of the bulk pre-oriented pyrolytic graphite plug shell. The objectives of these tests were to evaluate the "Pyroid" for use as a material for the plug shell. The latest report available, APL/X-134[27], indicated that the "Pyroid" plug was tested and rated fairly successfully for 25.4 sec when a failure for a supporting insulation drove the plug into the outer housing causing failure of the nozzle. The tests were conducted with the aluminized propellant.

(C) Burning rate pressure exponents 0.7 can be obtained with aluminized DB propellants containing a variety of added oxidizers such as AP, HMX or AN, by incorporating one of the following: 3% tri-n-butylphosphate, 10% NGu, 13% AN and BDNPA.

(U) It was extremely difficult to extinguish highly aluminized propellants by dp/dt.

Ref 28. Campbell, P. B., Total Impulse Control in Solid Propellant Rocket Motors, CPIA Pub 18, v. 1 (C), Lockheed Propulsion Company, Redlands, Calif.

III, A, Preliminary Design (cont.)

(C) Two techniques for controlling the total impulse of solid-propellant rocket motors using conventional high-performance propellants have been successfully demonstrated in preliminary static tests. The first provides control by incremental impulse additions; the design investigated consisted of three end-burning charges (discs) of a nitroplastisol-type propellant stacked on top of one another and separated by inhibitor. Each charge was provided with an igniter on its upper surface (beneath the inhibitor) so sequential ignition could be produced on command after burnout of the adjacent charge had occurred. Pertinent motor design details and the test results obtained are briefly discussed.

(C) In the second technique investigated, extinction of internal-burning grains of rubber-base composite propellant was achieved by rapid depressurization, the method previously studied by Povinelli and Ciepluch using small slab specimens. Five-pound charges of propellants incorporating 5 and 15 or 16% aluminum were tested in chambers 4 in. in diameter by 10 in. long under conditions of rapid depressurization to ambient pressures corresponding approximately to sea level and 150,000 ft. Decay of the combustion process was traced by high-response measurements of chamber pressure and luminosity. The effects of propellant composition and depressurization conditions on extinction characteristics are interpreted in terms of existing theories of solid propellant combustion.

Ref 29. Anderson, F. A., Strand, L. D., and Strehlaw, R. A., An Experimental Investigation of the Low Pressure Combustion Limits of Some Solid Propellants, Bulletin of the Interagency Solid Propulsion Meeting III (C), pp. 157-186, July 1963.

(C) The minimum pressure limit of combustion in motor firings has been determined for several propellants. This minimum pressure limit, or extinction pressure, has been found to be independent of the propellant grain geometry but strongly dependent on L* (the ratio of the free-chamber volume to the nozzle-throat area) and on the propellant ballistic properties.

(C) For a given L*, P_c increases on changing the AP/Al ratios from 80/0, 72/8 to 64/16, all at 80% total solids.

(C) The L* instability associated with the minimum pressure limit does not appear to be related in any way to the higher pressure combustion instability normally characterized by high-frequency pressure oscillations.

Ref 30. Ciepluch, C. C., Spontaneous Reignition of Previously Extinguished Solid Propellants, NASA Technical Note D-2167, March 1964.

III, A, Preliminary Design (cont.)

(U) Results of this investigation show propellant compositions could be extinguished by sudden depressurization provided that the characteristic time of the expansion process was less than some critical value. However, in some cases, depending on the operation conditions the extinction was only temporary and the propellant would spontaneously reignite. In each propellant composition there is a minimum ambient pressure below which reignition was never obtained. This reignition pressure limit was considerably higher than the self-sustaining combustion limit. Depressurizing at higher rates could increase the ambient pressure limit for reignition. The analysis of the results indicated that the reignition phenomenon was similar to a gas phase ignition mechanism and the energy required for ignition probably resulted from a combination of residual combustion gas and the residual heat in the propellant surface. In order to achieve permanent extinguishment in the atmosphere, some method of removing heat must be employed. This can be done through the use of a secondary purge.

Ref 31. Ciepluch, C. C., Effect of Composition on Combustion of Solid Propellant During a Rapid Pressure Decrease, NASA Technical Note D-1559, December 1962.

(U) The response of solid-propellant combustion to a pressure transient was studied in an apparatus that could be vented at a variable rate. The principal measurement was the time required for the pressure to decrease to one-half its initial value. The data are presented and discussed in terms of the maximum value of the time required to extinguish combustion. The value was decreased by an increase in aluminum or ammonium perchlorate concentration and was increased by an increase in binder concentration. An increase in the average particle size of ammonium perchlorate resulted in a decrease in this time. The addition of aluminum oxide produced a decrease in the time while the addition of potassium fluoride increased it.

(U) Analysis of the results suggested that hot-particles retention at the surface of the propellant was a major cause of the continuance of combustion in a rapidly decreasing pressure field.

Ref 32. Sehgal, R. and Strand, L., Low-Pressure Combustion, JPL Space Programs Summary No. 37-32, Vol. IV (C), pp. 109-112.

(C) Effects of oxidizer particle size and aluminum concentration and particle size on L* extinguishment was investigated. For nonaluminized propellants, the slope of log L* versus log p_e is -2n, as predicted theoretically. The slope of L* versus p_e is affected by the presence of Al, the concentration and particle size of Al. The L* extinguishment of propellants with coarse Al approach the behavior of nonaluminized propellants. The variation in oxidizer particle size has a negligible effect on L* versus p_e.

2. Preliminary Tradeoff Study

(C) The purpose of the preliminary tradeoff study task was to define the following criteria necessary for a single-chamber controllable solid rocket motor:

(a) Steady-state and transient combustion parameters
(b) Instant response after long periods of storage
(c) Ignition systems
(d) Termination and thrust modulation capability
(e) Insulation thermal degradation
(f) Motor reconfiguration (scale-up or scale-down)

These areas were to be investigated and defined within the following motor parameter boundary conditions:

(a) Mean thrust (nominal)--4000 lbf
(b) Specific impulse--240 to 250 lbf-sec/lbm--design goal standard delivered in BATES motors
(c) Four to seven stop-restarts
(d) Throttling range--3:1 minimum
(e) Propellant weight--500 lbm (nominal)
(f) Mass fraction--goal 0.80

a. Steady-State and Transient Combustion Parameters

(C) The various parameters that fall within this general category are the propellant L*-critical pressure relationship, the minimum operating pressure for variable thrust, the propellant burning rate exponent, the overall motor thrust ratio, and the motor environmental pressure. For this parametric study, these were varied over the following ranges:

(1) Extinguishment pressure (L* extinguishment), psia	5 to 25
(2) Minimum operating pressure, psia	50 to 100
(3) Burning rate exponent ($\underline{n}$)	0.60 to 0.70
(4) Thrust ratio ($\overline{F}$)	3:1 to 10:1
(5) Back Pressure (P_a), psia	0 to 15

These ranges were selected as they were considered to be the normal range of operation for a controllable solid rocket motor. Extinguishment pressures lower than 5 psia require excessive area changes, and higher extinguishment pressures than 25 psia have a tendency to degrade propellant performance. Operating pressures lower than 50 psia have a tendency to degrade propellant

performance. Operating pressures lower than 50 psia have a tendency to degrade propellant performance. Operating pressures lower than 50 psia usually result in inefficient combustion, and pressures higher than 100 psia require excessively high maximum operating pressures to attain thrust variation. Propellant burning rate exponents less than 0.60 require large nozzle throat area changes to effect thrust variation, and those higher than 0.70 are very susceptible to slight variations in nozzle throat area or propellant surface area, thus making the controllability of the motor a very delicate problem. Thrust ratios of less than 3:1 do not meet the work statement requirements, and those higher than 10:1 require large variations in pressure and throat area, thus penalizing mass fraction. The back-pressure range selected covers operation from sea level to deep space, the entire range over which the controllable solid rocket motor is expected to operate.

(U) Figures III-1 through III-15, inclusive, show the motor chamber pressure as a function of nozzle throat area ratio for constant thrust ratios and burning rate exponent, with three different minimum operating pressures. It can be seen from these plots that the lowest burning rate exponents require the highest operating pressure for a given thrust ratio and also require the largest nozzle throat area variation. As the extinguishment pressure is decreased from 25 to 5 psia, the nozzle throat area variation to attain a given thrust variation is increased. As the minimum operating pressure is increased from 50 to 100 psia, the maximum operating pressure is also doubled, resulting in a lower attainable mass fraction. From these data, it can be concluded that the best combination of operating parameters uses the lowest minimum operating pressure consistent with good combustion efficiency, the maximum L* extinguishment pressure propellant, and the highest propellant burning rate exponent available. All of these data on Figures III-1 through III-15 are presented at zero back pressures. To see the effect of back pressure on the other parameters, Figure III-16 was prepared. This figure shows the chamber pressure as a function of throat area ratio for a thrust ratio of 5:1, a minimum operating pressure of 50 psia, and an extinguishment pressure of 15 psia. In addition to vacuum and 15 psia conditions, the intermediate back pressures of 5 and 10 psia have been shown, since during atmospheric flight the effective back pressure at the base of the motor is a function of velocity, shape, and altitude. For all of the vacuum data presented, the nozzle expansion ratio was arbitrarily set at 10:1 at the minimum operating pressure. At all other back pressures, the nozzle expansion ratio was set to that value which would provide an exit pressure equal to one-half ambient at the minimum operating pressure (the point at which flow separation normally occurs). It appears from this figure that the nozzle design for operating at back pressures of 15 psia will deliver more thrust variation than that designed for operating at vacuum over the same motor pressure range. This conclusion is substantially correct; however, the nozzle designed for sea level operation-- or rather, the motor designed for sea level operation-- will not provide the same thrust variability when operated at vacuum. This

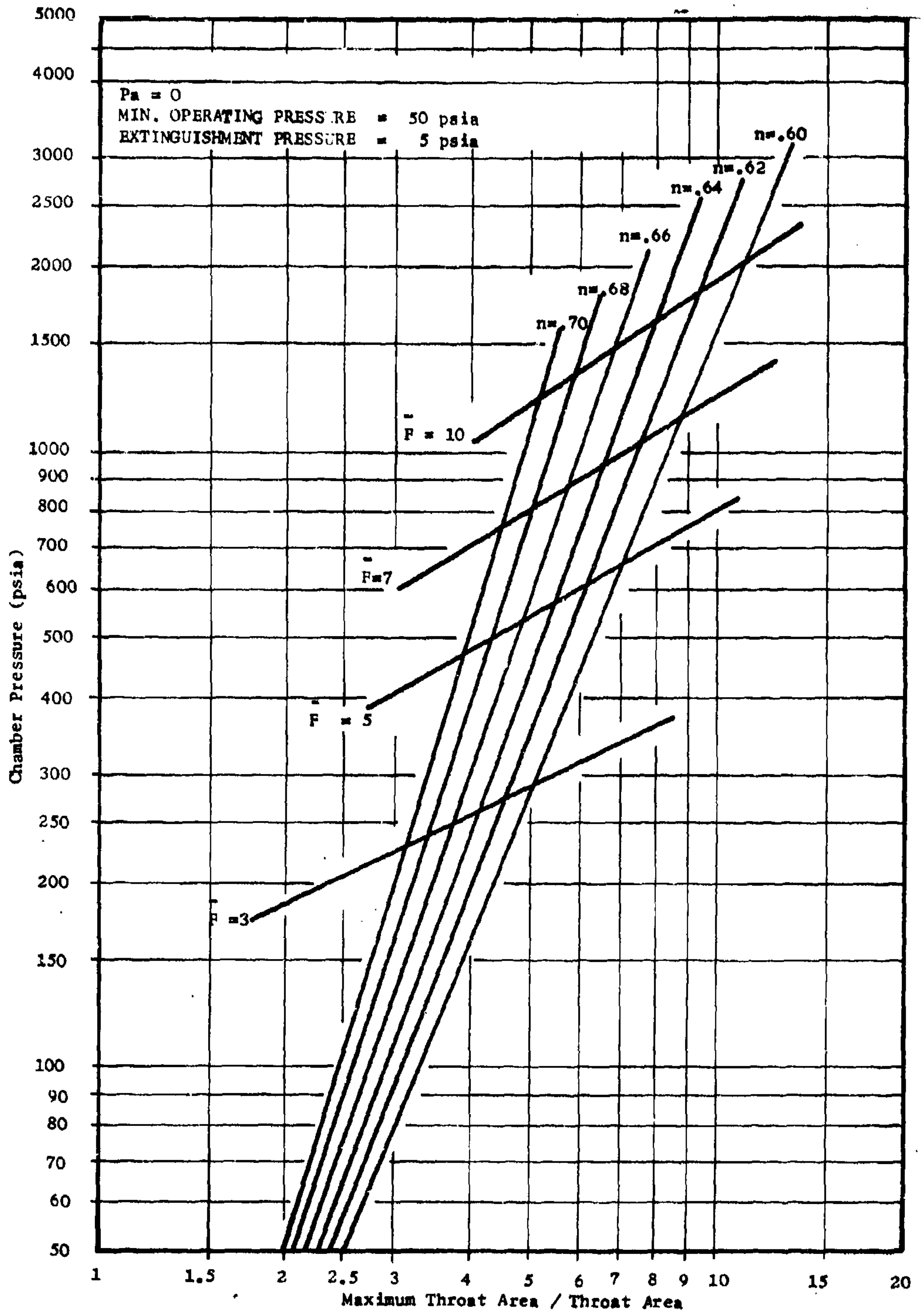

Nozzle Design Curves $P_{min} = 50$, $P_{ext} = 5$

Figure III-1

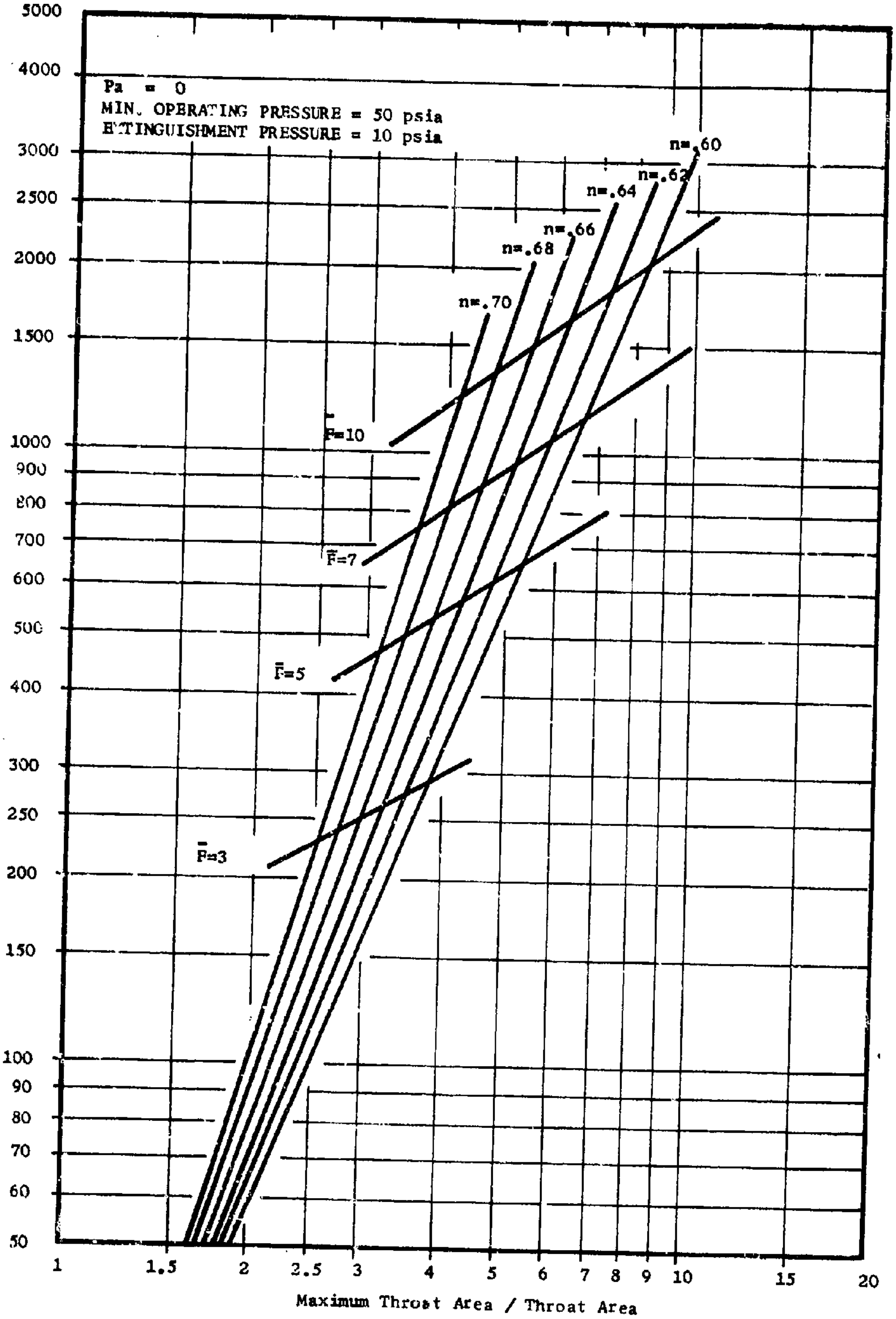

Nozzle Design Curves $P_{min} = 50$, $P_{ext} = 10$

Figure III-2

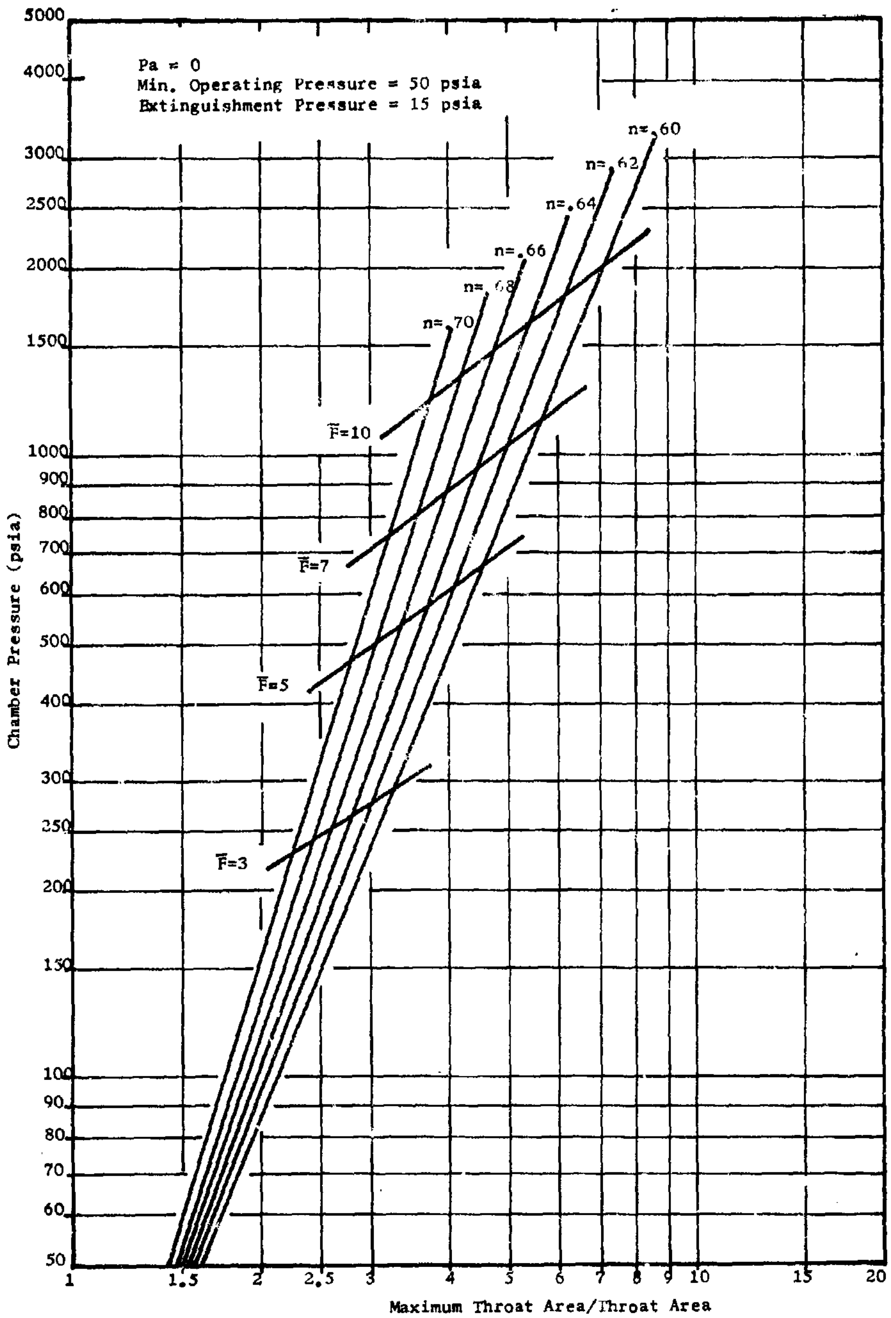

Nozzle Design Curves $P_{min} = 50$, $P_{ext} = 15$

Figure III-3

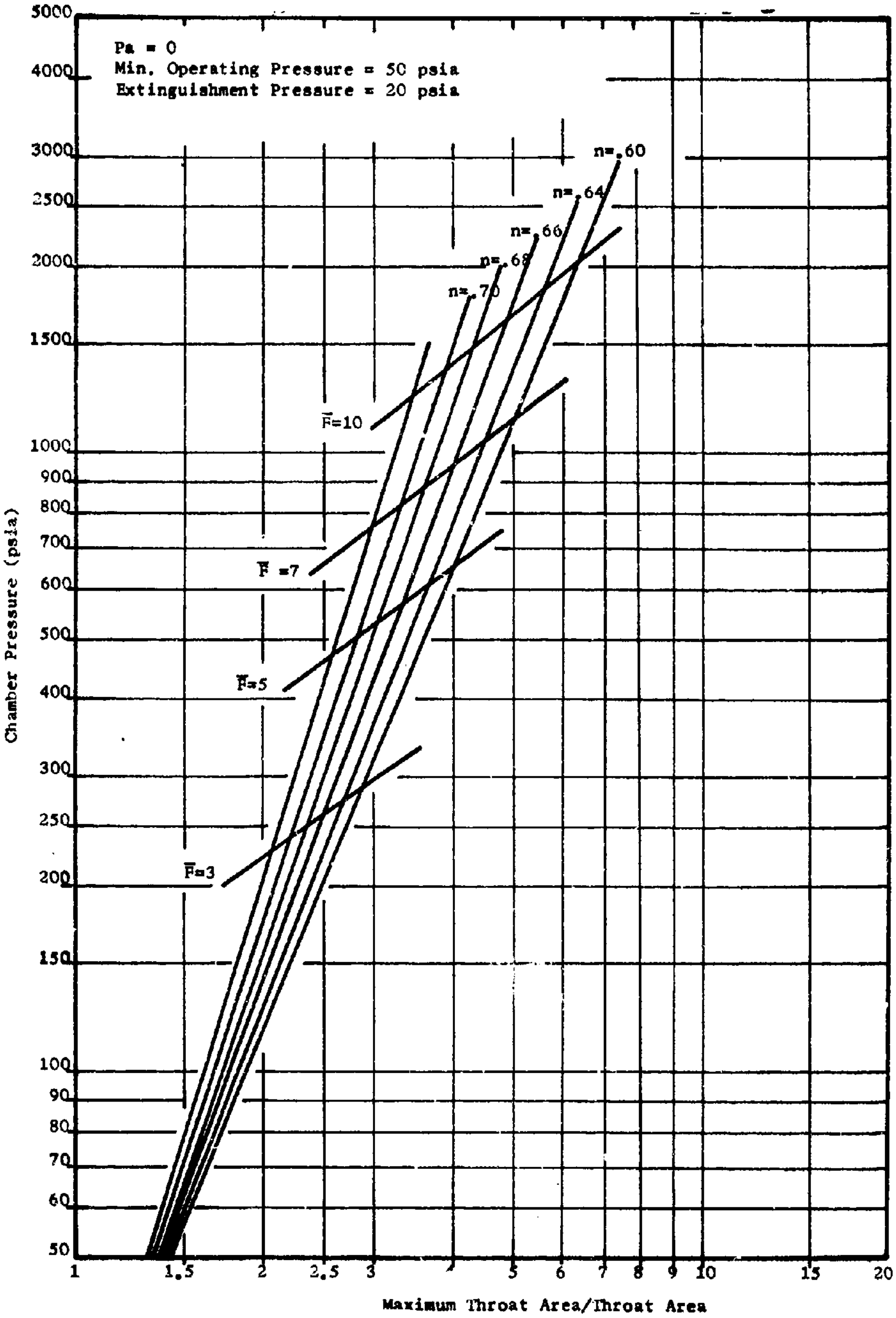

Nozzle Design Curves $P_{min} = 50$, $P_{ext} = 20$

Figure III-4

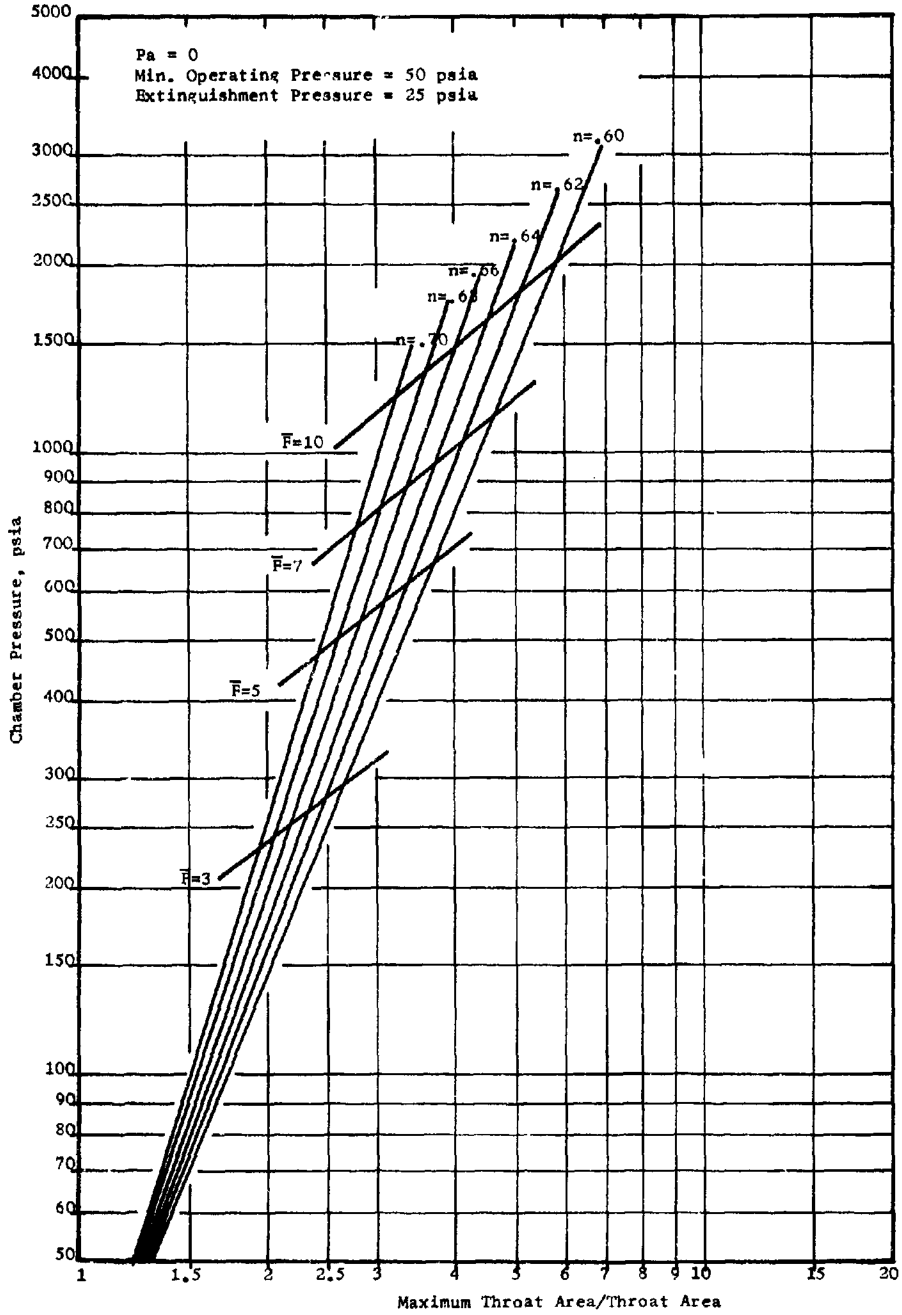

Nozzle Design Curves $P_{min} = 50$, $P_{ext} = 25$

Figure III-5

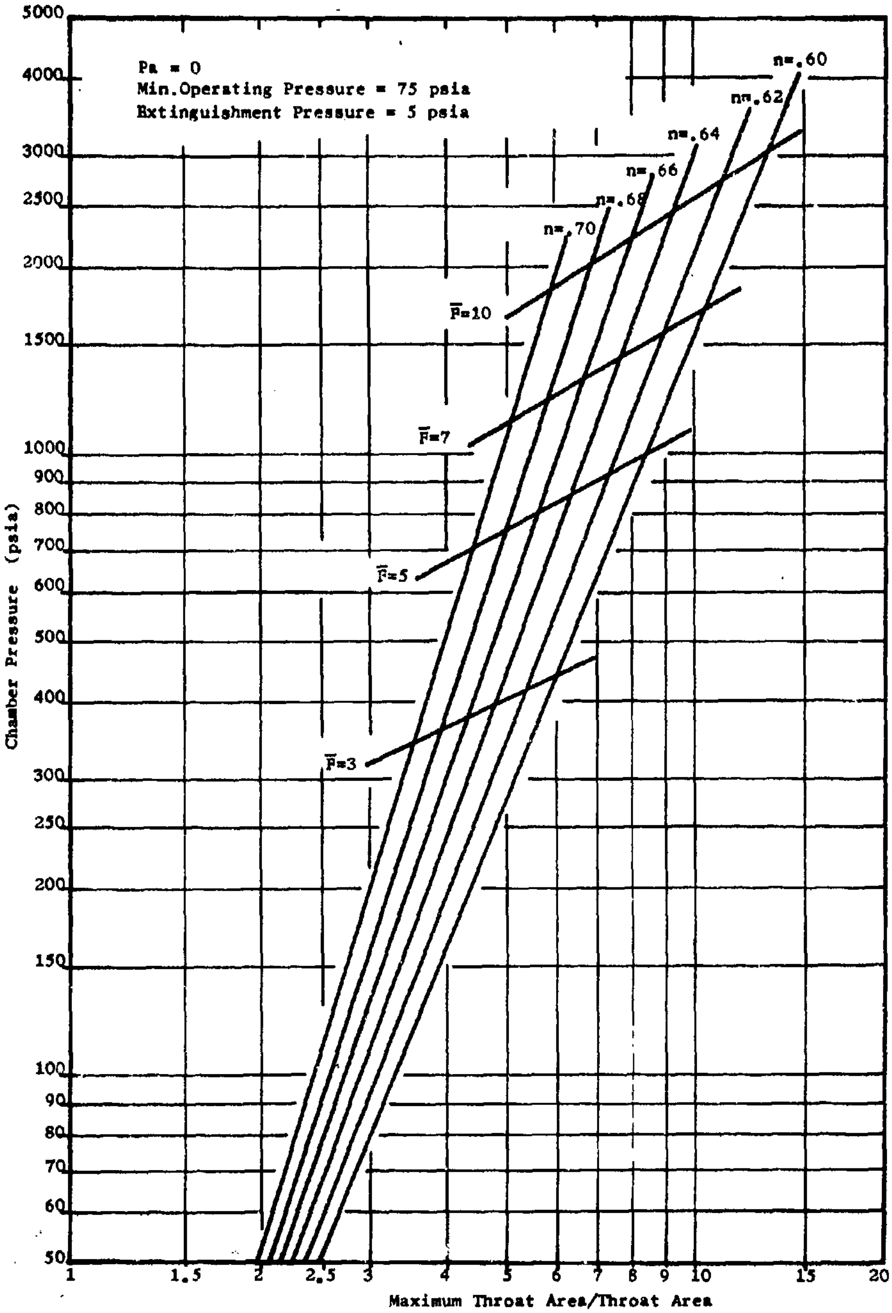

Nozzle Design Curves $P_{min} = 75$, $P_{ext} = 5$

Figure III-6

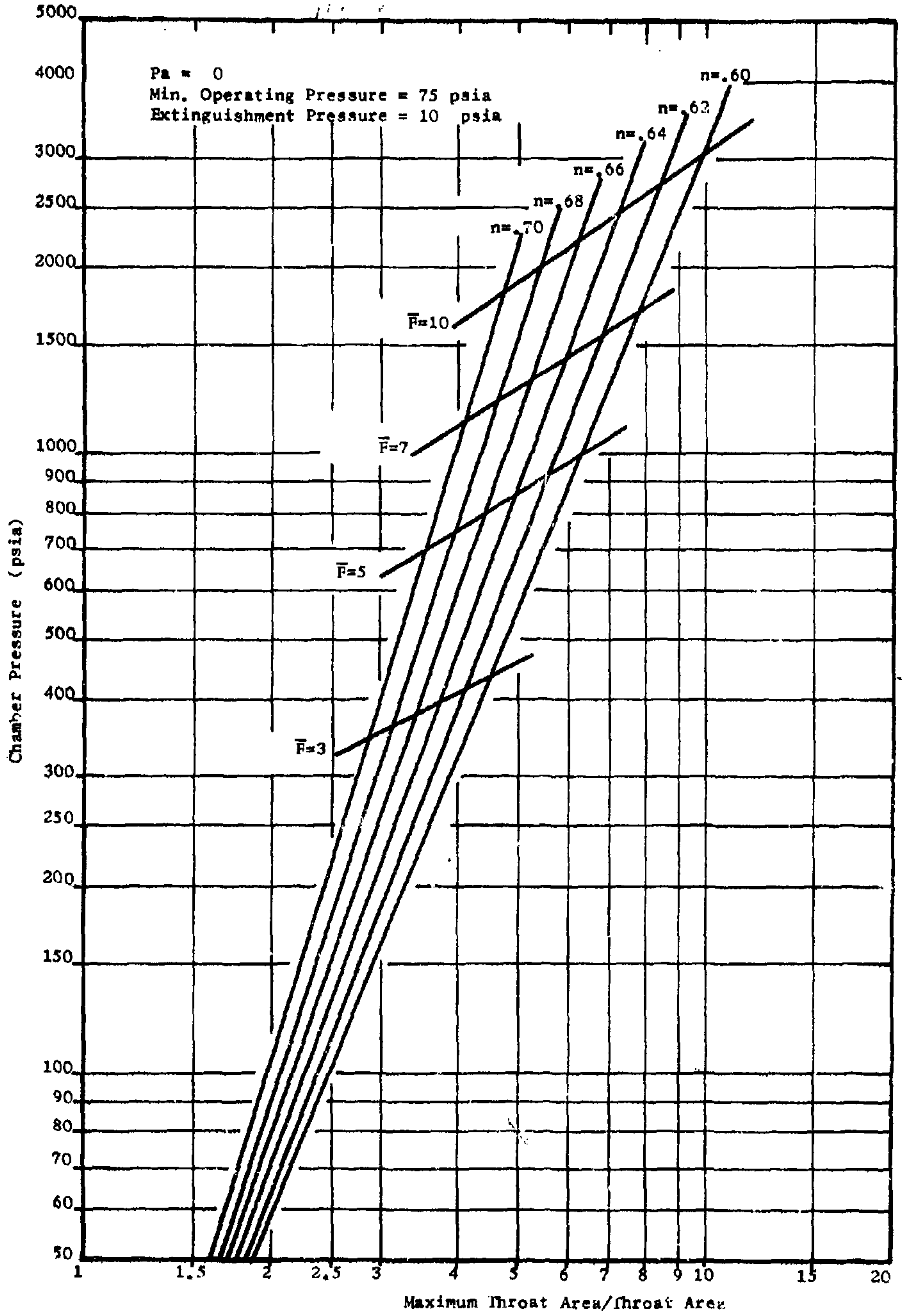

Nozzle Design Curves $P_{min} = 75$, $P_{ext} = 10$

Figure III-7

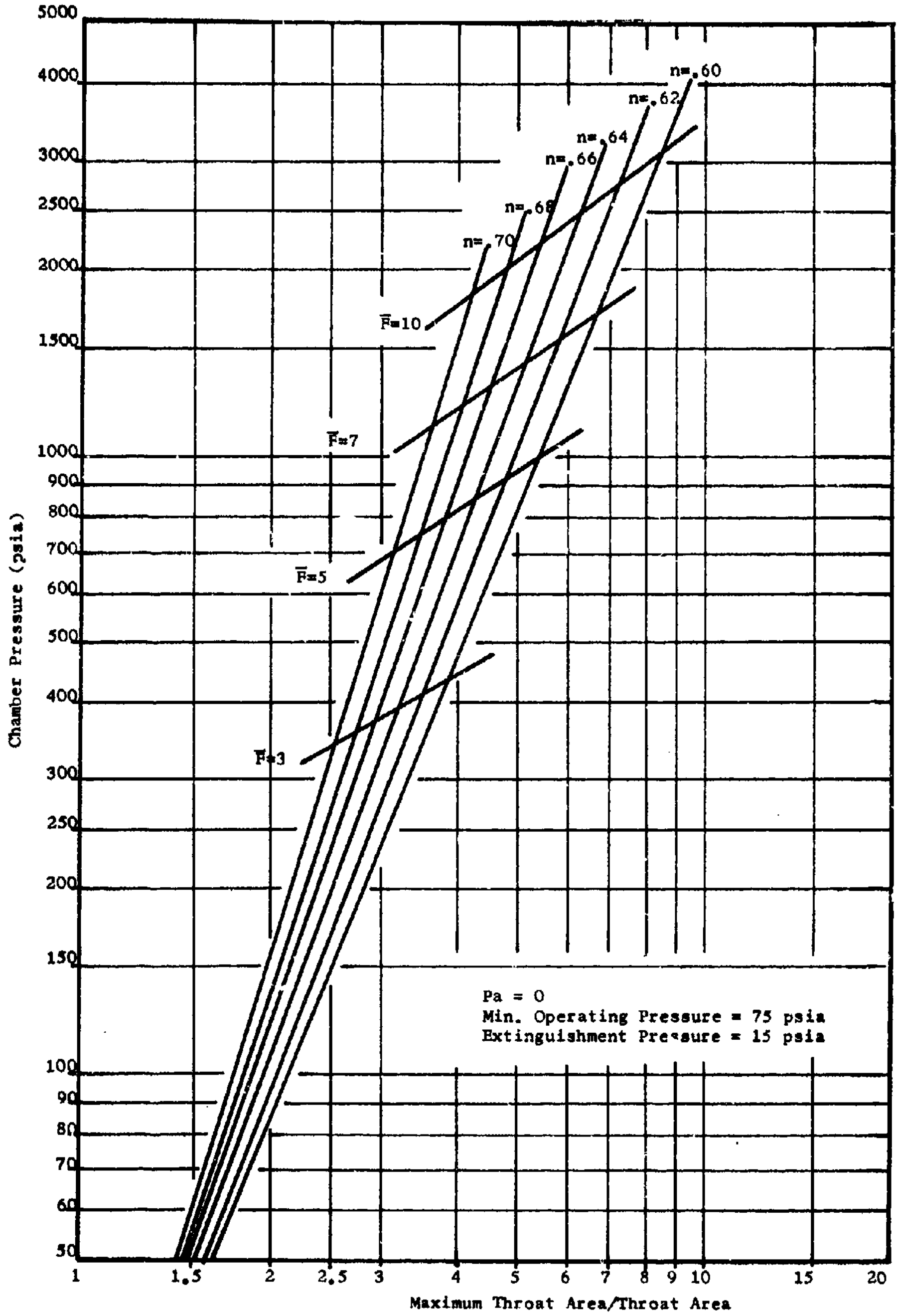

Nozzle Design Curves $P_{min} = 75$, $P_{ext} = 15$

Figure III-8

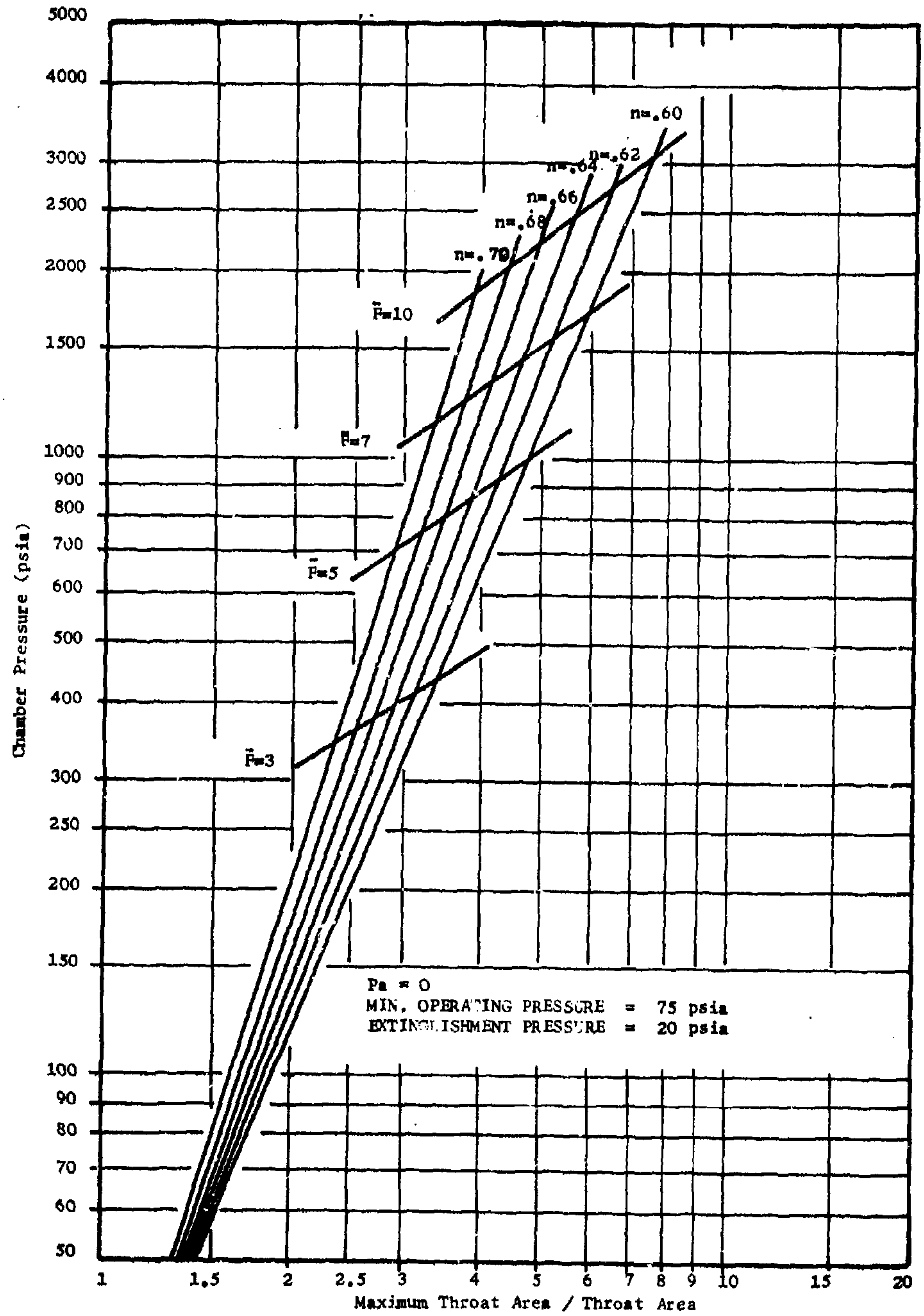

Nozzle Design Curves $P_{min} = 75$, $P_{ext} = 20$

Figure III-9

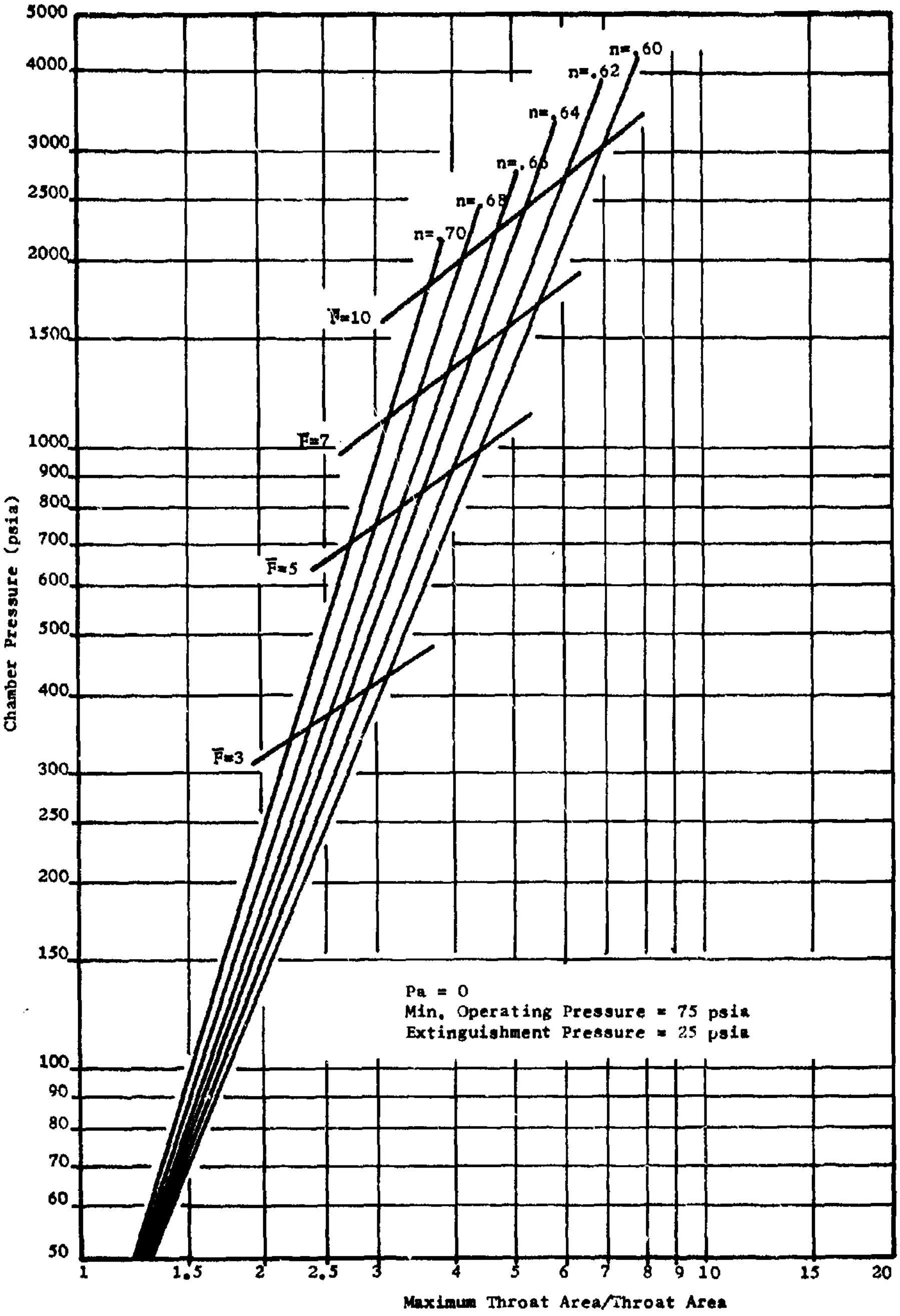

Nozzle Design Curves $P_{min} = 75$, $P_{ext} = 25$

Figure III-10

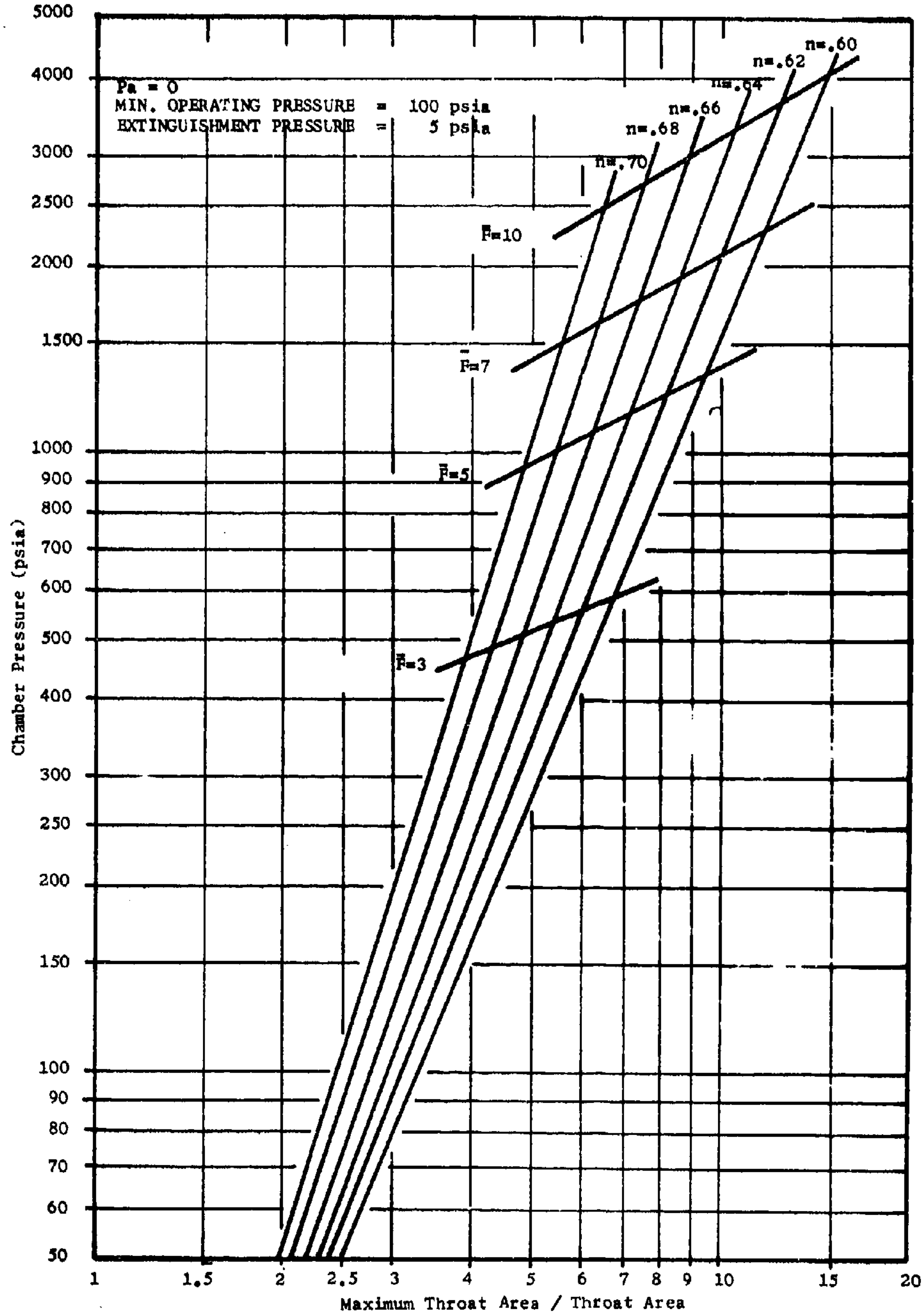

Nozzle Design Curves $P_{min} = 100$, $P_{ext} = 5$

Figure III-11

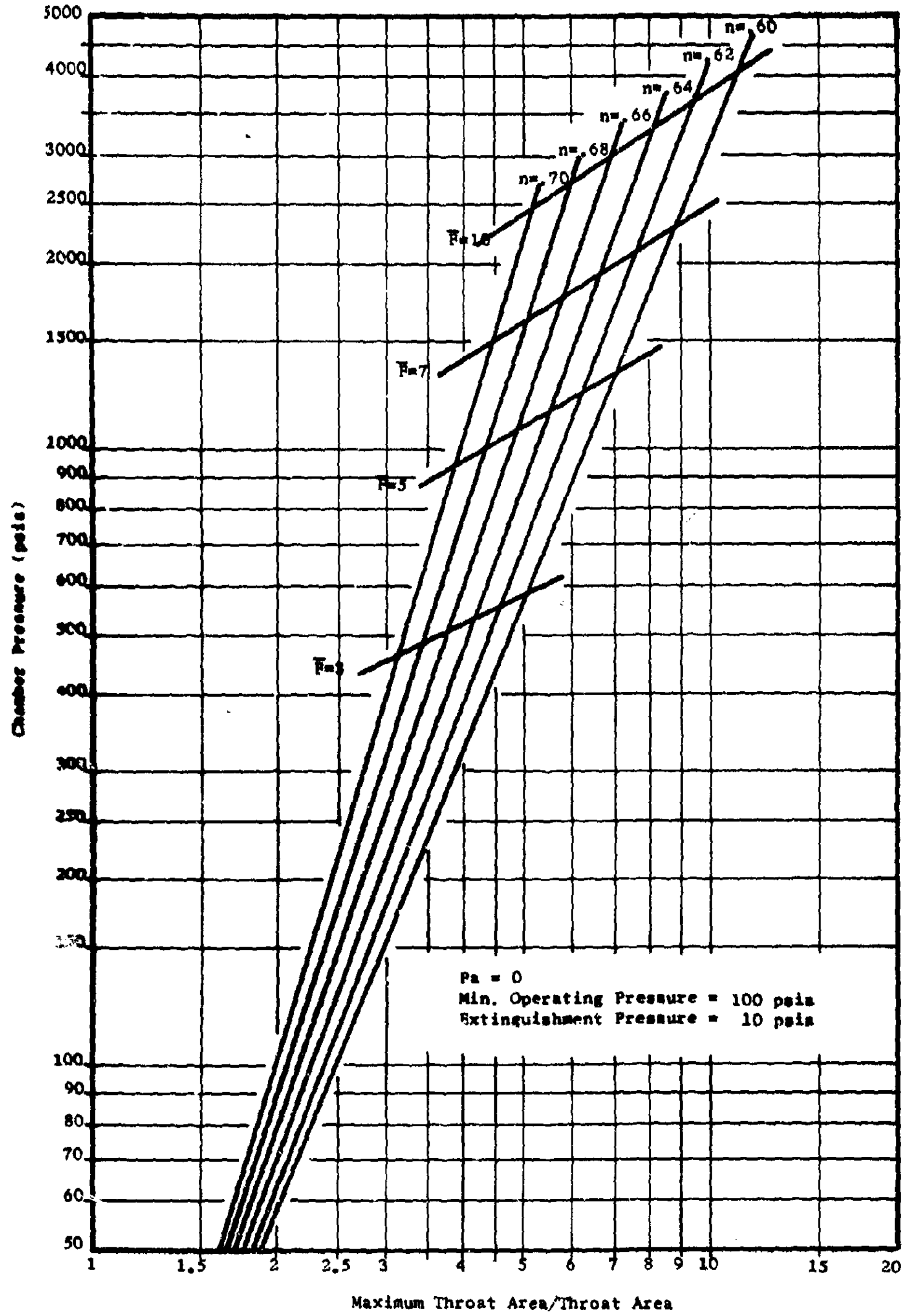

Nozzle Design Curves P_{min} = 100, P_{ext} = 10

Figure III-12

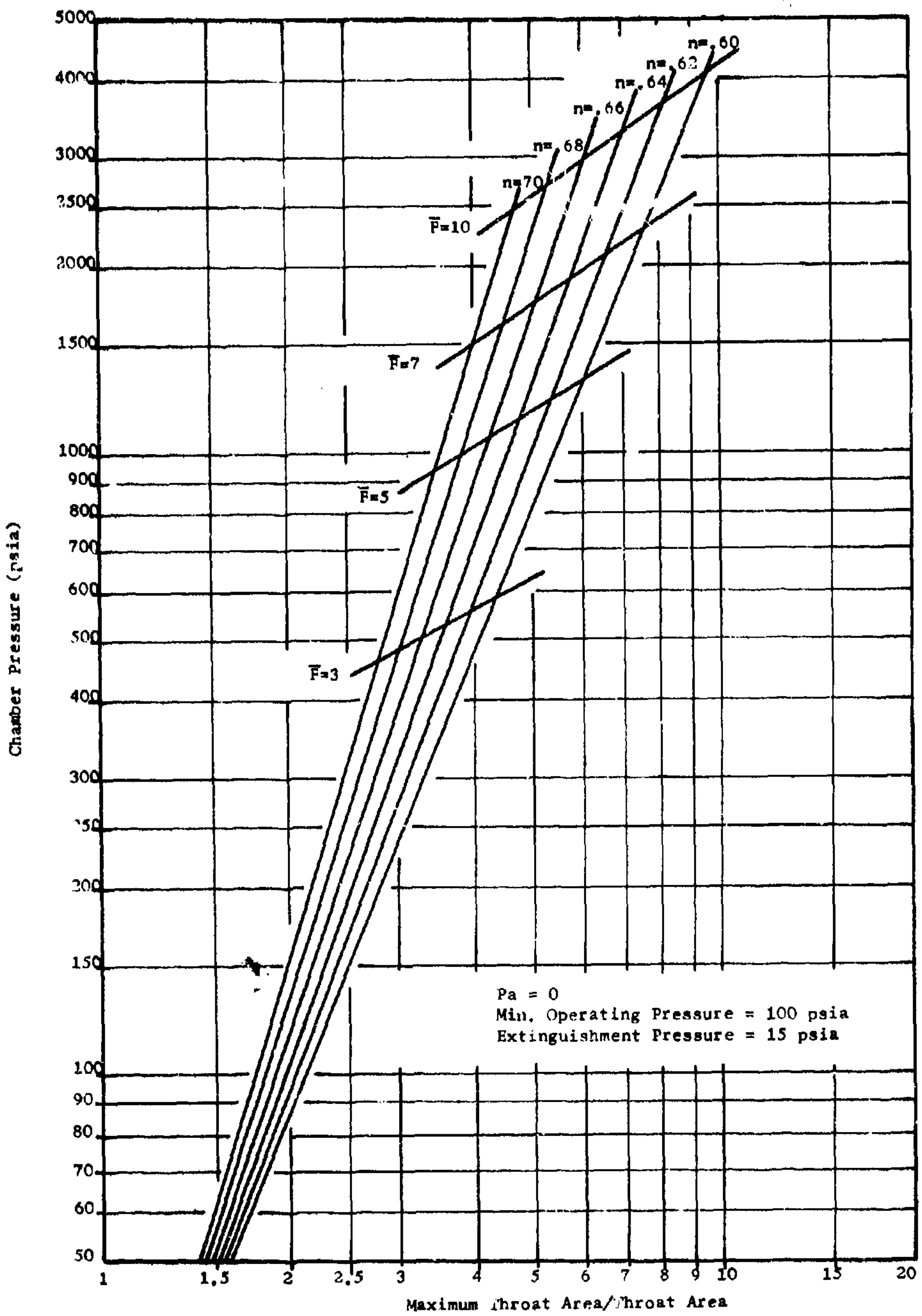

Nozzle Design Curves $P_{min} = 100$, $P_{ext} = 15$

Figure III-13

THIS REPORT HAS BEEN DELIMITED

AND CLEARED FOR PUBLIC RELEASE

UNDER DOD DIRECTIVE 5200.20 AND

NO RESTRICTIONS ARE IMPOSED UPON

ITS USE AND DISCLOSURE.

DISTRIBUTION STATEMENT A

APPROVED FOR PUBLIC RELEASE;

DISTRIBUTION UNLIMITED.

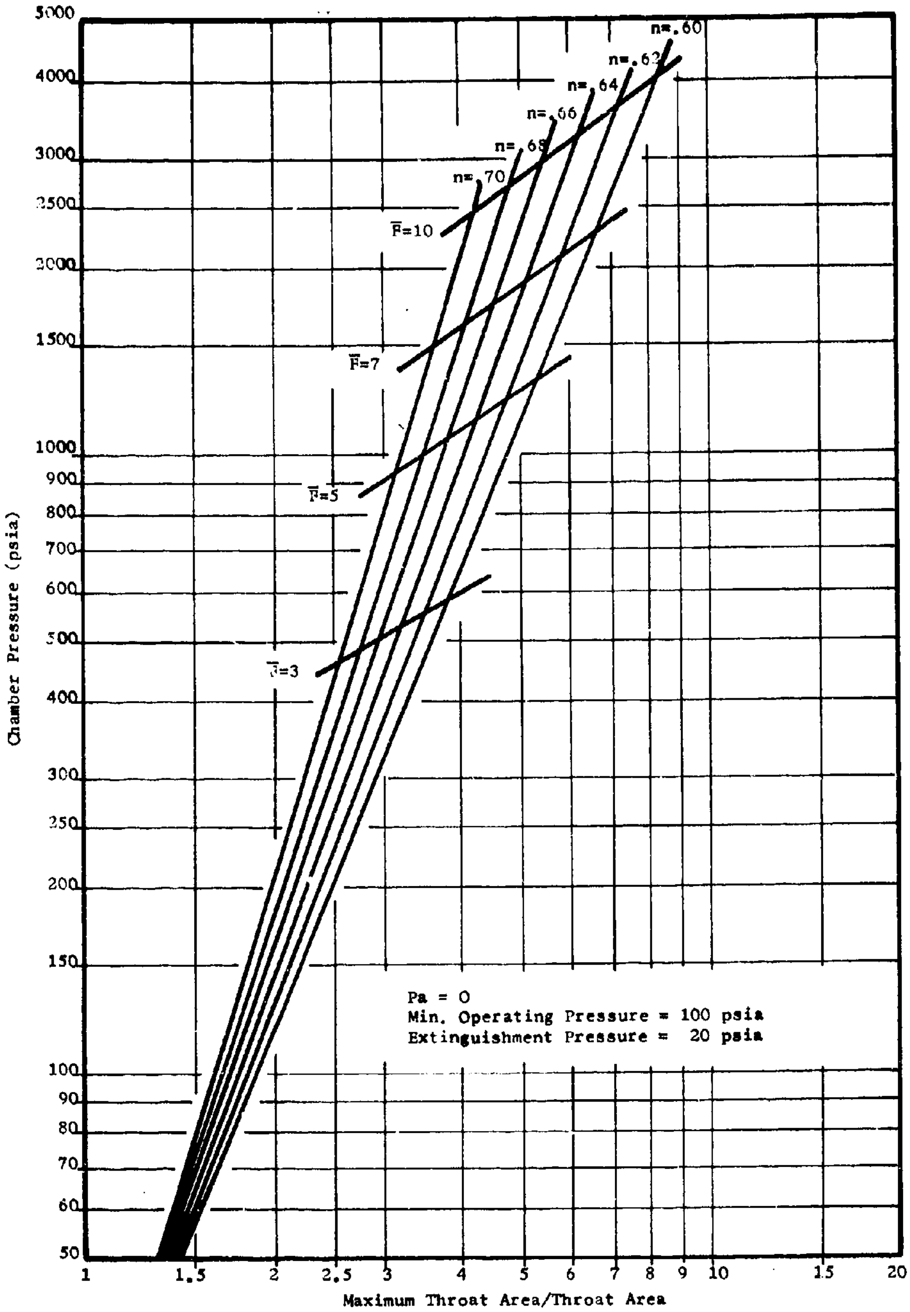

Nozzle Design Curves $P_{min} = 100$, $P_{ext} = 20$

Figure III-14

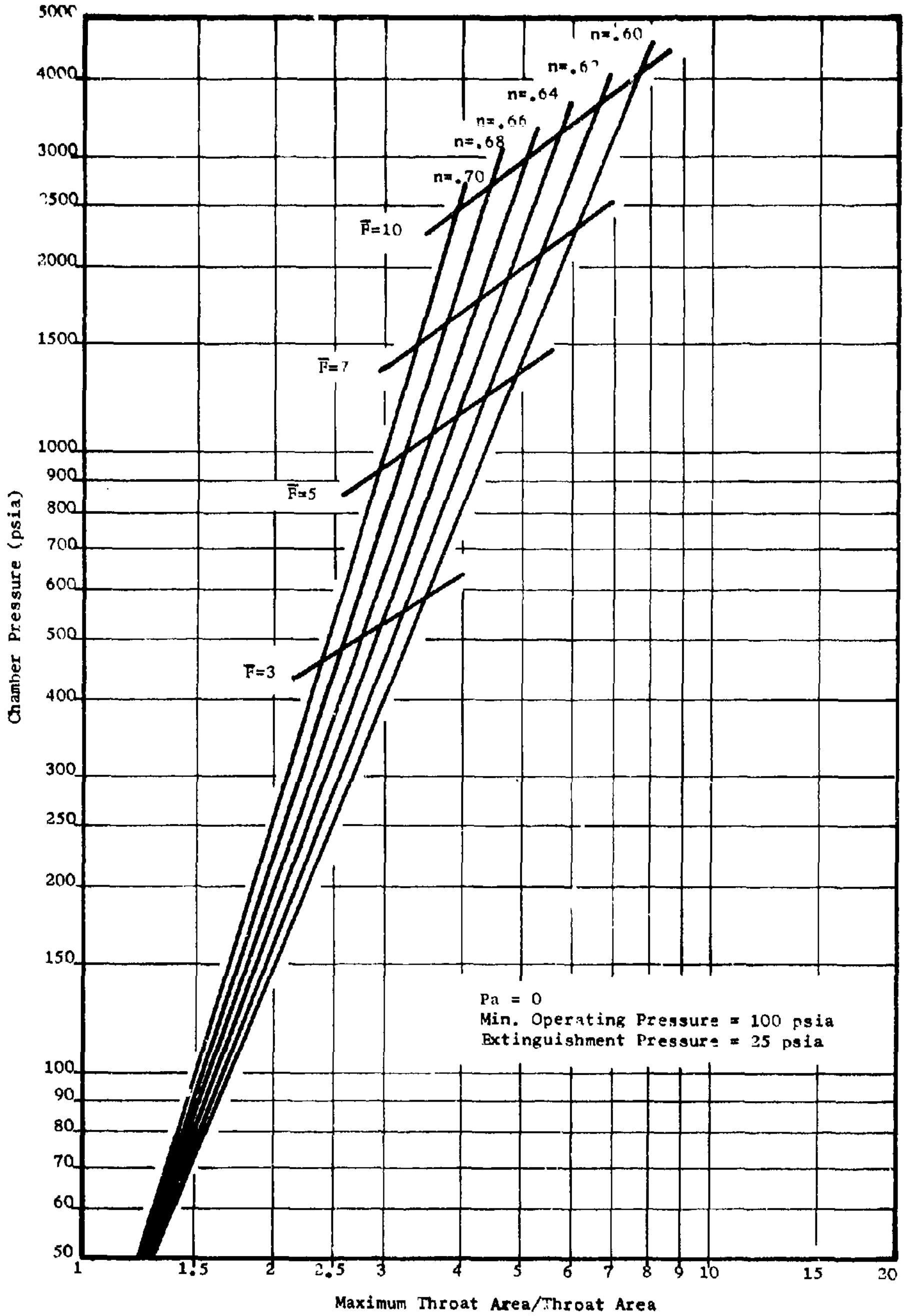

Nozzle Design Curves $P_{min} = 100$, $P_{ext} = 25$

Figure III-15

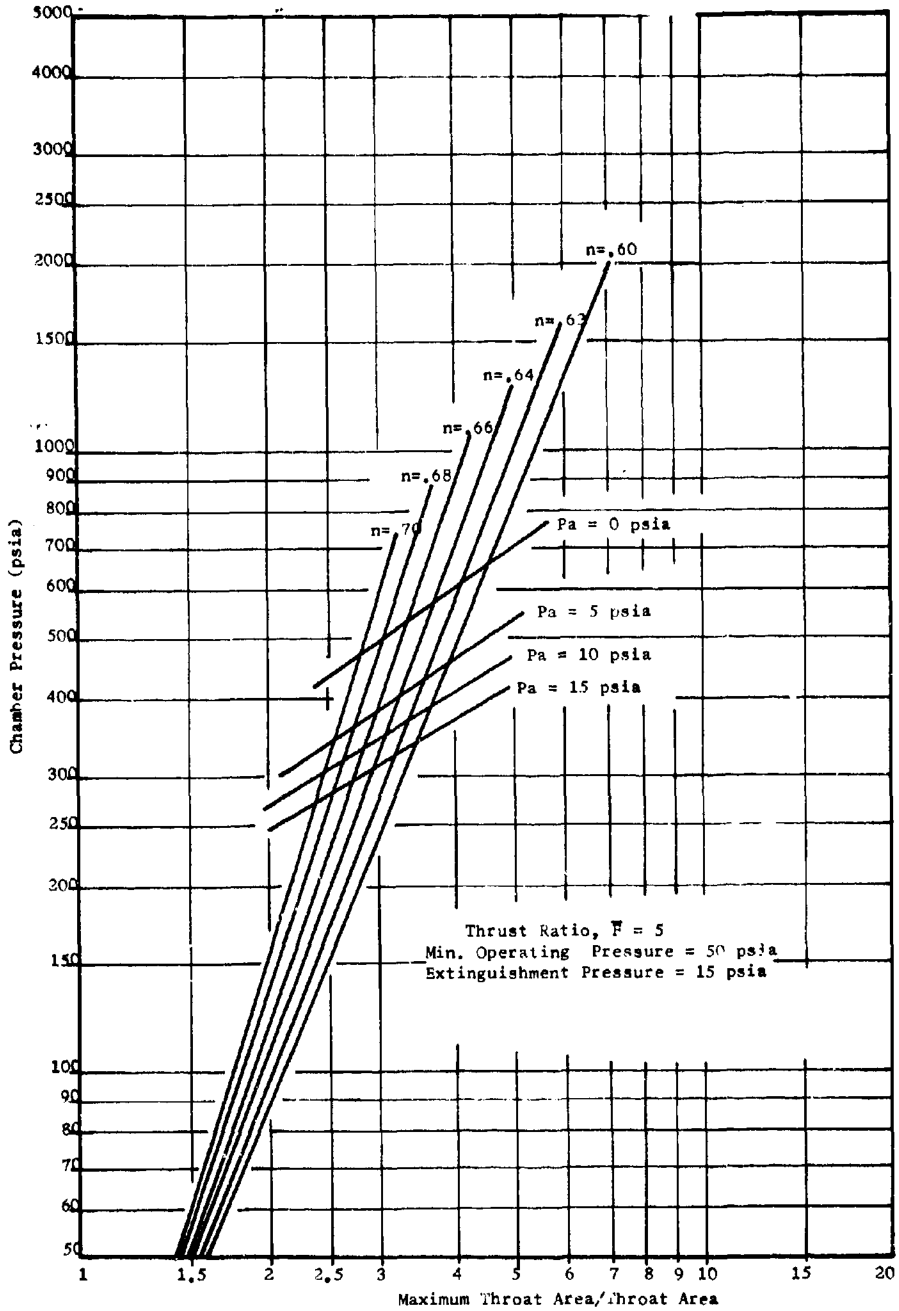

Effect of Back Pressure

Figure III-16

is attributable to the larger variation in thrust coefficient within the atmosphere. For example, a nozzle designed to deliver a thrust variation of 3:1 at sea level will experience a 42% change in thrust coefficient over its operating range, whereas a nozzle designed to deliver a 3:1 thrust variation at altitude will only experience a 4.5% thrust coefficient change over its operating range, the difference being made up by the larger pressure and area changes required for the altitude nozzle. Thus, it can be concluded that, to meet the motor operating requirements, the nozzle and motor must be designed to meet the operating requirements at zero back pressure because this point will require the highest motor operating pressure and the largest nozzle throat-area variation.

b. Instant Response After Long Periods of Storage

(U) To meet the requirements of instant response after long periods of storage, it is necessary to use design techniques which effectively eliminate any components which require prefiring thermal conditioning or "warm-up." This places a limitation on the design of the ignition system and the nozzle. Standard solid propellant rocket motor pyrotechnic ignition systems meet this requirement because they are usually squib-initiated and solid-grain-boosted, neither of which are extremely sensitive to temperature. Nozzle designs are limited only by eliminating the use of cooled nozzles which require preheating of the coolant, other types of cooled nozzles being quite acceptable. Nozzle control systems, specifically the actuation system used to effect nozzle throat area variation, must be instantaneously ready for use, thus possibly placing a limitation on the starting time of self-contained power-pack systems, and may require that some provision be made to hold pressure during the period of shutdown. Gaseous actuation systems are limited by the requirement that temperature affects the pressure during long periods of storage; thus a minimum allowable temperature must be placed on the gas accumulator and possibly heater strips provided to limit this temperature.

(U) The most severe limitation that is placed on the motor design by this requirement is that placed on the propellant. Space storability of propellants for long periods of time result in excessive degradation of physical and thermodynamic properties, causing losses in performance and excessive ignition delays. Thus, propellant selection must be made considering the space storability requirement, specifically in binder selection.

c. Ignition Systems

(U) One of the requirements of this program was to use state-of-the-art ignition systems to effect the multiple ignition requirements of the motor. Standard pyrotechnic igniters were to be used in the initial tests of the fullscale motors, with some consideration given to improvement in ignition characteristics and motor mass-fraction. This tradeoff study was

thus limited to pyrotechnic ignition systems. The areas that were considered were the size of the individual igniters, the possible sequencing of igniters, and the type of multiple pyrotechnic ignition system used.

(U) In order to give the system the maximum amount of flexibility, it was decided that the igniters had to be sized to accommodate ignition at any free volume of the motor. Only the first igniter could be sized with any set motor free volume--propellant surface area--grain configuration. Therefore, the ignition system consisted of one igniter sized for first ignition and five igniters sized for ignition at near web burnout.

(C) Types of igniters considered included the individual canister igniters adapted to a common manifold similar to those employed by Thiokol Chemical Corp.[19] and Amcel Corp.[5] using current igniter propellants and using advanced high burning rate propellants; wafer-pulse motor igniters similar to those developed by Lockheed Propulsion[21,22] using high burning rate propellants; and internal burning shell-pulse motors using conventional igniter type propellants. These four types of igniters are shown on Figures III-17 through III-20, inclusive.

(C) An analysis of the various types of igniters, including the adapters required, indicates that the conventional propellant canister type igniters could be designed with an ignition system mass-fraction in the range of 0.20 to 0.30. By changing to the advanced high burning rate propellants, the volumetric loading of the igniter was increased considerably, thus improving the potential ignition system mass fraction to between 0.40 to 0.50. By going to a wafer-pulse motor design, the mass fraction of the igniter could be in the range of 0.60 to 0.65; whereas the internal burning shell pulse motor was limited to about a 0.50 to 0.60 mass fraction. Of the four types of multiple pyrotechnic ignition systems considered, all but the internal burning-shell pulse motor have been successfully demonstrated in motor programs; however, none has been employed in the proposed manner.

(C) In addition to the mass fraction tradeoffs on the ignition system type, the reliability of the individual systems must be considered. The individual canister-type igniters would have the inherent reliability of an individual igniter with the only limitation being the burst diaphragm. Should one igniter fail to fire, the remaining igniters could be fired in any sequence because they are all the same size and function independently. It is believed that the reliability of the pulse igniter can be developed to the same level predicted by LPC[21,22] for the pulse motor; however, if a pulse of the pulse igniter fails to fire, the ignition capability of the motor is immediately dropped to zero unless some provision has been made for breaking up and ejecting the unburnt propellant in the pulse that misfired. The problem with this is the added pyrotechnic material that would be deposited in the main motor case and the ignition overpressure that could result. Based on these considerations, it was decided that the individual canister-type of ignition system be used for the first fullscale tests of this program.

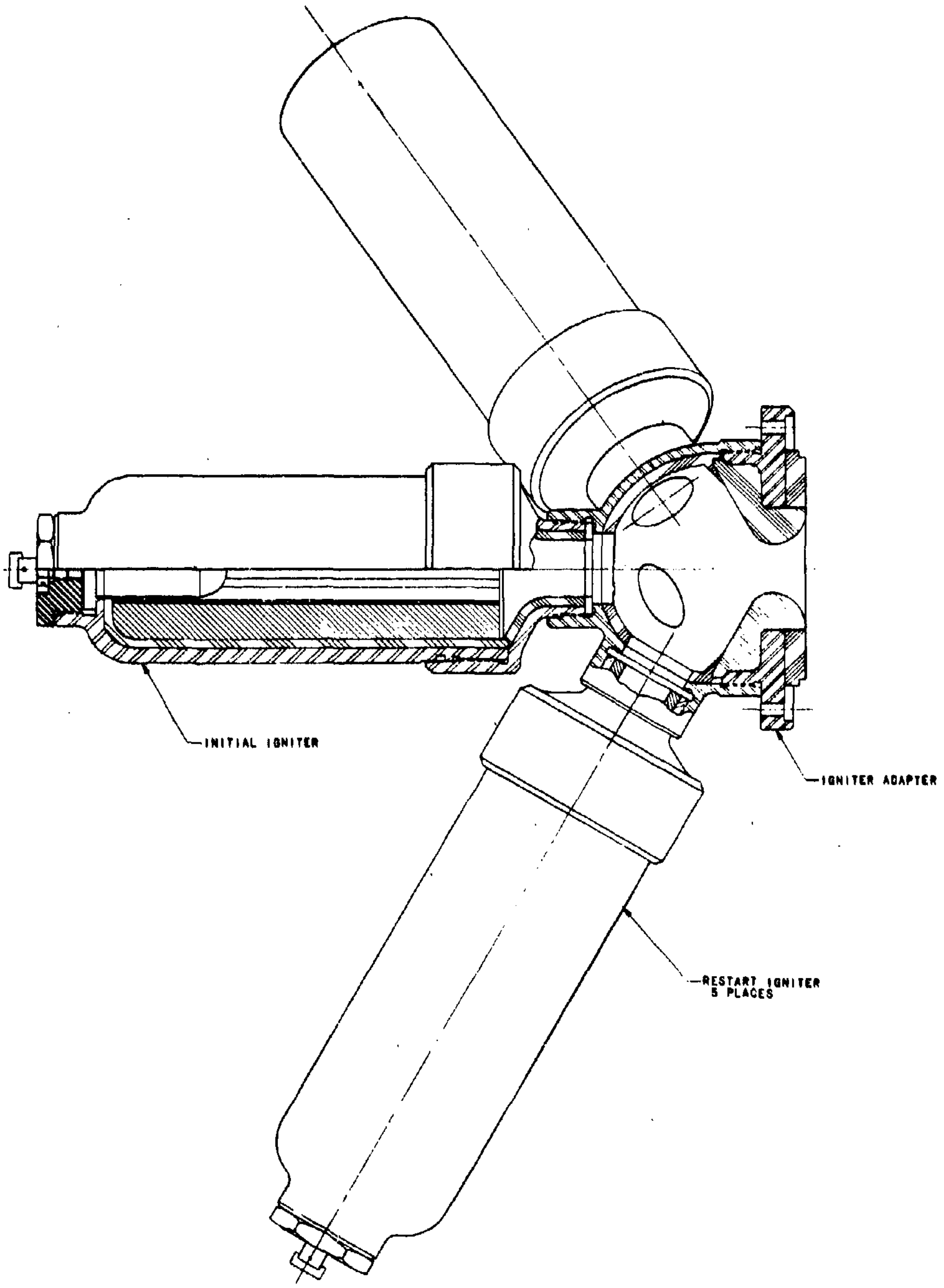

Canister Ignition System - Conventional Propellant

Figure III-17

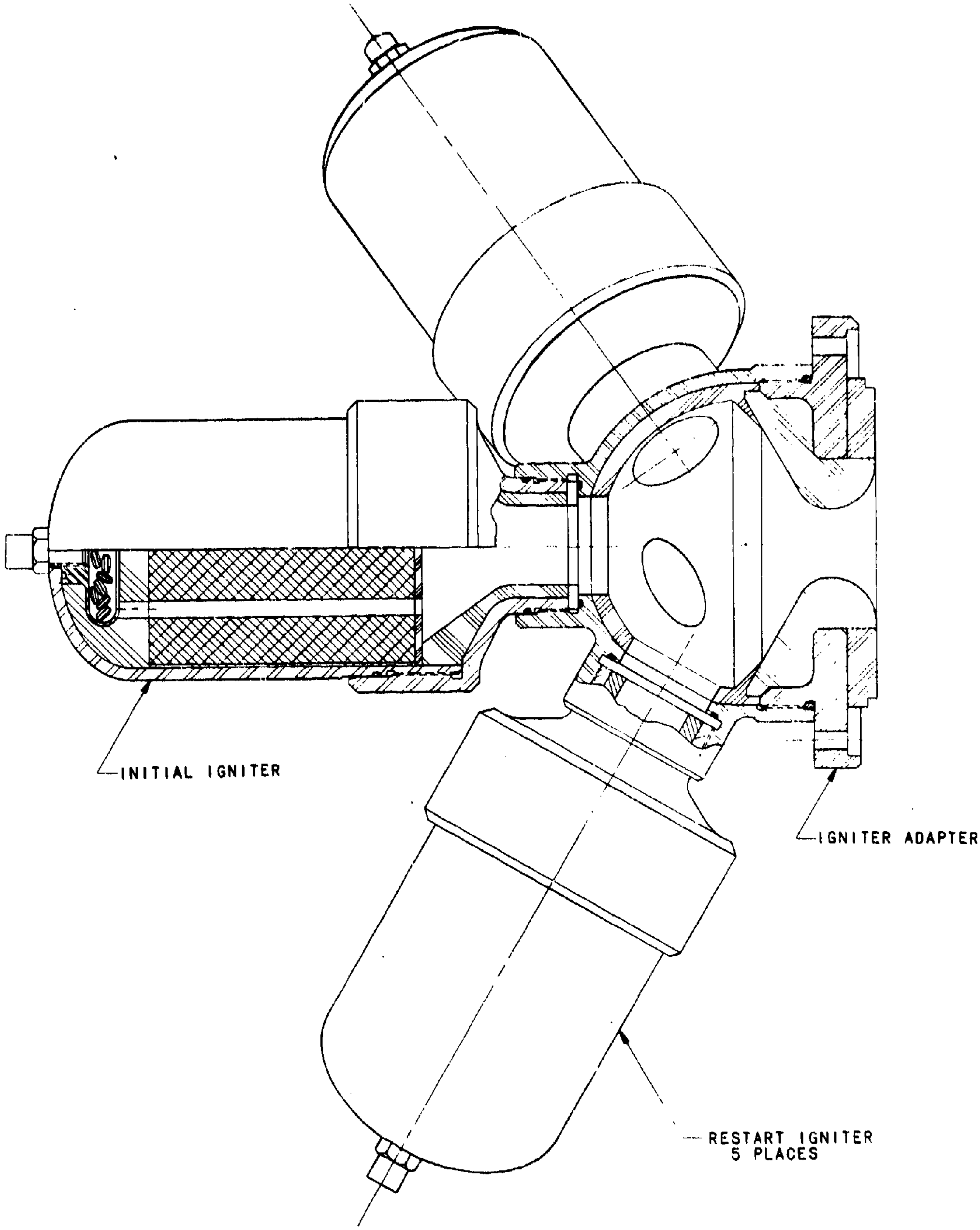

Canister Ignition System - High Burning Rate Propellant

Figure III-18

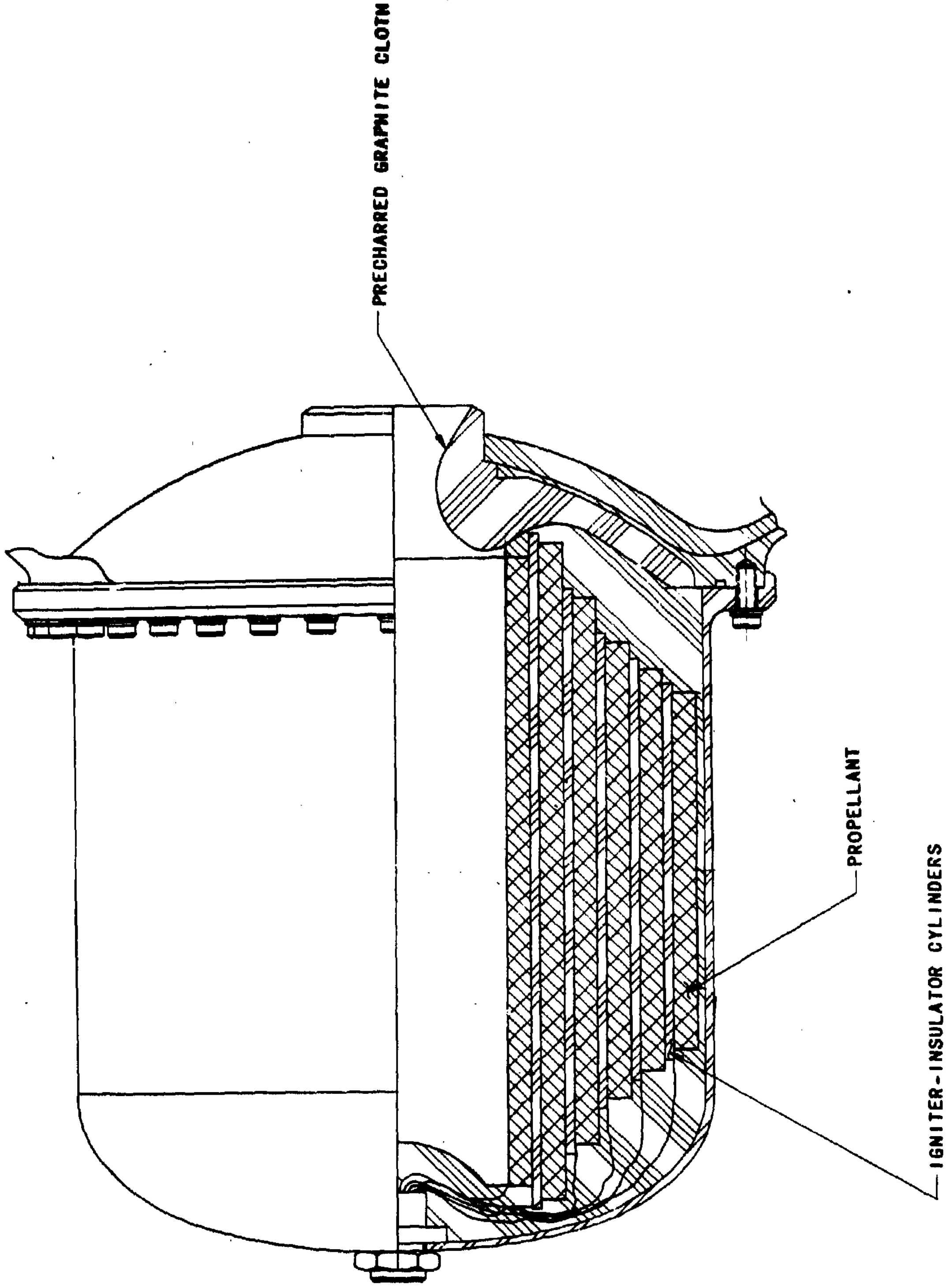

Pulse Ignition System - Internal Burning Shells (u)

Pulse Ignition System - Internal Burning Shells

Figure III-19

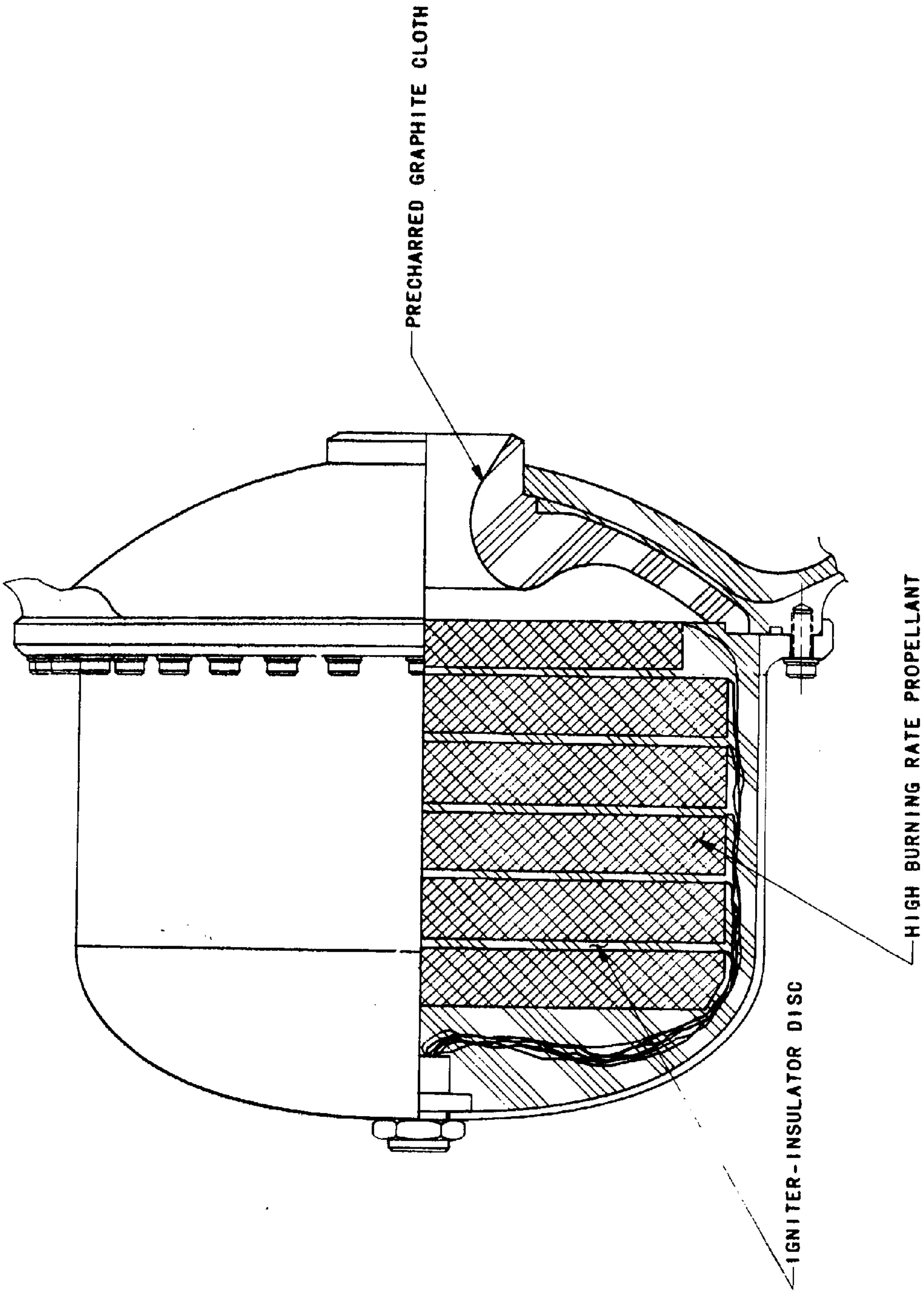

Pulse Igniton System - End Burning Wafers (u)

Figure III-20

d. Termination and Thrust Modulation Capability

(U) As shown graphically in Section "a" of this preliminary tradeoff study, the thrust modulation capability is a function primarily of the propellant burning rate exponent "n" and the nozzle throat area variation. The ability to achieve propellant extinguishment by the L* technique depends upon the motor free volume, maximum nozzle throat area, and, again, the propellant burning rate exponent. The ability to achieve extinguishment by rapid depressurization depends again upon the motor free volume, maximum nozzle throat area, and the rate of change of area capability. Because of the complex interrelation of motor and propellant parameters, the termination and thrust modulation capability tradeoff was conducted for a specific motor size and is presented in Section III,A,4 where the details of the motor preliminary design are discussed.

e. Insulation Thermal Degradation

(U) Considerable emphasis has been placed on determination of the actual thermal environment in the nozzle of the controllable solid rocket motor. In addition to the literature survey, discussed previously, and the cold flow program, discussed in the next section, thermal analyses were conducted to check the predicted temperature-time history of the various insulation materials being considered. From the results of these three methods of investigation, it was determined that material requirements vary considerably depending upon their placement in the movable pintle nozzle. Pintle housing and strut insulation material must have a very low conductivity, a low temperature of ablation, and a char layer that is readily removed by the low Mach-number gases flowing over it. In addition, this insulation char layer must have a very low density and have a low specific heat, thus minimizing the amount of heat storable. This later requirement will minimize the possibility of reigniting the propellant grain by radiation. Of all the insulation materials considered, the rubber base materials most closely meet these requirements.

(U) For flame liner application, the selection of the material depends upon the rate of heat input, the allowable thermal degradation, and the allowable dimensional change from firing to firing. Near the throat of the movable pintle nozzle, for example, the heat flux is high and the requirement that dimensional stability be preserved is dominating; thus, the insulative flame liner material must be one which most closely meets these requirements. Most of the reinforced phenolic materials lose dimensional stability as the resin system is sublimated during heat soak. The amount of dimensional change that occurs during this resin outgassing can be minimized by precharring the material before final machining, thus effectively graphitizing the plastic part yet maintaining a large percentage of the desirable insulative properties of the original material. The resulting material is well suited for use in high-Mach-number flows because of its good erosion

resistance, and its dimensional stability makes it an ideal material for use on the pintle and pintle insulating hood because these must maintain a close tolerance due to the relative motion of the two components during nozzle area changes.

(U) For backside insulation, especially under graphite, tungsten, or pyrolytic graphite, the material must have a low conductivity both in the original state and in the semicharred state. In addition, these materials must exhibit a high compressive strength in the charred state. The materials that were found to be good for this application are the asbestos phenolics and the high-silica phenolics. Magnesium hydroxide is an ideal insulation material; however, the outgassing of water vapor somewhat limits its applications. Pyrolytic graphite, with the proper grain orientation, is one of the best insulation materials for use on the backside of the refractory flame liners. The cost of this material in shapes other than plate is somewhat prohibitive because of the difficulty in holding tight tolerance without grinding the parts. If the pyrolytic graphite parts are machined to tolerance by grinding, cutting of the laminates limits the usefulness of this material as an insulator. Simple cylinders of pyrolytic graphite will be used as backside insulation for the pyrolytic graphite washered throat inserts in the pintle and the outer throat.

(U) Where a high thermal resistance is required yet very little space is available, zirconium oxide coating was selected as the best method of thermal protection of metallic structures. This material is easily applied by flame spray and the resulting coating can be ground to tight tolerances and smooth finishes. Other flame spray applied coatings are available for use as insulative barriers; however, the state-of-the-art is more advanced in the use of zirconium oxide than any of the other oxides, thus assuring a more repeatable product and improving reliability.

f. Motor Reconfiguration

(U) This specific task was directed toward an evaluation of the length-to-diameter ratio. Two computer programs were employed to evaluate the change in motor mass fraction as the diameter and thrust are varied, and, secondly, the attainable range of a missile on a typical air-launched mission as the diameter, thrust, and number of thrusting periods are varied. Both mass fraction and range are plotted as a function of the motor operating pressure in addition to the other variables.

(C) The mass-fraction graphs, Figures III-21, III-22, and III-23, utilized a computer program that was originally written for evaluation of various motor sizes that employed a movable pintle nozzle and had stop-restart capability. Because of the unknown ignition requirements, however, these data are presented incorporating a fixed weight for the ignition system for all of

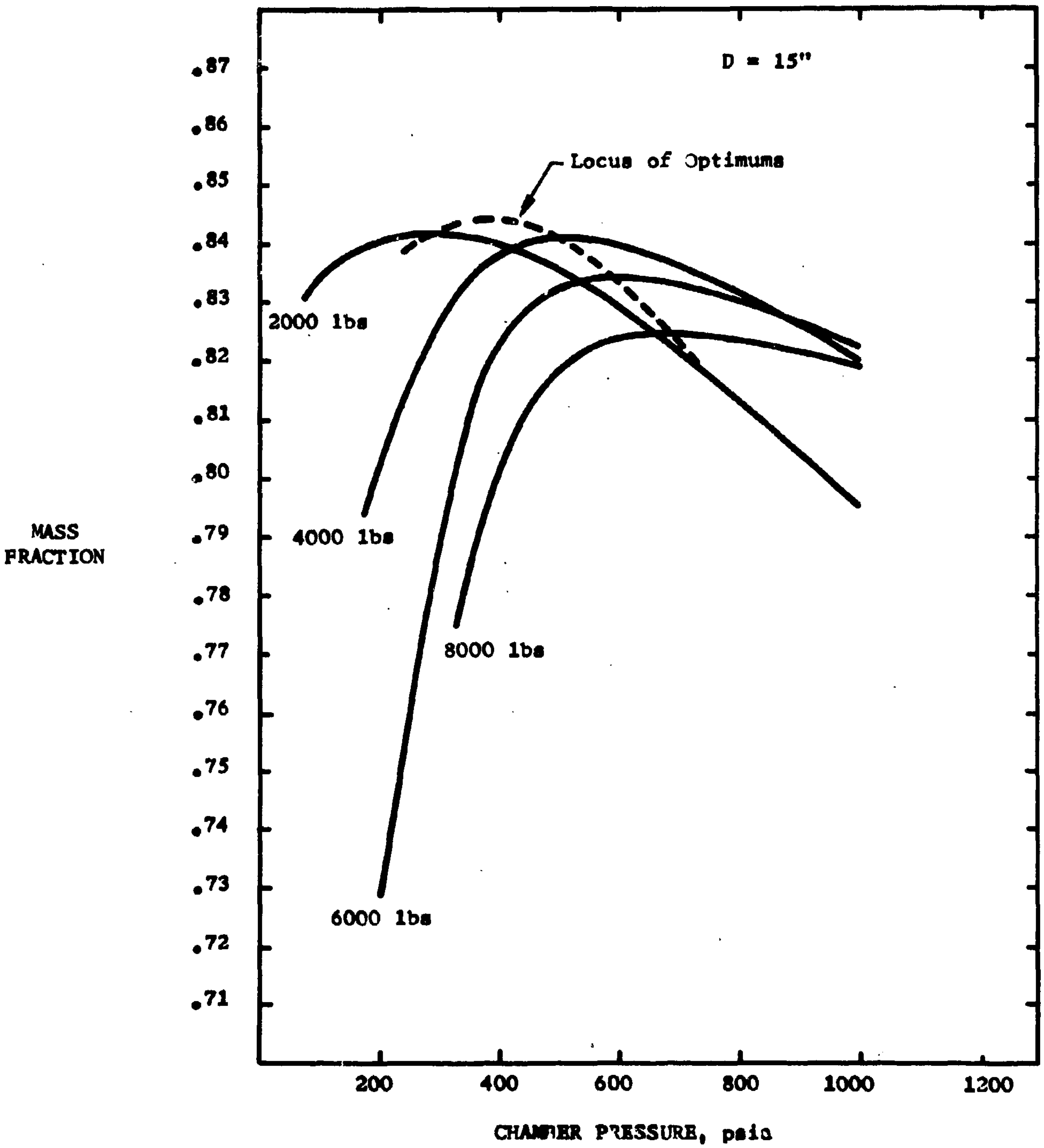

Trade-Off Study, Mass Fraction for 15-in.-Diameter (u)

Figure III-21

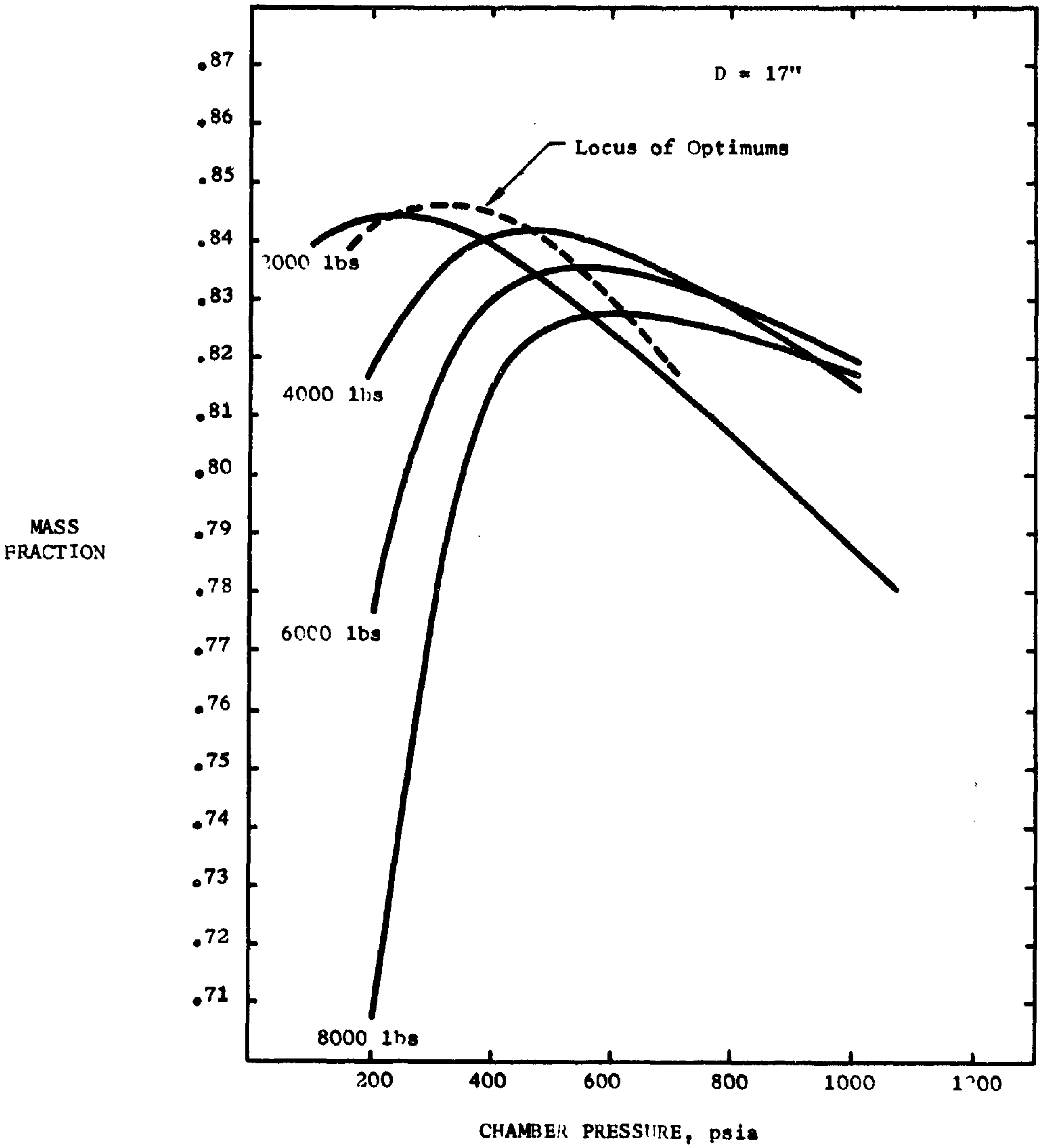

Trade-Off Study, Mass Fraction for 17-in.-Diameter (u)
Figure III-22

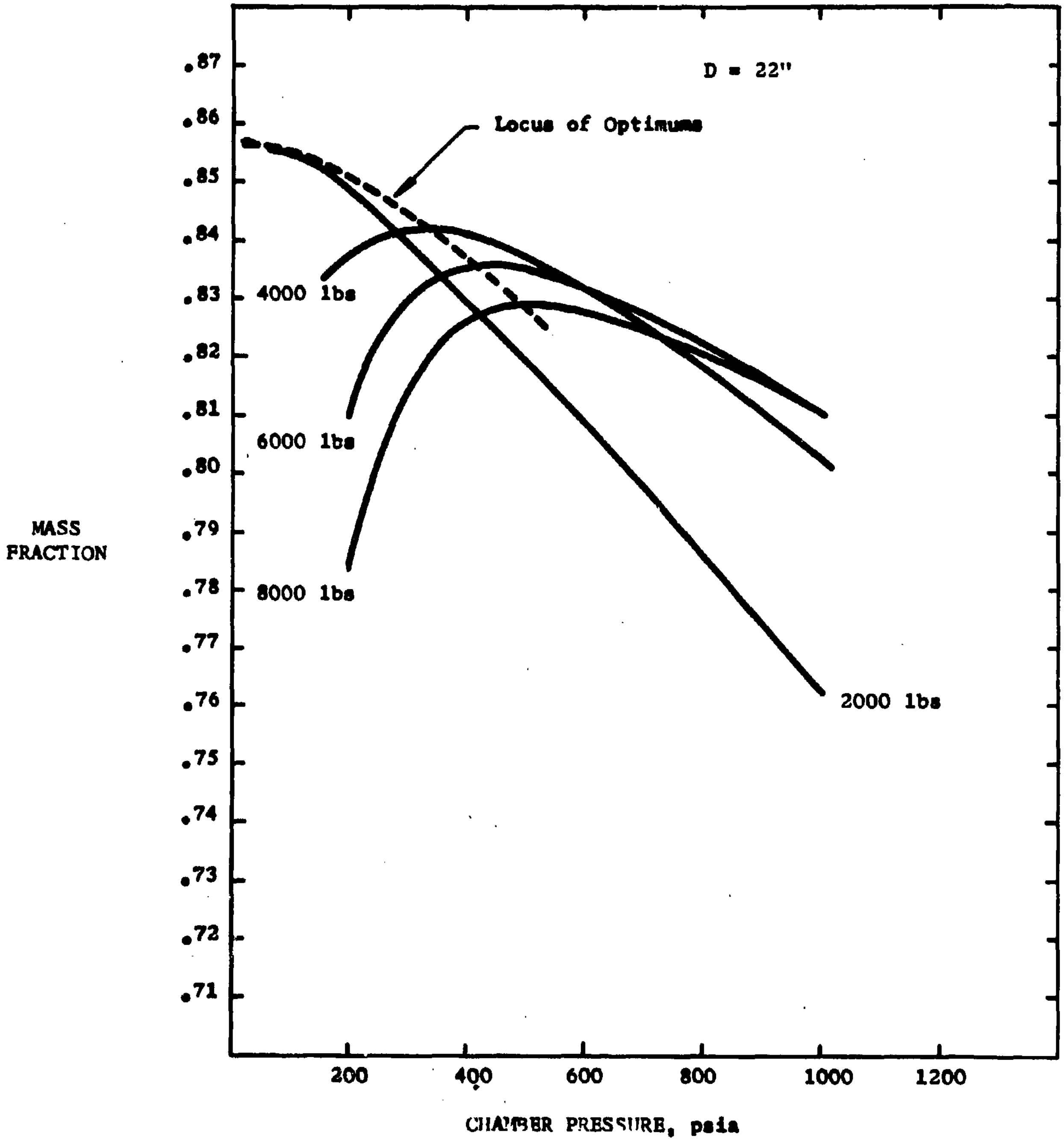

Trade-Off Study, Mass Fraction for 22-in.-Diameter (u)

Figure III-23

the motors evaluated. For purposes of evaluating the relative effect of configuration changes, these plots can be used without placing too much significance on the actual mass fraction value. For a multiple stop-restart motor with actual size igniters, the calculated mass fraction will be somewhat less than those presented on these figures. The general trend of these data indicate that, as the motor diameter is increased and the chamber pressure and thrust held constant the potential mass-fraction increases. Since the maximum operating pressure of the controllable solid rocket motor design is in the area of 700 psia and the maximum thrust is in the area of 8000 lb, by comparing the potential mass fractions of this point it can be seen that the optimum diameter occurs somewhere between 17 and 22 in. If the maximum thrust level were decreased, the optimum diameter would also decrease. A much greater increase in mass fraction can be achieved by decreasing the maximum operating pressure as the peak mass fractions for all of the thrust levels considered occurred at pressures lower than 600 psia. This latter change can be accomplished by using a propellant with a higher burning rate exponent as was shown in the first section of the preliminary tradeoff study discussion.

(C) Figure III-24 depicts the range of a missile using a propulsion system with a diameter of 15, 17, or 22 in. and operating at a constant thrust level of 2000, 4000, 6000, or 8000 lb. The trajectory of this missile was level at 500-ft altitude; launch was at Mach 0.55 with a boost-coast phase during which the angle of attack was varied to maintain level flight; and range was determined as the point at which the missile had coasted down to a Mach number of 0.70. Each of the motors started with a propellant loading of 500 lb and a total payload of 400 lb. The total weight of each missile varied as the mass fraction of the individual propulsion system varied.

3. Cold-Flow Testing

(U) The controllable solid rocket (CSR) motor configuration utilizes a pintle-type nozzle that is subject to complex flows in the throat entrance region, flows that change in character with a change in plug axial position. A one-dimensional analysis of the accelerating flow was believed inadequate to describe conditions in the annular passage and two-dimensional consideration presents excessive complexity in solution. Because heat-transfer analysis of heat flux to the boundaries requires definition of location magnitudes of mass-velocity, solution to define the boundary flow characteristics is important.

(U) For this reason, cold-flow experiments using simulated CSR internal geometry were conducted to provide direct measurements of static pressure distributions along the flow boundaries upstream of the variable throat station.

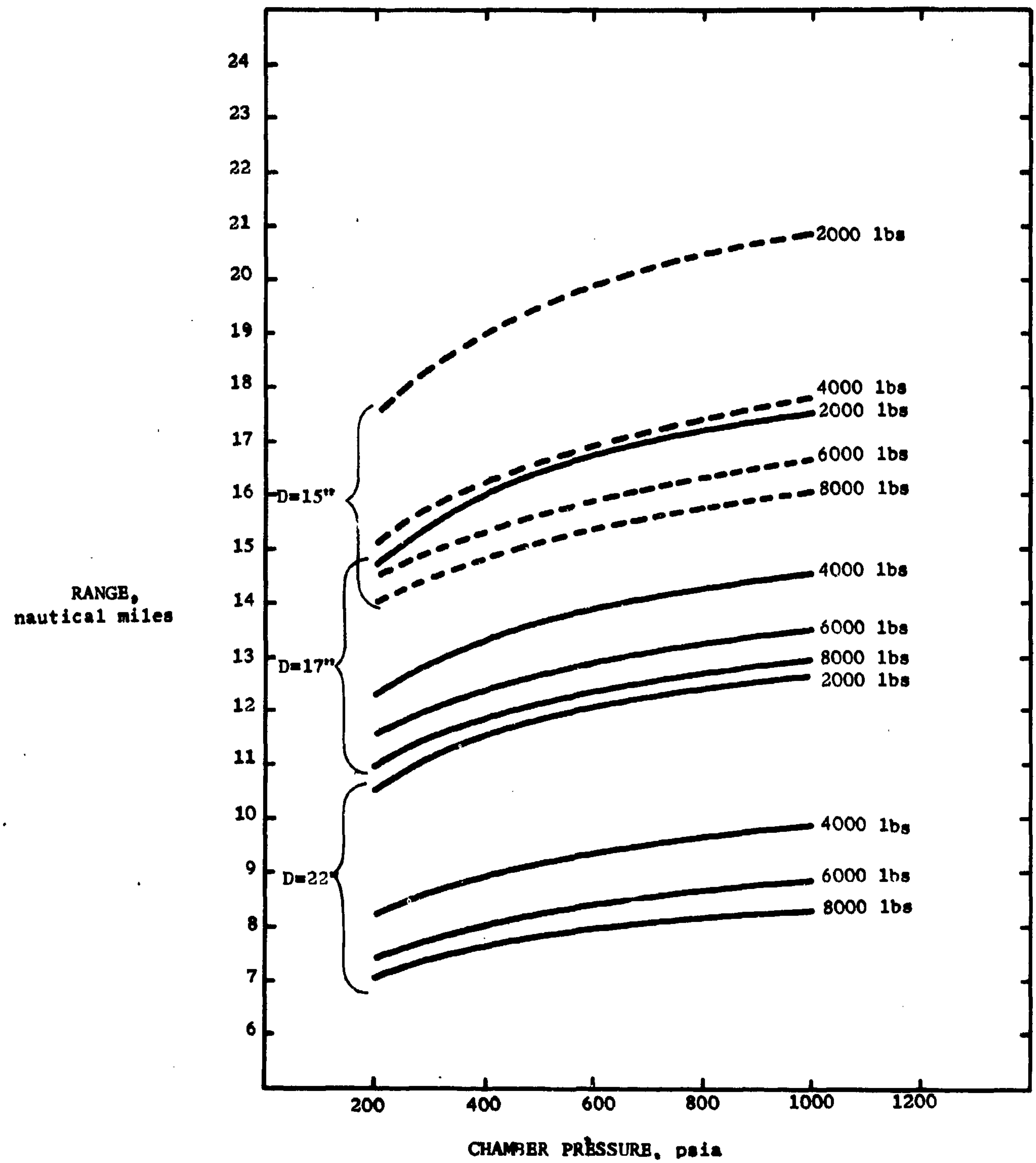

Trade-Off Study, Range vs Pressure, Thrust, and Diameter (u)

Figure III-24

III, A, Preliminary Design (cont.)

(U) A series of seven experimental cold-flow data tests was conducted in the Aerojet Aerophysics Laboratory in August 1965. These tests were made using a scale model of the plug-and-sleeve internal contours of the nozzle configuration, duplicating the actual motor contours upstream of the minimum throat station sufficiently to assure aerodynamic simulation. Four plug axial positions were evaluated so as to define changes in flow boundary characteristics with plug translation. A sufficient number of check and repeat tests were made to establish data validity and applicability. Definition of the test series is provided in Figure III-25.

(U) The model system was fabricated of laminated mahogany components designed to be inserted, for the test runs, in an existing three-dimensional test fixture. Translation of the plug was achieved through use of a manually-operated traverse mechanism originally designed for nozzle-throat flow-profile measurement. Assembly of the model components is shown in Figure III-26 (the test fixture is not included). Figure III-27 is a photograph of the test fixture installed in the laboratory preparatory to conducting the experiments.

(U) Check and repeatability runs were conducted to assure the adequacy of the simulation, particularly in respect to the replacement of motor sleeve struts with a disc-and-hole system in the model. Moreover, the accuracy and repeatability of plug axial position were established through repetition of selected data runs.

(U) Recorded data for these experiments consisted of photographic records of mercury multimanometry. Static pressure orifices, distributed in axial rows along the nozzle entrance flow boundaries, were located in the model as indicated on the data plots of this report. Recorded local static pressures were ratioed to stream total pressure and reduced to Mach number using isentropic relationships. Values of mass-velocity* were determined for faired values of Mach number, again using isentropic relationships. Although the Mach number distributions strictly apply for the flow of air, the mass-velocity ratio is, in effect, dependent one-dimensionally only on model geometry and can be used in analysis of propellant gas flow effects.

(U) Presentation of the data distributions along unsymmetrical surfaces is difficult in view of point of reference. The method used in the data plots of Figures III-28 through III-32 depends on definition of a surface

*The mass-velocity ratio (Pv/p*v*) is defined as the ratio of the product of density and velocity in a local region of flow to the corresponding product (mass velocity) that would exist if the flow were accelerated to reach the local speed of sound in that region.

Run No.	Plug Position*	Remarks
1	0	Minimum Throat
2	34.3	
3	68.5	
4	100	Maximum open area
5	100	Rerun of Run 4 at higher total pressure
6	0	Repeat of Run 1
7	0	Repeat of Run 1 with plug and outboard boundary rotated 30° relative to sleeve and sleeve support

* Distance of plug face forward of minimum throat position in percent total travel

Data Run Listing

Figure III-25

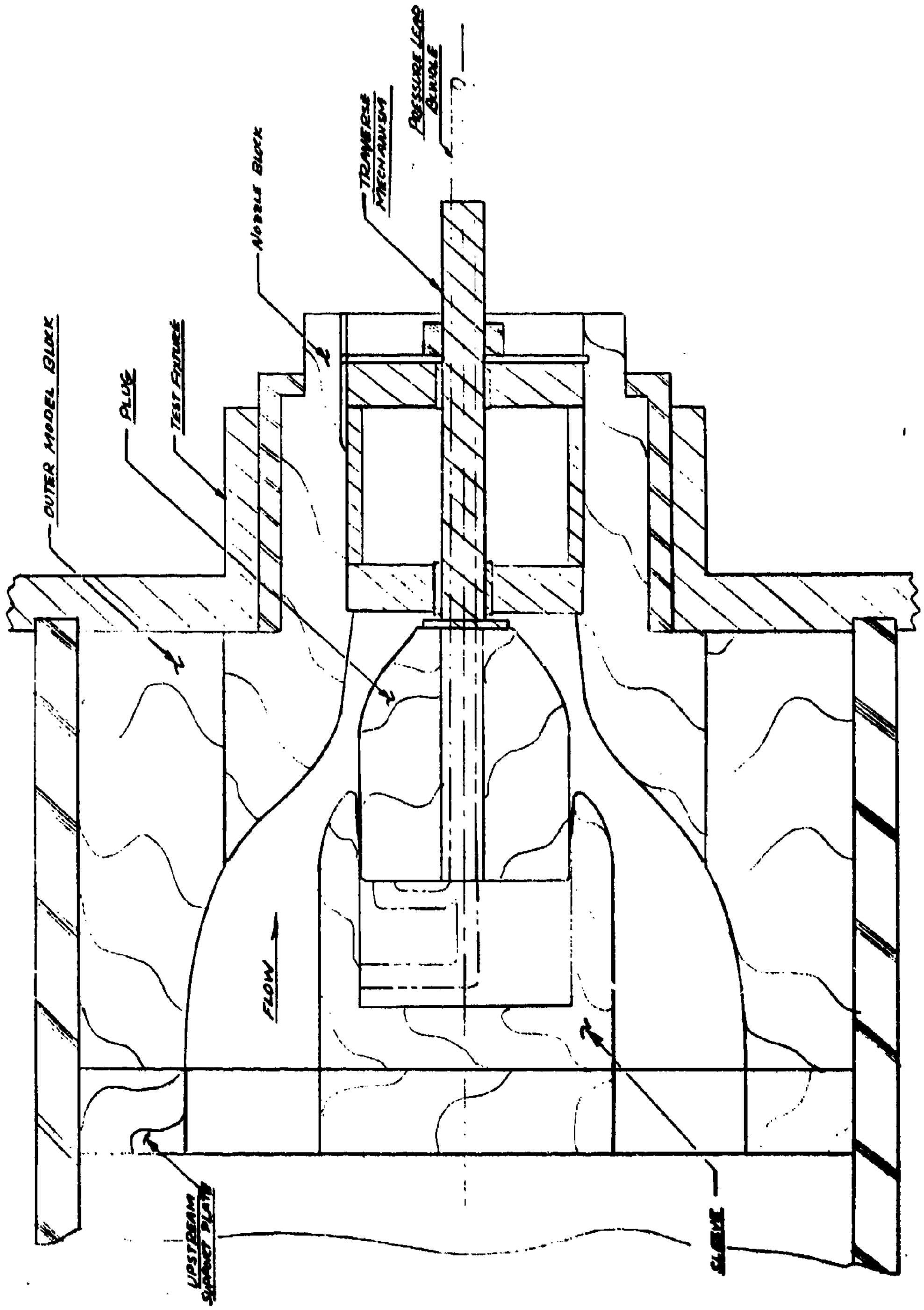

Cold Flow Model

Figure III-26

Test Fixture Installation - Cold-Flow Tests

Figure III-27

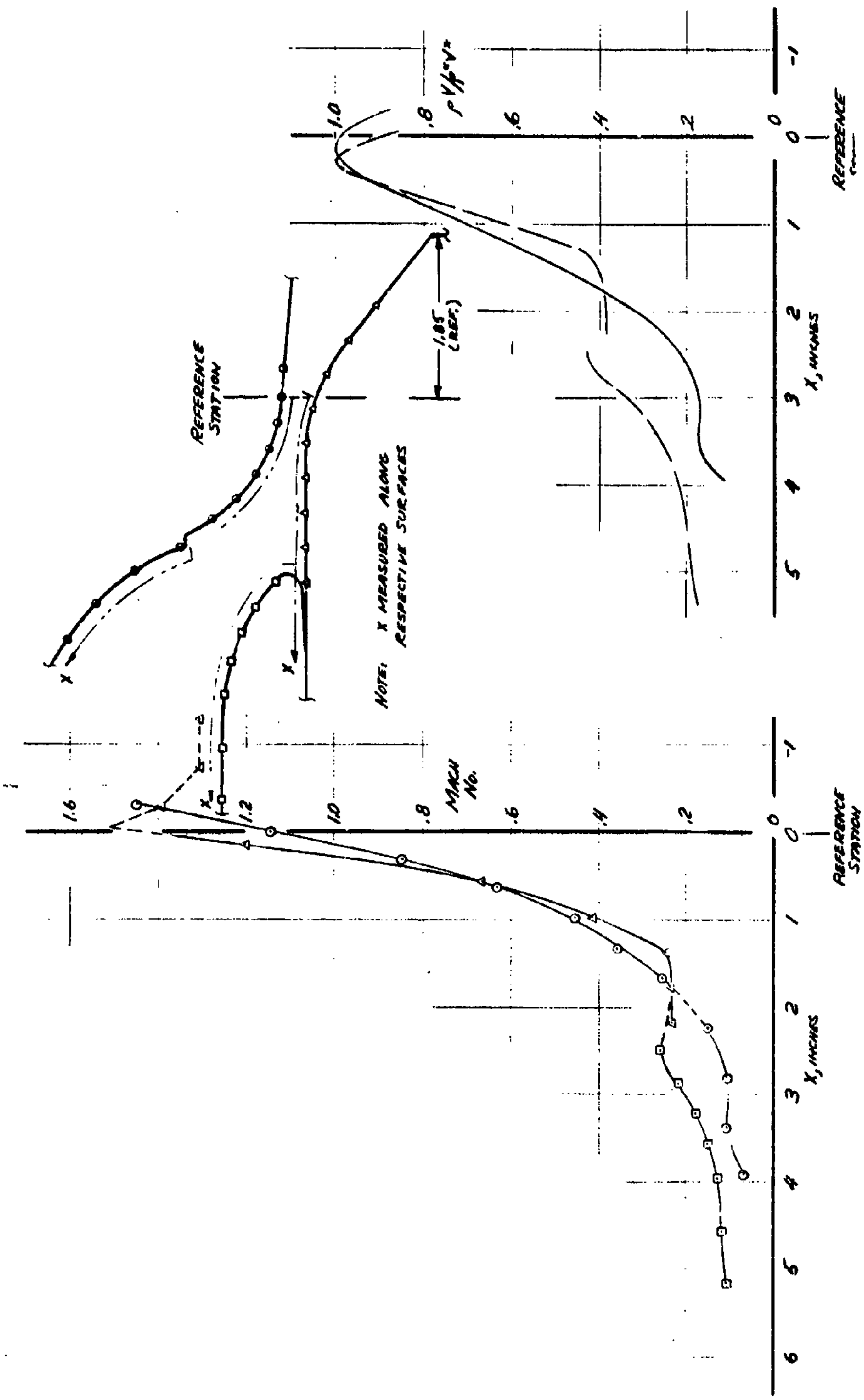

Cold Flow Test Data - Run 1 - Minimum Throat Position

Figure III-28

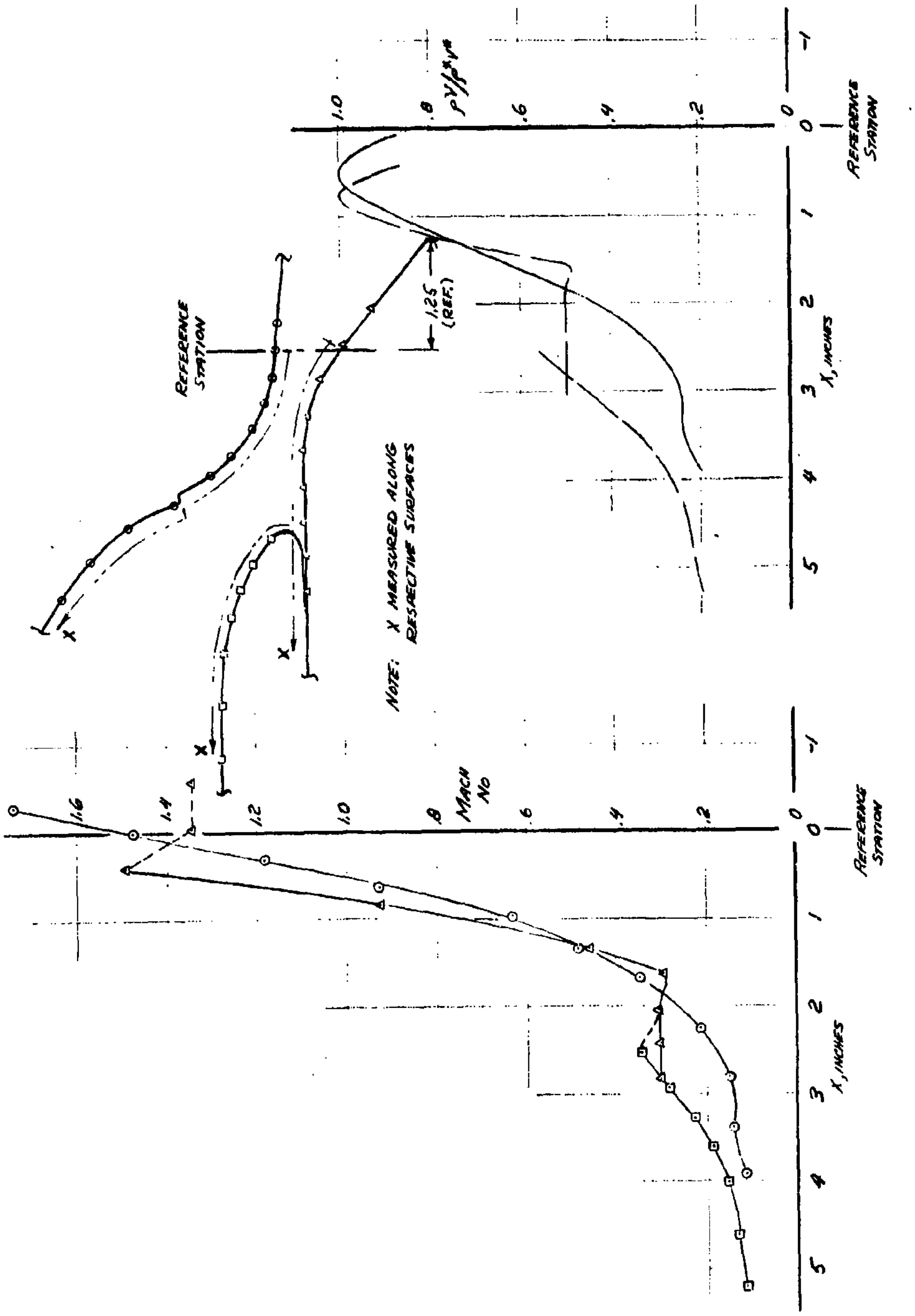

Cold Flow Test Data - Run 2 - Pintle 34.3% Retracted

Figure III-29

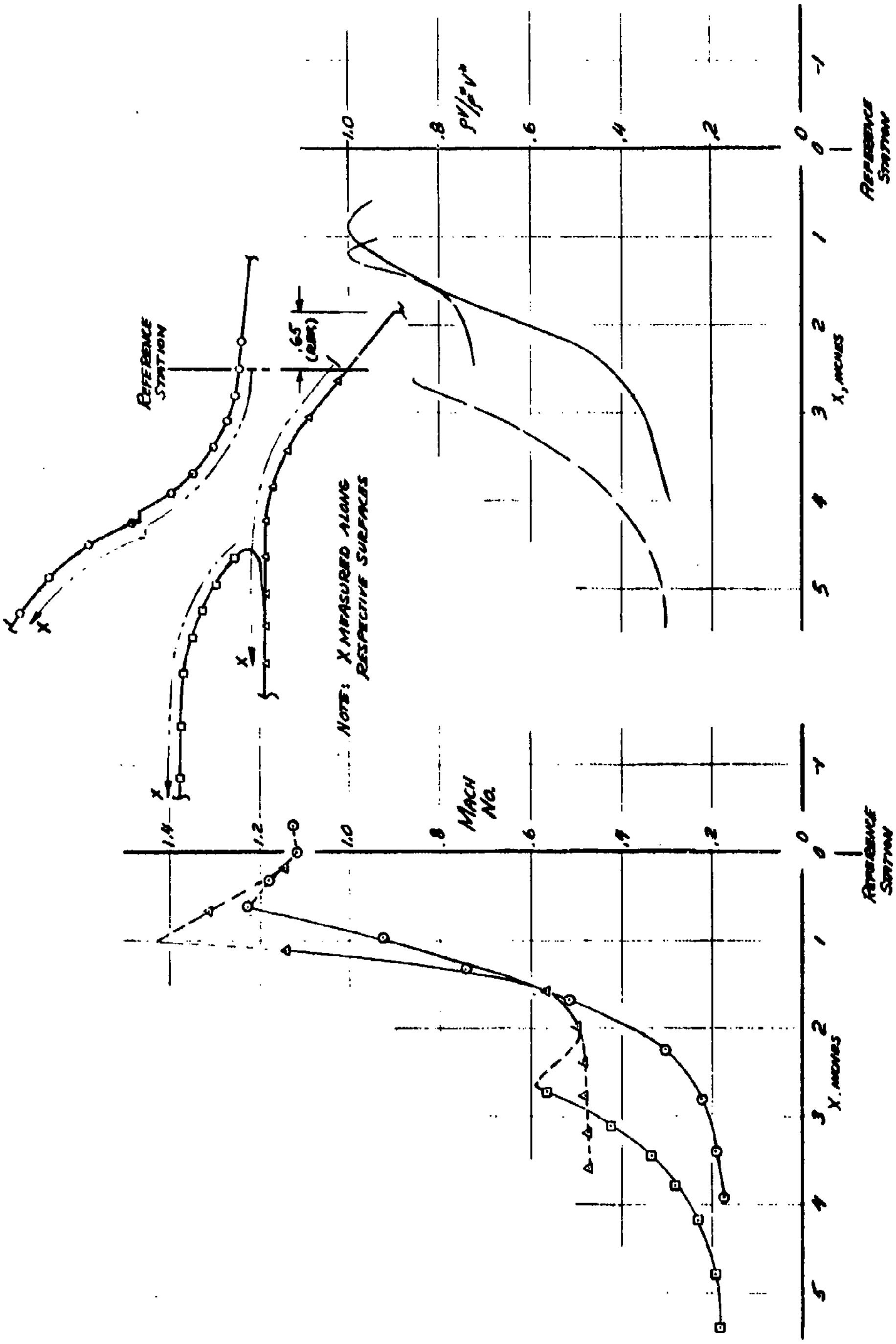

Cold Flow Test Data - Run 3 - Pintle 68.5% Retracted

Figure III-30

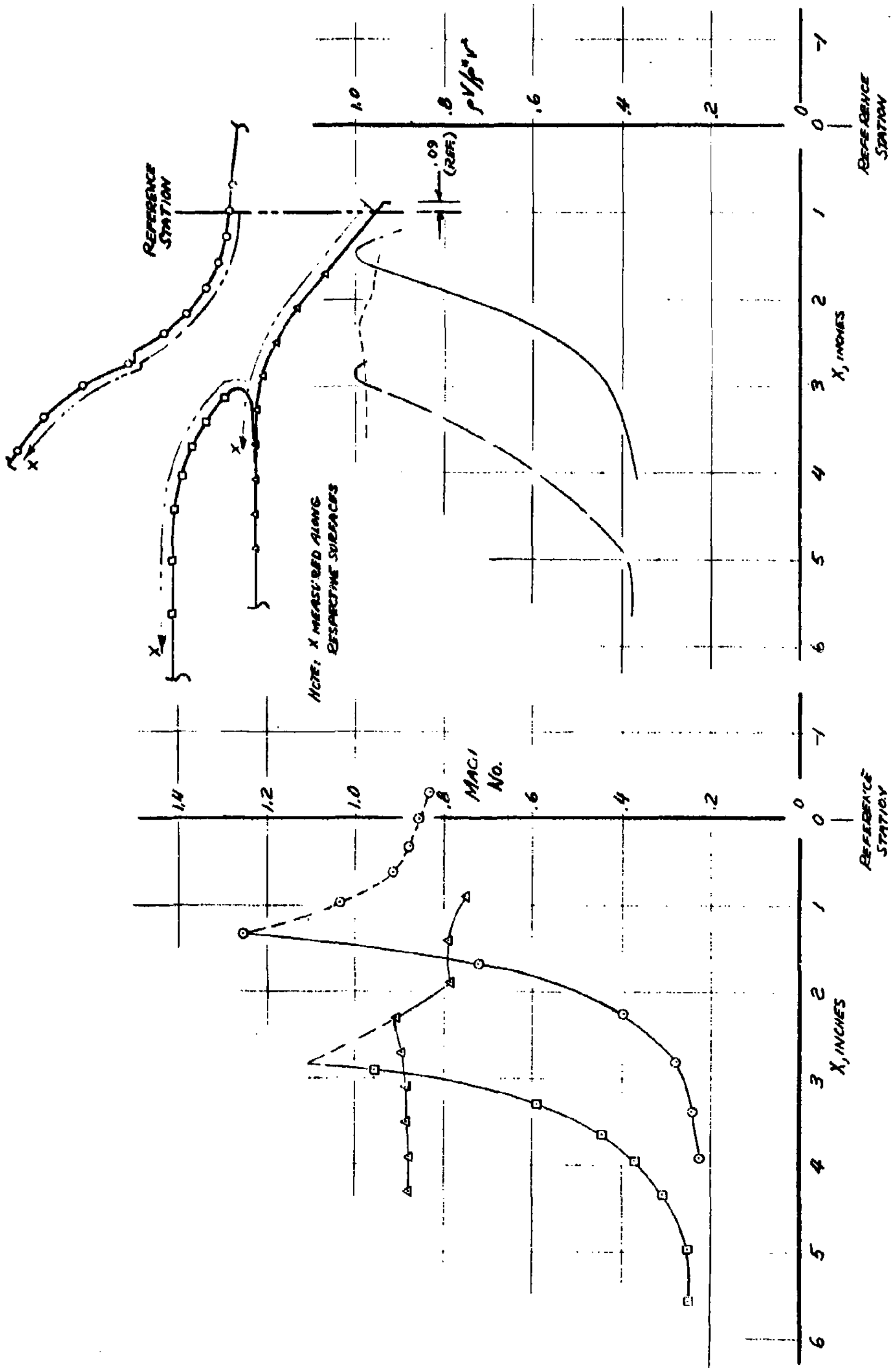

Cold Flow Test Data - Run 5 - Pintle 100% Retracted

Figure III-31

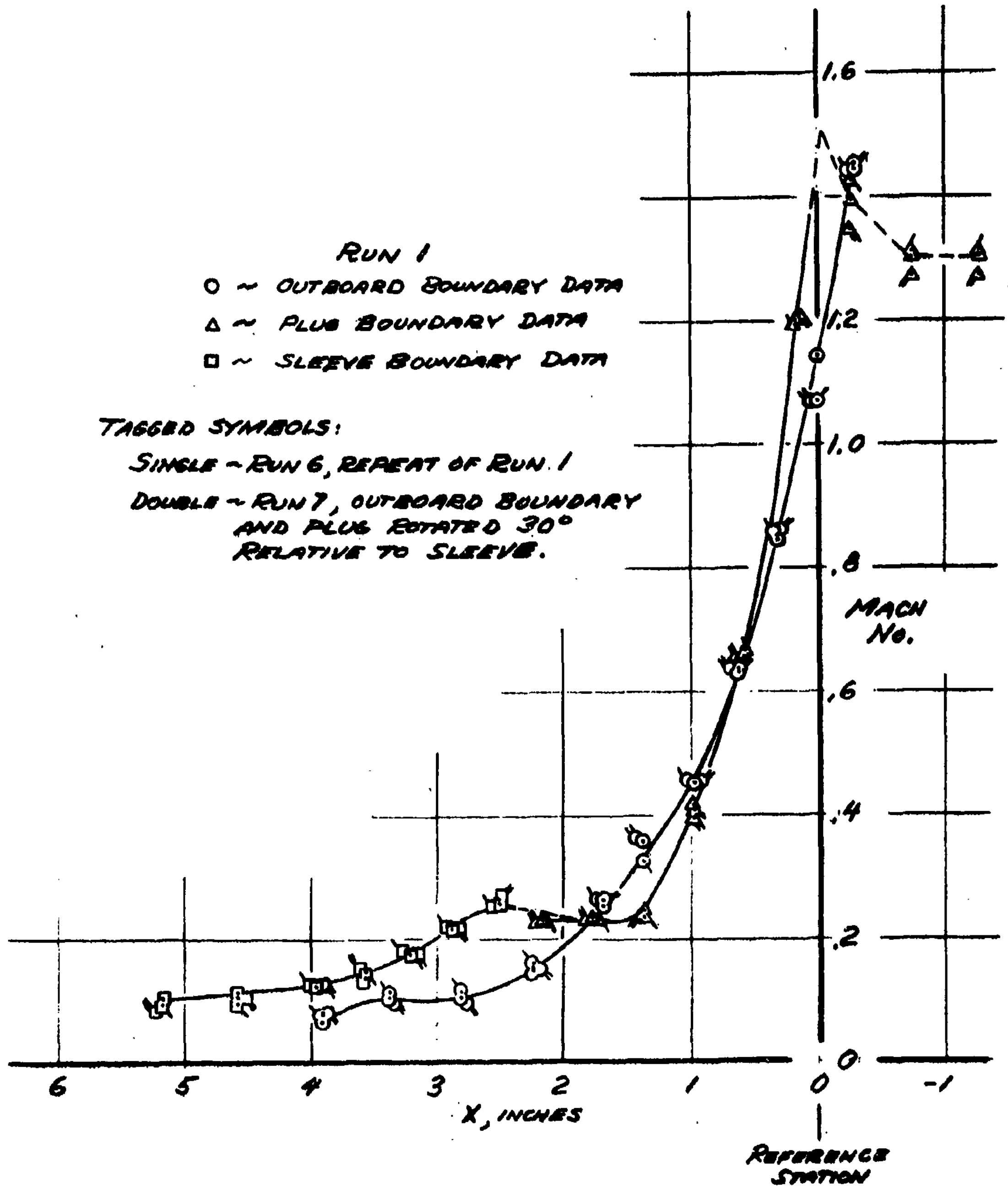

Cold Flow Test Data - Repeatability Check on Run 1

Figure III-32

coordinate, X. For the outer flow boundary, X is the same for all tests; for the plug and sleeve, X has a different origin for each plug position. The general reference point for the surface coordinate is the minimum radius station (from the motor center line) for the outer flow boundary of the actual motor. The origin for the plug and sleeve coordinate is maintained at a station radially inboard of this reference point, regardless of plug position. A full (model) scale line drawing of the flow boundaries is included for each configuration of Figures III-28 through III-31 defining both the existing geometry and the pressure orifice locations. The pressure orifices are related to the surface coordinate in the Mach number plots, thus tying the system together.

(U) The data describes exactly the translation of the effective throat location as the plug is retracted into the sleeve. Moreover the change in flow acceleration over the sleeve surface as a function of plug position is clearly evident, and the flow separation at the plug-sleeve juncture is described by the associated slope discontinuity of the data distributions.

(U) The general data repeatability as shown in Figure III-32 is considered good. The curve fairings used are identical to those of Figure III-28, thus validating the data used in Figure III-28 and, by inference, in Figures III-29, III-30, and III-31. The effect of plug and outer boundary rotation relative to the sleeve and sleeve support system is seen to be negligible.

(U) An analysis of the data was made to determine the mass-velocity distribution and compare this to corresponding information based on one-dimensional flow analysis. A deviation was expected on the basis of the flow passage asymmetry which should result in local regions of flow acceleration and deceleration. The analysis, however, showed that this deviation was primarily located in a region of relatively low Mach number (0.25 to 0.4) for which heating rates are generally less than 50% of maximum values. Mass-velocity in this region was computed to be approximately 10% less, based on one-dimensional flow, than measured in the actual experiments.

(U) Subsequent to completion and data reduction, the configuration of the variable throat nozzle was changed in such a way as to provide a generally reduced flow convergence rate in the entrance region. As a result, the applicability of the aerodynamic measurements was considerably reduced.

(U) The lower nozzle entrance convergence rates for the modified flow contour reduce the possible error in this region to below that for the original design evaluated experimentally. As a consequence, the recommended procedure for heat-transfer analysis for the new contour used the flow parameters determined on a one-dimensional basis with the knowledge that the possible error is indeed small.

4. Preliminary Motor Design

(U) A preliminary motor design was prepared to meet the performance criteria outlined in Section III,A,2. This preliminary design is a result of judicious application of current technology. Though it does not represent necessarily an optimum configuration for any specific application, it does demonstrate that the performance criteria can be met with a reasonably lightweight motor. The purpose of this design was to establish a basic configuration from which the heavyweight motor will be designed.

(C) The preliminary motor design, shown in Figure III-33, will deliver a maximum thrust of 8258 lb at altitude with a chamber pressure of 660 psia. A 3:1 thrust modulation is achieved by opening the throat and reducing the chamber pressure to 110 psia with the further possibility of a 5:1 variation by operating at a minimum chamber pressure of 50 psia. The nozzle is sized to reduce the chamber pressure to approximately 15 psia for extinguishment with a propellant having a 0.6 burning rate exponent. The actuation system was sized to provide a frequency response of 10 cps to assure extinguishment by rapid depressurization.

(C) The propellant parameters used in preparing this design were selected from those that have been demonstrated to be attainable under Contracts AF 04(611)-9889[1] and AF 04(611)-9962[2]. These are: a burning rate exponent of 0.60, a burning rate of approximately 0.10 in./sec at 100 psia, a standard specific impulse of 240 lbf-sec/lbm, and an average density of 0.063 $lb/in.^3$.

(C) Figures III-34, III-35, and III-36 were prepared to show the chamber pressure, the mass flow rate, and the vacuum thrust as a function of nozzle throat area, respectively. All of these plots have the throttling range and the extinguishment range marked. To meet the requirements of 3:1 thrust variability, about a nominal 4000 lb of thrust, a nozzle throat area variation of slightly over 2:1 is required, from 8.25 to 16.80 $in.^2$; however, the throttling range is sized to accommodate a nozzle area variability of over 2.8:1, from 6.75 to 19.0 $in.^2$, yielding the desired 5:1 thrust variability. The extinguishment range covers the nozzle areas from 19.0 to 30.4 $in.^2$.

(C) Figure III-37 depicts the L*-P_c operating map of this controllable solid rocket motor for propellants with burning rate exponents of 0.60, 0.625, and 0.65 to show the variation with exponent. Also superimposed on this figure are the data from two of the current extinguishable propellants, indicating that the sizing of this motor for L* extinguishment at 15 psia is reasonable with current propellants.

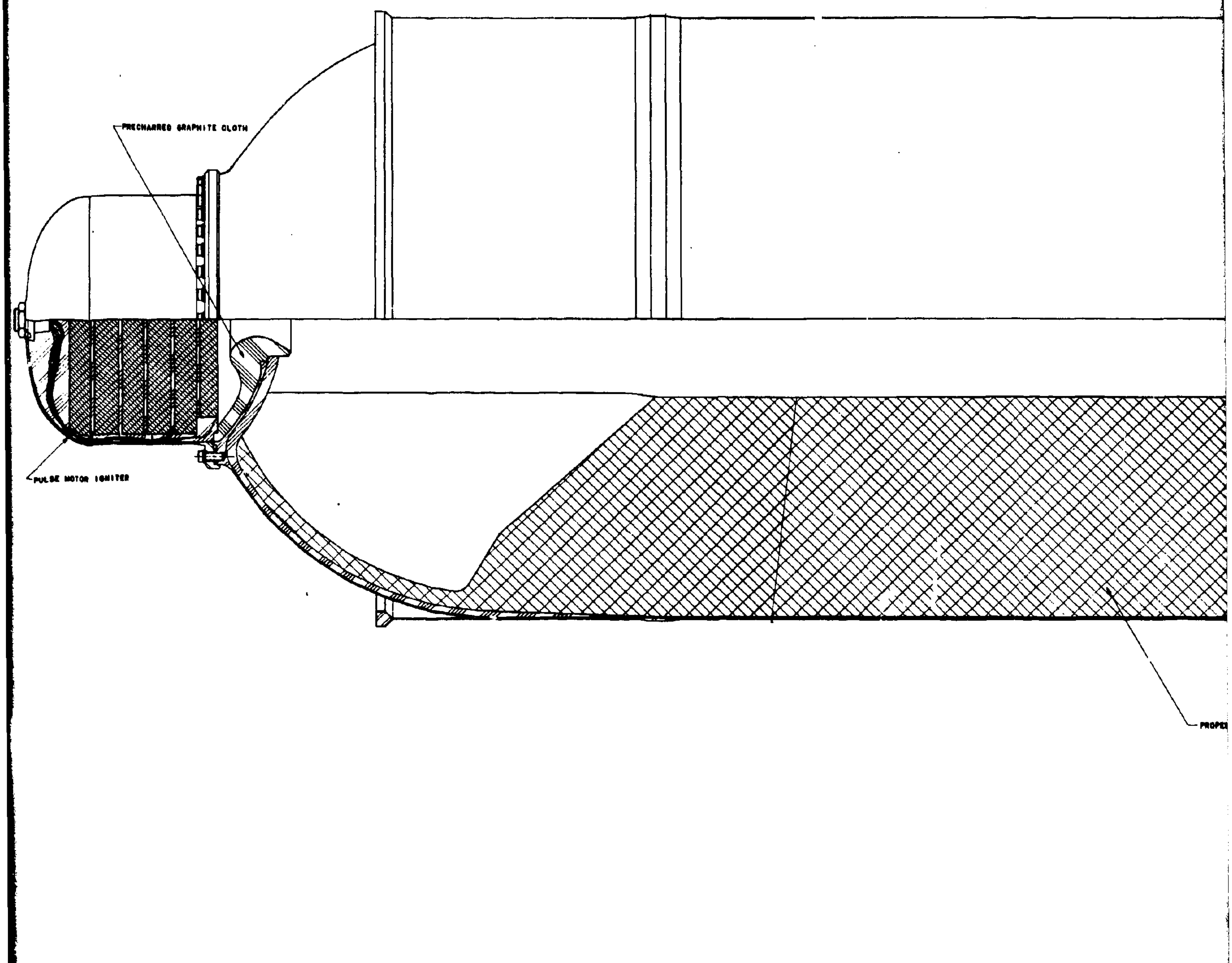
PRECHARRED GRAPHITE CLOTH
PULSE MOTOR IGNITER

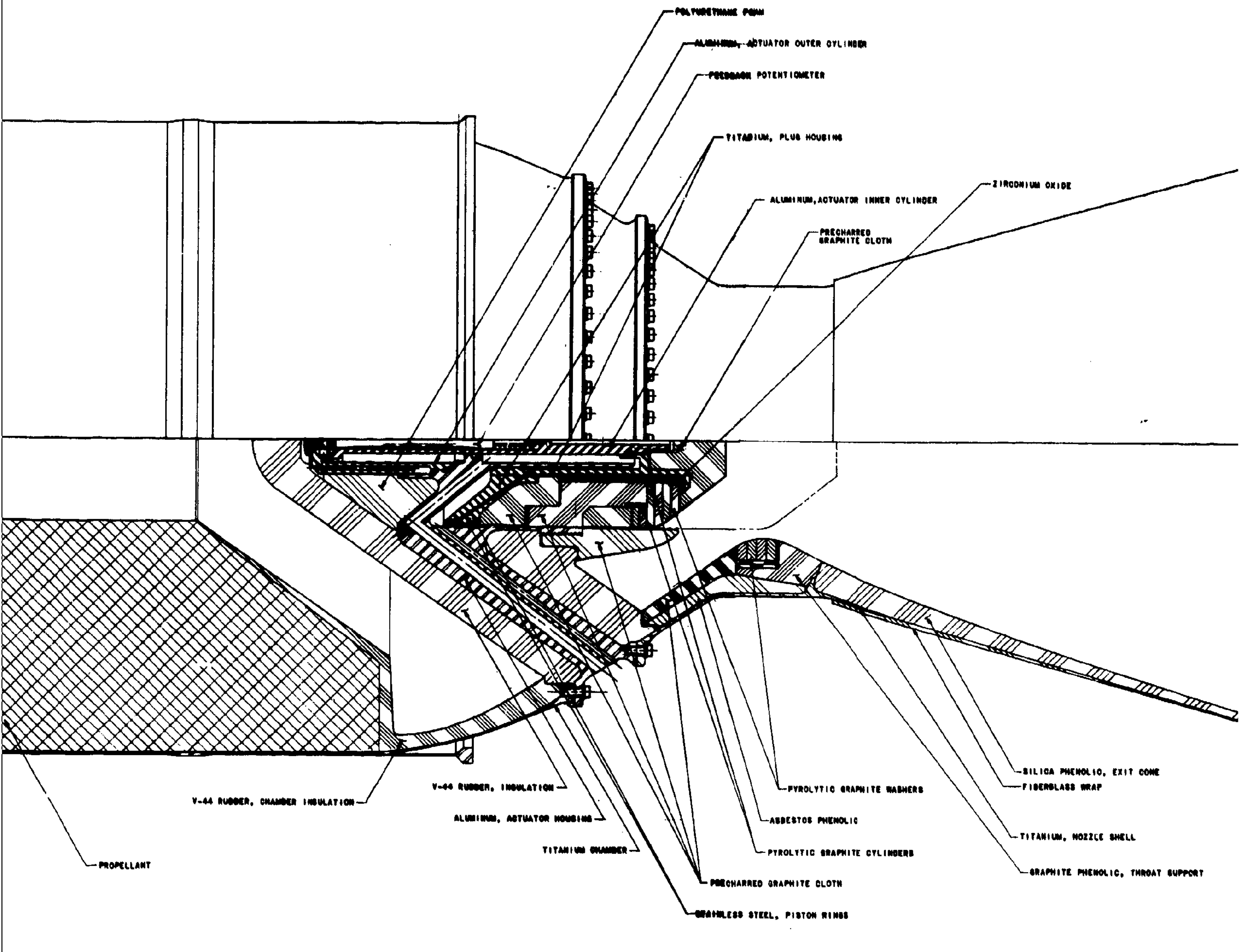

Preliminary Motor Desig

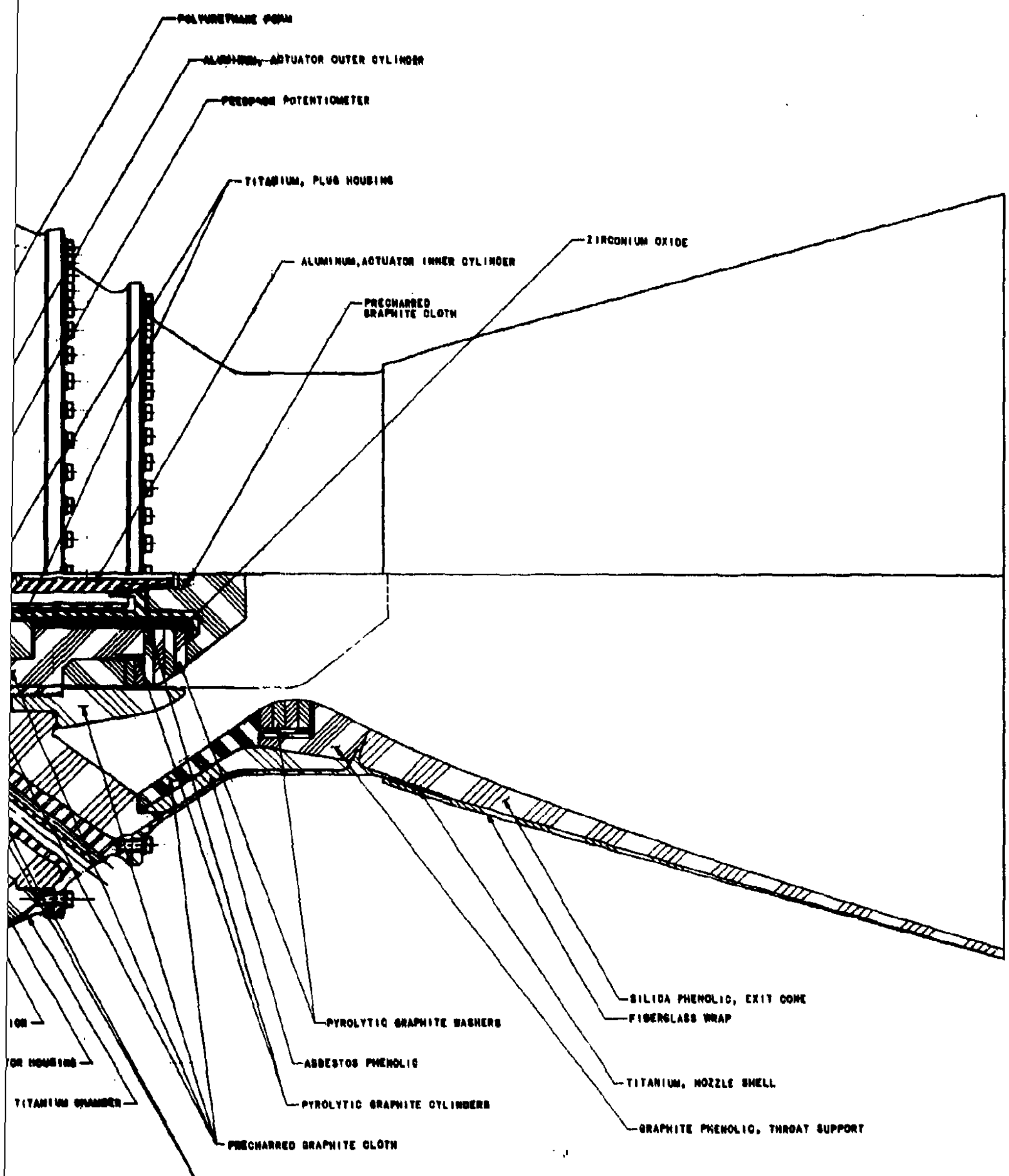

WEIGHTS	
CASE	34.09
INTERNAL INSULATION	61.11
NOZZLE	40.84
PLUG AND HOUSING	37.06
IGNITER INERT	8.13
HYDRAPAC	9.20
TOTAL INERT	190.43
MAIN PROPELLANT	697.06
IGNITER PROPELLANT	12.76
TOTAL PROPELLANT	709.82
TOTAL MOTOR WEIGHT	900.25
MASS FRACTION	0.788

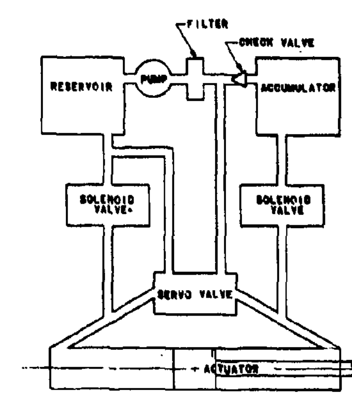

PLUG ACTUATION SYSTEM SCHEMATIC

Preliminary Motor Design - Controllable Solid Rocket Motor (u)

Figure III-33

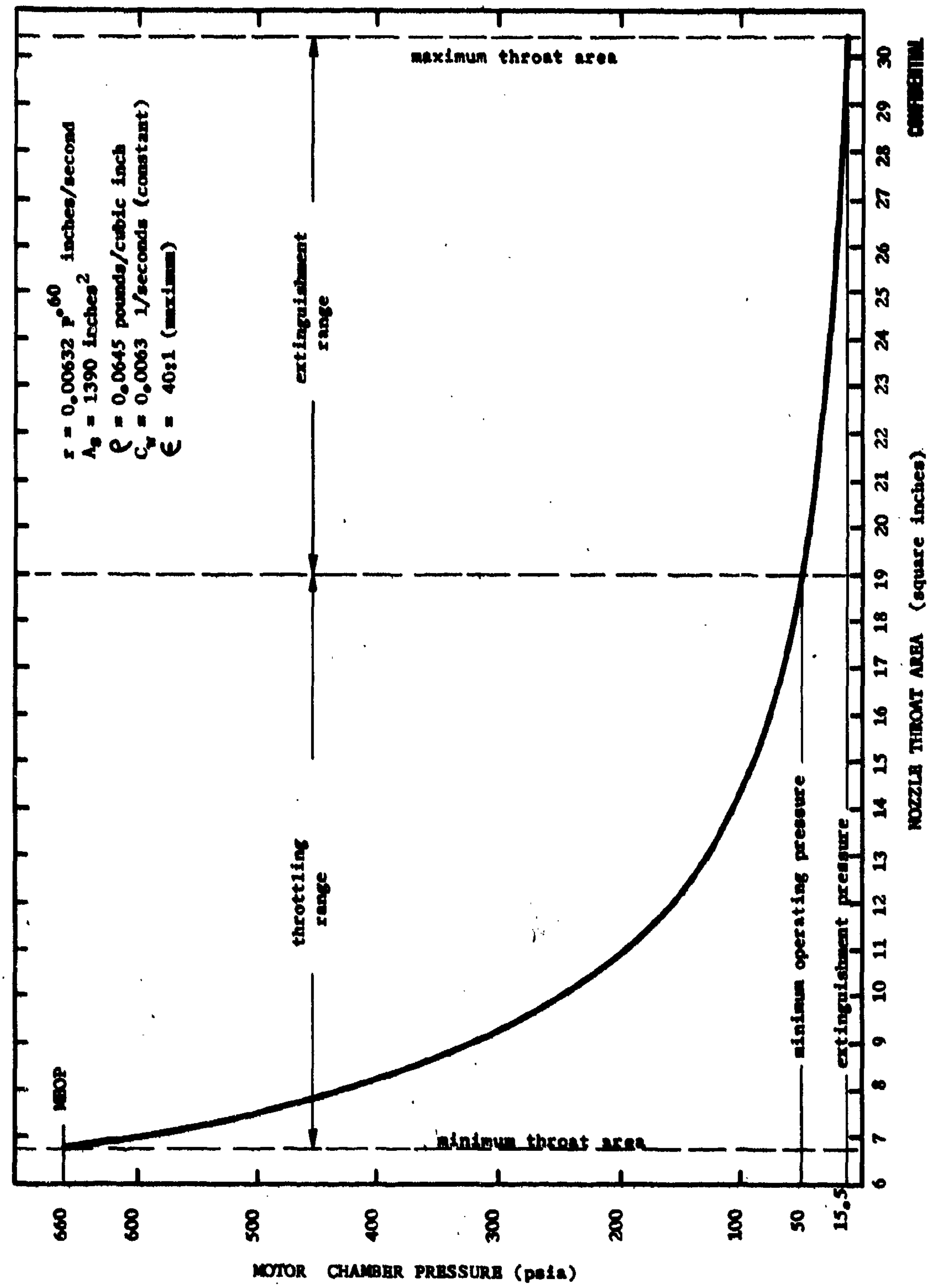

Controllable Solid Rocket - Full Scale Motor Data - P_c vs A_* (u)

Figure III-34

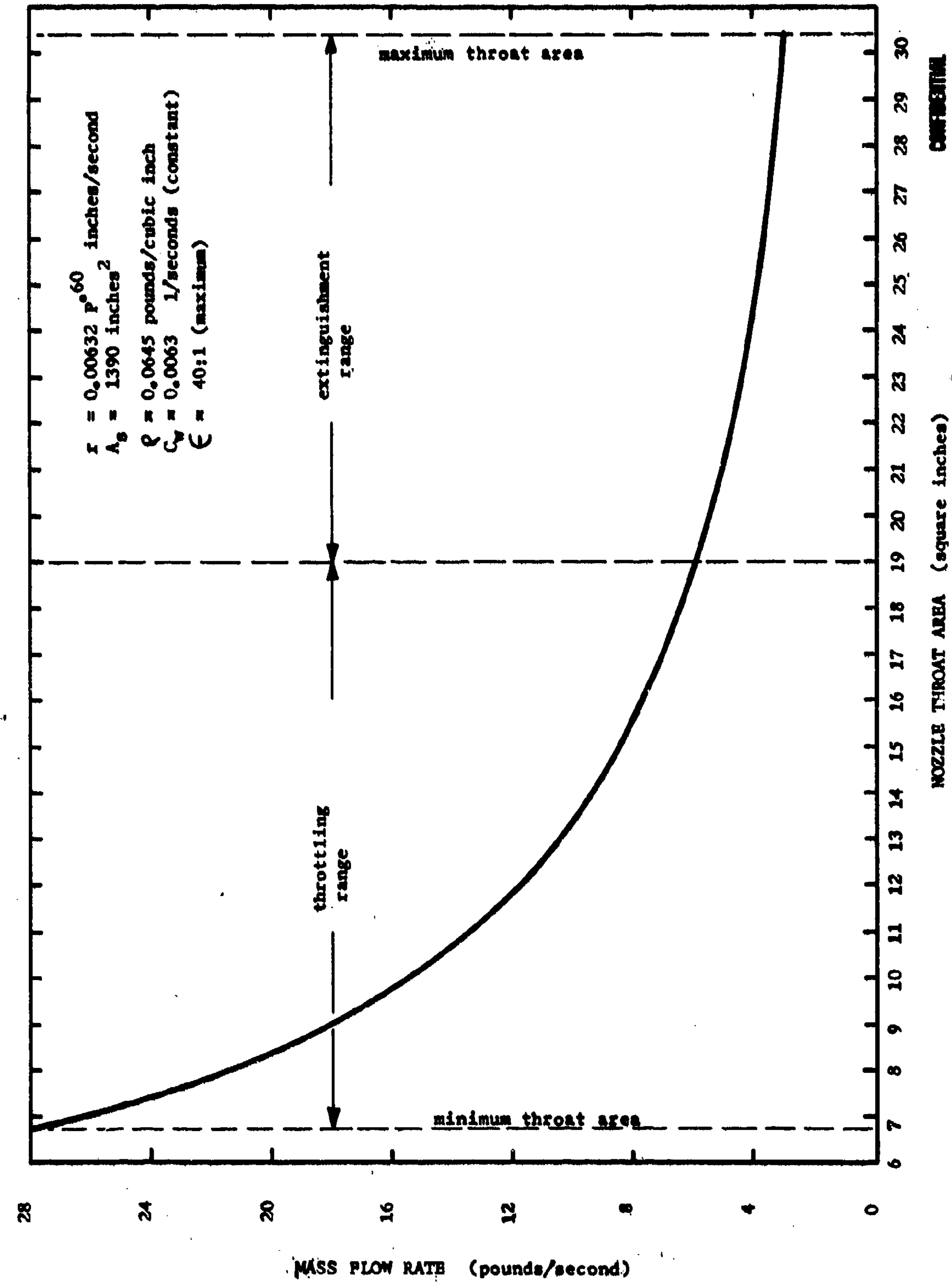

Controllable Solid Rocket - Full Scale Motor Data - $\dot{m}$ vs A_* (u)

Figure III-35

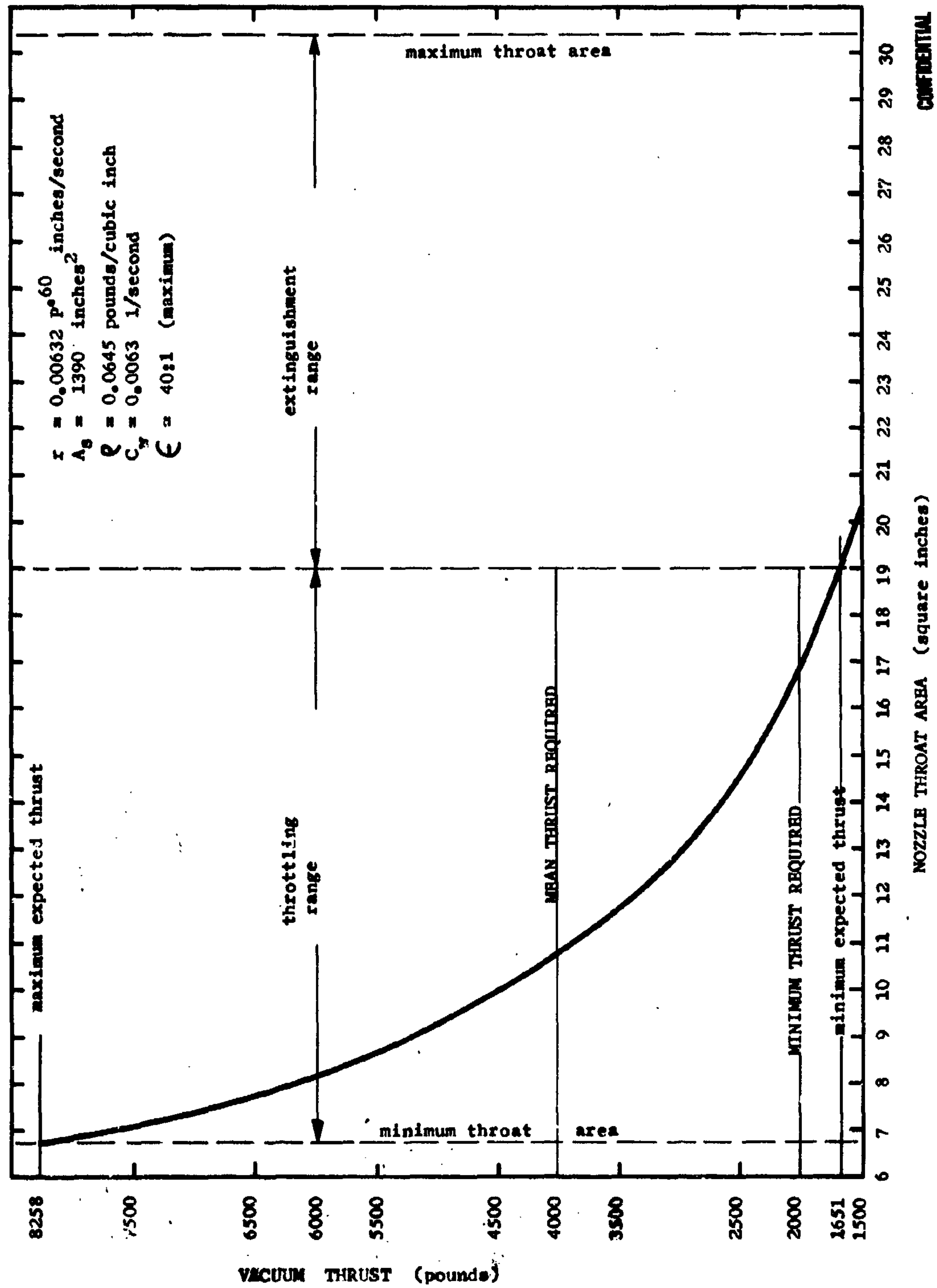

Controllable Solid Rocket - Full Scale Motor Data - F vs A_* (u)

Figure III-36

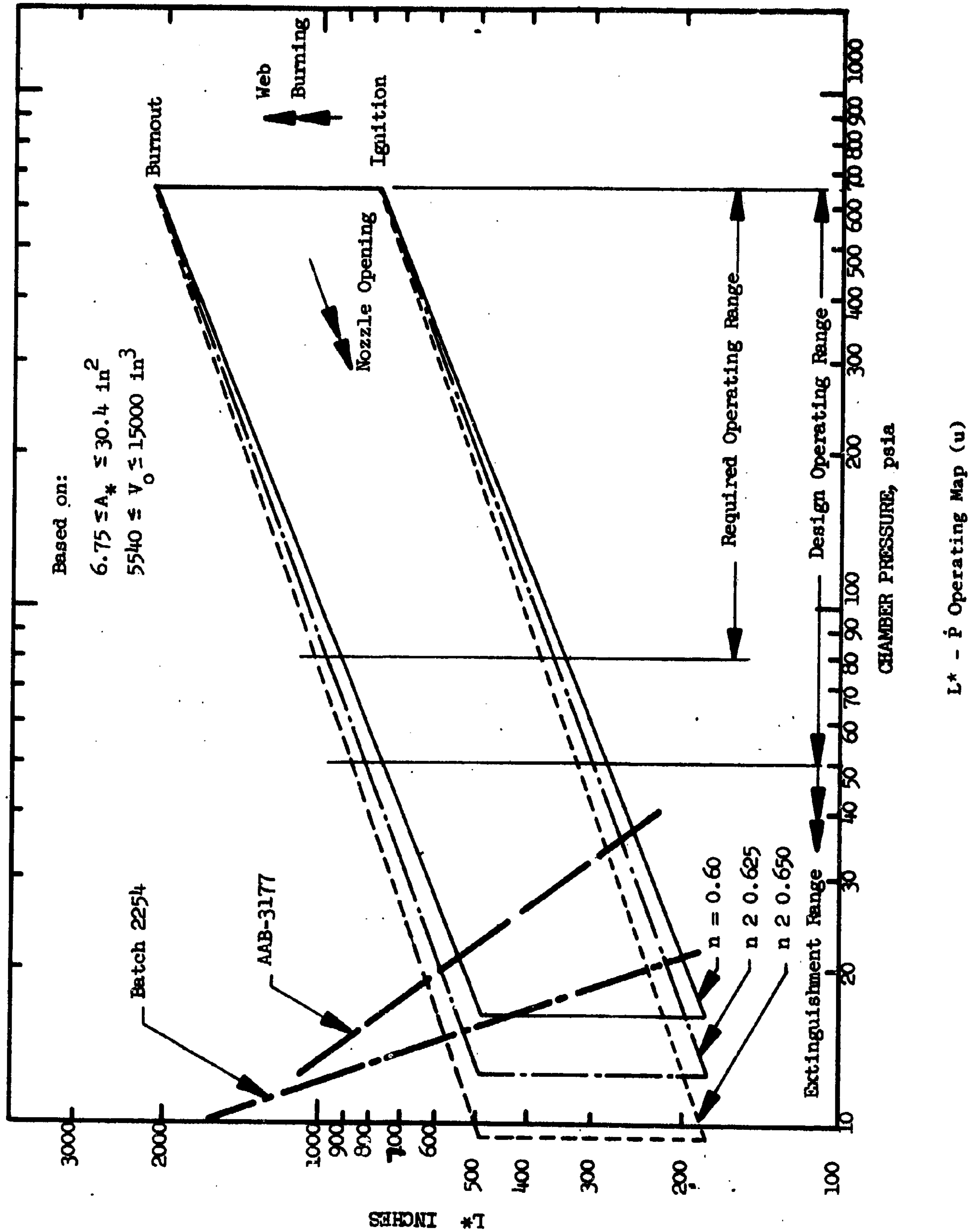

Figure III-37

(C) The P-dot extinguishment of the motor is dependent upon the motor free volume, the magnitude of the nozzle area change, and the rate of nozzle area change. To determine the P-dot extinguishment capability of the preliminary design motor, the theoretical depressurization rate was calculated at initial, middle web, and web burnout free volume for three nozzle opening rates from maximum chamber pressure to maximum nozzle area. This analysis was conducted using the computer program described in Appendix C of Reference 1. The thrust spike associated with these pressure transients was also determined. Figure III-38 shows the expected pressure transients, and Figure III-39 the thrust transients. From an extinguishment standpoint, the worst case occurs at the maximum free volume. The depressurization rate for this condition is presented in Figure III-40 with the predicted extinguishment for two current propellants superimposed to compare the expected motor response with that required for extinction. It can be seen from this figure that this motor is theoretically capable of permanently extinguishing either of the two propellants considered, at as low as 2.5 cps nozzle response. For this figure, a burning rate exponent of 0.60 was selected because this is the most conservative value in predicting the rate of pressure decay during a rapid nozzle area change. This figure agrees with those derived during the rocket motor tests of Contract AF 04(611)-9889[(1)]. For all cases of permanent extinguishment experienced in that program, the trace of actual motor depressurization rate as a function of motor pressure crossed the theoretical extinction line at or below 100 psia.

(C) The nozzle expansion ratio was limited to the case diameter. The largest expansion ratio that will fit within this envelope is 40:1. Figure III-41 depicts a plot of the nozzle optimum altitude as a function of nozzle throat area, as the area varies from a minimum of 6.75 in.^{2} to a maximum value of 30.4 in.^{2}. The only areas of interest are those from 6.75 to 19.0 in.^{2} as values beyond that range are only attained during a command to extinguish. As can be seen from this figure, the only point at which the nozzle is operating in an optimum environment is at the throat area setting of 8.5 in.^{2}. For smaller areas, the nozzle is underexpanded. For areas over 15 in.^{2}, the nozzle may run separated; however, this is near the minimum thrust range of operation, and is not considered to be critical.

(U) A detailed discussion of the design of each specific component is contained in the following sections.

a. Case

(U) Because of the generally inconclusive results of the trade-off study on motor diameter and L/D, it was decided that the case size should be selected considering tooling availability for the development phase of the program. A review of applicable tooling indicated that the fabrication and processing tooling and handling fixtures fabricated for use with the

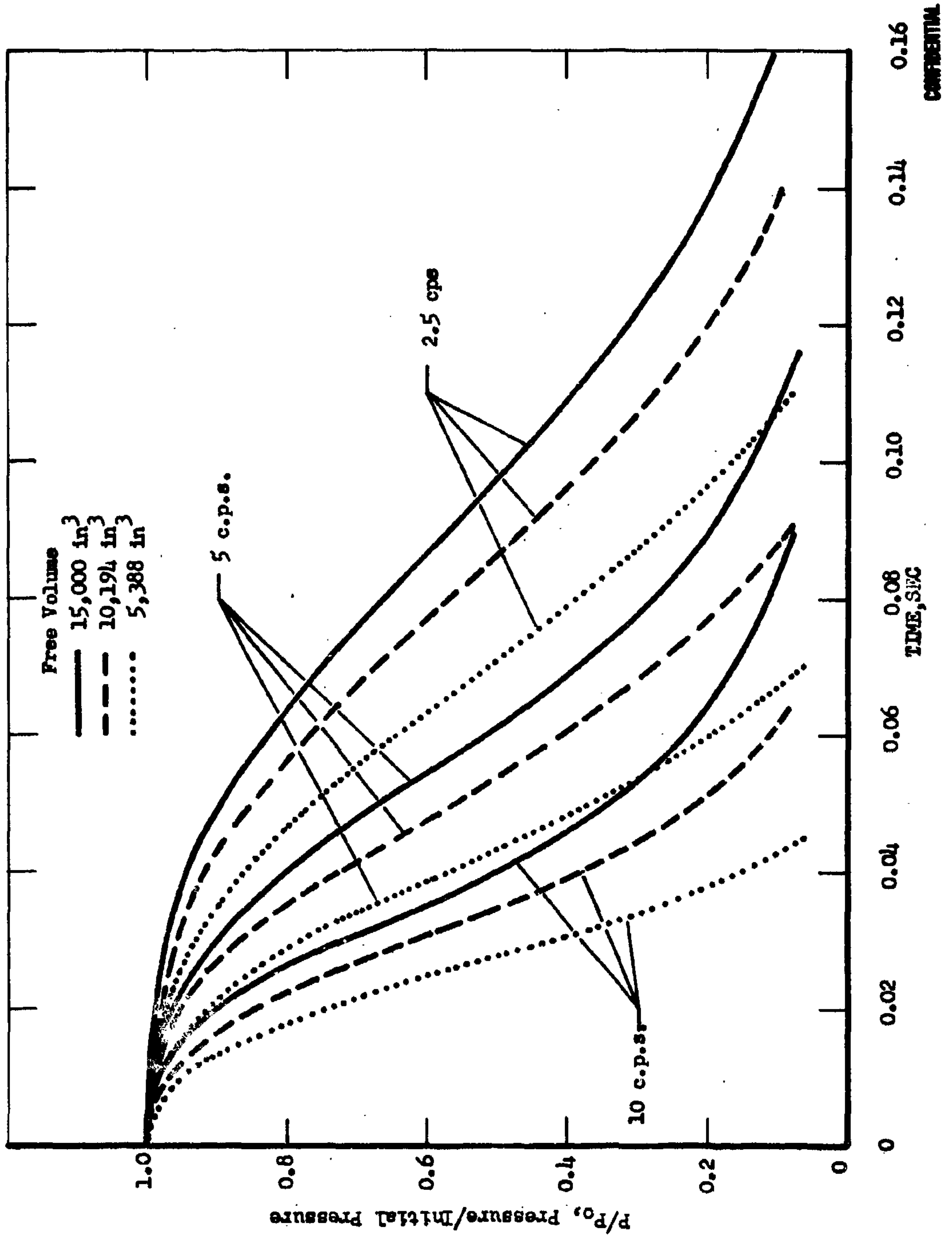

Controllable Solid Rocket - Full Scale Motor Data - P/P_o vs Time (u)

Figure III-38

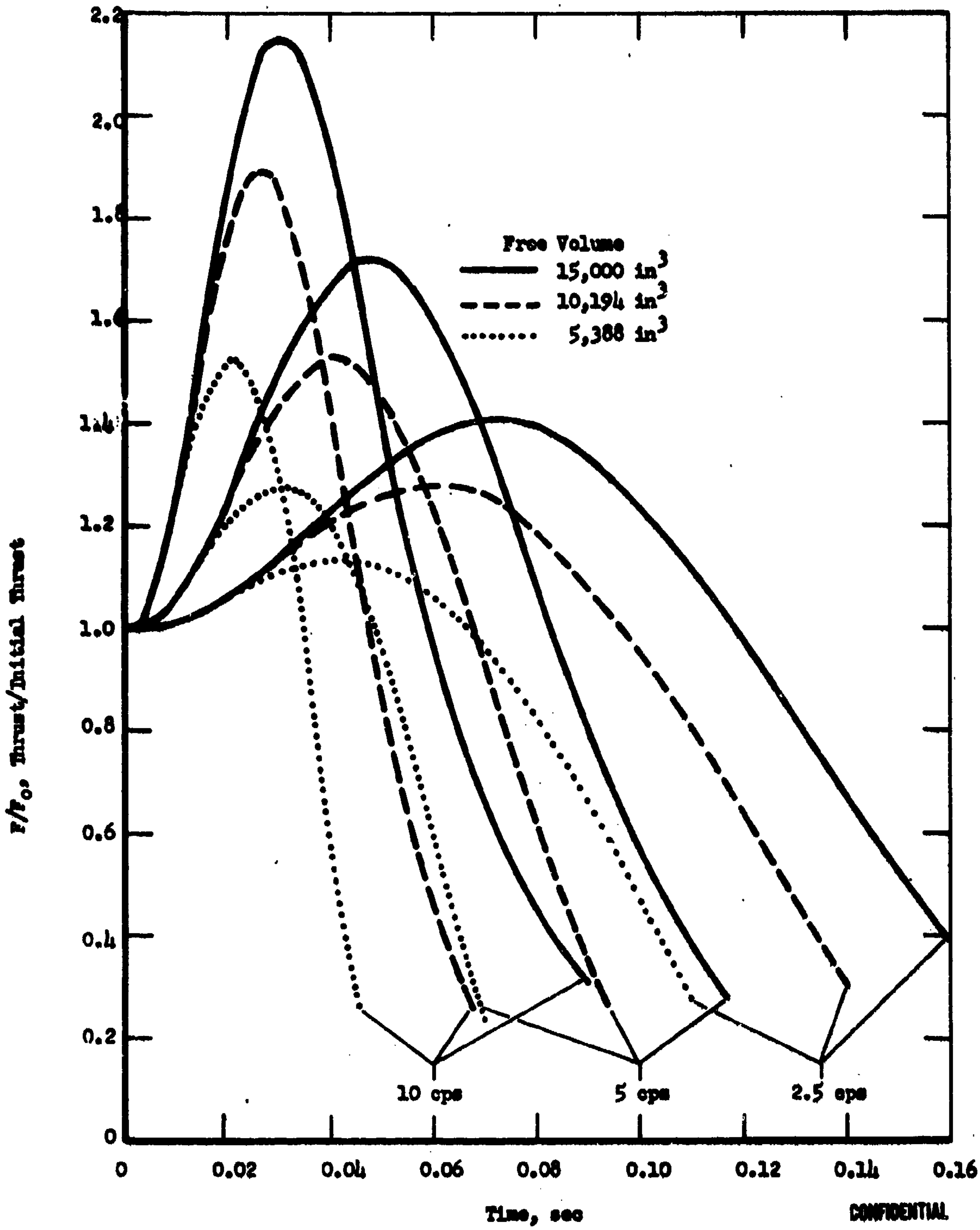

Controllable Solid Rocket - Full Scale Motor Data - F/F$_o$ vs Time (u)

Figure III-39

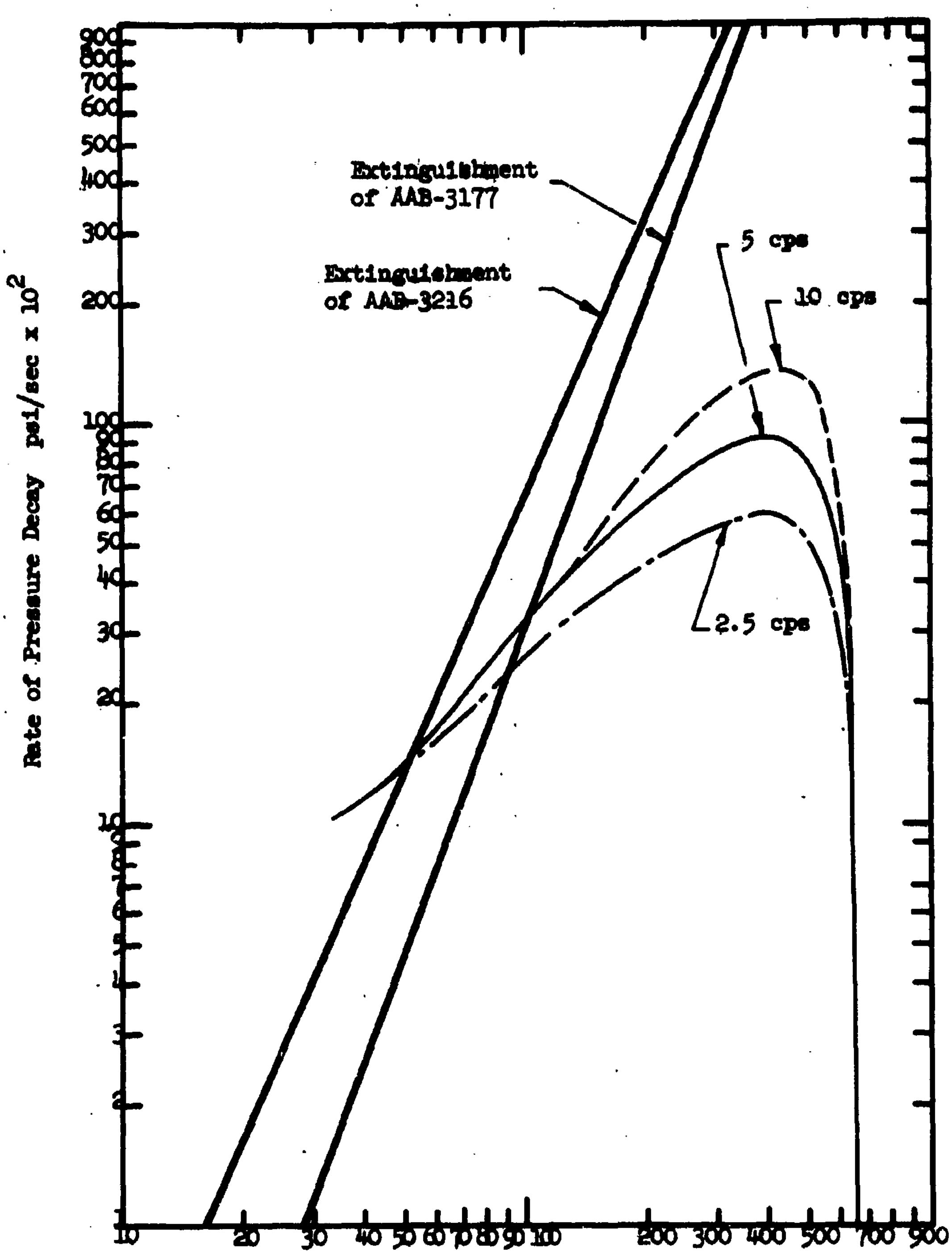

Ṗ Transient - Operating Map (u)

Figure III-40

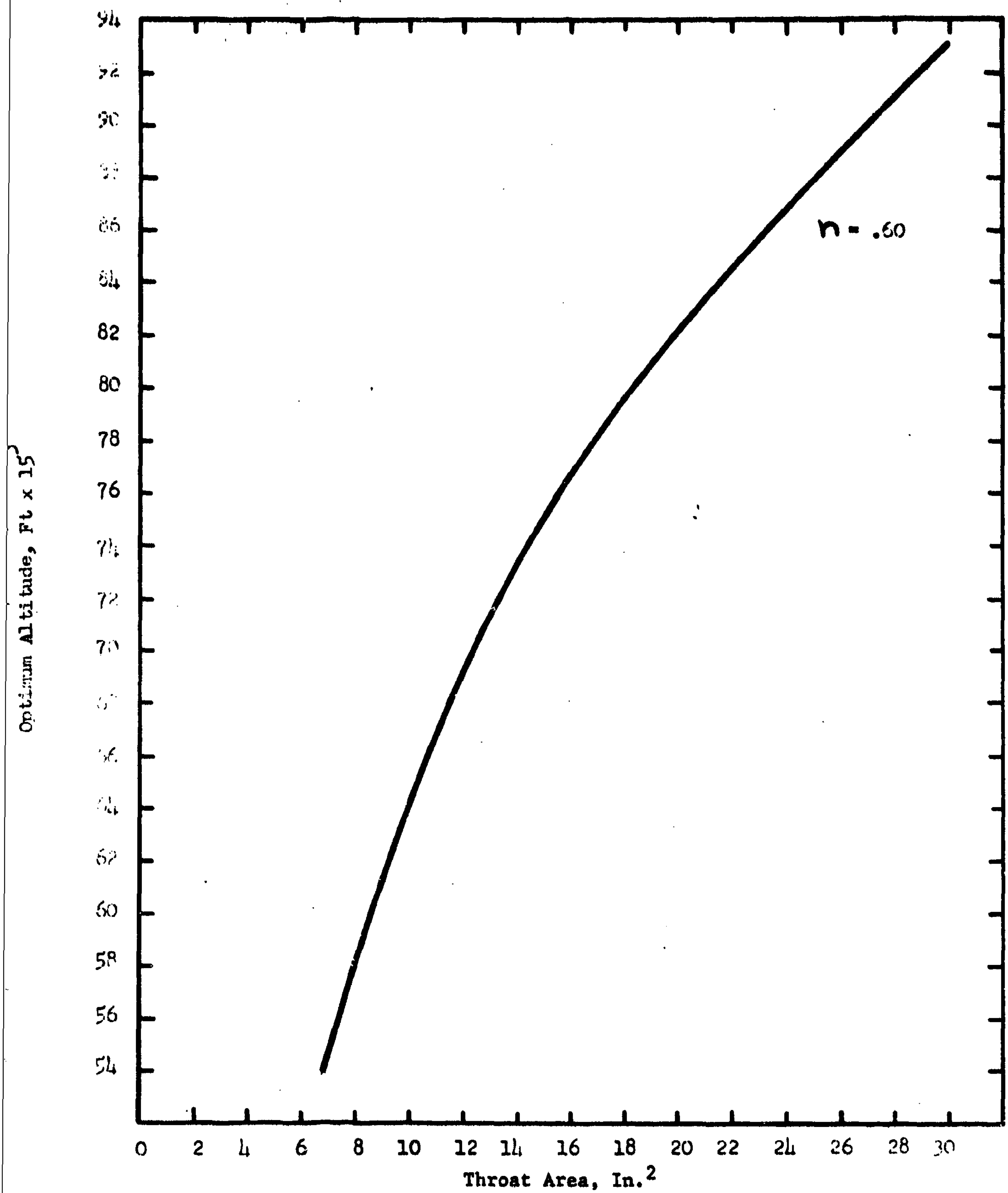

Optimum Nozzle Operating Altitude (u)

Figure III-41

30KS-8000 motor were available. The motor diameter was, therefore, established at 20 in. The case was designed considering 6Al-4V titanium at 165,000 psi ultimate tensile strength. The design is compatible with the fabrication technique of using two head forgings and a center ring forging welded together then machined to dimension.

b. Case Insulation

(U) In establishing the preliminary motor case insulation design for this motor, a Buna-N rubber based compound called V-44 (asbestos-silica loaded acrylonitrile-butadiene rubber) has been selected on the basis of its excellent mechanical, physical, and thermal properties. These properties are shown in Figure III-42. The material is completely elastomeric, yet sufficiently tough to provide thermal insulation and maximum resistance to an erosive environment. The reliability of this material and its processing techniques has been proved in the production of Polaris glass-filament motor case, Minuteman titanium motor cases, and the motor case for the 100-in.-dia motor program.

(U) In establishing the preliminary motor-case insulation design for this motor, the V-44 insulation erosion rates were based on results from statically fired second-stage Minuteman motors. A summary of data from 11 motor firings is shown in Figure III-43. The exposure times of the insulation in various locations in the preliminary design motor were determined from a study of the grain configuration as the propellant is consumed. These factors were then used to establish the thicknesses in case insulation. In addition, a theoretical analysis was conducted to determine the insulation thickness required to prevent the inside surface of the case from exceeding 400°F during motor operation.

c. Igniter

(U) The igniter for this motor is in itself a small pulse motor. This configuration was found to be the lightest weight system. The design details were based on the technology reported in LPC[21,22] and associated company-funded programs at Aerojet.

(C) Five of the six pulses are sized for ignition at maximum motor free volume. The first pulse is sized for the initial free volume. This pulse operates for 0.29 sec at 1000 psi and contains approximately 2 lb of high-burning-rate propellant. The remaining pulses operate for 0.20 sec at 2000 psi and contain approximately 2.5 lb of propellant. The entire igniter has a mass-fraction of approximately 0.62.

		V-44
Specific Gravity	gm/cc	1.287
Hardness	Shore A	83
Ultimate Tensile Strength	psi	1,600
Ultimate Elongation	%	200
Nitrogen Permeation	(1)	4.0×10^{-4}
Water Absorption(2)	%	0.13
Material Loss Rate(3)	in./sec	0.0018
Weight Loss	lb/sec	0.108
Backside Temperature Rise(4)	seconds	10
Thermal Conductivity at 250°F	Btu/ft^2/hr/°F/in.	1.59
Specific Heat at 50°F	Btu/lb°F	0.41
Heat of Ablation at 950 Btu/ft^2-sec	Btu/lb	8350

(1) N_2 permeation is determined at a pressure of 350 psi, and the units are ft^3/ft^2/mil-thickness/psi differential/24 hours.

(2) Water Absorption - increase in weight of test specimen after 30 min. absorption at 900 psi.

(3) Material loss rate and weight loss specimens are exposed for 30 sec to oxyacetylene-torch tests.

(4) Backside Temperature rise is for a specimen 0.060 in. thick and for a 300°F increase.

Properties of Gen-Gard V-44

Figure III-42

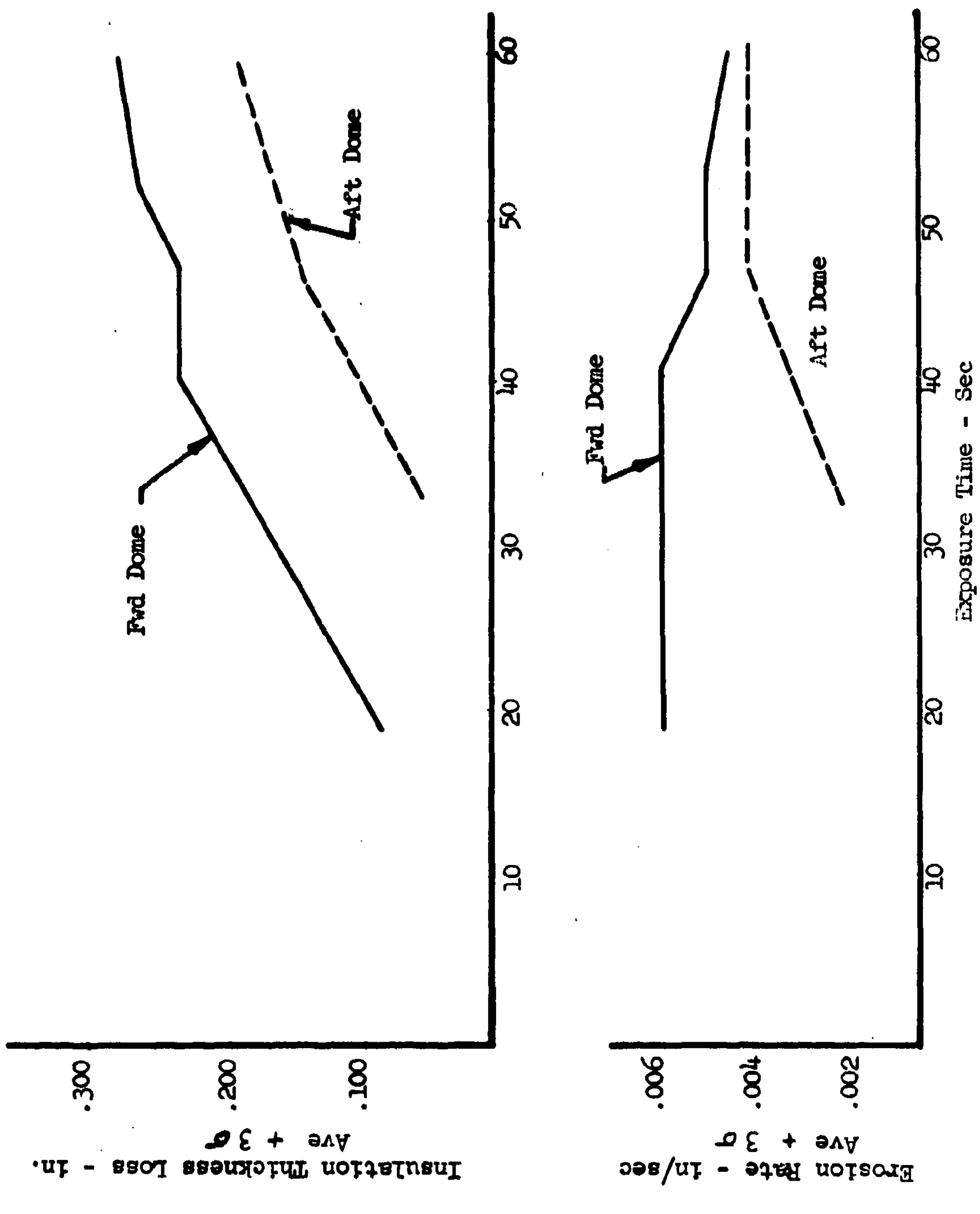

Summary of Erosion Data for Gen-Gard V-44

Figure III-43

d. Nozzle

(U) The philoslphy for the nozzle design was one of operating the flame barrier at high temperature to limit the total heat input, insulating immediately behind the flame barrier to restrict the heat flow into the structural component during the firing, and provide sufficient heat sink behind the insulator to absorb the heat which soaks through after the firing without reaching excessively high temperature.

(C) For a representative nozzle design, six separate thermal analyses were conducted to screen candidate configurations. A one-dimensional analysis was used with these screening checks. Three outer shroud material stack-up combinations were used; a configuration using edge-oriented pyrolytic graphite washers (Figure III-44), one using a tungsten insert (Figure III-45), and one with a pyrolytic graphite coating (Figure III-46). The duty cycle used consisted of full duration plus cooling. Both full duration and high pressure (660 psi for 27.5 sec) and low pressure (115 psi for 75 sec) were checked for all nozzles to determine which was the most severe. A summary of the runs and a comparison of the pertinent results are tabulated below:

Case	Configuration	Pressure	Maximum Surface Temp, °F*	Total Heat Input, Btu/ft^2
1	Pyrolytic graphite washers	Low	4460	21,500
2	Pyrolytic graphite washers	High	5030	20,900
3	Tungsten ATJ backup	Low	4720	17,400
4	Tungsten ATJ backup	High	5080	16,200
5	C-Direction pyrolytic graphite	Low	4940	6,000
6	C-Direction pyrolytic graphite	High	5270	2,960

*At throat

(U) As noted in this table, the order of preference from a thermal standpoint is (a) C-direction pyrolytic graphite with ATJ graphite backup, (b) tungsten with an ATJ graphite backup, and (c) pyrolytic graphite washers. This classification is based only on the amount of heat that is absorbed during a firing and that is subsequently released or expelled from the nozzle without causing undue deterioration. The best method for reducing

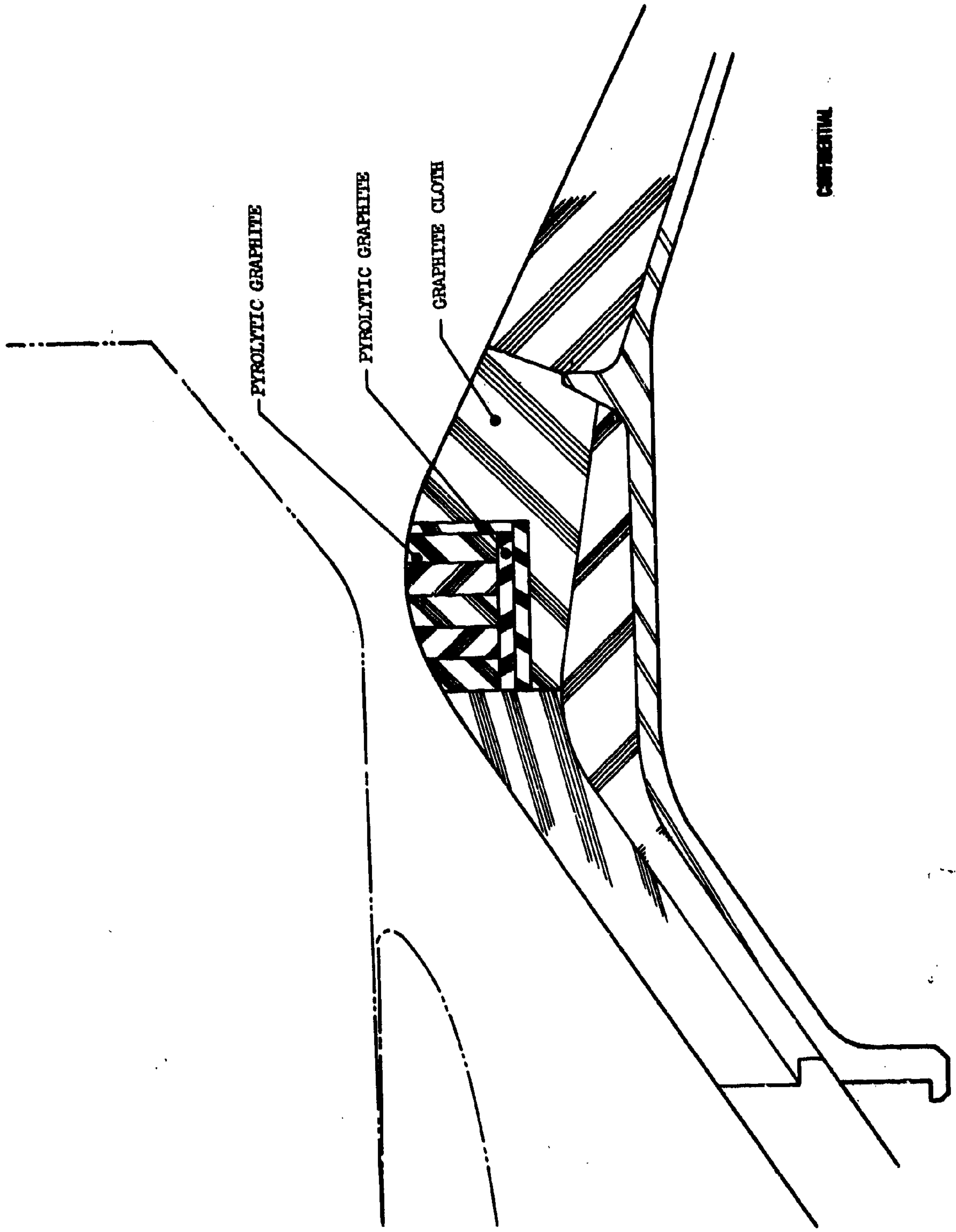

CONFIDENTIAL

Outer Shroud with Pyrolytic Graphite Washered Throat Insert (u)

Figure III-44

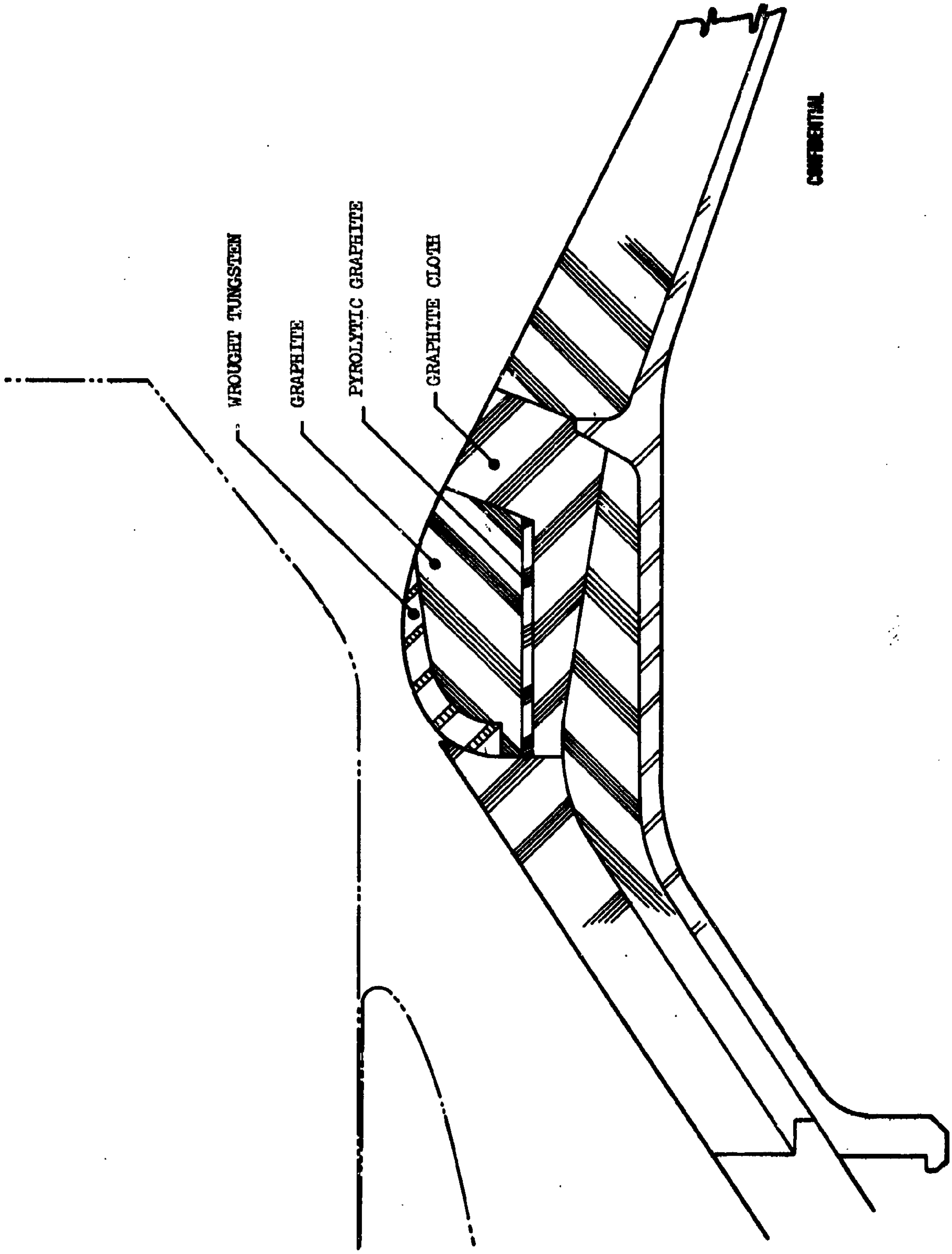

Outer Shroud with Tungsten Throat Insert (u)

Figure III-45

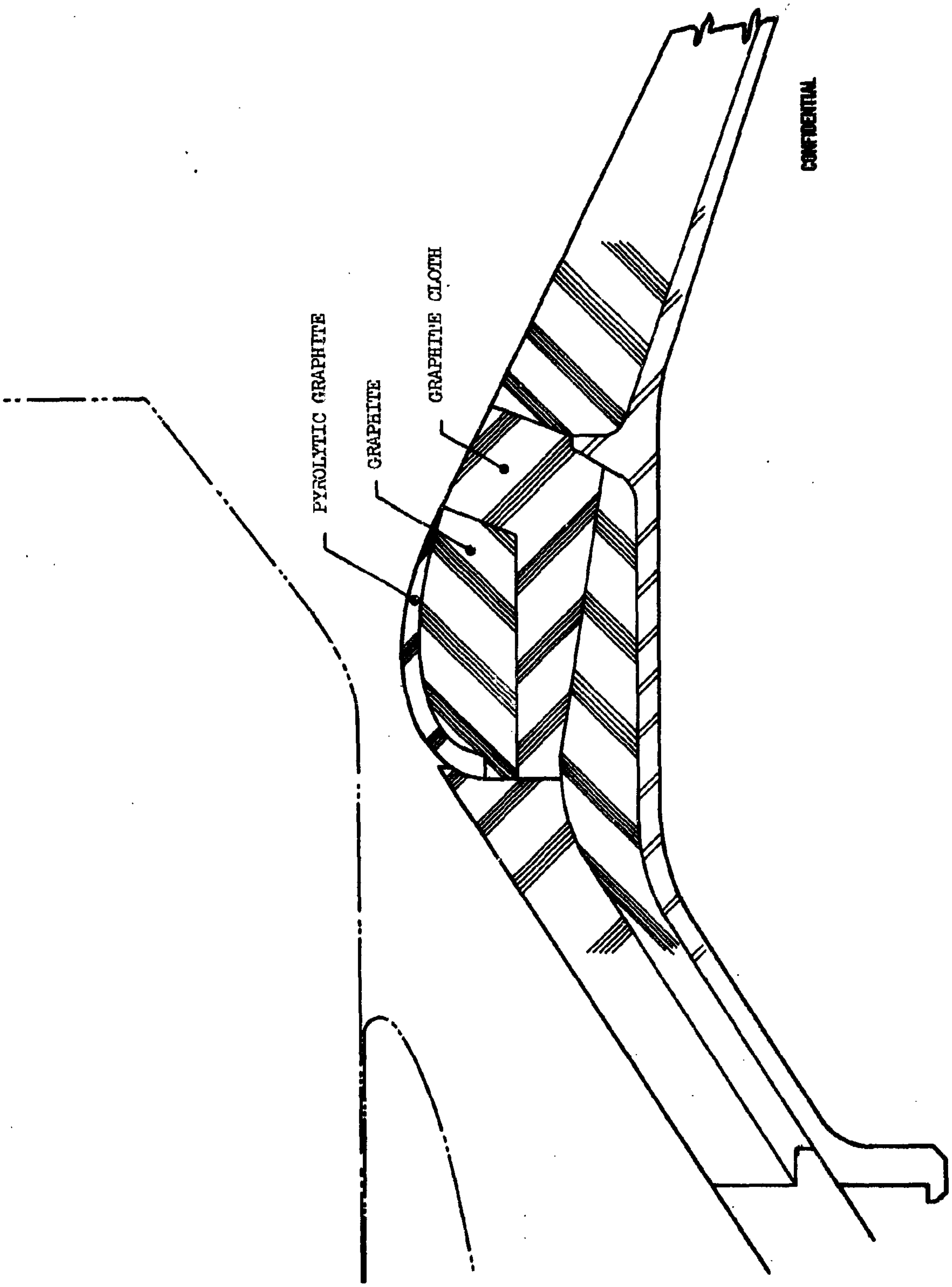

Outer Shroud with Layered Pyrolytic Graphite Throat Insert (u)

Figure III-46

the total heat input is to operate all exposed surfaces at a high temperature. This reduces the temperature difference between the exhaust gas involved which decreases the instantaneous heat flow. Typical input has a function of firing time for each configuration investigated as presented in Figure III-47.

(C) A C-direction pyrolytic graphite ATJ is one design which produces the desired features of high surface-temperature and low heat input. From the above table, these values were found to be 4940 to 5270°F surface temperature and 6000 to 2960 Btu/ft^2, respectively; however, the problem of thermal stress and delamination of pyrolytic graphite makes this design approach beyond the present state-of-the-art. Recent attempts to utilize this approach by Philco Aeroneutronics Division[17,18] resulted in radial cracking and delamination of the shell at the throat. Some encouraging results, however, have been reported. The successful testing described by Allegany Ballistics Laboratory[27] with the use of bulk pyrolytic graphite "pyrode" shows that, with some further materials development, this approach might be entirely feasible for restartable nozzles.

(U) The next two designs indicate temperature and heat input of the same relative orders of magnitude and the selection between them must then be based on other considerations. As a result, the pyrolytic graphite washer configuration was selected because the influence of temperature cycling on the grain growth of mechanical properties of tungsten has been shown by Philco Aeroneutronics Division[17,18] and others to adversely affect the cycling capability of the design.

(U) To provide an estimate of nozzle degradation, the thermal calculation was continued with the edge-oriented pyrolytic graphite washers. The shroud was allowed to cool by radiation from the exit cone. The temperature distribution after 480 sec was given in Figure III-48. As noted, the maximum temperatures occur in the pyrolytic washers and are approximately 2000°F. Structural temperatures are a nominal 800°F indicating that cooldown after maximum heat input does not compromise the design.

(C) The design of the movable pintle introduced the additional design constraints. Because of its basic shape, there is a physical limit to the amount of heat sink that can be used behind the insulation. In addition, thermal expansion of the flame liner is unrestricted in a radial direction. For this application, it is desirable to use materials that have a minimum expansion in this direction to avoid problems with binding the pintle housing. Edge-oriented pyrolytic graphite washers were selected for this area with a tungsten washer at the throat. For comparison of heat input, a pintle consisting of a thin tungsten shell backed with a magnesium hydroxide insulator was evaluated. A comparison of the two was shown in the following tabulation:

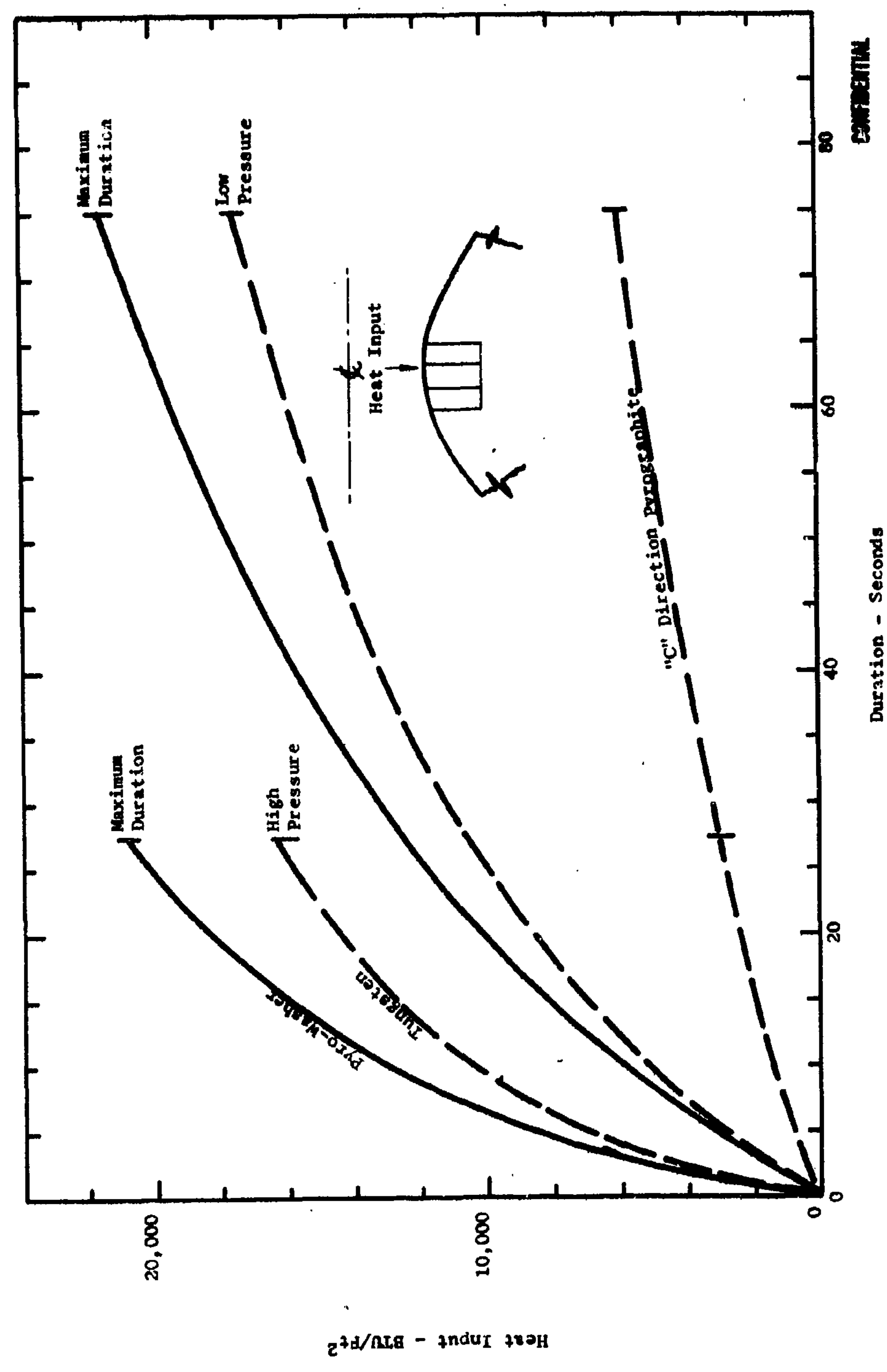

Total Heat Input vs Test Duration for Three Outer Throat Inserts (u)

Figure III-47

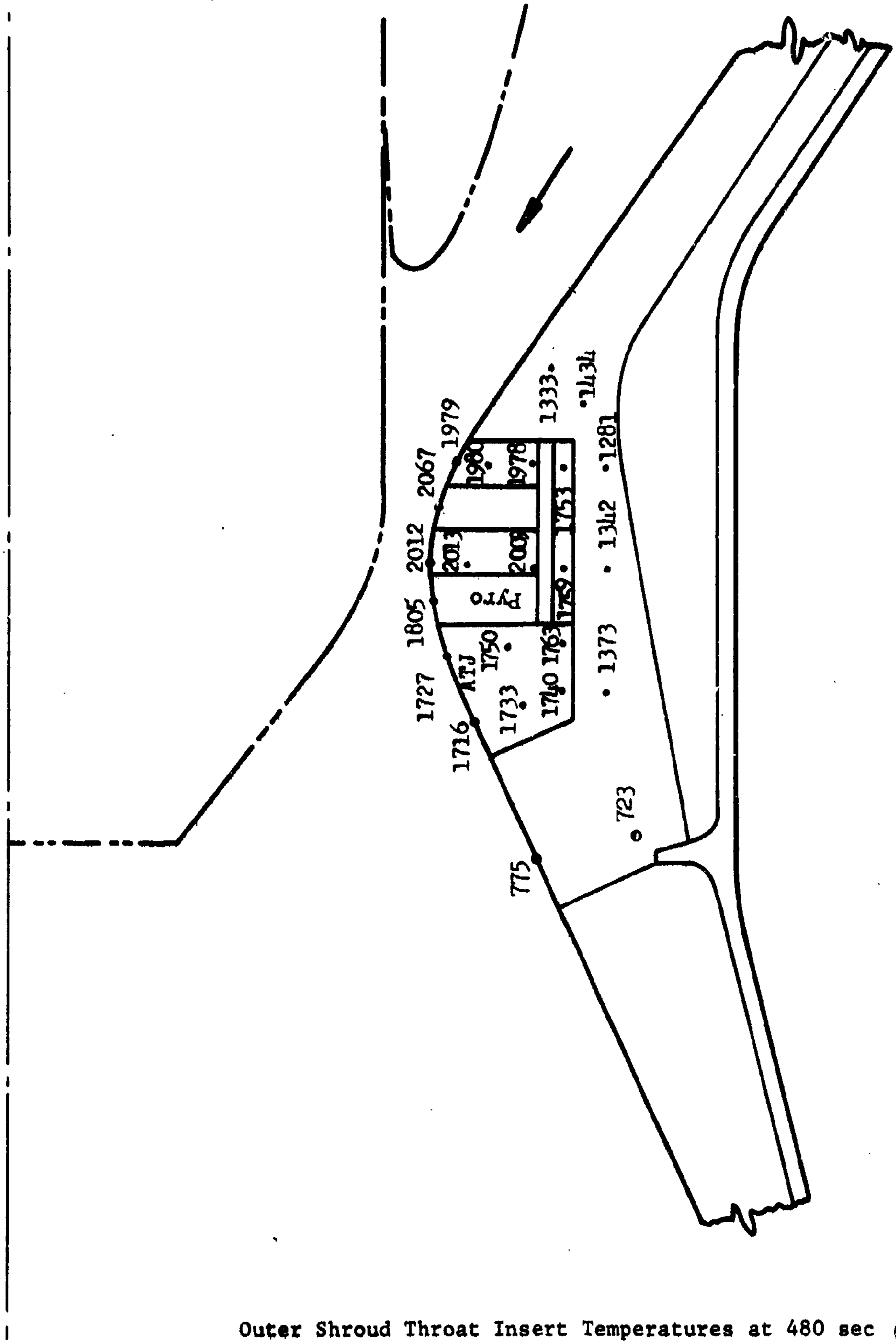

Outer Shroud Throat Insert Temperatures at 480 sec (u)

Figure III-48

III, A, Preliminary Design (cont.)

Case	Configuration	Pressure	T max, °F	Total Heat Input, Btu/ft^2
1	Pyrolytic washer	Low	4790	12,200
2	Pyrolytic washer	High	5060	17,100
3	Tungsten--$Mg(OH)_2$	High	5400	4,400

(C) A curve of heat input to the pintle as a function of firing time for each case investigated is presented in Figure III-49. Again the advantage of operating at high surface-temperatures is readily apparent by noting the relative heat inputs. Complete thermal evaluations of the pyrolytic graphite design were made for both the high and low chamber pressures. Resulting temperature distributions are presented in Figures III-50 and III-51, respectively. In both cases, the temperature distribution at burnout indicates a satisfactory design. Surface temperatures of the pyrolytic graphite washers are not excessive and structural components indicate negligible temperature rise.

(C) By continuing the thermal analysis into the cooldown cycle, the results shown in Figures III-52 and III-53 were generated. Cooling rates were based on thermal radiation from the exit plane. Again the structural temperatures are within tolerable limits, the maximum values (1100°F) occur on the interior titanium shell. The heat soak into the seal area of the integral actuator was also determined. Heat in this area will not be a problem as evidenced by the temperature in this region on the order of 210°F. These temperatures are sufficiently low that it appears that no problem will exist with a commercial actuator in this area.

(C) The nozzle for the preliminary motor design shown in Figure III-33 therefore reflects the result of this preliminary material stackup analysis. Both the outer shroud and pintle throat sections are designed using pyrolytic graphite washers backed with a pyrolytic graphite sleeve further backed with insulation. Wherever possible, asbestos phenolic was used as a backup insulation to use the superior thermal insulation properties demonstrated on the subscale tests conducted by Philco Aeroneutronics[17,18]. The critical entrance section utilizes precharred cloth to minimize the erosion, spallation and cracking. Insulation of the pintle actuator housing is V-44 rubber molded in place around the assembly.

(C) The movable pintle actuation system consists of an integral hydraulic actuator mounted within the strutted housing assembly. This configuration produces a lightweight compact actuation system which requires that a minimum amount of hydraulic fluid be pumped, thus facilitating rapid motions for depressurization extinguishment. Hydraulic pressure to operate this actuator is supplied by hydropac system designed by Convair, Inc. This hydropac unit, similar to that developed for use in helicopters, is shown on

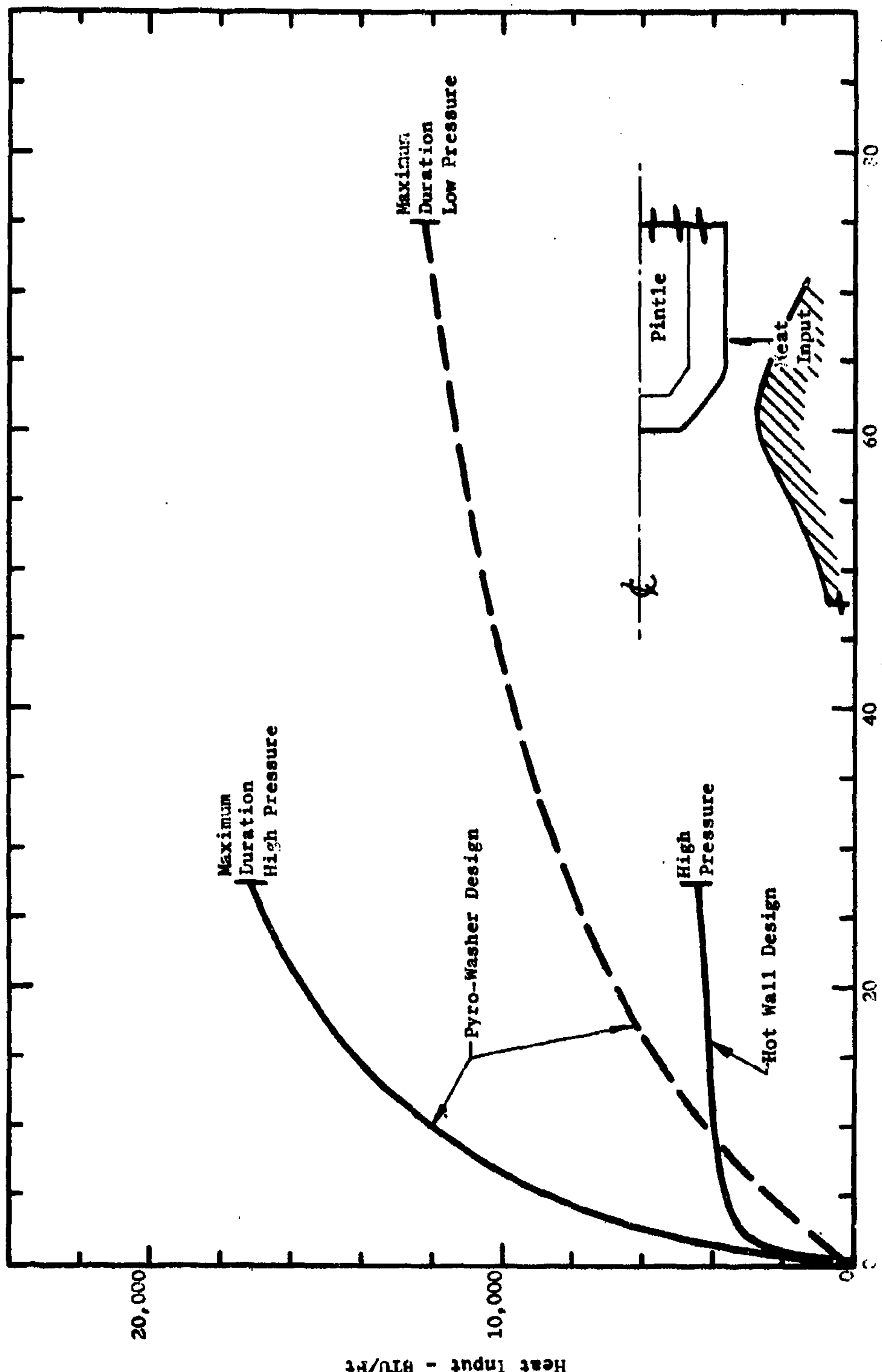

CONFIDENTIAL

Total Heat Input vs Test Duration for Various Pintle Designs (u)

Figure III-49

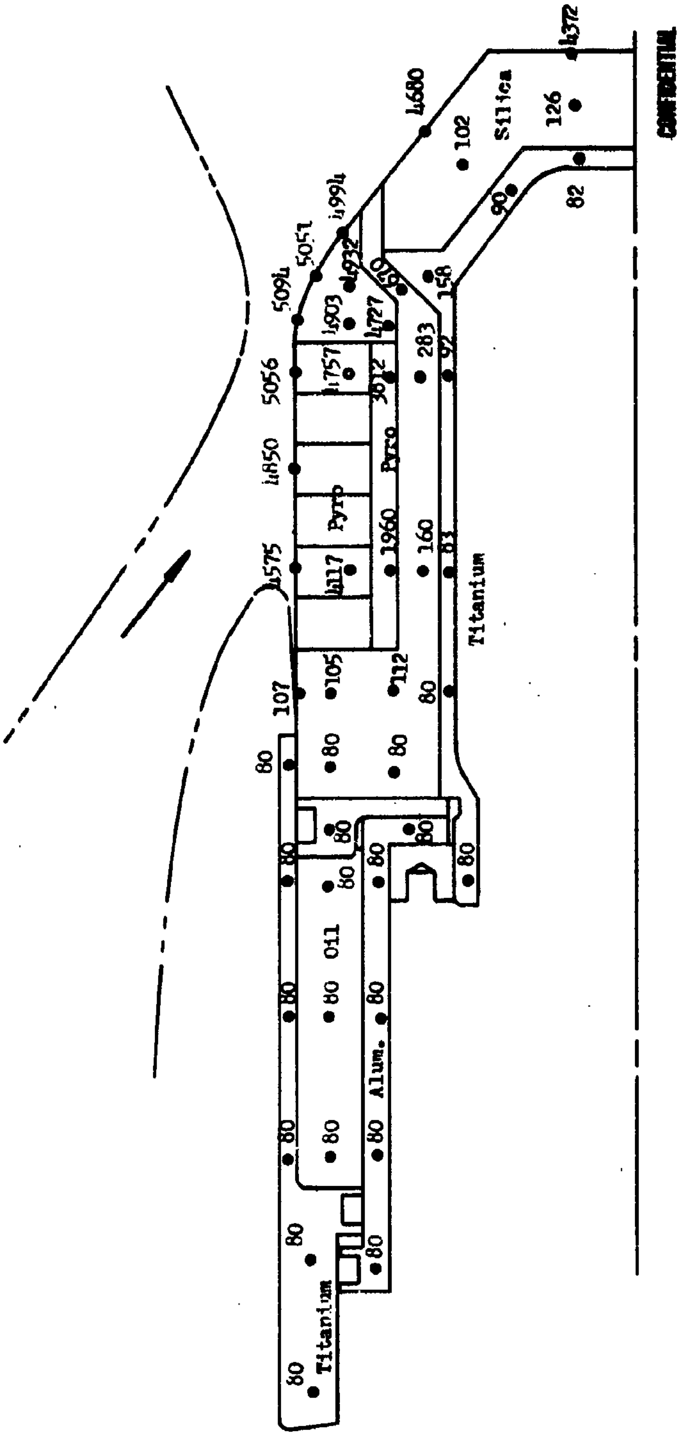

Pintle Temperature Distribution at Burnout - High Pressure (u)

Figure III-50

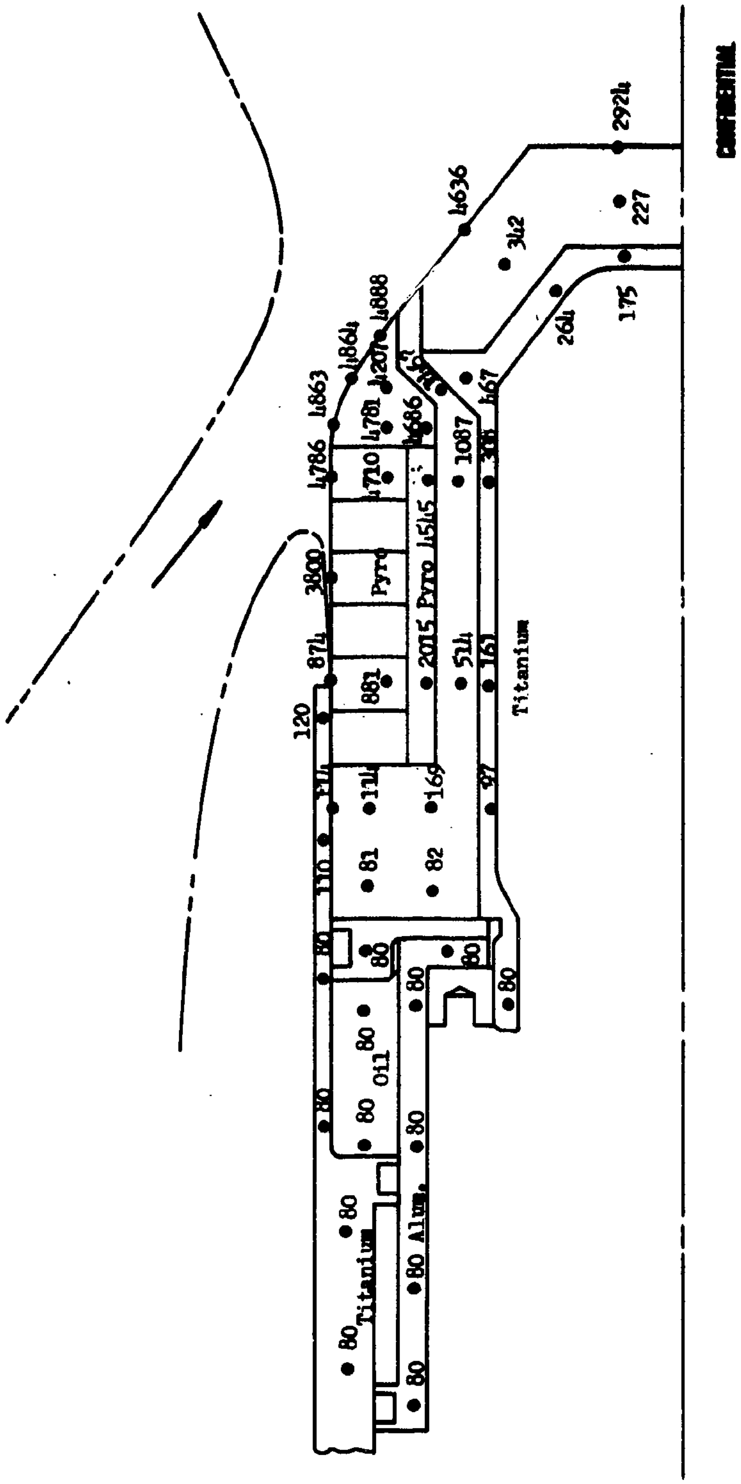

Pintle Temperature Distribution at Burnout - Low Pressure (u)

Figure III-51

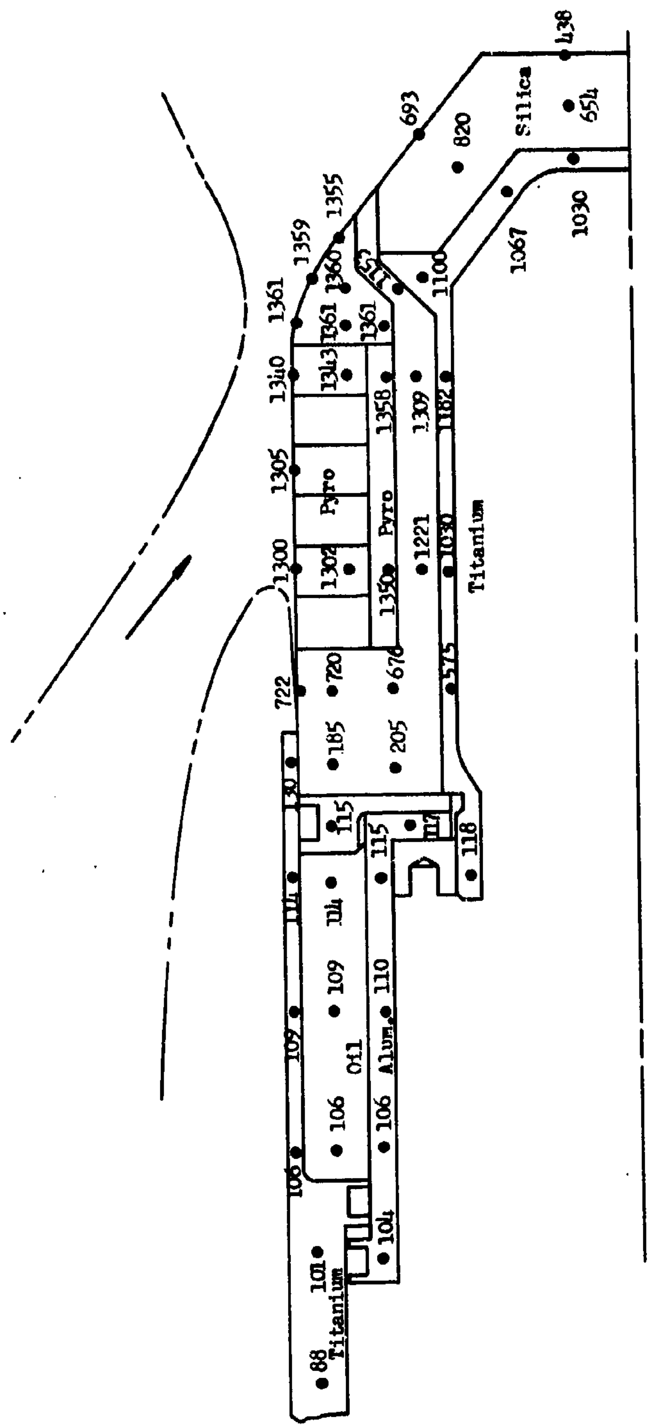

CONFIDENTIAL

Pintle Temperature Distribution at 480 sec - High (u)

Figure III-52

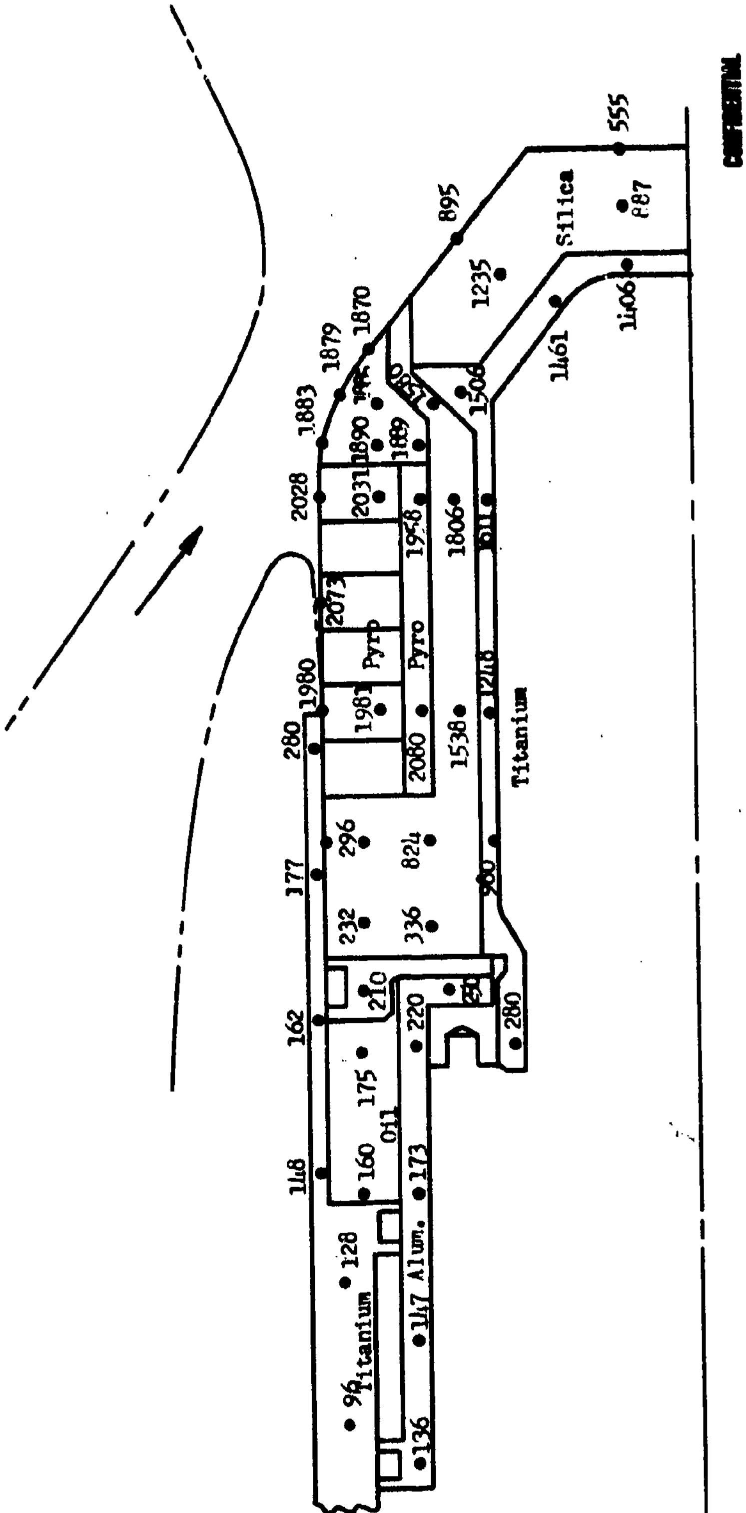

Pintle Temperature Distribution at 480 sec - Low Pressure (u)

Figure III-53

Figure III-54. The schematic of the hydraulic system is shown on Figure III-33. As shown on the schematic, for normal thrust modulation operation, the hydraulic fluid is pumped by an electric-motor-driven pump through the servovalve to reposition the pintle. For rapid motions, as required by rapid depressurization extinguishment, the servovalve system is bypassed by opening two solenoid valves, and the hydraulic fluid forced through the actuator directly from a gas pressurized accumulator. After extinguishment this accumulator is then recharged to full pressure.

(U) The summary of the detailed weight breakdown and the resulting motor mass fraction is shown on Figure III-33. Charged against the weight of this motor is everything required to make it a self-contained unit except the electrical power supply. This includes the motor case, nozzle, igniter, hydraulic actuator, and hydraulic power supply system.

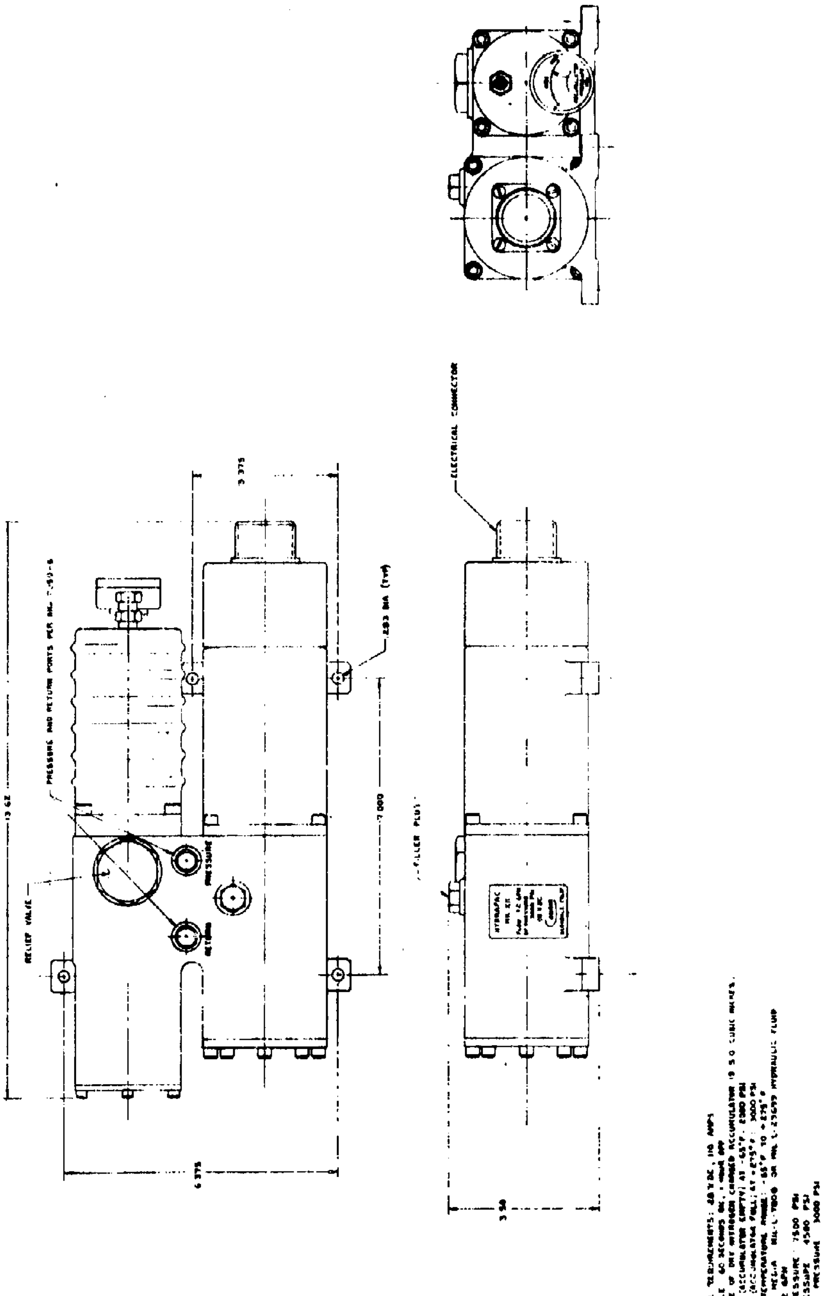

Hydrapac MK-XII, Conair, Inc.

Figure III-54

III, Technical Discussion (cont.)

B. PROPELLANT TAILORING

(U) The purpose of the propellant development phase was to tailor propellant AAB-3177, which was developed for extinguishability by rapid depressurization ($\dot{p}$) and L* on previous programs[1,2], to meet the more stringent requirements for this application. The main objectives were improved extinguishability by p and L* at all back pressures, higher specific impulse and higher burning rate pressure exponent; satisfactory mechanical properties, bondability and processing characteristics were also essential.

1. Propellant Modification and Testing

(U) Formulation studies were initiated to establish the ballistic solids and binder modifications necessary for tailoring of propellant AAB-3177 to meet the program requirements listed in Figure III-55. The objective of this effort was the provision of an optimum balance of ballistic, extinguishment, mechanical, bonding and processing properties. The approaches included (1) the necessary adjustment of ballistic solids to attain the required specific impulse, (2) evaluation of selected additives and oxidizers particle-size-distributions to increase the burning rate pressure exponent, and (3) tailoring the binder to provide satisfactory mechanical, bonding and processing properties.

a. Adjustment of Solids for I_s

(C) The polybutadiene propellant AAB-3177 which exhibited satisfactory extinguishment properties, n, r, and processing characteristics on the recent extinguishment programs[1,2] was modified to contain a higher ratio of aluminum to NH_4ClO_4 and slightly higher solids in order to produce the required I_s of 240 lbf-sec/lbm. Several modifications of AAB-3177 which had been evaluated for burning rate and n in laboratory-scale batches and which were expected to produce the required I_s based on thermodynamic calculations are presented in Figure III-56. The formulation of AAB-3177 is included for comparison. The first five batches (2061, 2082, 2060, 2081, and 2254) evaluated 5 and 10% $KClO_4$, 1 and 3% NaCl and total solids of 86, 88 and 89%. All formulations were expected to produce the required I_s except Batch 2081 with an I_s of 239. Increasing the NH_4ClO_4 concentration by 1% at the expense of binder in this formulation was expected to increase the I_s to 240 as indicated in Batch 2254. Alternatively, the NH_4ClO_4 level can be increased 1% at the expense of NaCl and also produce an I_s of 240 as in Batch 2559. Although Batches 2061, 2082 and 2060 met the I_s requirement, they were unsatisfactory due to low n. The last two batches (2254 and 2559) which met the ballistic requirements of this program were evaluated for extinguishability, mechanical properties and bondability.

Property	Requirements		Current Status: Batch 2254		Current Status: AAB-3216	
I_s, lbf-sec/lbm, 15° half-angle, 1000/14.7 psia	240		240		240	
Density, lbm/cu in.	0.064		0.066		0.0655	
Extinguishment						
Critical depressurization rate						
P_c, psia	50	100	50	100	50	100
$\dot{P}_{cr}$, psia/sec	1400	2700	700	3300	1300	6400
Extinction by L*						
L*, in.	180 - 500		275	890	242	
P_e, psia	40 - 20		30	12	4-6	
n (for throttling ability)	0.6		0.6(1)		0.63(2)	
r, in./sec at 100 psia	0.08 - 0.12		0.086(1)		0.130	
Mechanical Properties						
Propellant-to-Liner Bond	To be defined per final motor design		Adequate for subscale motors			

(1) Cured Strand Data
(2) 3KS-500 Motor Data

Summary of Propellant Requirements and Achievements (u)

Figure III-55

Batch No:	2061	2082	2060	2081	2254*	2559	AAB-3177
Ingredients							
NH_4ClO_4							
70/30, +48/MA**	65.0	70.0	50.0	60.0	61.0	-	64.0
35/15/50, +48/SS/MA**	-	-	-	-	-	61.0	-
$KClO_4$	5.0	5.0	10.0	10.0	10.0	10.0	10.0
Al (27 μ)	15.0	15.0	15.0	15.0	15.0	15.0	15.0
NaCl	1.0	1.0	1.0	3.0	3.0	2.0	3.0
PBD-Imine	14.0	12.0	4.0	12.0	11.0	-	13.0
PBD-Epoxy	-	-	-	-	-	12.0	-
Expected I_s, lbf-sec/lbm	243	244	241	239	240	240	235
Solid Strand Burning Characteristics							
r at 100 psia, in./sec	0.082	0.086	0.082	0.076	0.086	0.098	0.082
n	0.51	0.056	0.56	0.63	0.60	0.70	0.62
Castability	Good	Good	Good	Good	Fair	Good	Good

* 10-lb batch, all others are 1-lb batches
** +48 = Over 48 mesh
SS = Slow speed Micro-Pulverizer ground (~ 130 microns)
MA = Mikro-Atomizer ground (3-9 microns)

Modification of AAB-3177 for Specific Impulse Increase (u)

Figure III-56

b. Formulation Modifications to Increase n

(C) Two new methods of increasing the burning rate pressure exponent (n) above 0.60 have been developed. The data in Figure III-57 indicate that n can be increased up to 0.78 by using a different oxidizer particle size distribution, as indicated by comparing Batches 2254 and 2503. Although the concentration of NaCl was decreased in this case from 3 to 2% which would tend to decrease n, the use of the HN oxidizer blend in Batch 2503 more than compensated for the effect and produced a substantial increase in n. In later propellant studies the HN oxidizer blend of 35/15/50, plus 48/SS/MA* was used in place of the ME blend of 70/30, plus 48/MA to obtain the benefit of higher n values.

(C) It was also shown in Batches 2422, 2443 to 2445, 2471 and 2472 that reasonably low concentrations 2% of $CoSiO_3$ can be used to increase n from 0.59 to 0.68, when replacing either NaCl or binder. It was significant to find these two methods of increasing n above a value of 0.60, since this was expected to be a difficult problem.

c. Epoxy vs Imine Cure

(C) The epoxy curing system for the carboxy-terminated PBD binder has several inherent advantages over the commonly used imine curing system. The epoxy system is much less sensitive to moisture and various additives which will be evaluated for their effect on extinguishability, has slightly better castability and might be cured at a lower temperature (110 versus 135°F) thereby producing lower strain and stress requirements for a given motor design. The main disadvantage to using an epoxy system in this application is the reduction of approximately 10% in burning rate pressure exponent caused by substituting an epoxy for an imine cure. This effect on n is shown by comparing Batches 2060 versus 2169 and 2503 versus 2559 in Figure III-58 and confirms the findings of the $\dot{p}$ program[1]. Fortunately, the increase in n produced by using the HN oxidizer blend is sufficient to permit the use of the epoxy system with assurance of obtaining a satisfactory value of n, as in Batch 2559.

* +48 = Over 48 mesh
SS = Slow Speed Mikro-Pulverizer ground (~130 microns)
MA = Mikro-Atomizer ground (3 - 9) microns)

Batch No:	2254	2503	2422	2443	2444	2445	2471	2472
Ingredients								
NH_4ClO_4								
70/30, +48/MA*	61.0		-	-	-	-	-	-
35/15/50, +48/SS/MA*	-	61.0	-	-	-	-	-	-
45/15/40. +48/SS/MA*	-	-	61.0	61.0	61.0	61.0	70.0	70.0
Al (27 μ)	15.0	15.0	15.0	15.0	15.0	15.0	14.0	14.0
$KClO_4$	10.0	10.0	10.0	10.0	10.0	10.0	-	-
NaCl	3.0	2.0	2.0	1.5	1.0	-	-	-
$CoSiO_3$	-	-	-	0.5	1.0	2.0	1.0	2.0
PBD-Imine	11.0	12.0	12.0	12.0	12.0	12.0	15.0	14.0
r_{100}, in./sec	0.036	0.085	0.092	0.086	0.092	0.098	0.104	0.110
n	0.60	0.78	0.59	0.63	0.65	0.68	0.62	0.68
P_{DL}, psia	1.1	1.0	2.3	2.1	2.4	3.4	0.9	0.7

* +48 = Over 48 mesh
SS = Slow Speed Mikro-Pulverizer ground (~130 microns)
MA = Mikro-Atomizer ground (3-9 microns)

Effect of Oxidizer Particle Size Distribution and $CoSiO_3$ on "n" (u)

Figure III-57

Batch No:	2060	2169	2503	2559
Ingredients				
NH_4ClO_4				
70/30, 48/MA	60.0	60.0		
35/15/50, 48/SS/MA			61.0	61.0
$KClO_4$	10.0	10.0	10.0	10.0
Al (27)	15.0	15.0	15.0	15.0
NaCl	1.0	1.0	2.0	2.0
PBD-Imine	14.0	-	12.0	-
PBD-Epoxy	-	14.0	-	12.0
Solid Strand Burning Characteristics				
r at 100 psia, in./sec	0.082	0.086	0.085	0.098
n	0.56	0.47	0.78	0.70
Castability	Good	Very Good	Poor	Good

Effect of Epoxy vs Imine Cure System on "n" (u)

Figure III-58

d. Selection of Propellant and Liner for Subscale Motors

(C) Two modifications of AAB-3177 were considered for use in the subscale motor tests. A comparison of the composition, mechanical and bonding properties for the two propellants is given in Figure III-59. The mechanical properties of both propellants appeared adequate for this application in spite of the high solids loadings of 88 and 89%. The specific impulse density and n values of both propellants also met the program requirements as indicated in Figure III-55. The burning-rate pressure exponent of AAB-3216 is significantly higher than Batch 2254 (0.69 versus 0.60) and was one reason for choosing propellant AAB-3216 for the subscale motors. This propellant also had a significant advantage in processability, or castability, because of its lower solids content.

(U) Four liners which are commonly used with PBD propellants were evaluated for bondability to propellant with Batch 2254. The data in Figure III-59 indicated that three of the liners were satisfactory for this application. The best bond was obtained with Liner-858 which was selected for use in the subscale motor.

(C) The burning rate of propellant AAB-3216 from a 150-lb batch had been determined over the pressure range of approximately 100 to 600 psia, using four different types of specimens in order to establish a correlation among them. The different types of data are compared in Figure III-60. The propellant burning rate determined in a 3KS-500 motor using a 6-lb grain normally agrees with the burning rate observed in larger motors and was therefore considered a standard for burning rate determination. The burning rates measured with uncured and cured strands are slightly different from each other and from 3KS-500 data, as shown in Figure III-60. Cured strand data are used primarily for screening purposes and uncured strand data are used for batch qualification before casting. On other programs the burning rates determined with "small grains" agree well with data from 3KS-500 motors. The small grain, 1-62-in.-dia x 0.40-in. ID x 2.50-in. long, is made by casting and curing propellant in a phenolic tube with Teflon end plates and a core; both ends of the grain are restricted before firing in a closed bomb. The cost of a small grain firing in the Crawford bomb is less than one-tenth the cost of a small motor firing and, therefore, the small grains are used in place of motors whenever their results correlate well with motor data. In Figure III-60 it is seen that n is virtually the same in small grains and 3KS-500 motors, but the burning rate is 11.5% lower in the small grains. Because of this difference, the use of 3KS-500 motors for the primary determination of burning rates was to be continued.

Ingredients	Batch 2254 wt%	AAB-3216 Batch 65-60 wt%
NH_4ClO_4		
70/30, +48/MA	61.0	
35/15/50, +48/SS/MA	-	61.0
$KClO_4$	10.0	10.0
Al (27 μ)	15.0	15.0
NaCl	3.0	2.0
PBD-Imine	11.0	-
PBD-Epoxy	-	12.0
	100.0	100.0
Mechanical Properties, 77°F		
S_{nm}, psi	90	104
γ_m, %	23	23
γ_b, %	25	26
E_o, psi	562	598
Shear Strength, psi (77°F) Propellant/liner/insulation composite		
Liner SD-850-2	21	
Liner SD-858	46 (P)**	
Liner SD-862	37 (P)**	
Liner SD-864	38 (P)**	
Processability		
Brookfield Viscosity, poise		
135°F	-	17,600
150°F	-	13,600
Potlife, hours	-	>8

* Double-plate specimens tested in shear
** Failure occurred in the propellant

CONFIDENTIAL

Composition, Mechanical, Bonding, and Processing Properties of Preliminary Candidate Propellants (u)

Figure III-59

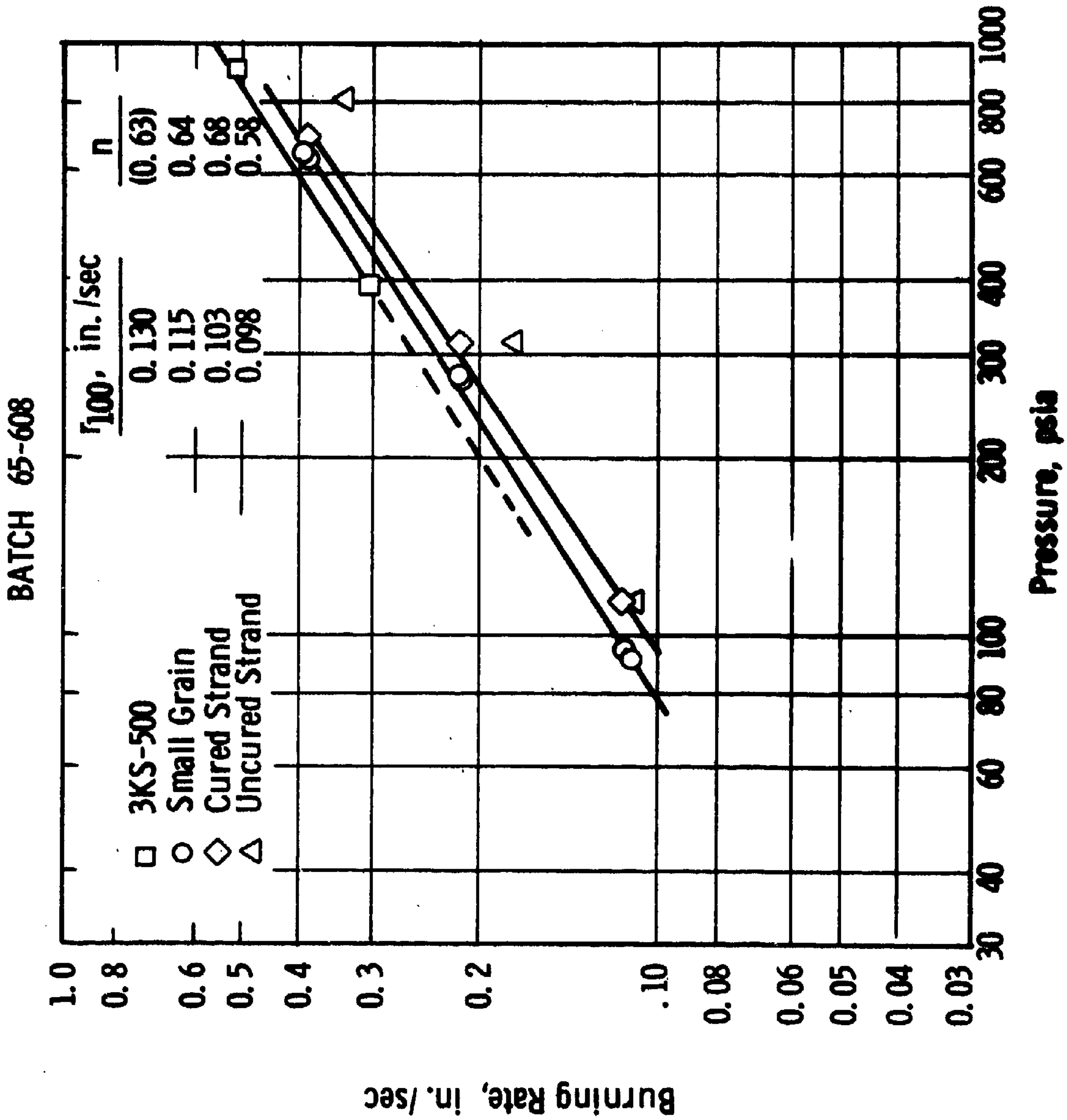

Burnign Rate of AAB-3216 (u)

Figure III-60

e. Extinguishability Screening Test Apparatus

(C) Previous extinguishment studies[2,30] have indicated that although sea level back pressure increases the $\dot{p}$ required for extinguishment, it is, nevertheless, possible to achieve permanent extinguishment of solid propellant motors at sea level by rapid depressurization techniques; on the other hand, there is no assurance that composite propellants can be permanently extinguished at sea level by L* techniques. For this reason the $\dot{p}$ extinguishability screening tests are conducted with sea level back pressure while L* screening tests are normally done in vacuum, with the exception of those which are for the purpose of testing new additives which have been incorporated specifically for improving extinguishability by L* instability at sea level.

(U) A sketch of the $\dot{p}$ extinguishability screening motor assembly is shown in Figure III-61. This motor is a modified 1KS-250 motor containing a cartridge-loaded end-burning grain of nominal 0.5-lb weight. The motor is fitted with a dual nozzle assembly such that the chamber pressure is controlled initially by a small-diameter outer-nozzle held in a swing-away device. Venting is accomplished on command by activating an explosive nut assembly which releases the swing-away device, allowing the outer nozzle to deflect out of the gas stream. Pressure decay then follows; the rate of depressurization may be regulated by the difference in the throat areas of the outer and inner nozzles and the chamber free-volume. The chamber pressure is monitored by both Taber and Kistler transducers and recorded on a Visicorder oscillograph. The Taber transducer is used mainly to indicate the chamber pressure at the start of the venting process. Because of its faster and smoother response, the Kistler transducer is used primarily for determination of the depressurization rates.

(U) The variable-volume screening motor which is used to determine the L* extinguishment characteristics of various propellants is shown in Figure III-62. The motor case is water cooled to eliminate the need for insulation and simplify the moving forward-seal design. The grain is bonded to a propellant support stand which, in turn, is attached to the piston which acts as the forward closure of the motor. Two cast-iron piston rings act as scrapers to remove oxide and metallic deposits from the cylinder wall, while a fluoro-elastomer O-ring provides the positive gas seal. The position of the piston and consequently the motor free-volume and L* range is controlled by the lock-nuts on the threaded shaft to which the piston is attached. All L* screening firings use a cylindrical grain which is 3.0-in. in diameter, 2.0-in. long, weighs approximately 1 lb and burns on the circumference and one end.

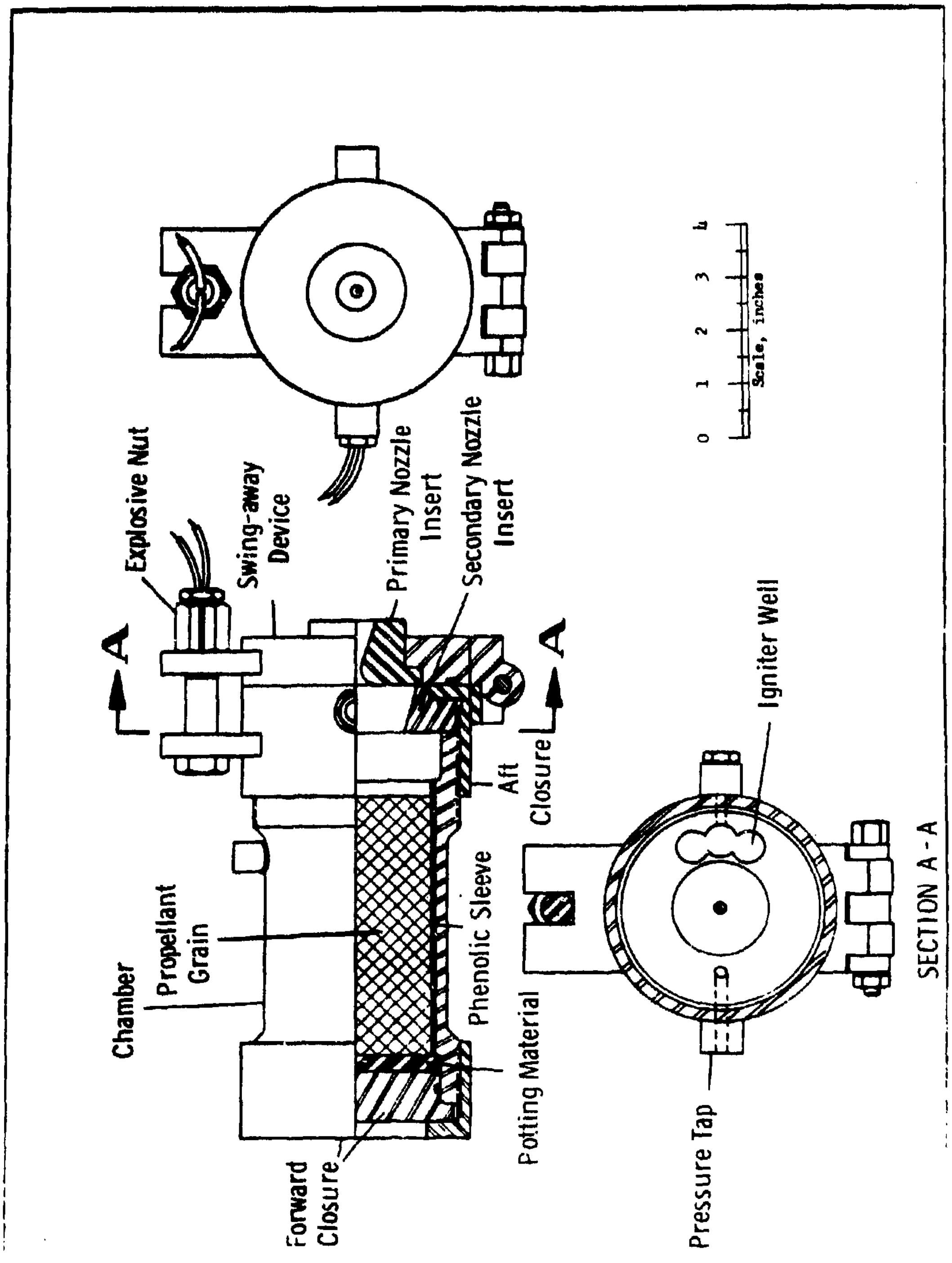

Rapid Depressurization Screening Motor

Figure III-61

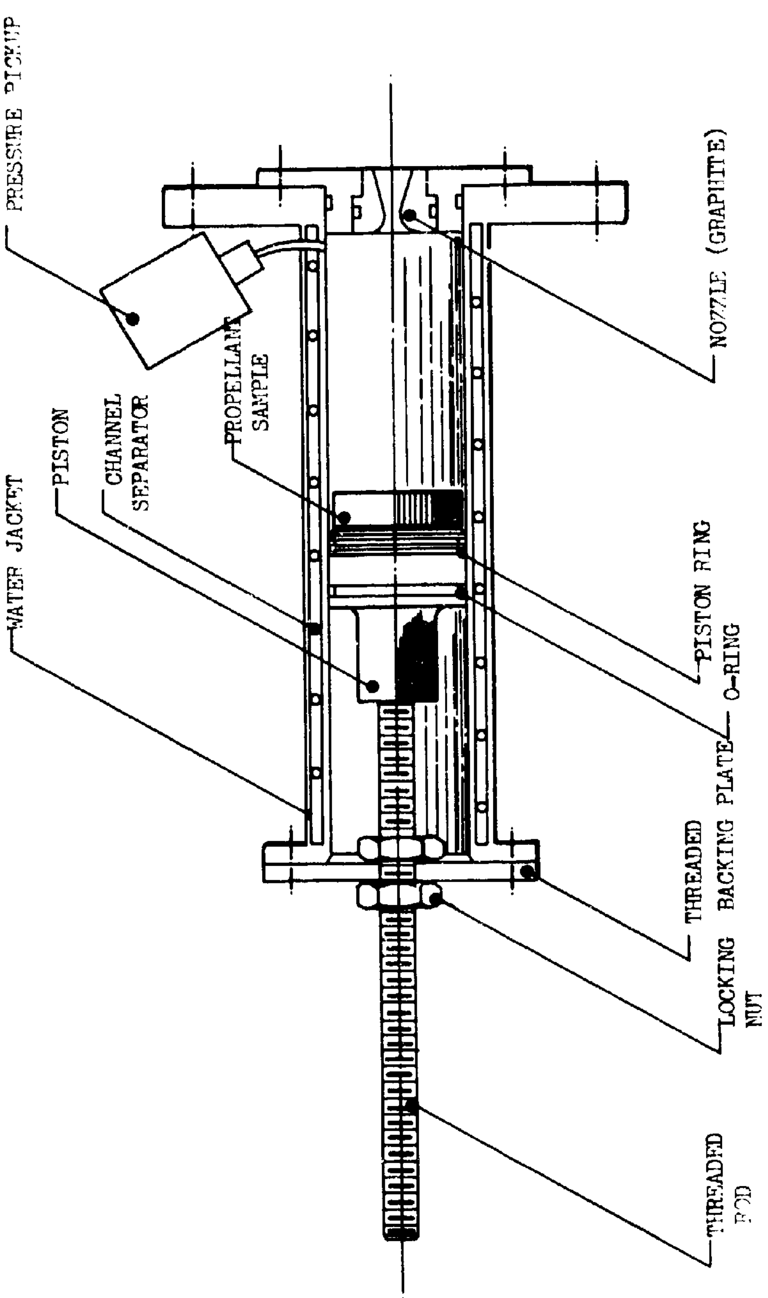

Variable Volume Motor - L* Extinguishment Program

Figure III-62

Property	Requirements and Goals	Current Status AAB-3220
Extinguishment		
Critical depressurization rate(1)		
p_c, psia	40	40
$\dot{p}_{cr}$, psia/sec	< 1500(1)	500(1) (sea level)
Extinction by L*		
L*, in.	180-500	391 695
p_e, psia	10-40	19 19 (vacuum)
n (for throttling ability)	≥ 0.60	0.66(2)
r, in./sec at 100 psia	0.08-0.12	0.093(2)
T_c, °F at 500 psia	≤ 5820	5814
Propulsive Performance:		
I_s, lbf-sec/lbm, 15° half-angle 1000→14.7 psia	≥ 240	238
Density, lb/in.^{3}	≥ 0.064	0.0655
Mechanical Properties, 80°F		
Constant Strain, %	> 4	To be determined
Elongation, %	>10	36
Propellant-to-Liner Bond		
Tensile Stress, psi	>17	162
Shear Stress, psi	>16	85
Processability	Adequate for existing equipment	Excellent; 36,000 poise 12 hr after end of mix.

(1) See Figure 68.
(2) Solid strand data.

Summary of Requirements and Achievements (u)

Figure III-63

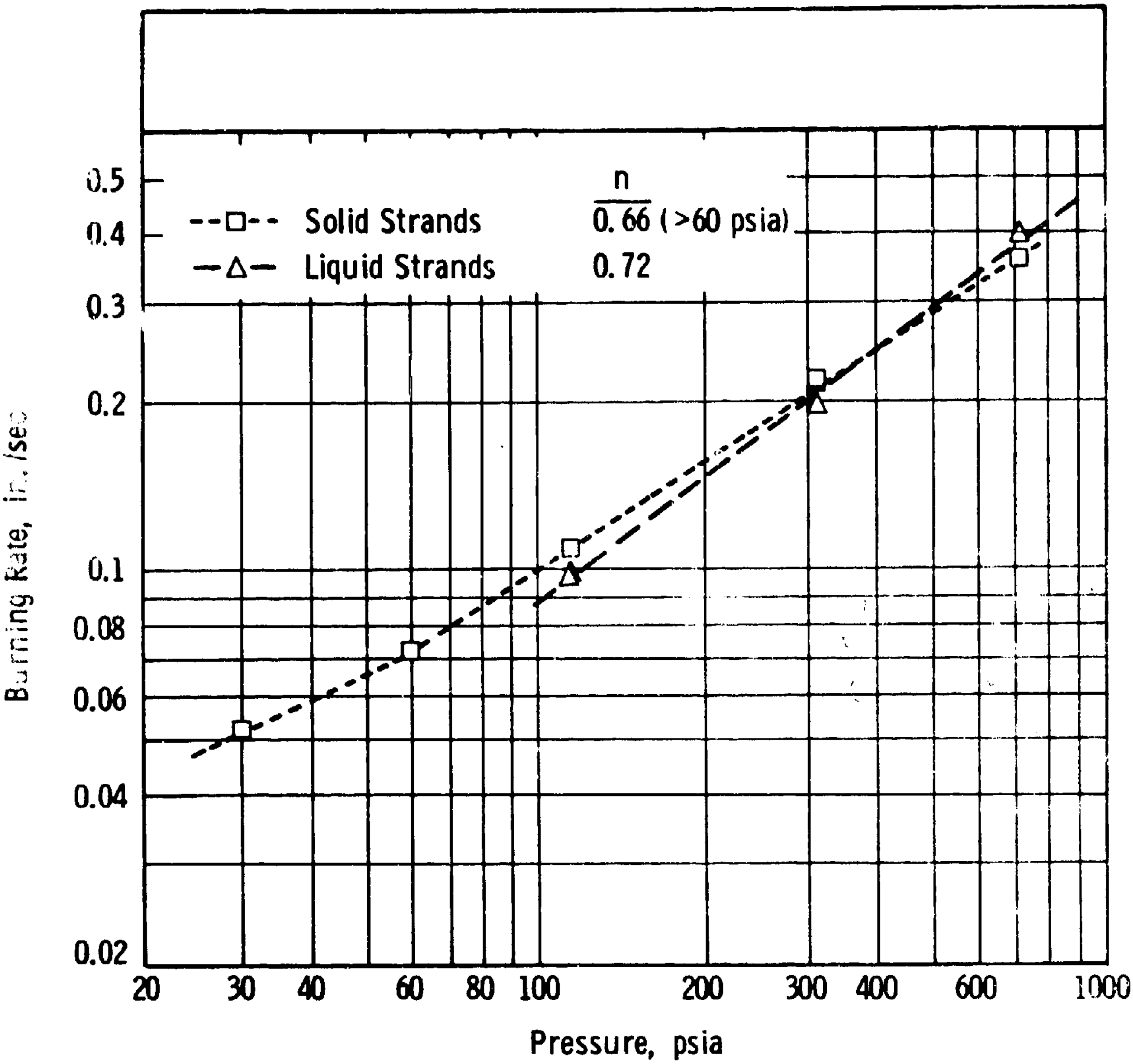

Burning Rate vs Pressure for AAB-3220, 2200-lb Batch No. 1-60D-001

Figure III-64

Product		Chamber	Chamber	Exhaust
	P, psia	1000	500	14.7
	T_c, °F =	5814	5703	3458
HCl		0.3428	0.3411	0.4226
N_2		0.2139	0.2138	0.2147
H_2O		0.4318	0.4251	0.3895
H_2		0.9686	0.9601	1.0412
O_2		0.0003	0.0005	0.0000
O		0.0019	0.0028	0.0000
OH		0.0262	0.0307	0.0005
Cl		0.0297	0.0366	0.0028
NO		0.0017	0.0019	0.0000
H		0.1236	0.1513	0.0090
CO		0.9229	0.9228	0.9085
CO_2		0.0507	0.0509	0.0652
PN		0.0001	0.0001	0.0003
PO		0.0005	0.0005	0.0004
Al		0.0006	0.0008	0.0000
AlCl		0.0150	0.0169	0.0000
$AlCl_2$		0.0237	0.0210	0.0004
$AlCl_3$		0.0004	0.0003	0.0000
AlO		0.0003	0.0004	0.0000
Al_2O		0.0001	0.0001	0.0000
AlOCl		0.0001	0.0001	0.0000
Al_2O_3(l)		0.2765	0.2768	0.2964
K		0.0083	0.0102	0.0007
KCl		0.1337	0.1324	0.1436
K_2O		0.0012	0.0008	0.0000
Product Quantity				
Moles gas product / 100g propellant		3.2982	3.3212	3.1950

AAB-3220, Theoretical Equilibrium Gas Composition

Figure III-65

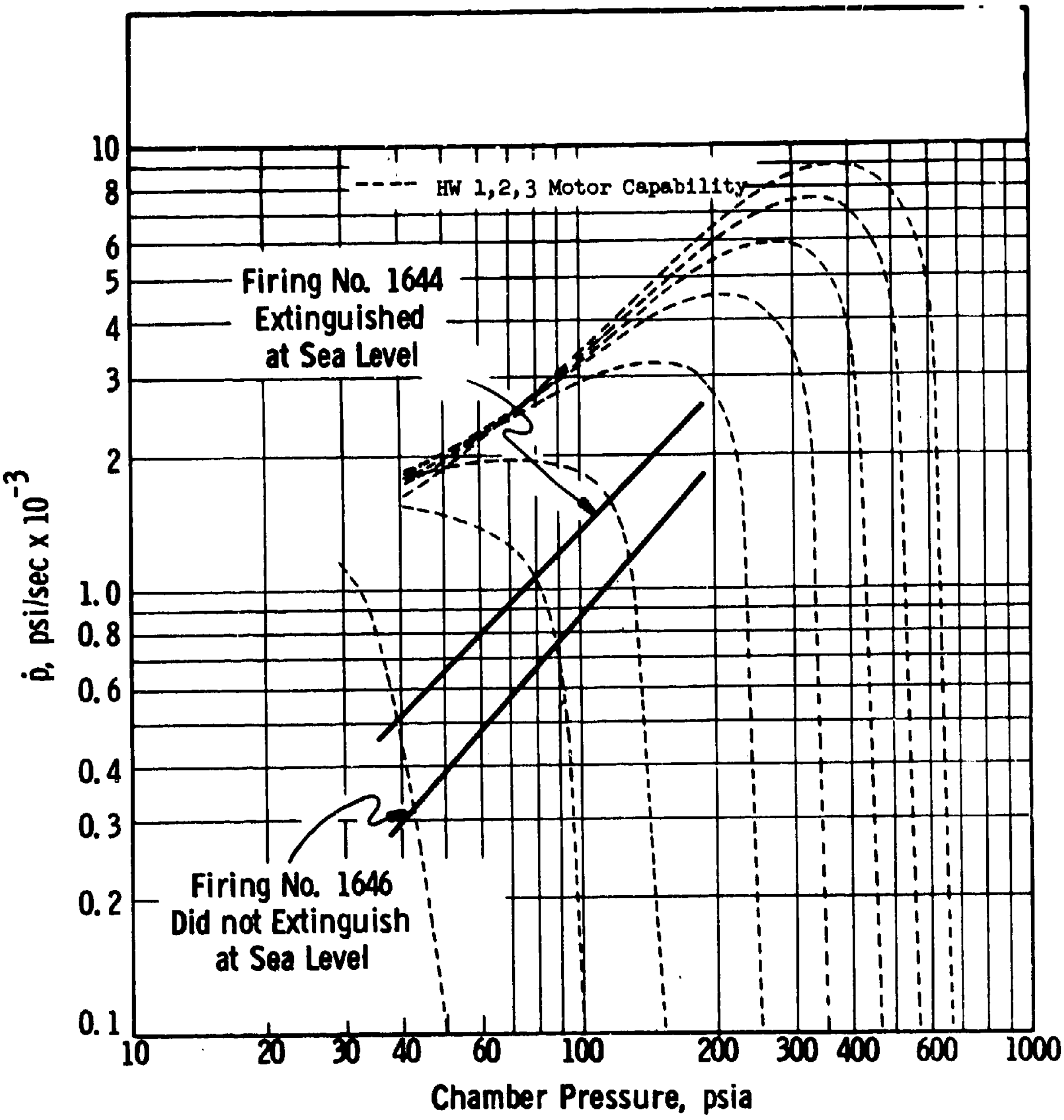

Depressurization Rate vs Chamber Pressure for AAB-3220 and HW-1 Motor Capability Near Burnout, F = 5.0 cps (u)

Figure III-66

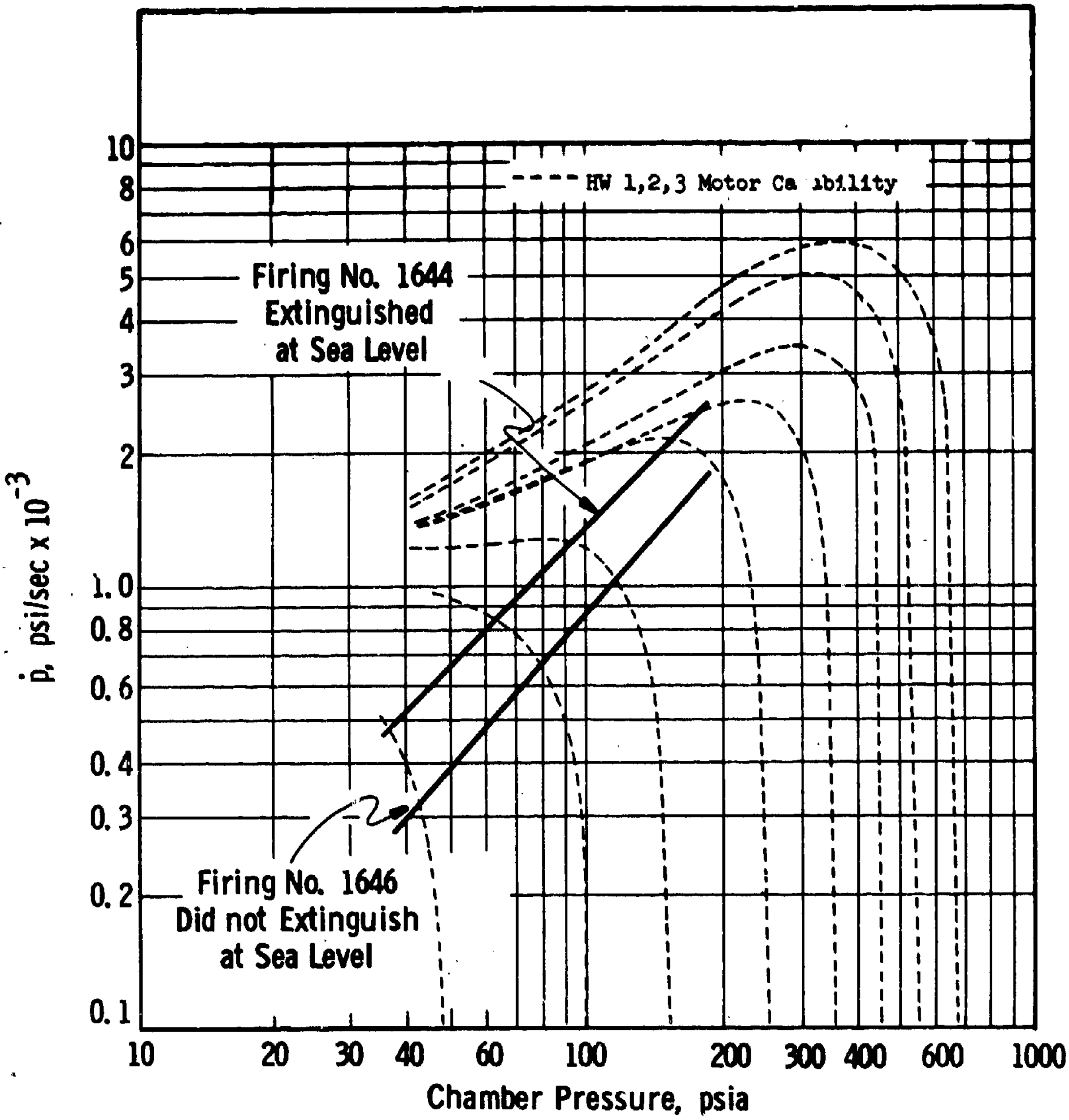

Depressurization Rate vs Chamber Pressure for AAB-3220 and
HW-1 Motor Capability Near Burnout, f = 2.5 cps (u)

Figure III-67

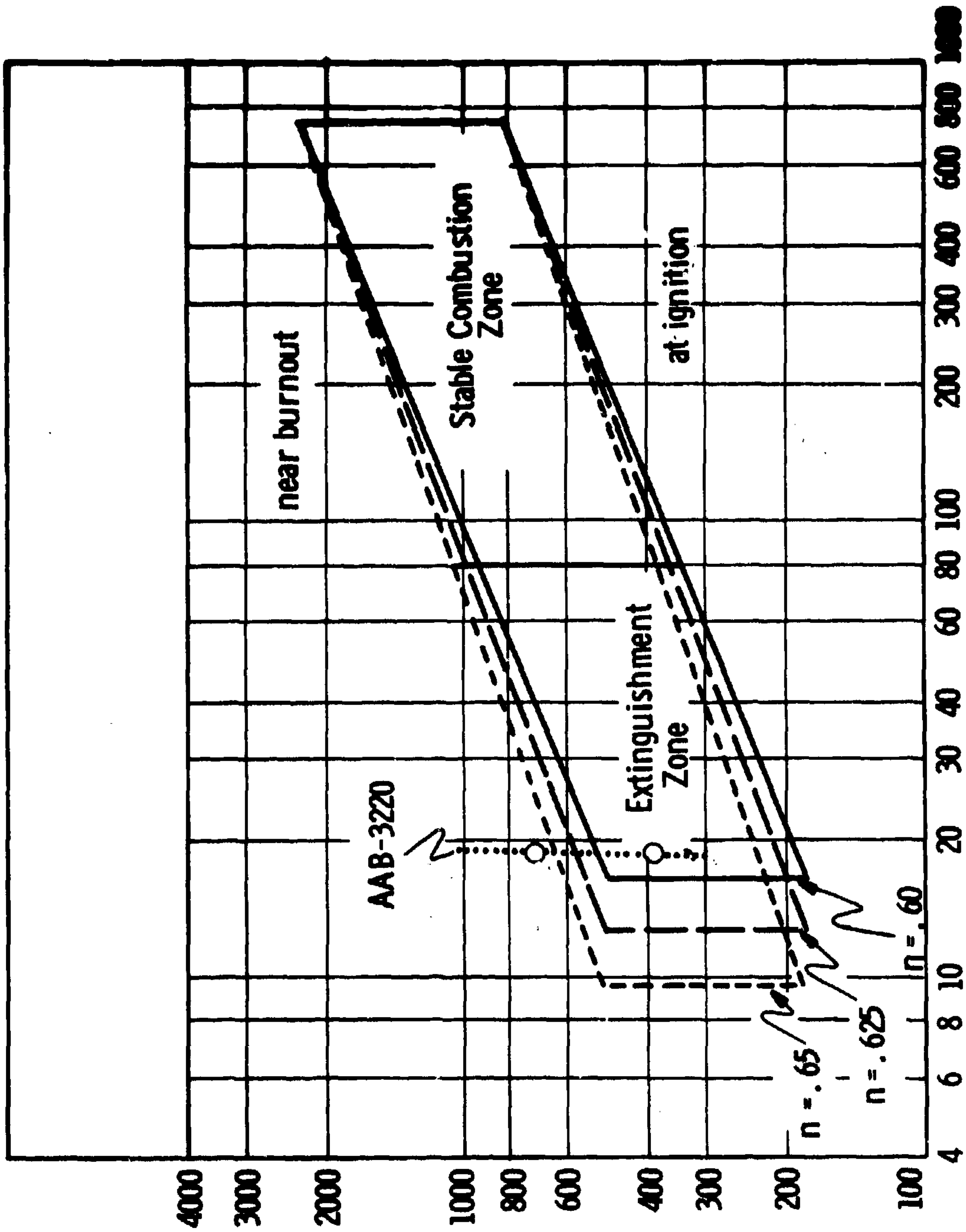

L* vs Chamber Pressure for HW-1, 2 and 3, L* vs P_e for AAB-3220 (u)

Figure III-68

capabilities plotted in Figure III-66 assumed a pintle response of 5.0 cps while those in Figure III-67 assumed 2.5 cps.* It can be seen that the depressurization rates calculated for the fullscale motors at either 5.0 or 2.5 cps should be more than sufficient to extinguish this propellant at sea-level back pressure when the starting chamber pressure is equal to or higher than 200 psia. Although no screening motor was fired at 100-psia starting chamber pressure, it appears that extinguishment would probably occur. The L* extinguishment characteristics of AAB-3220 determined in screening motor firings at vacuum are shown in Figure III-68, with the L*-pressure range which is expected in fullscale motor firings. The L*-p_e relationship determined in the screening motor falls in the "extinguishment zone" of the fullscale motor. This indicates that the fullscale motor should be capable of extinguishing this propellant by L* techniques at vacuum back-pressure, and the L*-p_e relationship is such that it probably will not interfere with the stable combustion zone for throttling. In the L* screening motor firings in the pressure range below approximately 50 psig, a significant amount of condensable material in the exhaust stream was deposited on the nozzle, partially restricting the throat area. Chemical analyses indicated that this deposit was composed of approximately 40% Al_2O_3, 40% KCl, 12% Al, and 8% unidentified mixture containing boron (probably BPN igniter material). Deposition of these materials is not expected to be severe during normal operation of the fullscale motor; however, it may become a problem in firings of very short duration and at low pressures.

(C) Prior to processing propellant AAB-3320 in production equipment (2200-lb batch size) the propellant was processed in a 60-lb batch using the same lots of raw materials which are available for production-scale batches to ensure that processability and rate of cure were satisfactory. The potlife of this batch was shorter than desired, while cure was very rapid, indicating that the cure-catalyst concentration should be reduced. The catalyst level was reduced from 0.04 to 0.025% in the 2200-lb batch, which exhibited excellent castability and potlife with a satisfactory rate of cure. Tentative action limits were established for quality control of this first production-scale batch (No. 1-60D-001). These limits are tabulated in Figure III-69 with the

---

* Other assumptions:

$r = 0.005\ p^{0.65}$ in./sec	$B = 0.25$
$A_s = 1270$ in.^{2}	$\alpha = 3.76 \times 10^{-4}$ in.^{2}/sec
$V_o = 15{,}000$ in.^{3}	$T_o = 6480°R$
$\rho = 0.067$ lb/in.^{3}	$M = 32$
$C_w = 0.00658$ sec^{-1}	$\gamma = 1.20$

	Minimum	Maximum	Batch 1-60D-001
NH_4ClO_4			
MA, Fisher subsieve, microns	3	9	5
SS, % through 100 mesh screen	45	75	46, 43
% through 150 mesh screen	20	45	27, 25
+48, % through 48 mesh screen	0	2	1
$KClO_4$			
HS, % through 200 mesh screen	65	90	67
% through 325 mesh screen	85	98	92
NH_4ClO_4, blend			
% Moisture	0	0.05	0.007
Submix			
% Moisture	0	0.05	0.013
Acid equiv/100g	0.0276	0.0292	0.0283
Premix			
% Moisture	0	0.05	0.013
% Solids	56.0	56.8	56.2
Propellant			
% Solids	85.5	86.5	86.1
Liquid density	1.809	1.819	1.813
Liquid strand burning rate*	0.094	0.104	0.099

* Data from previous batches:

10-lb, No. 3419, $r_{100} = 0.097$

60-lb, No. 65-752, $r_{100} = 0.101$

Action Limits for AAB-3220

Figure III-69

measured values for the 2200-lb batch. All analyses are within limits, although the percent of SS ammonium perchlorate through the 100 mesh screen is marginal; this oxidizer was accepted in this case since other size sieve analyses of it were satisfactory. The rate of viscosity increase at 135°F of this propellant is shown in Figure III-70. The viscosity is still satisfactory for casting 12 hr after the end of the mixing operation; this should be more than adequate for casting three fullscale motors from one propellant batch. The effect of catalyst concentration on viscosity buildup is also illustrated in Figure III-71, with data from 10-lb batches of propellant. Catalyst concentration provides a useful tool for controlling potlife.

(U) The explosive characteristics of propellant AAB-3320 were determined before processing a production-scale batch. The results of these safety tests tabulated in Figure III-71 are typical of a Class 2 or ICC Class B propellant.

(U) The tensile properties of propellant AAB-3220 from the 2200-lb batch have been determined over the temperature range of -40 to 150°F. These properties listed below appear to be more than adequate for this application.

T, °F	S_{nm}, psi	γ_m, %	γ_b, %	E, psi
150	102	28	30	536
77	130	32	36	624
-40	290	26	35	2263

3. Propellant Burning Rate Discrepancies

(U) Propellant tailoring efforts had been terminated during the third quarter of Contract AF 04(611)-10820, after the second heavyweight motor test as it appeared that AAB-3220 propellant would meet the basic needs of the program. These first two tests demonstrated variable thrust at sea level and the second test, HW-2, demonstrated that the controllable solid rocket motor could be extinguished at sea level, although permanent extinction could not be maintained. On the basis of these tests, it seemed probable that some of the funds allocated to continue propellant tailoring could be diverted to areas elsewhere in the program that were indicating higher than estimated costs. The propellant work was halted at a point which would allow immediate reinstatement of this work with little loss of effort if such a move were indicated later in the program.

(C) With the firing of HW-3, Runs 003 and 004, it became apparent that AAB-3220 would be marginal in meeting the program requirements on the

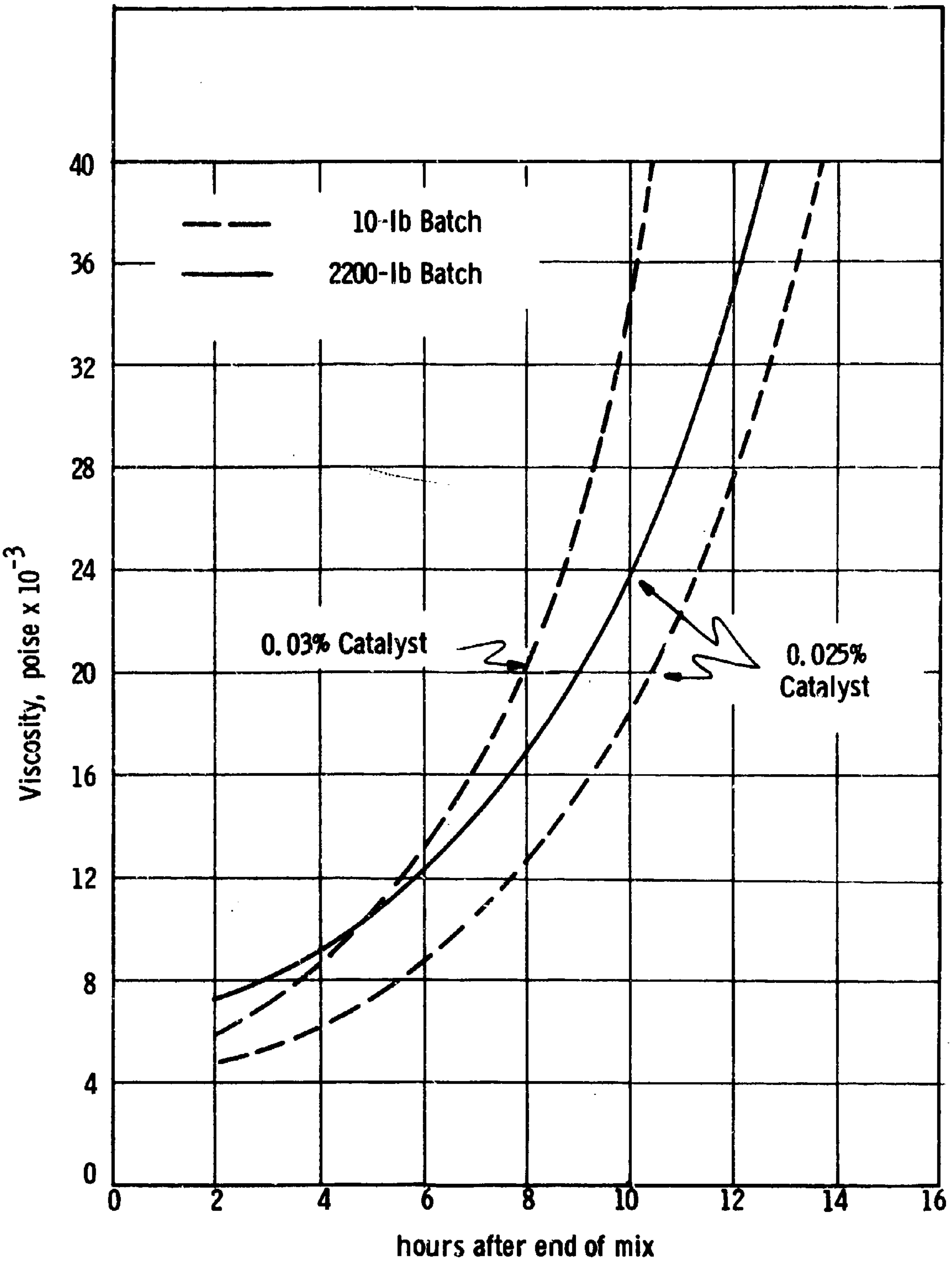

Viscosity Increase of AAB-3220 at 135°F

Figure III-70

Impact Sensitivity Bureau of Mines 50% Fire Point	38.5 cm/2Kg
Autoignition Temperature	571°F
Temperature Stability 180°F, 48 hr	
2-in. cube	No change
1-in. cube	No change
No. 8 Blasting Cap	
2-in. cube	Negative (burn 38 sec) Negative (burn 39 sec)
Unconfined burning, 2-in. cube	39 sec
Woodblock 1/2 in. x 2 in.	
(a) No. 8 Blasting cap, no booster	Negative
(b) 5 gram tetryl booster	Negative
(c) 5 gram tetryl booster 0 Attn.	Negative
(d) 5 gram tetryl booster 0 Attn.	Negative
(e) 5 gram tetryl booster 0 Attn.	Negative
(f) 5 gram tetryl booster 0 Attn.	Negative
NOL Sleeves	
(a) 0 Attn.	Negative
(b) 0 Attn.	Negative
(c) 0 Attn.	Negative
(d) 0 Attn.	Negative
(e) 0 Attn.	Negative
(f) 0 Attn.	Negative
Recommended Military Explosive Classification:	Class 2
Recommended ICC Classification:	Propellant Explosive Class B

Explosive Safety Tests of AAB-3220

Figure III-71

basis of both burning rate and P-dot extinguishment. Motor HW-2, fired during the third quarter of the program, indicated that the burning rate of AAB-3220 propellant in the 'Finocil' grain configuration used in the single-chamber controllable solid rocket motor was somewhat higher than would be expected from the 3KS-500 burning rate motors. Even taking into consideration the scaleup factor on the batch size, the burning rates at low pressures were considerably out of line. This factor, in itself, was not a major problem area so long as the propellant could be successfully extinguished at altitude. When motor HW-3, Run 004, could not be extinguished at what was thought to be in excess of 60,000 foot simulated altitude, a decision was made to reopen the propellant evaluation effort in an attempt to either find a different formulation which would better meet the needs of the CSR motor or to correct the burning rate difficulty with AAB-3220 so that the minimum chamber pressure attainable in the fullscale CSR would be low enough to permit reliable extinguishment. This propellant re-evaluation effort was thus initiated after a meeting with the Air Force technical personnel at AFRPL, Edwards Air Force Base.

a. Propellant AAB-3220 Retesting

(C) Some investigative work was immediately initiated as soon as it was determined that AAB-3220 could not be readily extinguished in the fullscale CSR at altitude. This was started simultaneously with the investigations as to the other possible causes of the anomaly in HW-3, Run 004, that were previously discussed. During the course of the propellant investigations, it was postulated that the burning rates that were determined in the 3KS-500 motors and the Crawford Bomb Motor (CBM) tests were low due to the heat loss to the surrounding environment, namely the chamber walls. Data that had been taken on the batch of propellant that was used in the first three heavyweight motors was compared to that back calculated from firing HW-2. These data are presented on Figure III-72.

(C) From Figure III-72, it is apparent that considerable deviation exists between the burning rates calculated from the CSR motor and those measured in the subscale motors, specifically at pressures below 100 psia. An attempt was made to calculate the mass flow coefficient of the propellant gas in the CSR motors. The values calculated, 0.0067 and 0.0063 1/sec, were in very good agreement with the theoretical value of 0.00658 1/sec that was predicted for this motor. As the theoretical value was used to back calculate the burning rate from the CSR and the only other values used were measured thrust and measured chamber pressure, it was determined that the values calculated were probably a very good indication of what could be expected in this motor. It was then hypothesized that reignition of the motor HW-2 was due to the higher temperature of the grain immediately after extinguishment and aided by the heat flux from the hot insulation. This higher temperature profile in

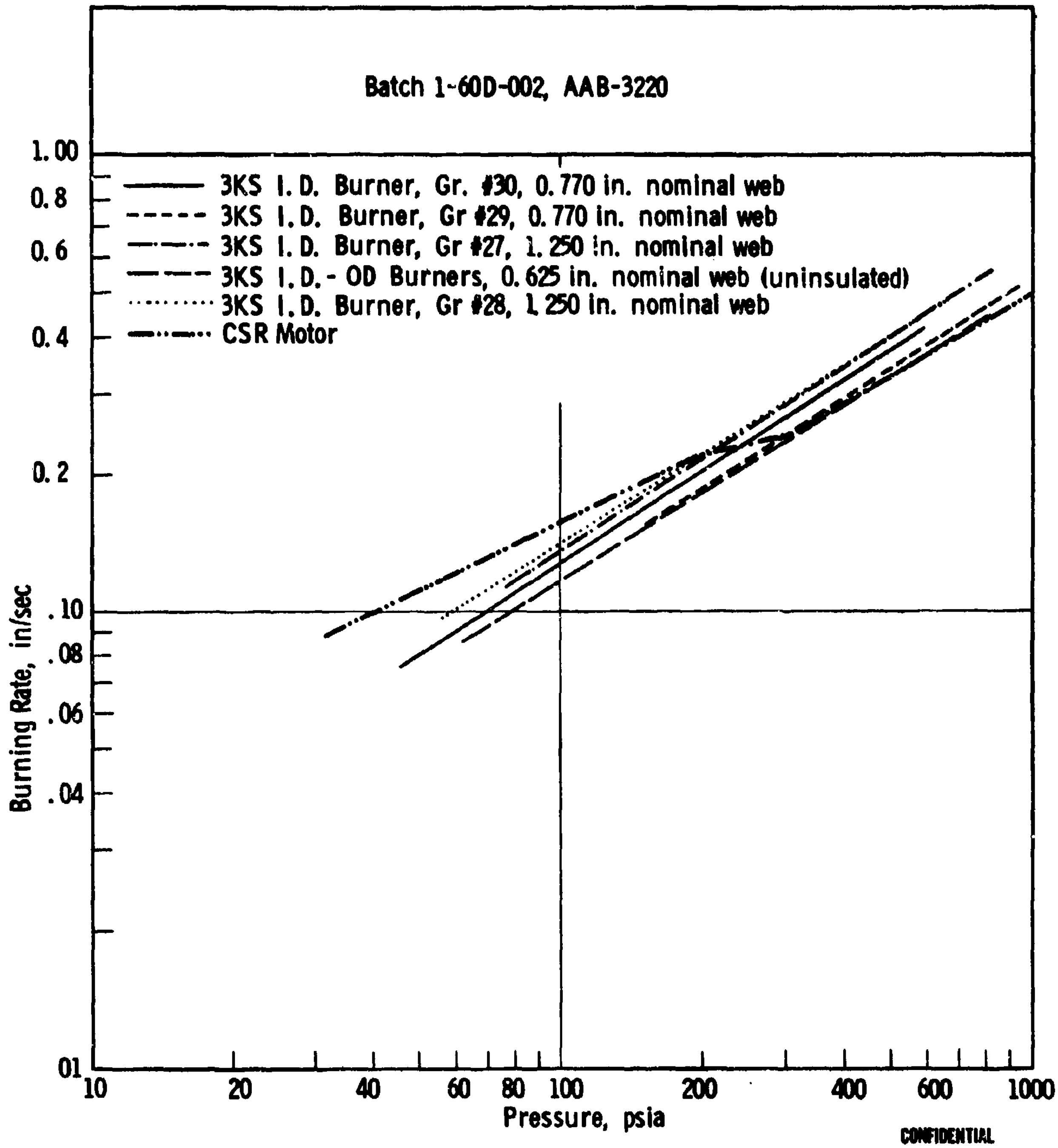

Burning Rates of CSR 002 and Subscale Motors (u)

Figure III-72

the propellant may be the cause of the indicated high burning rate at low pressure. When this hypothesis was investigated, it was found that the burning rate for the first 0.60 seconds may be slightly higher than normal; however, this effect could not possibly last for the 5 seconds that HW-2 indicated high burning rates.

(C) A second approach was to re-analyze the small motor firing data taken from the same batch as that cast into the first three heavyweight motors. These motors were 3KS-500 burning rate determination motors, using n internal and external burning cylinder of approximately 6 pounds of propellant. From the grain configuration, these firings should have been neutral; however, in each case they were slightly progressive, when fired at low pressures. The possibility of aluminum oxide deposition on the nozzle throat insert was investigated and found to be far too small to account for the progressivity. The only remaining possibility that would explain this progressivity is that the grain did not burn evenly and that the inside diameter burned at a higher rate than did the outside diameter. To further investigate this possibility, the ID-OD-end burning grains were re-investigated. These grains should burn regressively at a pressure regressivity of 28% as they have a surface area regressivity of about 13%. These firings, however, had only a 5% to 0% regressivity, thus they also burned more progressively than anticipated.

(C) The other type of grain used to measure burning rate is the Crawford Bomb Motor. This motor used small ID burning grains which are quite accurate at high pressures, but were also low at the low pressures. As these are internal burning grains, the fact that they were low eliminated the possibility that grain configuration was the cause of the burning rate discrepancy. It was therefore hypothesized that the cause of the low pressure burning rate discrepancy was heat loss to the motor case and nozzle in the small motors, depressing the burning rate. This theory appeared to be consistent with all of the small scale motor data, including the CBM. By calculating the difference in internal and external burning rates required to explain the progressive burning of a neutral grain configuration, it was found that the internal burning rate would have to be approximately 25% higher than the average burning rate that was quoted at the average pressure. Although this is not enough of a difference to explain the total deviation between the small motor and the fullscale CSR motor, it is definitely in the correct direction.

(C) Since the heat losses to the environment in the small motors consisted of a large percentage of the heat available in the propellant gasses, the parameter to be considered in the determination of burning rates at low pressures is the heat loss per unit mass flow. This parameter becomes

progressively greater as the chamber pressure, thus the mass flow is decreased. This becomes a very important part of the P-dot and L* extinguishment process as the residence time of the gas in the chamber is increased as the pressure is lowered, thus the heat loss from any given amount of gas is increased as the pressure is lowered. It was therefore indicated that the P-dot and L* data that had been taken from the screening test motors was also probably not that which would be indicative of the fullscale motor.

(C) All of the small scale burning rate motors and the P-dot and L* screening test motors had been fired as uninsulated motor cases on previous programs with considerable success in predicting the performance. These tests, however, were all fired at high chamber pressures where the heat loss per unit mass flow is low. In conjunction with the Air Force, it was decided to repeat the testing of AAB-3220 at low pressures using insulated motor cases. These data, although still in process of being reduced, give an indication that the burning rates have not changed much from those fired in uninsulated motors. Considerable attention was directed toward the selection of the appropriate insulation to use in these motors. It appeared that the rubber insulations with fairly high heats of ablation and low conductivities were much better than the paper-phenolics although the latter were more readily available in the proper size tubes. The paper-phenolic insulations seemed to absorb sufficient heat from the propellant gas to depress the burning rates almost as much as the bare steel chamber walls. When rubber insulation was used, the burning rates at low pressures came fairly close to those calculated from the CSR motor. For P-dot and L' screening tests, the extinguishment requirements are probably more sensitive to heat loss than are the burning rates, as even the paper-phenolic insulators were sufficient to indicate a definite difference in rates of depressurization required to extinguish propellant from those predicted in the uninsulated motor cases.

b. Conclusions

(U) From the results of this limited program it was determined that heat losses in small motors play a very important part in the effective burning rate exhibited in these motors. Although the cause is apparently known, correction of the problem has yet to be attained. Insulation of the chambers improves the situation, yet it does not solve the problem because the amount of heat absorbed by the insulation is sufficient to depress the burning rate in motors with a very small amount of propellant. As shown on Figure III-73, the insulated motors required a higher P-dot for extinguishment.

(U) Increasing the size of the motor will help to solve the problem, yet this approach will increase the cost of development of propellants and require that new propellants be investigated in large batch sizes--a prohibitive solution. It is therefore necessary to use scaling techniques to

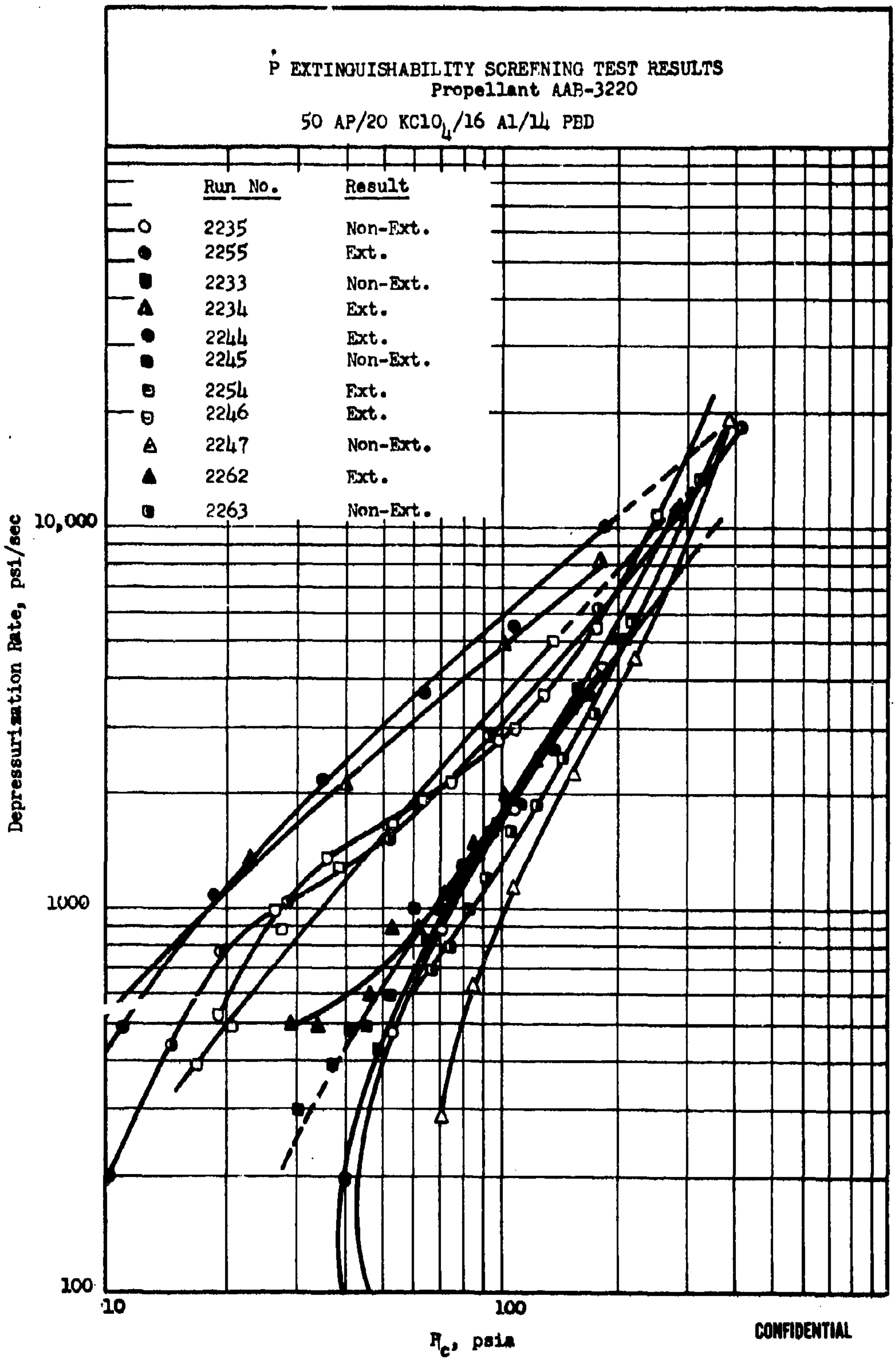

CONFIDENTIAL

P-dot Extinguishability Screening Test Results (u)

Figure III-73

predict the low pressure burning rate of propellants in full-size motors at low pressures by comparing the rates measured in the test-tool-type firings of a propellant that has been tested in full-size motors to those of the new propellant and ratioing the results. More effort is required in this area since all formulations are not expected to be scalable using results of a limited few configurations that have data over a large range of motor sizes.

4. Propellant AAP-3249

(C) At the time that the propellant tailoring effort was stopped, there were a few alternate formulations that had not received as much work as AAB-3220, however appeared to offer lower rates of depressurization than AAB-3220 with about the same specific impulse. These formulations were all nitro-oxidizer. These formulations are shown below as compared with the heavyweight CSR propellant, AAB-3220.

Ingredient	Propellant Compositions by Weight %			
	AAB-3220	Batch-158	AAP-3249	Batch-467
AP	50.0	61.0	51.0	48.0
KC104	20.0	-	-	-
NQ	-	15.0	15.0	20.0
Al	16.0	2.0	10.0	10.0
NaCl	-	-	3.0	-
PBD	14.0	-	-	-
NPPU	-	22.0	21.0	22.0

(C) The burning rates that were derived from the solid strand test method are shown on Figure III-74. As can be seen from this figure, the burning rate of Batch-158 was indicated to be higher than that of AAB-3220. This by itself would require that the extinguishment characteristics of this formulation be quite a bit more easily attainable than those of AAB-3220. The burning rate of Batch-467 was lower than that of AAB-3220 at the high pressure end only. This was an undesirable characteristic in that all it would accomplish was to lower the maximum thrust level that can be attainable with the CSR design as it stood. As the burning rate of this propellant was approximately the same as that of AAB-3220 at the low pressure end, the same minimum pressure attainable in the CSR with AAB-3220 would limit this Batch-467 formulation from attaining a L* extinguishment.

(C) The burning rate of AAP-3249 was in the correct relative position in the areas of low pressure, however, the high pressure characteristics were similar to Batch-467 with the same limitation on the maximum thrust level. AAP-3249 would be a fairly good selection from the thrust variation stand if it were as extinguishable as AAB-3220 in that the minimum pressure attainable

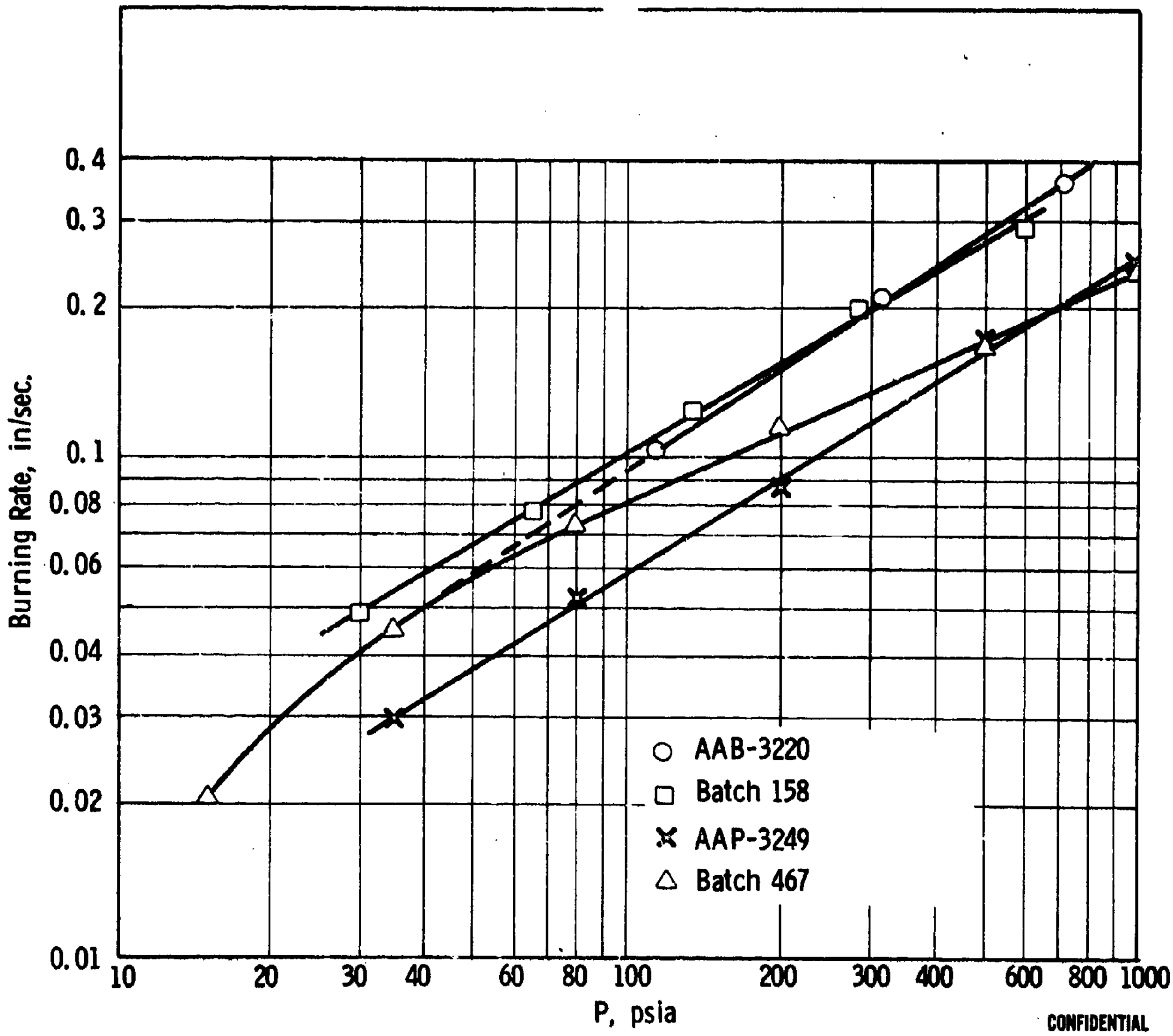

Solid Strand Burning Rates (u)

Figure III-74

III, B, Propellant Tailoring (cont.)

in the CSR motor as now designed is less than 10 psia. The limitation at the high pressure end could be easily eliminated for a propellant with so low a burning rate at the low pressure end of the scale. A simple change in the diameter of the outer throat insert would drastically reduce the nozzle minimum throat area without materially affecting the maximum throat area. The minimum area was at this point approximately 6.25 square inches and the maximum throat area was approximately 28.5 square inches for the lightweight series. By decreasing the minimum area by 2.25 square inches, the chamber pressure and maximum thrust attainable would be greatly increased with only a 2.25 square inch change to the 28.5 square inch maximum area. This would limit the minimum pressure attainable to approximately 14 psia - only a 4 psi change.

(C) The extinguishment characteristics of these three alternate propellants were quite different. In the first place, all were apparently more easily extinguished by P-dot than was AAB-3220. EAch had a definite "break-even-venting-line" where half of the motors fired are permanently extinguished and the other half fail to extinguish. These P-dot versus P traces are presented for Batch-158, AAP-3249, and Batch-467 on Figures III-75, -76, and -77, respectively. From these data, it can be seen that AAP-3249 was the most easily extinguishable of the three, with a P-dot requirement of -1800 psi/sec and Batch-467 with a requirement of about -600 psi/sec at 100 psia. As these tests were conducted in the insulated chambers described above, they are considered to be fairly good indicators of what can be expected in the fullscale CSR motor.

(C) Although all three propellants were acceptable from an extinguishability standpoint, only AAP-3249 had a direct and inexpensive solution to the maximum attainable thrust problem. This propellant was therefore selected for the lightweight motor test series. The expected delivered impulse of AAP-3249 was 237 plus seconds, standard. The oxygen balance of this propellant was approximately 2.5 times that of AAB-3220, therefore some increased surface regression of the carbon type nozzle materials was expected; however, due to the lower flame temperature, less than 5300°F, the thermal problem was expected to be less severe than that caused by AAB-3220.

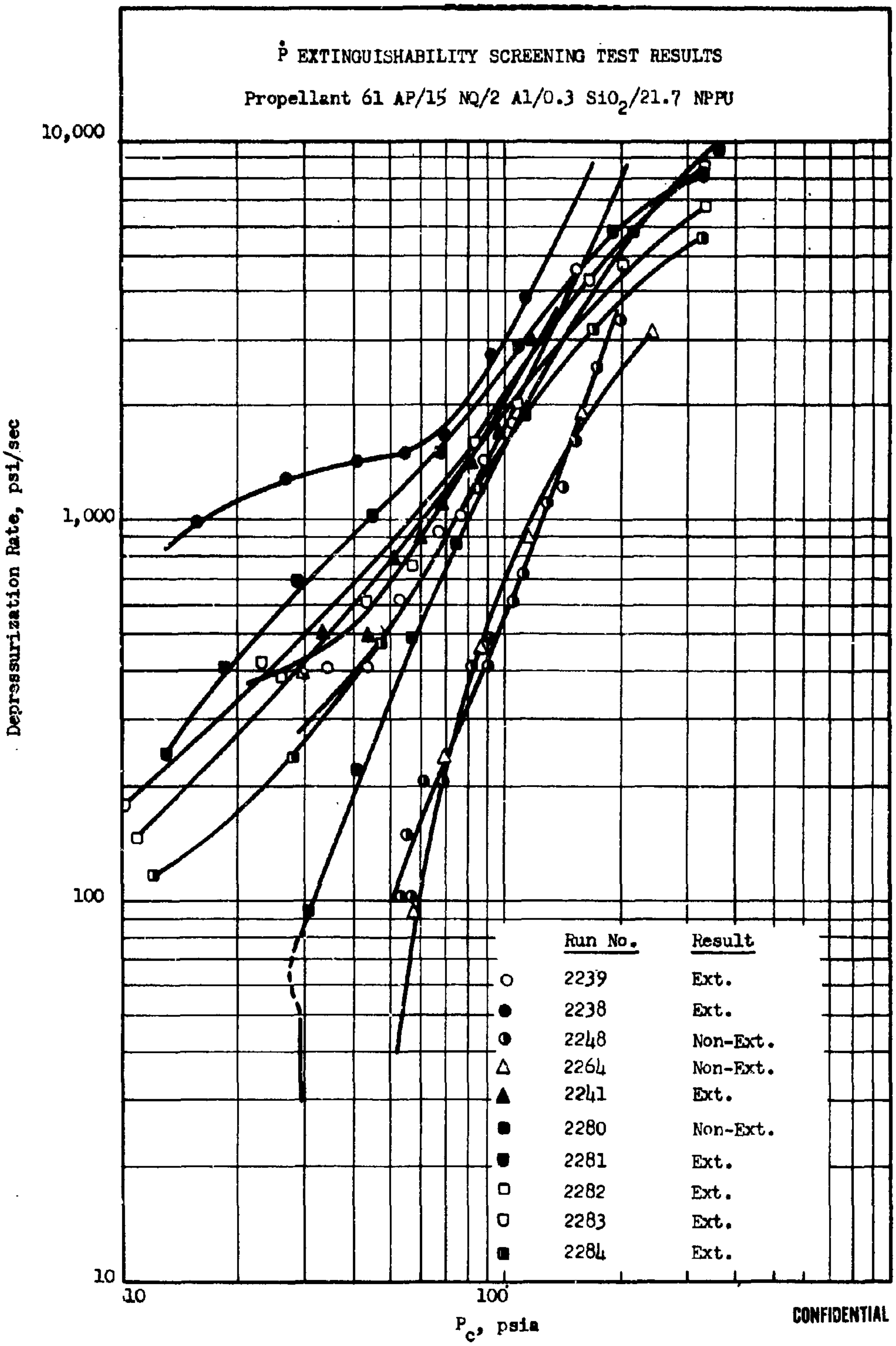

P-dot Extinguishability Screening Test Results (u)

Figure III-75

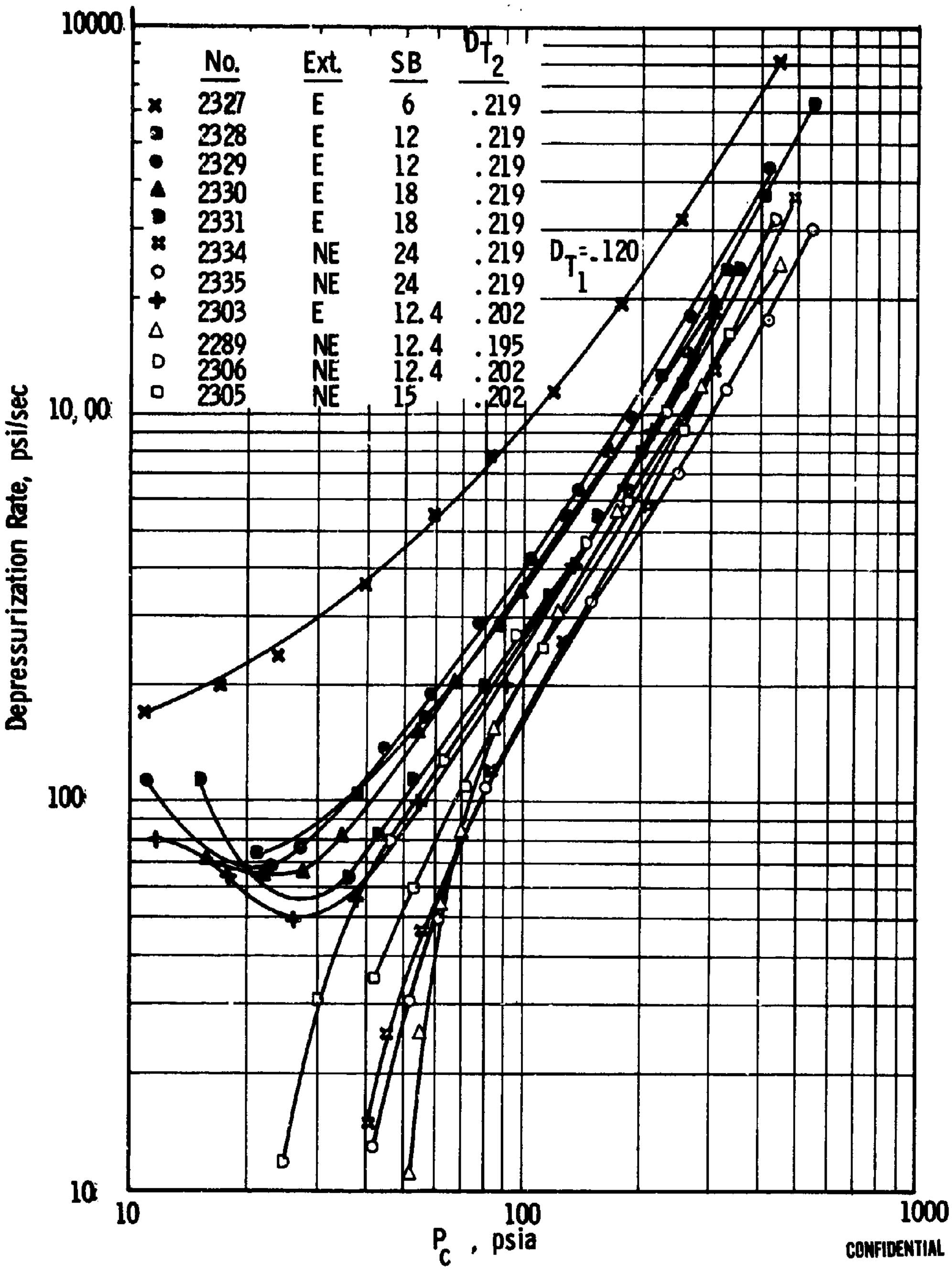

P-dot Extinguishability Screening Test Results (u)

Figure III-76

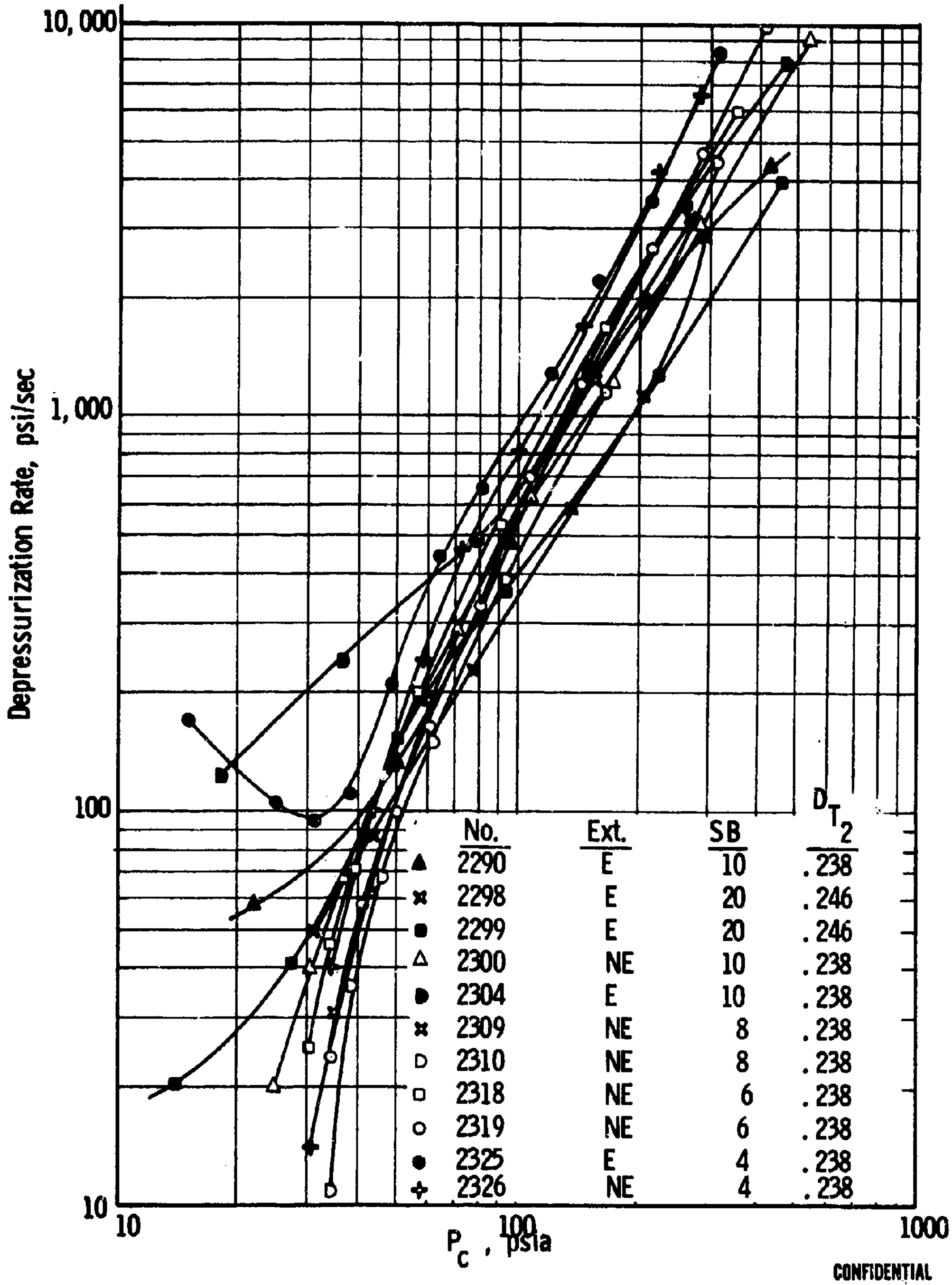

P-dot Extinguishability Screening Test Results (u)

Figure III-77

III, Technical Discussion (cont.)

C. SUBSCALE MOTOR DEVELOPMENT

(U) The objective of the subscale motor design and testing was to determine the validity of the approaches developed in the preliminary design effort through the fabrication and testing of these concepts on a subscale motor. A total of six tests employing 10KS-1000 motor hardware were conducted. The motors were cast with AAB-3216 propellant in an internal and end-burning grain configuration. The nozzle throat area and propellant burning surfaces were sized to provide a chamber pressure ranging from 300 to 400 psia. Average web duration was approximately 14.0 sec. The pintle and outer throat materials as well as several design features were selected on the basis of the preliminary designs that are available at this time. Different pintle housing and strut insulations are being utilized in order to evaluate the effectiveness of ablating and non-ablating materials.

(U) Because radiation of feedback from the pintle housing to the propellant surface was anticipated as being a major problem, these tests attempted to determine the amount of energy feedback that would be seen. Instrumentation was installed under the propellant at various locations along the length and around the circumference of the motor, and was exposed upon propellant burnout to record the temperature rise due to radiation feedback from the pintle housing.

(U) In addition to radiation feedback measurements the nozzles were instrumented in such a manner as to confirm the thermal analysis and to determine the heat-soak characteristics of the design.

(U) No attempt was made to extinguish these motors. The nozzle components from the first tests were visually examined for erosion and potential problem areas and then mounted on the next motors and refired. After these firings, the components were visually examined and installed on the final motors for firing. After the third set of firings the nozzles were visually examined and sectioned for thorough analysis. All thermal data were reduced and utilized in confirming or altering the fullscale design analysis as well as the design approach.

1. Subscale Motor Design

a. Nozzle Description

(U) The subscale nozzle of the CSR program was similar to the fullscale nozzle, namely, a shrouded pintle configuration as shown in Figure III-78. It consists basically of a pintle or inner throat mounted in a center housing which is supported by two struts located just upstream of the outer or conventional portion of the nozzle.

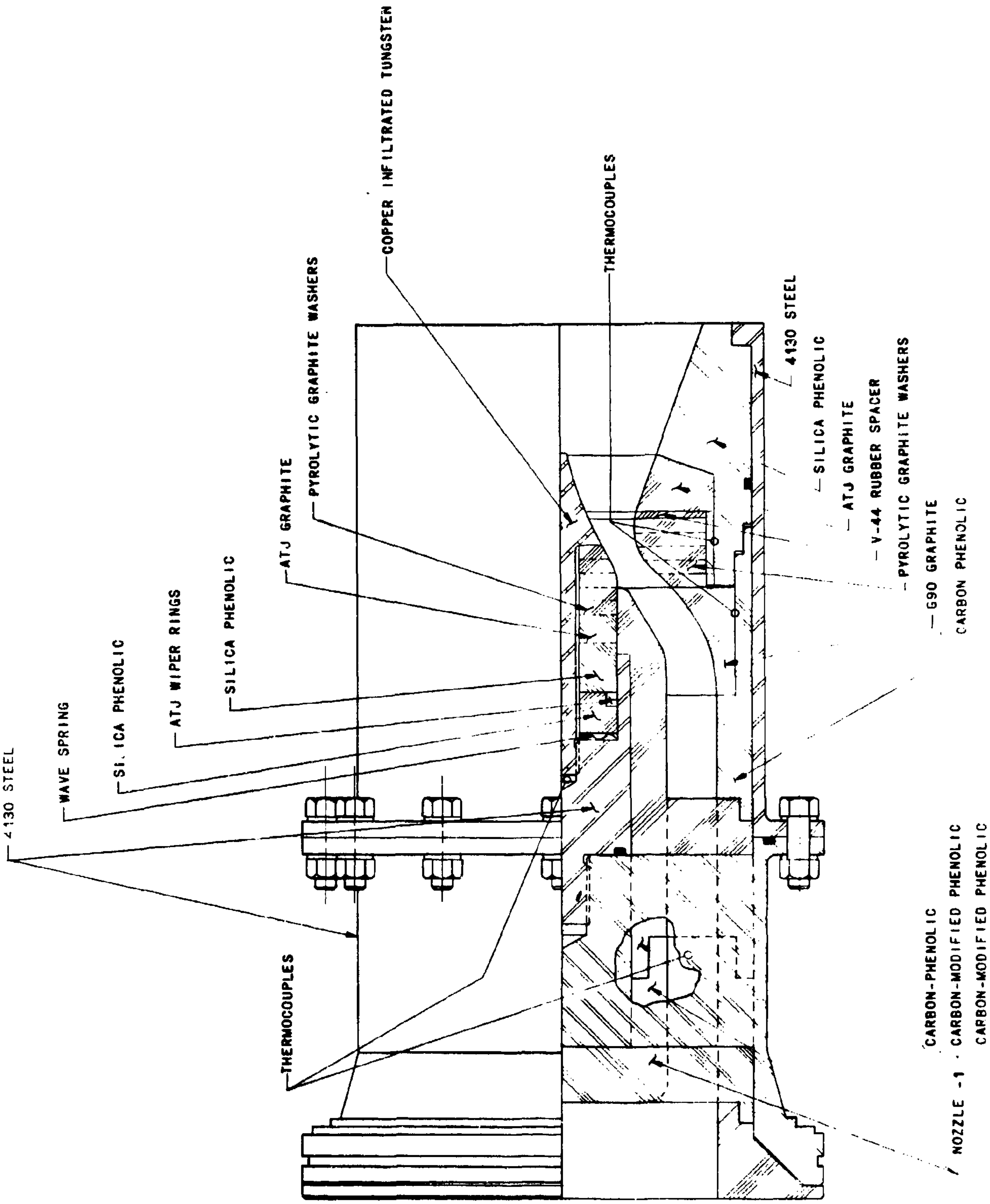

Nozzle Assembly - Subscale Test Motor Initial Design

Figure III-78

III, C, Subscale Motor Development (cont.)

(U) To facilitate fabrication and assembly, advantage was taken of the configuration and the assembly was made of two subassemblies. One subassembly, the upstream portion, consisted of the strutted housing with the pintle or inner throat mounted in it. The other subassembly downstream consisted of the conventional nozzle assembly or shroud. The two subassemblies were bolted together.

(U) The pintle or inner throat was constructed of edge-oriented pyrolytic graphite washers and an aft portion of ATJ graphite retained by a copper-infiltrated tungsten center bolt which was threaded into a 4130 steel pintle adapter. The adapter is recessed and partially encloses the pintle assembly. The adapter was in turn threaded into the centerbody of the strutted housing. Thermal insulation between the pyrolytic graphite washer stack and the main body of the pintle adapter was provided for by means of a molded silica phenolic spacer. Thermal expansion of the pyrolytic washer stack during firing was provided for by means of two wavy springs located between the silica phenolic spacer and the main body of the pintle adapter. Also, prevention of flame washing back into the wavy spring area was provided for by means of two ATJ graphite wiper seals located between the silica phenolic spacer and the ID of the recessed portion of the adapter.

(U) The center body and strutted housing as well as the pintle adapter and a portion of the pintle were protected from the motor combustion products by means of two molded pieces of insulation which overlap and join at the longitudinal midpoint of the struts. The upstream piece of housing insulation covered the upstream half of the housing center body, struts and outer housing while the downstream portion of the housing insulation covered the pintle adapter and a portion of the pintle as well as the downstream half of the center body, struts, and outer housing. In each instance the insulation consisted of a one-piece molding of the chosen material finish machined to the final configuration. Different materials were employed in the two different nozzle assemblies. In one configuration both the upstream and downstream insulators were made of a random fiber elastomer modified carbon phenolic. In the other configuration a straight random fiber carbon phenolic was used in the downstream piece while a castable rubber was employed in the upstream piece. The downstream subassembly or shroud portion of the nozzle was constructed in much the same manner as a conventional nozzle. The entrance section consisted of a parallel to center line carbon phenolic tape-wrapped tube in conjunction with a G-90 graphite entrance cap. In addition to being upstream of the G-90 cap, the carbon phenolic piece also backed it up and provided thermal insulation to the nozzle housing. The throat insert or nozzle outer throat consisted of edge-oriented pyrolytic graphite washers as in the pintle or inner throat. The pyrolytic washer stack was encased in a pyrolytic graphite cylinder which provides a thermal insulation ability as well as a

smooth, hard surface over which the pyrolytic washer stack may slide during thermal expansion. Thermal expansion of the pyro-stack was accommodated by use of a crush washer and the first section of the exit cone. The first section of the exit cone was an ATJ graphite ring and was referred to as the throat retainer. The entire throat assembly consisting of the pyro-stack, the pyro cylinder, the expansion washer and the ATJ graphite ring was backed up by and retained by one piece of molded chopped silica phenolic cloth which also served as the nozzle exit cone. The entire unit was in turn retained in a 4130 steel housing which as mentioned above was bolted to the upstream nozzle subassembly, (strutted housing).

b. Choice of Materials and Design Features

(U) Material selections were made in accordance with the objectives of the subscale portion of the program. Of primary importance was the evaluation of two different types of pintle housing and strut insulations. Because of the possible detrimental effects of radiation back to the propellant surface by an insulator that retains its char layer, materials were chosen that are expected to have a low char thickness. Also, since erosion was of great importance in this area, it was considered. Since it was difficult to prescribe the exit material that may meet both requirements it was decided to evaluate two different materials, one that has a definite known small char and one that had better erosion resistance. Therefore, a rubber was selected for the low char material. To improve erosion resistance, a carbon phenolic material was selected for better erosion resistance. Since the standard carbon and graphite phenolics are known for their deep hard char capability a variation of carbon phenolic with not as good erosion resistance but better charring characteristics was employed. The carbon phenolic selected employed an elastomer modified resin system. Stacked pyrolytic graphite washers were selected for the throat inserts on both the pintle and the outer throat since this was the material selected for the fullscale design.

b. Radiant Heat Measurement

(U) In order to attain thermal data on the possibility of ignition of the propellant remaining in the chamber after a pulse, two methods were considered. First, since the major mode of heat transfer inside the chamber after tailoff is by multiple radiation reflections, the obvious measurement method would be total intensity radiometer. However, the problem of installation of such a device to view inside a chamber together with the possibility of clouding any lens system with aluminum oxide provide a most formidable problem. Thus, this method was discarded in favor of a direct temperature measurement method.

(U) Thermocouples were designed and fabricated for the purpose of measuring the radiation feedback from the pintle housing. These thermocouples employed a rugged construction necessary to withstand the vibrational environment experienced in a rocket motor firing. They consisted basically of a thin platinum disk, 5 mil thick with two separate chromel-alumel wires spot-welded on the upper surface. This assembly, which was covered with a thin coat of Pliobond was mounted on a V-44 rubber insulator which is in turn mounted in a 0.5-in.-dia stainless-steel housing. The entire assembly, shown in Figure III-79, is constructed in such a manner as to be pressure sealed.

(U) Two 10-KS-1000 chambers were modified in such a manner as to accept the instrumentation per Figure III-80. A series of 0.5-in.-ID Swagelok fittings, were welded along the length and circumference of the chamber and the chamber wall has been bored through. When the instrumentation was inserted into the fittings, butted up against the back side of the propellant grain, and tightened according to the manufacturers recommendations, a 2000-psi sealed assembly was attained.

(U) Additional thermocouple instrumentation was installed in the nozzle assemblies for the purpose of confirming the thermal analysis and determining the heat soak and cool-down characteristics of the subscale design. Five thermocouples were installed in each assembly. Spring-loaded thermocouples were used in order that contact between the thermocouple and the heat source would be maintained throughout the firing and during cooldown thus allowing for component movement due to vibration and thermal growth. The pintle adapter and strutted housing were modified in such a manner as to place a spring-loaded TC probe against the aft end of the copper-infiltrated-tungsten bolt. The other four thermocouples were located behind the G-90 entrance cap and behind the outer pyrolytic graphite washer stacked throat in each of two planes, either in line with the struts or 90° away from them.

(U) All four thermocouples were spring loaded against the material desired by means of an 0.125-in.-dia stainless-steel thermocouple probe assembly. These assemblies were inserted through 0.125-in.-dia holes drilled through the backup insulators and held in place by means of Conax pressure fittings welded to the nozzle housings.

2. Subscale Motor Test Results

(U) The objectives of this program were twofold: (1) the determination of materials for use on a pintle nozzle subjected to multiple firings, and (2) the determination of the radiation feedback to the propellant grain from the hot nozzle-components after extinction. The program plan for the subscale motor program was to design two nozzles using different materials

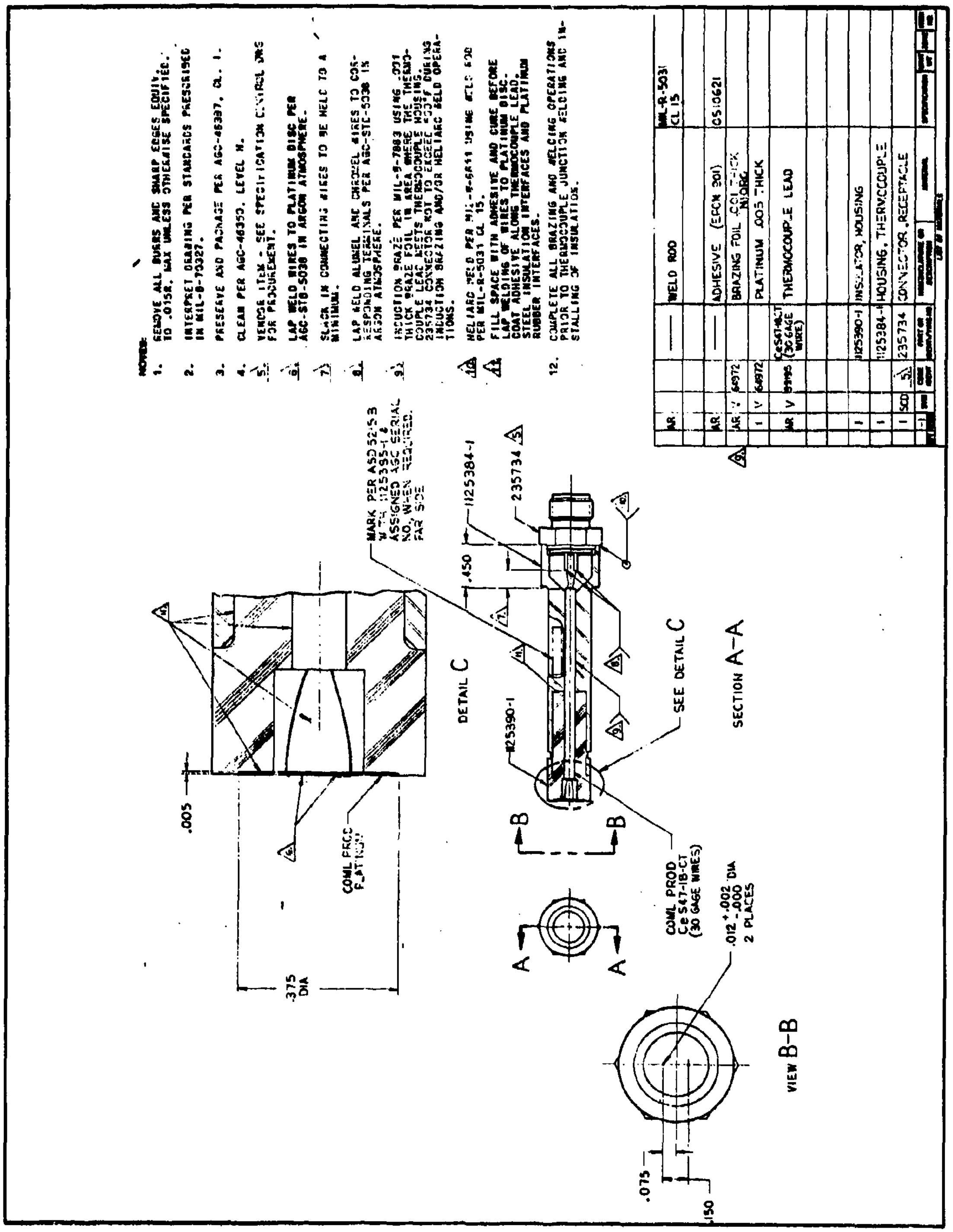

Thermocouple Assembly

Figure III-79

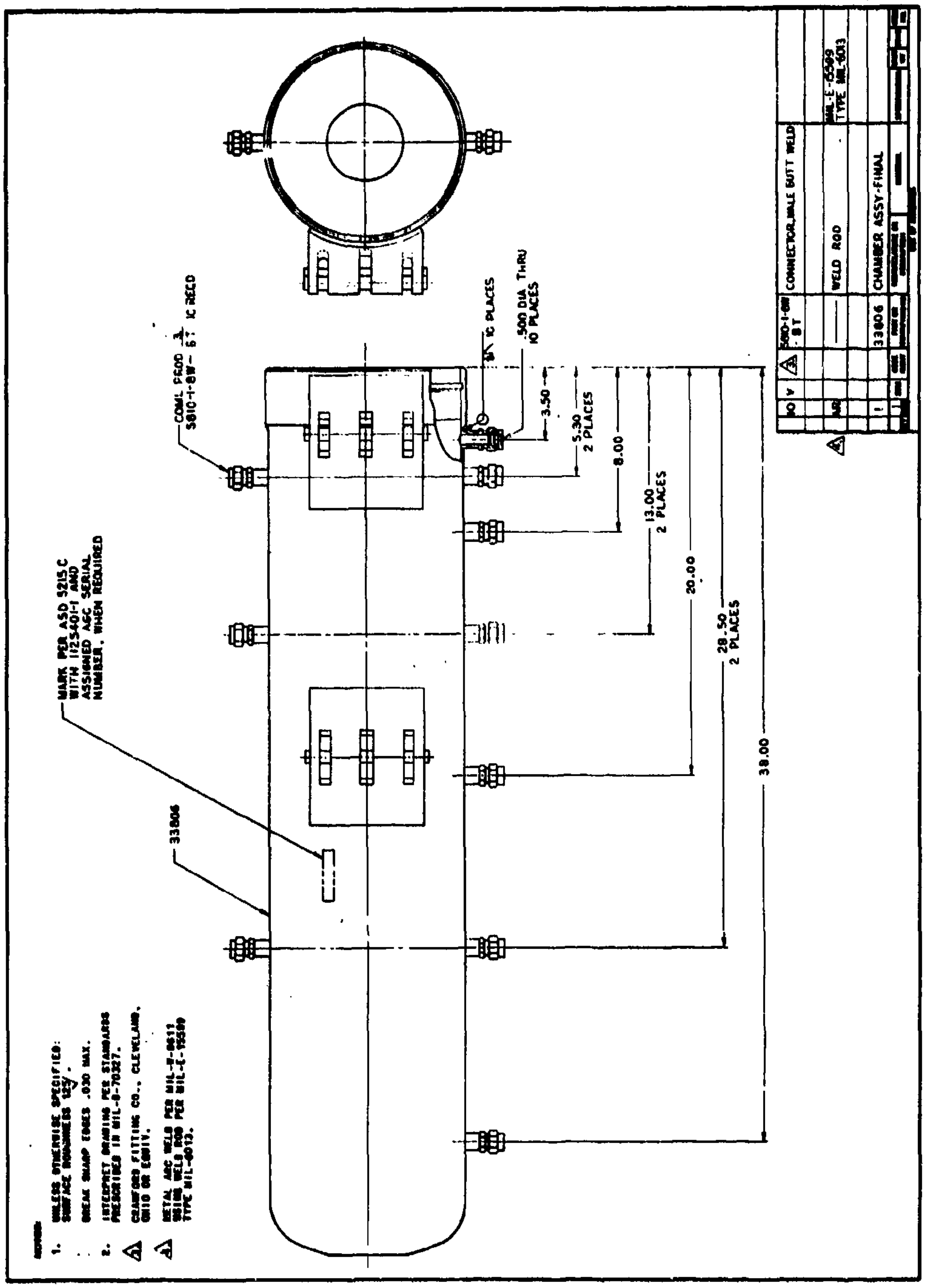

Instrumented Chamber

Figure III-80

and fire each nozzle three times to determine the relative performance of each material when subjected to multiple firings. Two of the motors were equipped with thermocouples in the chamber wall insulation to determine the radiation feedback after propellant burnout. Because of failures of the pintle support rod, this plan was modified from the original plan to test fire two nozzles three times each, with the following result: one nozzle outer throat was fired a total of four times, the second nozzle outer throat was fired a total of two times, one pintle was fired twice, and one pintle was fired once. The following sections will describe in detail each of the tests, the nozzle components tested, and the data acquired.

a. Subscale Motor Test CSR-DN-01S-BH-001

(U) The first subscale motor to be tested was provided with a subscale fixed pintle nozzle SN 1, PN 1125233-3 as shown on Figure III-81. This nozzle was equipped with the following material selections:

Component	Material
Insulator, Housing	MX 4925, Random Fiber Carbon Phenolic
Insulator, Housing Fwd	Coast - Elastomer Mod., Carbon Phenolic
Insulator, Housing Aft	MXCE-280 - Elastomer Mod., Carbon Phenolic
Entrance Cap	G-90 Graphite
Insulator, Entrance Cap	MX-4926 Parallel to Centerline Carbon Phenolic
Exit Cone	MX-2625, Silica Phenolic
Retainer, Throat	ATJ - Graphite
Throat	Pyrolytic Graphite Washers
Spacer, Throat	Uncured V-44 Rubber
Insulator, Throat	Pyrolytic Graphite Cylinder
Pintle Pilot (Support)	Copper Infiltrated Tungsten
Throat, Inboard (Pintle)	Pyrolytic Graphite Washers
Spacer	Silica Phenolic
Pintle Spacer	ATJ - Graphite

These components were assembled as shown on Figure III-81 and provided with thermocouple instrumentation to verify the thermal environment, both during and after the firing. One thermocouple was spring-loaded behind the copper-infiltrated tungsten pintle support rod (TN-1); two thermocouples were located behind the G-90 graphite entrance cap (TN-2 and TN-3), one in line with a strut, and one 90° from a strut; two thermocouples were located behind the outer throat (TN-4 and TN-5), one in line with a strut and one 90° from the strut; and one thermocouple was located in the strut. The numbering system of the thermocouples in this nozzle is consistent with the numbering system used for the entire subscale motor program; thus on the remainder of the tests to be discussed, the location of the thermocouples will not be reiterated.

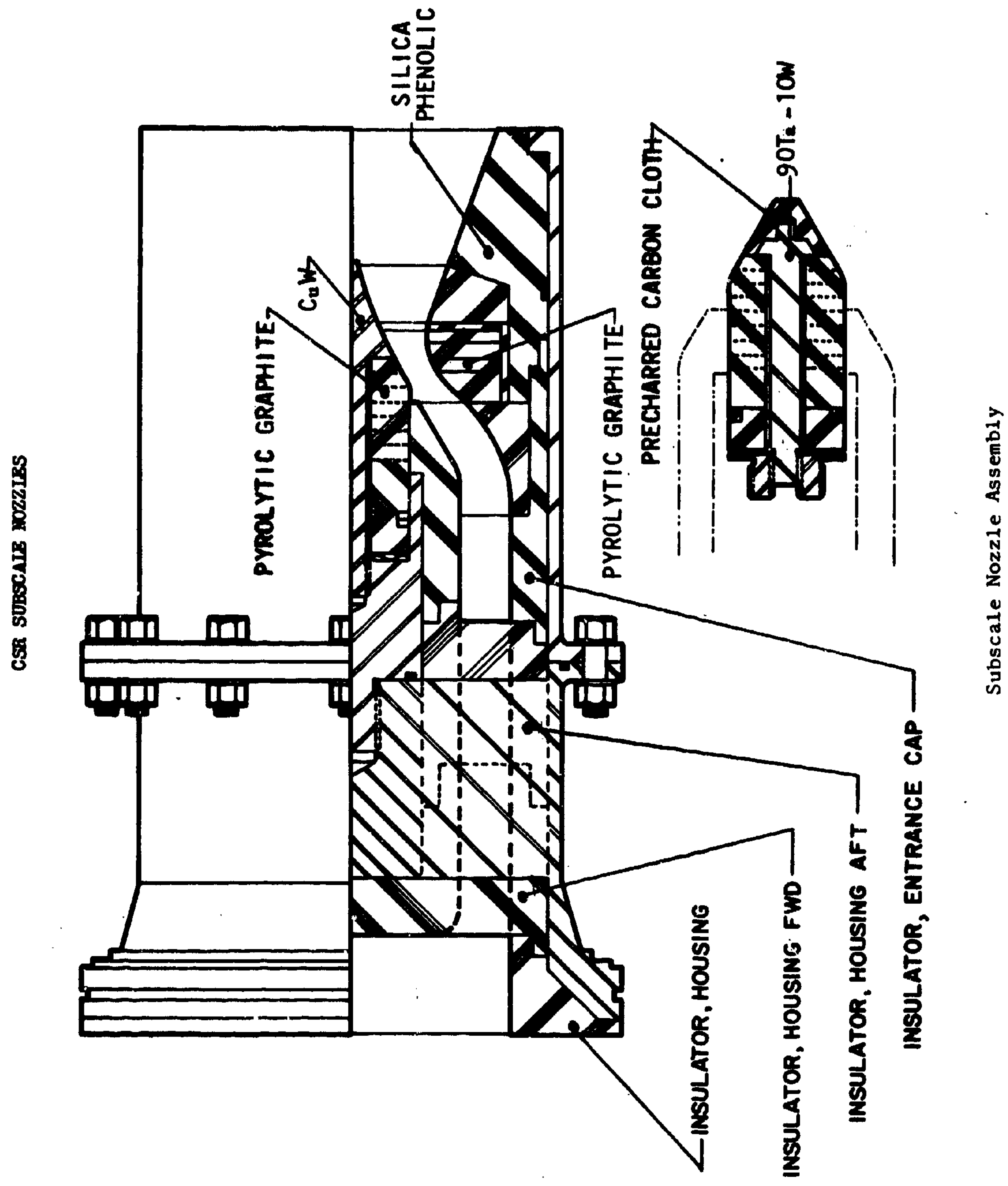

Figure III-81

(U) In addition to the thermocouples, the motor was instrumented with two pressure pickups located in the igniter plenum chamber and in one load cell to measure the thrust. The motor setup in the test stand is shown on Figure III-82 and -83. To avoid the postfire burning of the insulation materials, a 'halo' of nitrogen gas was formed by a nitrogen ejector ring mounted to the aft end of the nozzle. The nitrogen was activated at motor tailoff and provided a drop of less than one-half psi in the motor, effectively blocking the influx of oxygen from the atmosphere, and thus eliminated almost all of the postfire combustion of the plastic materials normally associated with a sea level static test firing. This ring covered with silicon rubber insulation and connected to the flex hose, can be seen on Figures III-82 and III-83 on the aft end of the nozzle. The entrance section of the nozzle and the aft end of the nozzle are shown on Figures III-84 and III-85, respectively, prior to the first test-firing.

(U) Motor CSR-DN-01S-BH-001 was test-fired 20 October 1965. Ignition was normal, with a slight ignition spike to a maximum pressure of 555 psia at 0.07 sec, dropping to a nominal pressure of 445 psia at 0.20 sec at igniter burnout. Web burning following igniter burnout was normal, indicating no erosion of the throat until the T plus 5 sec, at which point the pintle ejected, causing a pressure drop to 275 psia. Burning was regressive from this point until web burnout at T plus 9.0 sec. The pressure-time trace and the thrust-time trace of this motor are shown on Figure III-86. Instrumentation continued to run for a total elapsed time of 9.0 min to check the heat soak of the nozzle components. The temperature-time history for the six thermocouples on this nozzle are shown on Figure III-87. The significance of the temperatures will be discussed in more detail in the section on thermal analysis.

(U) Review of the thermal analysis and the structural analysis of the pintle pilot (support rod) indicated that a positive margin of safety existed for this part; however, the margin was extremely slight. The remaining portion of the pintle pilot was examined and subjected to a pull test to establish the quality of the material. The results of this test indicated that the ultimate tensile strength of the material was only 76,100 psi, and the elongation was 1 1/2% in a 1.0-in.-long specimen. These are somewhat below the expected values, accounting for the failure in this part.

(U) Visual analysis of the remainder of the nozzle yielded the following information:

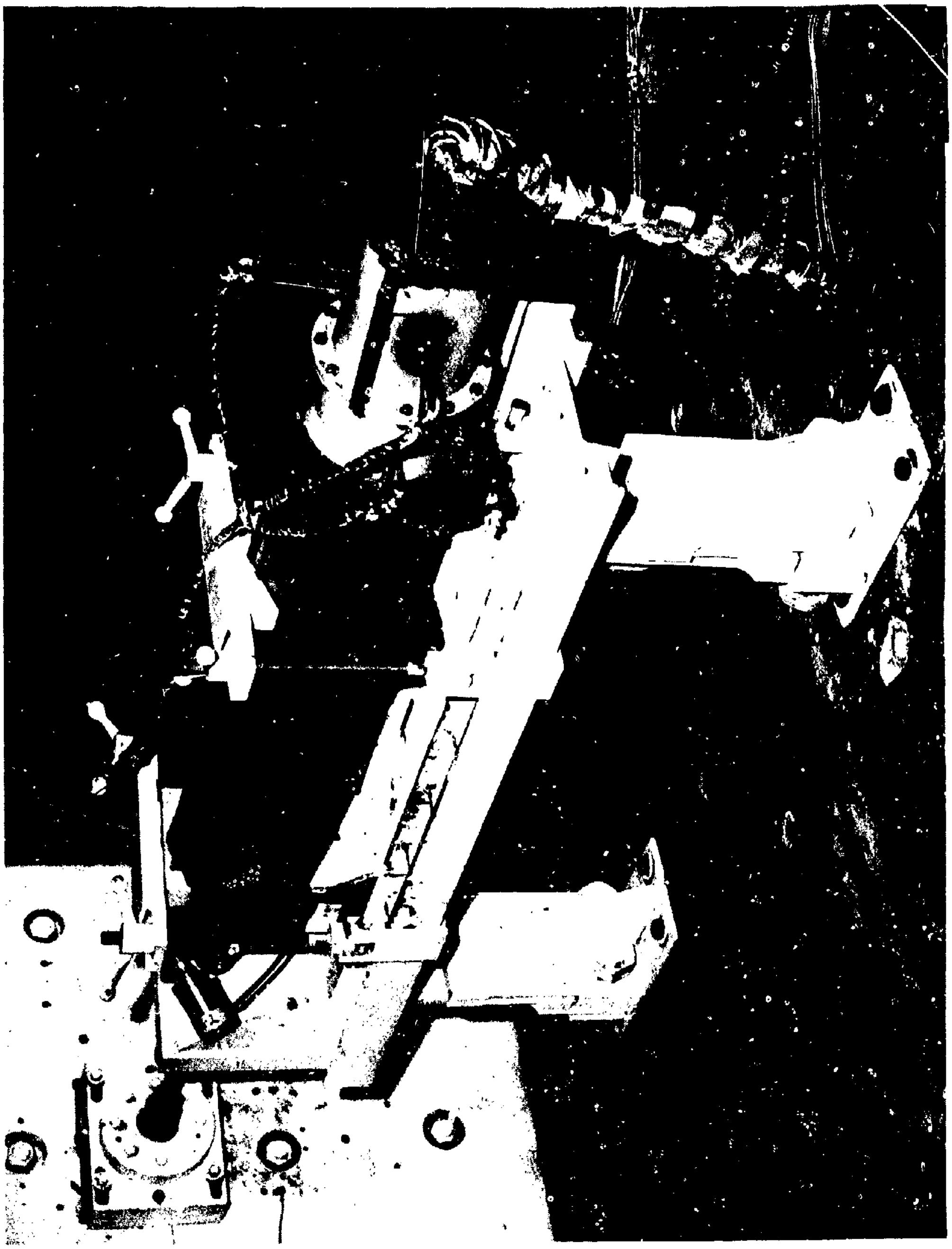

Test Setup, 3/4 Aft View, CSR-DN-01S-BH-001, Prefire

Figure III-82

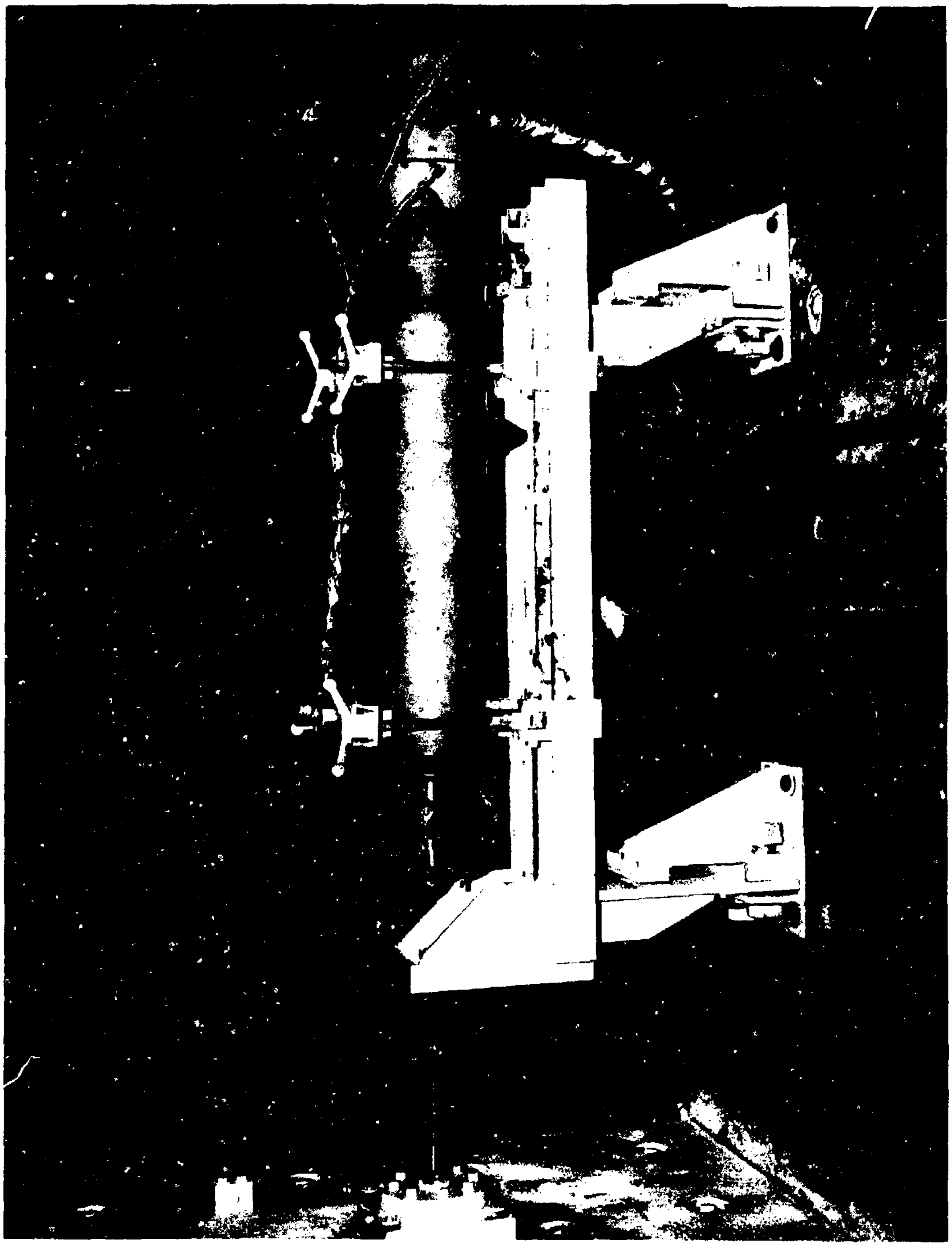

Test Setup, 270° View, CSR-DN-01S-BH-001, Prefire

Figure III-83

Entrance Section, CSR-DN-01S-BH-001, Prefire

Figure III-84

Nozzle Closeup, CSR-DN-01S-BH-001, Prefire

Figure III-85

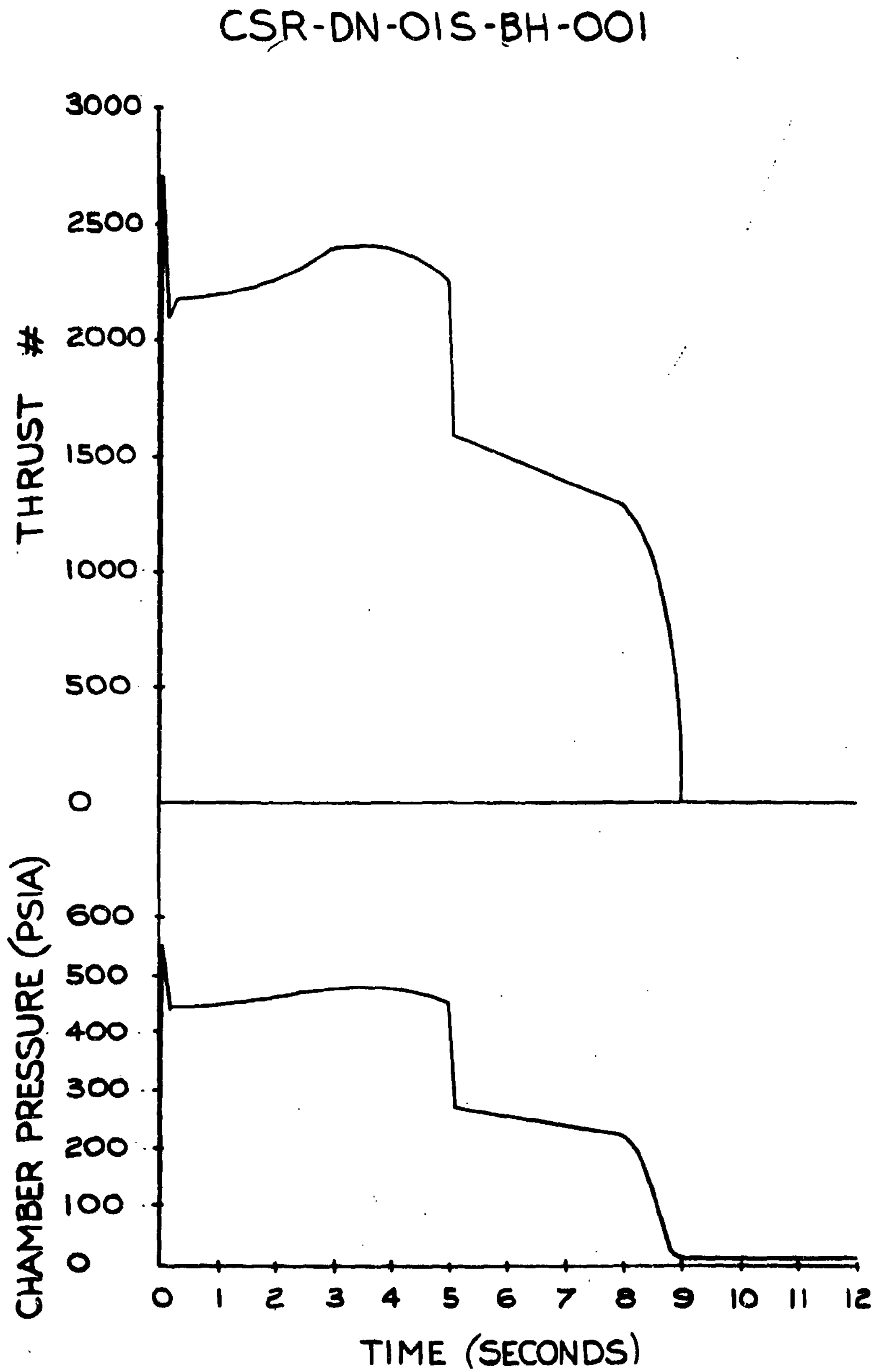

Pressure-Time and Thrust-Time History, CSR-DN-01S-BH-001

Figure III-86

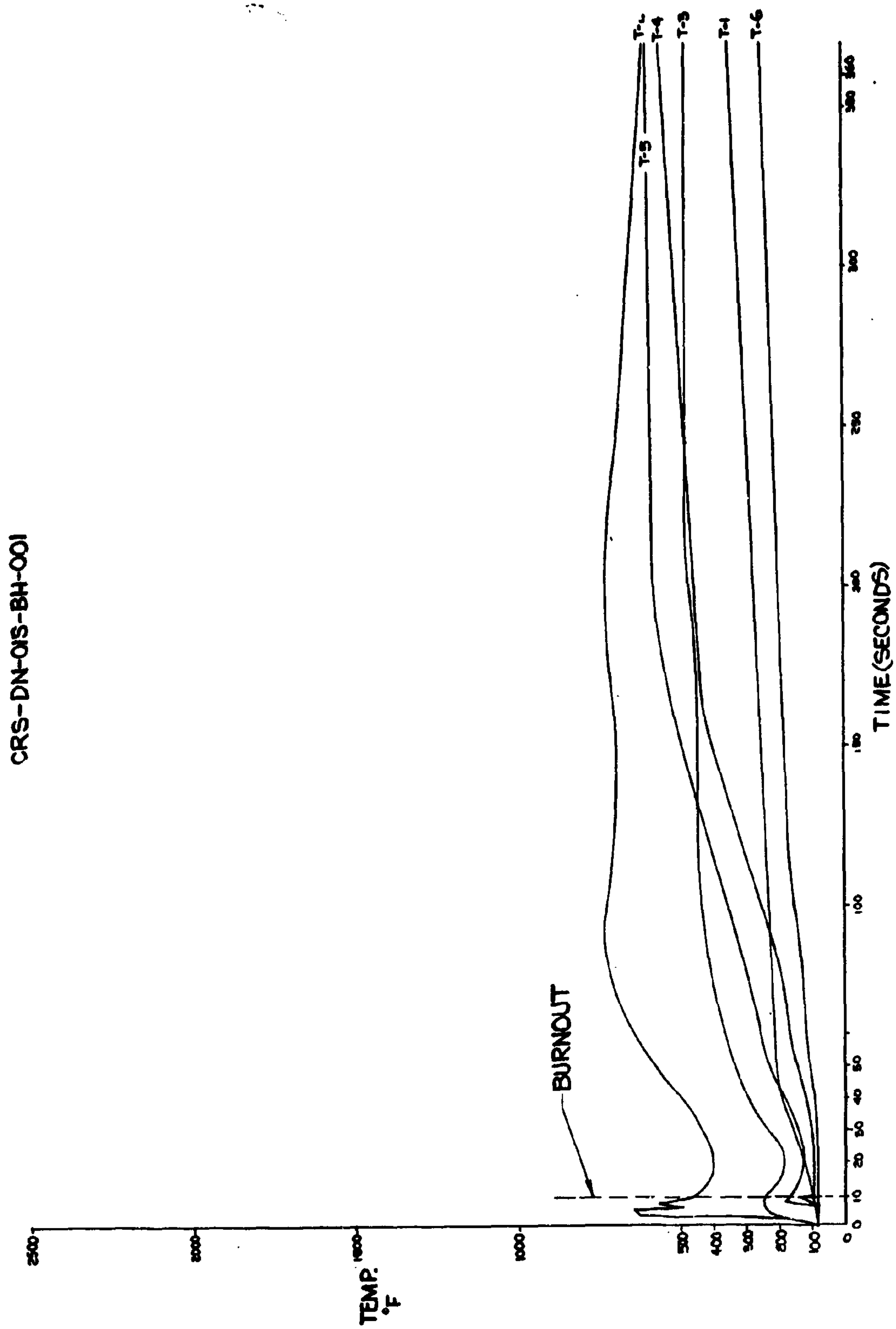

Temperature-Time History, CSR-DN-01S-BH-001

Figure III-87

Component	Condition
Insulator, Housing Aft	Severely cracked, 1/16-in.-wide by 1/2-in.-deep all around the circumference
Insulator, Housing Fwd	Slightly cracked on fwd face; some bubbles
Insulator, Housing	Slightly delaminated
Insulator, Entrance Cap	Some delamination
Entrance Cap	Excellent condition; feather edge broken off 180°
Throat	Excellent condition; no delaminations; no erosion

Because the pintle pilot was broken and had separated at the interface of the inner throat insert, all of the pyrolytic graphite washers had ejected with the pintle pilot rod end. The graphite and the silica phenolic spacers were intact, with no sign of heat damage. The wavy spring behind the silica phenolic was still in a springy condition, with no permanent set. The paint on the housing behind the G-90 graphite entrance cap was scorched, indicating that temperatures in excess of 300°F had been seen in this area. On future tests, it was decided to install a thermocouple on the outside of the housing behind the entrance cap to determine the exact temperatures experienced in this area. This thermocouple will be designated as TN-7 on tests 002 through 006, inclusive.

(U) Although this motor was only fired for 9 sec, and the last four seconds were at a relatively low pressure, the severe cracking of the aft housing insulation indicated that this will be a problem area in the design of the heavyweight motor nozzle. For the refiring of nozzle SN-1, it was decided to machine-off the cylindrical portion of the aft housing insulator back to the struts and to replace it with a cylinder of MX-4926 carbon phenolic wrapped 30° to the center line. To avoid a recurrence of the pintle pilot failure, the pintle pilot was replaced with one fabricated from 90% tantalum--10% tungsten and protected on the aft end by a cap of silica phenolic. No changes are anticipated in the inner throat area because the outer throat performance indicated that pyrolytic graphite washers would perform successfully in this area. All other components on nozzle SN-1 were considered in good enough condition to be refired.

b. Subscale Motor Test CSR-DN-01S-BH-002

(U) The second subscale motor was provided with nozzle SN-2, PN 1125233-5-Modified. This nozzle was modified because it was equipped with the same copper-infiltrated tungsten pintle pilot as nozzle SN-1 that failed in this area. By reanalyzing this component, it was determined that a hole drilled axially in the end of the pintle pilot to a depth of 2.5 in. at a

diameter of 0.125 in. would probably relieve the thermal stress portion of the load sufficiently to allow the component to withstand the test firing. This modification was initiated because it was impossible to disassemble the component without completely destroying the pintle. Because of the questionable quality of the copper-infiltrated tungsten material, this component was given only a moderate chance of success. Other areas of the nozzle in which the materials differed from those of nozzle SN-1 were:

Component	Material
Insulator, Housing Aft	MX-4925, Random fiber carbon phenolic
Insulator, Housing Fwd	SD-850-15D Rubber cast in place
Insulator, Housing	SD-850-15D Rubber cast in place

These components were assembled and provided with the same thermocouples as was Motor 001. Thermocouple TN-7 was also placed on the outer case structure for the reasons previously discussed. This motor was set up in the test stand similar to Motor 001, and the nitrogen halo was also provided as before. The remainder of the exposed copper-infiltrated tungsten pintle pilot was covered with a thin layer of Shaugeenan to reduce the initial thermal shock.

(U) Motor CSR-DN-01S-BH-002 was fired 28 October 1965. Ignition was normal with the maximum ignition spike pressure of 600 psia occurring at 0.08 sec. At igniter burnout (0.200 sec), the chamber pressure stabilized at 445 psia. The chamber pressure followed the surface area web relationship, indicating that the throat area remained constant throughout the test. Total web action time was 8.00 sec as expected for the pressure range of the motor. The pressure-time and thrust-time plots are shown on Figure III-88.

(U) Since the data from this test indicated that the motor performed as expected, the instrumentation was permitted to record for a total of 16.0 min. The temperatures from the seven thermocouples on this motor followed very closely to the temperatures predicted from the thermal analysis. The temperature-time history is shown on Figure III-89. The results of this test will be discussed in more detail in the section on thermal analysis.

(U) Visual analysis of the nozzle after the test indicated that the drilled hole in the pintle pilot apparently relieved the thermal stresses sufficiently to withstand the maximum stress time period and to survive the firing. Attempts to disassemble the pintle stackup proved futile without destroying the components, so it was decided to proceed with the retesting of this pintle without a more detailed inspection of the pintle pilot support rod. Visual analysis of the remainder of the nozzle yielded the following information:

CSR-DN-01S-BH-002

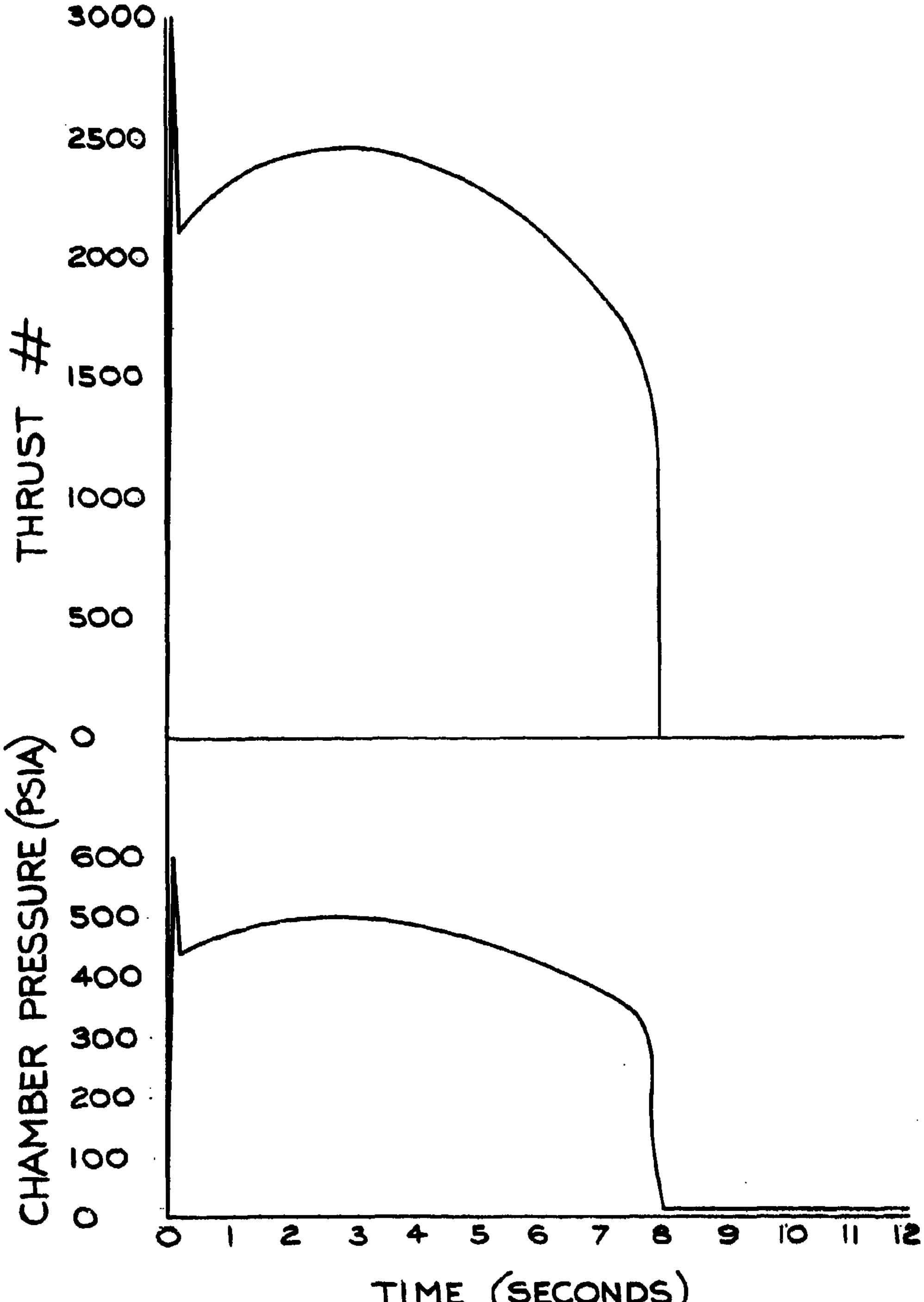

Pressure-Time and Thrust-Time History, CSR-DN-01S-BH-002

Figure III-88

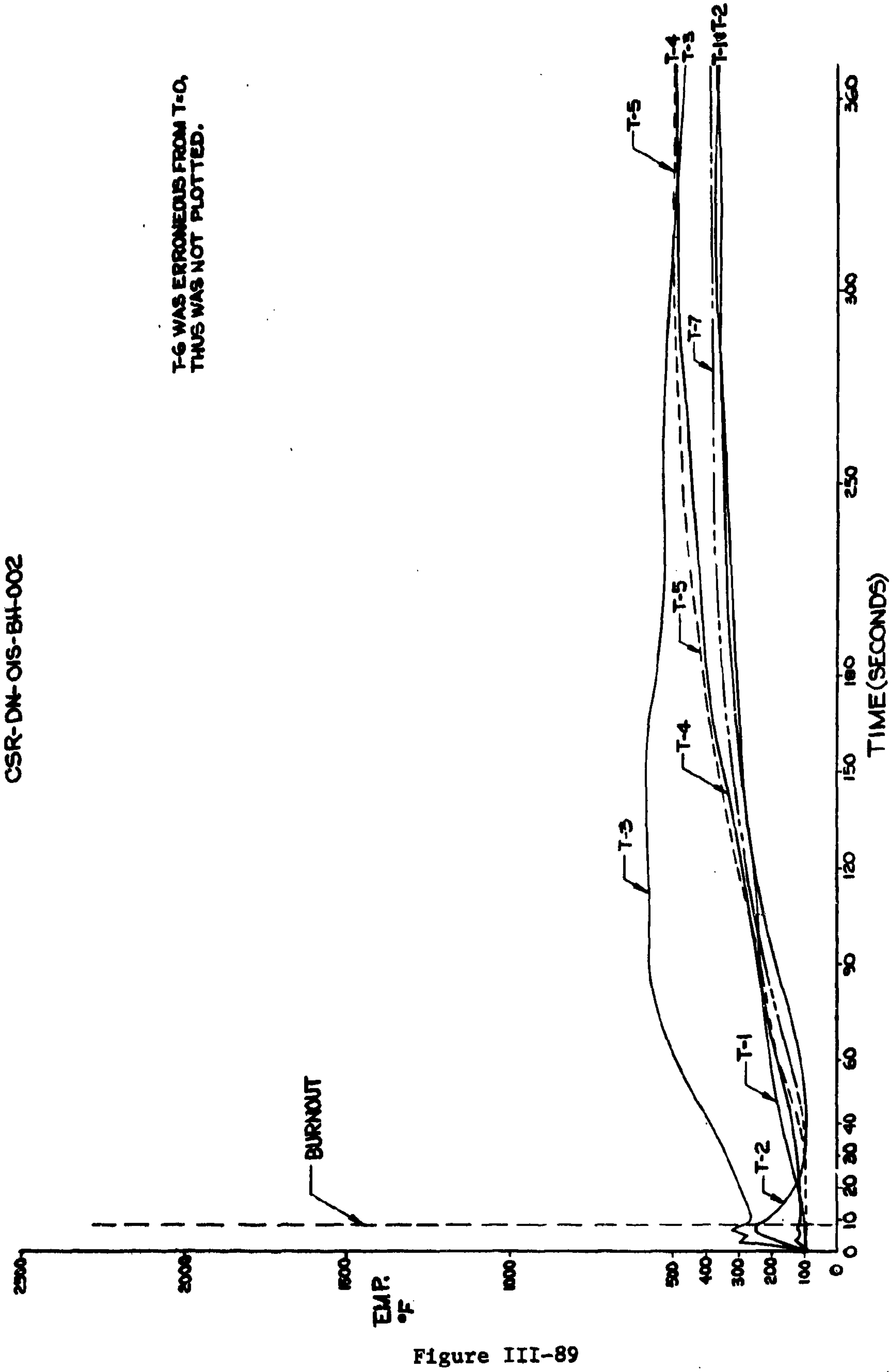

Temperature-Time History, CSR-DN-01S-BH-002

Figure III-89

Component	Condition
Throat, Inboard	The pyrolytic graphite washers were in excellent condition with no delaminations or erosion. Each washer was free to rotate.
Insulator, Housing Aft	Negligible erosion on this component; however the same cracking was in evidence on the cylindrical section covering the pintle.
Insulator, Housing Fwd	Deep gouging and very uneven erosion. Rate of erosion over 30 mils/sec.
Entrance Cap	Excellent condition; no erosion of graphite or cracking.
Throat	No cracking, delamination, or erosion of pyrolytic graphite.

(U) This motor was fired at full chamber pressure for the full duration of the test, with no major problems of any type experienced by the nozzle. One point of interest was the hard char formed on the SD-850-15D rubber. This material has performed very well in motor cases as chamber wall and aft closure insulation; however it is not considered usable in the pintle nozzle as strut housing insulation because of the severe erosion. Neither the insulator, housing aft, section that covers the pintle nor the insulator, housing forward was considered reusable. Thus these parts were removed by machining and replaced with Gen-Gard V-44 rubber. Since the pintle could not be inspected more closely, it was determined that the only method of determining the reuse properties of this component was to refire it as-is.

c. Subscale Motor Test CSR-DN-01S-BH-003

(U) The third subscale motor was provided with the same nozzle fired successfully on Motor 001 with the changes described in the discussion of Motor 001. To repeat, these changes were the replacement of the pintle pilot with one fabricated from 90% tantalum--10% tungsten and provided with a silica phenolic cap to limit the oxidation of the 90-10 alloy, and the replacement of the cylindrical section of the insulator, housing aft with a carbon phenolic tape-wrapped component wrapped 30° to the nozzle center line. The buildup of the new pintle assembly is shown on Figure III-90 with the fully assembled pintle shown on Figure III-91. The nozzle assembly is similar to that shown on Figure III-81 with the exception of the pintle pilot and pintle end-cap components. This nozzle was attached to Motor 003 in a manner similar to the first two nozzles and set up in the same test stand with the nitrogen halo. On this motor, however, thermocouple TN-1 was nonoperative because of breakage within the nozzle. Thermocouples 2 through 6, inclusive, were repositioned to place them in more intimate contact with the flame liner

90 Tantalum--10 Tungsten Pintle Buildup

Figure III-90

Figure III-91

backup materials and eliminate the thermal lag through the interface between the flame liner materials and the insulators. In addition, all the thermocouples were rotated so that they were 45° from the plane of the struts.

(U) Motor CSR-DN-01S-BH-003 was test-fired 11 November 1965. This motor fired as scheduled with no anomalies. The total firing duration was 8.0 sec, with the maximum pressure attained being 475 psia at 0.10 sec. The pressure-time history followed the web-surface area, thus indicating that the nozzle throat area remained constant. The pressure-time and thrust-time histories are shown on Figure III-92. The thermocouple instrumentation was permitted to record for a full 20.0 min to attain the maximum heat-soak history of the nozzle. These data are shown graphically on Figure III-93 and discussed more fully in the section on thermal analysis.

(U) Visual analysis of the nozzle components after the test indicated that all components had performed successfully. The only part requiring replacement is the silica phenolic pintle pilot cap. This is merely an oxidation-retardant; thus it was expected to erode and/or melt during the test. One major point of interest is the performance of the 30° angle-wrapped carbon phenolic section which was used to replace the cylindrical segment of the insulator, housing aft. This component, shown in Figure III-94, was in excellent condition after the test, with no evidence of the cracking that had been present on the first two motor tests. The slight delamination of this component in evidence near the struts is due to an overwrap of carbon phenolic parallel to the nozzle center line. This overwrap was used as a fix to bring the billet from which this component was fabricated up to the required outside diameter. This was not a designed-in feature, but only an improvisation to meet the firing schedule. It can also be seen on this figure that the pintle throat insert (pyrolytic graphite washers) is in excellent condition as is the MXCE-280 aft-housing insulation. It should be noted that this is the second firing on this aft-housing insulation; yet there does not appear to be any noticeable erosion or cracking of this component.

(U) The forward housing insulation, Coast's elastomer modified carbon phenolic material, performed very well with only slight gouging in the areas of the struts. This material formed a very hard char during the first test, which apparently remained intact during the second exposure. On this test, as on Motor 001, there was no noticeable change in the G-90 entrance cap and only slight delamination of the insulation material upstream of the entrance cap. The feather edge of the G-90 graphite which had broken off over an arc of 180° during the first firing was unchanged by the second exposure. The ATJ graphite outer throat support was slightly gouged downstream of the outer throat; however, this component is in good enough condition to be refired.

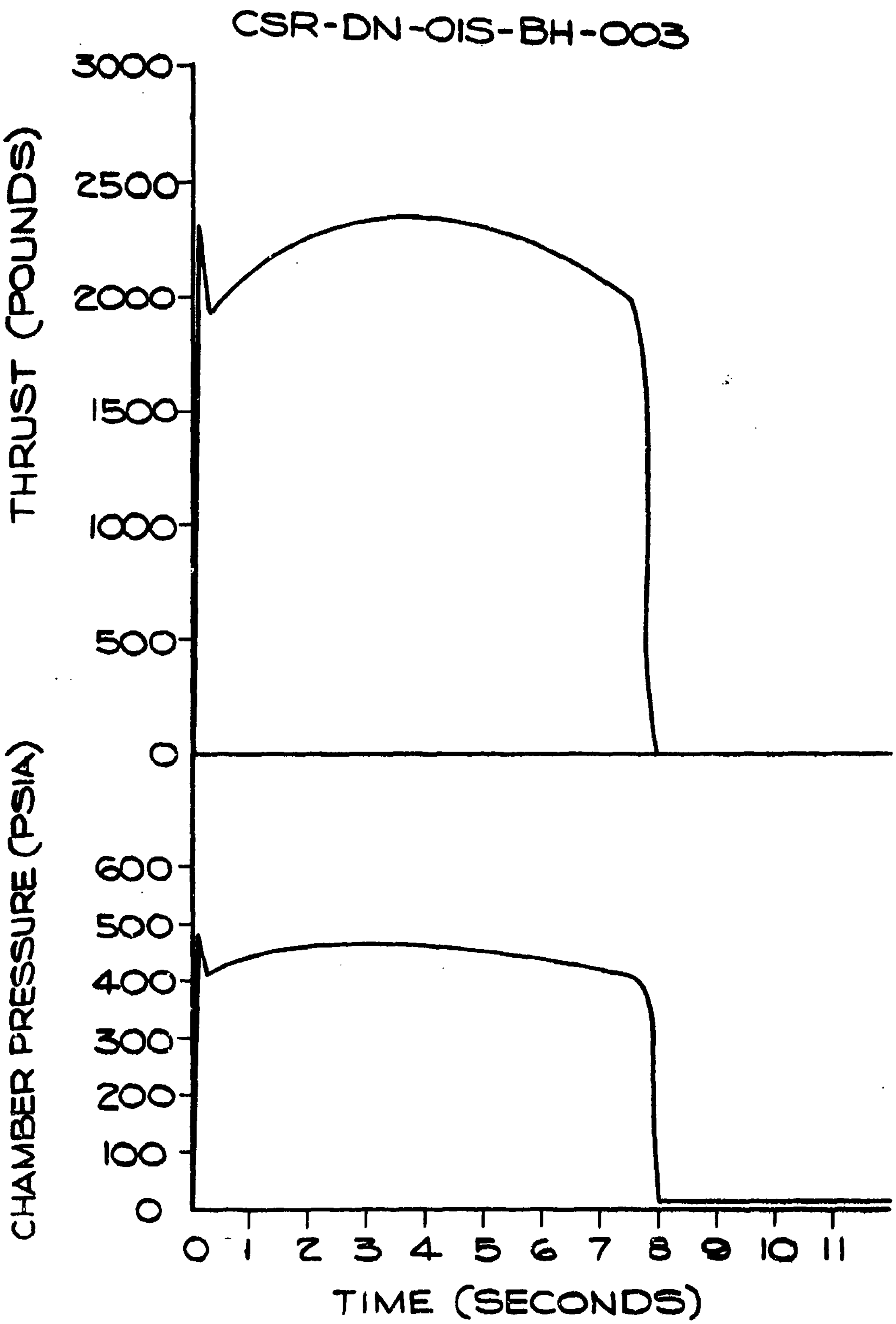

Pressure-Time and Thrust-Time History, CSR-DN-01S-BH-003

Figure III-92

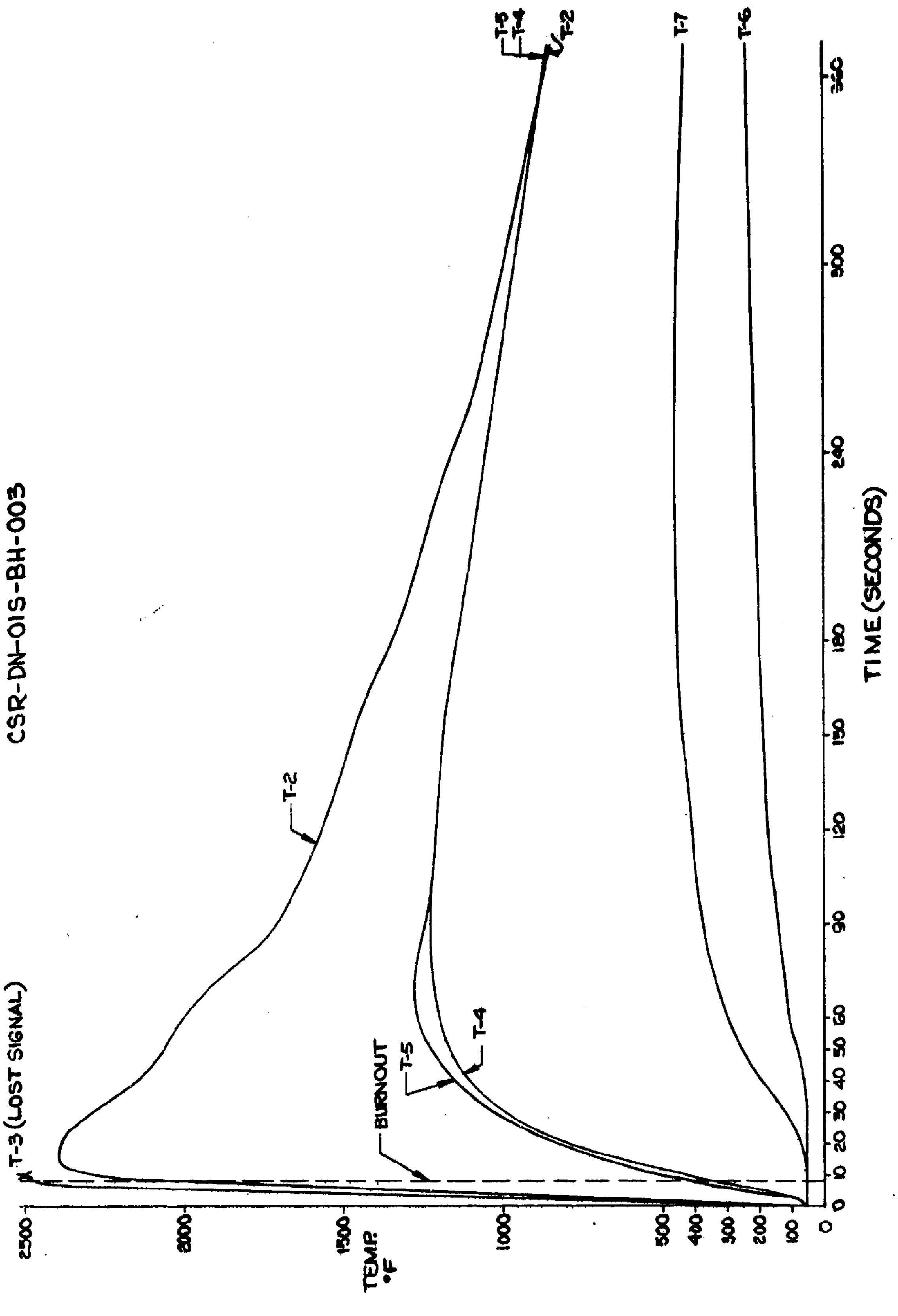

Temperature-Time History, CSR-DN-01S-BH-003

Figure III-93

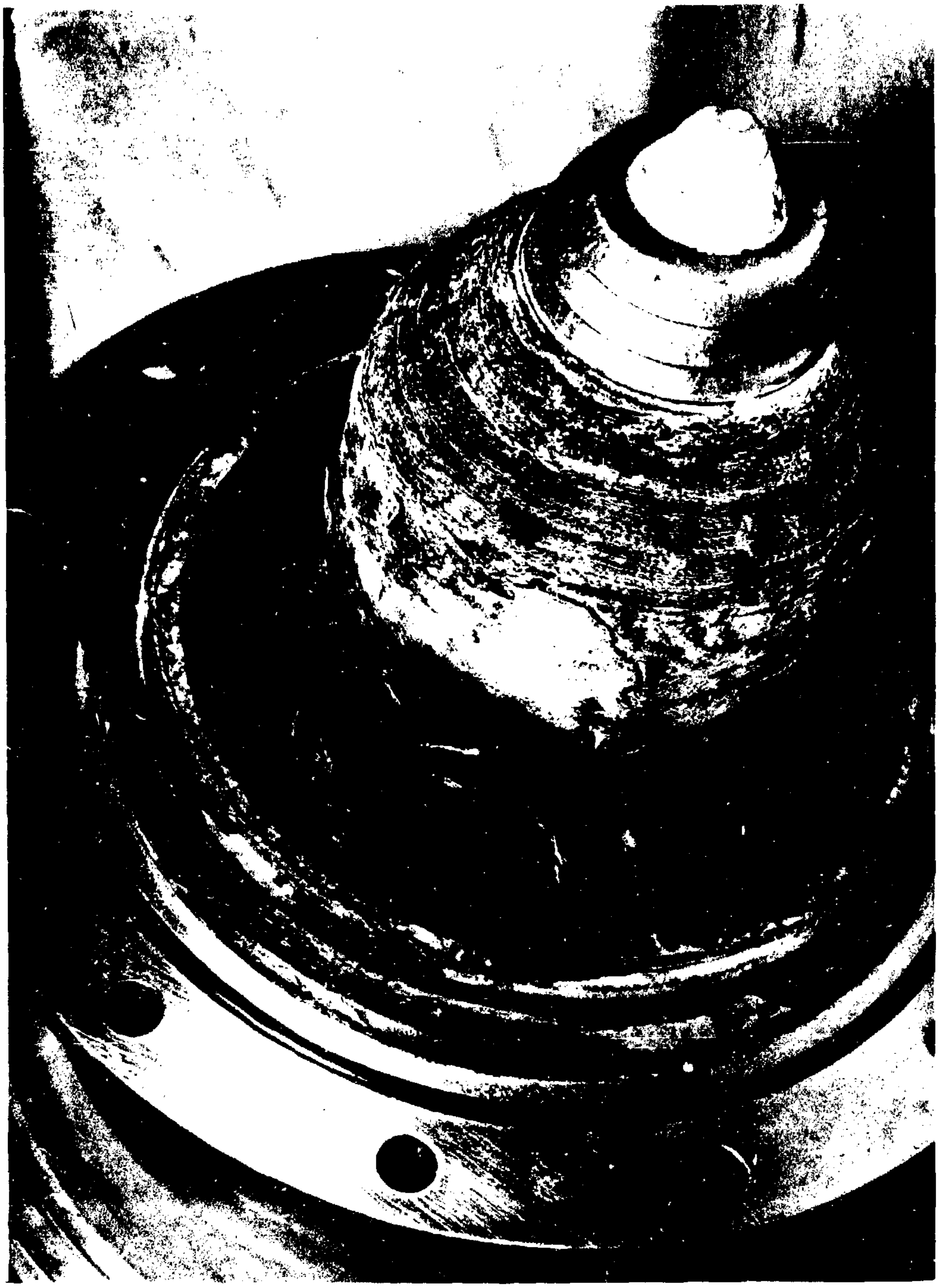

Postfire Pintle Assembly, CSR-DN-01S-BH-003

Figure III-94

(U) On the basis of this visual analysis, it was determined that this nozzle could be refired with the replacement of the pintle pilot cap only. All other components were considered reusable.

d. Subscale Motor Test CSR-DN-01S-BH-004

(U) This motor was fitted with the refurbished version of nozzle SN-2, as fired on Motor 002. Refurbishment of nozzle SN-2 consisted of replacement of the cast SD-850-15D rubber insulation with V-44 rubber and the replacement of the cylindrical section of the aft-housing insulator with V-44 rubber. The exposed face of the copper-infiltrated tungsten pintle pilot was reinsulated with Snaugeenan-SS for thermal shock protection as in Test 002.

(U) Subscale Motor CSR-DN-01S-BH-004 was tested 11 November 1965. Ignition was normal and smooth, with a maximum pressure of 445 psia experienced at 0.1 sec. The test progressed normally for 4.2 sec, at which time the pintle ejected, dropping the chamber pressure to 225 psia and extending the test duration for 10.3 sec. The pressure-time and the thrust-time histories for this test are presented on Figure III-95. Thermocouple instrumentation was permitted to record for over 19 min to determine the heat-soak characteristics of the nozzle. Although the pintle ejected at 4.2 sec, the data attained by the thermocouples are usable when the appropriate corrections are made to the heat flux of the nozzle at that time period for the calculated thermal analysis. These data will be discussed in the section on thermal analysis. The temperature-time history of this nozzle is shown on Figure III-96.

(U) Visual analysis of the postfired nozzle components indicated that the pintle pilot rod had broken off slightly upstream from the point where separation of Motor 001 pintle occurred. This part had broken very close to the bottom of the 0.125-in.-dia hole that had been drilled in the pintle pilot rod to reduce thermal stresses. The ejected portion of the pintle was located and examined for probable causes of the failure. It was determined that the component had apparently cracked during the first firing (Motor 002) during the cooldown portion of the test and been undetected because of the inability of disassembling the nozzle without destroying the components. From the failure of the copper-infiltrated tungsten rod on Motors 001 and 004, it was determined that the physical properties of this material are too unpredictable for it to be used as a primary structural member in the design of the rocket nozzle. The ductility and toughness of the 90-10 alloy make it a far superior material even though it must be protected from the oxidizing environment and can only be used at lower temperatures than tungsten.

CSR-DN-01S-BH-004

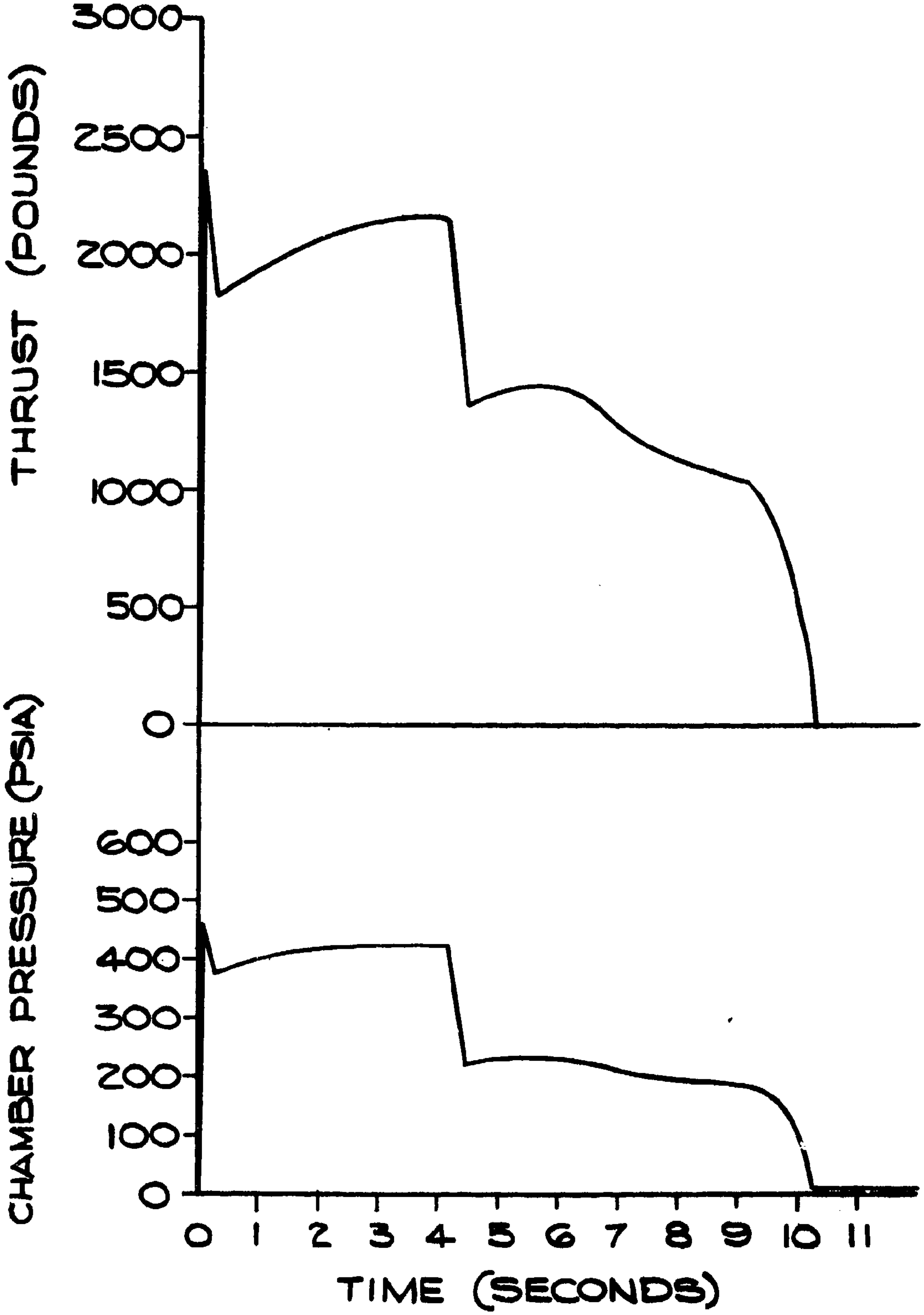

Pressure-Time and Thrust-Time History, CSR-DN-01S-BH-004

Figure III-95

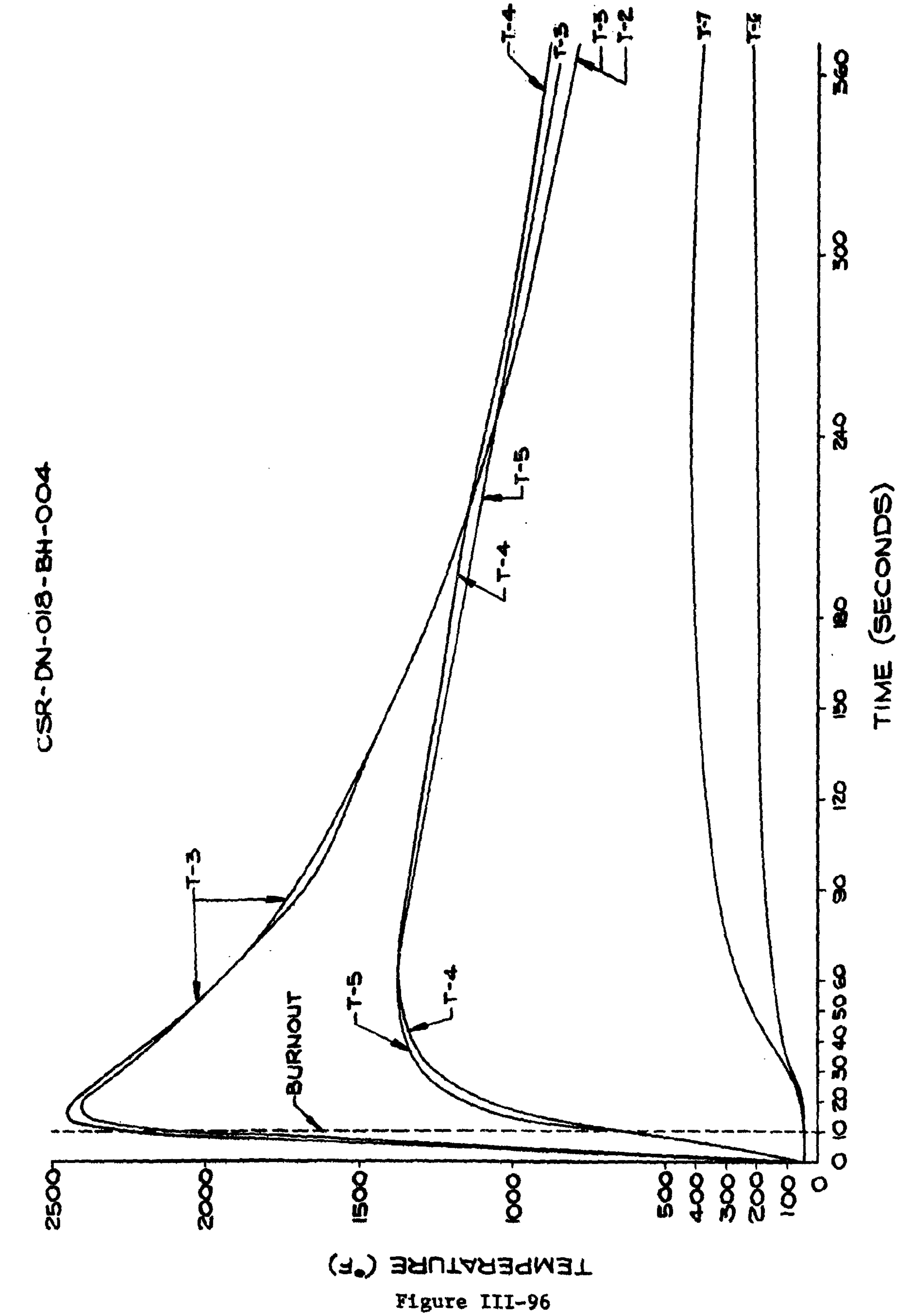

Temperature-Time History, CSR-DN-01S-BH-004

Figure III-96

III, C, Subscale Motor Development (cont.)

(U) The performance of the GenGard V-44 rubber was far from satisfactory both in the forward housing insulation area and as a pintle support insulation. Insufficient data were available to accurately predict the performance of the V-44 in these areas because the Mach number of the gas passing through the struts and over the pintle support insulation varied from 0.28 to 0.19. Usable data for the design of insulation using V-44 rubber is limited to Mach numbers somewhat less than 0.10. From the results of this test, it is evident that this material should not be used on the full-scale nozzle at Mach numbers higher than 0.05 because the erosion rate will exceed the allowable rate at values above this point.

(U) The performance of the remainder of the nozzle was similar to that of nozzle SN-1 on Motor 003; all performed satisfactorily. The throat exhibited no delamination or erosion, the entrance cap was not cracked or eroded, and the entrance cap insulator was only slightly more delaminated than on the first firing of this nozzle. Because of the long tailoff of Motor 004, some aluminum oxide was deposited on the pyrolytic graphite throat insert.

(U) Because of the excessive deterioration of the insulation of the pintle strutted housing, and the loss of the second pintle, it was determined that this nozzle would not be refurbished for another test firing. Nozzle SN-1 with the 90-10 alloy pintle pilot was selected to be refired on the last two motors.

e. Subscale Motor Test CSR-DN-01S-BH-005

(U) Subscale Motor 005 used a chamber that had been reworked to include 16 thermocouple bosses used to mount "heat flux meters" to measure the radiation feedback from the hot nozzle parts after the test. Nozzle SN-1 was installed on the motor complete with the nitrogen halo that had proved to be so successful on the previous four motor tests. The test setup is shown on Figure III-97. The ring stand and equipment shown immediately aft of the motor is an experimental thermocouple for measurement of exhaust gas temperatures. This is not related to the Controllable Solid-Rocket Motor Program, and thus will not be covered in this report.

(U) Motor CSR-DN-01S-BH-005 was test fired 16 November 1965. This motor was the third firing of nozzle SN-1 and the second test firing of the pintle assembly of this nozzle. Ignition was normal and smooth without any noticeable ignition spikes. This is probably attributable to the rather cool temperature of the day and the length of time that this motor spent in the bay outside of the conditioning cell prior to firing. Maximum pressure attained during this test was 475 psia at about 3.0 sec, with web burnout occurring at 8.4 sec. One disappointing aspect of this test was the circuit

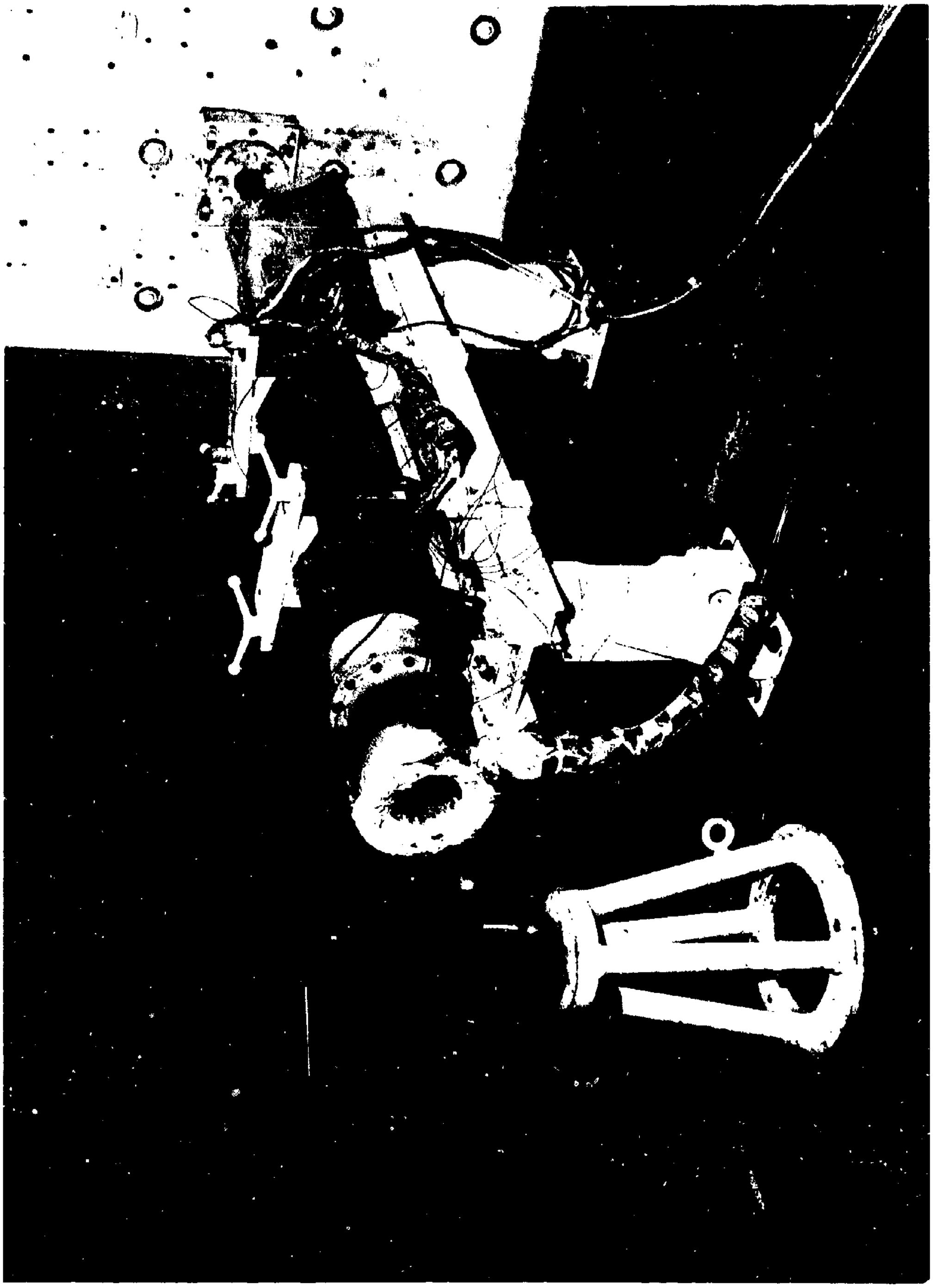

Test Setup, CSR-DN-01S-BH-005, Prefire

Figure III-97

failure in the transmission lines between the bay and the control room, resulting in the loss of all of the thermocouple data. After the precalibrations and probably during the countdown, an open circuit condition between Bay W-5 and Control Room W-3 occurred, blocking all of the data from the 14 thermocouples on this motor.

(U) Postfire analysis of the nozzle components yielded the following information:

Component	Condition
Throat	The pyrolytic graphite was in excellent condition with no erosion and no delamination.
Entrance Cap	The G-90 graphite has developed a small longitudinal crack; still no erosion.
Insulator, Entrance Cap	The carbon phenolic, parallel to center line wrap is only slightly delaminated.
Insulator, Housing Fwd	The elastomer modified carbon phenolic is beginning to show signs of some gouging, yet maintains a hard char.
Pintle Assembly	The pintle housing insulator is beginning to show some signs of delamination, yet is still in usable condition.

(U) The pintle pilot cap of silica phenolic either melted or eroded as on the previous firing of this nozzle, and will therefore have to be replaced before the nozzle can be refired. That is the only repair necessary on this nozzle prior to refiring it on Motor 006. The pyrolytic graphite washers on this pintle assembly had the same appearance as on Motor 003 after the first firing of this assembly. All washers were free to spin and had a total accumulated gap of about 0.015 in. Small surface-blistering occurred during the first test of this nozzle and increased to a much more noticeable extent during this test. MXCE-280 material has an apparently lower erosion rate and less susceptibility to local gouging than does the Coast material; however, both are acceptable for this use. Both materials are subject to surface cracking of the hard char that is formed, but both seem to have had the ability to hold this char during the subsequent tests.

(U) Because of the uniform pressure-time trace of this motor and the rather close correlation with the thrust-time trace, it is evident that the condition of the nozzle throat remained constant throughout the test

firing. Only minor aluminum oxide deposition was found on the throat insert after the test, and this was probably deposited during the tailoff. The pressure-time and thrust-time histories of this motor are shown on Figure III-98. There was very little damage to the silica phenolic exit cone after three thrusting periods. One minor gouge was seen on the lower right-hand quadrant of the exit cones; however, this was beginning to form during the second test (Motor 003), and is probably due to a local defect in the molded component. This gouge was located very close to the point at which flow separation is expected to occur due to the overexpansion of the nozzle at sea level.

f. Subscale Motor Test CSR-DN-01S-BH-006

(U) Subscale Motor 006 was also equipped with the modified chamber to record the radiation feedback from the hot nozzle-components after the test. This motor was set up in the test stand similar to that of Motor 005. The same exhaust gas measurement device appears on this motor aft of the nozzle as was on Motor 005, but with a little more sophisticated supporting device. Because of the loss of all thermocouple leads in the previous test, the circuit on these thermocouples was rechecked on the final countdown.

(U) This motor was fitted with nozzle SN-1, making this the fourth firing of that nozzle and the third firing of the pintle assembly and the pintle housing insulator. For this test, a cap of precharred carbon phenolic was used on the end of the pintle pilot in place of the silica phenolic used on the two previous tests. This cap was fabricated from a layup of flat laminates.

(U) Subscale Motor 006 was test-fired 18 November 1965. Ignition was normal and smooth with the maximum motor pressure occuring at approximately 1.0 sec at a level of 501 psia. The pressure-time trace was slightly regressive; however, checking the thrust-time trace with the pressure-time trace, it was concluded that the propellant grain had more surface area exposed initially and burned regressively from the onset of combustion. The pressure-time and thrust-time traces are shown on Figure III-99.

(U) On this motor all of the thermocouple data were recorded for the full 20 min, yielding valuable radiation feedback data for the design of the fullscale motor. The nozzle temperature-time history is shown on Figure III-100. These temperatures will be discussed in more detail in the section on thermal analysis. The locations of the six chamber thermocouples are shown on Figure III-101. The temperatures of these thermocouples are shown on Figure III-102. It is noteworthy that the maximum temperature attained was in excess of 1100°F--more than sufficient to ignite most solid propellants. This would imply that it will be necessary to maintain the fullscale motor at a very low L* after extinction to avoid inadvertent reignition. This will be covered in more detail later in the report.

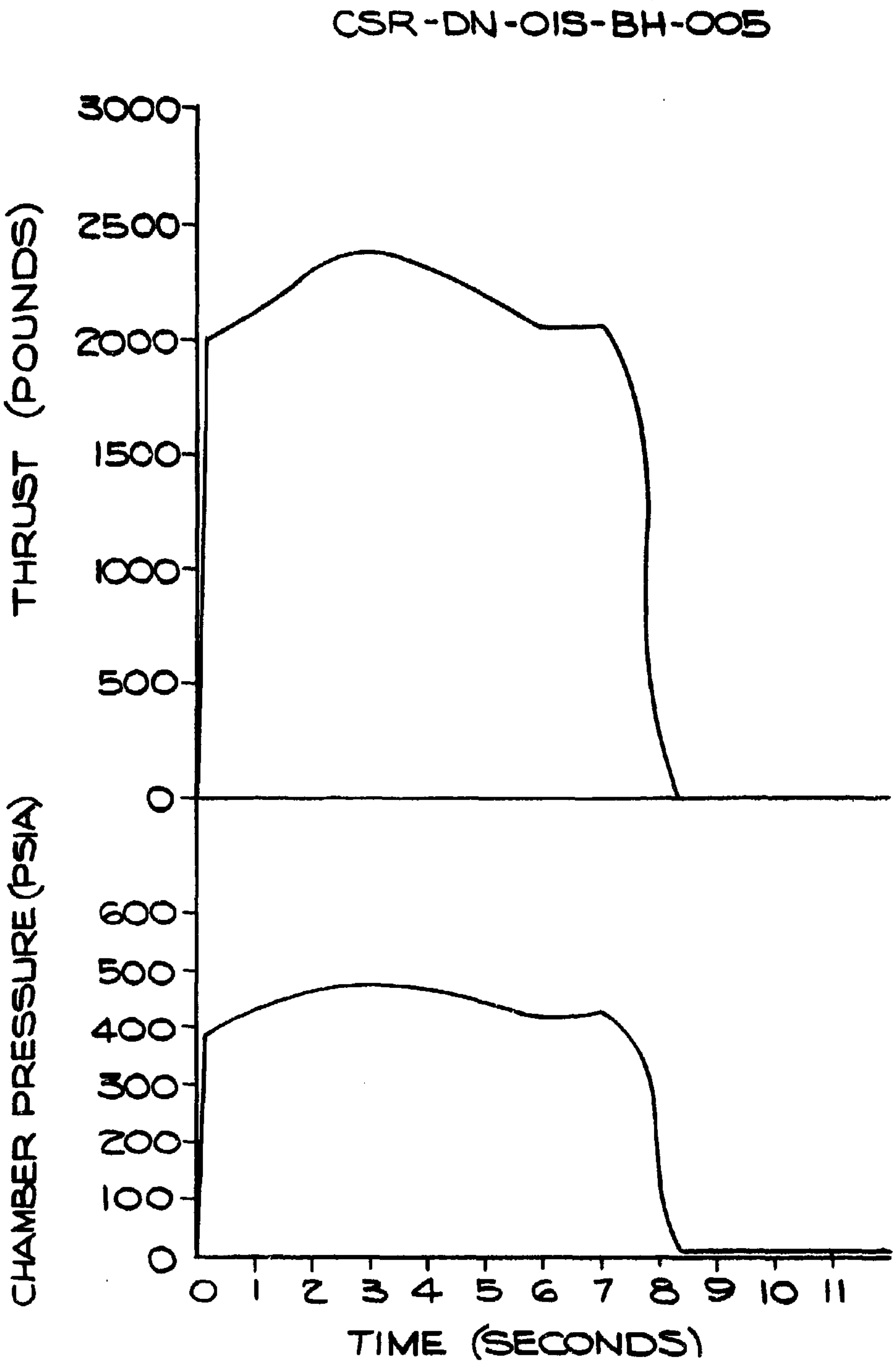

Pressure-Time and Thrust-Time History, CSR-DN-01S-BH-005

Figure III-98

CSR-DN-01S-BH-006

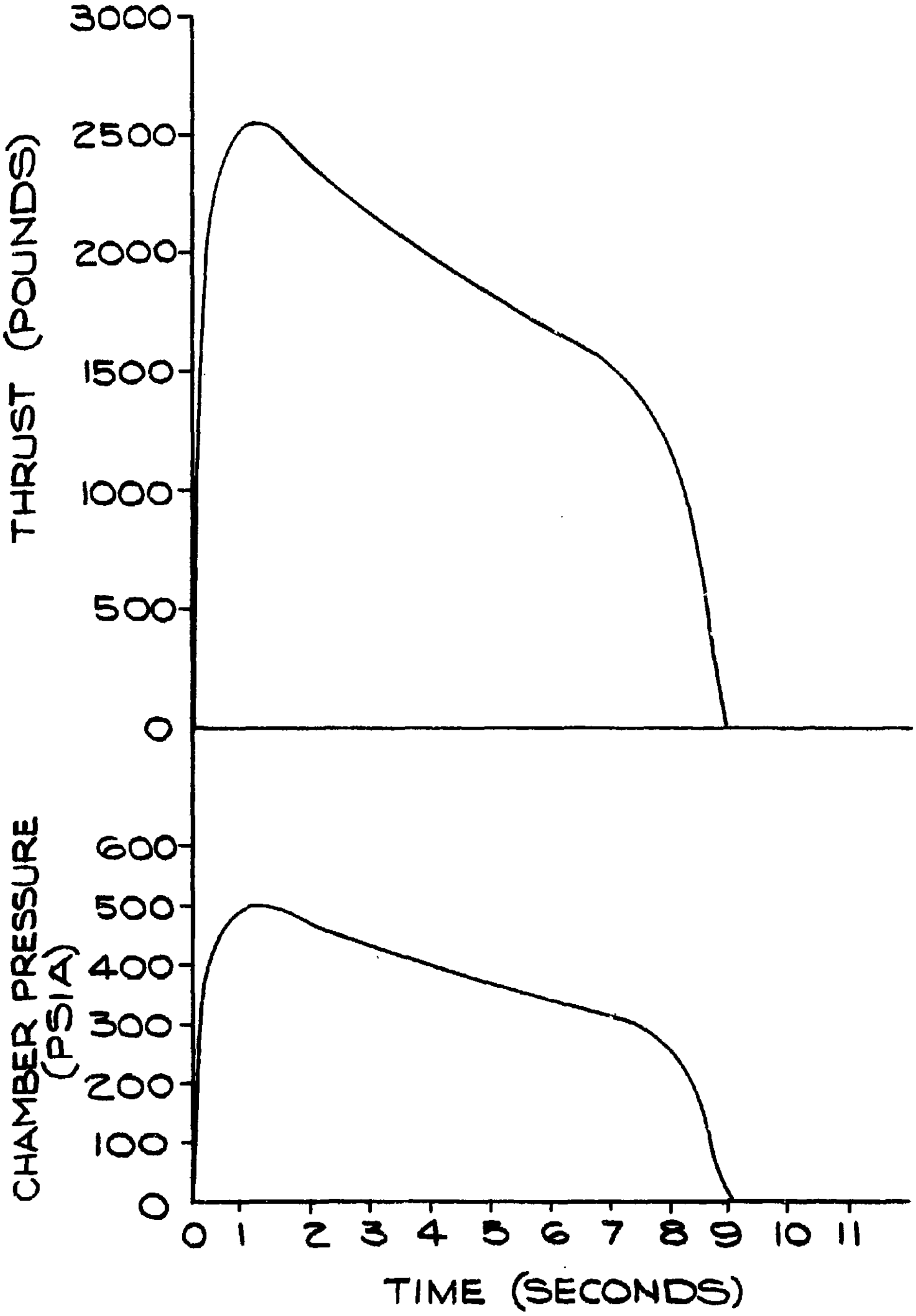

Pressure-Time and Thrust-Time History, CSR-DN-01S-BH-006

Figure III-99

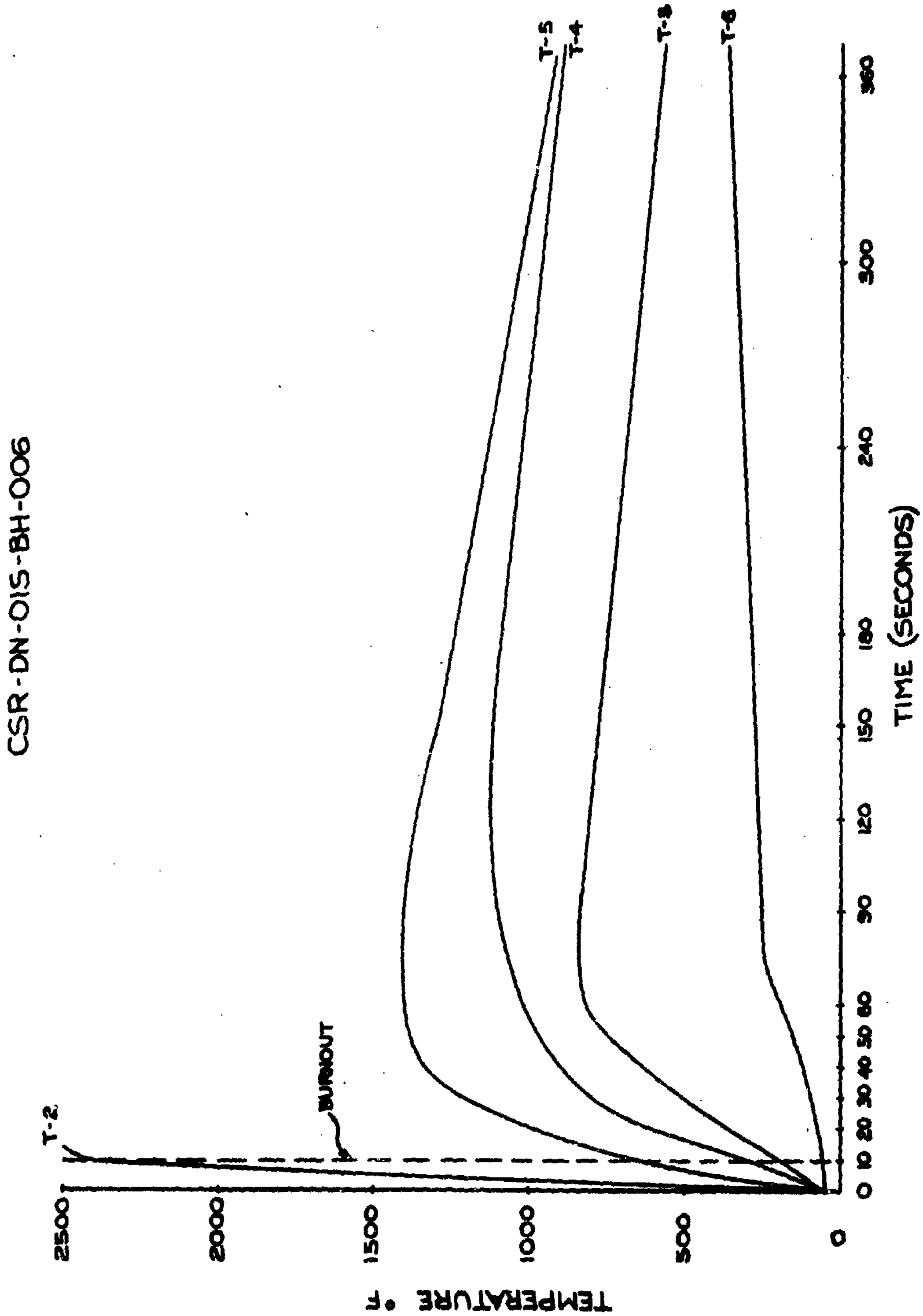

Temperature-Time History, CSR-DN-01S-BH-006

Figure III-100

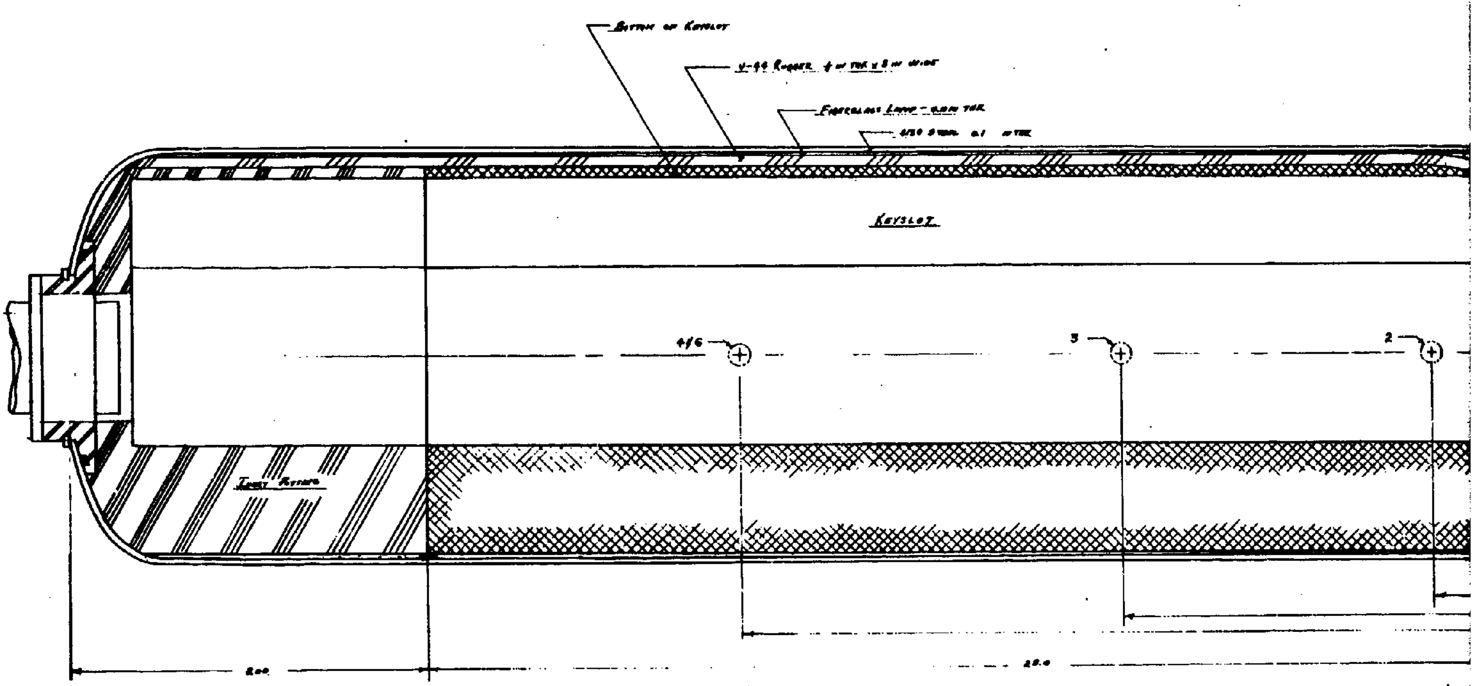

Bottom of Keyslot
Keyslot
4/6
3
2

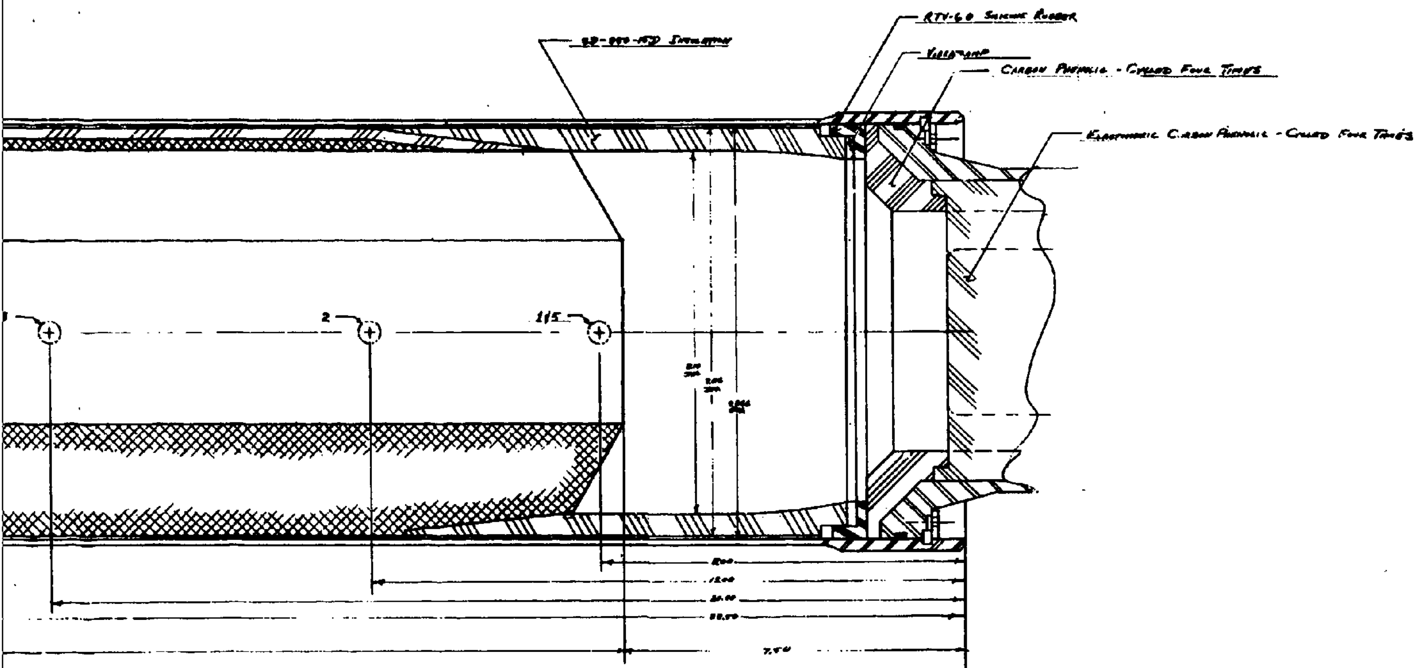

Chamber Thermocouple Locations, CSR-DN-01S-BH-006

Figure III-101

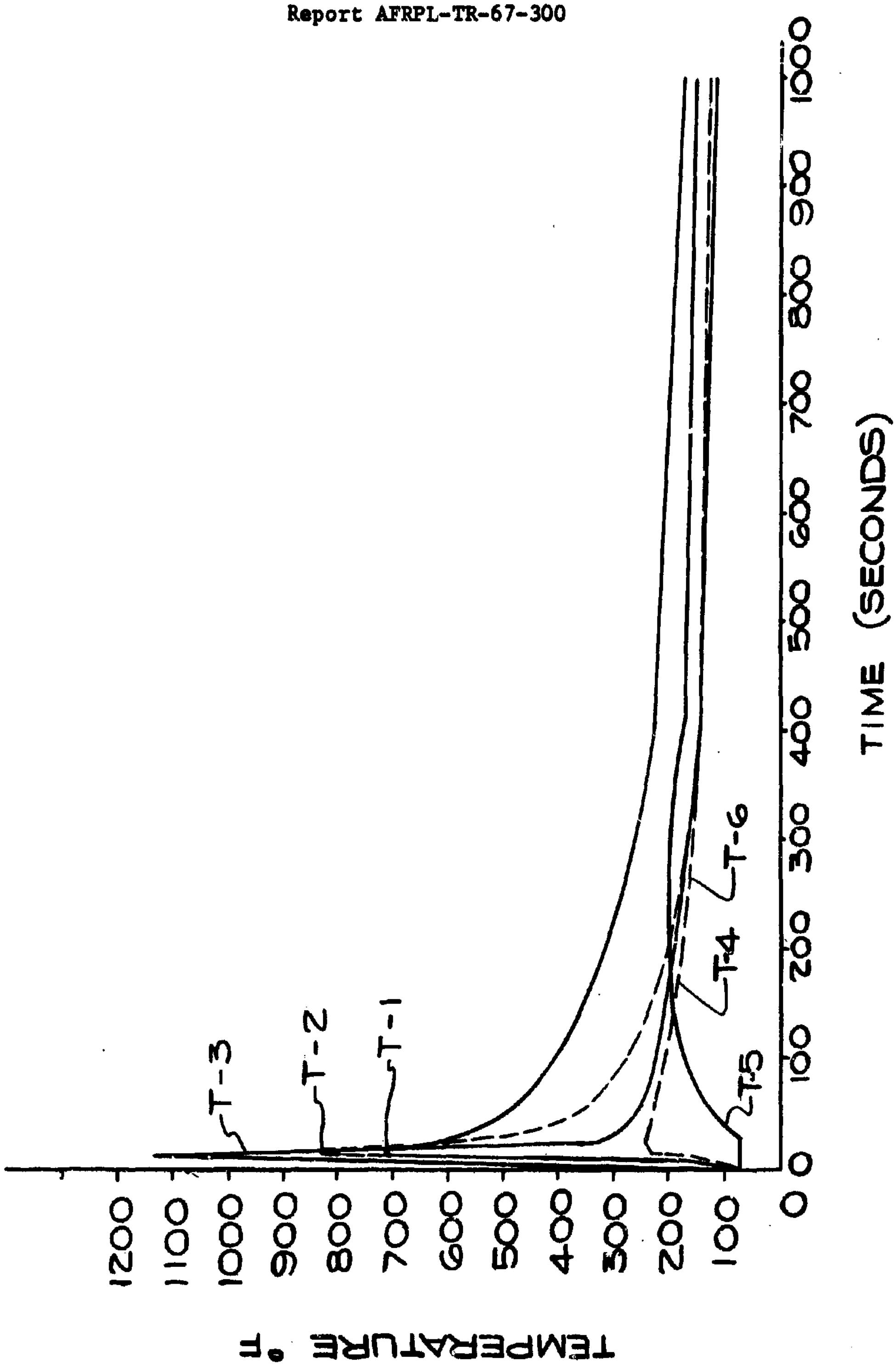

Chamber Thermocouple Data, CSR-DN-01S-BH-006

Figure III-102

(U) Postfire visual analysis of the components of nozzle SN-1 indicated that this nozzle had survived the firing and was completely intact. One point of interest was the performance of the precharred carbon phenolic pintle pilot end cap. As opposed to the silica phenolic end caps that were used on Motors 003 and 005, this material eroded only slightly and could be considered refirable. This component can be seen on Figure III-103. Also shown on this figure is the angle-wrapped carbon phenolic pintle housing insulation. This component delaminated only slightly on the third test, and was in sufficiently good condition to be refired with a high confidence of success. The carbon phenolic tape formed a hard char which apparently did not erode on the cylindrical surface. The conic surface near the pyrolytic graphite washers eroded slightly baring a portion of the fourth washer. The pyrolytic graphite washers withstood the test firing as expected; but the last washer showed some signs of delamination. The aft housing insulation, MXCE-280, was in the same condition after this test as it was after Motor 005. This material had been subjected to a total of four test firings without loss of insulating properties and with a minimal erosion. Apparently, the hard char that was formed after the first test protected the virgin material through the remainder of the test program.

(U) The forward housing insulation, Coast's elastomer modified carbon phenolic, withstood the four test firings; however, the erosion of this material was much greater than that of the MXCE-280. This insulation can be seen on Figure III-104. The entrance cap, G-90 graphite, that had developed a longitudinal crack after the third exposure is shown on Figure III-105. The longitudinal crack had lengthened and widened slightly, but this component is still in condition to be refired. The entrance cap insulator, parallel to center line wrapped carbon phenolic, delaminated slightly on this firing as on the past three tests; however, it also is in condition to be refired. The throat insert, pyrolytic graphite washers, are in excellent condition, with no erosion or delamination after four test firings.

(U) The throat support, ATJ graphite, and the exit cone, silica phenolic molded, are shown on Figure III-106. These components withstood the four firings in excellent condition, and are suitable for refiring. The slight gouging that was apparent in the exit cone after the third test firing, Motor 005, had not increased during the fourth test.

3. Summary of Subscale Program

(U) The subscale motor design and test program was a very valuable portion of the overall development program for the single-chamber controllable solid rocket motor because it pointed out the potential problem areas in the design of a restartable nozzle. One specific potential problem that was observed in this program was the cracking and delamination of the pintle housing insulator. This component in the fullscale motor is one of the most

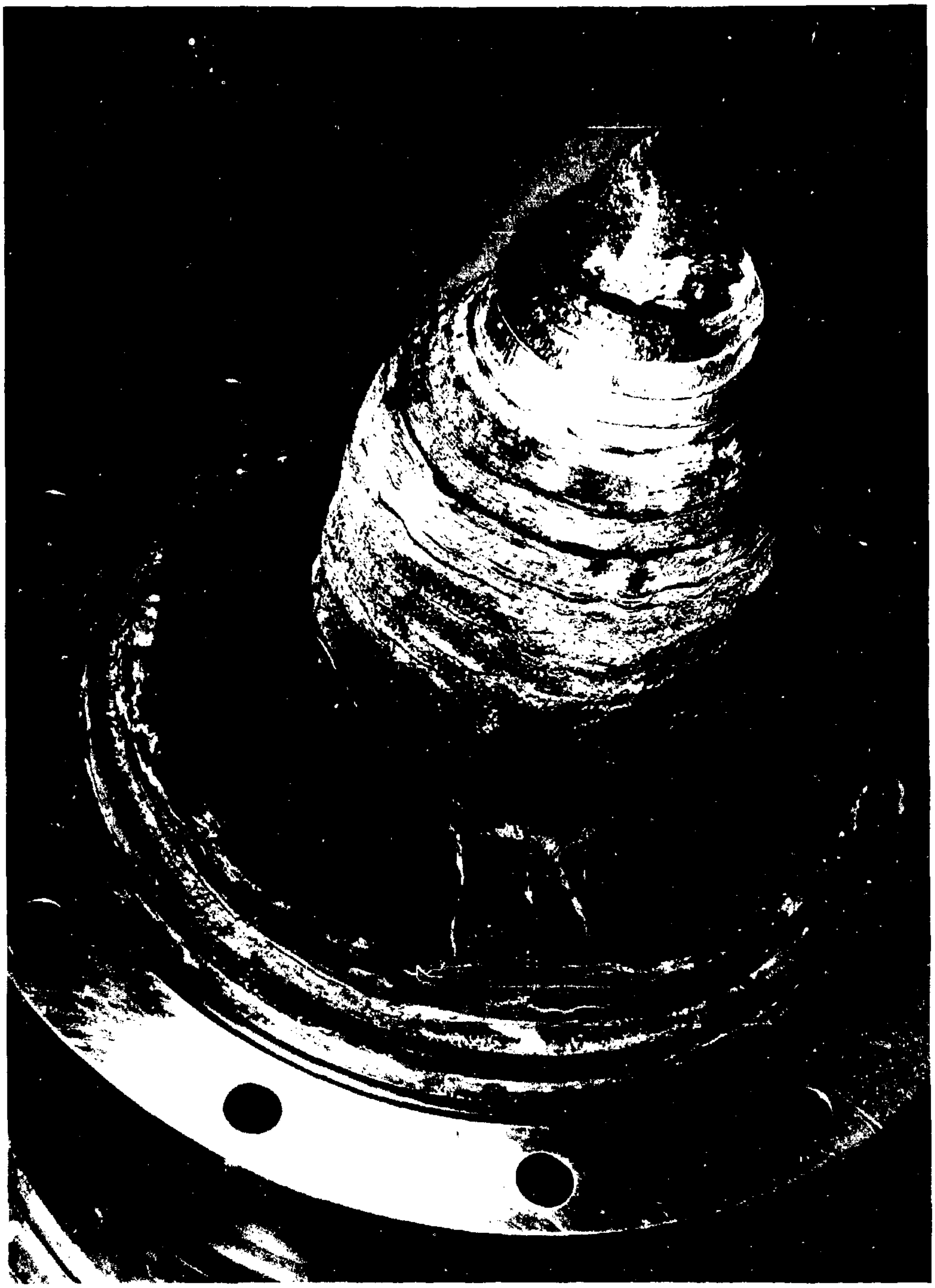

Pintle Assembly, CSR-DN-01S-BH-006, Postfire

Figure III-103

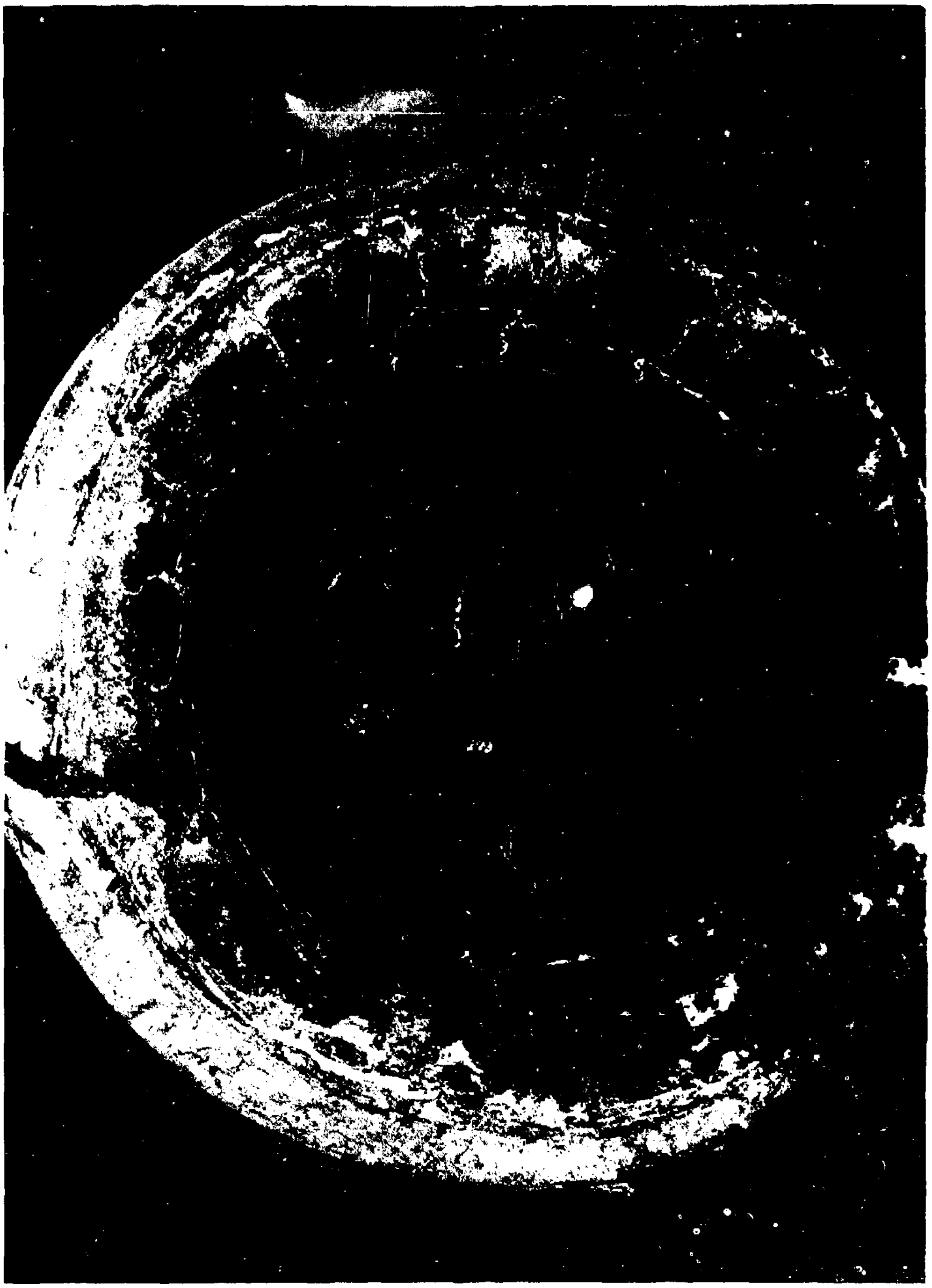

Insulator Housing Forward CSR-DN-01S-BH-006, Postfire

Figure III-104

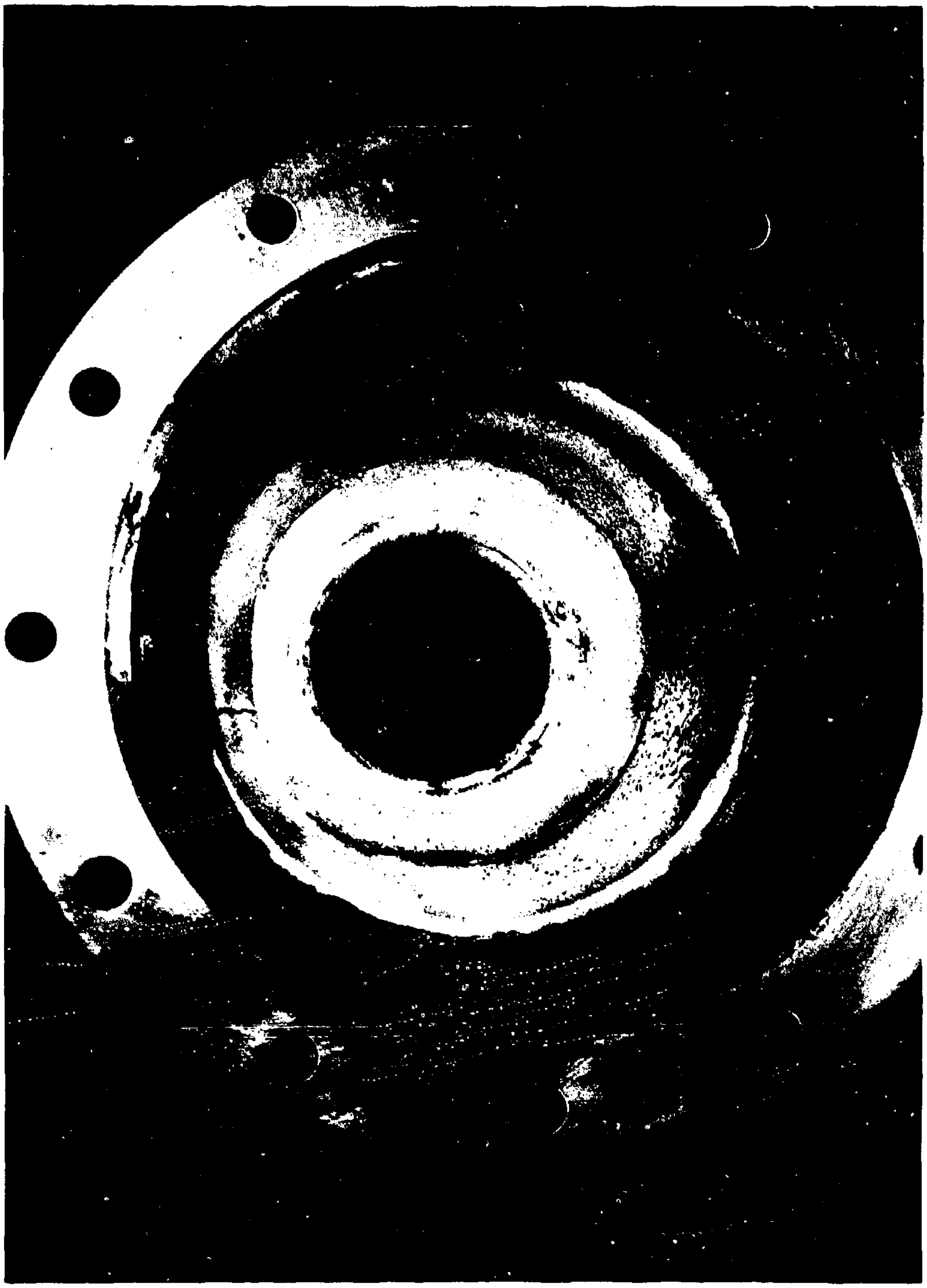

Nozzle Entrance, CSR-DN-01S-BH-006, Postfire

Figure III-105

Aft View, Nozzle, CSR-DN-01S-BH-006, Postfire

Figure III-106

III, C, Subscale Motor Development (cont.)

critical of the nozzle parts because a separation of a portion of this insulator could result in a catastrophic failure of the motor by blocking the nozzle throat. During the subscale motor program, four different materials and three fabrication techniques were used in this area; thus, a good comparison of performance of materials was attained. The most promising technique and material combination for the fullscale motor was the angle-wrapped carbon phenolic that fired successfully on three tests. This was used on the fullscale motor for the initial test firing to determine the effectiveness of design in a scaled-up motor.

(U) During this subscale program, the housing insulation that was found to be the optimum of the ones tested was the MXCE-280 elastomer modified carbon phenolic material. Although the Mach number in the fullscale motor nozzle design is much lower than that of the subscale nozzle, this material will be used to ensure that the first design is conservative. Former design of the fullscale nozzle strut housing insulation incorporated GenGard V-44 rubber. Because of the poor showing of this material in a similar application in the subscale nozzle, its use was discontinued for the fullscale nozzle. This material was still used as the chamber and aft dome insulation because of its superior performance in this area.

(U) The additional change to the fullscale design as a result of the subscale tests is the incorporation of 90 tantalum-10 tungsten alloy as the pintle support rod. This material performed remarkably well in the oxidizing atmosphere of the subscale motor; thus it was expected to perform equally well in the fullscale motor should the pintle end-cap insulation fail.

III, Technical Discussion (cont.)

D. HEAVYWEIGHT MOTOR DEVELOPMENT

1. Heavyweight Motor Design

(U) The objectives of the heavyweight motor development were twofold: (1) to verify and improve the design of the rocket motor components and (2) to develop the data necessary to successfully design controllable rocket motors of any size.

(U) To accomplish these objectives with the minimum risk and with the minimum expenditure the following criteria were set for this phase: (1) The heavyweight motor shall have no mass fraction goal. (2) Conventional state-of-the-art hardware materials shall be employed wherever possible. (3) Both L* and $\dot{P}$ extinguishment shall be demonstrated. (4) During the first test no nozzle actuation will be accomplished. (5) The design must be capable of restart after any combination of previous firing and heat soak. (6) All testing shall utilize a chamber pressure feedback servocontrol system. The heavyweight motor design that is presented in the following sections was designed within the above requirements.

a. Case Design

(U) The basic case diameter was set at 20 in., as previously described. The overall length was set on the basis of propellant loading and nozzle envelope. To determine the basic wall thickness, material, and heat treatment, a tradeoff study was conducted to evaluate the motor case weight, motor potential mass-fraction, and the allowable operating pressure as a function of case thickness. The potential mass-fraction tradeoff was run to cover the possibility of using the same case for both the heavyweight and the lightweight motor development efforts. The basic shape of the motor was set by the existing welding and machining tooling for the 30KS-8000 motor in an effort to accelerate the schedule and conserve funds. Based upon this shape, a case weight analysis was conducted in terms of "basic wall thickness" and percentage of basic wall thickness. This case weight was then added to estimated weights for lightweight components such as the nozzle system, the ignition system, the motor insulation, and the actuation system to determine the potential mass fraction of a lightweight motor using this "heavyweight" case.

(C) To complete the tradeoff, an estimate of the allowable variation in minimum nozzle area and maximum propellant surface area was made. This percent of variation represents the point at which the motor case is calculated to rupture from overpressure in terms of basic wall thickness. From these plots, a basic wall thickness of 0.070 to 0.075 in. was selected as the maximum allowable without dropping the potential mass fraction of the motor below 0.70 using the steel case. This selection provides for an

III, D, Heavyweight Motor Development (cont.)

unscheduled variation of nozzle area (below minimum) and propellant surface area (above maximum) of over 33%, as safe a margin as possible without going to excessive thick-wall cylinders. It was decided to remain in the thin-wall cylinder category to evaluate any problems of case deflection during the heavyweight program and solve them during this phase as opposed to encountering them farther downstream in the lightweight program.

(U) The detail drawing of the chamber is presented in Figure III-107. This chamber is fabricated from Ladish D6AC Steel Alloy, with a heat treatment of 200,000 psi ultimate. The basic fabrication technique uses two dome forgings and one cylindrical forging, rough-machined, welded, heat-treated, and final-machined. The apparent excessive length of the forward skirt was required to accommodate the available machining and handling tooling without modification as this tooling is still in use in the 30KS-8000 program. A 5-in. forward boss diameter was selected to allow a maximum amount of clearance for possible future mating with a multiple ignition system. The aft boss diameter was set at the minimum required to allow adequate nozzle clearance for the strut mounted movable pintle nozzle. Both forward and aft bosses are equipped with the "shear lip" design to minimize the stresses at the discontinuity. By using the three-piece forging technique all longitudinal welds were eliminated leaving only two girth welds at thickened cylindrical sections. Skirt wall thickness was sized to accommodate the excessive thrust spikes expected during rapid depressurization extinguishment transients.

(C) The design loads on the motor case were 1385 psia (chamber pressure is not expected to exceed 1200 psia); chamber thrust of 117,000 lb (this is not expected to exceed 70,000 lb); igniter thrust of 6000 lb (this is not expected to exceed 3200 lb; and motor weight of 1500 lb including handling tooling design loads. The chamber was sized to the ultimate strength of the material. For areas that indicated a negative margin of safety, the stresses were recalculated using biaxial allowable strengths. Bosses were checked using flat-plate hydrotest fixtures as boss restraints to cover the stress condition. As a result of these analyses, it was determined that under the design loads imposed, the chamber would operate without rupturing; however, local yielding could occur at pressures in excess of 1280 psia, an unlikely condition without catastrophic failure of either the nozzle, the grain, or the ignition system.

b. Grain Design and Case Insulation

(U) The design objectives of the grain configuration were: (1) The motor must be capable of extinguishment as shortly after first ignition as practical; (2) the grain exhibit as nearly neutral a surface area-web thickness relationship as possible; (3) the grain design and insulation design be mated to assure a low stress combination as the physical properties

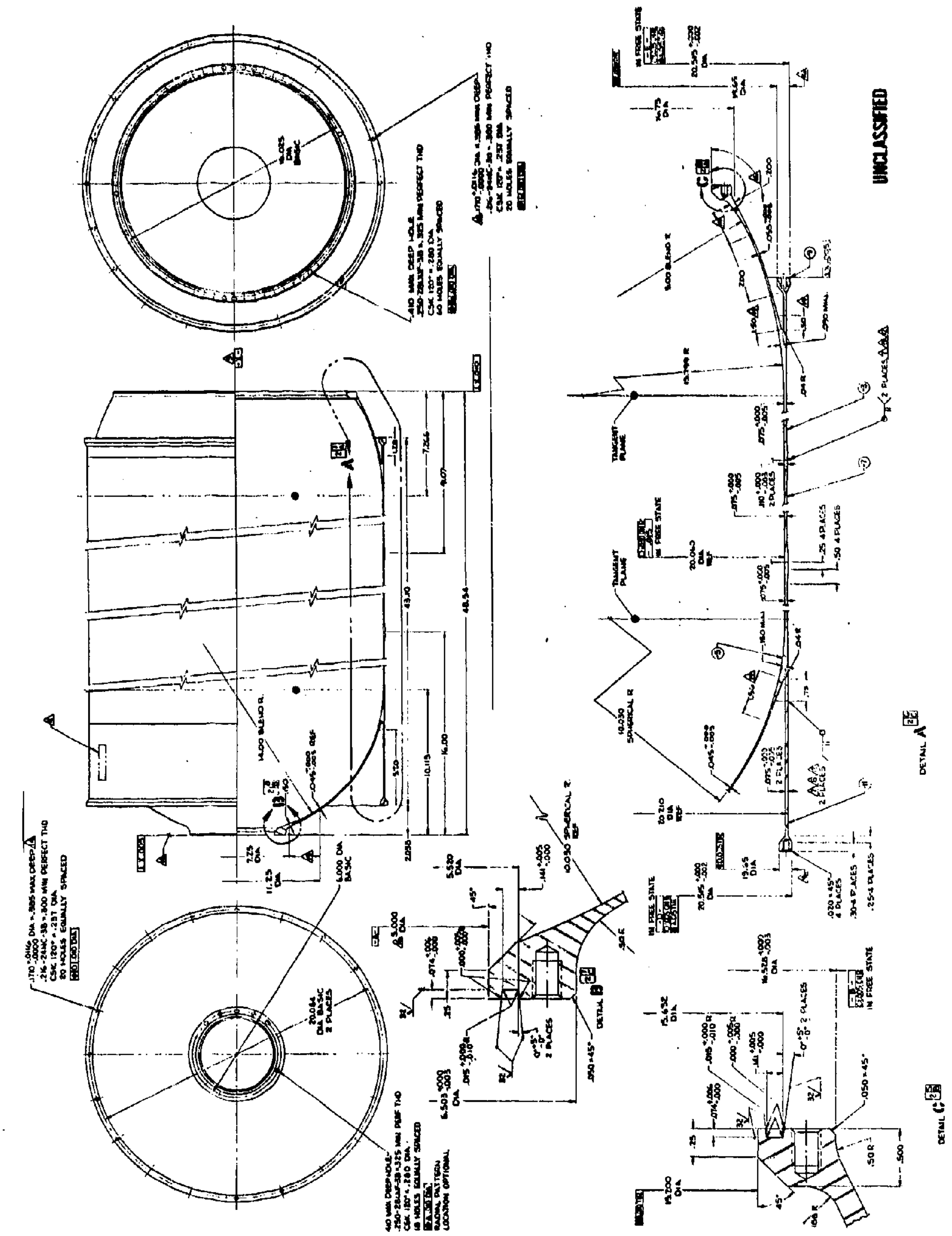

Chamber, 20-in.-Diameter, Dwg 1125271

Figure III-107

of extinguishable propellants are not yet well defined; (4) the grain be protected on the aft face by a restriction to minimize the probability of reignition after extinction due to radiation feedback from the hot nozzle components; and (5) the bond between the insulation and the propellant grain be capable of withstanding the heat soak after firing without separation. Following these criteria, a grain configuration and insulation combination has been designed. This design is shown on Figure III-108.

(1) Grain Configuration

(U) The grain configuration selected for use on the fullscale motor is an aft end restricted, internal burning, finocyl with six symmetrical 1/2-in. wide fins. This design was selected in preference to other large web grain shapes since it provided better performance control, preferable structural support, and better ignition response. In addition, the finocyl limits the chamber insulation exposed to flame to that located near the forward head of the motor where the mass flux and velocity are low, thus the heat flux is low. For stop-restart designs this is a requirement as degradation of chamber insulation will continue after extinguishment until all heat absorbed during the firing pulse has been dissipated.

(C) The surface area requirements set on the grain configuration were based upon the expected propellant ballistic properties. Propellant studies indicated that a propellant burning rate of about 0.100 in./sec at 100 psia with an exponent of approximately 0.65 would probably be available for the heavyweight motor series. From the nozzle design and chamber design used, it was decided to limit the average grain surface to a maximum value of 1300 in.^{2} and the maximum deviation from this average to plus or minus 5% to control motor operating pressure and duration. The final design, with the aft face fully restricted, has an average burning surface area of 1278 in.^{2} and a maximum deviation of plus or minus 4 1/2%.

(C) Calculations were run to determine the expected pressure-time characteristics of this grain configuration in the controllable solid rocket motor, first with the nozzle at minimum throat area and second, with the motor operating at an average thrust level of 2000 lb. With the nozzle set at the minimum throat area, 6.75 in.^{2}, an action time of approximately 21.8 sec was expected with an integrated average pressure of 655 psia. The maximum pressure expected, 740 psia, occurs both at the 6-sec point and at the 21-sec point, just prior to web burnout. The minimum pressure expected occurs at ignition and is about 510 psia. During web burning, a saddle was expected at about 13 sec with the minimum pressure dropping to 570 psia.

(C) All calculations were based upon single-start ambient propellant temperature. If the motor was restarted with the propellant

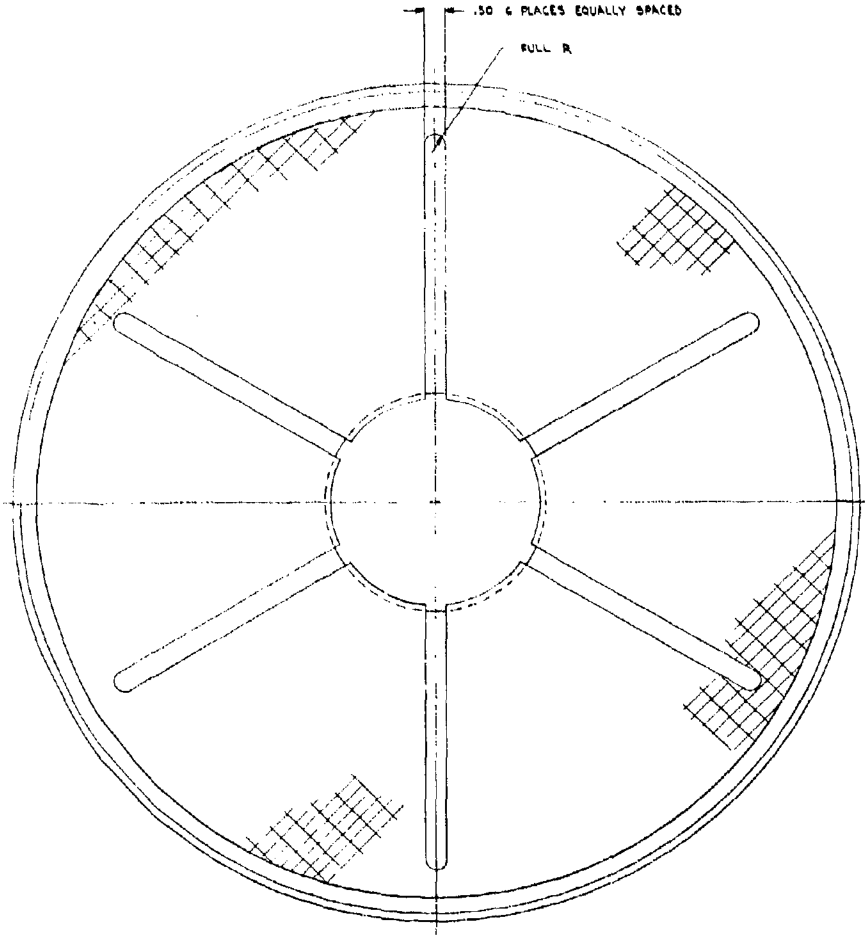

SECTION A-A

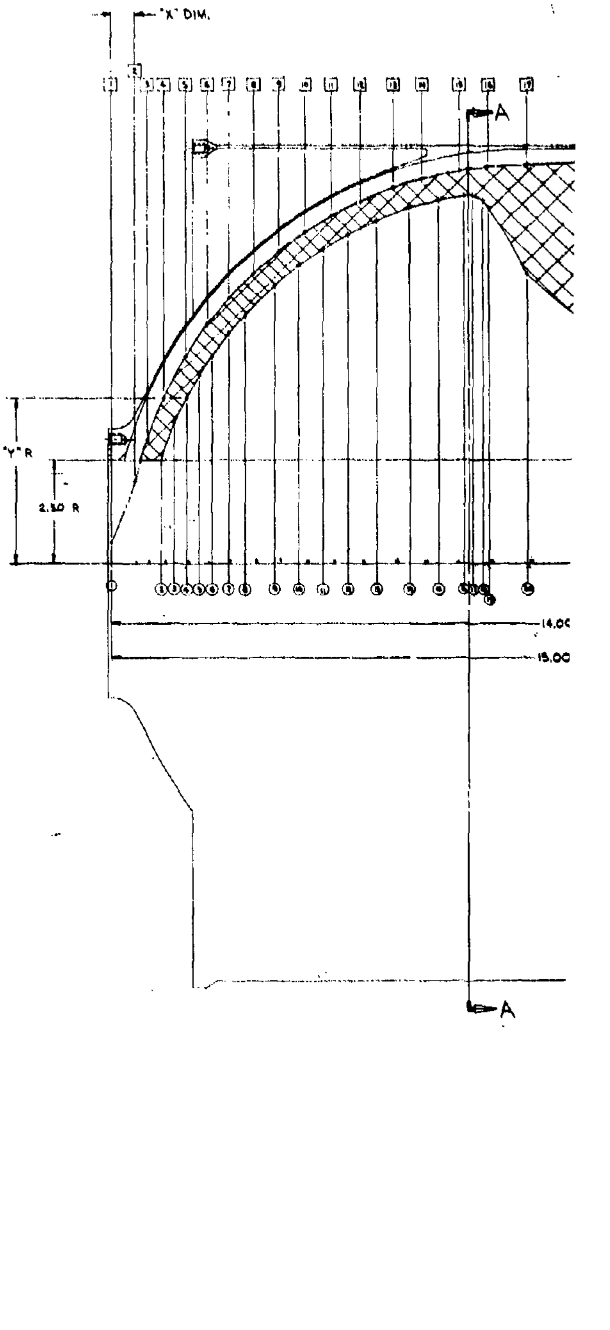

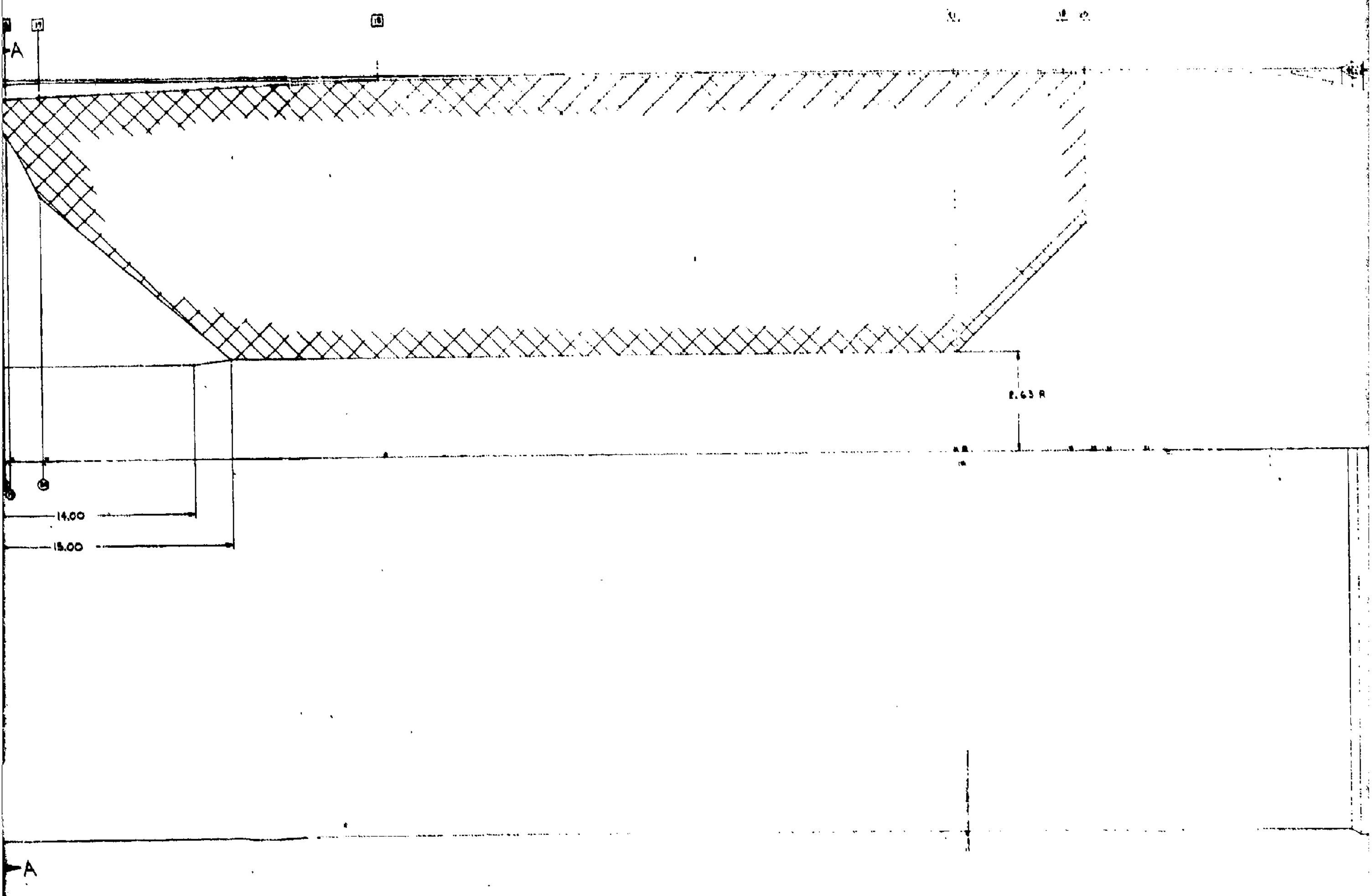

Grain Configuration for the Ful

Figure III-1

U

GRAIN ENVELOPE POINTS

#	'X' DIA.	'Y' R
1	0	.5
2	.88	2.0
3	.88	3.0
4	1.25	4.0
5	1.77	5.0
6	2.30	5.8
7	2.9	6.4
8	3.4	7.0
9	4.0	7.83
10	4.65	8.0
11	5.3	8.4
12	6.0	8.75
13	6.8	9.10
14	7.5	9.3
15	8.4	9.5
16	9.1	9.6
17	10.03	9.85
18	19.0	10.03
19	37.07	10.03
20	37.64	8.06
21	38.2	2.88

FIN EXTERIOR POINTS

#	'R' DIA.	'Φ' R
1	0.	2.40
2	1.2	2.40
3	1.8	3.4
4	1.8	4.0
5	2.1	4.85
6	2.4	5.0
7	2.8	5.55
8	3.2	6.0
9	3.9	6.7
10	4.8	7.2
11	5.1	7.6
12	5.7	7.95
13	6.4	8.3
14	7.2	8.6
15	7.8	8.8
16	8.5	8.9
17	8.7	8.9
18	8.95	8.8
19	9.1	8.6
20	10.	7.

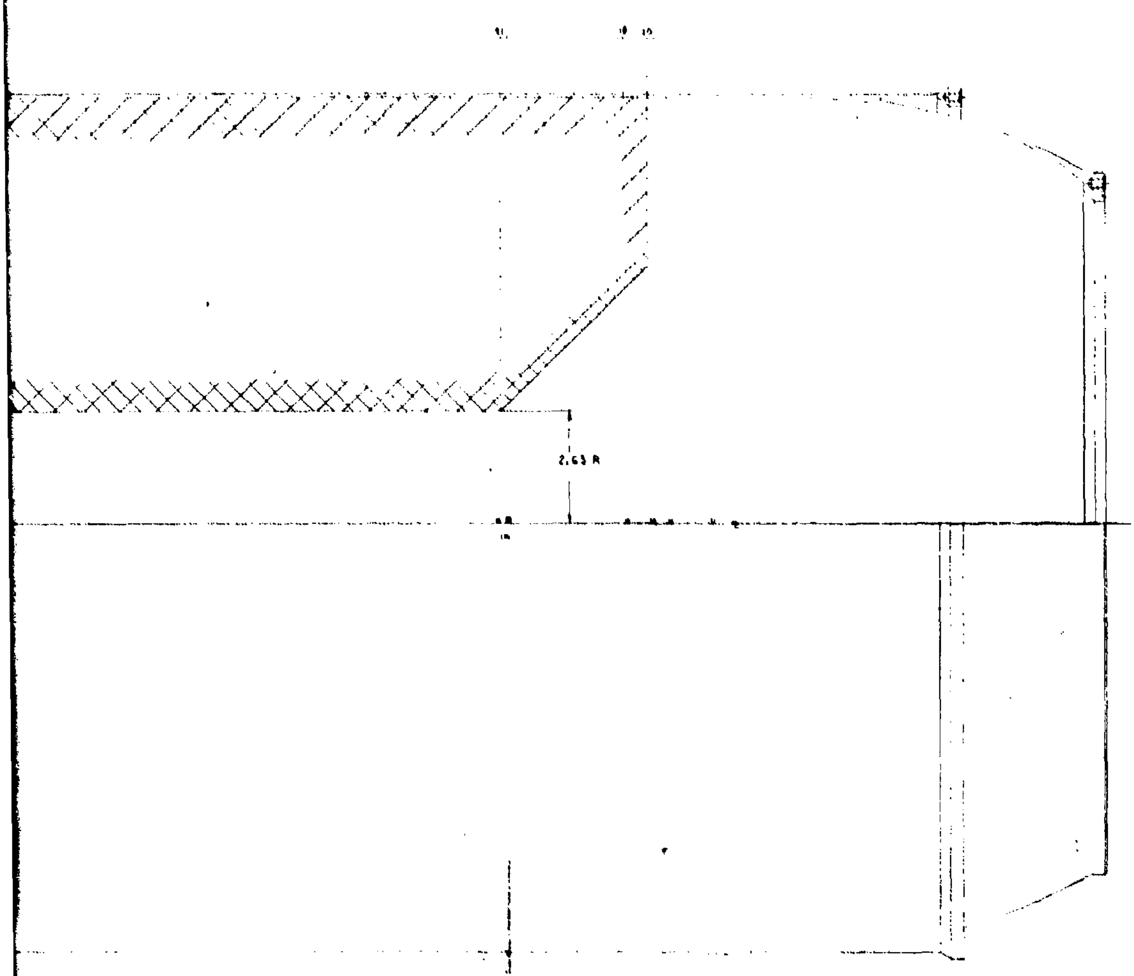

Grain Configuration for the Full Scale Motor Design (u)

Figure III-108

at an elevated temperature these predicted values would be much lower than the actuals as extinguishable propellants by nature have high susceptibility to temperature, i.e., high π_k.

(C) With the pintle in the minimum thrust condition, 2000 pounds thrust, the average operating pressure was expected to be approximately 79 psia. The web time for this configuration was in excess of 87 sec.

(2) Case Insulation

(U) In establishing the motor case insulation design for this motor, an acrylonitrile-butadiene rubber compound (Gen-Gard V-44) was selected based on its mechanical, physical, ablative, and fabrication properties. This material may be used as either a premolded-cured-in-place material or as a layup-bagged-cured-in-place insulation making it adaptable to the needs of the controllable solid rocket motor from both a design and schedule standpoint.

(U) Gen-Gard V-44 uses an asbestos filler material to greatly improve its ablation characteristics and make it a usable material even in the relatively high Mach number flow regions, as proven by Skybolt, Minuteman, and Polaris experience. The thermal cycling characteristics of this material over the range of -30 to plus 140°F temperatures have been demonstrated. For higher temperatures, thermal cycling tests have been conducted using plasma-arc equipment. These latter tests indicate less erosion would be experienced during stop-restart motor operation with cooldown to ambient between cycles than during a single cycle of the same total exposure time.

(U) Insulation thicknesses for the fullscale motor were selected by first determining the absolute minimum thicknesses required at maximum firing duration. These thicknesses were based on the gas velocities, average mass-flow rates, and exposure times in the proposed design and on the maximum insulation loss rates observed in the Polaris, Minuteman, and 120-in.-dia motors, scaled to the operating conditions of the proposed motor. To incorporate a margin of safety, these minimum thicknesses were uniformly increased and the contour smoothed to facilitate fabrication.

(U) The resulting insulation--grain configuration is shown on Figure III-109 with the insulation thicknesses called out for the axial stations marked on the figure. To improve the grain stress condition for initial propellant cure and for thermal cycling a released boot concept was employed. This boot, a uniform 0.060-in. thick V-44 component, is released from the forward boss, axially aft for 13.5 in. A 2-in.-wide band is bonded to the chamber insulation to assure boot retention. The released length

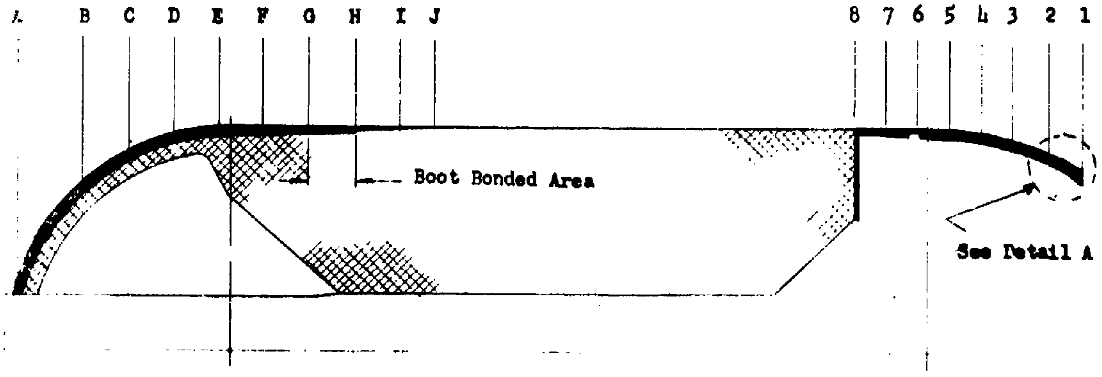

FWD CLOSURE

Location X Axis, Inches	Maximum Exposure Time at Star Points Secs	Predicted Thickness Loss at Star Points, Inches	Insulation Plus Boot* Actual Thickness	Maximum Exposure Time 30° from Star Points, Secs	30° Predicted Thickness Loss from Star Points Inches	Insulation Plus Boot* Actual Thickness
A 0.4	81	.324	.400	81	.324	.400
B 3.5	81	.324	.400	48	.192	.300
C 5.5	81	.324	.400	38	.152	.250
D 7.5	81	.324	.400	33	.132	.230
E 9.5	81	.324	.400	31	.124	.220
F 11.5	26	.104	.200	26	.104	.200
G 13.5	17	.068	.170	17	.068	.170
H 15.5	5	.020	.120	5	.020	.120
I 17.5	0	0	.100	0	.0	.100
J 19.0	0	0	.030	0	.0	.030

* Uniform Boot thickness 0.060 ± .010"

AFT CLOSURE

Location X Axis, Inches	Max Exposure Time, Secs	Predicted Thickness Loss, Inches	Actual Thickness
1 0	88	.528	.900
2 1.5	88	.528	1.070
3 3.0	88	.440	.750
4 4.5	88	.440	.610
5 6.0	88	.352	.550
6 7.5	88	.352	.460
7 9.0	88	.264	.360
8 10.5	88	.176	.250

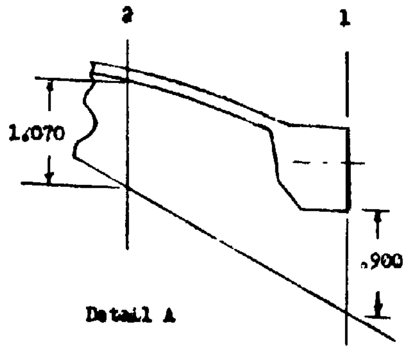

Detail A

Insulation Profile - Grain Superimposed (u)

Figure III-109

completely covers the area of the grain that contains the fins; thus the stress risers are compensated for without added excessive insulation and without compromising the design of the finocyl.

c. Igniter Design

(U) The criteria used for the multiple pyrotechnical ignition system design were: (1) the ignition system be capable of providing first ignition and a minimum of five reignitions at any web conditions, (2) the ignition system be current state-of-the-art for the heavyweight motors, (3) the ignition system operate satisfactorily both at sea level and at simulated high altitude, and (4) each igniter be capable of preventing accidental ignition during handling and prefire preparations. One additional requirement is that all six igniters be capable of being installed prior to first motor ignition and withstand the thermal environment of all six motor pulses without inadvertent ignition.

(U) To meet these criteria, experience from the Minuteman Development Program was employed. The concept selected uses the Minuteman propellant igniter and the same propellant that was used through Wing V. A set of ignitability calculations were run to determine the energy requirements of the heavyweight motor. These calculations assumed that the main motor propellant had the same ignition characteristics as AAB-3177, an extinguishable propellant formulation developed during the previous year's work on Contract AF 04(611)-9889. To simplify the design and fabrication of the ignition system, it was decided that only two sizes of igniter would be used. One size was designed specifically for first ignition of the motor and the second was sized for last ignition. In actual use, one of the first-ignition cartridges and five of the last-ignition cartridges would be used in the motor. Nozzle throat area corrections will be used to control the motor bore pressure for intermediate ignitions using the last-ignition cartridges. To control the motor bore pressure, it is necessary to have some means of determining the web thickness remaining after each firing. This will be determined by a simple integration of the thrust-time trace with the I_{sp} estimated from the average operating pressure.

(U) The ignition system for the three heavyweight motors is depicted on Figure III-17 with cartridge details shown on Figure III-110. An insulated ruptured diaphragm is used to protect the unfired igniters during motor burning. All igniters use the same nozzle, with the individual cartridges running unchoked. The actuation of the igniter is accomplished by firing an EBW squib developed on the Polaris Program, into an initiator containing 30 grams of 2D size boron potassium nitrate pellets. These, in turn, ignite the main charge of ANP-2758 Mod 1 propellant. The first ignition is accomplished using a mass flow rate of 6.27 lb/sec at 1000 psia operating pressure

NOTES:

1. IDENTIFY WITH PART NO. 1125533 AND APPROPRIATE SUFFIX NUMBER, REV LTR TO WHICH ASSEMBLY IS MFD AND INSPECTION STAMP PER ASD 5215N.
2. INTERPRET DRAWING PER STANDARDS PRESCRIBED IN MIL-D-70327.
3. CLEAN INNER METAL SURFACE OF CHAMBER PER TT-C-490, METHOD II
4. INSULATE INTERIOR SURFACE OF IGNITER CHAMBER WITH SD-850-15 PBAN TER-POLYMER INSULATION. INSULATION FORMULATION AND INSTALLATION PROCEDURE TO BE SPECIFIED BY DEPT. 4730.
5. ANP-2756 MOD I PROPELLANT FORMULATED AND CAST PER AGC-36026/28, TYPE I. IN ADDITION TO THE REQUIREMENTS OF AGC-36026/28, THE CURED PROPELLANT SHALL EXHIBIT THE FOLLOWING PROPERTIES:

MAXIMUM TENSILE STRENGTH	75 PSI, MINIMUM
ELONGATION AT MAXIMUM TENSILE STRENGTH	25%, MINIMUM
INITIAL MODULUS	250 PSI, MINIMUM

6. APPLY MIL-T-5524 LUBRICANT TO THREADS.
7. TORQUE RETAINER TO 100 ± 25 FT-LBS.
8. LUBRICATE "O" RING WITH MIL-L-4343 GREASE.
9. FOR STORAGE PRIOR TO INSTALLATION APPLY POLYETHYLENE SHEET OVER OPEN END OF IGNITER AND SECURE WITH TAPE. TAPE SHALL COVER ALL THREADS.
10. PERFORM ELECTRICAL CONTINUITY CHECK OF EBW SQUIB PER O.D. 21849 PRIOR TO INSTALLATION.
11. TORQUE TO 120 ± 5 IN-LBS.
12. INSPECT PROPELLANT GRAIN CONFIGURATION PER T-
13. BOND 1125531-1, INITIATOR, TO 1125532-1 OR -3, CHAMBER, WITH AGC-34285 CEMENT.

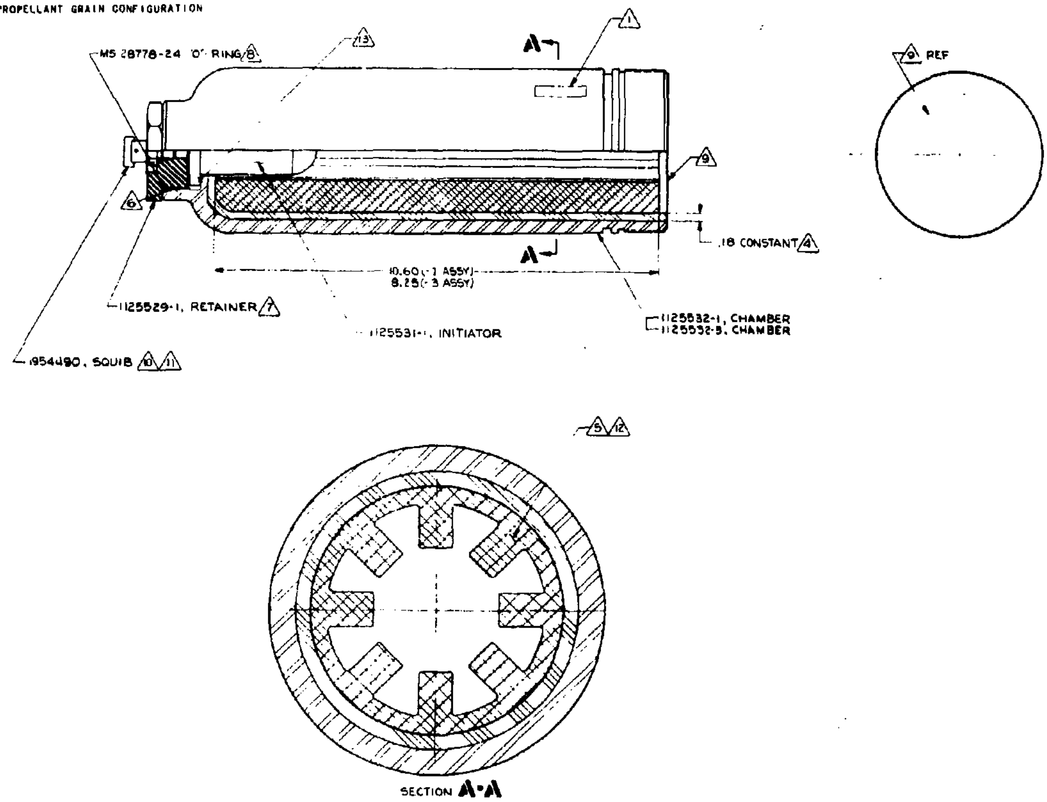

Igniter Assembly, Controllable Solid Rocket Motor

Figure III-110

for a duration of 0.290 sec, the average energy input to the grain surface being 119 cal/cm^2. The total propellant weight in the first-ignition cartridge is 2.06 lb. The other five igniters deliver 2.59 lb of propellant at a maximum mass flow rate of 12.55 lb/sec over a duration of 0.200 sec with the average operating pressure being 2000 psia.

d. Nozzle Design

(C) The nozzle design for the heavyweight motor is a more conservative approach to the same concept that was outlined in the preliminary design. Briefly, this nozzle is a strut-mounted, hydraulically actuated, movable pintle, shrouded nozzle with the area variability between 6.75 to 30.40 in.^{2} and a maximum expansion ratio for altitude testing of 40:1. The nozzle pintle and strut mount are designed such that pressure loading on the pintle will always be in the direction of increasing nozzle throat area, thus making the rapid opening requirement for $\dot{P}$ extinction easier to meet and effectively making the nozzle "failsafe." Each of the nozzle components will be discussed individually in the following sections giving the material selections and design considerations. The complete nozzle design is depicted on Figure III-111.

(1) Pintle

(C) The pintle design uses a stacked pyrolytic graphite washer insert, retained by a silver-infiltrated tungsten ring as the inner throat liner. Immediately upstream of the pyrolytic graphite and downstream of the tungsten, pre-charred carbon cloth inserts are used to complete the flame liner. These inserts are nested in an asbestos-reinforced phenolic insulator. The insulated assembly is supported on 90 tantalum-10 tungsten alloy rod and backed by a steel piston. The nose cap of precharred carbon cloth is supported by a molybdenum bolt. The steel piston uses two standard automotive piston rings and one high temperature O-ring to clean the cylindrical sealing surface of foreign objects and maintain a positive sliding gas seal during pintle operation, respectively.

(C) The material selections were based upon the results of the literature survey as well as the expected thermal environment of the pintle. It was determined that pyrolytic graphite is an excellent flame liner material for multiple exposure usage so long as the surface temperatures are maintained below an acceptable level. Although refractory metals are not considered good choices for reuse under normal rocket motor conditions, the selection of silver-infiltrated tungsten was predicated upon the strength of the sintered tungsten at elevated temperatures, the added conductivity of the infiltrated material over the sintered metal, and the added toughness of the

FULL SCALE HW-1 NOZZLE (U)

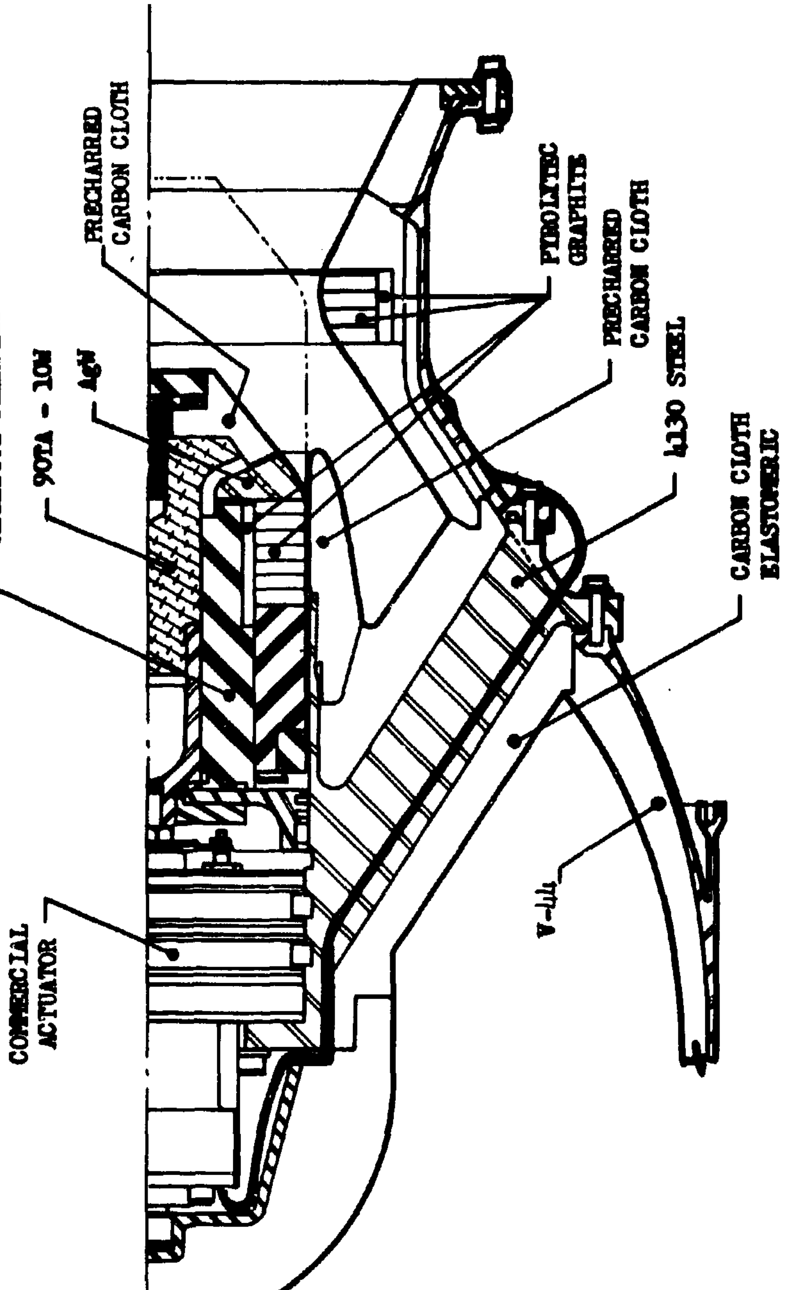

Nozzle Assembly Heavyweight Motor HW-1 (u)

Figure III-111

infiltrated material. The use of precharred carbon cloth insulative material as subsonic and supersonic flame liner material is based upon the low erosion rate of this material and its dimensional stability under reheating cycles. By minimizing the volatiles in the material through precharring, components are less susceptible to spallation, delaminating, and swelling--all of which cause loss of dimensional stability with subsequent clearance problems between sliding components. The basic insulation material, asbestos reinforced phenolic, was selected on the basis of its low conductivity and high compressive char strength.

(2) Pintle Housing

(C) The pintle housing is a three strutted component, fabricated from a single forging of either 4130 steel or 6Al-4V titanium alloy and heat treated, in either material, to 150,000 minimum yield strength. The outer diameter of this component forms a portion of the aft motor closure between the chamber and the outer throat structure. This method of design allows for ready access to the pintle subassembly and/or the outer throat subassembly, greatly simplifying the buildup of the subassemblies and the top motor-assembly. The inner cylindrical section of the pintle housing forms the actual pintle sleeve and also forms the outer portion of the hydraulic fluid transfer manifold. Each of the three struts is provided with two bored holes. Two of the struts contain the hydraulic fluid passages from an external hydraulic test stand to the transfer manifold, while the third contains the passage for position feedback lines. Each of the struts contains an air bleed line to vent the volume between the hydraulic actuator and the forward side of the pintle piston. Insulation of the pintle housing consists of MXCE-280, molded in place. A separate insulative cap of MXCE-280 is used to protect the actuation system and divert the gas flow to the annular passages between the struts.

(3) Hydraulic Actuator

(U) The hydraulic actuator is a specially designed unit, supplied by Conair, Inc., specifically to meet the requirements of both precise and rapid pintle positioning. The basic actuator-manifold housing will be fabricated from a single aluminum billet to eliminate leakage and tolerance problems. A single-ended rod and unbalanced area piston will be used to compensate for the unbalanced loading on the pintle. Porting of the actuator-manifold and the strut housing will be designed to accommodate a response rate of 10 cps for the 1/2-cycle rod retraction stroke, providing for the rapid area changes necessary to accomplish $\dot{P}$ extinguishment. The system is designed to operate at a nominal pressure of 3000 psi using MIL-L-7808 oil as the power transfer medium. The fluid was selected based

on its high temperature operating characteristics and low coking characteristics at elevated temperatures. A cushion is supplied in the blind side of the actuator to snub the last 1/8-in. of stroke, limiting the impact at the end of the 10 cps stroke. For safety purposes, the actuation system will be proof tested at 6000 psi and designed for burst at 7500 psi.

(U) Each actuation system will be equipped with a linear potentiometer with a 10,000 ohm coil and 0.003-in. resolution to accurately measure pintle position. The potentiometer will be housed within the actuator-manifold housing such that it is exposed only to the vented volume between the actuator and the pintle piston. The lead lines to the potentiometer are potted into the volume behind the actuator such that they can be fed through the bore in the strut provided for them.

(4) Nozzle Shroud

(C) The nozzle shroud, or outer throat and exit cone, is designed as a two part assembly with the break in the two parts occurring at an expansion ratio of 10:1 based on minimum nozzle throat area. This split was required to allow for sea level testing of a motor designed for altitude operation. The flame liner materials that were selected for use were the same as those used in the pintle for similar application. Pyrolytic graphite washers are used on the throat insert material to make use of their high resistance to surface regression and good restart capability. Graphite cylinders are used on the backside of the washers to permit a free sliding surface for thermal expansion. In the subsonic flow region, graphite phenolic flame liner material is used in place of the precharred material used on the pintle. For the outer throat insert, the tolerance control problem is not as severe as in the pintle; thus, the lower conductivity and better ablation characteristics of the uncharred material can be used. Backside insulation of this insert and the throat insert is an asbestos filled phenolic, high pressure molded and machined to required dimensions. Immediately downstream of the throat insert, graphite phenolic is used as the nozzle flame liner material for the same reasons as it was used upstream of the throat. The expansion cone liner is silica phenolic, tape wrapped parallel to centerline for maximum erosion resistance. The same material is used to line the extension to the expansion cone. The structural material used for the outer shroud is either 4130 or 6Al-4V titanium alloy heat treated to 150,000 psi minimum yield strength. As this shroud design is similar to a conventional nozzle and all of the design techniques used in the shroud have been proven in conventional nozzles, the heavyweight design need not be as conservative in this area.

2. Pressure Feedback Servocontrol System

a. Design of Initial System

(U) The purpose of the pressure feedback servocontrol system is to control the thrust generated by the single-chamber controllable solid rocket motor and to stop-restart this motor on command. The initial system is shown on Figure III-112 in a simplified circuit diagram. This system incorporates safety interlocks, manual operation, and preprogrammed operation. The manual operation mode will allow selection of the igniter, fire-switch operation, thrust variation, and emergency stop-restart. After manual operation of the fire switch, the system can be controlled by preprogrammed thrust-parameter input either from a programmed signal generator or tape reader. Safety interlocks protect the motor from inadvertent ignition and from overpressure.

(U) The control system operates in two modes, position and force control, utilizing two feedback loops. This system ensures that the nozzle pintle is in the proper position before starting the motor. During the ignition transient, position control is employed to eliminate plug motion during possible ignition pressure spikes. After the ignition transient has decayed, the system is automatically switched to force control. This change of mode is initiated by a time-delay timer. The automatic shutdown system incorporates a failsafe manifold on the servovalve that rapidly places a hydraulic bias on the valve to activate extinguishment under excessive chamber pressure conditions. Activation of this emergency shutdown system automatically terminates the action of the force control loop, bypassing the servovalve and driving the pintle open to effect P extinguishment.

(C) Thrust control is achieved by a force feedback signal that consists of the measured chamber pressure multiplied by a nozzle throat area that is calculated from a potentiometer signal that indicates nozzle pintle position. By comparing the feedback force parameter with the input command, an error signal results in directional motion of the pintle to correct the error. Damping is achieved by use of a compensation network in the servo controller. It is expected that thrust control can be attained within plus or minus 10% over the operating range of 2000 to 8000 lb of thrust. At lower thrust levels, the accuracy of the control will fall off rapidly due primarily to the inaccuracy of the method of calculating nozzle throat area from nozzle position. To simplify the electrical circuitry in the controller, a second power equation of pintle position will be used to calculate the nozzle throat area. This equation is accurate to within plus or minus 3% over the variable thrust range; however, the accuracy is much less as the nozzle throat is opened into the extinguishment range. L* extinguishment can

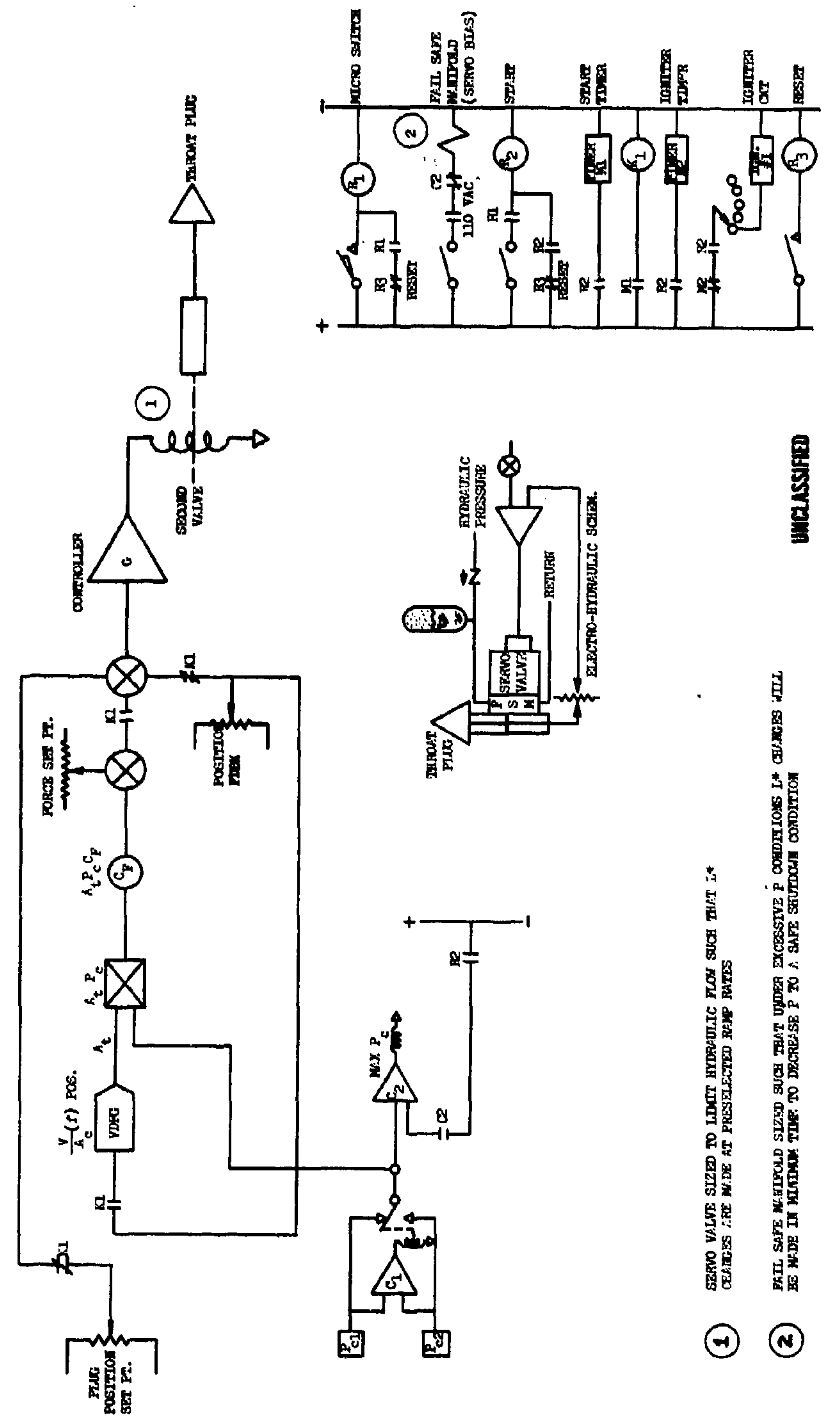

Pressure Feedback Servocontrol System Schematic

Figure III-112

still be attained by simply commanding zero-force output, although the path to zero force will not necessarily follow the input path.

(U) The sequence of operation of the system shown on the diagram is described in the following paragraphs. This description assumes that all switches and relay contacts are initially in the position shown on the diagram.

(U) First, one of six igniters is manually selected. The servo failsafe manifold switch is made. This removes a hydraulic bias on the valve. The plug position command signal is applied to the controller summing junction through the normally closed contacts of relay K_I. The error signal resulting from the summing of the position command signal, and the plug position feedback signal, activates the hydraulic system placing the plug in the desired position for ignition. When this position is attained, a start position signal activates relay R_1 and locks it in through a set of its own contacts. R_1 contacts arm the start circuit; thus assurance is made that the proper plug position is obtained before starting the motor. Closure of the start switch energizes relay R_2 and locks it in. Contacts of R_2 relay provide closure for a signal to the igniter and timers M_1 and M_2. Timer M_2 de-energizes the igniter circuit. Timer M_1 is set to a predetermined value necessary to achieve steady-state operation. On time out, normally open contacts of time M_1 close and energize relay K_1, effecting a mode transfer from position control to force control through relay K_1 contacts. The resultant force parameter feedback-command error signal activates the hydraulic system as previously described.

(U) Chamber pressure is obtained from voltage comparator C_1, monitoring a pair of transducers. This dual transducer system minimizes the possibility of a low chamber pressure due to line clogging or transducer failure. Voltage comparator C_2 monitors maximum chamber pressure and, when triggered, will lock in and de-energize the failsafe manifold, applying a hydraulic bias to the valve terminating the action of the force control mode and effecting emergency extinguishment. The entire system is reset by closing the reset switch, thus returning all relays to the de-energized position.

(U) Two types of shutdown are provided: one, by the control system emergency stop and the second, by reducing the force command to zero. If the failsafe manifold is de-energized by either comparator, C_2, triggered by maximum chamber pressure, or by manually opening the failsafe switch, a hydraulic bias is applied to the nozzle plug control valve which will effect a P shutdown motion on the pintle.

(U) This control system was simulated on both a special test fixture and on an analog computer to minimize development on actual motor firings. System accuracy and repeatability was established by comparing force command against actual measured force during static testing. The calculated force based on motor chamber pressure and nozzle pintle position will be compared to measured thrust. At steady state, command force and force feedback are equal; therefore, the response of the control feedback loop, to a step input command, can be determined from this baseline.

(U) The measurements required for the operation of the control system are nozzle pintle position and motor chamber pressure. The accuracy of the control system depends directly on these two measurements, thus a major effort was made to increase the reliability of these measurements. The accuracy of the calculated nozzle throat area has been previously discussed and can only be improved by incorporation of an extensive electrical network to solve a seventh power equation. For purposes of this program, this complexity was not deemed necessary as only a minor improvement could be expected to result. Currently, Aerojet's Solid Rocket Test Operations is measuring pressures to plus or minus 0.38% one sigma with a bias of 0.19% at both sea level and simulated altitude. Motor thrust measurement accuracy is dependent upon the test stand, and for the purpose of system accuracy definition (steady-state operation) a 1% one sigma will be adequate.

b. Final Pressure Feedback Control System

(U) For the first three test firings of the controllable solid rocket motor, a "breadboard" control system was employed to vary the thrust and extinguish the motors. This breadboard system employed the PC-12 computer circuitry that was to become the final control system; however, this circuitry was temporarily patched into the stationary equipment in control room W-3 at Aerojet's Sacramento Solid Rocket Test Facility. All of the timing and amplifying functions required by the control system, other than those inherent in the computer, were externally supplied using available control room facilities. As this setup was not compatible with the program requirements of firing motors at the Arnold Engineering Development Center, an integrated, portable console was designed and fabricated to provide all of the control functions necessary to fire, vary thrust, and extinguish the single-chamber controllable solid rocket motor. This integrated system required inputs in the form of 28 vdc - 10 amp, 115 vac - Single Phase - 60 cycle - 10 amps, and the normal motor feedback signals of chamber pressure, pintle position, and thrust to completely control the CSR motor. As the two power supply requirements are available in almost any motor test facility, including portable test units, the CSR motor can be test fired at any facility without special setup and at nominal cost. A brief description of the console and its operation is provided in the following paragraphs.

(U) The pressure feedback control system, as packaged in a Stantron F1500-25 console cabinet, is shown on Figure III-113. The console incorporates illuminated push button switches, indicators, meters monitoring pintle position, chamber pressure and thrust. A hand operated "throttle" is provided to give the test conductor manual control over the controllable solid rocket motor. The system is also provided with the flexibility of remote programmer input if it is found more desirable to test the CSR with a preselected program rather than manually. The console houses a 3-shelf PC-12 analog computer, sequence control circuits, pressure transducer conditioning circuitry, interface connector panel, igniter select and firing circuit.

(U) The console consists of four sections: (1) the console lid, Figure III-114, which incorporates the indicators and controls; (2) the sequence circuitry, Figures III-115 and -116 and (3) the computer section, Figures III-117 and -118; and (4) the interface connection panel, Figure III-119.

(1) Console Lid

(U) The console lid is divided into three sections: (1) indicator, (2) control, (3) igniter selector. The indicators provide visual display of the mode of the sequence circuitry at all times. Indication is given by the meters of plug position, chamber pressure and thrust. The light indicators functions are:

(a) FSM Energized - This function indicates when the failsafe manifold is energized and the servo valve is electrically operable, assuming that the hydraulic pressure is up.

(b) Sequence Ready - This function indicates that the proper chain of events prior to rocket fire has been achieved and igniter can be fired.

(c) TCPS - This function indicates that thrust chamber pressure switch has been actuated. A sustained chamber pressure will assure a timing out of the MTCPS TIMER and the combination "PRESSURE SWITCH-TIMER" circuit will initiate a transfer from the position mode to the force mode.

(d) MTCPS and MIGN - These functions indicate the time out of the two timers used in the circuits. The MTCPS timer is used in conjunction with a comparator to initiate transfer from position to force mode and the MIGN timer opens the igniter firing circuit.

(e) Position Mode/Force Mode - This indicator indicates the pintle control mode that is in effect. The position mode allows control of the pintle with the plug position pot. The force mode allows control with the thrust control throttle.

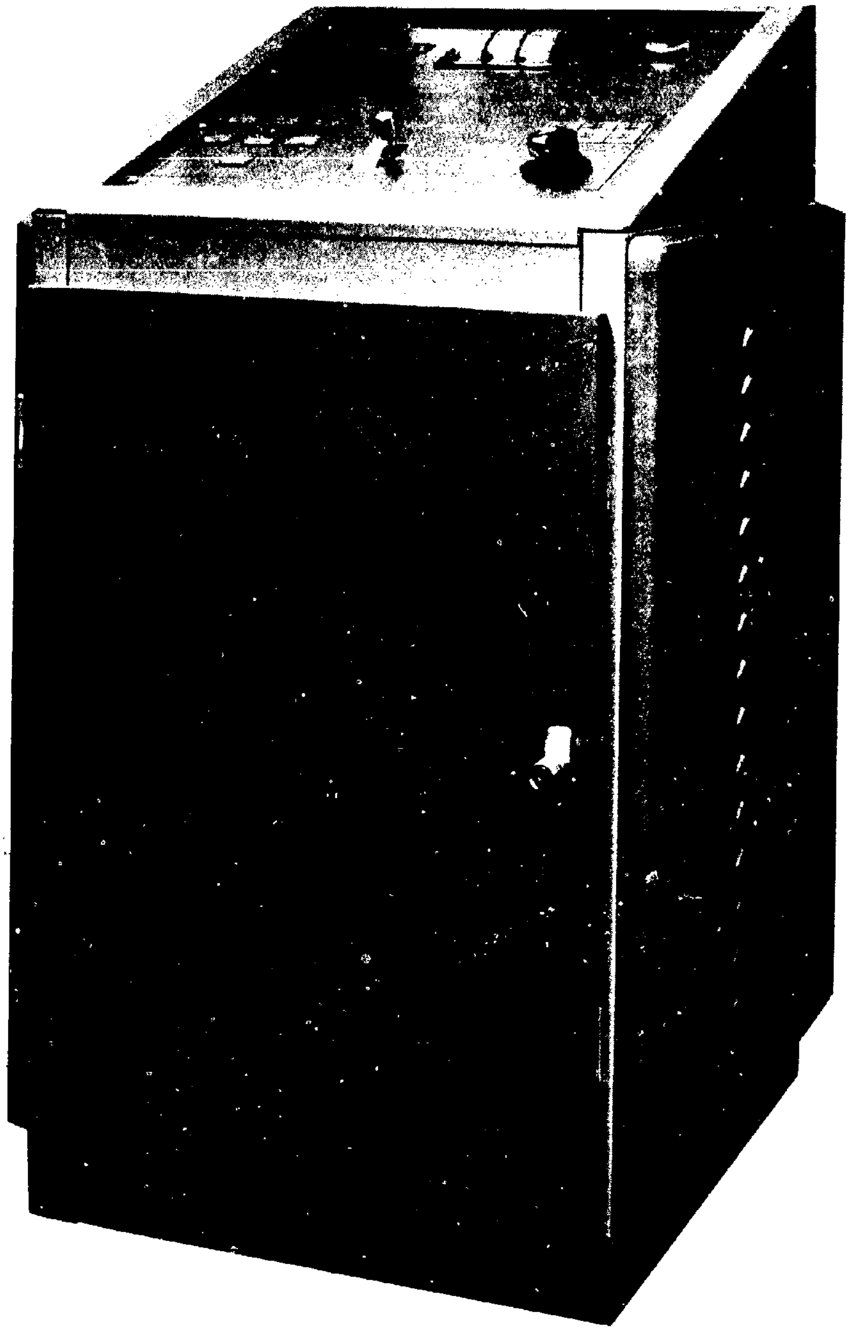

Pressure Feedback Control Console

Figure III-113

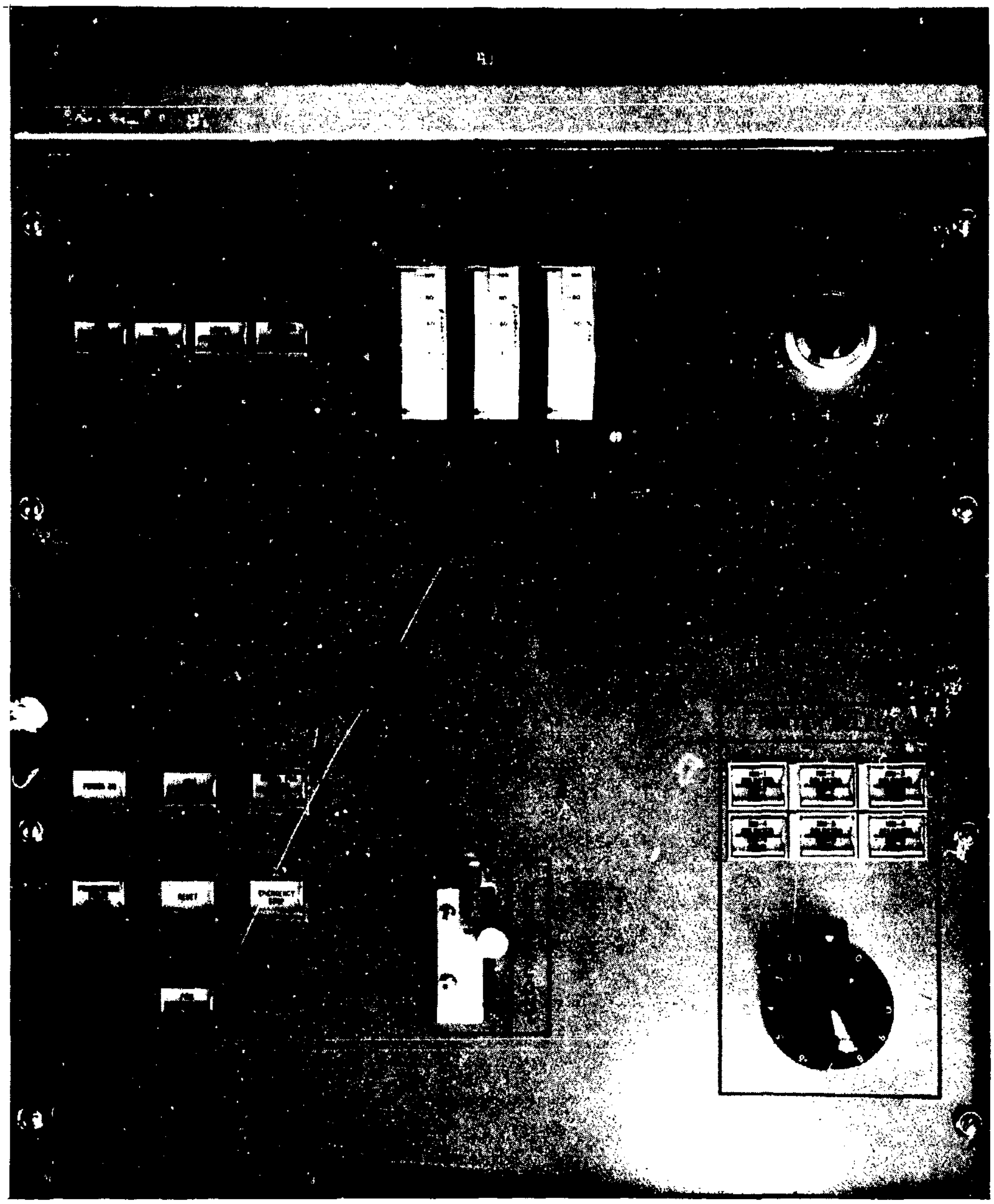

Console Lid

Figure III-114

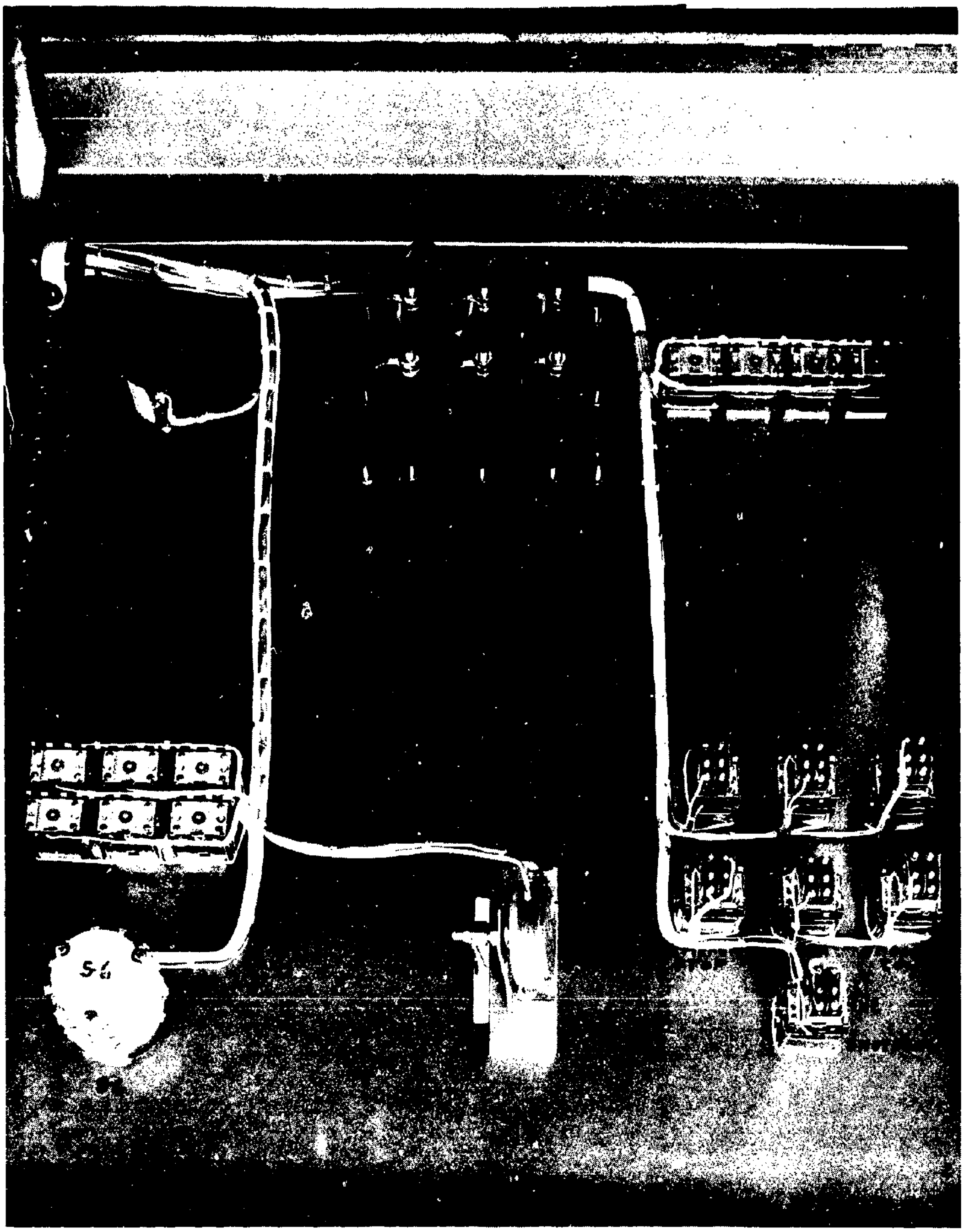

Console Sequence Circuitry

Figure III-115

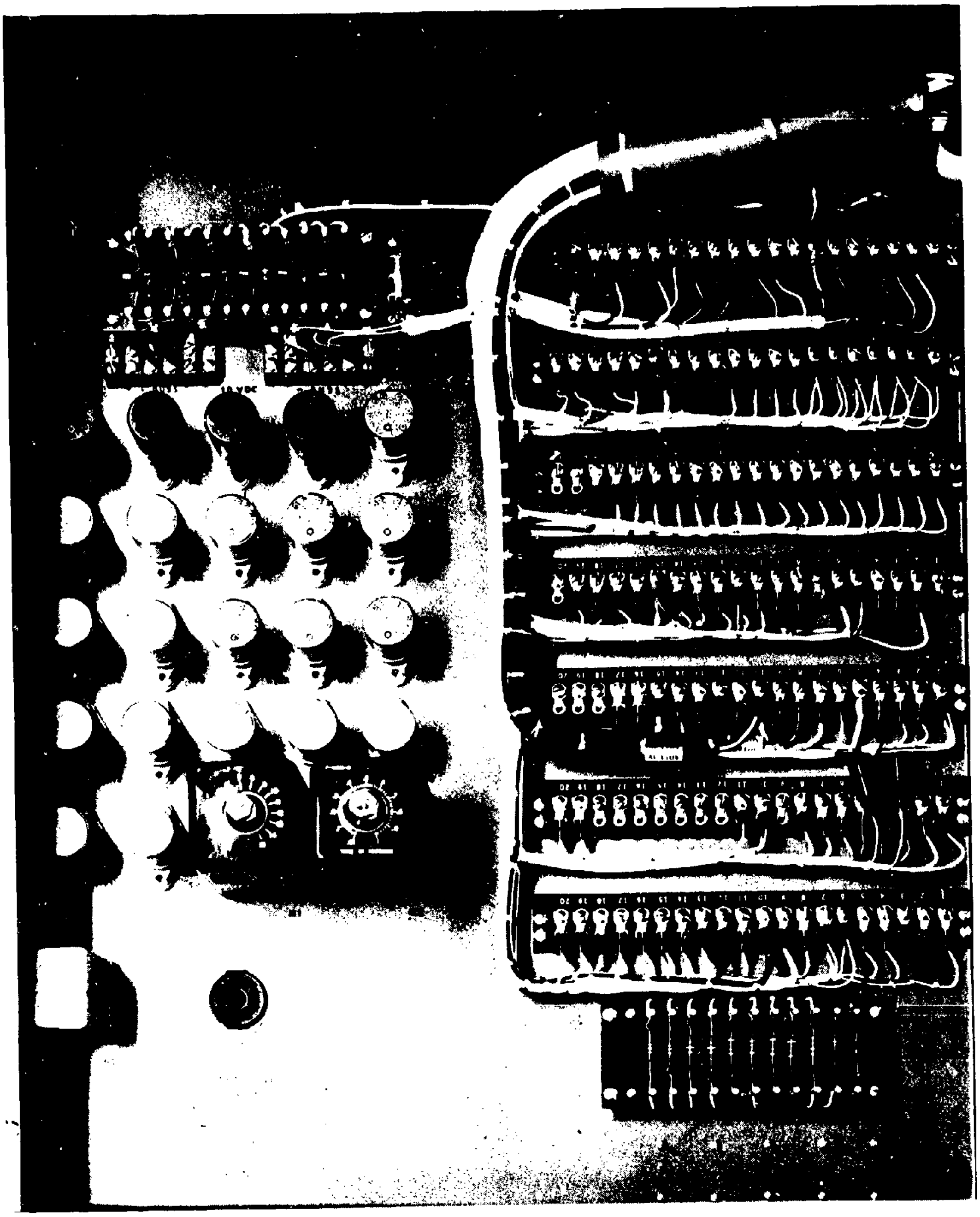

Console Sequence Circuitry

Figure III-116

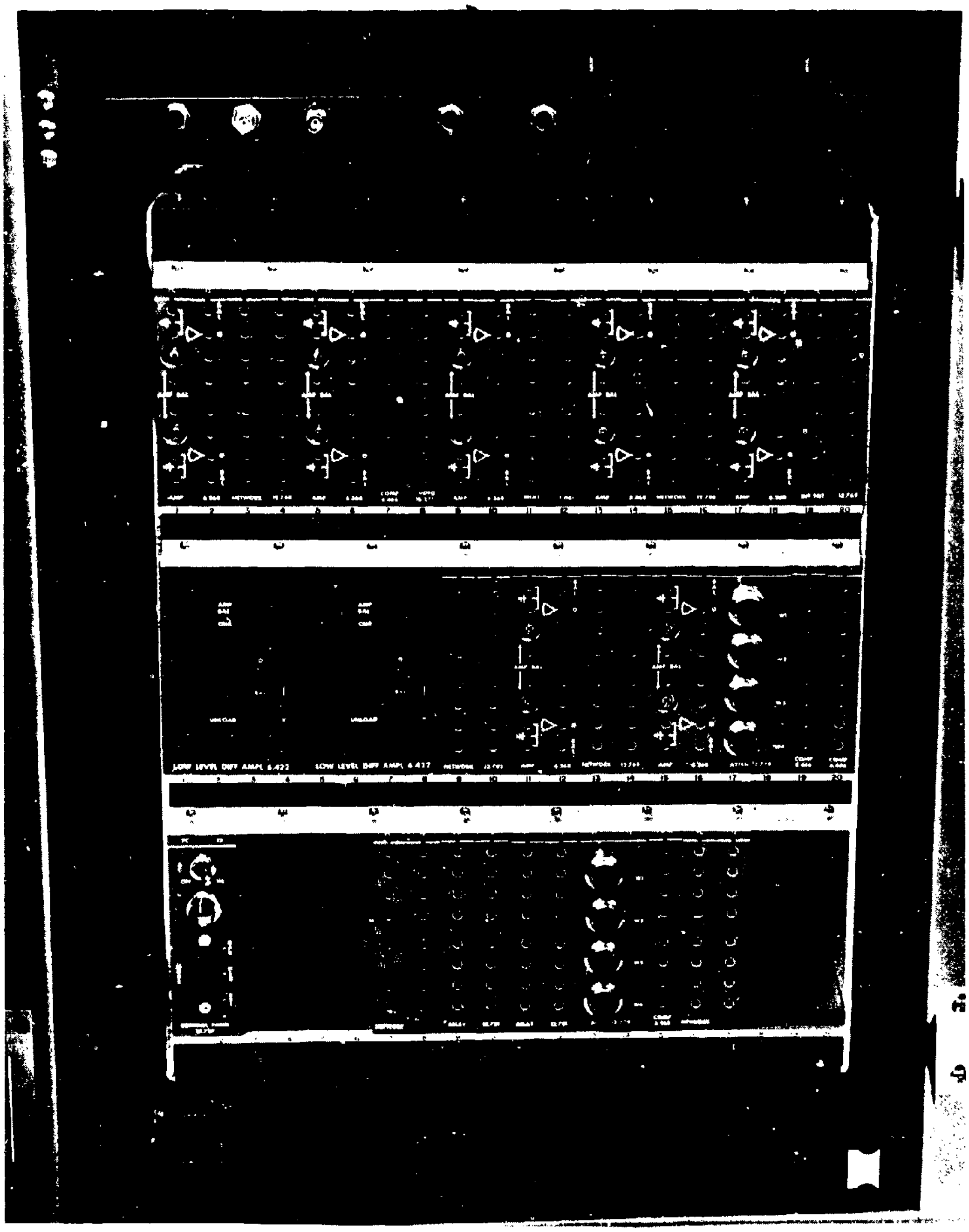

Console Computer Section

Figure III-117

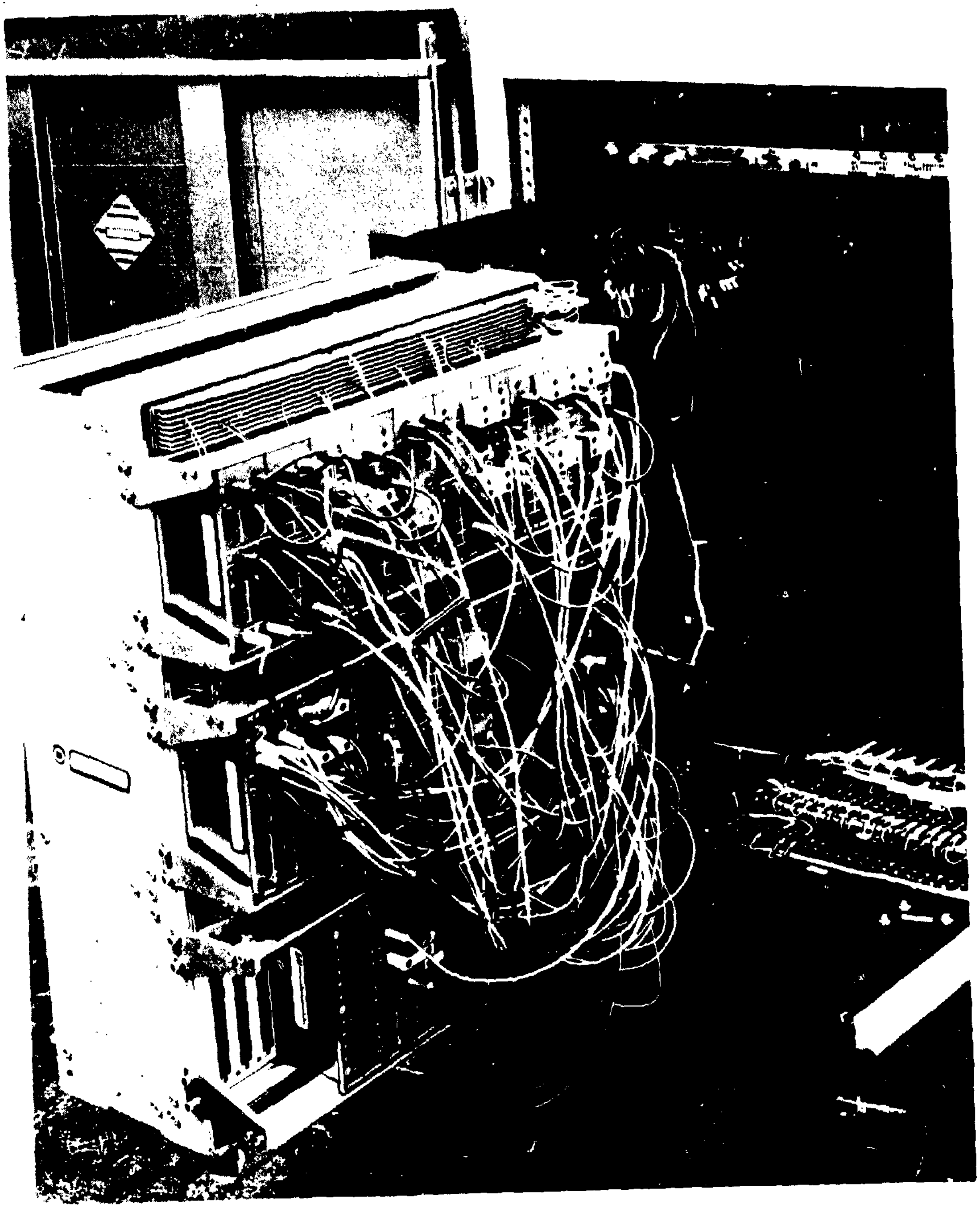

Console Computer Section

Figure III-118

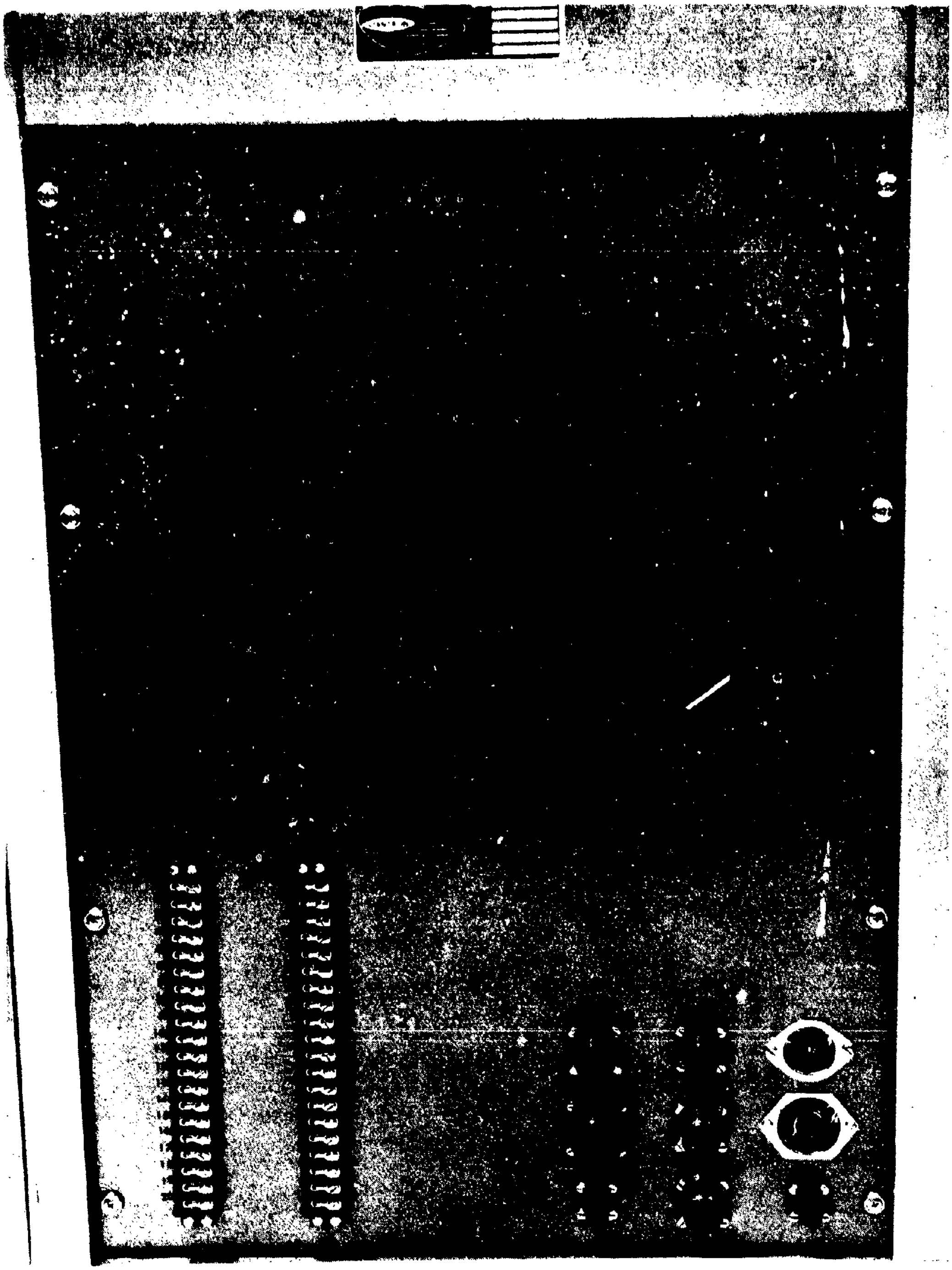

Console Interface Connection Panel

Figure III-119

III, D, Heavyweight Motor Development (cont.)

(U) The control section of the lid consists of 7 push button indicators, a throttle lever and a rotary potentiometer. The push buttons allow the application of power to the console, arming, firing, and resetting. Positioning of the plug and thrust control are achieved with the rotary pot and throttle respectively.

(U) The igniter selector switch allows selection of any one of six igniters. The igniter selected is indicated. The output signal is a 28 vdc signal that may be used to actuate the select relay. On firing of the selected igniter the "IGN-X FIRED" light goes on, thus indicating the igniter circuit pulsed with the firing signal. The "IGN-X FIRED" light will stay on until console power has been removed. Reset does not affect the lights.

(2) Sequence Circuitry

(U) The purpose of the sequence circuit is to provide control of the failsafe manifold, plug position, igniter select, etc., so that a firing can be safely initiated, terminated and the motor restarted if desired. The sequence circuit provides initial position power to the failsafe manifold allowing positioning of the plug in the start position before the firing can be initiated. On placement of the plug in the proper position the signal to the failsafe manifold is transferred to the READY-MALF circuit and the sequence ready circuit is energized. Automatic shutdowns are initiated on the opening of READY-MALF circuit by loss of ac power, high Pc, loss of dc power, or manually, by actuation of the emergency stop button. The mode of the sequence circuit is displayed at all times by the console indicators. A timer checkout circuit is incorporated in the console to facilitate checkout and setting of the two timers used in the sequence circuits.

c. Computer Section

(U) Servo control is affected by the use of a Pace PC-12 analog computer consisting of the following components:

(1)	Dual dc Amplifiers	7 each
(2)	Lo Level Amplifiers	2 each
(3)	Relay Comparators	4 each
(4)	$(1/4)^2$ Multiplier	1 each
(5)	Integrator	1 each
(6)	Four Potentiometer Network	2 each
(7)	Variable Diode Function Generator	1 each

(8)	Quad Relay Module	2 each
(9)	Inverter Network	3 each
(10)	Custom Network	2 each

and respective patching modules. The servo control system operates in two modes, the position mode and the force mode utilizing two feedback loops.

(U) Prior to the firing and during the start transient period the position mode is used to place the plug in the desired position. On decay of the start transient and in steady state, the system is automatically switched to the force mode. In the force mode thrust may be varied as desired by use of the thrust control throttle or by means of a programmed force input. The force feedback signal is obtained by sensing the plug position and converting it to throat area in the variable diode generator and multiplying it with chamber pressure in the $(1/4)^2$ multiplier. The error signal resulting from the summation of the demand force signal and the force feedback signal activates the hydraulic system controlling the nozzle movement. Optimum damping is achieved by use of proper amplifier gains.

(U) The relay comparators are used to monitor the plug position and chamber pressure and to initiate switching signals to the sequence circuitry.

(U) The lo-level amplifiers incorporate a gain of 333. The input to these amplifiers from the transducers monitoring the chamber pressure is increased to 10 volts maximum. A comparator circuit is used to monitor the Pc signal; the comparator circuit is adjusted to automatically switch to the transducer providing the highest Pc signal. This system minimizes the possibility of a low chamber pressure due to line clogging or single transducer failure.

(U) Comparators are also used to monitor the plug position and to monitor levels of chamber pressure to initiate mode transfer or emergency shutdown due to excessive chamber pressure.

d. Console-Rocket Motor Interface Panel

(U) The rear panel of the console is provided with terminal strips and connectors to provide interface with the rocket motor and with instrumentation for monitoring and recording purposes. The interface cables to the console required are as follows:

III, D, Heavyweight Motor Development (cont.)

(1) 28 vdc 10 amps

(2) 115 vac 1-phase 60 cycle 10 amps

(3) Thrust monitoring signal from instrumentation (10 vdc max.)

(4) Position feedback potentiometer

(5) Pc transducer #2

(6) Pc transducer #1

(7) Servo valve

(8) Igniter select relays and firing pulse to EBW unit

(9) Failsafe manifold

(10) Instrumentation signal for recording servo voltage, plug position, percent throat area, force feedback, chamber pressure Pc, and programmed force.

Connections are also provided on the rear terminal strip to allow a "hands off" firing of the motor by means of an external programmer i.e., the arming, firing and resetting of the console may be accomplished by external control.

e. Operation

(U) The sequence circuitry allows positioning of the plug prior to rocket fire, for checkout, measurements or setup purposes. The sequence ready circuit ensures that the plug is in the proper position before igniter fire can be initiated. The READY-MALF circuit locks in the signal to the failsafe manifold and initiates the shutdown in case of a high Pc, loss of power or in case the emergency shutdown button is actuated. The emergency shutdown button can be used in case a relay in the shutdown circuit malfunctions.

(U) Rocket extinguishment may be accomplished by either P-dot or L* commands. P-dot command extinguishment is accomplished by de-energizing the failsafe manifold; thus, the servo valve is bypassed and a hydraulic bias placed on the actuator rapidly driving the pintle to the shutdown position. The pintle may be shuttled to the shutdown position from maximum displacement in 50 milliseconds. P-dot command shutdowns are accomplished by pressing the Fire-Shutdown Switch or the Emergency Stop Switch. L* command shutdowns are accomplished by retracting the Thrust Control throttle towards the 0% position. As the Fire-Shutdown Switch is an alternate action switch, Reset and Arming cannot be accomplished until the switch is placed in its initial position. This is indicated by a continuous reset light.

III, D, Heavyweight Motor Development (cont.)

(U) Restart of the motor is accomplished by selecting an igniter, resetting, arming and applying power to the failsafe manifold. With hydraulic pressures up and the plug position potentiometer set, the plug will track to the start position and Sequence Ready. The sequence of operation is as follows:

(1) Computer on, switch in operate position.

(2) Console power on - 15 minute warm up.

(3) Hydraulic power on - pressure up.

(4) Actuate 'Initial Position Power'.

(5) Arm

(6) Place plug in initial position by dialing potentiometer to desired start position. All green board when this position is attained.

(7) Set thrust control throttle to desired start thrust.

(8) Select igniter to be fired.

(9) Fire motor.

(10) After TCPS indicates, throttle motor by moving hand throttle or motor can be controlled by external programmer signals into the console.

f. Modification to Circuitry

(U) During the initial usage of this computer, some difficulty was experienced due to the non-constant mechanical gain of the rocket motor system over the wide range of operating pressures. To compensate for this non-constant gain, a variable gain network was incorporated into the circuit. This variable gain network operated on the measured chamber pressure of the motor, correcting the electrical gain input such that at high chamber pressures the electrical gain was lowered and at low chamber pressures the electrical gain was raised. This compensation was introduced during the lightweight test series after testing LW-3 and considerably improved the control capability of the system.

3. HW-1 Test Firing CSR-DA-01S-BH-001

(C) The primary objective of this test firing was to determine overall motor performance and to perform initial shakedown of all components with the pintle held in a fixed position. This was the first test of all components with the pintle held in a fixed position. This was the first test of all components (with the exception of the igniter, which was tested to verify the configuration and ballistics). A secondary objective of this first test was sea level extinguishment very near the end of web burning. Preliminary estimates of the web burning time were made, based on the burning rates determined by both 3KS-500 motor data and solid strand data. These data indicated that the duration would most probably be 27 sec, assuming that the aerodynamic throat area of the nozzle was 96% of the geometric throat area of the nozzle.

(C) On this basis, it was determined to attempt extinguishment at the 25-sec point unless an anomaly occurred earlier, at which time extinguishment would be commanded prematurely. An overpressure shutdown system was supplied which would automatically command extinguishment if the chamber pressure exceeded 1000 psia. In addition, the test conductor was supplied with a "kill" button in the event erratic combustion or a leak occurred, and it was recognized in time to save the .otor.

(U) Figures III-120 through III-128 depict the motor prior to test firing as set up in the test stand. The hydraulic control panel is clearly shown in Figures III-121 and III-122. Special brackets mounted to the aft test stand ring and the hydraulic lines were used to eliminate the flexing of the hydraulic tubes at the point where they were welded to the strutted housing. These brackets are shown in Figure III-123.

(U) Also shown on Figure III-123 (and more clearly in Figures III-124 through III-126) is the nitrogen ejector ring mounted on the aft face of the nozzle at the exit plane. The purpose of this ring is to provide a curtain of nitrogen after motor shutdown to halt the entry of air and thus avoid post-burning of the insulation. On the deck below the center of the motor, as shown in Figure III-124, a solenoid valve was located in the nitrogen purge line so that this purge could be initiated immediately at the command for solution.

(U) On Figure III-125, the potted lead lines can be seen at their point of attachment to the nozzle to the right side of the nozzle slightly above the motor centerline. Figures III-125 and -126 show the nozzle installed in the motor with the pintle in the firing position for this test, and the fully retracted (extinguishment) position, respectively. The igniters and the chamber pressure transducers are shown in Figures III-127 and III-128.

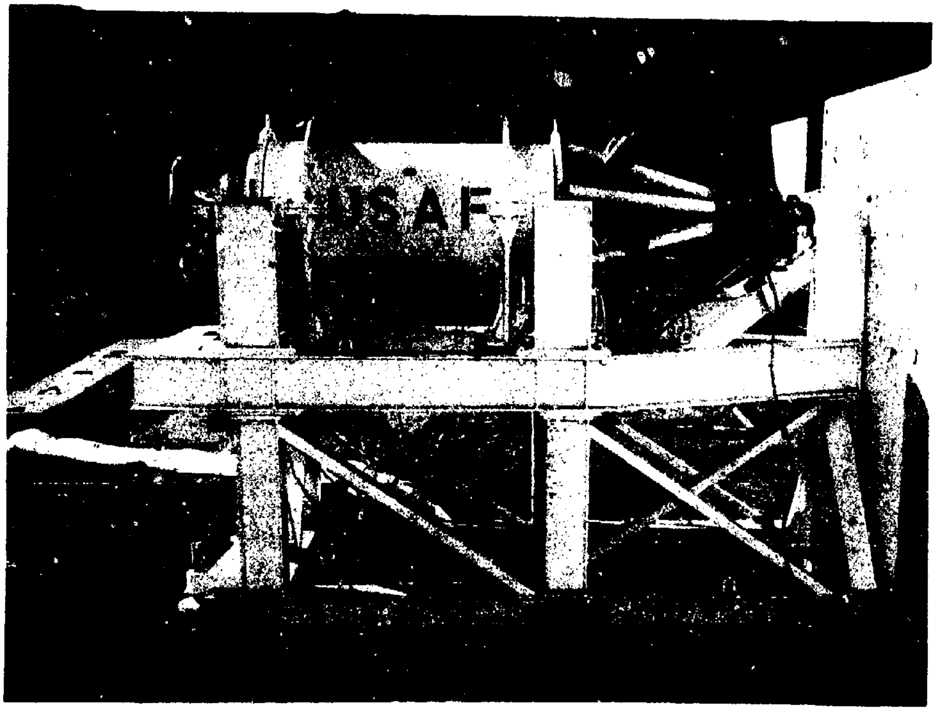

Overall 90° - Starboard HW-1 - Prefire

Figure III-120

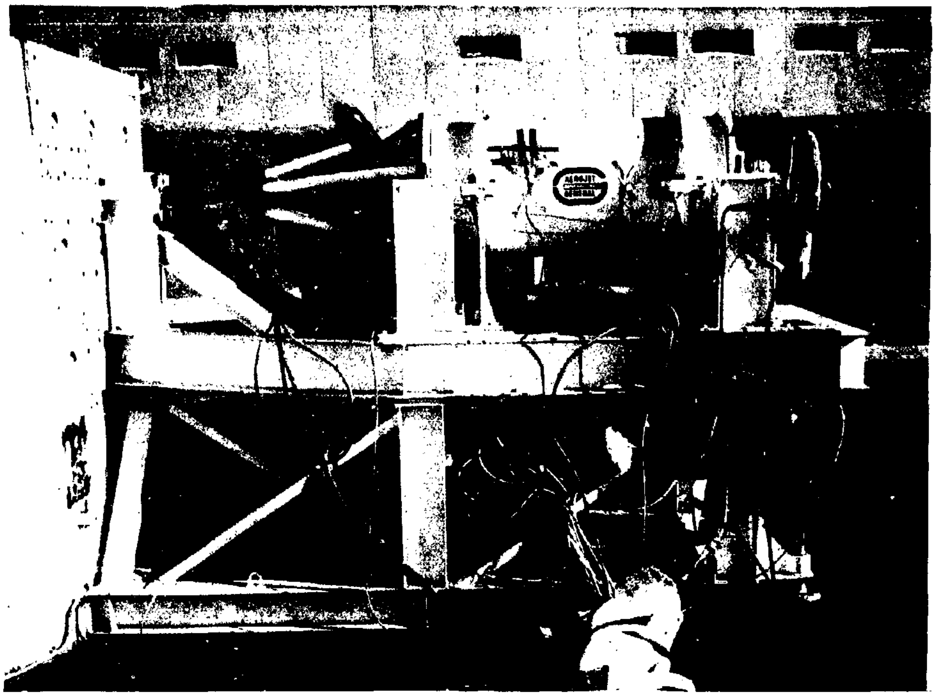

Overall 90° - Port HW-1 - Prefire

Figure III-121

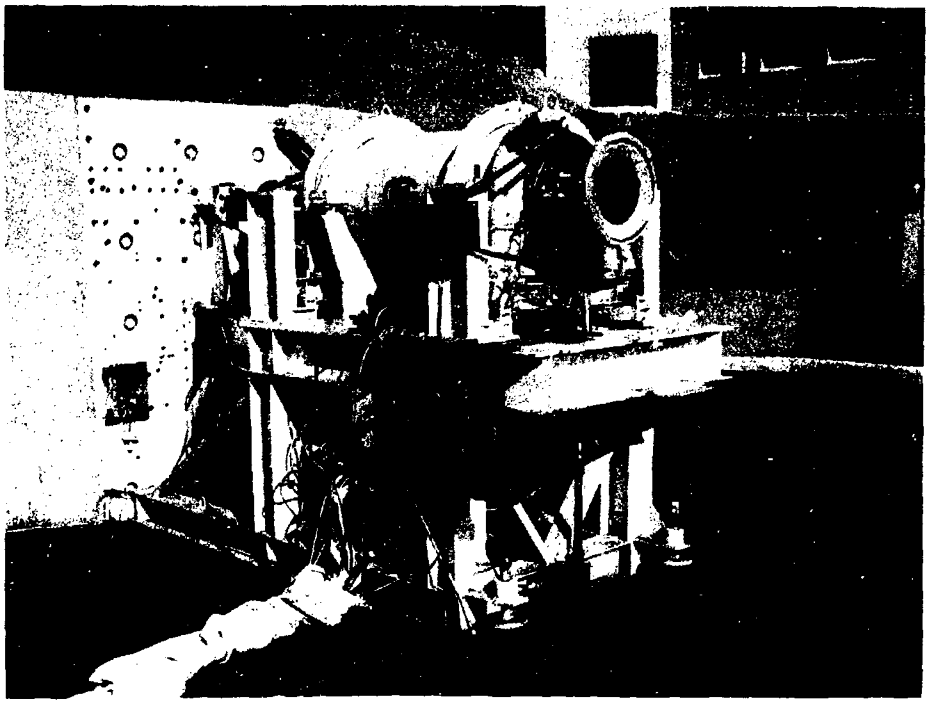

3/4 Aft, Port, HW-1 - Prefire

Figure III-122

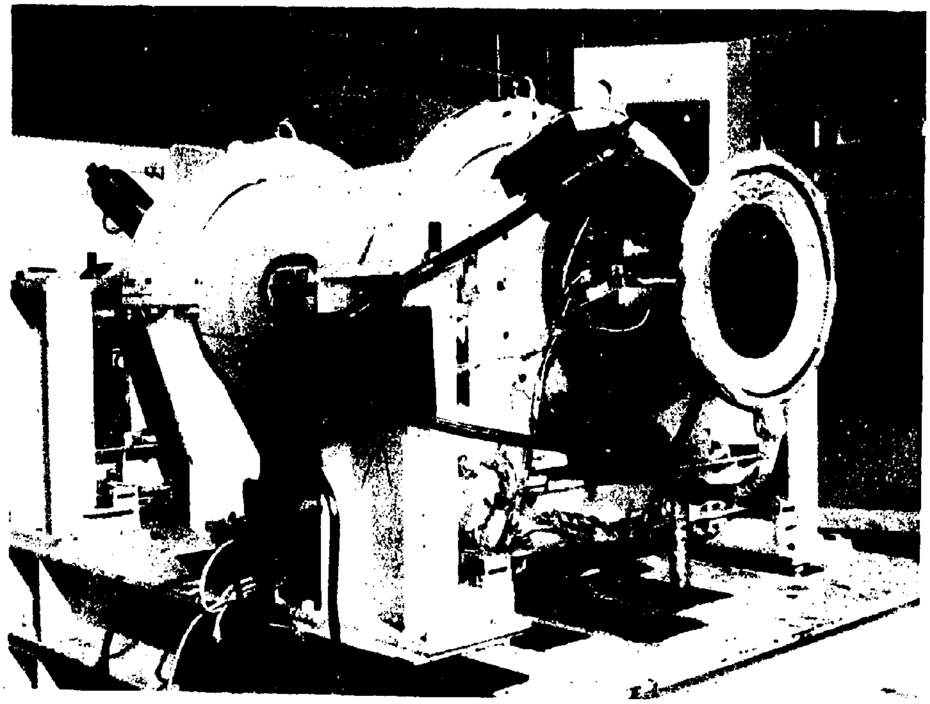

C/V 3/4 Aft, Port, HW-1 - Prefire

Figure III-123

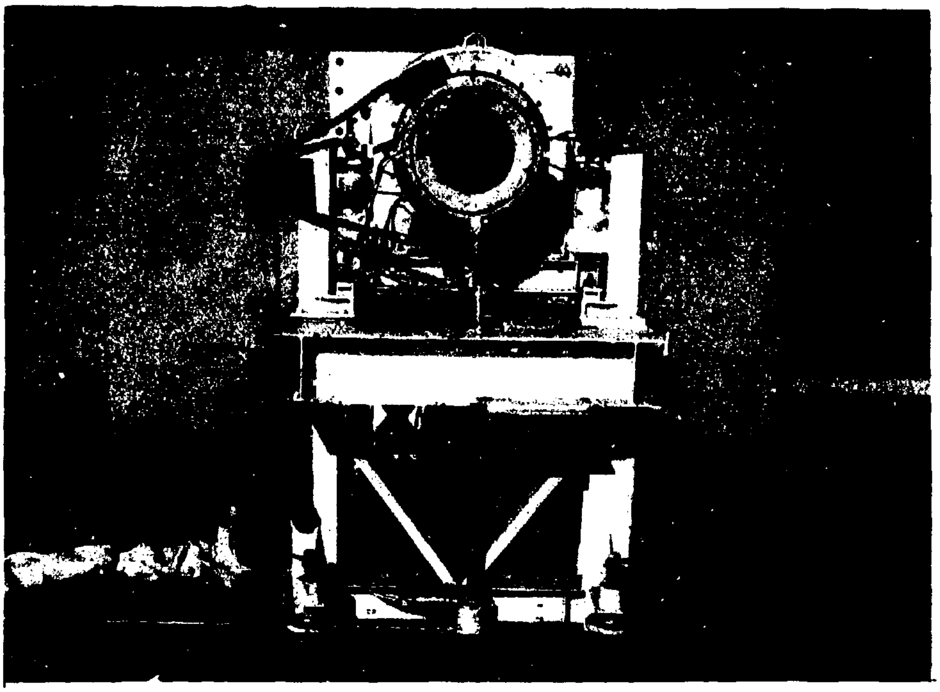

Aft Overall HW-1 - Prefire

Figure III-124

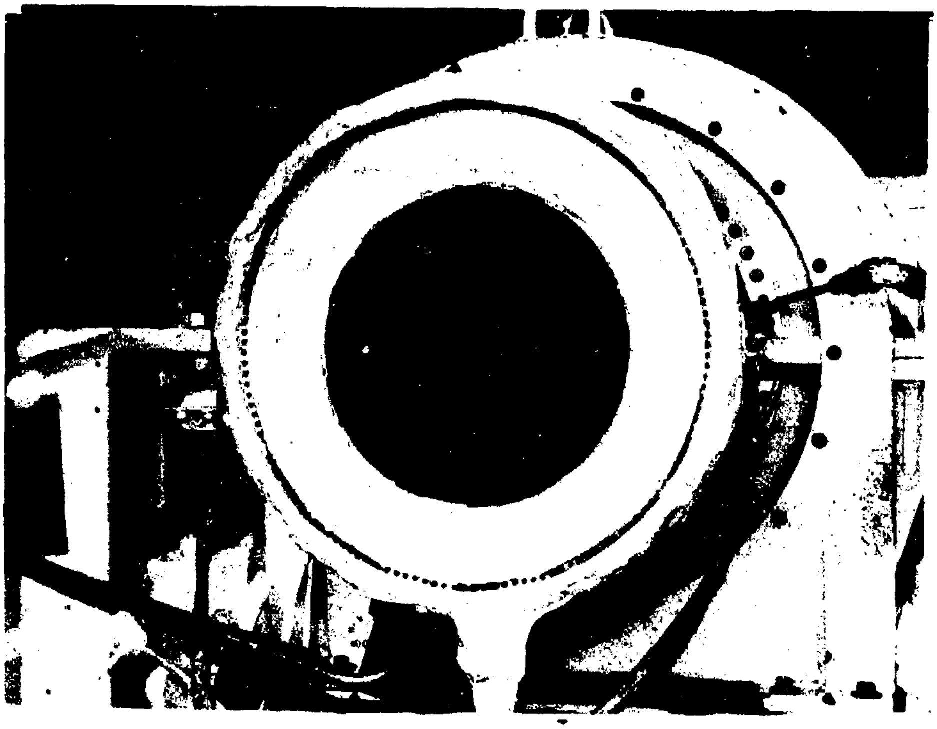

C/V Nozzle - Firing Position HW-1 - Prefire

Figure III-125

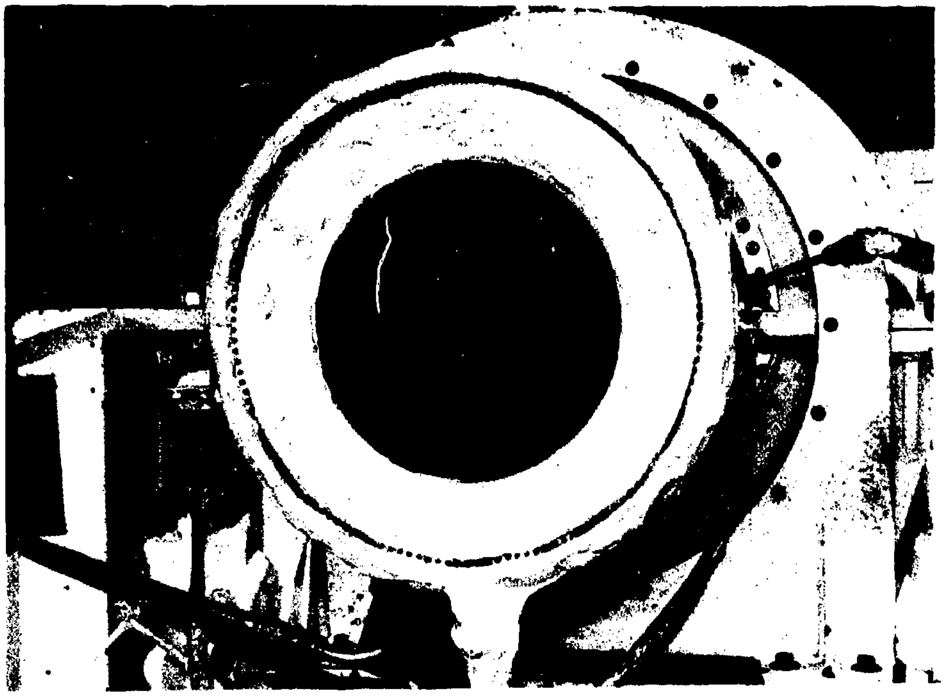

C/V Nozzle - Extinguishment Position HW-1 - Prefire

Figure III-126

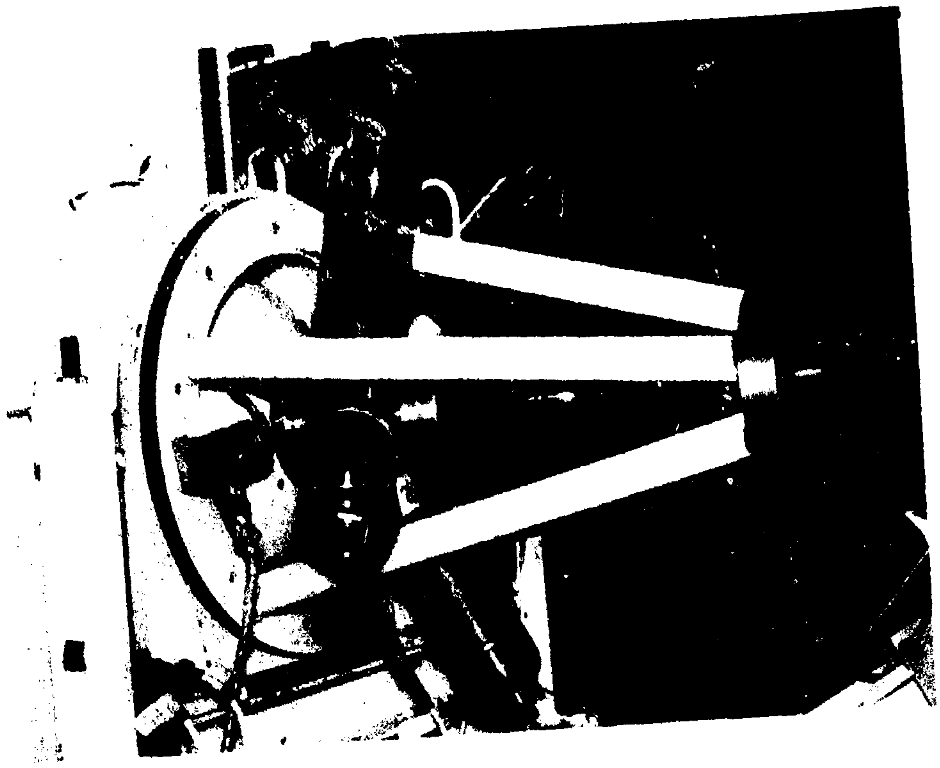

C/V Nozzle - Extinguishment Position HW-1 - Prefire

Figure III-127

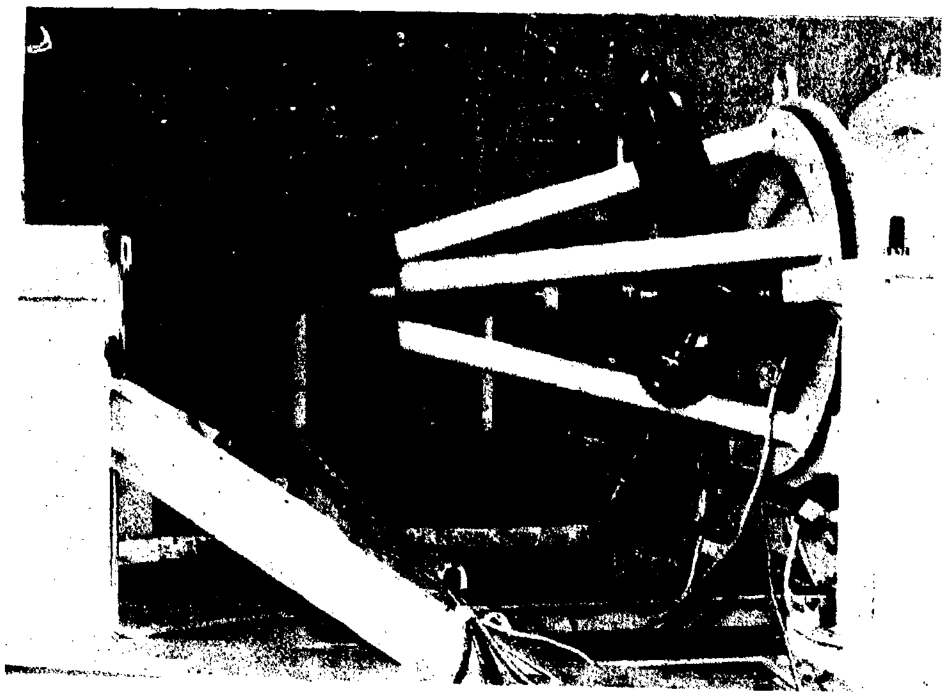

Igniters, Starboard, HW-1 - Prefire

Figure III-128

(U) For this first test, only the igniter canister on the centerline of the motor is live, the other canisters being empty or filled with unmachined insulation. The center igniter was equipped with an exploding bridge wire squib initiator, the others being plugged in the event the rupture discs failed. Also shown in Figure III-128 is the flexure rod between the axial thrust load cell and the thrust takeout ring. This flexure was used to avoid erroneous weight readings.

(C) Controllable solid rocket HW-1 was statically test fired at 1450 hours on 11 February 1966 from Test Bay W-4 of Aerojet's Solid Rocket Test Facility in Sacramento. The motor fired normally for the full 25-sec duration and extinguishment was automatically commanded by the programmer at that time. The pintle withdrew completely within 120 millisec as expected. Coincident with the extinguishment command, a nitrogen ejector ring began to flow a curtain of nitrogen aft of the nozzle exit plane, blocking the entry of any oxygen-bearing air and preventing excessive after-burning of the insulation. At the T plus 35-sec point, the pintle was commanded to re-position to firing configuration to prevent radiation from melting the pintle housing structure. This re-positioning did not occur until the 65-sec point because the vent valve in the hydraulic control panel was jammed in the open condition and had to be recycled before the pintle could be moved.

(C) The motor was treated as a typical hangfire because of the possibility that there was live propellant remaining, and the area remained closed for 30 min. Nitrogen was permitted to flow for 15 min after extinguishment command. At T plus 30 min, the area was reopened and the motor was visually inspected. Four hot spots were found on the case approximately 9 in. forward of the aft skirt boss (Figures III-129 and III-130). Some small pieces of charred carbon phenolic elastomeric material were found approximately 5 to 10 ft aft of the nozzle exit, indicating that they had been ejected during the extinguishment transient, not during the test firing. All of the propellant was consumed during the test.

(U) With the exception of the hot spots mentioned above, the motor hardware appeared to be in excellent condition after the test firing, as can be seen in Figures III-131 through III-135. Figures III-132 and -133 show the nozzle from close to the motor. It can be seen in these figures that the nozzle apparently survived without noticeable damage. Slight deposits of hollow aluminum oxide bubbles occurred on the pintle tungsten insert, most likely during the 1-sec tailoff. The walls of these bubbles were approximately 0.020-in. thick, and the bubbles could be removed with light finger pressure; thus, they must have occurred during tailoff, or the gas flow would have caused them to separate and eject from the motor. Figures III-134 and III-135 depict the forward end of the motor. All six of the igniter canisters were intact, without any evidence of heat.

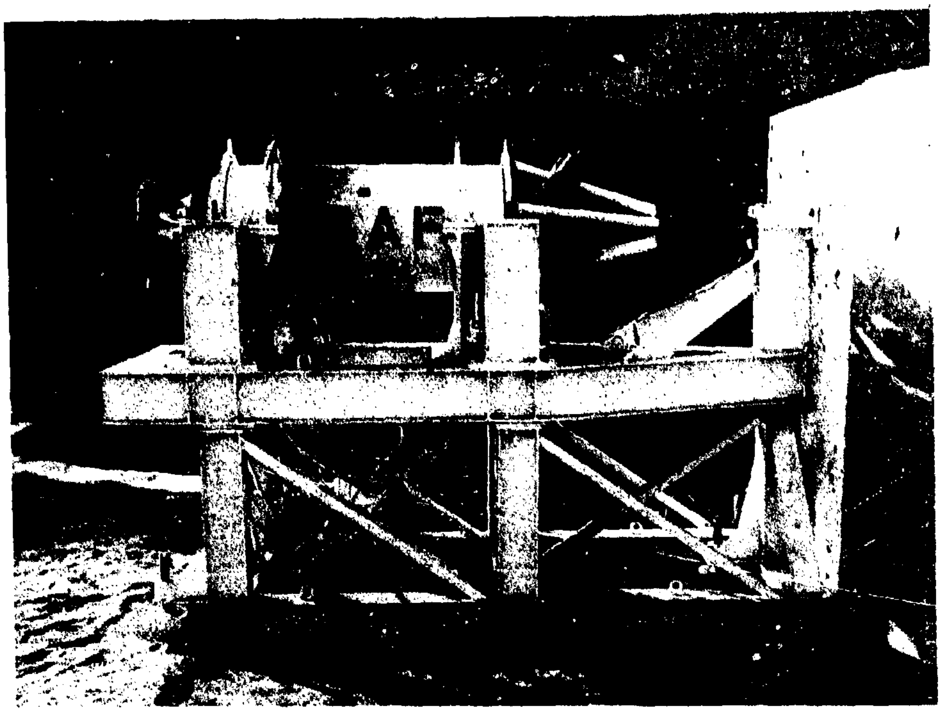

Igniters, Port, HW-1 - Prefire

Figure III-129

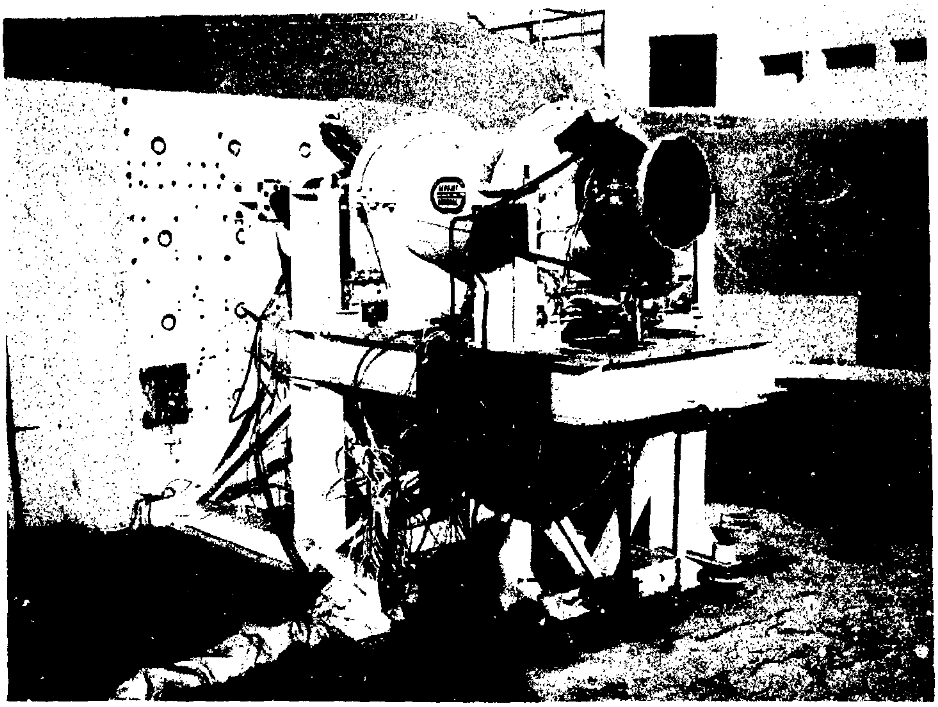

3/4 Aft, Port, HW-1 - Postfire

Figure III-130

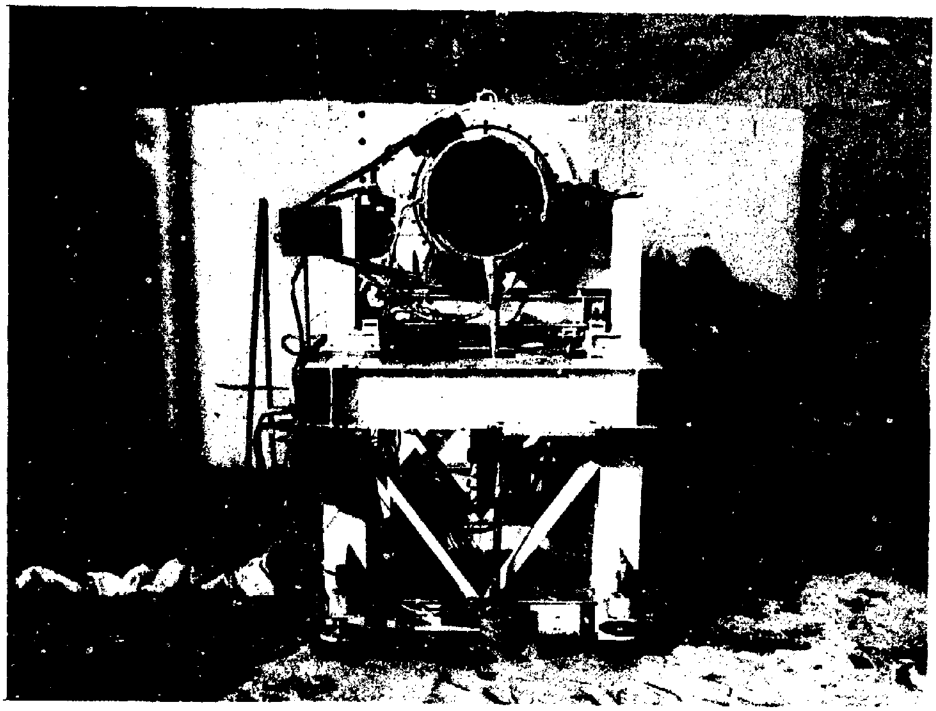

Aft Overall, HW-1 - Postfire

Figure III-131

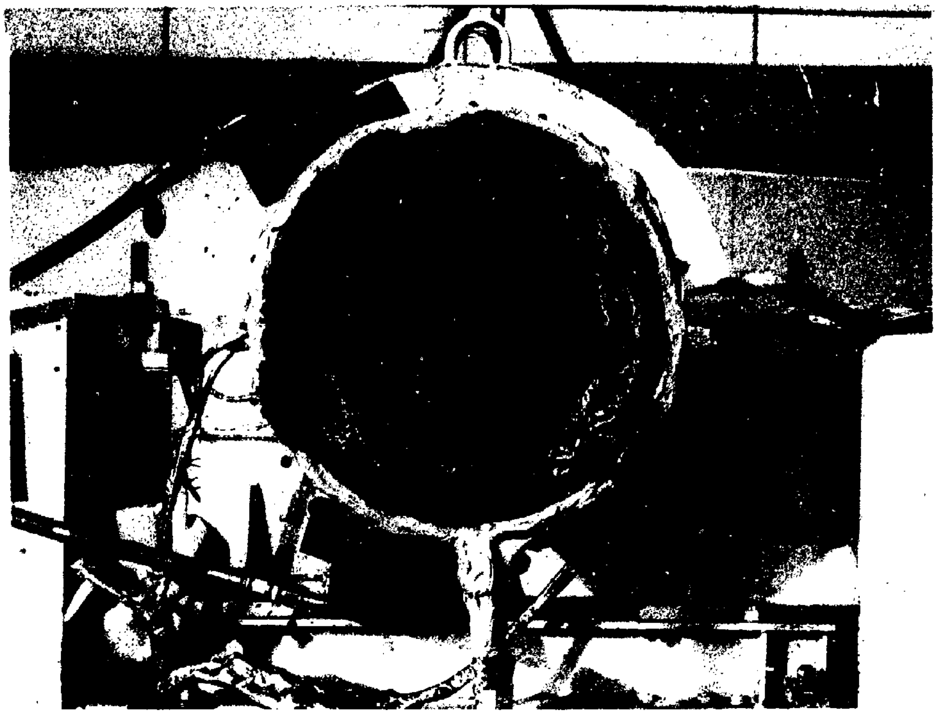

C/V Nozzle, HW-1 - Postfire

Figure III-132

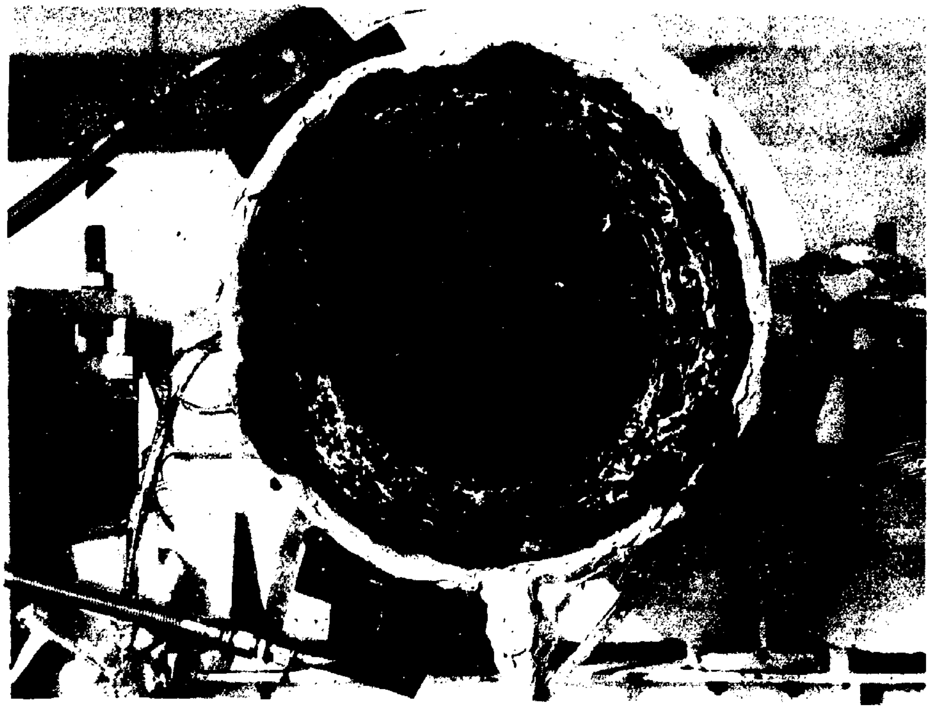

C/V Nozzle, HW-1 - Postfire

Figure III-133

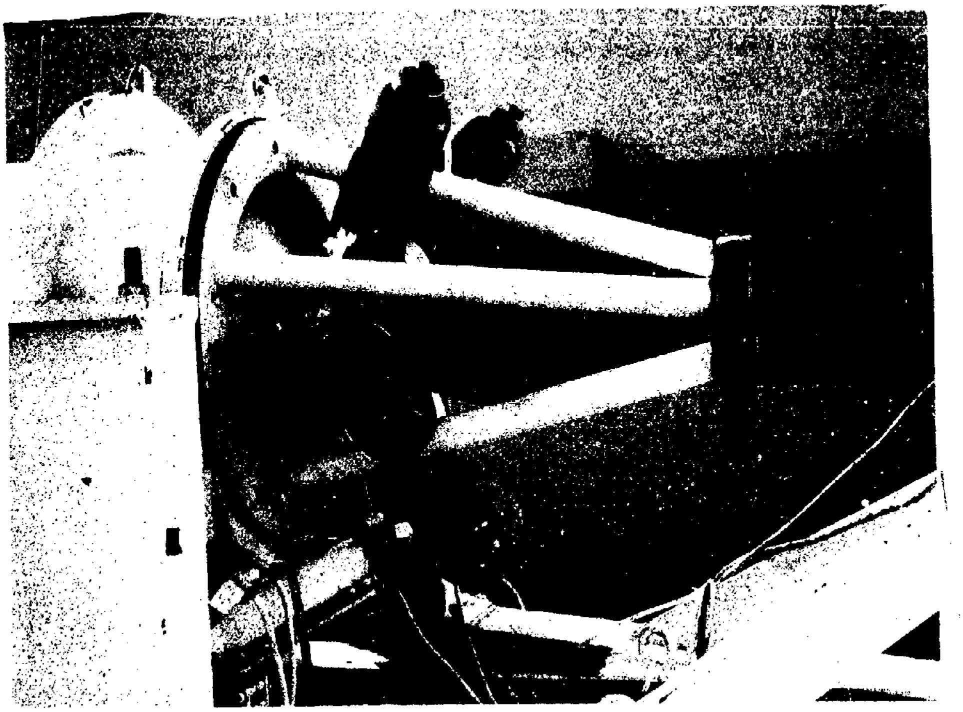

Forward Closure, HW-1 - Postfire

Figure III-134

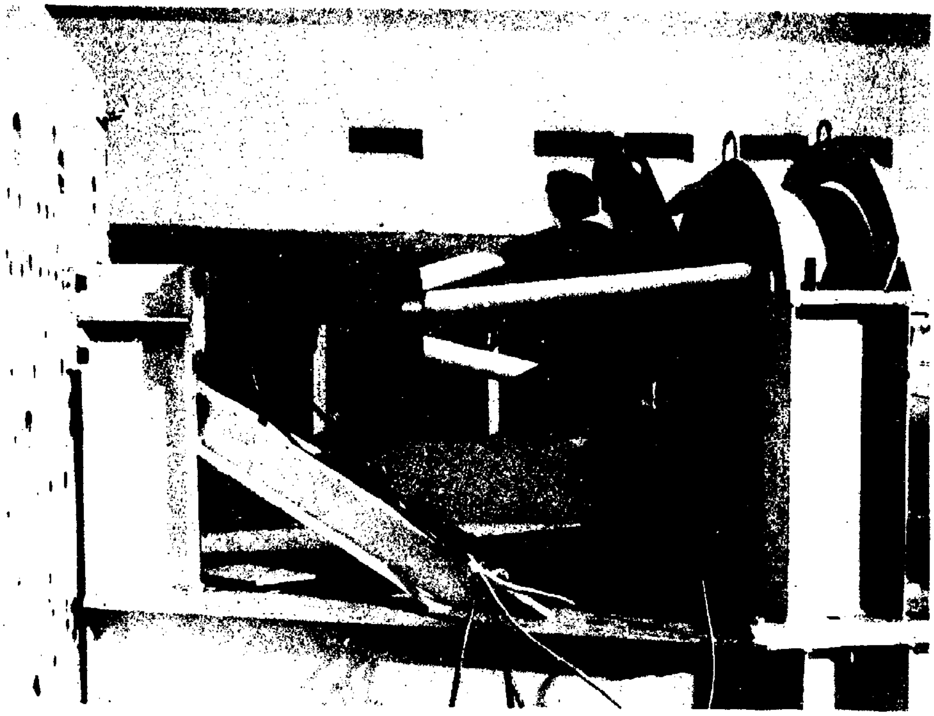

Forward, Port, HW-1 - Postfire

Figure III-135

(C) Review of the test data indicated that ignition was normal and smooth, with the maximum pressure reaching 490 plus psia and averaging 475 psia during the 270-millisec igniter functioning time. At igniter burnout, the chamber pressure dropped to 365 psia, with the remainder of the pressure time trace showing a progressive rise to 478 psia at 8 sec, a regressive drop to 295 psia at 24.3 sec, and tailoff from 24.3 sec until extinguishment command at 25.0 sec. Chamber pressure was ambient from 25.147 sec on. The thrust-time and pressure-time traces followed each other exactly, as can be seen in Figure III-136. Peak thrust was 6600-lb during ignition and 6500-lb during the web burning at the 8-sec point.

(C) Analysis of the position feedback signal from the potentiometer mounted within the nozzle pintle indicated that the pintle drifted over 0.200 in., closely following the pressure trace. Although the servo valve received a signal to counteract this drift, the differential pressure gage in the actuation system indicated that the servo valve shuttle did not respond to the signal and that the actuation system remained blocked. The nozzle throat area was calculated from the pressure-time and thrust-time traces. At the zero position of the pintle, the aerodynamic throat area was 8.99 in.^{2}. During the test, the pintle drift resulted in apparent nozzle throat area variation from an aerodynamic low of 8.42 in.^{2} to a high of 9.45 in.^{2}, exactly following the pintle drift indication.

(C) It was estimated that the restriction on the aft face of the propellant began to burn through approximately 5 sec after fire switch. Analyses of the films of this firing indicate that the chamber hot spots began to become evident at approximately 19 sec, with the initial indications occurring 2.5 in. forward of the restrictor face. Due to the loss of the restriction, the grain did not follow the pressure-time trace that had been predicted, and premature burnout occurred prior to extinguishment command. Therefore, the second objective of this test could not be met.

(C) Because this motor was hung from four load cells during the test, a continuous weight loss was recorded during the firing. Each load cell contains two bridge circuits, thus two sets of weights were recorded and summations made. The "A" side of the load cells indicated that 596 lb of material were lost during the test, the "B" side of the load cells indicated the 594 lb were lost; thus, the average loss of material of 595 lb was used during the data analysis. This number compared almost exactly with the known propellant loading, the restrictor used, and the igniter propellant loading. These three loadings sum to 594 lb. The weight loss is shown plotted as a function of time on Figure III-137.

(U) On the basis of these data, an analysis of the test was made. It was determined from this analysis that the restriction material on the aft face of the grain is not sufficient to protect the propellant for the entire

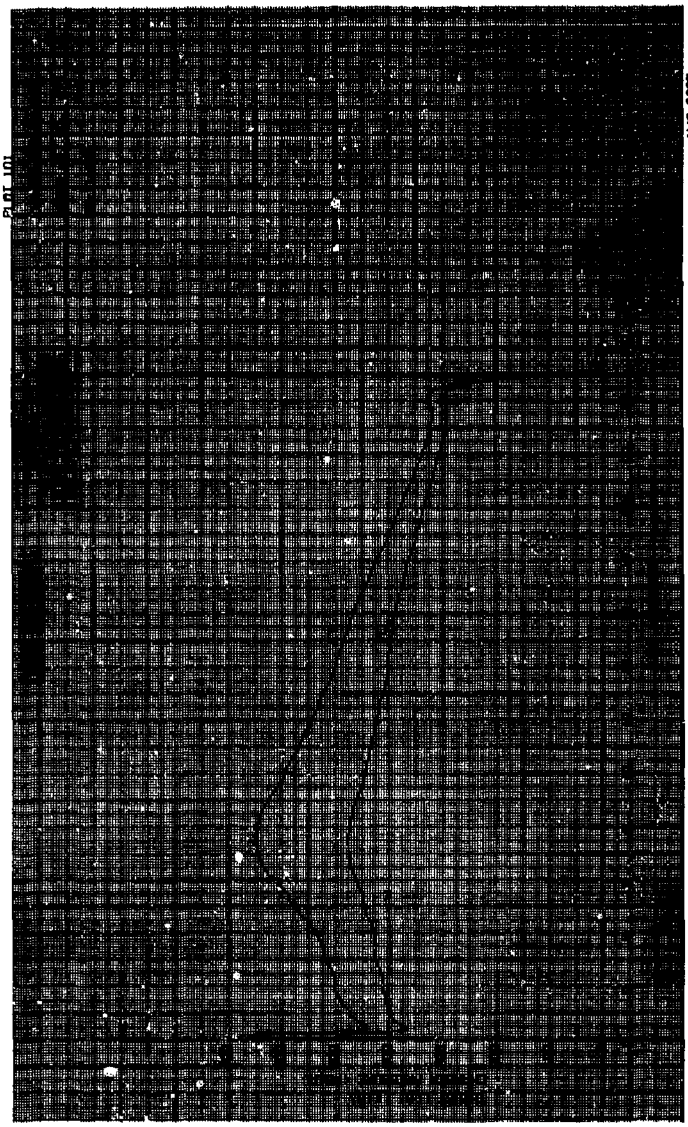

Thrust-Time and Pressure-Time, HW-1

Figure III-136

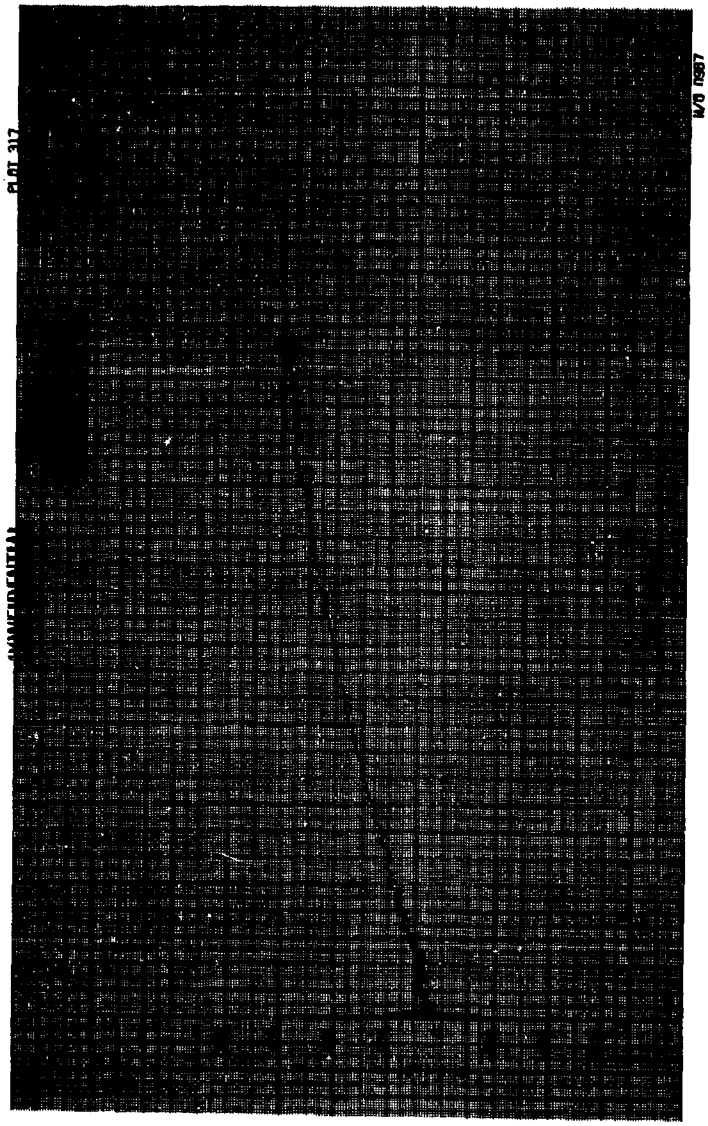

Weight Loss-Time, HW-1

Figure III-137

duration of the firing; thus, this will be thickened on future tests. In addition, more chamber insulation is required under the propellant near the restricted aft face in the event that the thickened restriction also burns through. These changes in motor insulation will be incorporated on all future tests.

(C) Summary of these test data yielded the following performance data:

Duration:	25.147 sec to P_c = 14.7 psia
Thrust:	4880 lb average 6600 lb max. during ignition 6500 lb max. during web burning
Pressure:	395 psia average 499 psia max. during ignition 478 psia max. during web burning
Weight loss:	595 lb average
I_s Delivered:	206.24 lb-sec/lb
I_s Corrected:	239 plus lb-sec/lb
Impulse:	122,707 lb-sec
Pressure-time:	9912 psia-sec
Nozzle area:	8.99 sq in. geometric set point 8.45 sq in. aerodynamic at set point 8.86 sq in. average aerodynamic 9.45 sq in. maximum aerodynamic

The corrected specific impulse was determined from a thrust coefficient correction to optimum expansion at a 15-degree half-angle from 1000 psi to atmospheric pressure. The nozzle aerodynamic throat areas were determined by the measured thrust and measured pressure and calculated based upon the variable thrust coefficient.

(C) As previously discussed, the motor case developed four hot spots originating approximately 2.5 in. forward of the aft face of the grain restrictor material. These hot spots indicate that the restrictor burned through locally as opposed to tearing off. If the restrictor had torn off, a hot band would have been in evidence rather than local hot spots. With the

exception of the four hot spots, where the 0.030-in.-thick insulation was burned through, the remainder of the motor insulation survived the test in good condition. Measurements of the aft closure insulation material loss indicate 0.112 in. to 0.496 in. of the V-44 rubber were lost from the maximum motor diameter to the nozzle attachment flange.

(U) The ignition system survived intact with no noticeable insulation loss either in the fired canister or in the igniter housing. The igniter throat did not appear to erode. Some of the V-44 rubber insulation on the downstream face of the igniter boss flange did char and fall off during removal of the igniter from the motor, as can be seen in Figure III-138. The condition of the igniter throat insert is good enough to permit the reuse of this piece of hardware for multiple igniter testing.

(C) Prior to disassembly of the nozzle, the only areas that appeared to have been affected by the test were the pintle entrance cap insulation and the strutted housing insulation between the struts. These areas both used MXCE-280 carbon-phenolic-elastomeric insulation molded in place over the supporting structure. These parts are shown in Figures III-139, -140, and -141, respectively. The char depth of this insulation varied from 0.25 to 0.30 in. and had cracked loose from the virgin material at the char interface, as can be seen in Figures III-139a and -139b. It was this material, especially from the entrance cap, that was found 5 to 10 ft aft of the motor after the test. From an external view of the nozzle, all other areas appeared to be in excellent condition.

(C) Disassembly of this nozzle proved to be a far more difficult task than was anticipated because the basic structural members did not receive sufficient heat to break the bonds formed by the Epon 921 adhesive that was used during the assembly process. The EC-801 sealant material used during the assembly also was intact, further complicating the disassembly of the unit. Removal of the pintle and actuator from the strutted housing proved to be a very difficult task because the chrome and nickel plating on the aftmost inch of the housing had flaked and become wedged between the pintle piston and the housing.

(C) This flaking was probable caused by the excessive heat radiated to the housing from the pintle during the 40 sec that the pintle remained retracted due to the valve stickage in the actuation panel. On future tests this time will be held to a maximum of 10 sec or less. The housing will be reusable after some rehabilitation of the chrome plating and renewal of the external insulation. Damage to the plating can be seen in Figure III-140a. Damage to the MXCE-280 insulation around the outside of the pintle housing was caused during disassembly of the nozzle. This insulation had to be chipped away before the aft insulator could be removed because the bond did not break due to heat.

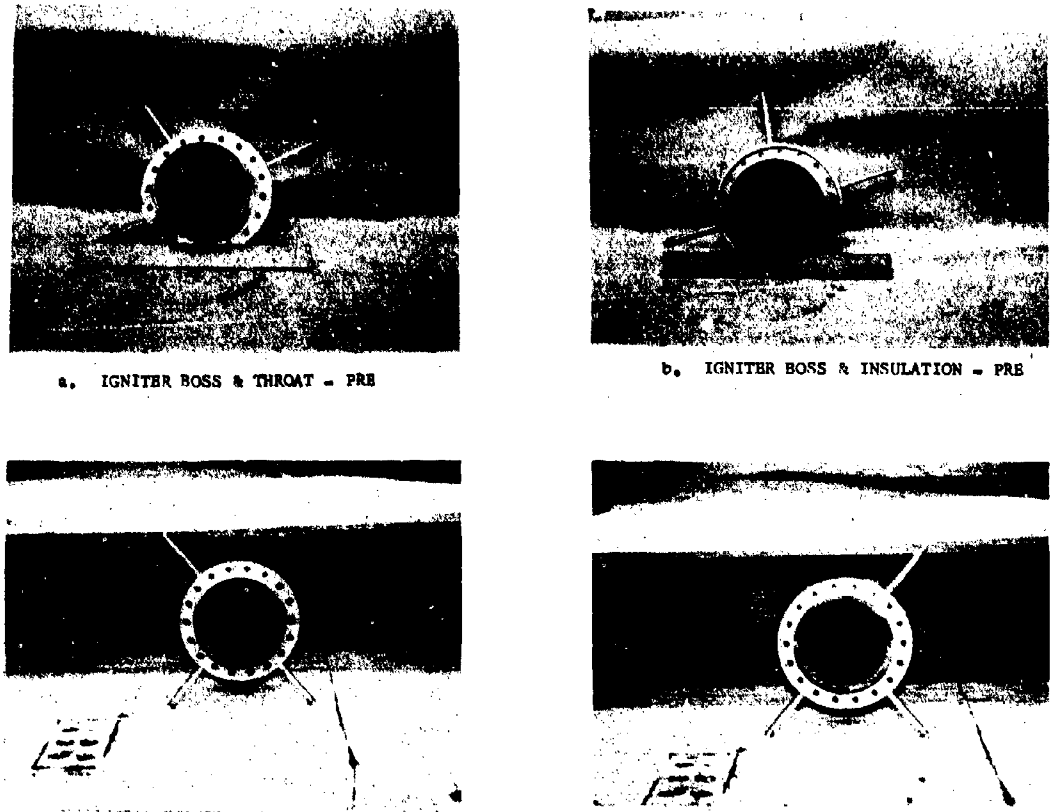

a. IGNITER BOSS & THROAT - PRE

b. IGNITER BOSS & INSULATION - PRE

c. IGNITER BOSS & THROAT - POST

d. IGNITER BOSS & INSULATION - POST

UNCLASSIFIED

Igniter Boss HW-1 Prefire and Postfire

Figure III-138

CONFIDENTIAL

a. NOZZLE - POST FIRE

CONFIDENTIAL

b. NOZZLE - POST FIRE

CONFIDENTIAL

c. POST FIRE - PINTLE & STRUTTED HOUSING

CONFIDENTIAL

d. POST FIRE - PINTLE & STRUTTED HOUSING

Nozzle HW-1 - Postfire (u)

Figure 139

a. STRUTTED HOUSING - POST

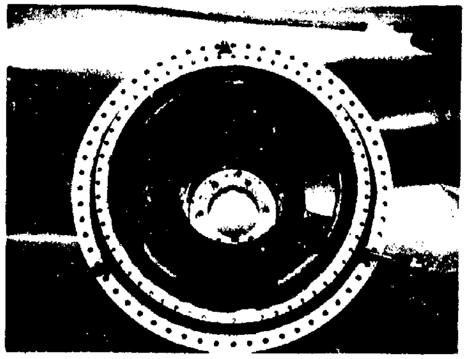

b. STRUTTED HOUSING - POST

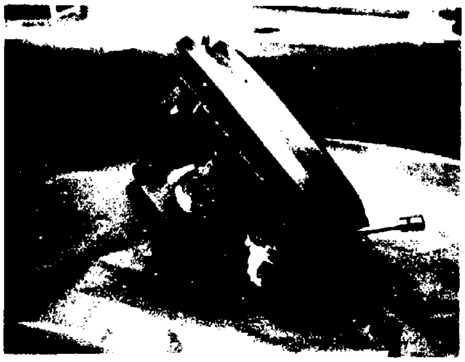

c. STRUTTED HOUSING - POST

d. STRUTTED HOUSING - POST

CONFIDENTIAL

Strutted Housing, HW-1 - Postfire (u)

Figure III-140

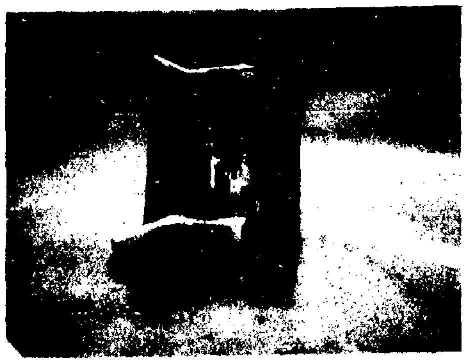

a. OUTER NOZZLE INSERTS - POST

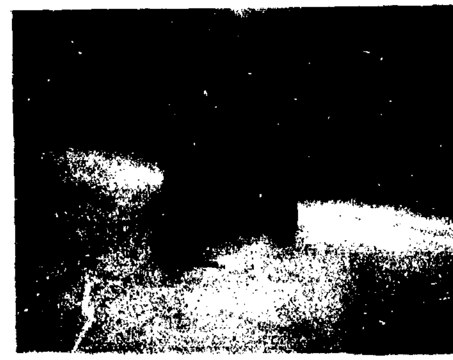

b. AFT INSULATOR - POST

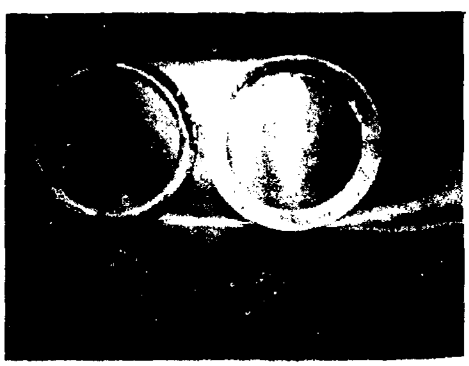

c. PYROLYTIC WASHERS - POST

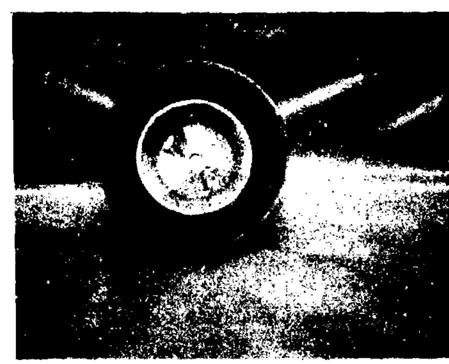

d. ENTRANCE CAP - POST

CONFIDENTIAL

Nozzle Hardware, HW-1 - Postfire (u)

Figure III-141

(C) The actuator survived the test in excellent condition; however, it was badly damaged during the subsequent disassembly process and will require extensive repairs prior to reuse. This is shown on Figure III-142. The pintle pyrolytic graphite was in excellent condition with no erosion as was the precharred carbon phenolic insulator immediately forward of it. The acrylic plastic ring had started to sublime slightly indicating that 500°F gas had reached this area. The pintle structural materials were untouched as was the wavy spring. The pintle insulators were also in excellent condition with no char. The end cap insulation, precharred carbon phenolic, was eroded slightly but had only lost 0.100 in. of material. The silica phenolic disc on the end of the pintle had charred to a depth of 0.12 in. The piston rings and all O-rings in the pintle assembly were intact with no evidence of having been exposed to excessive heat. These components are shown in Figures III-139 and III-142.

(C) The outer throat survived the test without any evidence of damage. The throat approach and the throat support components had slight erosion; however, the pyrolytic graphite throat insert had no erosion. The asbestos phenolic insulator was not charred, indicating that the carbon phenolic throat approach and the throat support are capable of providing sufficient insulation for the housing without the asbestos. These components are shown in Figure III-141.

(C) Probably the most surprising result of this nozzle test was the appearance of the aft pintle housing insulator. This component was manufactured from a snap-cured billet of carbon phenolic material, MXC-51, which was provided as a last minute substitute by Fiberite Corporation. The performance of this parallel to centerline wrapped part exceeds the performance of all the other insulation-type materials exposed to the flame in this firing. Erosion was minimal (less than 2 mils/sec average) and the component did not delaminate during the test--the most probable form of failure for this type of part. The last (aftmost) inch of the part was completely charred through; however, dimensional stability was maintained. This part is shown sectioned in Figure III-141 and installed in the nozzle in Figure III-139. Future nozzles will use this material.

(C) Thermal paint was used on some of the nozzle components during the assembly process to determine the maximum temperatures attained during this test. In all, this proved to be somewhat disappointing as the results were difficult to interpret and the paint did not adhere to the components as well as was expected. This could in part be due to the inexperience of the personnel using the technique; however, the use of this paint will be more limited in future tests. One area where the paint did indicate a temperature rise was in the pintle entrance cap cavity. The surface temperature of the actuator body and the entrance cap support exceeded 644°F but did not exceed 1180°F.

a. PINTLE STRUCTURE - POST

b. PINTLE INSERTS - POST

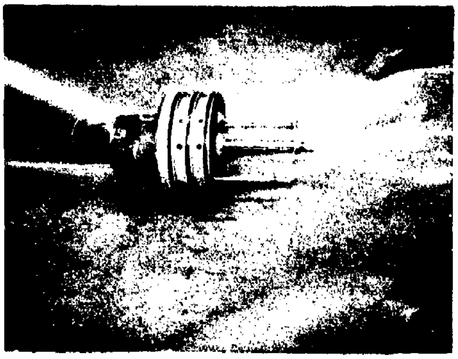

c. ACTUATOR - POST

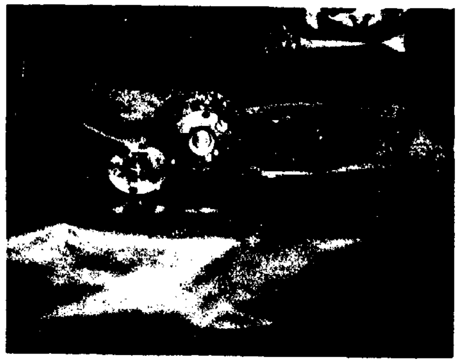

d. ACTUATOR - SNUBBER REMOVED - POST

CONFIDENTIAL

Pintle and Actuator HW-1 - Postfire (u)

Figure III-142

Because the insulation of the potentiometer lead lines had melted, it was evident that some hot gas did get into the entrance cap cavity. The most probable point of entry for this gas is between the strutted housing and the insulation molded around this housing. Because of the different shrinkage rates of the metal and the insulation, an adequate gas seal between the two does not exist. From the appearance of the remainder of the components that may have been exposed to this gas, it is believed that the thermal paint reflected only the surface temperature of the part, not the mean part temperature. Because the actuator body is aluminum, it is expected that there would be some indication of temperature elsewhere on the body had a portion reached in excess of 600°F. This, however, was not the case as the remainder of the actuator saw no noticeable temperature rise. On these data it is concluded that gas reached the inside of the entrance cap causing the thermal paint to "kick-over" and melt the wire insulation that protects the potentiometer lead lines as they pass through the strut. As this area cannot be sealed with any degree of certainty, future tests will incorporate potentiometer lead lines with a higher tolerance for heat.

(C) On the basis of this test firing it was determined that the basic design of the heavyweight series of the Controllable Solid Rocket Motor is sound and can be expected to withstand any of the duty cycles to which it will be subjected from a thermal standpoint. The changes in restrictor thickness and chamber wall insulation that were indicated by this test have been incorporated in the design and will appear on subsequent motors starting with HW-2. A possible change in the formulation of the MXCE-280 insulation was indicated; however, this will not be changed until after further testing. Sufficient material thickness is available to ensure protection in the event of char layer loss during subsequent tests; thus, this does not contribute any potential failure modes to HW-2 or HW-3.

4. HW-2 Test Firing CSR-DA-01S-BH-002

(U) The primary objective of this test firing was controlled thrust variation and sea-level extinguishment. The chamber pressure feedback control system was used to control the motor output for both the thrust variation and the extinguishment mode of this program. The operation of this control system consists of two control modes, position control of the pintle for ignition transients and force mode for variable thrust control. In addition to these two modes of control, the system has safety circuitry which, when activated, will bypass the force mode control and attempt motor shutdown by rapid depressurization if the chamber pressure exceeds a preset value.

(C) For this test firing, the initial pintle position was set to ignite the motor at a nominal chamber pressure of 400 psia. Position control mode was maintained for the first 0.400 sec to avoid any interference from the

igniter during force mode control. The force parameter is the multiple of chamber pressure times nozzle throat area and is equivalent to thrust divided by thrust coefficient. As the thrust coefficient varies so drastically with expansion ratio at sea level, it was decided to avoid the complexity of this added parameter in the computer circuitry of the control system for this program. For this test, three force stations were to be input in steps for the first 8 sec of the test, at which time the first sea-level extinguishment was commanded. The extinguishment position of wide open nozzle was to be held for 5 sec, to T plus 13 sec; then the pintle was to be position mode replaced to initial ignition conditions. If the motor failed to extinguish or failed to maintain permanent extinction, the force mode control circuit would be automatically reactivated by chamber pressure. At this point, a variable thrust step input program would be used to control the motor until web burnout.

(U) Some trouble was experienced during the motor setup prior to test firing in that the failsafe manifold, used to achieve high response rates by bypassing the servo valve, failed under pressure twice at the return port chamber cover plate. A rather unusual procedure was used to repair the failsafe manifold so that HW-2 test firing could proceed on schedule. Two large C-clamps were used to hold the top plate to the manifold body.

(C) Controllable solid rocket motor HW-2 was statically test fired at 0142 hours on 26 March 1966 from Test Bay W-4 of Aerojet's Solid Rocket 8 sec until extinguishment was commanded. The pintle was withdrawn from minimum throat area to maximum throat area in 0.040 sec by the failsafe manifold. Chamber pressure dropped to atmospheric in 0.140 sec and held at that level for approximately 1.17 sec. During this motor down-time, a nitrogen halo at the exit of the nozzle was flowing to block the entry of oxygen in an attempt to halt reignition. Chamber pressure rose from 14.5 to 55 psia at 9.5 sec without any change in nozzle position indicating that reignition had occurred. At T plus 13 sec, the pintle was repositioned and the motor followed the variable thrust program until burnout.

(U) After burnout, the motor pintle remained in the fully extended position for approximately 5 min. At 5 min, the hydraulic pressure was shut down and the failsafe manifold forced the nozzle into the retracted position as this manifold requires a minimum of 2200-psi hydraulic line pressure to be in the operative position. Approximately 5 min elapsed before the anomaly was noted and the hydraulic pressure reactivated and the pintle re-extended as required by the test plan. Unfortunately, the thermal damage to the strutted housing chrome and nickel plating on this motor was the same as on HW-1. The only way of avoiding this on future tests is by the installation of a separate bypass valve to be used only after firing and to block pintle actuation by the failsafe manifold.

(C) Preliminary analysis of the data from HW-2 indicates that the motor performed all of the thrust variations satisfactorily and did extinguish for a short period of time; however, the motor reignited and burned steadily at a low pressure of 55 psia. Ignition was smooth and uneventful as in HW-1. The maximum pressure at ignition was approximately 435 psia, regressing to a low of 365 psia at igniter burnout. At 0.400 sec, the pressure feedback control system switched from position mode control to force mode control and called for a thrust parameter (chamber pressure times area) output of 3500 lb. Responding to this input, the nozzle began to close down the throat, causing the chamber pressure to rise to a high of 620 psia and finally stabilize at a pressure of 565 psia and hold this value for the duration of the 3500 lb command. On command to decrease the force level to 2000 lb, the nozzle opened until the pressure reached a low of 165 psia. When the maximum force input of the system, 5000 lb, was given at T plus 5 sec the nozzle closed to the minimum throat area and the chamber pressure climbed to a high of 915 psia. At extinguishment, T plus 8 sec, the chamber pressure dropped to 14.3 to 14.5 psia, slightly below atmospheric. This decrease below atmospheric is natural because the nitrogen ejector ring at the aft end of the nozzle will produce a slight vacuum in the motor. As was previously stated, the motor remained at 14.5 psia for 1.17 sec, at which time the pressure rose smoothly to 55 psia where stable combustion existed until T plus 13.5 sec, at which time the force mode control system asked for and received an output of 3500 lb.

(C) After repositioning to the 3500 lb point, the motor followed the force mode control system input and varied thrust from a low of 2050 lb to a high of 4625 lb just prior to burnout, in steps of 350, 600, 400, 1150, and 550 lb, respectively. The maximum controlled thrust was 8600 lb, which occurred at T plus 7 sec at a pressure of 915 psia. The minimum controlled thrust was 2050 lb, which occurred at T plus 20 sec at a pressure of 95 psia. In actuality the minimum thrust was 1250 lb which occurred at T plus 10.3 sec and held until T plus 13.4 sec; however, this occurred during position mode control at a pressure of 55 psia with the nozzle at the extinguishment position. Thus, it is not considered as a variable thrust point in this test firing. Thrust-time and pressure-time data are presented as they were plotted by the X-Y plotter of the ADC data acquisition computer (Beckman) system on Figure III-143.

(C) During this test firing, a total propellant and insulation loss of 558 lb was experienced. This coincides very closely with the total weight of propellant in the main grain, the igniter grain, and the restriction material in the motor. The weight loss is shown plotted as a function of time on Figure III-144. Another interesting parameter that was plotted by the computer is the thrust divided by the pressure. This plot is shown as Figure III-145.

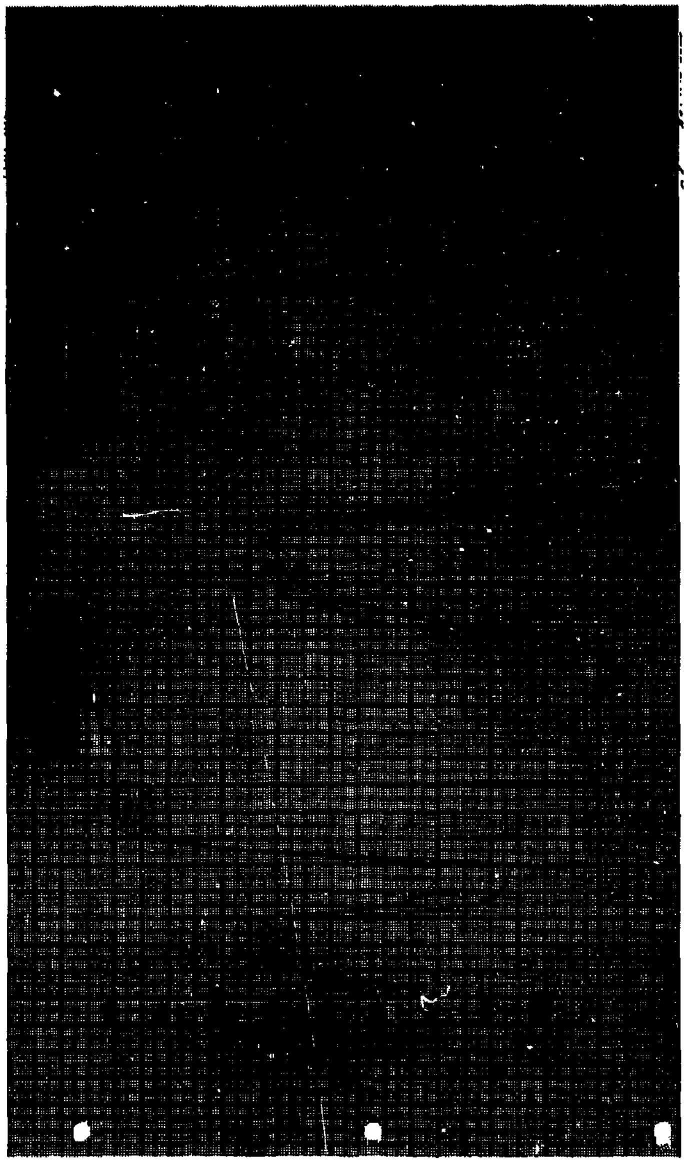

CONFIDENTIAL

Thrust-Time and Pressure-Time, HW-2 (u)

Figure III-143

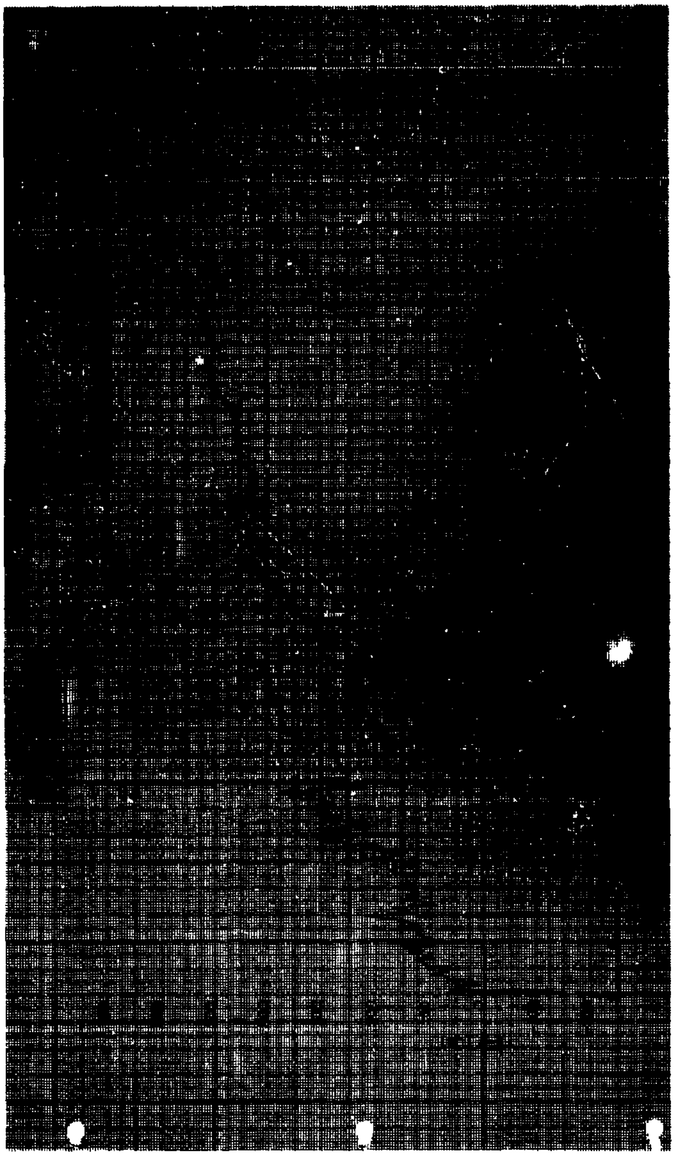

CONFIDENTIAL

Weight Loss-Time, HW-2 (u)

Figure III-144

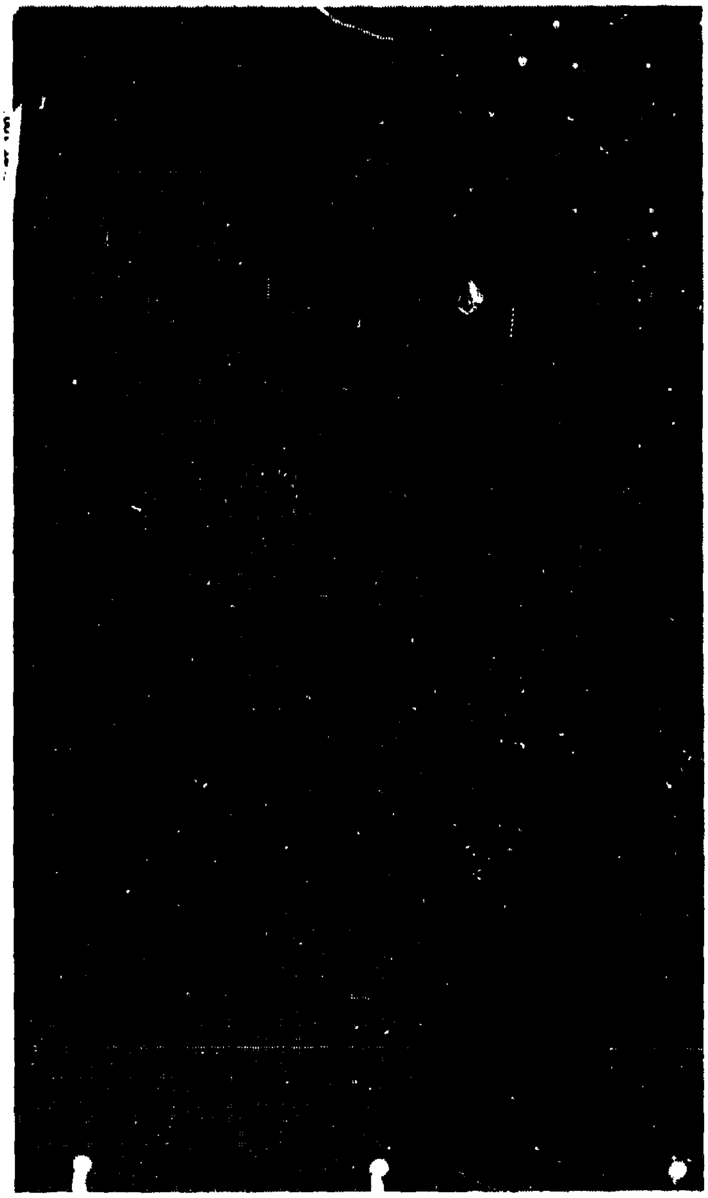

UNCLASSIFIED

Thrust/Pressure vs Time, HW-2

Figure III-145

The main use of this plot is the determination of the aerodynamic throat area of the nozzle. As the thrust divided by the pressure is equal to the thrust coefficient times the throat area and the thrust coefficient is a function of the nozzle only for any chamber pressure and expansion ratio, a parametric plot of various Cf x A* as a function of A* can be made for various pressures and the actual aerodynamic throat area can be derived by picking off the area at the appropriate pressure. This same technique was used to determine the aerodynamic throat areas in the test of HW-1. One other point of interest is the indication that there was a thrust spike at T plus 8 sec when extinction by rapid depressurization was commanded. Although the sampling rate used for the plots was too slow (0.076 sec) to catch the spike on the plot as the spike occurred within 0.025 sec, the thrust divided by pressure plot caught the indication that the chamber pressure dropped before the thrust dropped; thus, this figure shows a spike. The actual thrust spike was 14,100 lb, which is a multiplication factor of approximately 1.64 times the 8600 lb just prior to extinction command. The areas calculated by the pressure feedback system computer are used for the determination of force mode output from pintle position are shown plotted on Figure III-146. These areas are not the same as the aerodynamic areas because the position versus area plot fed into the variable function generator of the control system was in error (see Figure III-146). Corrections will be made before the next test firing.

(U) The various nozzle throat areas as a function of pintle position are shown on Figure III-147. These areas are the geometric minimum area, the aerodynamic throat area as calculated from the data of HW-2, and the program input area to the PC-12 computer variable function generator. For the test firing of HW-1, the input to the variable function generator was equal to the geometric calculated throat area. Analysis of the test data indicated that the actual aerodynamic area was somewhat smaller than the geometric area at the specific pintle position that HW-1 was fired. To compensate for this apparent boundary layer effect, the entire curve was shifted and input to the PC-12 computer for HW-2. Reduction of the data from HW-2 indicated that this shift was excessive in the range of small nozzle areas and in the exact opposite direction in the midrange of pintle travel. Apparently, the boundary layer effects at the small nozzle throat area range is not as great as originally indicated by the test results of HW-1; thus, the corrected area pintle position function will be input on HW-3 and HW-4. Further corrections to this function will be input from the data of HW-4 if they are necessary. The variable thrust control range of this nozzle is the stroke from 1.65 to 3.50 strokes. From 0.0 to 1.65, the pintle is in the extinguishment range of travel; thus, corrected flow areas are not as important as in the variable thrust range. The difficulty in accurately calculating the nozzle throat area in the midrange of pintle

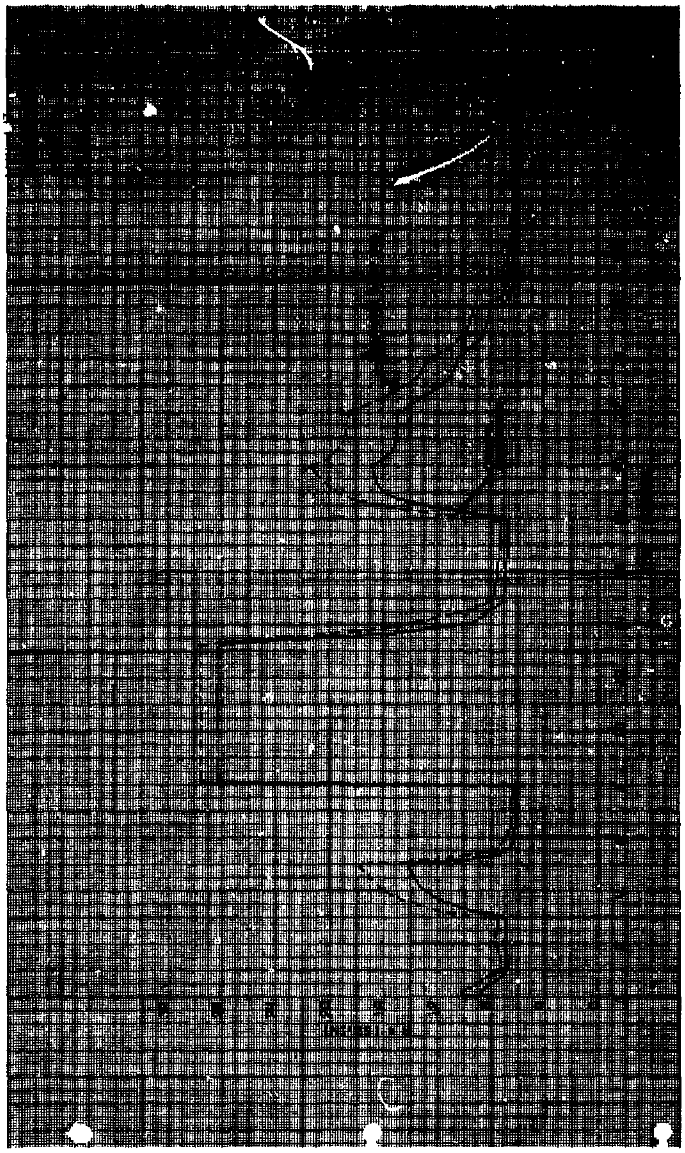

Calculated and Aerodynamic Nozzle Throat Areas, HW-2

Figure III-146

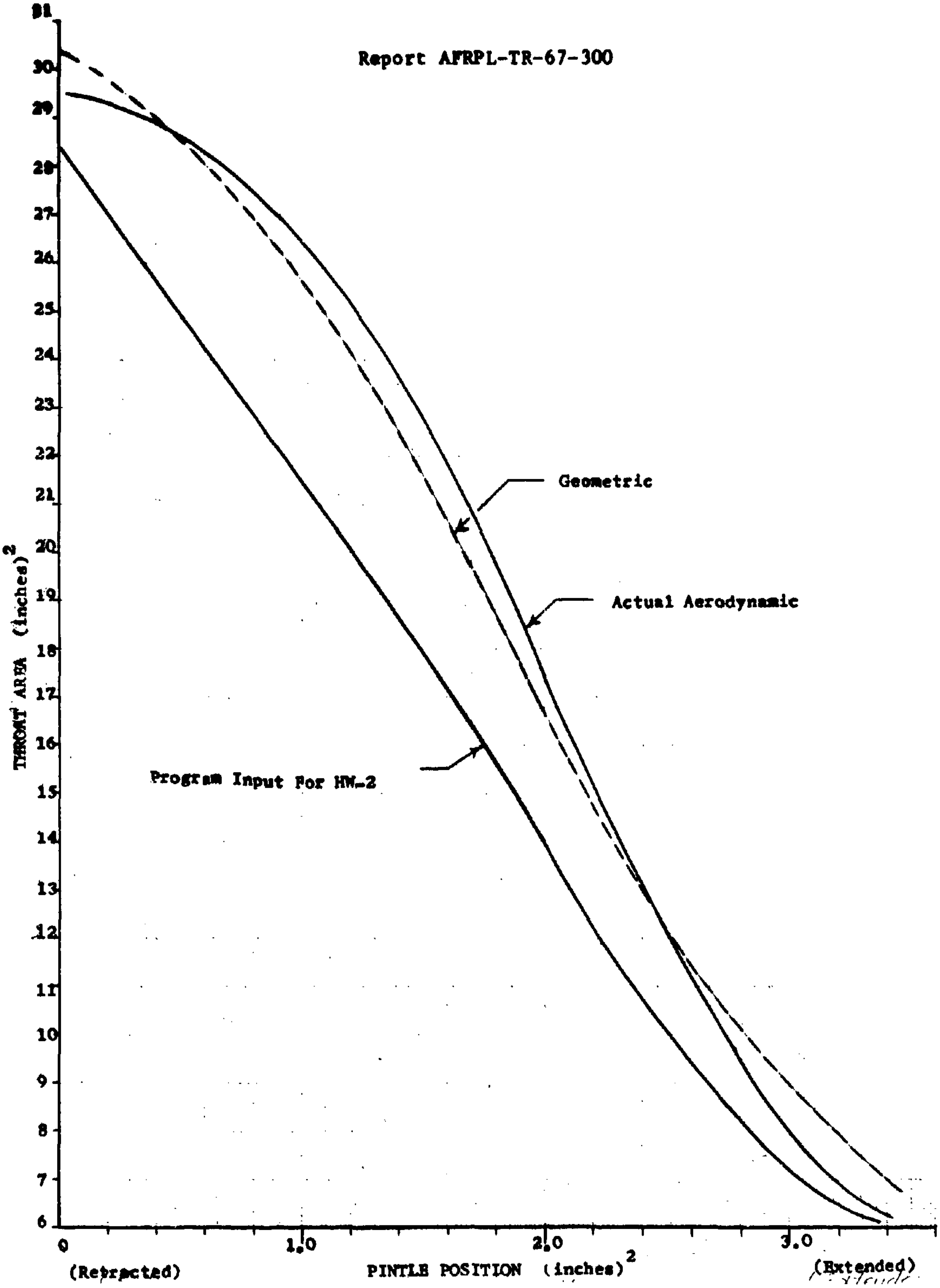

Pintle Position vs Area

Figure III-147

travel is probably due to the angularity effect of the throat and the fact that this propellant contains a high percentage of solids in the exhaust stream.

(C) The final data plot presented for HW-2 is the input versus time and the motor output versus time for the force parameter on which the motor control was dependent (Figure III-148). It should be noted that in most cases the output of the motor was larger than the input program desired. This was caused by the amplifiers between the system multiplyer and the system signal comparator circuits. The amplifier setting was based upon the theoretical motor and determined by the aid of an analog computer to match the system gains. It can be seen that as the motor propellant burned out and the motor free volume increased, the system gains more closely approximated the theoretical calculations; thus, the output more closely matched the input signal at the stability point (zero error). This deviation will be corrected on future tests because the amplifier settings will be modified and the actual motor responses increased by use of a larger servo valve (3.0 gpm).

(C) Summary of the test data yielded the following performance data:

Duration	30.5 sec to P_c = 14.7 psia This included 1.17 sec of extinguished motor grain and 3.8 sec of very low pressure combustion
Thrust	8600 lb controlled maximum 2050 lb controlled minimum 1250 lb with the nozzle wide open and the system on position control
Pressure	915 psia controlled maximum 95 psia controlled minimum 55 psia stable minimum (nozzle open) 14.3 psia with grain extinguished and ejector functioning
Weight Loss	558 lb
I_s Delivered	206.8 lb-sec/lb
I_s Corrected	239 plus lb-sec/lb
Impulse	115,599 lb-sec

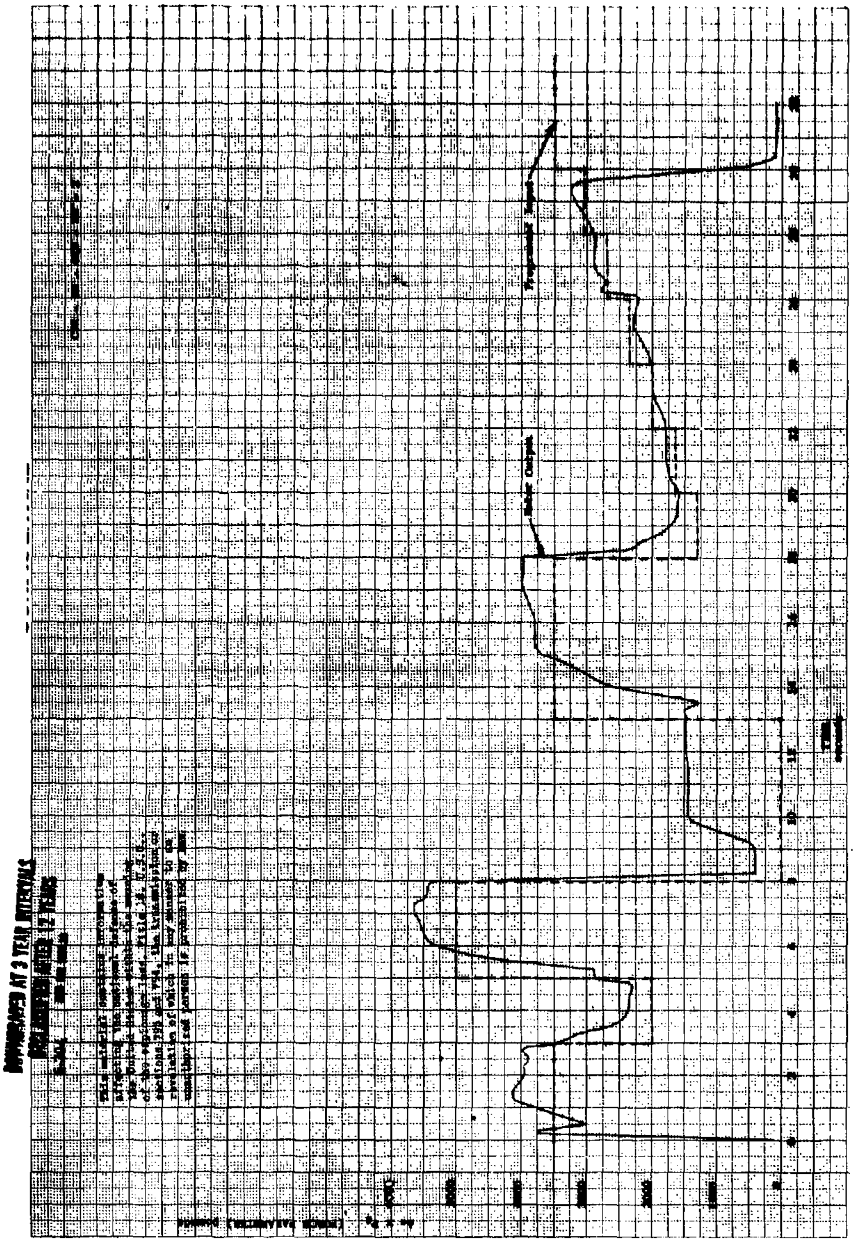

CONFIDENTIAL

Motor Input-Time and Output-Time, HW-2 (u)

Figure III-148

Pressure-Time	10,050 psia-sec
Nozzle-Area	6.30 sq in. aerodynamic minimum 30.4 sq in. aerodynamic maximum
Thrust Spike	14,100 lb for 0.025 sec

The corrected specific impulse was determined from a thrust coefficient correction to optimum expansion at 15-degree half-angle from 1000 psi to atmospheric pressure. The nozzle aerodynamic throat areas were calculated as previously stated using measured thrust and measured pressures. All other data are as measured from the test firing without modification with the exception of the addition of atmospheric pressure.

(U) The motor case and insulation of HW-2 survived the test in excellent condition without any hot spots on the case and with only a minor loss of insulation. The actual measured insulation loss has not been determined as of this report; however, it is approximately the same as that of HW-1 from visual evaluation.

(U) The ignition system survived the test also in excellent condition. Once again, no erosion was experienced at the igniter throat and the internal igniter insulation was in good shape, similar to HW-1.

(C) Prior to disassembly of the nozzle, this unit appeared to be in better condition than HW-1 in that the char and cracking of the MXCE-280 was less pronounced and flaking of the material had not occurred. Due to elimination of the majority of the bonding surfaces in this nozzle it was much easier to disassemble than HW-1. Components that survived the test firing also survived the disassembly procedure unlike their counterparts in the first heavyweight nozzle. There was no erosion of the pyrolytic graphite or the silver-infiltrated tungsten in the pintle and only slight erosion of the precharred carbon phenolic ring forward of the pyrolytic graphite in the pintle. The acrylic plastic ring was more than 50% sublimed on this nozzle as compared to only about 20% sublimed in the first test. The actuator was in excellent condition but the cap seals on the static O-rings apparently had been cut during installation on this nozzle. No melting of the potentiometer lead line insulation occurred on this test because the wires were insulated with Teflon and covered with a shrink-fit rubber sleeve. The piston rings and O-rings were in excellent condition as were all of the structural components. Although the silica phenolic disc which insulates the 90-10 tantalum-tungsten nut blew off at about 8 sec, and this nut was exposed for over 22 sec, the component was intact with no noticeable melting or oxidation.

(C) The outer throat assembly was intact without any erosion of the pyrolitic graphite and only minor erosion of the throat approach, throat support, and exit section. This nozzle had less erosion than HW-1 on the carbon phenolic components. The entrance cap was charred to a depth of approximately 0.25 in.; however, this char was in place on the cap, although it was slightly cracked. The strutted housing and aft insulator cap were charred slightly; however, both were reusable. The strutted housing chrome plating was damaged on this test as on HW-1 for the same reason--pintle retraction and hold while still hot. These components can be rehabilitated without loss, however, because only the last inch was damaged on each.

(C) This test firing verified the conclusions drawn on the basis of HW-1; i.e., the controllable solid rocket motor design is sound and can be expected to withstand any of the duty cycles to which it will be subjected. In addition, this test proved that the use of a pressure feedback control system is feasible for static testing and can be used without running into instabilities. By using this system it is unnecessary to second-guess the internal ballistics of the motor and force the motor to conform to steady-state equations during actual transient behavior. Analysis of the data indicated that extinction at sea level was momentarily attained and, therefore, this should be a goal on future tests. Analysis of the films indicated that combustion of a nonaluminized fuel was responsible for reignition. The most probable suspect in this motor is the SD-844-1 material, which is used as an end grain restriction.

(C) Controlled thrust variation in excess of 4:1 was attained on this test; this is more than ample to meet the work statement requirements.

(U) The failure of the vent side of the failsafe manifold was traced to the hydraulic circuit downstream of the hydraulic panel and is not a valve problem. The sizing and the length of the return lines combined to restrict the hydraulic fluid flow, thus causing a pressure buildup in the failsafe manifold and deformation of the cover plate. This problem is being rectified for future tests. For HW-2, the two C-clamps worked well during the test as they overpowered the problem rather than provided a solution.

5. HW-3 Test Firing CSR-DA-01S-AH-003

a. First Test

(U) The primary objective of motor HW-3 test firing was to determine the altitude extinguishment capability of the fullscale heavyweight controllable solid rocket motor. As had been shown in the firing of HW-1, it was possible to extinguish the CSR motor at sea level, however with the configuration tested it was impossible to maintain permanent extinction. HW-3 was scheduled for the first simulated altitude test of a fullscale CSR motor of the same configuration as HW-1 to determine the effect of altitude on the ability of the motor to attain permanent extinction. This motor was therefore set up in the W-7 altitude tank at Aerojet's Sacramento Solid Test Facility. This facility was equipped with a diffuser designed for the CSR at mid-mass flow configuration. A hydraulically operated trap-door was provided at the diffuser outlet so that altitude could be maintained after motor shutdown to prevent reignition. In addition to the diffuser and trap-door, the altitude facility was equipped with a nitrogen ejector capable of handling 5 pounds/second gas flow at a backpressure of approximately 1 psia. This ejector system could be remotely isolated from the altitude facility by a hydraulically operated butterfly valve so that the tank could be pumped down using the mechanical vacuum pumps to conserve the supply of nitrogen for the actual run.

(C) The CSR motor, HW-3, was scheduled for a total of four thrusting periods, each to be terminated using the rapid depressurization mode of extinguishment. To match the motor output to the diffuser design, it was decided to fire the motor at a chamber pressure of approximately 550 psia. At this pressure, the motor was calculated to flow at approximately 27 pounds/second through an aerodynamic throat area of 7.5 square inches, making the effective expansion ratio approximately 36:1. The exit pressure was calculated to be approximately 1.25 psia, closely matching the tank pressure for which the diffuser was designed. At a mass flow rate of 27 pound/second, the web duration was calculated to be slightly over 20.8 seconds, thus each pulse was determined to be 5 seconds in duration to permit the four thrusting cycles planned.

(C) Sequencing of the various facility items was a very critical portion of this test. In order of activation the following functions were performed.

(1)	Start Tank Pump-down	T - 2 hours
(2)	Cut in Ejector	T - 20 seconds
(3)	Open Ejector to Tank	T - 15 seconds
(4)	Release Diffuser Trap-door	T - 1 second
(5)	Ignition Command to Motor	T - 0 seconds

(6)	Activate Trap-door to Close	T plus 4 seconds
(7)	Isolate Ejector from Tank	T plus 25 seconds
(8)	Shut-down Ejector Nitrogen	T plus 35 seconds
(9)	Vent Tank to Atmosphere	T plus 1 hour

The most critical of these functions were numbers (4) and (6) which involved opening and closing the trap-door at the exit end of the diffuser. By releasing the hydraulic pressure holding the door shut at T - 1 second, the door is held in place by the differential pressure (by the atmosphere) until the motor fires and pushes the door to 10 degrees open. At that point the hydraulic actuator is cut in the circuit and completes the door opening. Dry runs indicated that the trap-door required approximately 1 second to close, thus it was commanded to close at T plus 4 seconds, approximately one second before motor shutdown command. This timing was set to avoid if possible the entry of oxygen laden air after motor vent - allowing convective cooling to take place.

(U) For this firing, the motor was equipped with only one live igniter for each pulsing period rather than the four igniters being installed for each firing. This was necessary since the facility has not as yet been setup to handle more than one exploding bridge wire squib at a time. In addition, some problems have been encountered with the rupture discs in the multiple canister igniter design being used. These discs are fabricated from light gage nickel alloy and coined to hinge open yet remain retained by the hinge-flap. Due to the high rate of pressure rise in the igniter and the shock loading, the hinge concept is non-functional and the disc is ejected intact. As each disc is slightly larger than the common igniter udder throat passage, damage has been sustained by the throat insert due to the passage of these discs. This area is being redesigned for future altitude test motors to eliminate this problem. For HW-3, it was decided to fire all four igniters down the centerline port of the ignition system without rupture discs to avoid this problem.

(U) To measure the thermal feedback to the motor due to diffuser unloading and backflow during the run, thermocouples were spotwelded to the chamber and heat-flux probes were installed on the blast baffle. The chamber was wrapped with one ply of asbestos cloth to further protect the hardware from external heating. All of the instrumentation lines were wrapped with asbestos as were the thrust and motor weight load cells. Flash bulbs, wired into the ignition circuit, were provided to signal ignition to the camera that was trained on the diffuser entrance through a view port in the side of the tank wall.

(C) Heavyweight Motor, HW-3, was statically test fired at 0315 hours 30 April 1966, in the simulated altitude facility W-7 at Aerojet's

Sacramento Solid Test Facility. Ignition was smooth and the firing proceeded as programmed for the five second duration at which time the motor was successfully extinguished by the P-dot technique. Average chamber pressure of 550 psia was commanded and control was maintained; however, there was a low frequency oscillation (approximately 1 cps) with a 50 psi amplitude during the five second run. Altitude was maintained for approximately one hour after the test before the tank was opened.

(C) Review of the data from HW-3 Run 003 indicated that ignition was smooth and normal with maximum chamber pressure of 585 psia during the ignition transient being reached at approximately 0.270 seconds, igniter burnout time. The chamber pressure dropped to a low of 490 psia after igniter burnout and before force mode control was initiated at 0.500 seconds. When force mode control was cut in by the timer circuit, the chamber pressure recovered and began the low frequency oscillation previously discussed. With the exception of the first half second, the thrust delivered was smooth and averaged approximately 7600 pounds. At extinguishment command, the thrust spiked to approximately 12,800 pounds before dropping. The Thrust-Time and Pressure-Time plots for this test are presented in Figure III-149.

(C) The input to the control system was set at 4100 pounds, a multiple of the chamber pressure times the calculated nozzle throat area. This parameter was measured at the input point to the control computer, however an anomaly in the scale factor made the data unusable. The input force received was thus calculated from the feedback measurements and the error measurements. This calculated input as a function of time is presented on Figure III-150. As this is a calculated parameter rather than a measured parameter and since the first 0.500 seconds and all readings after 5.000 seconds are not indicative of the signals sent to the motor, these readings should be ignored. For the first half second the motor is on a pintle position control mode to allow for ignition and motor stabilization. At the five second point, when P-dot extinguishment is commanded, the control system is bypassed and the failsafe manifold is activated. The actual feedback signal from which the input was calculated is presented on Figure III-151. The same oscillations are present on this plot as were evident on the Thrust-Time and Pressure-Time traces. These oscillations were the result of increased gains in this control system over those used on HW-1 and HW-2 test firings. Due to the slow response of those two motors to input commands it was decided to increase the system gains until minor oscillations occurred in an attempt to keep the motor operating within the capability of the diffuser.

(C) As can be seen from Figure III-152, the Thrust/Pressure versus Time trace for HW-3, the minor oscillations are present, however they are out of phase with those of thrust and pressure. This trace is a measure

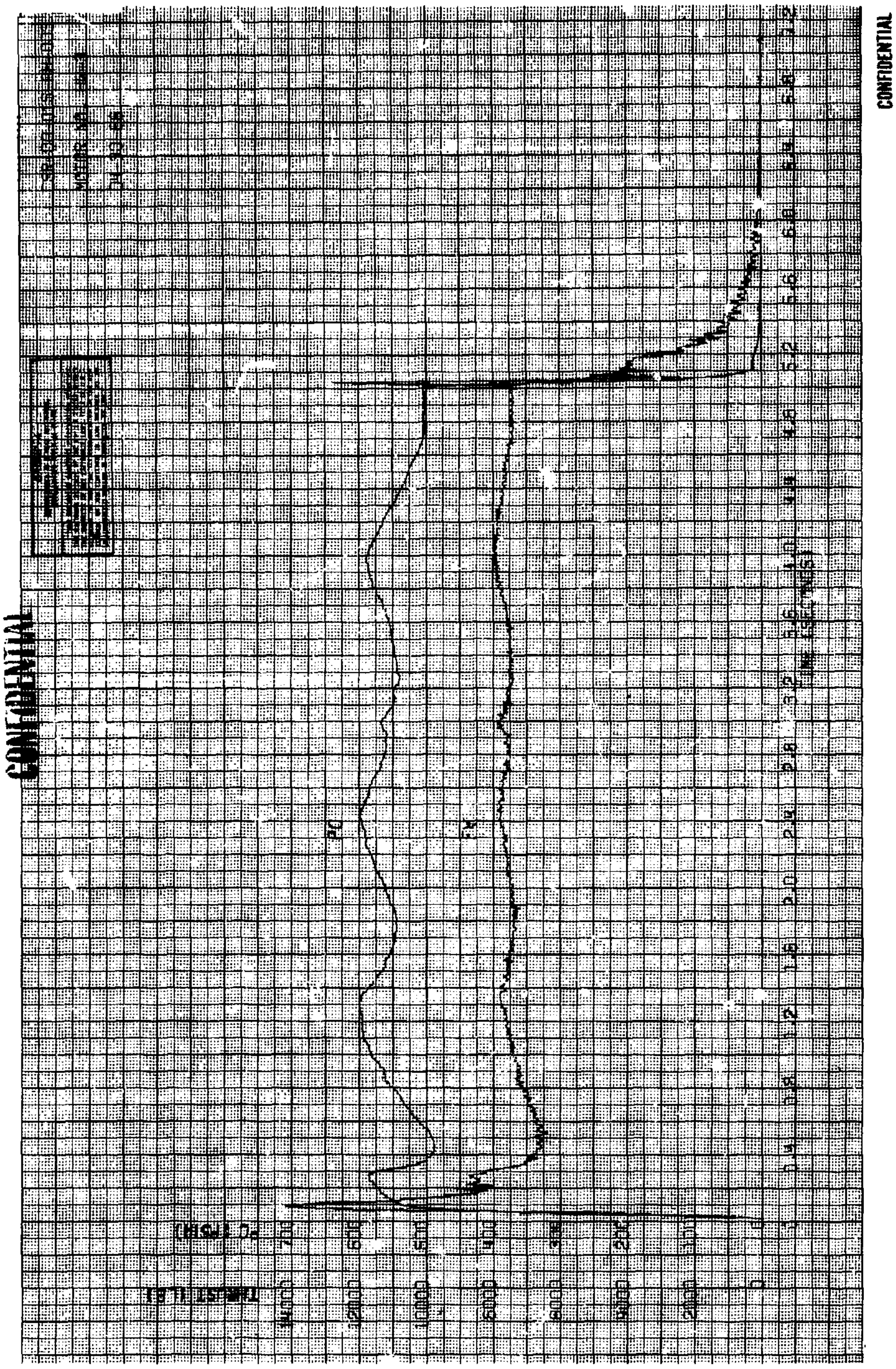

Thrust-Time and Pressure-Time, HW-3, Run 003 (u)

Figure III-149

Program Input-Time, HW-3, Run 003

Figure III-150

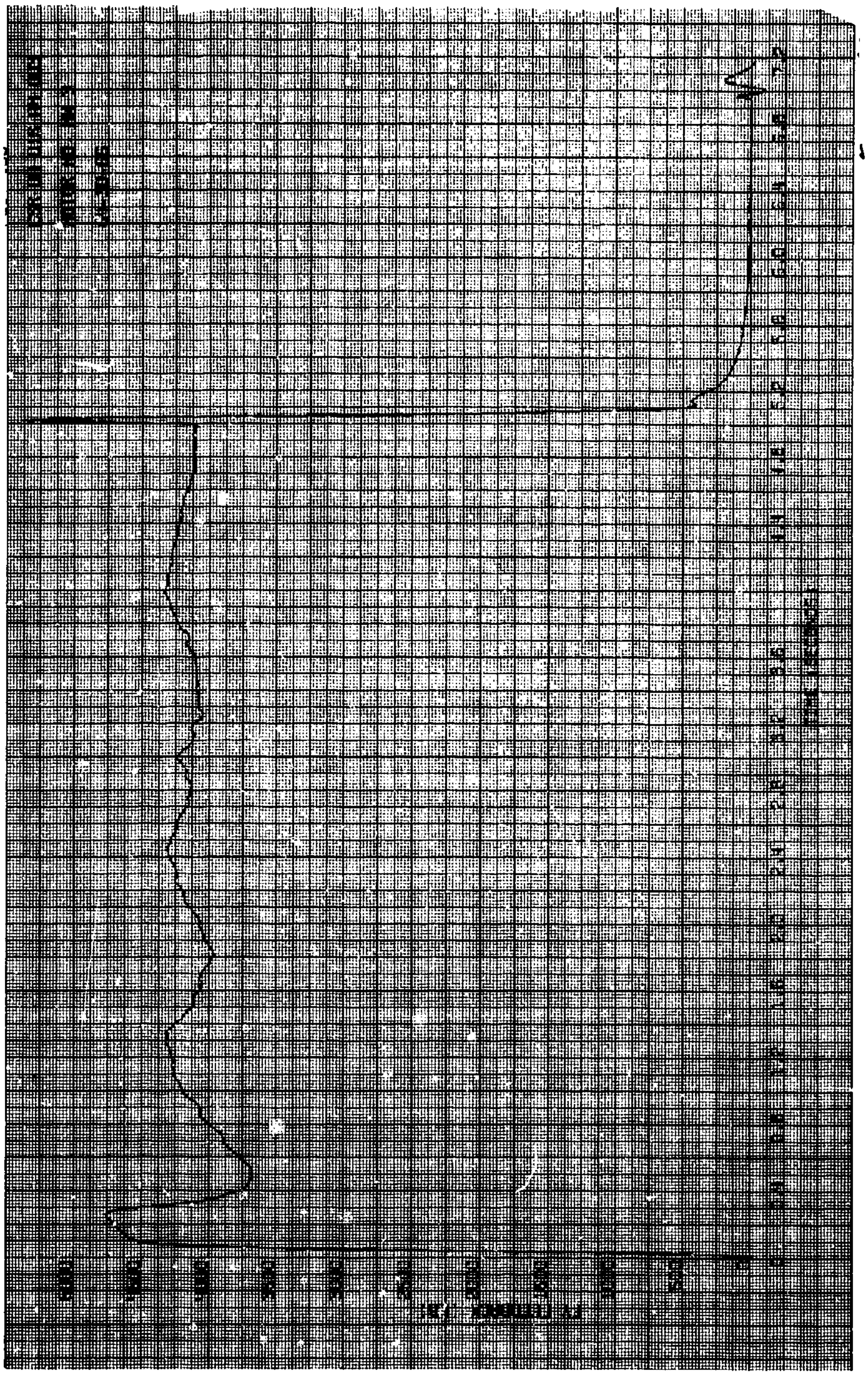

Feedback-Time, HW-3, Run 003

Figure III-151

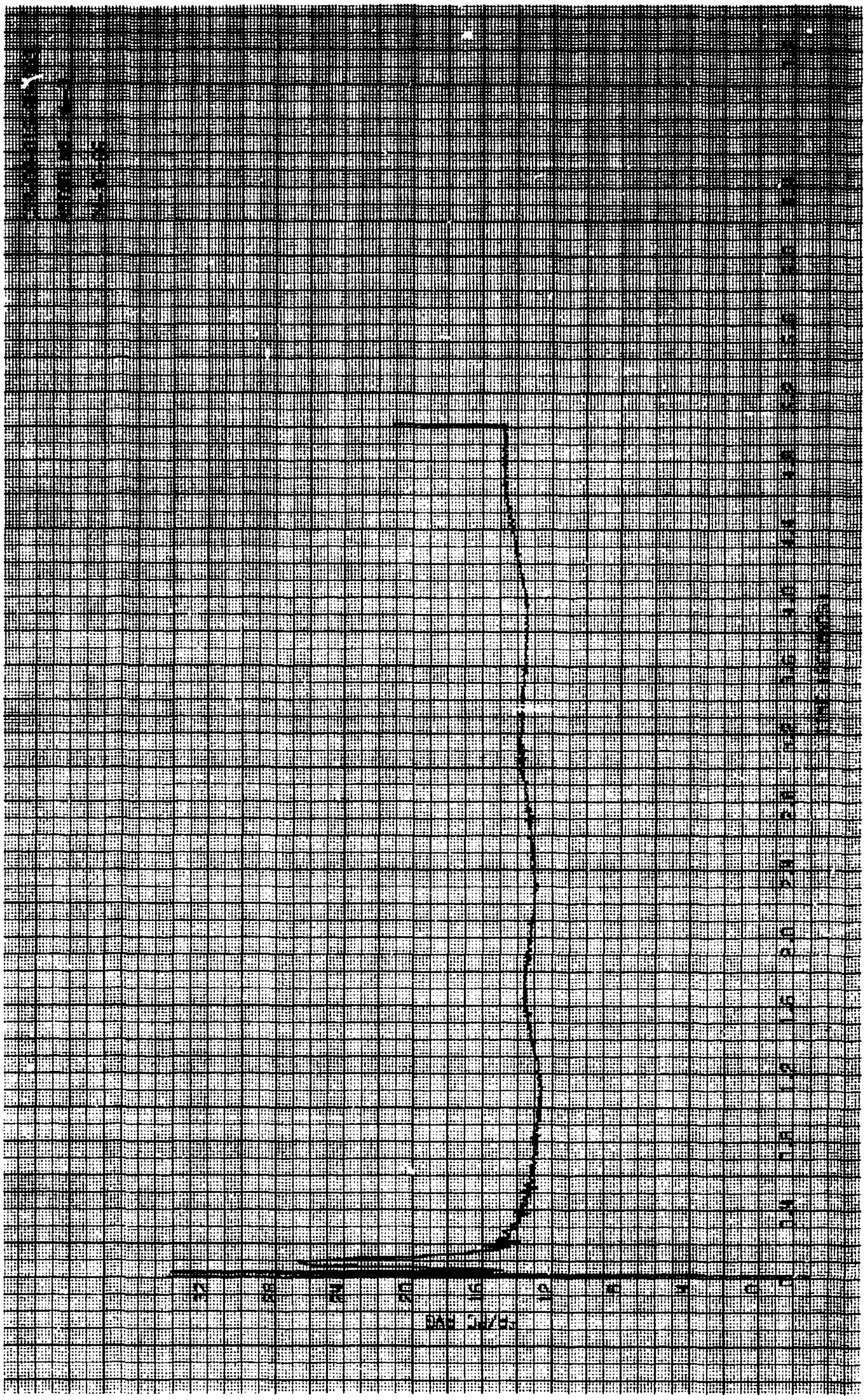

UNCLASSIFIED

Thrust/Pressure - Time, HW-3, Run 003

Figure III-152

of the nozzle throat area times the nozzle thrust coefficient as a function of time. The low amplitude-high frequency oscillations that are superimposed on the general trace are caused by the ringing of the test stand and do not reflect the motion of the pintle.

(C) This motor was test fired on a stand designed to continuously weigh the motor during the test. Four load cells are provided for this function. Figure III-153 is a trace of the sum of these load cells subtracted from the initial reading prior to fire-switch. The oscillations on this trace are caused by the ringing of the test stand and in no way reflect the mass flow rate at any time. At the 7 plus second point the oscillations are damping out and the apparent weight loss, counting the initial offset of 19 pounds, is approximately 140 pounds. The total motor impulse delivered in the first 5.100 seconds was 38,634 pound-seconds. Dividing this by the 140 pounds an average delivered specific impulse of approximately 272 seconds is derived. The average expansion ratio of the nozzle is 36:1 and the half angle is about 15 degrees. Expansion is close to optimum considering the diffuser pressure, thus correcting this value of specific impulse back to standard sea level, the propellant delivered a standard specific impulse of about 239 plus seconds as expected.

(U) The ejector system and diffuser system operated slightly better than designed as at no time during this firing did the pressure in the altitude tank exceed 0.40 psia and for the most part held at a level of 0.16 psia, or an equivalent altitude of approximately 100,000 feet. The design point for this system was 1.0 psia, or slightly over 60,000 feet. The differential pressure between the tank and the atmosphere was recorded and subtracted from the absolute atmospheric pressure. The result, the actual pressure in the altitude tank, is presented on Figure III-154 as a function of time.

(U) During the test, the heat flux gages recorded a thermal input to the flame baffle of less than 1.0 BTU/square foot-second. During the venting this value increased to approximately 4.0 BTU/square foot-second. The total rise in surface temperature of the chamber was somewhat less than ten degrees over the entire test and for approximately two minutes thereafter.

(C) In summary, the analysis of the test data from HW-3 Run 003 indicated that the motor yielded the following performance data:

Duration:	5.100 seconds to diffuser venting
Thrust:	7600 pounds average
	6500 pounds minimum
	8000 pounds maximum
	14,200 pounds ignition spike
	12,800 pounds extinction spike

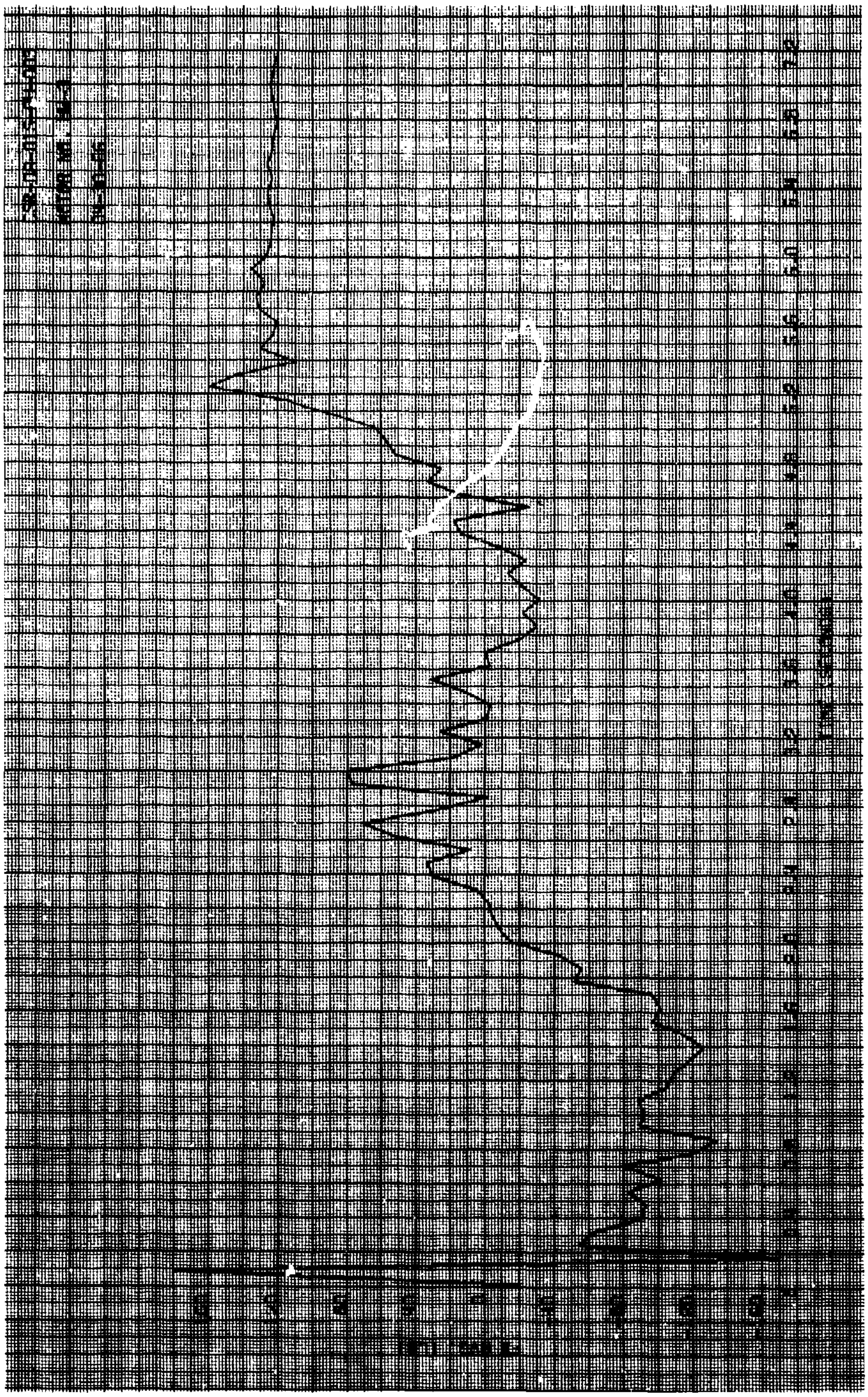

Weight Loss - Time, HW-3, Run 003

Figure III-153

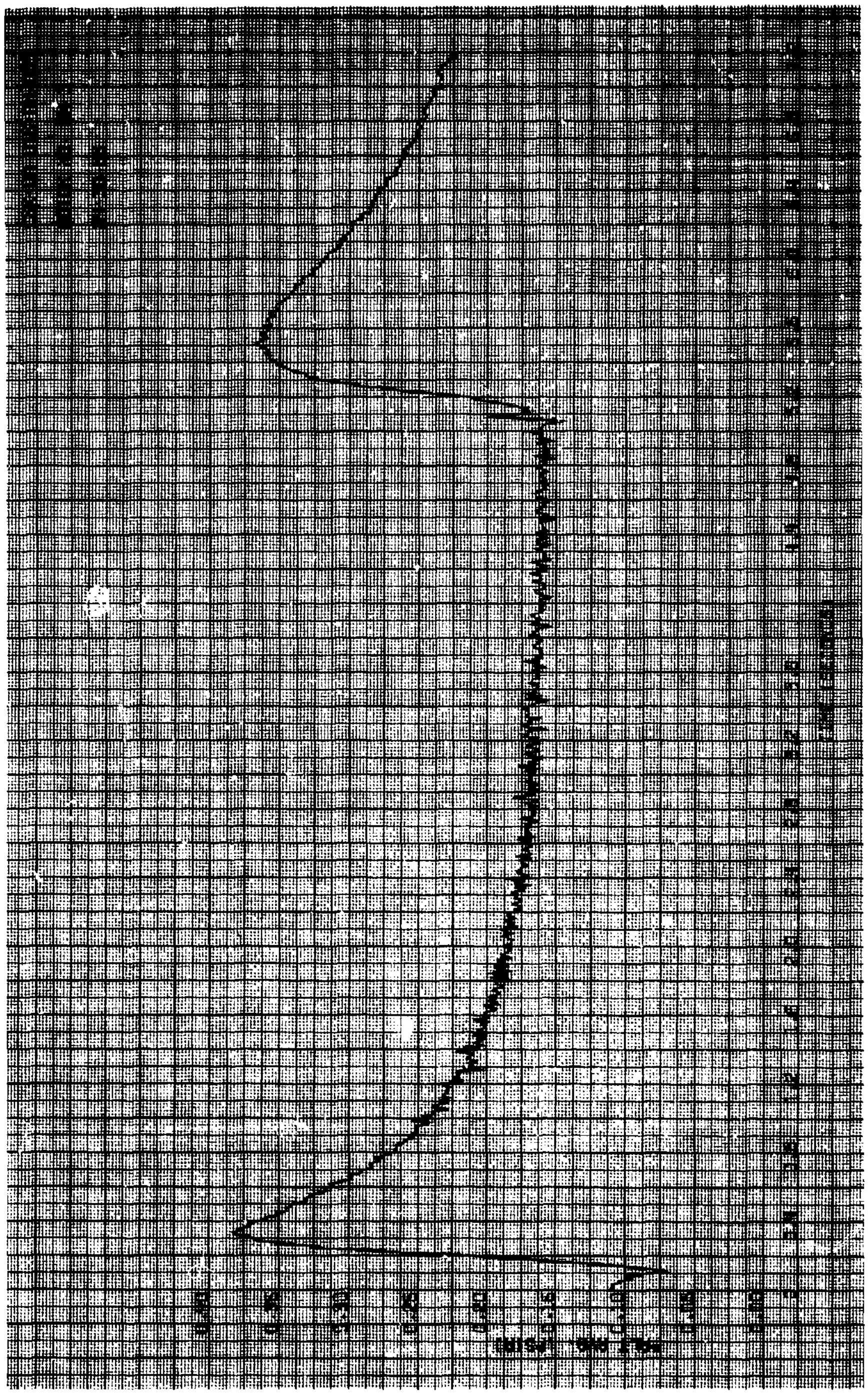

Altitude Tank Pressure - Time, HW-3, Run 003

Figure III-154

III, D, Heavyweight Motor Development (cont.)

Pressure:	548 psia average 480 psia minimum 600 psia maximum
Weight Loss:	140 pounds
I_s Delivered:	272 lb-sec/lbm
I_s Corrected: (SRO conditions)	239 plus lb-sec/lbm
Impulse:	38,634 pound-seconds (Does not include diffuser backflow)
Pressure-Time:	2,782 psia-seconds (to 5.10 sec)
Nozzle Throat Area:	7.50 square-inches average 7.35 square-inches minimum 7.95 square-inches maximum

The corrected specific impulse was determined from the thrust coefficient corrected to optimum expansion ratio at a 15-degree half angle from 1000 psi to atmospheric pressure. The nozzle throat area was determined from back calculation using the thrust divided by the chamber pressure and is based upon a variable thrust coefficient.

(U) As this was only the first firing of a scheduled four firing series on this motor, the motor hardware was not disassembled after this test. In general, the motor was in excellent condition after this first test with very little evidence of thermal degradation on any of the components. The only evidence that the motor had been subjected to a firing was on the exterior of the nozzle exit cone extension where the glass overlay had been peeled back during the diffuser unloading. Only the glass cloth was affected, the silica phenolic liner being in excellent condition.

(U) This being the first altitude firing and heat soak that the fullscale CSR motor had experienced, it was decided not to risk a subsequent failure on the leakage of an O-ring. The nozzle exit cone extension was therefore removed and the remainder of the motor repressure-checked. The major worry was the single Viton-A O-ring that seals between the outside diameter of the pintle piston and the strutted housing. This O-ring is subject to full chamber pressure with the backside of the O-ring vented through the struts to the tank pressure. All seals were found to be sound and the nozzle exit cone extension was replaced to make the motor ready for the second firing.

III, D, Heavyweight Motor Development (cont.)

(U) As the motor was being repositioned in the altitude facility and made ready for the second test, pintle position was rechecked and found to be in the same relative electrical and mechanical position as it was prior to the first firing, indicating that the linear potentiometer in the pintle actuator assembly had not experienced any noticeable temperature rise.

(C) On the basis of this first altitude test firing of the controllable solid rocket motor and the successful extinguishment of the propellant grain using the P-dot technique, it was shown that large motors (600 lb live grain) can be made and controlled as readily as the small motors (100 lb live grain) that were tested under the P-dot and L* extinguishment contracts concluded in 1965, Contracts AF 04(611)-9889 and AF 04(611)-9962, respectively. The motor performed as predicted and the control system maintained good control of the motor output even though the gains were set slightly too high for optimum control. From the results of this firing, there was no reason to believe that this motor could not be refired and extinguished successfully for the six thrusting periods that it had been designed. The one potential problem area that had been a source of worry prior to the test, namely the unloading of the gases trapped in the diffuser when the trap-door was closed during the extinguishment transient, appeared to cause no problems whatsoever during the actual test.

b. Second Test

(U) The only repairs made to HW-3 after the first test were those dealing with the external insulation in the area of the baffle and the exit cone. Both the blast baffle and the exit cone were reinsulated with the trowellable silicon rubber compound as is shown on Figure III-155. It should be noted in this figure that the clearance between the nozzle exit cone and the diffuser entry appear to be almost closed due to the trowellable insulation on the exit cone extension. This clearance, when compared with that of the first test of this motor apparently played a very important part in the outcome of HW-3 Run 004 as will be discussed later.

(U) On the forward end of the motor, the fired igniter that had been located in the boss on the motor centerline was removed and replaced with a large unfired igniter to avoid the problem of rupture disc ejection and subsequent igniter throat damage as was previously described.

(C) Motor HW-3 was fired for the second time at approximately 2305 hours also on 30 April 1966. This motor was programmed the same as the first test of this motor in an attempt to duplicate the data with the larger motor free volume present after the second pulsing period. Ignition was smooth and normal and the firing was without major incident until extinguishment

UNCLASSIFIED

Aft View, HW-3, Run 004, Prefire

Figure III-155

was commanded at T plus 5 seconds. Extinction did not occur, the trap-door closed on schedule, the door remained closed until T plus 12 seconds when it was manually commanded to open, hot gas back flow from the diffuser over the motor caused complete loss of nozzle feedback, and at some point prior to web burnout, the chamber burned through at the aft end as a result of exposure to this feedback gas.

(C) Review of the data from HW-3 Run 004 indicated that ignition was smooth with the maximum pressure attained being 500 psia at approximately 0.250 seconds, igniter burnout time. Shortly after igniter burnout, the motor chamber pressure dropped to a low of 355 psia due to the large initial throat area setting for ignition. The low pressure held until force control mode was cut in by the timer at T plus 0.500 seconds, at which point the chamber pressure began to recover to the programmed 550 psia. For the first five seconds of the test the chamber pressure oscillated about the 550 psia predicted value at a frequency of about .75 cycles per second and an amplitude of about 25 psi, both slightly lower than those experienced during the first run. The average thrust level for the first five seconds of the test was 7600 pounds and the average chamber pressure burning was slightly higher on the average for this second test than it was for the first test. On command to extinguish the motor chamber pressure dropped to a low of 32 psia and immediately recovered to an average pressure of 52 psia where it continued to burn for approximately five seconds. At the ten second point, the program called for the pintle to reinsert and the chamber pressure to recover to that of the motor at ignition prior to force mode control (about 350 psia). The chamber pressure only rose to 80 psia and immediately dropped back to 52 psia until about 11.2 seconds when it slowly began to climb. The peak pressure attained after this time occurred at 12.45 seconds and reached a value of 740 psia. Chamber pressure dropped immediately back to 52 psia and from this point until burnout of web, about 32-33 seconds, oscillated erratically about 100 psia with one spike reaching 230 psia.

(C) After the eight second point the data is for the most part worthless as the pintle feedback lines were burned through and any control forces input to the pintle were open-loop and entirely unrelated to those desired inputs. The point at which the chamber burnthrough occurred is not obvious from the data and was not evident from the films as the window clouded over at the five second point and remained that way for the remainder of the test. The chamber pressure and thrust as a function of time are shown in Figure III-156.

(C) Input to the control system was 4100 pounds, the same as that to Run 003. For this test as for the first test, the program input records were not usable, therefore this function was calculated from program output and the error signal from the computer circuit. Figure III-157 shows

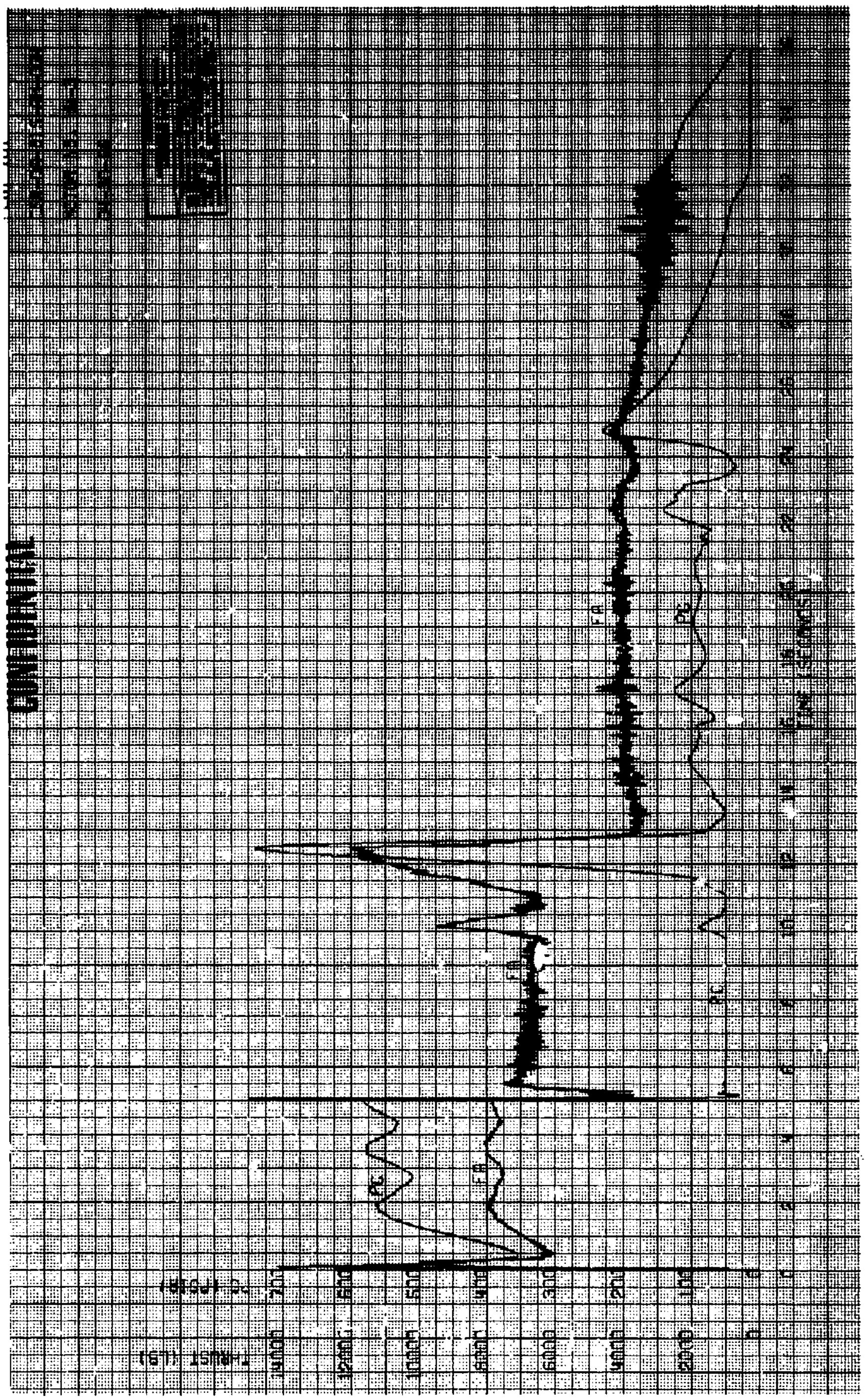

CONFIDENTIAL

Thrust-Time and Pressure - Time, HW-3, Run 004 (u)

Figure III-156

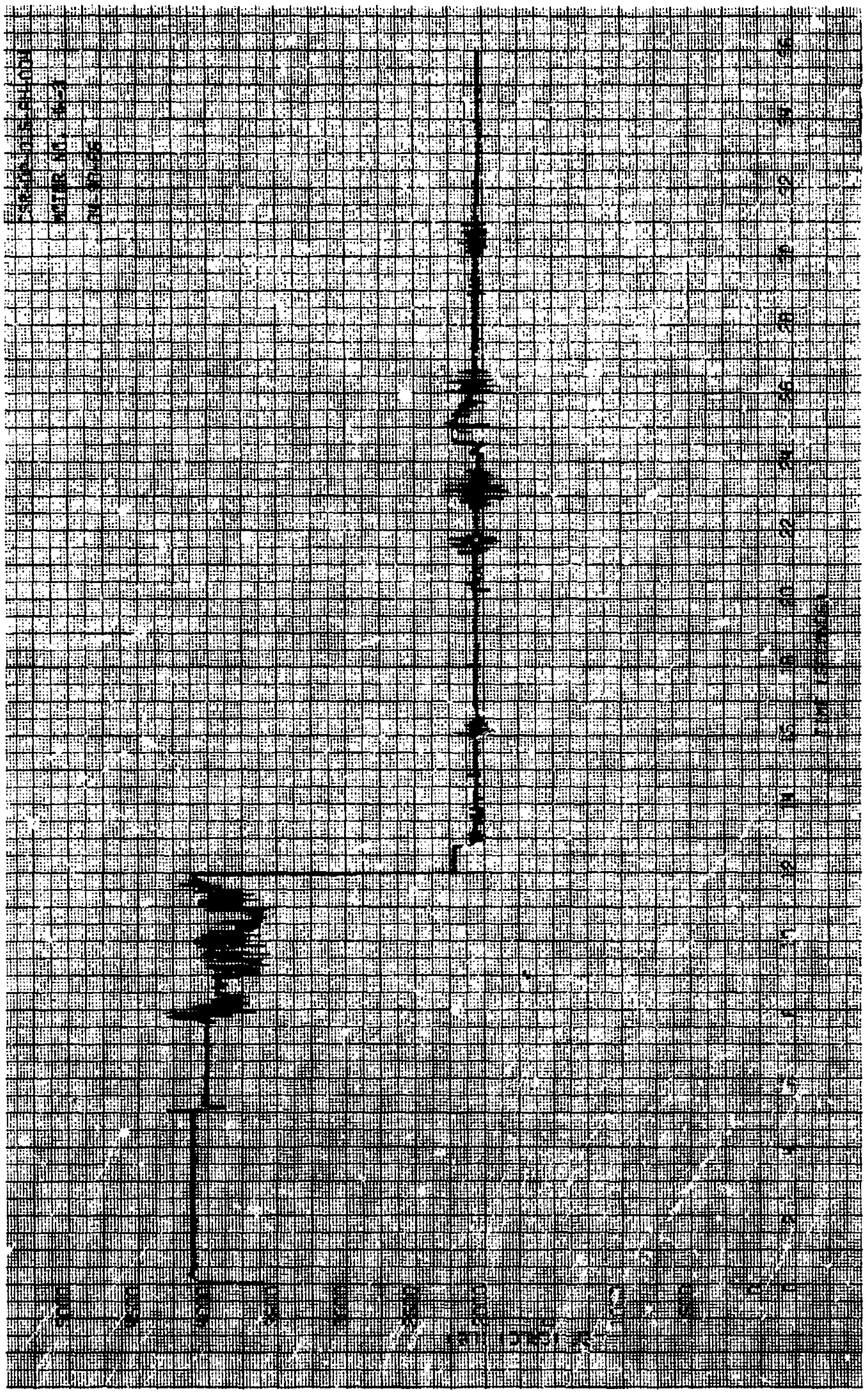

UNCLASSIFIED

Program Input, HW-3, Run 004

Figure III-157

the calculated input signal and clearly points out the time at which feedback was lost from the pintle signal and clearly points out the time at which feedback was lost from the pintle potentiometer, namely the 7.60 second point. This point is a usable data point although the programmer is being bypassed from the time of extinguishment command until the 10 second repositioning point. Even though it is not being used to control the motor from the 5 to the 10 second point, the computer is still calculating the feedback forces and attempting to compensate for them with signals to the servo valve. The servo valve is responding to the signals; however, the hydraulic supply to the servo valve is being shunted past the valve, through the failsafe manifold, and returned to the hydraulic supply cart. Figure III-158 shows the calculated feedback signal from the computer and indicates an incipient loss of feedback at the 7 second point with total loss at the 7.6 second point. All data on this figure beyond this time is worthless from an analysis standpoint.

(C) Figure III-159 depicts the measured thrust divided by the measured chamber pressure as a function of time. The high frequency oscillations in this plot point out the effect of the back flow of gas over the aft end of the motor and the ringing of the test stand from this excitation. This plot is useful in determining the aerodynamic throat area of the nozzle during the controlled portion of this test and, in addition, indicates that the chamber burnthrough most likely occurred at about the 24.5 second point where the plot indicates an incipient oscillation of increasing amplitude. Since there is no longer a blockage at the end of the diffuser, the only feasible explanation for this amplitude increase is gas leakage from the motor case at some point other than the nozzle.

(C) Although it is almost useless, the weight loss trace has been included to show the magnitude of the unsymmetrical loads that were felt by this motor after the 5 second point and due to the gas back flow. This plot is shown on Figure III-160. Stabilization of this parameter almost occurs at the 33-34 second point indicating a weight loss of about 400 pounds for the second test firing. Although this value is close to that which represents the remaining propellant after the first test, it is probably not accurate due to heat damage to the load cells and due to stand ringing.

(C) The absolute tank pressure is shown on Figure III-161 as a function of time. This plot clearly shows the effect of gas blow back on the environment of the altitude facility. From the 5 second point until the 12.5 second point the pressure in the tank is continuing to increase. At the 12.5 second point, apparently, the trap-door was commanded to open allowing some semblance of order for the remainder of web burning. This figure also verifies the 24.5 second point as the most probable point of chamber burnthrough.

UNCLASSIFIED

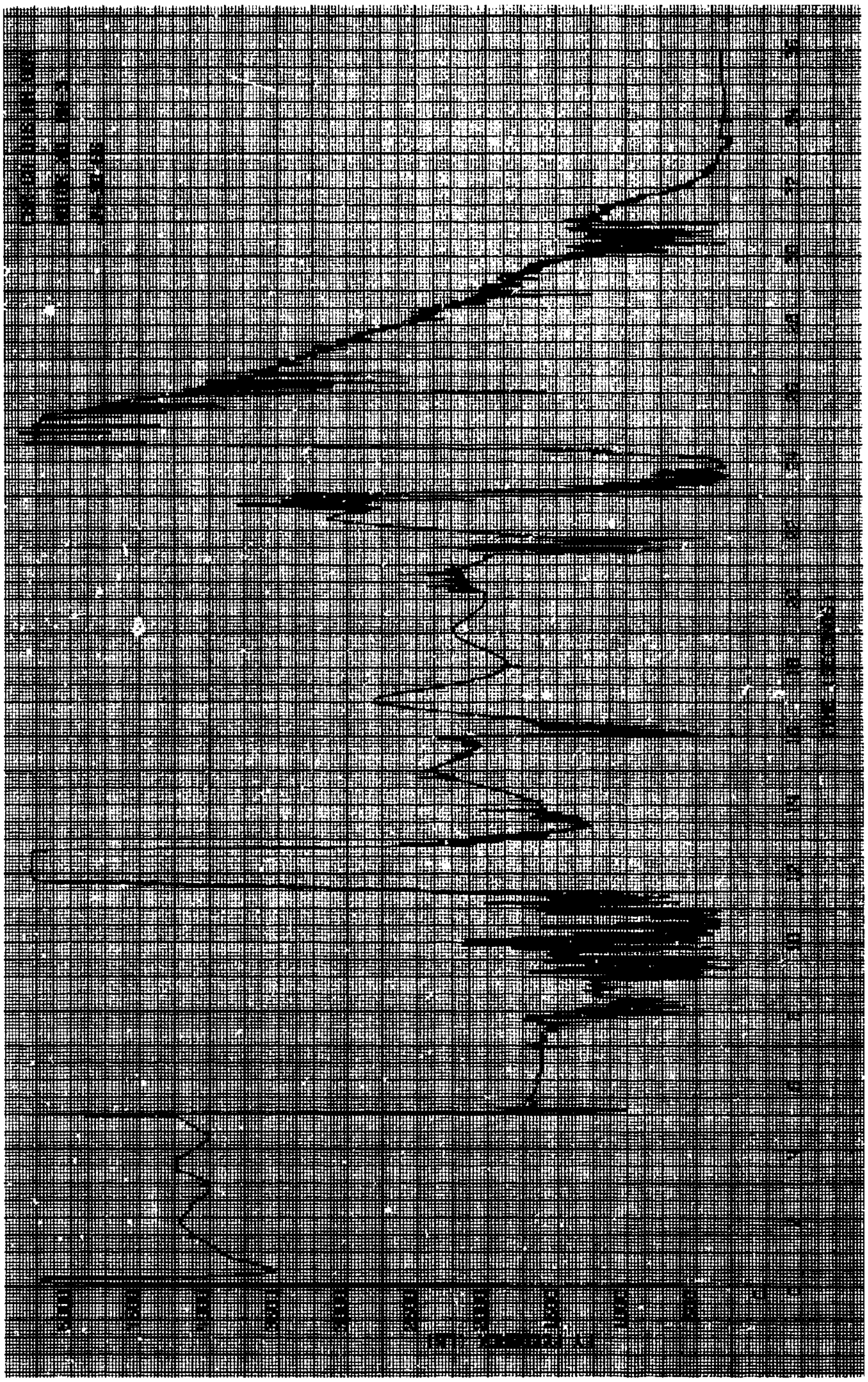

Feedback - Time, HW-3, Run 004

Figure III-158

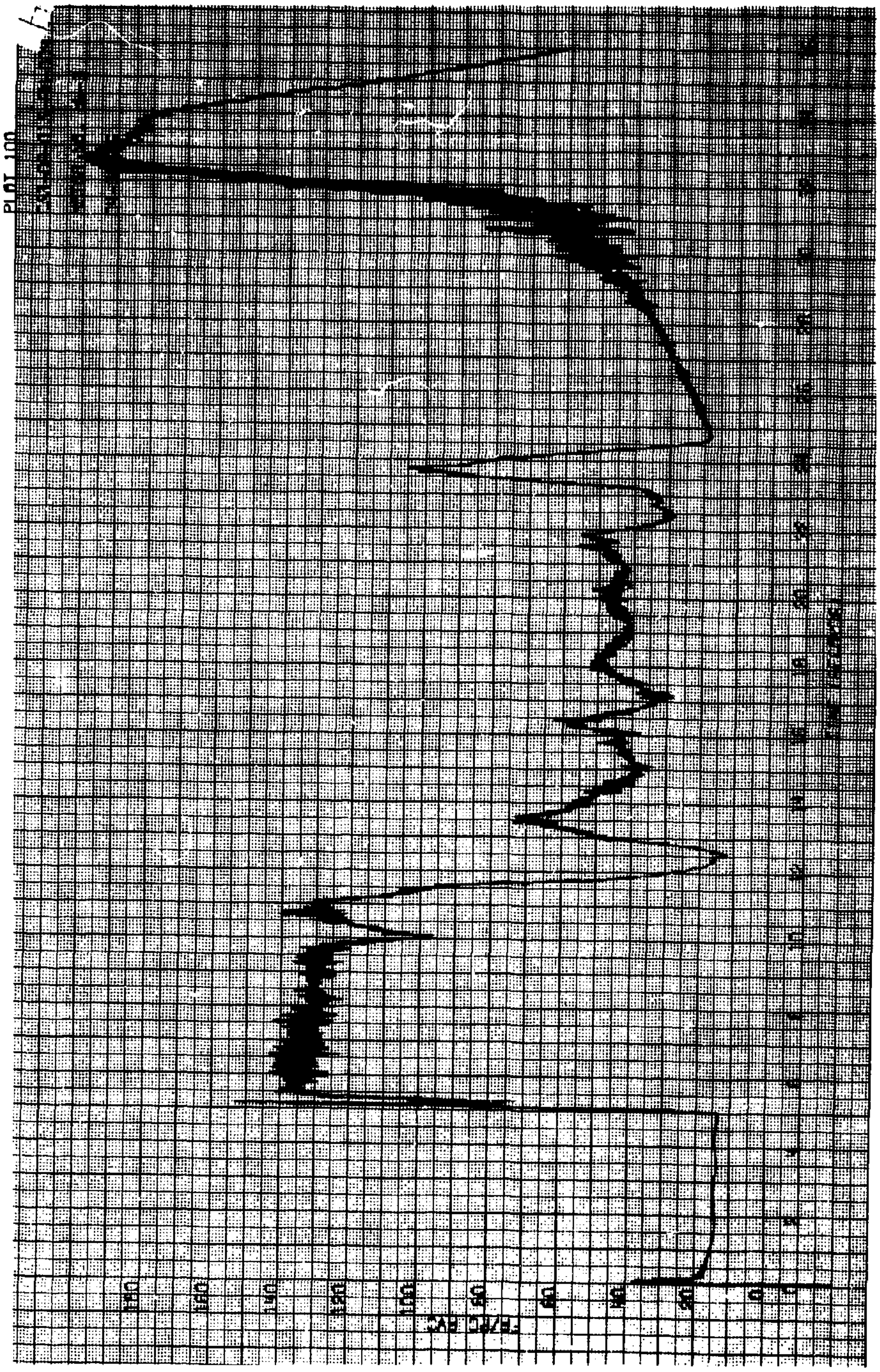

UNCLASSIFIED

Thrust/Pressure - Time, HW-3, Run 004

Figure III-159

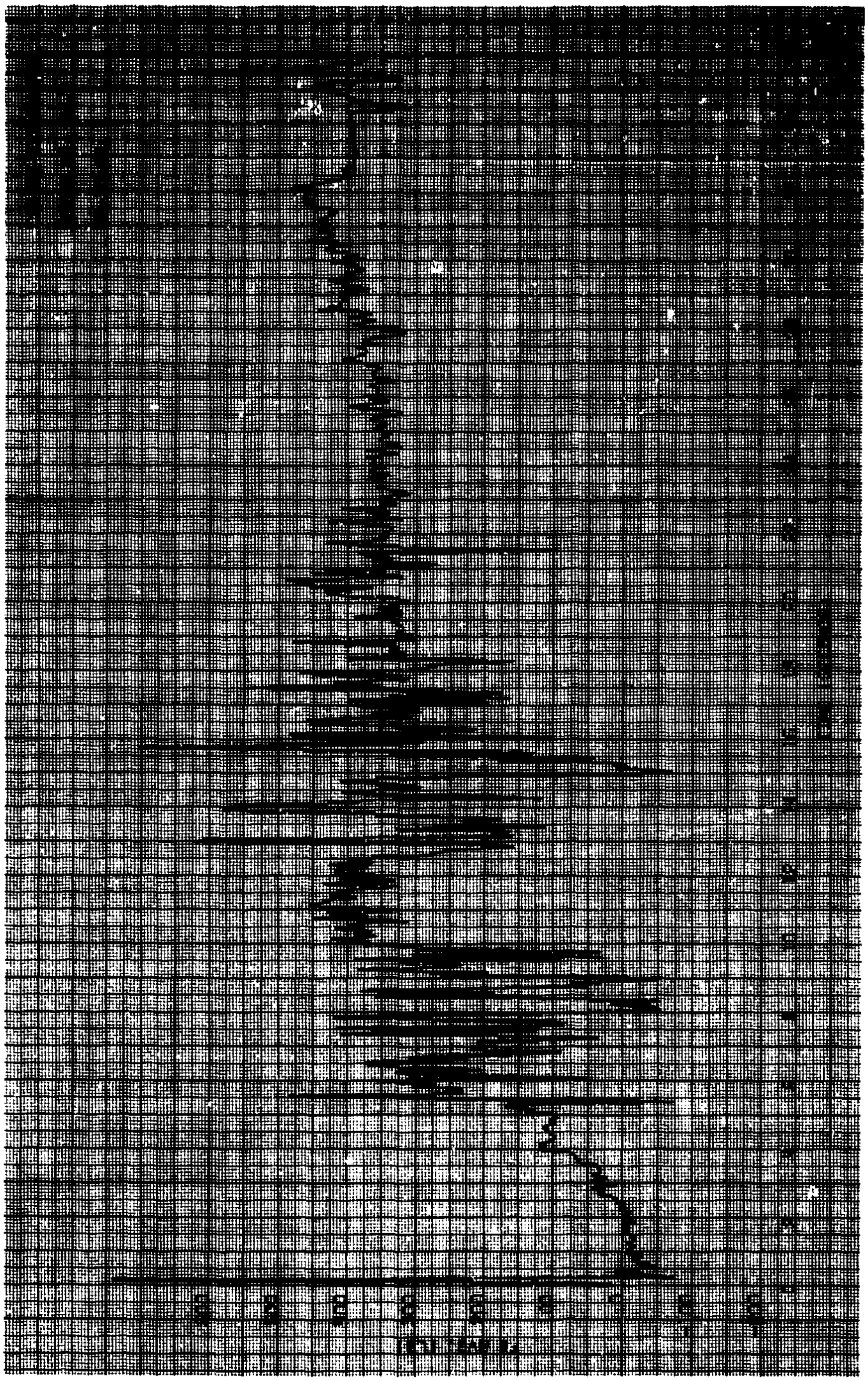

Weight Loss - Time, HW-3, Run 004

Figure III-160

UNCLASSIFIED

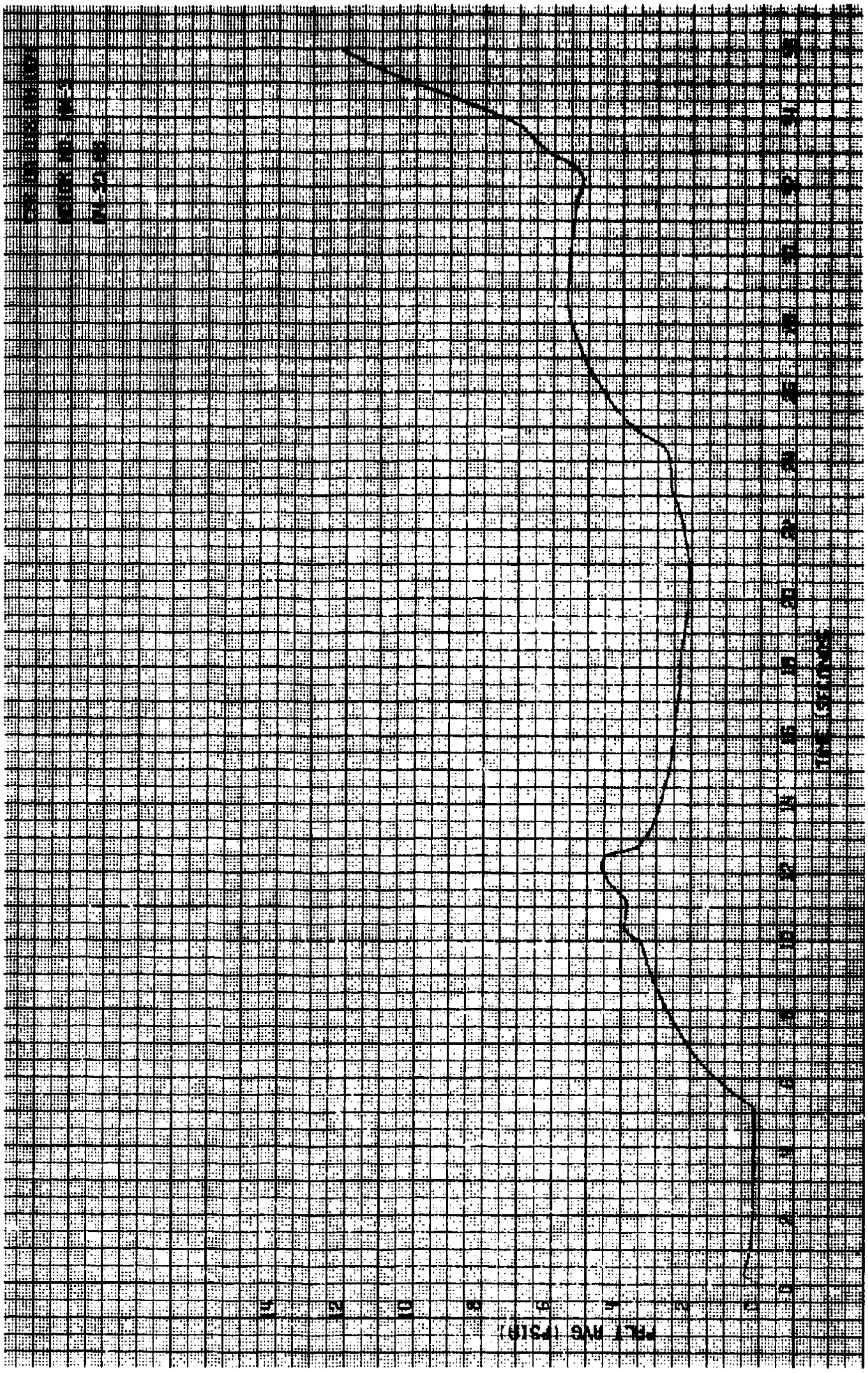

Altitude Tank Pressure - Time, HW-3, Run 004

Figure III-161

III, D, Heavyweight Motor Development (cont.)

(C) Figures III-162, -163, and -164 show the heat flux and chamber outside wall temperatures as a function of time. The severity of the environment can be seen from the rate of heat flux increase from the 5 second point on until loss of feedback from the heat flux meters. The most severe heating of the chamber occurred on the 180 and 270-degree side of the chamber. That is the side between the motor and the sidewall of the tank, away from the outlet to the nitrogen ejector. Loss of hydraulic pressure from the hydraulic circuit located on that same side of the motor verified the severity of the environment.

(C) In summary, the analysis of the test data from HW-3 Run 004 indicated that the motor yielded the following performance data up to the loss of pintle position (7.6 seconds):

Duration:	Not Applicable (about 33 seconds)
Thrust: (5 second Control Period)	7600 pounds average 6000 pounds minimum 8000 pounds maximum 14,200 pounds ignition spike 15,000 pounds extinction spike
Pressure: (5 second Control Period)	510 psia average 355 psia minimum 580 psia maximum
Weight Loss:	Estimated at 140 pounds for the first 5 seconds
I_s Delivered:	Estimated at 272 lb-sec/lbm
I_s Corrected: (Std. Conditions)	Estimated at 239 plus lb-sec/lbm
Impulse: (5.011 seconds)	38,183 pound-seconds
Pressure-Time: (5.011 seconds)	2585 psia-seconds)
Nozzle Throat Area: (5 second Control Period)	8.45 square-inches average 7.85 square-inches minimum 9.20 square-inches maximum

These values presented above do not include any data after the first 5 - 5.5 seconds of firing. The minimum pressure attained was 32 psia approximately and occurred after the pintle had been retracted in a P-dot extinguishment

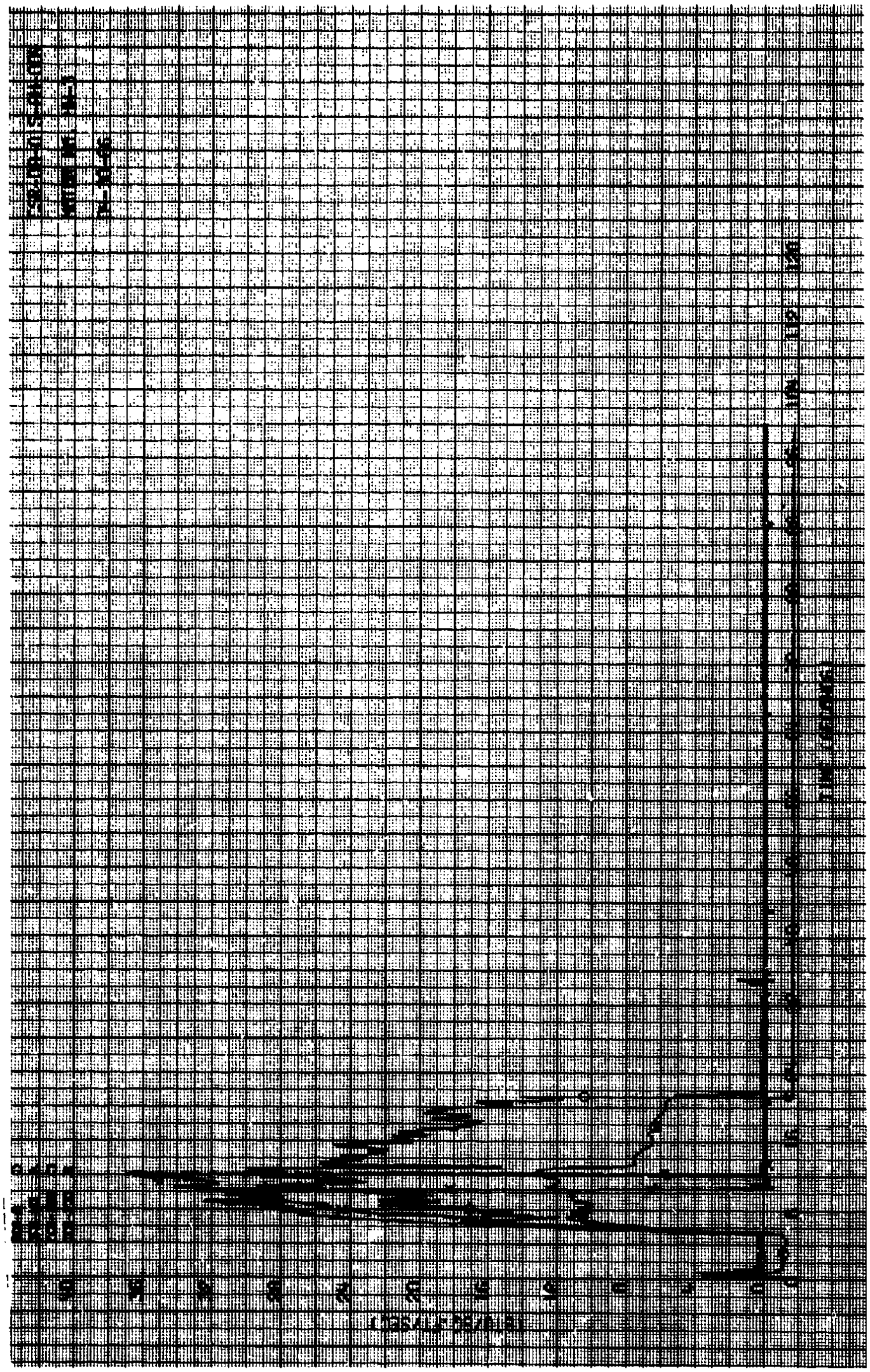

Heat Feedback - Time, HW-3, Run 004

Figure III-162

UNCLASSIFIED

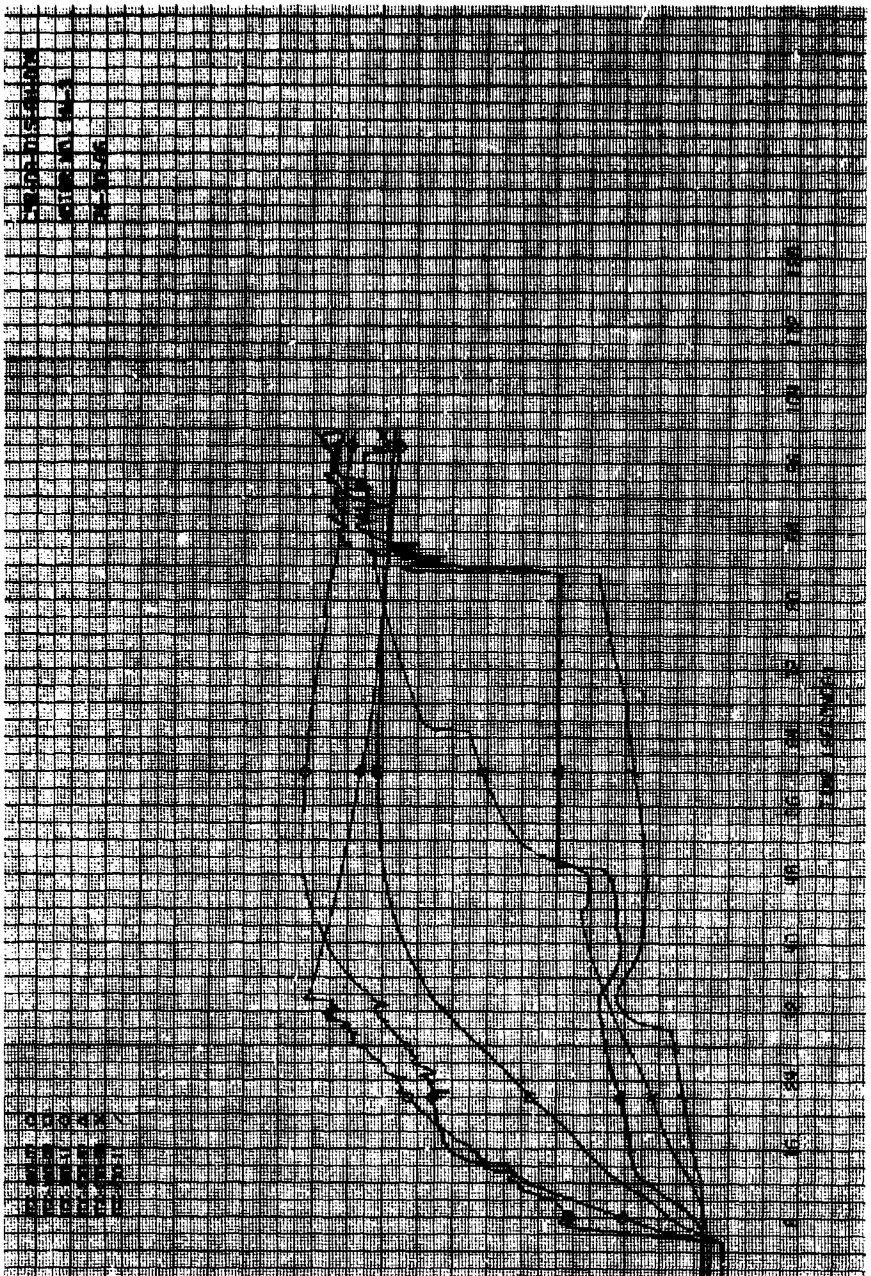

Chamber Thermocouples, HW-3, Run 004

Figure III-163

UNCLASSIFIED

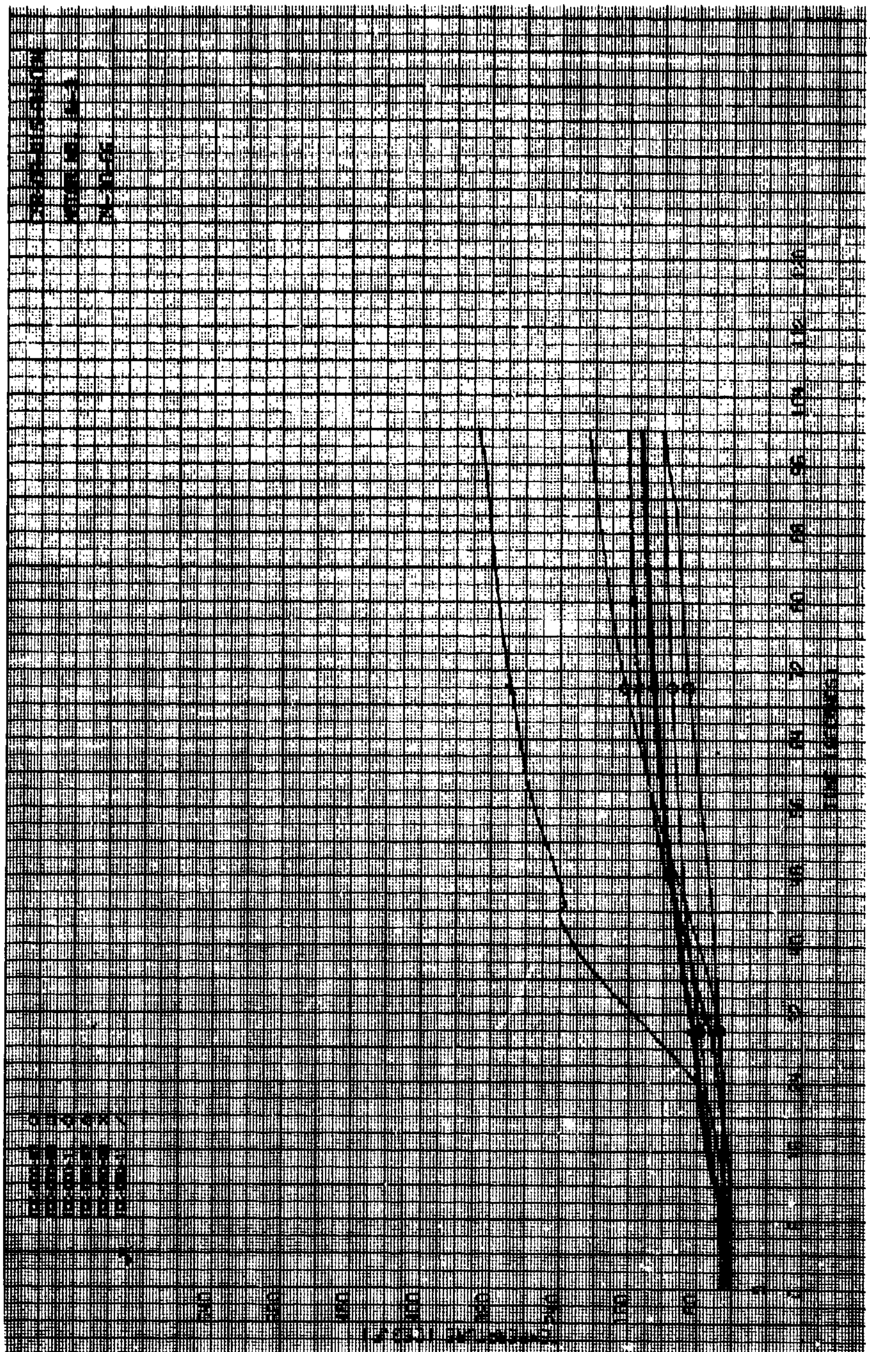

UNCLASSIFIED

Chamber Thermocouples, HW-3, Run 004

Figure III-164

mode. Stabilization occurred at 52 psia the same as it did on the aborted extinguishment of motor HW-2 fired at sea level. This indicated that the motor was reproducible in surface area, nozzle throat area, and burning rate with the pintle wide open. Cold flow testing of the nozzle after firing indicated that this wide open throat area was about 25.7 square inches rather than the expected 29 square inches and that the throat area was located between the outer throat insert and the aft insulator on the strutted housing. By removing this insulator and re-flowing the nozzle, it was determined that the actual sonic point moved back into the nozzle geometric throat plane and increased to a value of 28.5 square inches.

(C) With the exception of the hole burned in the aft end of the chamber, the hardware was in remarkably good condition considering the severity of the external heating. An overall motor view is shown on Figure III-165 and a closeup showing the hole in the chamber on Figure III-166. The hole in the chamber is on the side opposite the ejector butterfly valve in the altitude facility and was probably caused by the recirculatory gas flow feeding back from the blocked diffuser and forced to flow around the motor to the ejector inlet. As can be seen almost all of the silicon rubber insulation has been burned off or is charred through affording the motor little protection from the thermal environment. This material is a good external insulation when the thermal environment is primarily from radiant heat sources; however, it is limited in its ability to withstand direct impingement and high velocity flow.

(C) The aft end of the motor and a nozzle closeup view looking down the nozzle exit cone are shown on Figures III-167 and III-168 respectively. The hydraulic control panel can be seen on the lefthand side of the motor. This panel sustained some heat damage, but for the most part, was generally in better condition than normally would have been expected. This was due, most likely, to the convective cooling that it received from the 20-odd gallons of oil that leaked through it during the test and after the hydraulic line between the strut and the panel was burned through. This oil, while it probably protected the control panel, ignited at the motor and became an additional heat source leading to the eventual burnthrough of the case. As can be seen from the nozzle closeup the nozzle pintle and outer throat assembly were intact. There were some deposits of aluminum oxide and other condensed solids on the "A" section of the exit cone and on the exit cone extension, however the throat inserts were clean and appeared to be in excellent condition.

(C) Two views of the nozzle assembly as removed from the motor and with the exit cone extension removed are shown on Figures III-169 and -170. This nozzle has the same general appearance as those that were tested on HW-1 and HW-2 with the exception of the entrance cap. On this motor the entrance cap was insulated with molded GenGard V-44, an asbestos and silica filled nitrile rubber compound normally used as chamber sidewall insulation. From the appearance of the igniter canisters and the thrust tripod, it

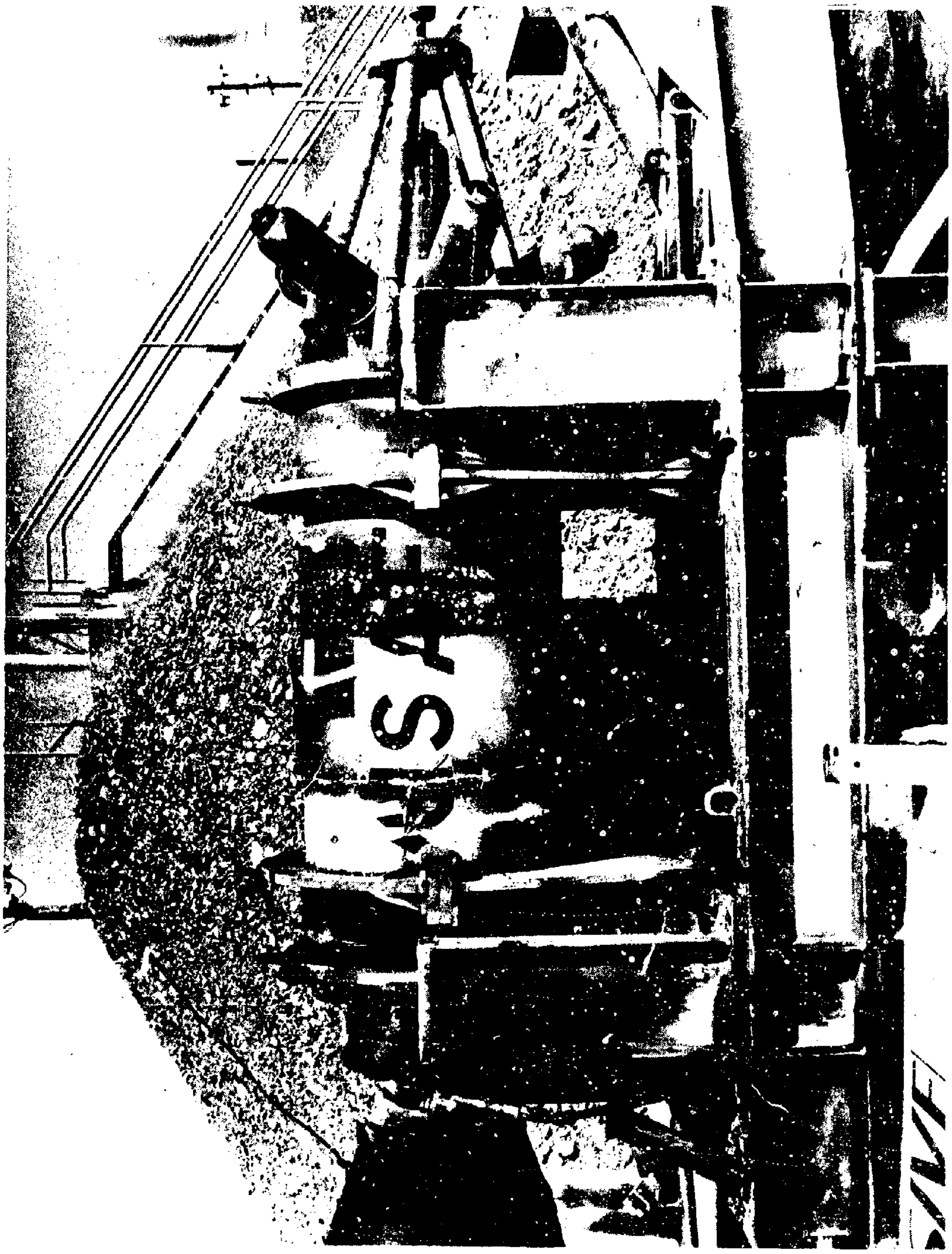

Overall View, HW-3, Run 004, Pcstfire

Figure III-165

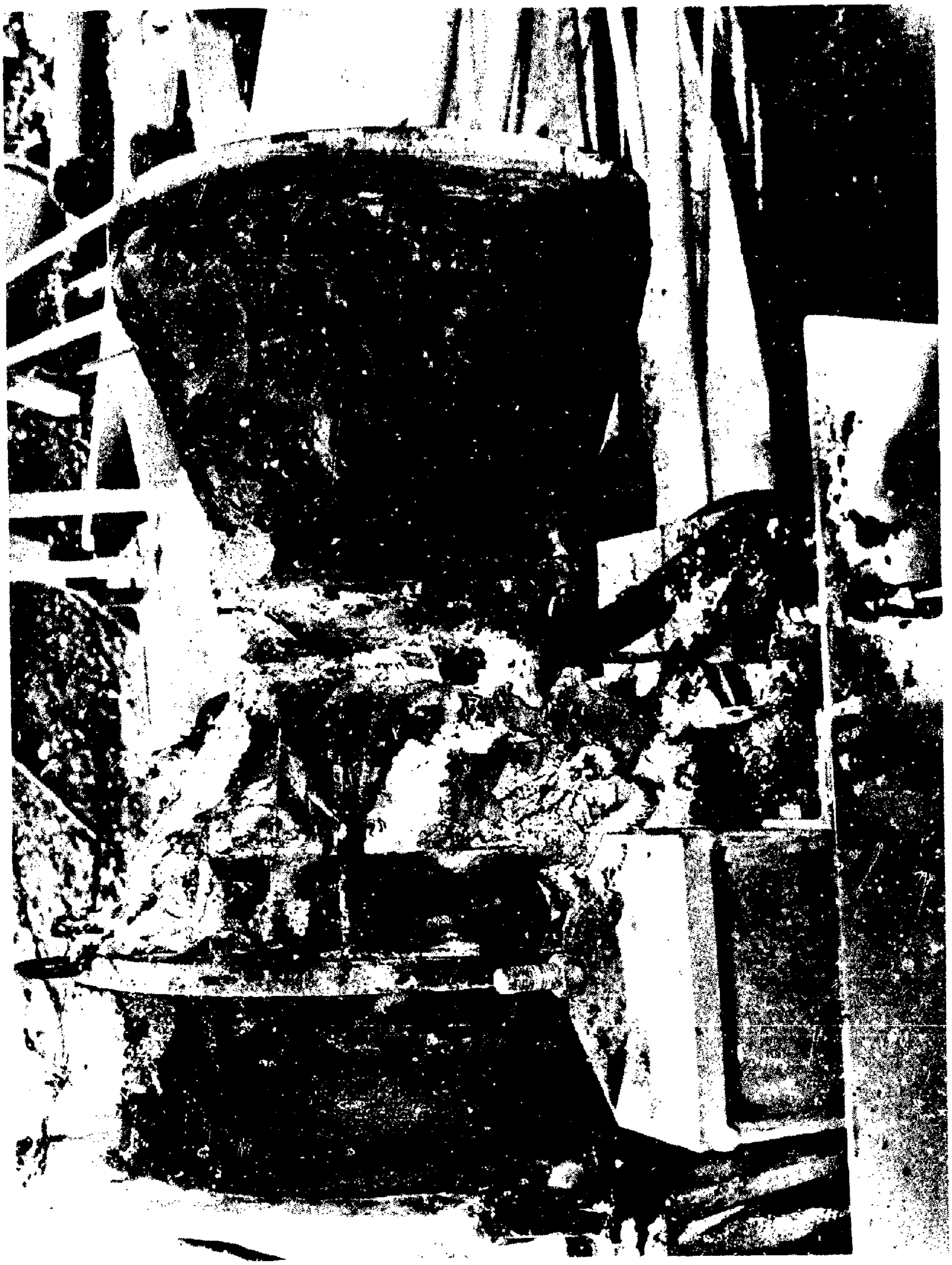

Rear-Side Closeup, HW-3, Run 004, Postfire

Figure III-166

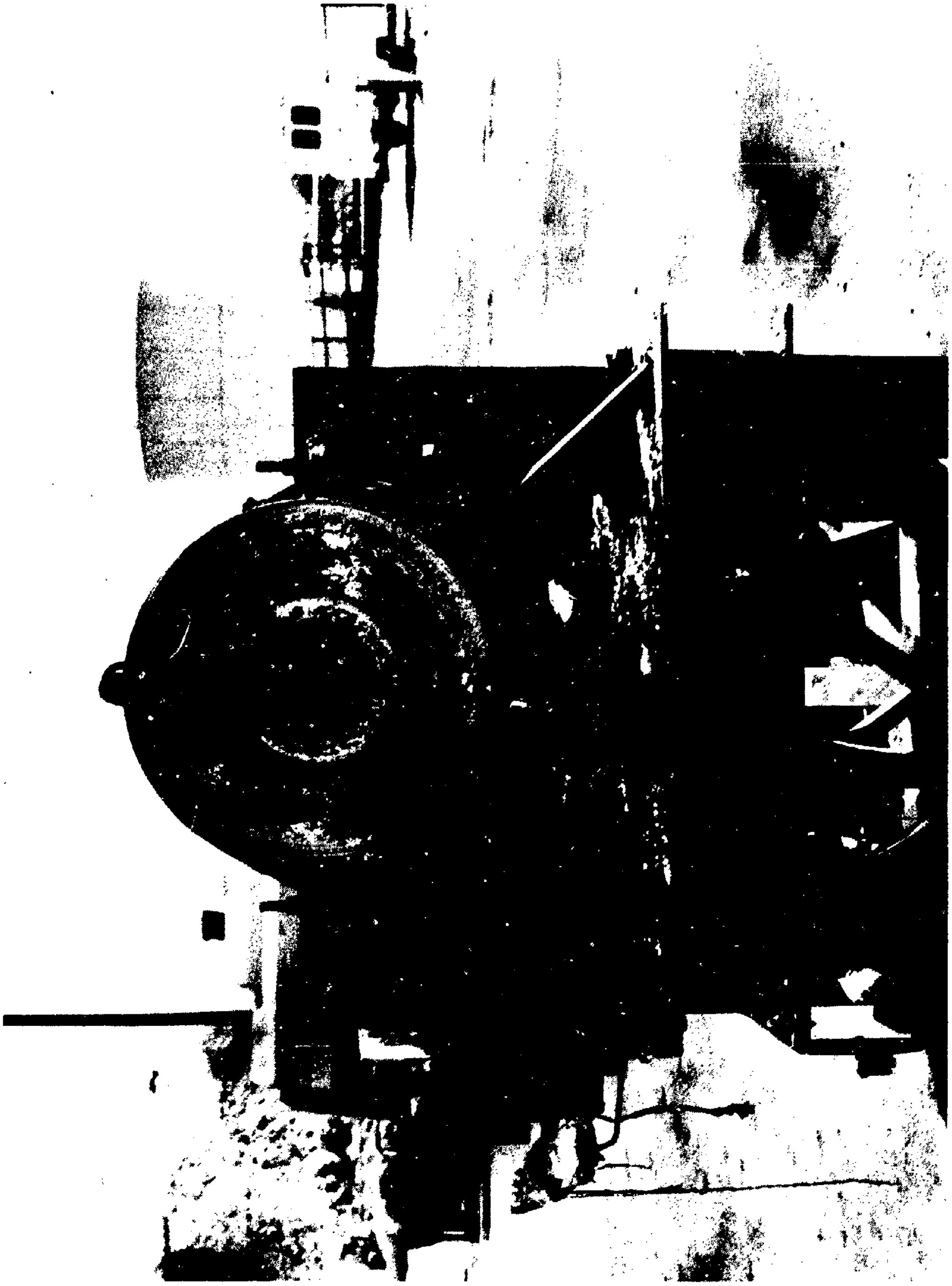

Aft View, HW-3, Run 004, Postfire

Figure III-167

Nozzle Bore Closeup, HW-3, Run 004, Postfire

Figure III-168

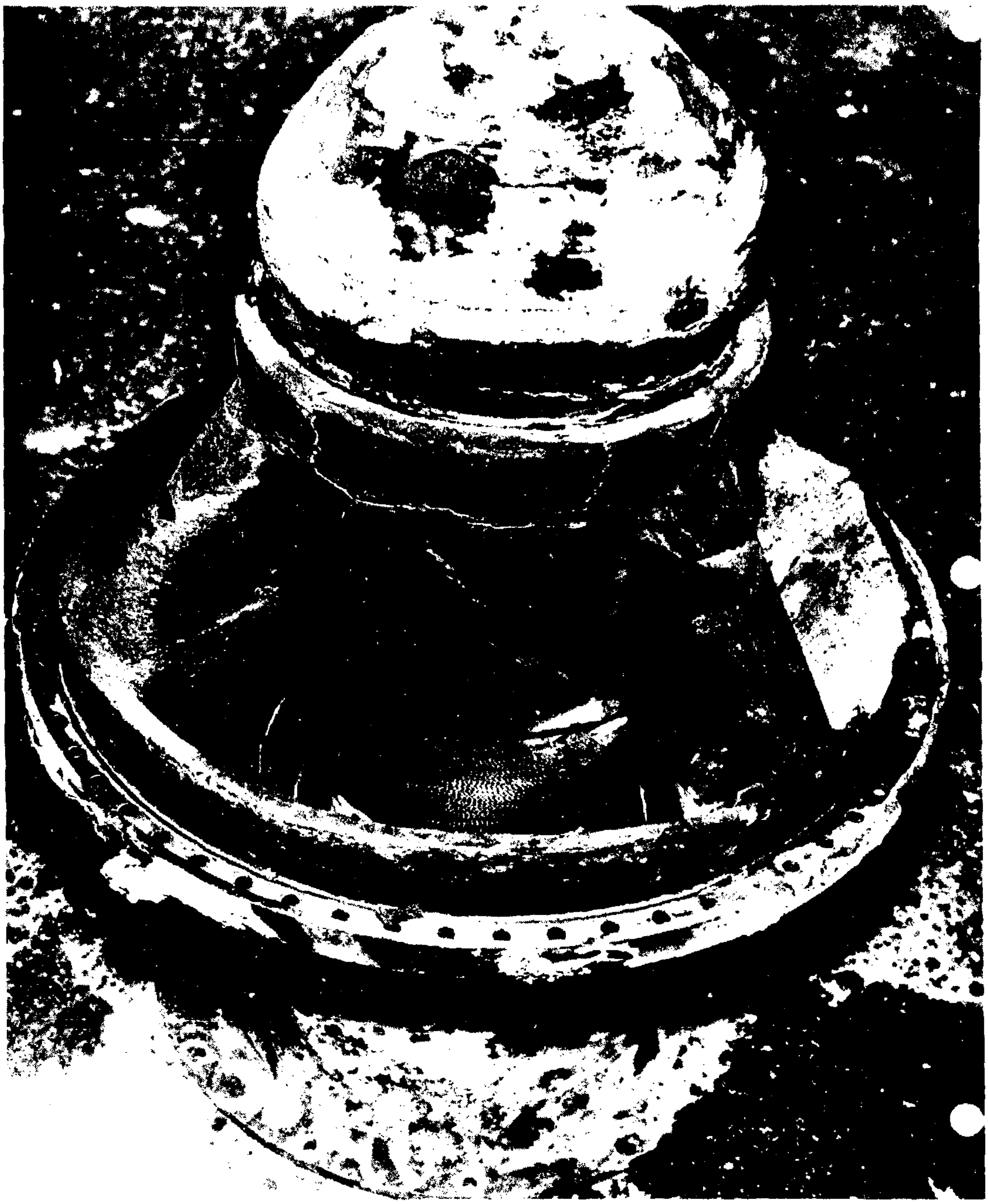

Nozzle, HW-3, Run 004, Postfire

Figure III-169

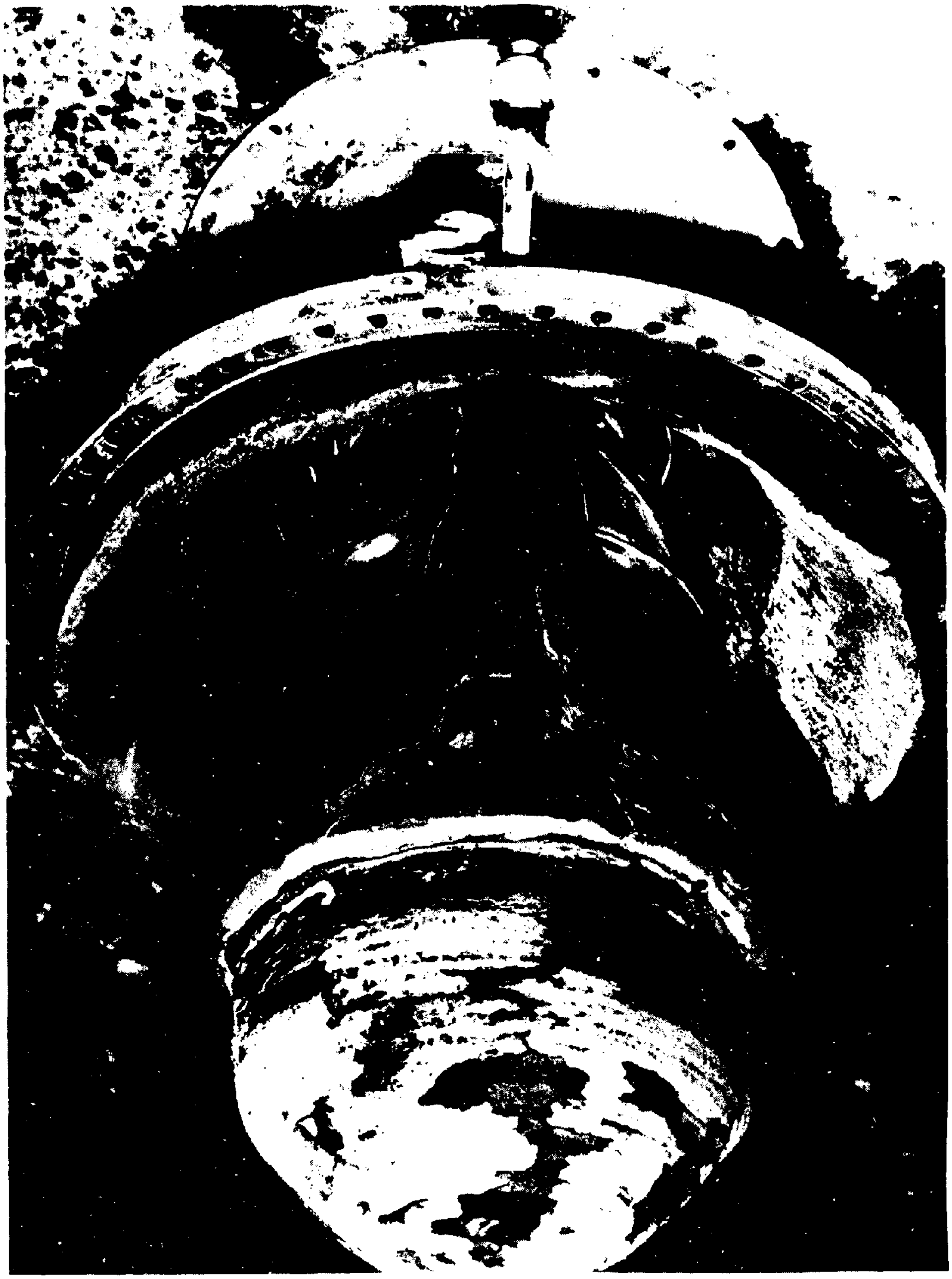

Nozzle, HW-3, Run 004, Postfire

Figure III-170

was evident that the environment at the forward end of the motor was only slightly less severe than that at the aft end.

(C) After the test, the nozzle was moved to the nozzle assembly area and careful disassembly of the components were undertaken. The exit cone extension was in excellent condition. The inside contour had suffered only deposition of condensed solids -- there was no erosion or ablation that could be measured and the parallel to centerline wrapped silica phenolic had not delaminated. The seal between the exit cone extension and the outer shell had been subjected to considerable heat; however, the O-ring was still very pliable and would be expected to function as designed on refire of the component. The glass-epoxy laminates that were overlaid to give added strength to the exit cone extension had peeled back and offered little to the structure. The steel flange, although blue over 75% of its surface, was still firmly attached to the liner and could be reused.

(C) The outer throat of the nozzle after firing and all of its components were in the same excellent condition that the same components were in firings HW-1 and HW-2. Only the steel shell showed any signs of the severe thermal environment to which this motor had been subjected. The graphite phenolic throat support where it was exposed to the flame and the "A" section of the exit cone had ablated slightly, less than 1/8 inch at the maximum point. The throat approach, also a graphite phenolic component had less than 0.030 inches of ablation. On this test, the asbestos phenolic shell insulator had started to char from the outside diameter, receiving probably more heat through the outer shell than through the throat assembly or the throat approach. The pyrolytic graphite washer stack used as the outer throat insert and the graphite backup ring were not damaged during this test nor was there any sign of erosion or delamination of the individual washers.

(C) The only visible points of damage to the strutted housing and pintle subassembly were to the strutted housing which was attached to the motor at the point of chamber burnthrough and to the entrance cap rubber insulation which has previously been discussed. One of the hydraulic tubes had been burned off and a portion of the shear lip was missing. The actuator withstood the test firing in excellent condition, and in fact, appeared to have been less heated than that fired on HW-1--a full duration sea level test. This is probably due to the better seal between the strutted housing and the strutted housing insulation on this part than on the first component molded. The inner bore of the strutted housing on this nozzle was in the best condition of any of the nozzles tested to date. This was a lucky coincidence as after 8 seconds into the second firing, pintle control was lost. Evidently, the pintle did not move back into the bore, but instead remained in the nozzle outer throat for the duration of this test.

(C) The components of the pintle and actuator were intact and from outward appearances, were in excellent and refirable condition. There was one notable exception to this, however, and that being a very critical component of this assembly. The main pintle O-ring was badly charred through and cracked. This O-ring seals between chamber gas and ambient pressure as the volume between the actuator and manifold assembly and the pintle assembly are vented through the three struts. In fact, all of the O-rings in the pintle subassembly were badly charred and cracked although not one of them showed any evidence of leakage. It is possible that the excess heat that was pumped into the strutted housing by the burning oil after the test firing was the cause of the O-ring cookout. The temperatures that were experienced were probably somewhere in the vicinity of 800 - 1000 degrees, as the metal components did not indicate anything more severe. All of these O-rings were fabricated from Viton A, a material which has proven good at temperatures up to 1000 degrees for short periods of time without failure.

(C) The remainder of the components in the pintle assembly were in good condition and some of them will be reused on the lightweight nozzle test motors. The pyrolytic graphite washers will be reused from all of the three heavyweight motors as will the pintle support structure and the 90-tantalum 10-tungsten nuts. The incipient problems indicated by the charred O-rings will receive a very careful design review prior to the first lightweight test firing. As an alternate to the material substitution discussed in the previous paragraph, the volume between the pintle assembly and the actuator-manifold assembly will be sealed off in future tests.

(C) The general conclusion drawn from firing HW-3 Run 004 is that the original failure was caused by inability to extinguish the motor without an automatic safety feature which would immediately open the trap-door at the end of the diffuser should the motor fail to extinguish. It was determined that all of the damage caused by this failure is attributable to the backflow of gas from the diffuser rather than any normal heat soak condition. In addition the after burning caused by the hydraulic leak probably contributed significantly to the damage.

(C) The above conclusion was drawn after a careful evaluation of the data as well as the components and comparison of the results of these analysis with the results of HW-1 and HW-2. To avoid a recurrence of this anomaly, it was necessary to determine exactly why the motor failed to extinguish the second time. There were three possibilities: (1) The rate of depressurization for any given pressure was much lower than that expected due to a mechanical failure in the components or a propellant grain crack; (2) The propellant requires a much higher than expected rate of depressurization in order to be successfully extinguished; (3) There was some external factor which caused extinguishment to be aborted.

III, D, Heavyweight Motor Development (cont.)

(C) A very careful analysis of the oscillograph traces of HW-3 Runs 003 and 004 and those of HW-1 indicated that the rate of depressurization for any given pressure was not out of line with that which would normally be expected at the given motor free volume and nozzle area change that transpired. Therefore, Item (1) was ruled out as the probable cause of the failure to extinguish HW-3 Run 004.

(C) Rerunning of the rapid depressurization screening tests using insulated motors it was found that it takes a much higher rate of depressurization to extinguish the propellant than was originally anticipated. This rate, however should have been within the capability of the CSR motor at the free volume in question. In fact, the rate was within the CSR delivered rate for Run 004 down to a pressure of about 60 psia, at which point the rate of depressurization suddenly began to decrease rapidly, indicating that some external influence was present.

(C) Only one thing could externally influence the rate of depressurization of a venting motor; a change in the venting area. This change in the venting area could be caused by a motion of the pintle or by an unchoking of the motor at the nozzle and a rechoking at some other point. Since the pintle did not move, it became evident that the motor was being choked at some point other than in the nozzle. Calculations were made to determine what the possible choke points were and it was found that the area between the diffuser and the nozzle exit cone extension was the most likely point. This probability was verified by a review of the motor setup for the two tests, Run 003 and Run 004. Whereas there was no silicon rubber compound between the nozzle exit cone extension for Run 003, this same area appears to have been almost closed for the second run. It has been calculated that this could have been the motor choke point at as high a chamber pressure as 60 - 70 psia, definitely causing a change in the rate of venting. If this became the "motor-throat", the "motor" would then consist of the standard CSR, the entire nozzle, and the entire 21-inch diameter by roughly 13 foot long diffuser. With the "motor" free volume encompassing all of these components, it is understandable that the rate of venting would be seriously reduced.

(C) Having established the most probable cause of the abortive extinguishment attempt on HW-3, the approach was taken to establish the most practical and quickest solution to the problem. It has been determined that the motor would most likely have extinguished successfully had the silicon rubber compound not been used on the nozzle and blocked the diffuser entrance. However, during the propellant re-evaluation P-dot screening tests in insulated motors, it became evident that an extinguishment problem would still exist as the motor free volume is increased due to the propellant consumption. Conservative estimates place the number of successful extinguishments that could be expected in the present CSR design as that number that could be conducted within the first 60 - 70% of propellant web. The last

30 - 40% of web would probably not be extinguishable due to the large free volume and the correspondingly slower rate of venting with the present nozzle design. From this determination, it became necessary to consider making a change in the motor as well as simply eliminating the diffuser problem. This motor change could be one of three changes in design: (1) Change the propellant to a more extinguishable formulation; (2) Increase the nozzle outer throat diameter by about 2 inches and the pintle by about 2.1 inches in order to increase the maximum nozzle throat area without changing the minimum area; and (3) Short cast the next motors with AAB-3220 to lower the minimum attainable pressure.

(C) Of the three alternatives, the most attractive from a design standpoint is the change in nozzle diameter as this would allow a better packaging of the nozzle pintle and actuator, provide more flexibility for structural design, and allow the use of the present propellant which is fully compatible with the grain design and the nozzle materials that have been demonstrated. This approach is, unfortunately, the most impractical from a cost and schedule standpoint. Major changes in the nozzle would require that new motor cases be fabricated with larger aft boss, that all nozzle hardware would be redesigned and new hardware fabricated before any further testing, and that a new actuator design be formulated for the increased loads imposed upon a larger pintle. This approach was ruled out for the remainder of Contract AF 04(611)-10820 due to the financial aspects. This contract was budgeted based upon reuse of the chamber and nozzle structural hardware. All processing tooling would also require rework if the chamber boss size was altered, causing cost and schedule problems. Therefore, only the other two alternatives could be used.

(C) Based upon a time and schedule analysis, it was decided to attempt to find a propellant formulation which was more easily extinguished than AAB-3220, that had the same physical properties, and that had a more favorable burning rate. A time limitation was placed upon this effort with the decision date to be mid-July 1966. If at that time a suitable propellant substitution could not be found, the lightweight motor series would be short cast to lower the minimum chamber pressure attainable with the current hardware and improve the extinguishability of the CSR motor. This last choice would result in a limitation of the thrust variability as well as lower the mass fraction of the motor.

6. Conclusions

(U) As a result of the heavweight development program it had been proven that fullscale movable pintle nozzles, used in conjunction with extinguishable propellants, could be mated to form a single-chamber controllable solid rocket motor. The technology in the area of materials application, propellant tailoring, and design of the full system had been shown. This technology; however, was not completely sufficient to permit the immediate

III, D. Heavyweight Motor Development (cont.)

development of a flight rated unit. It was, however, sufficient to permit the early transfer from the heavyweight development program to the lightweight development program. Problems had been encountered in this heavyweight development program; however potential solutions to these problems had been formulated and the lack of severity of the problems did not warrant extended heavyweight development effort.

E. LIGHTWEIGHT MOTOR DEVELOPMENT

1. Lightweight Motor Design (LW-1)

(C) The motor configuration for LW-1 consisted of a 20-in.-dia cylindrical case, cast with a modified "Finocil" grain configuration of AAP-3349 extinguishable propellant and equipped with a single canister igniter of conventional propellant grain design and a variable-area nozzle of movable pintle design for thrust variability and extinguishment. This motor contained approximately 570 lb of propellant in the main grain and 1.5 lb of propellant in the igniter.

(C) The propellant used on this series of motors consisted of an ammonium perchlorate and nitroguanidine oxidized formulation, with aluminum fuel and nitroplasticized polyurethane binder. A small quantity of sodium chloride (3%) was used to improve extinguishability. This propellant had a much lower burning rate than the AAB-3220 formulation used in the heavyweight series of motors. In addition, the P-dot extinguishment screening tests of the two propellants indicated that this formulation, AAP-3249, could be extinguished by depressurization rates almost an order of magnitude lower than those required to extinguish AAB-3220 at equivalent pressures.

(U) Because of the lower burning rate of this propellant it was necessary to modify the nozzle throat area to compensate for the loss of mass addition. In place of the 6.25 in.^{2} used for the heavyweight motor nozzle minimum area, a new minimum of 4.9 in.^{2} was required for the lightweight series. To accomplish this in the most expeditious manner, the outer throat insert was redesigned to a slightly smaller diameter, thus also lowering the maximum throat area attainable by 2.35 in.^{2} to a new value of about 27.75 in.^{2}. This change in the outer throat diameter induced a controls problem because it made the effective change in nozzle throat area with pintle position extremely sensitive. For an 8% change in pintle position, the change in motor operating pressure was over 80%. To compensate for this excessive sensitivity, the gains in the pressure feedback control system were cut back.

(C) This motor, being the first of the lightweight motor series, was assigned to check out the lightweight pintle liner system that had been designed into the expected lightweight motor configuration. This lightweight liner system consisted of the substitution of pyrolytic graphite washers in place of the silver-infiltrated tungsten insert used in the heavyweight motor design. Because of the results of a test of pyrolytic graphite washers in a similar application on the nozzle development program conducted at Arde-Portland (Contract AF 04(611)-10749), a reevaluation of the design was conducted prior to test firing. It was determined that under a given set of

circumstances it would be possible for the initial thermal expansion of the outside diameter of the pyrolytic graphite washers to load the washers in such a manner to cause immediate failure in plate bending before the expansion of the entire washer stack could compensate for the loading. To avoid this possibility, the washers were grooved at the outside diameter, 0.011 in. wide by 0.300 in. deep.

2. LW-1 Test Firing CSR-DA-01S-BH-005

(U) The primary objective of the test of motor LW-1 was to determine the system operating capability at sea level using a new propellant and a new design for the pintle liner. It had been shown in the sea-level tests of the heavyweight motor series that permanent sea level extinguishment could not be attained using AAB-3220 propellant in the grain configuration used. This new propellant, AAP-3249, had much lower P-dot extinguishability requirements, a lower burning rate, and no end-restriction material that could cause reignition. One of the objectives of this test was therefore another attempt to achieve extinguishment at sea level conditions. A variable-thrust program was designed for this test so that the burning rate of the propellant in the CSR motor could be calculated at a number of chamber pressures, because it was found in the heavyweight tests that the burning rate at low pressures did not agree with that measured in the small burning rate determination motors.

(C) The CSR motor, LW-1, was statically test-fired in Bay W-4, sea-level stand, on 10 August 1966 at approximately 0140 hr. The nozzle setup is shown in Figure III-171. It should be noted that for this test, one of the side igniter ports was used for initial ignition. Within 230 millisec after fire switch the pintle liner system was ejected, dropping the effective chamber pressure to a very low value, and voiding any further data from this motor test firing.

(U) Although the useful test data from this firing was severely limited because of the short duration, the data on heat soak and long-duration heating of the motor and nozzle components was useful in determining the points requiring redesign consideration. The effect of heat soak to the chamber sidewall was evident by the scorched paint on the cylindrical section of the chamber. This point of the chamber has only a very thin insulation liner that is not exposed to flame until propellant burnout occurs. The heat effects are the result of insulation after-burning, a condition not pertinent to the design of the single-chamber controllable solid rocket motor.

(U) The effect of pintle liner loss early in the test is evidenced by the appearance of the nozzle after firing as shown on Figure III-172. In the center of the nozzle, the pintle support structure can be seen in a

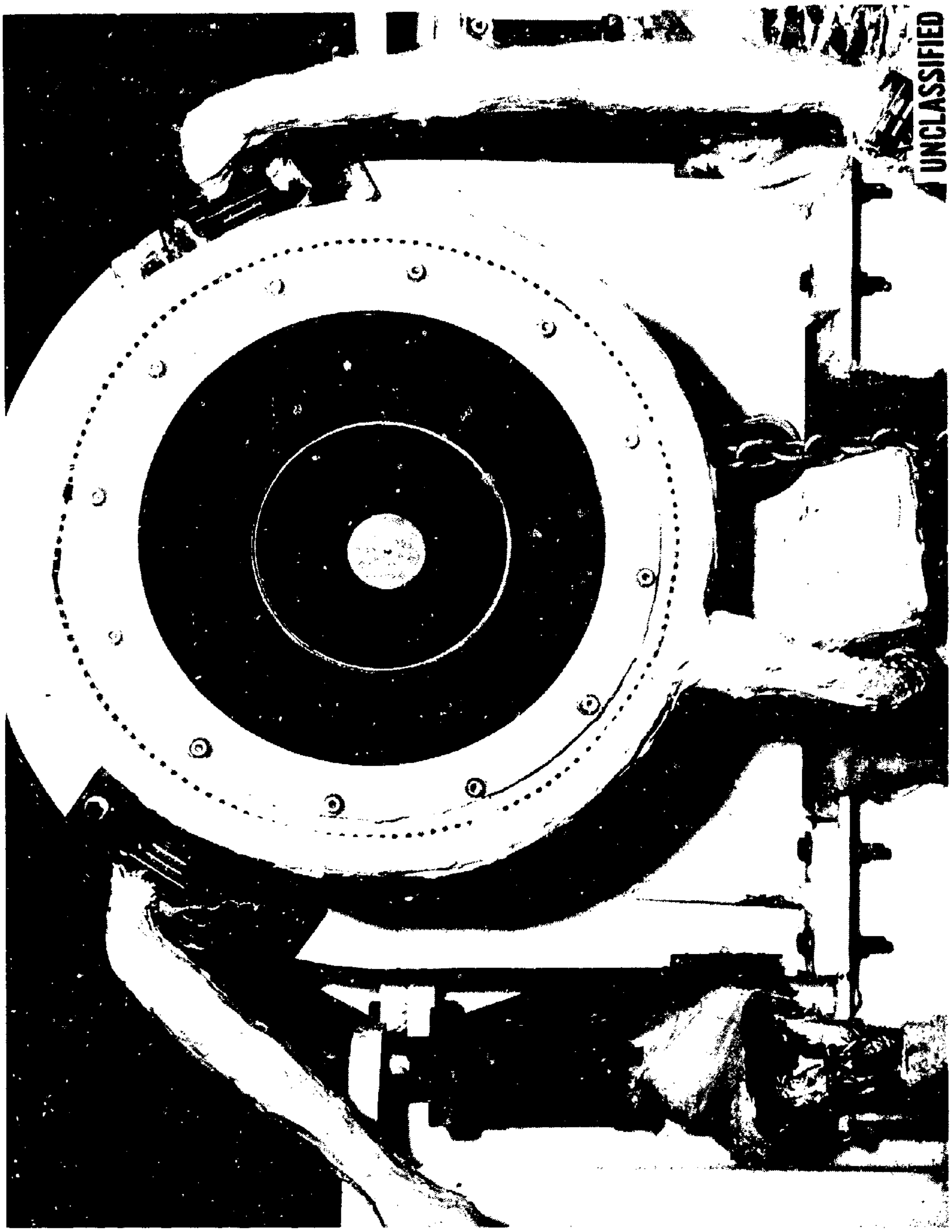

CSRM-LW-1 Prefire (Nozzle)

Figure III-171

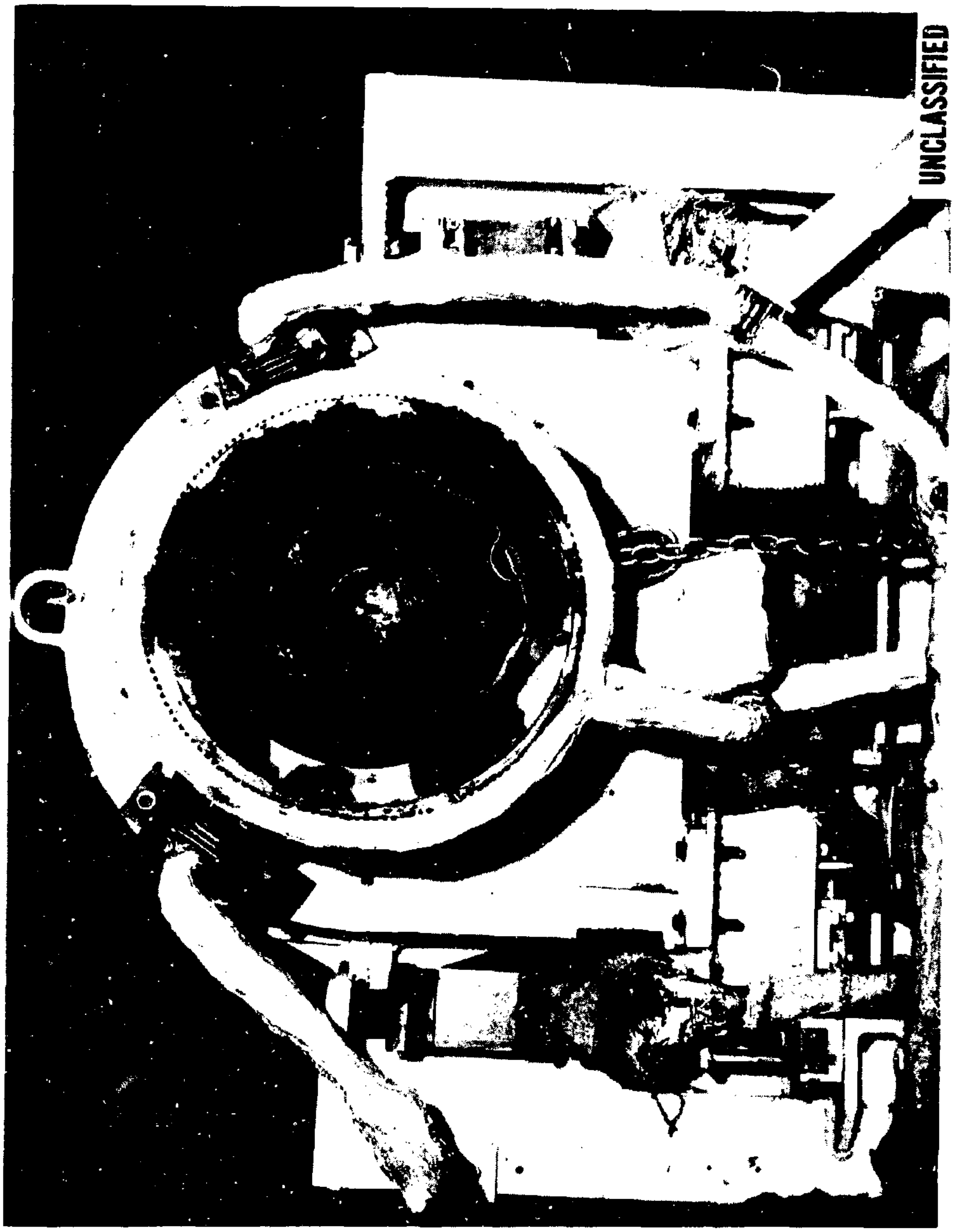

CSRM-LW-1 Postfire (Nozzle)

Figure III-172

partially oxidized state. This component, a 90-10 tantalum-tungsten retainer, withstood exposure to the flame for approximately 2 min without any insulative protection, accounting for the oxidation of the component. The deposits on the outer throat and the expansion cone are primarily aluminum oxide in a very soft condition similar in appearance and texture to porous slag. This material was easily removable by light finger pressure. The condition of the outer throat liner materials under this deposition was excellent with no noticeable material losses, delaminations, or deterioration. The overall appearance of the nozzle components indicates that the flame temperature of the exhaust gas was considerably depressed from the greater than 5200°F temperature expected from this propellant firing at nominal pressures.

(U) Disassembly of the nozzle indicated that the above conclusions were accurate because the amount of heat absorbed was actually less than would be expected in a short-duration high-thrust test-firing. This was the first test using silica phenolic elastomeric in place of the carbon phenolic elastomeric as a housing insulation material. The material was slightly charred; however, no cracking of the surface was evident as had been present on all previous tests using carbon phenolic elastomeric. The actuator was in excellent condition, with only slight indication of external heating. All of the liner of the pintle was ejected with the exception of the asbestos phenolic insulator sleeve, which eroded approximately 0.5 in. where it was exposed to the flame.

(C) On the basis of the firing of LW-1 using AAP-3249 propellant and a lightweight pintle liner system, it can be concluded that the pintle liner system will not withstand the pressure loading that material physical property data on pyrolytic graphite indicated. A laboratory test of the pyrolytic graphite component design was run using the pintle components that had been ordered for LW-3. This test was an attempt to duplicate the pressure loading condition that a rocket motor firing would place on the components. The total load input to the components was measured and the data was analyzed by the structural analysis group and compared to the analysis run on the initial design. The results indicated that the analysis was correct; however, the allowable physical properties used were incorrect. Data on the allowable shear stress indicated that 4800 psi could be used for analysis; the laboratory test indicated that the more accurate value would be closer to 2400 psi ultimate--low by a factor of 2. A redesign of the pintle to use pyrolytic graphite would require redesign of the lightweight Rene 41 support structure that had been fabricated for the lightweight series. It was therefore decided to continue the silver-infiltrated tungsten insert for the remainder of this program.

(U) Because of the short duration of the high-pressure phase of this test, there was no possibility of calculating any performance figures for this new propellant. An attempt was made to evaluate the low-pressure data; however, because of the condition of the pintle and the motion of the pintle during this portion of the test, it was decided to void all of the test data and rerun the test on the next motor.

3. Lightweight Motor Design Modification (LW-2 and LW-3)

(C) The motor configuration for LW-2 was similar to that fired for LW-1 in all respects except for the pintle design. The pintle for this motor used a one-piece lightweight Rene 41 support with the liner system identical to that successfully test-fired in the heavyweight motor development phase. Approximately 570 lb of AAP-3249 propellant was cast in the finocyl grain configuration and 1.5 lb of igniter propellant was contained in the single igniter canister.

4. LW-2 Test Firing CSR-DA-01S-BH-006

(U) The primary objective of the test of motor LW-2 was to determine the system operating capability at sea level using a new propellant and a new lightweight pintle support design. The input program for this firing was identical to that input to LW-1, because the firing of LW-2 had the same objectives as LW-1. This basic program input to this motor consisted of ignition and the first few seconds at constant mid-thrust, a slow full withdrawal of the pintle, a reinsertion of the pintle to maximum thrust as a step input, then a P-dot extinguishment. If the extinguishment is successful, the pintle will remain out of the throat for 3 sec before being returned to ignition set point where it would remain until chamber pressure either increases to 150 psia for 300 millisec, forcing a control system switch to force mode, or until the pintle cools if extinguishment is permanent. If the pressure rises after the reinsertion of the pintle, the remainder of the program was set up to vary thrust upward to maximum in a series of step inputs, then attempt a second P-dot extinguishment at the 44-sec point. This alternate program is then repeated for one more cycle in the event the second P-dot command does not result in permanent extinguishment.

(U) This program was designed to give some indication of the low-pressure operating characteristics of the lightweight CSR motor as well as to determine the sea-level extinguishability of AAP-3249 propellant in this motor at two different free volumes. During the test setup it was determined that the control system would have some difficulty in maintaining a constant thrust level near the maximum thrust condition, since stability of

the system is, in part, controlled by the rate of motion of the pintle with the corresponding pressure changes. As was discussed previously, the pintle sensitivity near the 100% point (fully in the throat) is such that an 8% movement of the pintle would result in an 80% change in chamber pressure, making control of the system very sensitive and inducing some oscillations in pintle motion, chamber pressure, and thrust.

(U) This motor, as with LW-1, was set up to reuse a fired igniter udder, necessitating that the first ignition be fired from one of the side ports rather than "down-the-bore", as originally designed. The hydraulic control panel used in this test is similar to that used on the heavyweight motors, complete with C-clamps as an added safety feature. A nozzle closeup with the pintle withdrawn is shown on Figure III-173.

(C) Lightweight motor LW-2 was statically test-fired at 2105 hr on 12 August 1966 from Bay W-4 at the Aerojet Sacramento Test Facility. Ignition was normal and smooth, with force mode switchover occurring at the 0.300-sec point, as expected. The motor followed the input program to the 9-sec point where P-dot extinguishment was commanded. Propellant extinguishment occurred at 10 sec, and was maintained until the 12-sec point when the pintle was reinserted to the start position. Chamber pressure responded within the first half second, and the motor went into a variable thrust program. The firing progressed normally until approximately 44 sec, at which point the pintle liner insert was ejected, the pintle slammed open, and the propellant burned out at a very low pressure. The forces on the pintle due to partial blockage of the throat area during ejection of the silver-infiltrated tungsten insert caused the pintle to open fully in less than 8 millisec. The shock loading on the actuator caused an extremely high hydraulic pressure buildup in the actuator, splitting the actuator housing and buckling the actuator rod. Because this occurred within the last inch of web, propellant burnout occurred shortly after (within 15 sec) the pintle insert was ejected. Considerable data were gathered on the motor performance, allowing a realistic evaluation of the lightweight motor system.

(C) During the firing of LW-2 an anomaly was noted in the data acquisition of chamber pressure late in the test firing. Two Tabor transducers, 0 to 1000 psi, were used to measure the chamber pressure and to feed-back to the control computer for force parameter calculations and motor control. The major disagreement between these two transducers during the test, and the fact that the igniter pressure transducer, a 0 to 3000 psig Tabor, agreed with first one of the transducers, then with the other, indicate that some transducer tube clogging occurred during the firing. Chamber pressure is therefore plotted as a function of time using the igniter pressure transducer data rather than the chamber pressure transducer data. This plot is presented in Figure III-174. Of significance in this plot are that

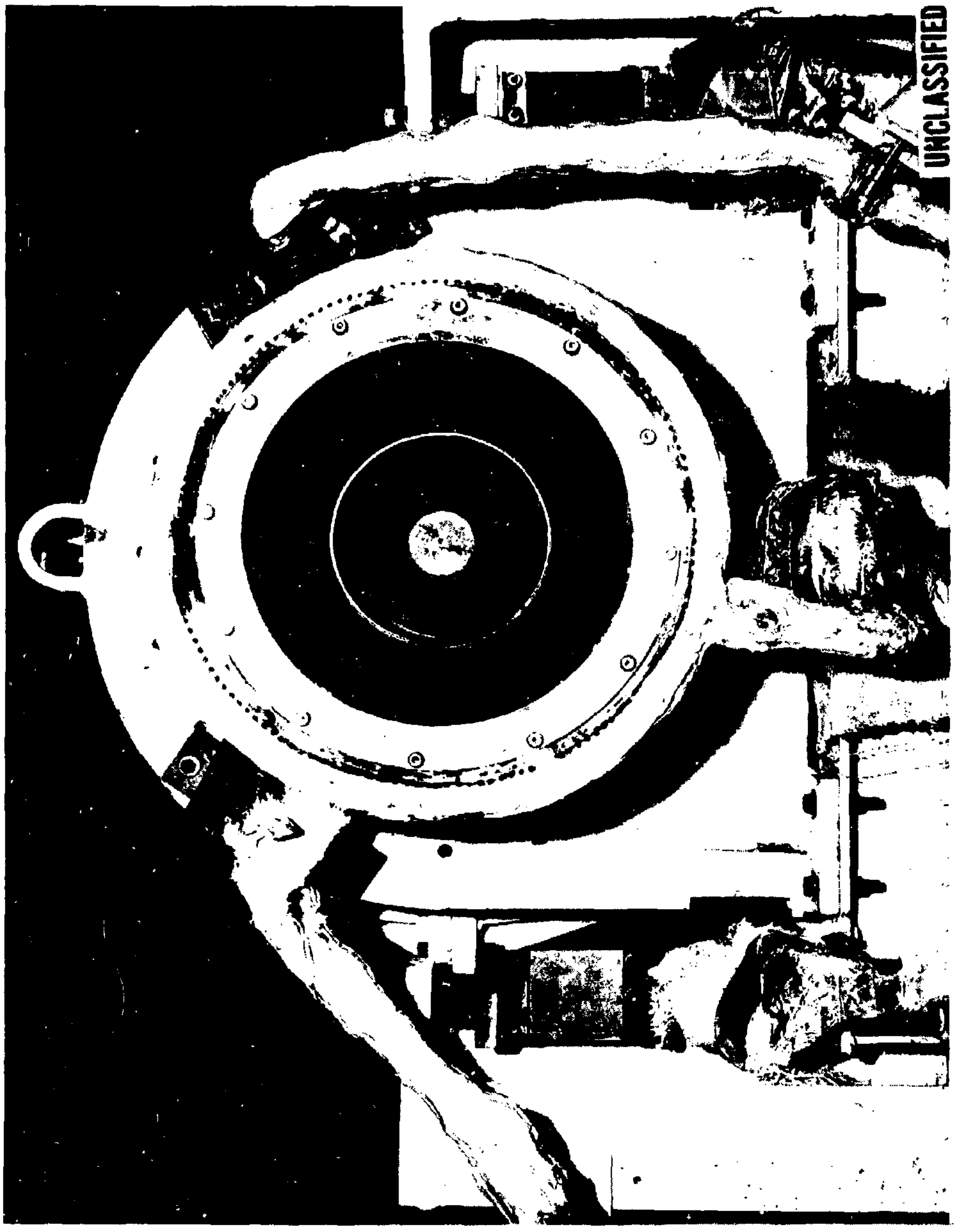

CSRM-LW-2 Prefire Nozzle

Figure III-173

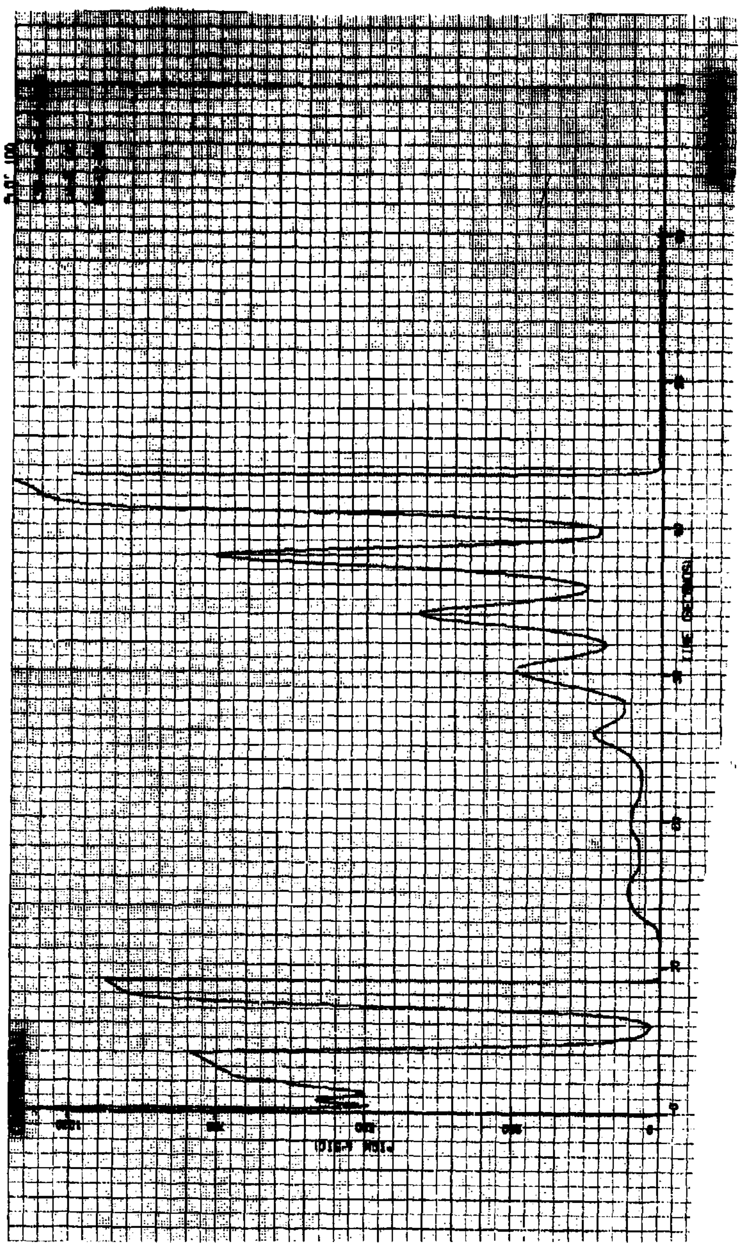

Pressure-Time Trace CSRM-LW-2 (u)

Figure III-174

(1) the chamber pressure was zero-gage from approximately 9.4 sec until approximately 12 sec, indicating that the propellant grain had been temporarily extinguished, (2) the chamber pressure was oscillatory from the 25-sec point until pintle liner ejection, with the amplitude of the oscillations increasing with chamber pressure as expected from the analog computer runs of this system, and (3) the maximum chamber pressure that the system experienced was over 1100 psi just prior to pintle withdrawal, indicating that the silver-infiltrated tungsten insert was partially blocking the throat just prior to its ejection.

(C) The input program to this motor as well as the force feedback are plotted on Figure III-175. As can be seen from this plot, the motor attempted to follow the input program; however, due to the depressed response inputs in the computer system, there was a definite response lag in the motor. Analysis of this plot, compared with the plots of error signal, chamber pressure feedback, nozzle throat area, and pintle position indicated that in addition to the critical stability problem caused by the sensitivity of pintle position to chamber pressure, a sticking servovalve compounded the controls problem. Because this was the fourth servovalve used on this motor, the others having to be replaced as the result of sticking during functional testing, it is highly probable that contamination was the major problem rather than sensitivity of the pintle position-chamber pressure consideration. This problem will be difficult to solve without the use of a self-contained hydraulic supply and control system because the portable hydraulic pressure cart requires long lines, frequent movement, and frequent addition of hydraulic fluid, all being factors conducive to insufficient cleanliness control.

(U) The problem of the sticking of servovalves is further pointed out by comparing the pintle motion plot with the differential hydraulic pressure time plot. Although an error signal exists, the pintle was stationary and the hydraulic pressure loading on the actuator was balanced rather than trying to overcome any aerodynamic or frictional loads. This condition limited the control of the pressure feedback control system on the CSR motor; however, it did not have any contributing effect on the subsequent failure of the silver-tungsten insert. The failure of this insert was attributed to poor-quality material.

(U) Another of the objectives of this test was to determine the effectiveness of the various insulation materials being considered for the igniter rupture discs. Two materials were being evaluated on this firing: a modified silicon rubber and the standard igniter insulation, SD-850. The temperature-time history of the igniter thermocouples indicated there was no noticeable difference in their insulative capability. From the control room television monitor it was difficult to determine that the motor had not failed, but had merely ejected a part of the pintle. Therefore, test procedure required that the bay deluge be initiated, completely inundating the motor.

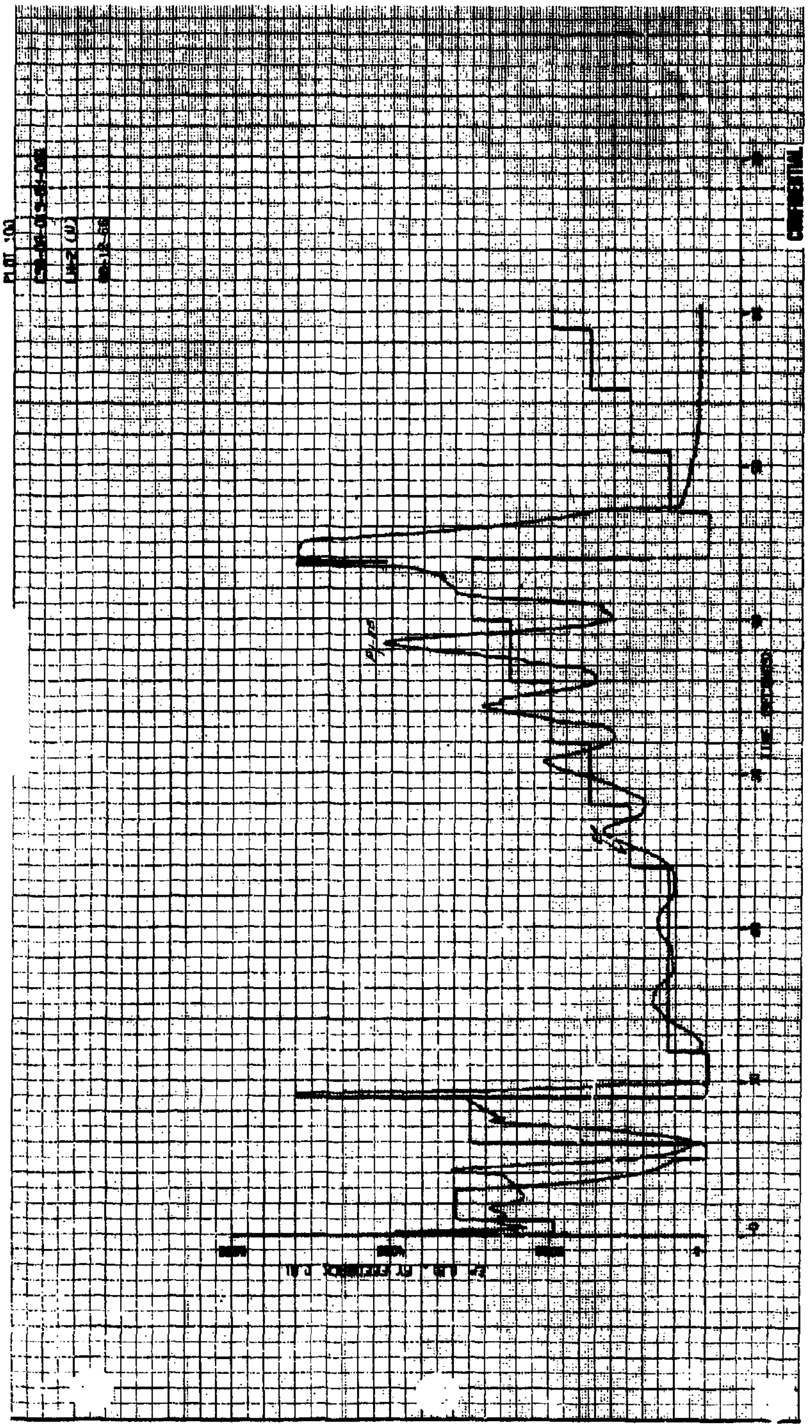

Force Mode Control Trace CSRM-LW-2 (u)

Figure III-175

III, E, Lightweight Motor Development (cont.)

(C) The performance figures are as follows:

Thrust	
Prior to extinguishment	5,250 lb maximum 324 lb minimum 10,500 lb spike
Subsequent to inadvertent ignition	5,275 lb maximum 700 lb minimum 14,500 lb spike
Chamber Pressure	1,050 psia maximum 30 psia minimum 1,220 psia at failure of pintle liner
Total Impulse:	
Prior to failure of pintle	91,000 lb-sec
Duration to Failure	43.5 sec

(C) It is interesting to note from the results of this firing that if the nozzle throat area is opened slowly, low-pressure stable combustion can be attained and controlled. This is witnessed by the stable 30 psia and 324 lb of minimum thrust obtained during this firing. The total variation in thrust achieved during this test was over 16:1 under controlled conditions. This value does not include any of the thrust spikes, nor does it consider the time during which the motor was extinguished. The 16:1 thrust variation was attained prior to the first command to extinguish. After the abortive extinction, a 7.5:1 thrust variation was achieved prior to failure of the silver-tungsten insert. Whereas the first variation of thrust from a low of 324 lb to a high of 5250 lb occurred over a pressure range from 30 psia to 953 psia, the second variation of thrust from a low of 700 lb to a high of 5257 lb occurred over the pressure range from 50 psia to 1050 psia. These data indicate that this motor can be operated from a low pressure of 30 psia to a high pressure of 1000 psia.

(C) Because of the combined effect of oversensitive linear pintle motion with chamber pressure and sticking servovalves, it was decided future motors would not be operated at the high end of the pressure scale, but will be held to pressures less than 600 psia. At a pressure of 600 psia, a sea-level firing will have a high thrust of approximately 4200 lb, giving a thrust variation of approximately 13:1. The altitude thrust variation of

this motor when fired at a back-pressure of approximately 0.25 psia will be approximately 5:1, operating at about 30 psia minimum--1000 lb thrust minimum to 540 psia maximum--5000 lb thrust maximum.

(C) On the basis of this firing, a burning rate was determined for AAP-3249 propellant over a range of pressures in the full-scale CSR motor. This burning rate was slightly higher at the low pressure end of the scale than was that determined by small motor tests. This is as expected, since this difficulty had first been experienced during the heavyweight motor development program, and was taken into account in the predictions for this firing. The results of LW-2 indicated that the burning rate exponent for AAP-3249 in the full-scale CSR motor is 0.528 and the burning rate at 100 psia is 0.095 in./sec. Although the burning rate exponent and the burning rate at 100 psia are slightly lower than the optimum design point for the hardware, both are acceptable for the remainder of the lightweight motor development phase.

(U) In general, the appearance of the hardware from motor LW-2 after the firing was good. Photographs taken of the motor while still in the test stand are presented as Figures III-176 and III-177. The absence of the characteristic dark band around the cylindrical section of the chamber can be accounted for by the use of the bay deluge system at the end of this test. A darkening is expected when a normal heat soak after web burnout occurs, especially pronounced during very low pressure firings as the heat-affected zone of the propellant is much thicker, allowing more heat to transfer through the thin chamber wall insulation at the cylindrical section of the chamber.

(U) A close-up view of the inside of the nozzle is shown on Figure III-177. It can be seen from this figure that the pintle throat insert is completely missing. Both the pyrolytic graphite and the silver-infiltrated tungsten are missing; however, the pintle support system is intact and, as was later found, is reusable. There are some light deposits of porous aluminum oxide on the top and bottom of the outer throat. These are due to the 10 to 15-sec tailoff of the firing after the pintle insert had been ejected.

(U) Of the disassembly photographs, those presented on Figure III-178 are the most significant in pointing out the effect of the loss of the pintle throat inserts. This figure depicts the actuator and manifold assembly in various stages of disassembly. The split of the actuator housing can be clearly seen with the snubber and potentiometer removed. The effect of the force input is attested to by the buckled actuator rod-piston assembly. As can be seen from those photographs, the only component that was adversely affected due to the ejection of the pintle liner was the actuator assembly. This item is expendable in the fail-safe type of design employed

CSRM-LW-2 Postfire

Figure III-176

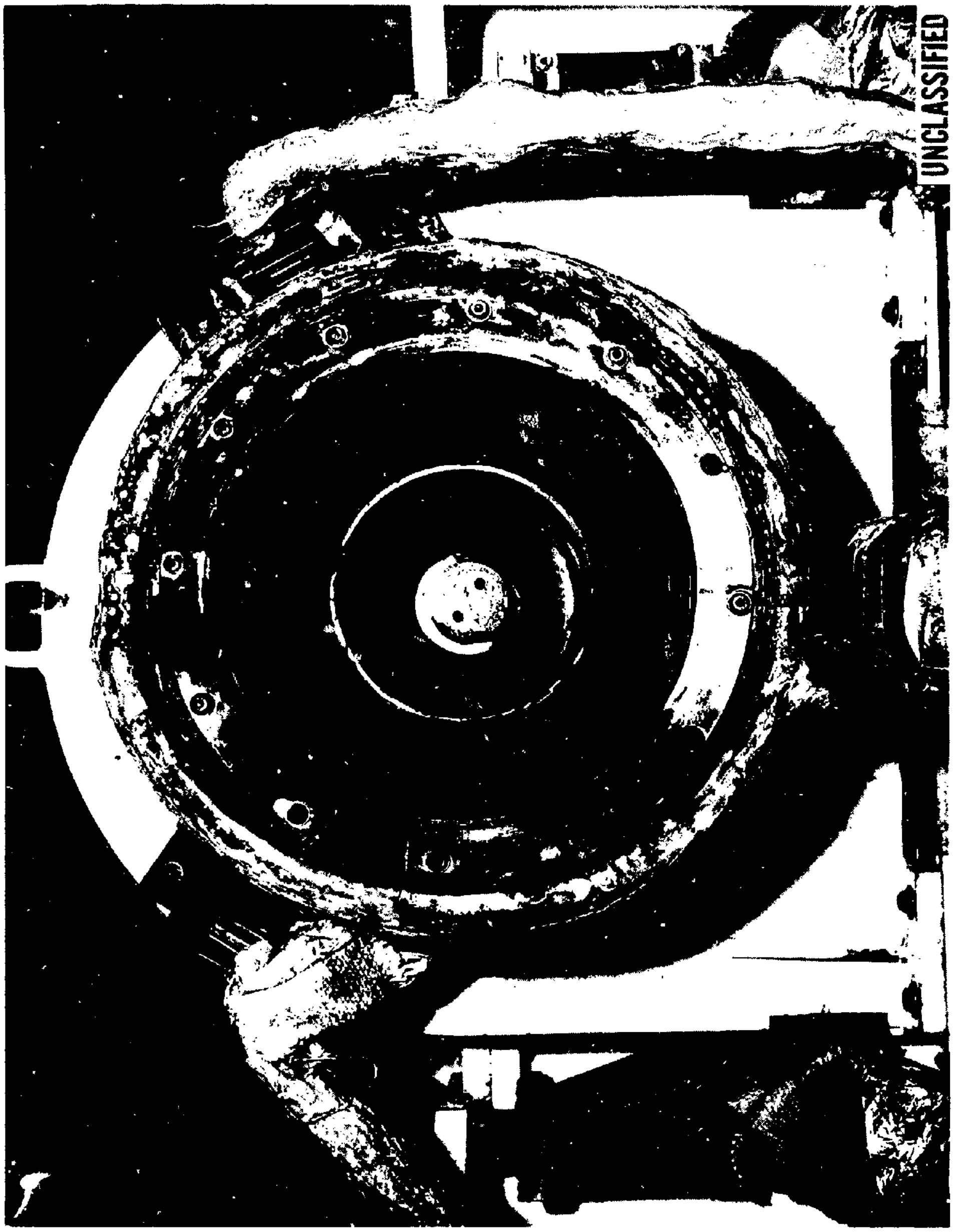

CSRM-LW-2 Postfire (Nozzle)

Figure III-177

a. Actuator Components, LW-2, Postfire

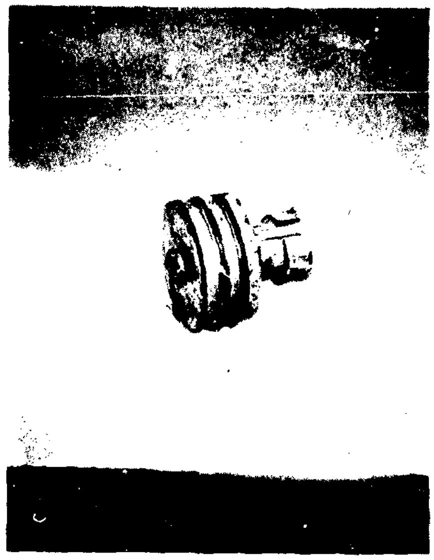

b. Actuator Housing, LW-2, Postfire

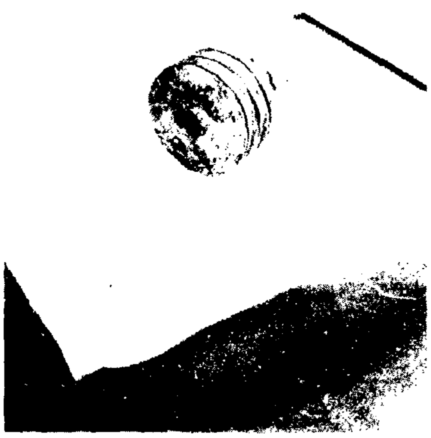

c. Actuator Housing, LW-2, Postfire

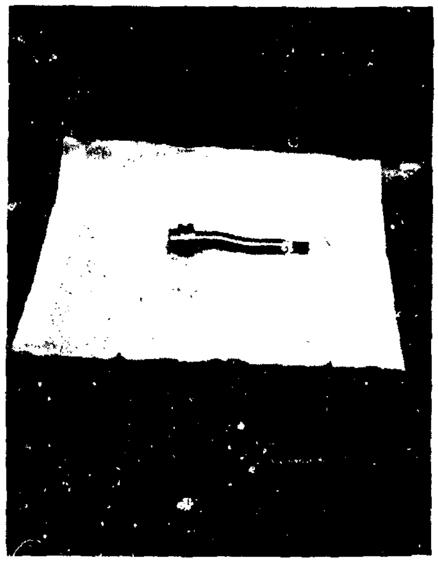

d. Piston & Rod Assembly, LW-2, Postfire

UNCLASSIFIED

CSRM-LW-2 Postfire (Actuator and Manifold Assembly)

Figure III-178

in the CSR, in that excessive chamber pressure will cause the pintle to open whether the maximum pressure dump switch operates as designed or fails to operate as it did on the firing of LW-2.

(U) The reason for the loss of the silver-tungsten insert in CSR motor LW-2 was established to be a material problem by analysis of the pieces of tungsten that were found after the test. Photomicrographic analysis of the structure of this component indicated that the quality of this part was far inferior to that which had been fired on the heavyweight series of CSR motors and had operated successfully.

(U) Since this problem was one of material property rather than one of a specific design, discussions with the raw material supplier as to corrective action were immediately initiated.

(U) On the basis of the firing of LW-2 it was concluded that propellant AAP-3249 will meet the need of the lightweight series of controllable solid rocket motors. This propellant performed as expected, with the exception of attaining permanent sea-level extinguishment. During the next test-firing, LW-3, more stable control of the motor was expected because new servovalves were purchased. The hydraulic system used for the ground testing of the CSR motors in this program is still a weak point in the system as pointed out by the contamination experienced in this test. Self-contained flight-type hydraulic control packages are suggested for elimination of this problem.

(C) Although the pintle insert failed very near to the end of this firing, this test is considered to have been successful in achieving its objectives. It was shown that AAP-3249 propellant is compatible with the CSR motor design; that thrust modulation far in excess of required rates can be achieved; that temporary extinguishment at sea level can be achieved so that permanent extinguishment at altitude is expected; and that the lightweight pintle support system is able to withstand design loads toward the end of the test when it has reached near its maximum temperature. On the basis of the above points, it was concluded that the CSR lightweight design should operate successfully for the remainder of the test series without requiring major redesign.

5. <u>LW-3 Test Firing CSR-DA-01S-BH-007</u>

(U) Motor LW-3 was assembled exactly the same as LW-2 and was to be a verification test prior to sending LW-4 to AEDC, Tullahoma, Tennessee for initial altitude testing. One change in the test setup of LW-3 was the incorporation of Raymond-Atchley 5 GPM Servovalve in the hydraulic control

circuit to improve the control of the motor by minimizing the possibility of valve stickage due to contamination.

(C) Motor LW-3 was statically test fired at sea level 1 November 1966. Objectives of this firing were controlled thrust modulation, prediction of ballistic performance, evaluation of a new control console network with variable gain capability, and final system checkout. The motor ignited normally with igniter burnout occurring at the 0.270 second point. Chamber pressure returned to the expected value after igniter burnout and stabilized within 0.100 seconds. At approximately 1.63 seconds, the silver infiltrated tungsten pintle insert began to break up and eject, with full liner ejection occurring at 1.70 seconds. Chamber pressure dropped to a very low value for the remaining 3 minute duration of the web burning.

(C) With the exception of the pintle support rod which sustained considerable oxidation damage, the remainder of the motor was in good condition, the other components being scheduled for reinsulation and reuse. Analysis of the silver infiltrated tungsten component parts found after the test indicated that thermal cracking had occurred and propagated rapidly to the surface of the insert, causing ejection of the insert and subsequent flame damage to the support structure. The thermal cracking condition was apparently caused by lack of silver infiltrant in several areas of the insert. To verify that pressure loading alone would not cause failure of the tungsten supported by the lightweight Rene' 41 support rod, direct load tests were conducted on a tensile test machine.

(C) On the basis of the results of LW-2 and LW-3 it was determined that the use of silver infiltrated tungsten as pintle throat insert material is an extremely unreliable practice as the quality of the silver infiltrated tungsten has been difficult to maintain constant. The components that failed on LW-2 and LW-3 would have been completely acceptable for use on conventional nozzles and most likely would not have cracked had they been used on outer throats. The unique conditions present in the pintle structure require that the material used for the throat insert be a highly reliable load carrying member, a condition which unfortunately silver infiltrated tungsten does not meet. It was therefore decided that a major pintle redesign be initiated to eliminate silver infiltrated tungsten from the pintle.

6. Lightweight Motor Design Modification (LW-4)

(C) An immediate redesign of the pintle for the remainder of the lightweight motors was initiated. This redesign was directed toward the removal of the silver infiltrated tungsten from the pintle, making use of pyrolytic graphite washers; however, supporting these washers so that the

combined stresses were well below that allowed from actual destructive tests of washers. Using an allowable interlaminar shear strength of 2300 psi from the results of these tests, a pintle design was formulated and analyzed. This final design is shown on Figure III-179.

7. LW-4 Test Firing CSR-DA-01S-BH-008

(C) Motor LW-4, with the new pintle design incorporated, was test fired at sea level on 27 December 1966. Objectives of this test firing were controlled thrust modulation, nozzle pintle design qualification for the pending AEDC tests, and an attempted sea level extinguishment, augmented by a nitrogen purge through the motor after P-dot initiation. In addition, the variable gain network in the control system was to be checked out since the test of LW-3 did not last sufficiently long to permit evaluation of this circuit.

(C) The motor was ignited as planned with peak pressure being held to approximately 560 psia. After ignition transient, the first input step to the motor was taken from the manual throttle on the pressure feedback control console. The motor's pressure and thrust responded to this input with a slight oscillation of low frequency and low amplitude for the first 10 seconds of the test. At the 10 second point, until P-dot at the 48 second point, the motor followed the input commands exactly -- no oscillations in either pressure or thrust indicating that the response variability circuit was functioning exactly as planned.

(C) At the 48 second point, P-dot was initiated. The chamber pressure dropped to atmospheric for 0.30 seconds at which time the nitrogen purge was initiated raising the internal motor pressure to about 30 psia. At the 50 second point the pintle was repositioned into the throat and the motor was returned to force mode control. Permanent extinction did not occur on this motor. From visual observations it appeared that the motor did not extinguish even temporarily either before or after the nitrogen purge. At 50 seconds, the motor had fully reignited. The control system was able to control the combination of hot gas and nitrogen until web burnout at 62 seconds.

(C) After this test, all motor components were in excellent condition. The operating pressure was somewhat lower than anticipated indicating that the burning rate of this propellant was slightly higher than that predicted from the analysis of the LW-2 test firing. Figure III-180 shows the pressure and thrust traces of this test. Since the combination of LW-2 and LW-4 gave a number of stable pressure points, the burning rate of the propellant was calculated from a combination of both of these tests. This burning rate was then used for the predictions of pressure and thrust for the AEDC test motors.

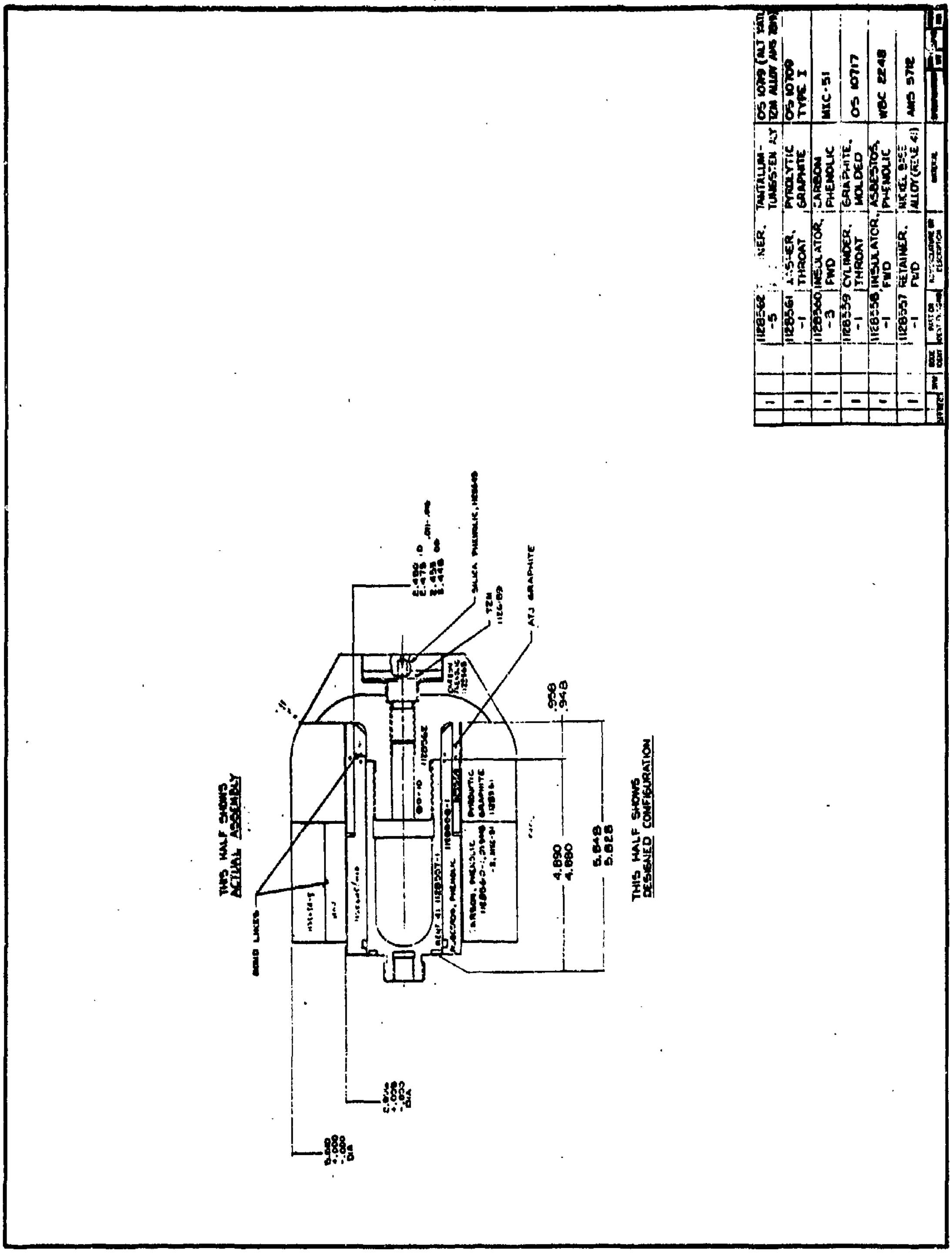

Pintle Design, Motor LW-4

Figure III-179

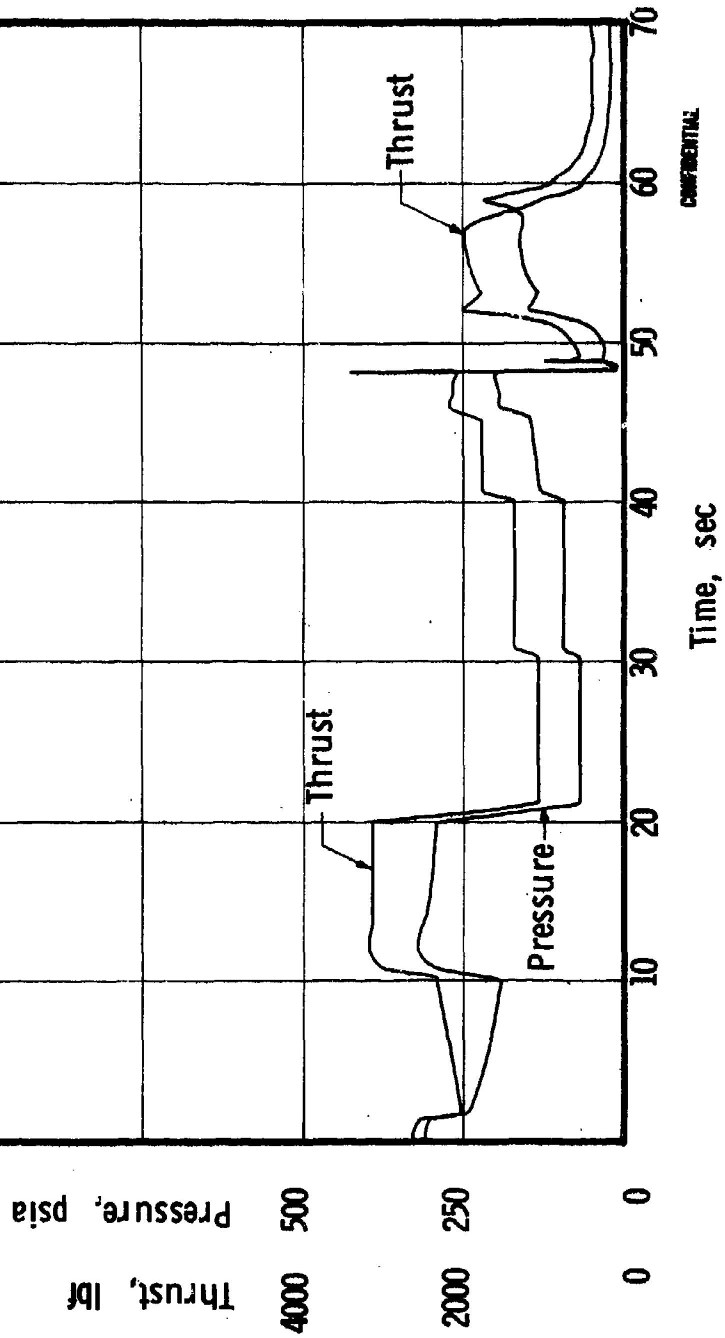

Pressure-Time, Thrust-Time, Motor LW-4 (u)

Figure III-180

8. Conclusions

(C) In summary, four motors were test fired in the Lightweight Motor Development phase of this program. Motor LW-1 failed shortly after ignition due to pyrolytic graphite washer ejection from the pintle. This ejection was attributed to the use of the wrong design limits for this material. Motors LW-2 and LW-3 made use of the heavyweight nozzle pintle insert design (silver infiltrated tungsten) however used a light-weight support rod of Rene' 41 in place of the 90-tantalum, 10-tungsten used in the heavyweight motor series. LW-2 ejected the pintle insert after only 1.70 seconds. Both malfunctions were attributed to thermal cracking initiating from lack of uniform infiltration material. Motor LW-4 made use of an all-pyrolytic graphite washer pintle insert design. This design performed as planned for the full duration indicating that the problem of pintle throat insert had apparently been solved.

(C) In the two attempts to attain sea level extinguishment during the Lightweight Motor Development series, permanent extinction was not achieved, either with or without the nitrogen purge. Both motors LW-2 and LW-4 achieved controlled variable thrust, with LW-4 indicating excellent control of the thrust level without the hunting and undershoot previously experienced.

(U) On the basis of the results of LW-4 it was determined that the remaining four motors would be tested at AEDC to demonstrate both thrust variation and stop-restart operating at altitude. All four of these motors were scheduled to use the LW-4 design in the pintle area.

F. AEDC DEMONSTRATION TEST SERIES

(C) The purpose of the AEDC demonstration test series was to demonstrate the feasibility of a single-chamber controllable solid rocket motor by firing each motor up to six times and demonstrating a thrust range from 6000 pounds to 2000 pounds at a simulated altitude of over 60,600 feet (1 psia backpressure). The motors were to be extinguished by both P-dot and L* and the duty cycle was to be variable. Thrust control was to be demonstrated by a pressure feedback control system and was to be held constant at any desired input thrust level within the variable thrust range. The control system was to compensate for changes in propellant burning surface.

(U) Four motors were involved in the AEDC demonstration test series: LW-5, LW-9, LW-10, and LW-11. Motors with the designation LW-6, LW-7, and LW-8 do not exist in this program as these numbers were assigned to the original processing of LW-9 through LW-11; however, a propellant cure problem necessitated the reprocessing of these three motors. The first motor to be tested at AEDC was LW-5 in January 1967. The final three motors were scheduled into AEDC in July 1967.

1. Design of Motor LW-5

(U) The Aerojet-General Corporation Single-Chamber Controllable Solid-Propellant Rocket (CSR) motor (Figure III-181) is a full-scale, lightweight development motor having the following nominal design characteristics:

Length, in.	90
Diameter, in.	20
Loaded Weight, lbm	720
Propellant Weight, lbm	570
Area Ratio Range	9.8 to 53.6
Thrust Range, lbf	840 to 8200
Chamber Pressure Range, psia	18 to 870

Motor weight and physical dimension data are presented in Table I.

(U) The cylindrical motor case is constructed of heat-treated alloy steel (Ladish D6AC) approximately 0.075 in. thick at the case wall and 0.050 in. thick at the forward and aft closures. The igniter manifold and the nozzle pintle assembly are attached to the motor case with shear lip bolted joints. Case-bonded asbestos-silica nitrol-rubber (Gen Gard® V-44) 0.060 in. thick insulates the motor case from internal heat. A release boot on the forward end of the motor is 0.060 in. thick and serves as a strain relief for the propellant grain.

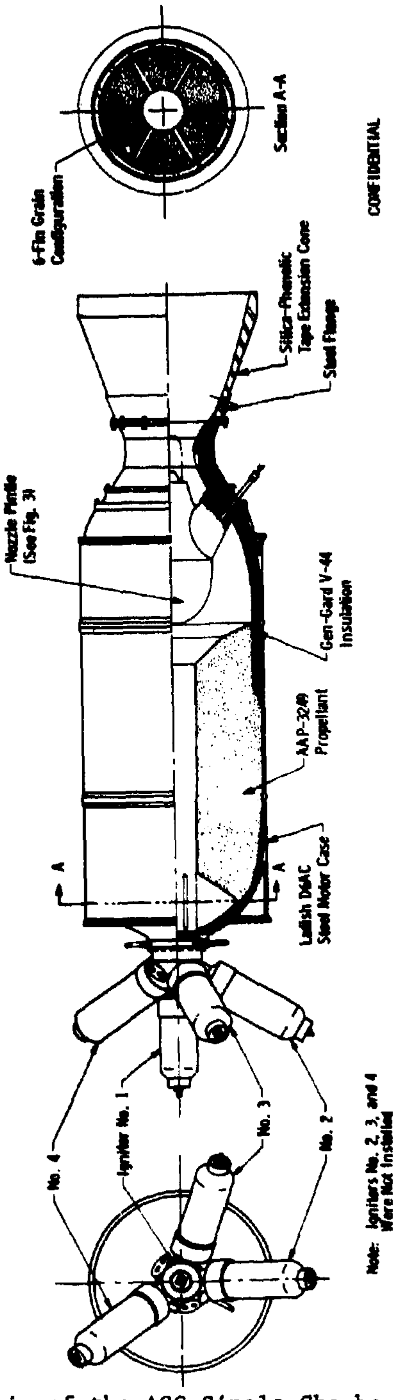

Schematic of the AGC Single-Chamber Controllable Solid-Propellant Rocket Motor

Figure III-181

Table I

Summary of Motor Physical Dimensions (u)

Motor Serial Number	LW-5
Manufacturer's Stated Propellant Weight, lb_m	564.0
Motor Assembly Weight, lb_m	
Prefire	715.99
Postfire	140.11
Expended Mass (AEDC), lb_m	575.88
Nozzle Exit Area, $in.^2$	
Prefire	268.80
Postfire[1]	267.57
Percent Change from Prefire	-0.46
Average	268.19

[1]Exhaust product deposition not removed prior to measurement.

III, F, AEDC Demonstration Test Series (cont.)

(C) The CSR motor contains AAP-3249 solid propellants (ICC Class B) which is composed of ammonium perchlorate (51%), nitroguanidine (15%), aluminum (10%), sodium chloride (3%), and nitroplasticized polyurethane binder (21%). The grain design has a neutral burning finocyl configuration (six symmetrical fins in the forward end and cylindrical center and aft ends) which burns both internally and on the aft face. The isentropic exponent of the propellant exhaust gases is 1.20.

(C) The igniter manifold contains bosses for mounting up to six igniter assemblies. The center-mounted igniter assembly contains 1.5 lbm of solid propellant and is used for the initial motor ignition. The five igniter assemblies located angularly around the igniter manifold each contain 3 lbm of solid propellant and are used for subsequent motor restarts. Only the center-mounted igniter was used in the test program reported herein. The igniter assembly contains ANP-2758 Mod I solid propellant, which is cast in a symmetrical eight-fin configuration (Figure III-182). Each igniter uses a Hi-Shear PE451-003 exploding bridgewire (EBW) power cartridge. A Polaris EBW firing unit supplies 1800 amp at 2000 v to the power cartridge. The firing unit capacitors are charged by a 2000-cps, 115-v rms-ac signal from a Polaris exploding bridgewire field charge unit. Both the electrical input to the charge unit and the triggering pulse are 28 vdc.

(C) The CSR motor has a variable-area nozzle assembly which utilizes a hydraulically actuated, centrally located nozzle pintle, strut-mounted from the aft closure (Figure III-183). From its fully retracted position, the pintle translates axially into an outer throat and exit cone assembly. The annular nozzle throat area varies from 5 to 27.25 in.^{2} as the pintle translates from the aft to forward position (3.5 in.). The hydraulic actuator consists of a piston-cylinder assembly equipped with a linear motion potentiometer. The actuator housing is constructed of aluminum alloy. The piston and rod are steel. Structural components of the nozzle are made of heat-treated 4130 steel. The structural components of the pintle are constructed of Rene-41® and TZM alloy (90% tantalum and 10% tungsten). The outer throat and pintle throat washer are fabricated from pyrolytic graphite and supported by an ATJ graphite washer. The pintle forward insulator, insulator cap, aft housing insulator, throat approach, and throat support are made of carbon-phenolic tape wrappings. The strut housing and entrance cap insulation are molded silica-phenolic elastomer.

(U) The contoured nozzle extension cone (Figure III-181) has an exit area of 270 in.^{2} and a half-angle of 13 degrees at the exit plane. The cone is constructed of silica-phenolic tape wrapped parallel to the centerline and bonded to a 4130 steel flange. The overwrap at the attachment flange is epoxy-impregnated glass.

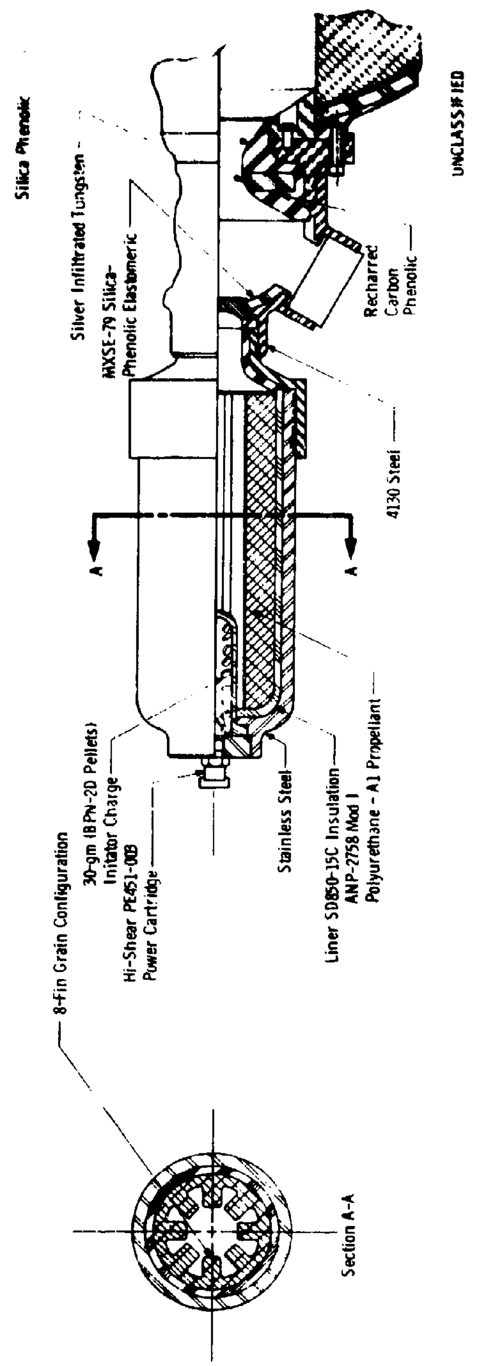

Igniter Assembly - Schematic

Figure III-182A

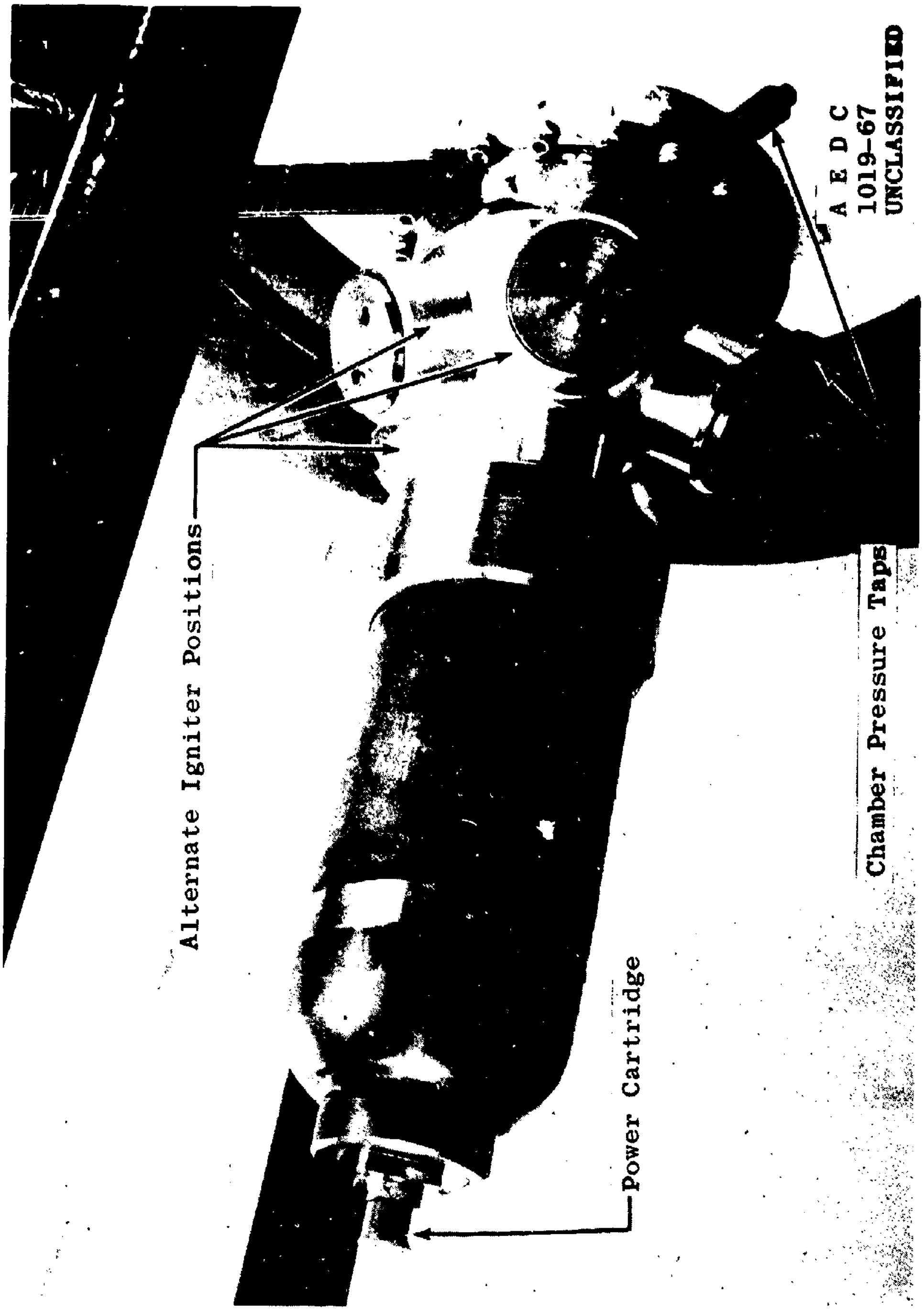

Igniter Assembly - Photograph

Figure III-182B

CONFIDENTIAL

(This Page is Unclassified)

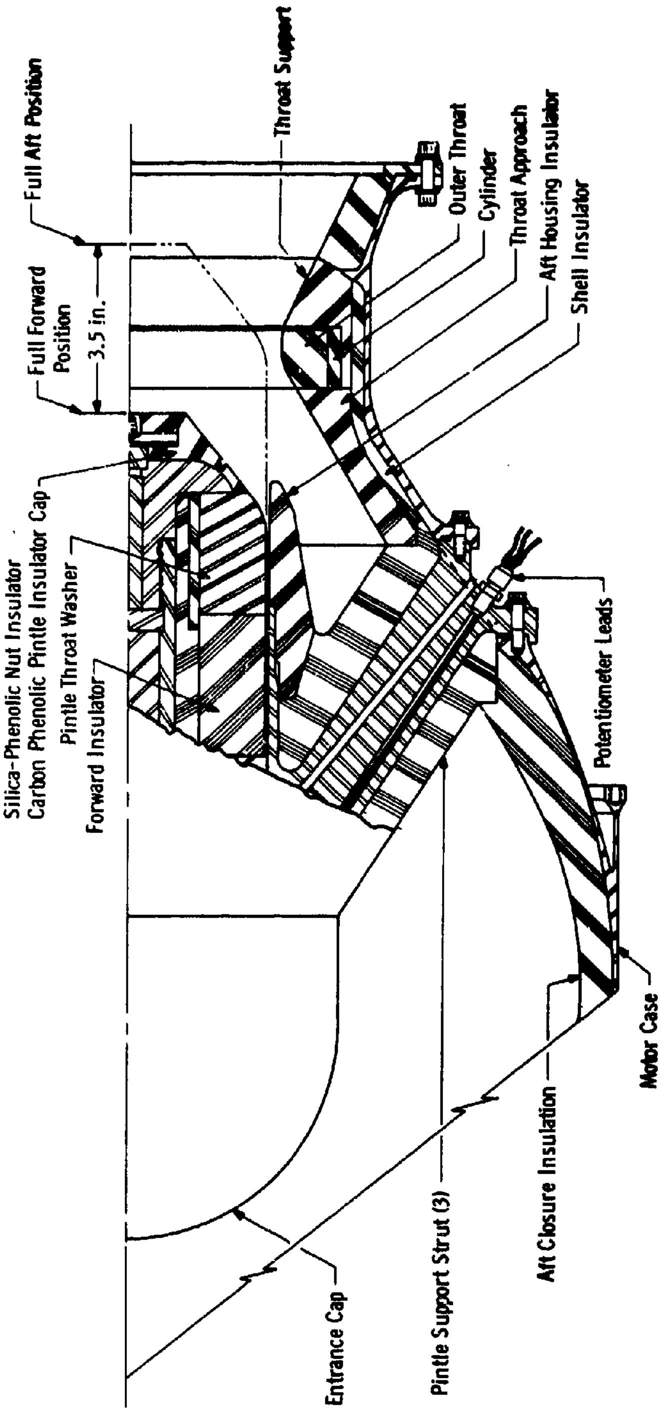

CONFIDENTIAL

Nozzle Pintle Assembly - Schematic

Figure III-183A

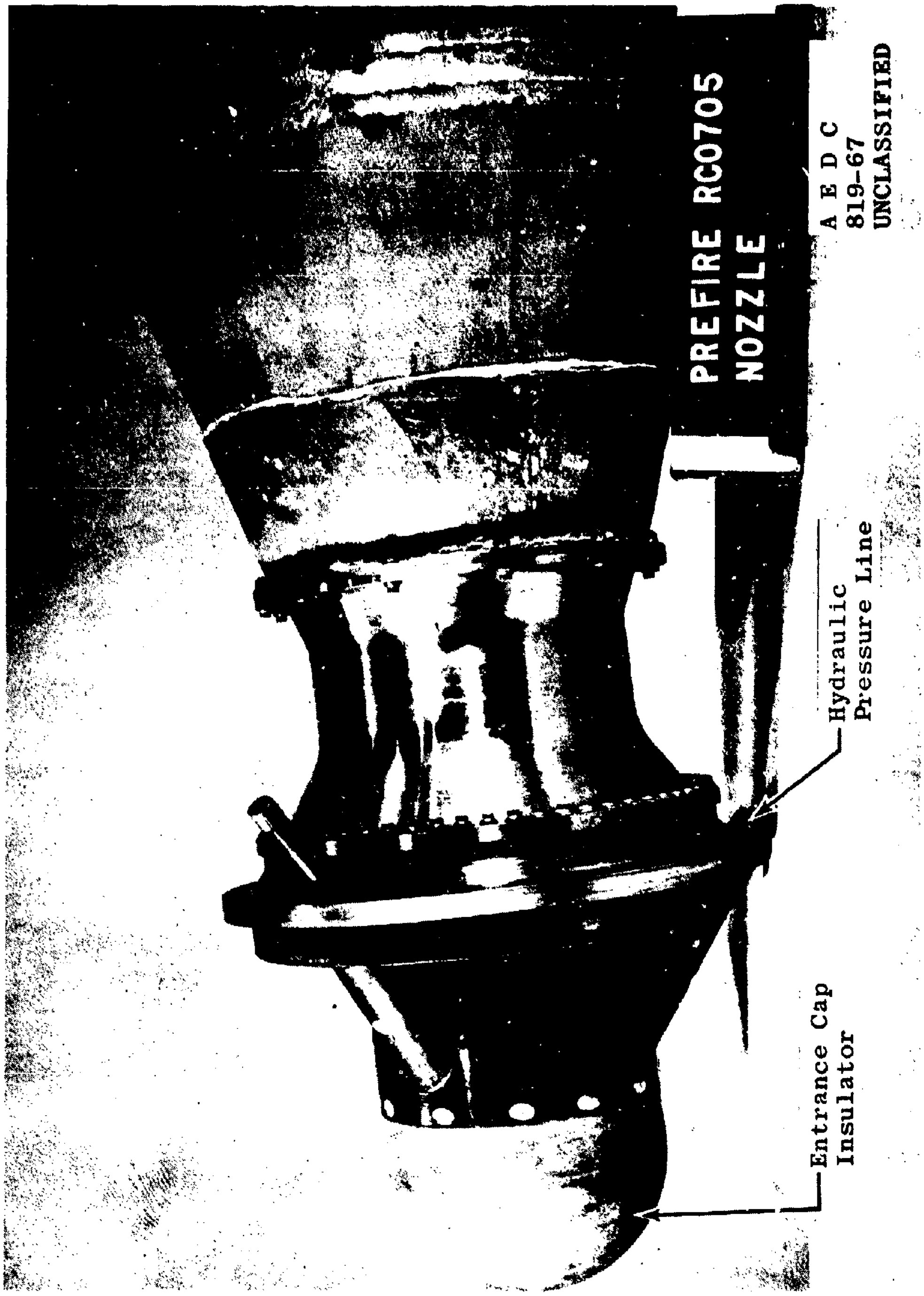

Nozzle Pintle Assembly - Photograph

Figure III-183B

III, F, AEDC Demonstration Test Series (cont.)

(U) The pintle actuator is operated by an electrically controlled hydraulic servosystem (Figure III-184). Pintle positioning is permitted by a hydraulic failsafe manifold. The manifold is a solenoid-actuated, spring-loaded, two-position, four-way valve. The manifold is normally energized during motor operation. When the failsafe manifold is either de-energized or the hydraulic supply pressure drops below 2500 psi, hydraulic pressure is diverted from the servovalve and forces the pintle to the full forward position, terminating motor thrust. When the manifold is energized, pintle control by the servovalve is accomplished with electrical signals from a process control analog computer console. The control console integrates a relay logic system with the closed-loop servosystem to provide monitoring and control of ignition, thrust modulation, and thrust termination. A block diagram of the control operation is presented in Figure III-185. Programmed thrust termination may be accomplished either by a programmed signal from the computer console to the servovalve or by de-energizing the failsafe manifold. Because of long lines between the hydraulic power supply cart and the motor assembly and the requirement for fast response, an oil accumulator (approximately 1-gal capacity) is provided near the servovalve to provide the necessary mass flow rate to the pintle actuator.

2. Test LW-5

(U) The motor assembly was tested in Propulsion Engine Test Cell (T-3).[1] A schematic and a photograph of the motor installation are shown in Figure III-186. The motor was mounted on a thrust cradle which was supported from the cradle support by three vertical and two horizontal double-flexure columns. Axial thrust was transmitted through the thrust pylon to two load cells mounted in a double-flexure column on the motor axial centerline. A remotely operated thrust stand calibrator was used to obtain pre- and post-firing axial thrust system calibrations.

(U) The hydraulic pump assembly used to actuate the pintle servovalve was located outside and adjacent to the test cell. The high-pressure hydraulic lines were connected to the valve, positioned perpendicular to the motor axial centerline (to eliminate thrust measurement interaction effects), and coupled to sealed junctions at the test cell wall.

(U) Pre-ignition pressure altitude conditions were maintained in the test cell by a steam ejector operating in series with the RTF exhaust gas compressors. During a test firing, the motor exhaust gases were used as the driving gas for the 30-in.-dia, ejector-diffuser system to maintain test cell pressure at an acceptable level.

[1] Test Facilities Handbook (6th Edition). "Rocket Test Facility, Vol. 2," Arnold Engineering Development Center, November 1966.

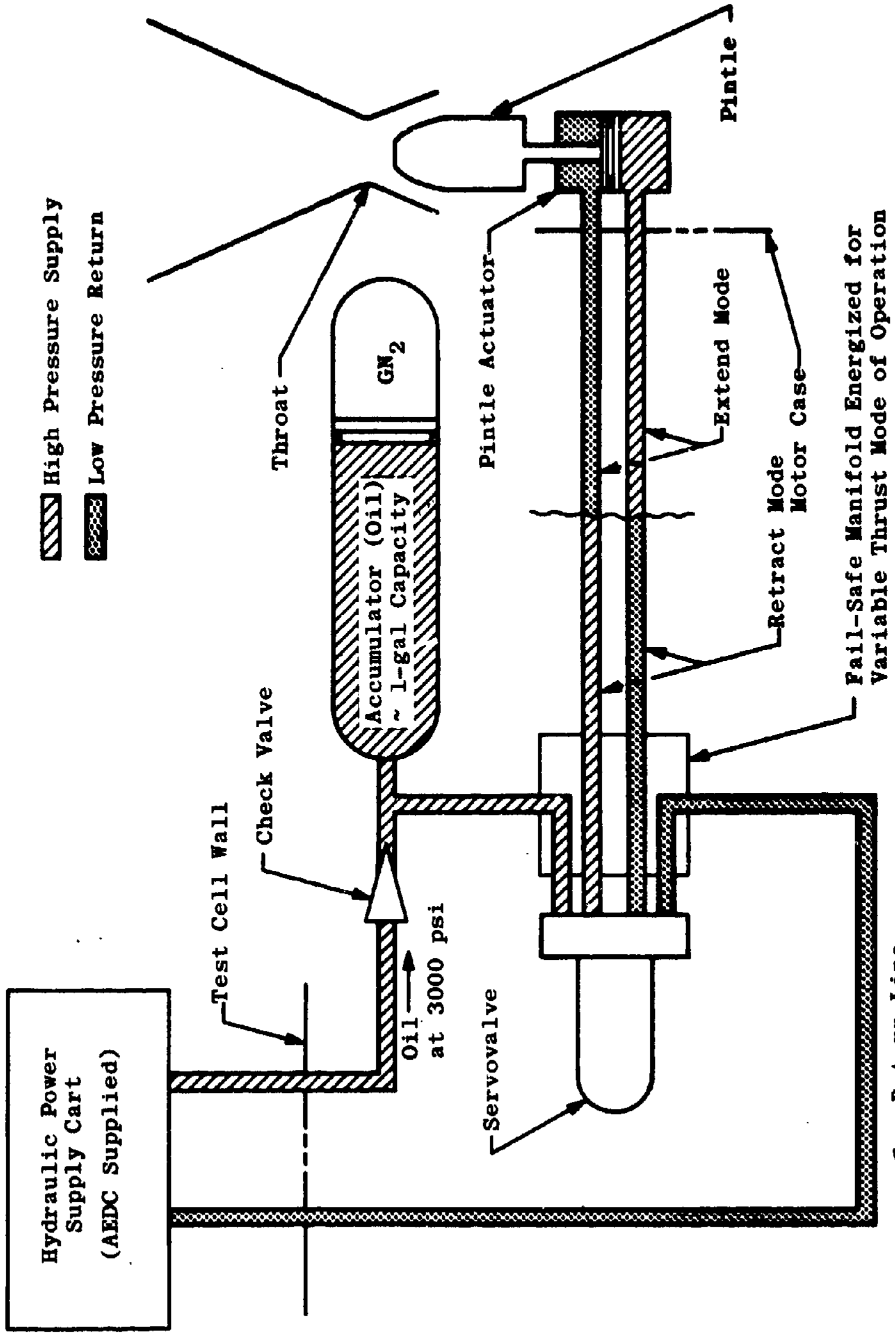

UNCLASSIFIED

Schematic of the Pintle Hydraulic System - Firing Mode

Figure III-184A

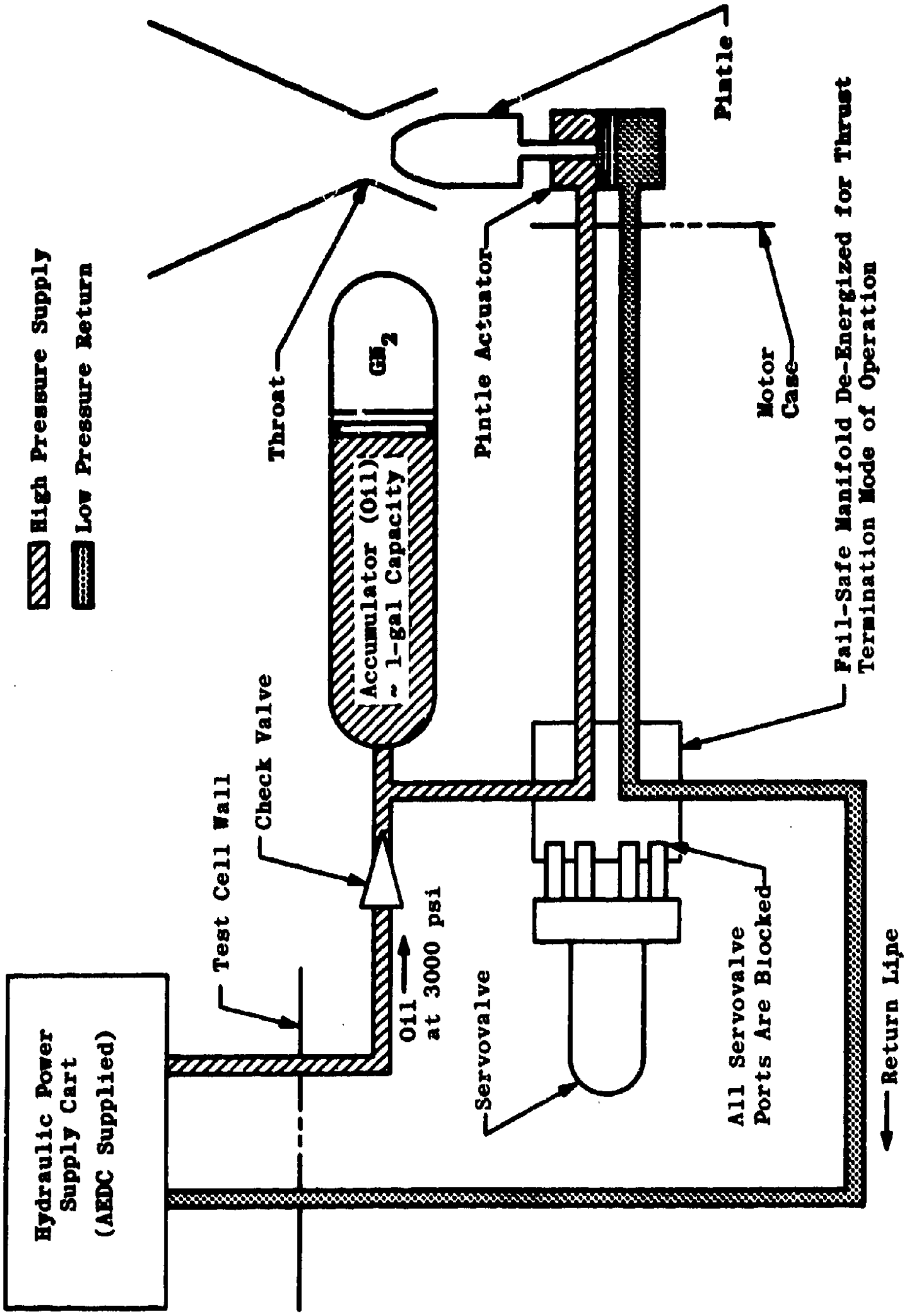

UNCLASSIFIED

Schematic of the Pintle Hydraulic System - Thrust Termination Mode

Figure III-184B

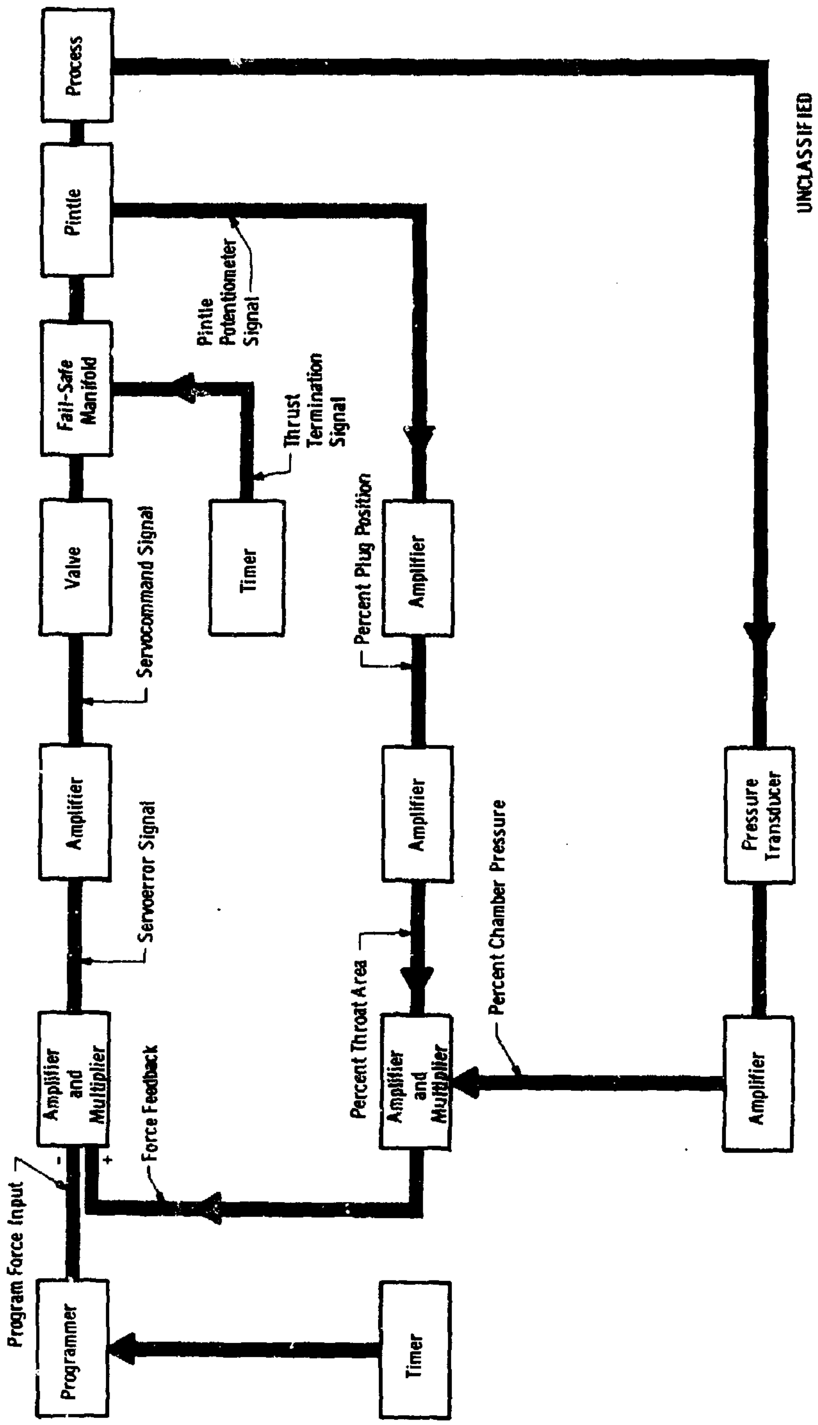

Block Diagram of the Nozzle Pintle Control System

Figure III-185

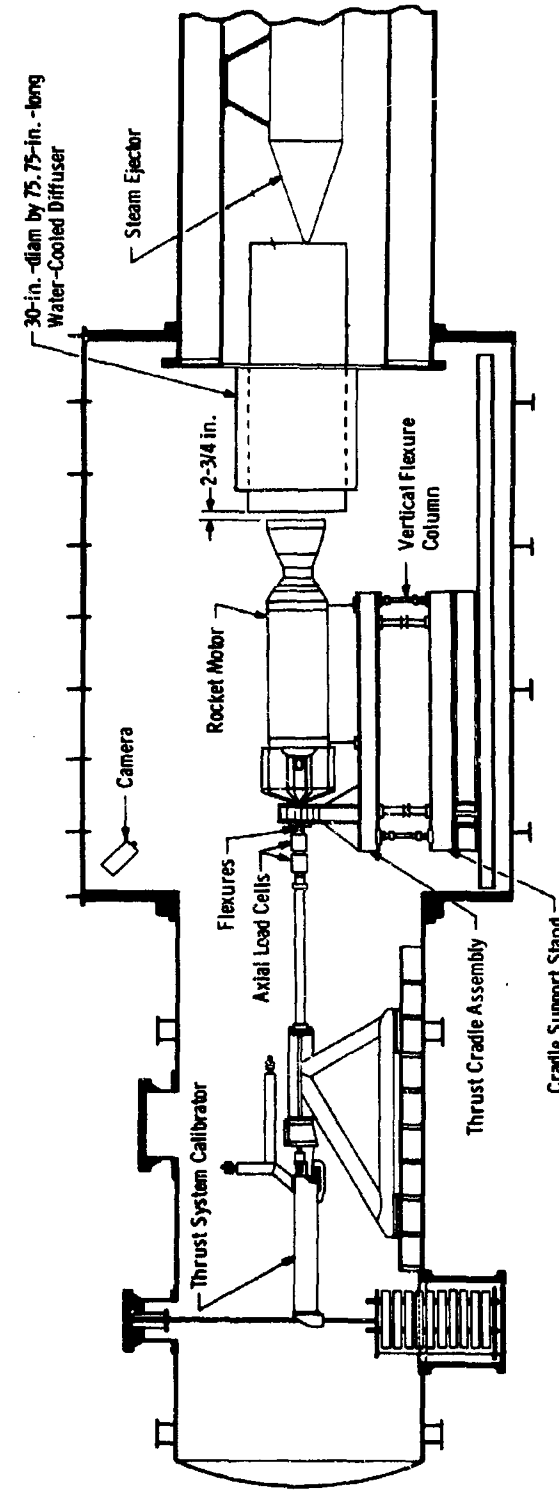

UNCLASSIFIED

Installation of the AGC Single-Chamber Controllable Solid-Propellant Rocket Motor in the T-3 Test Cell - Schematic

Figure III-186A

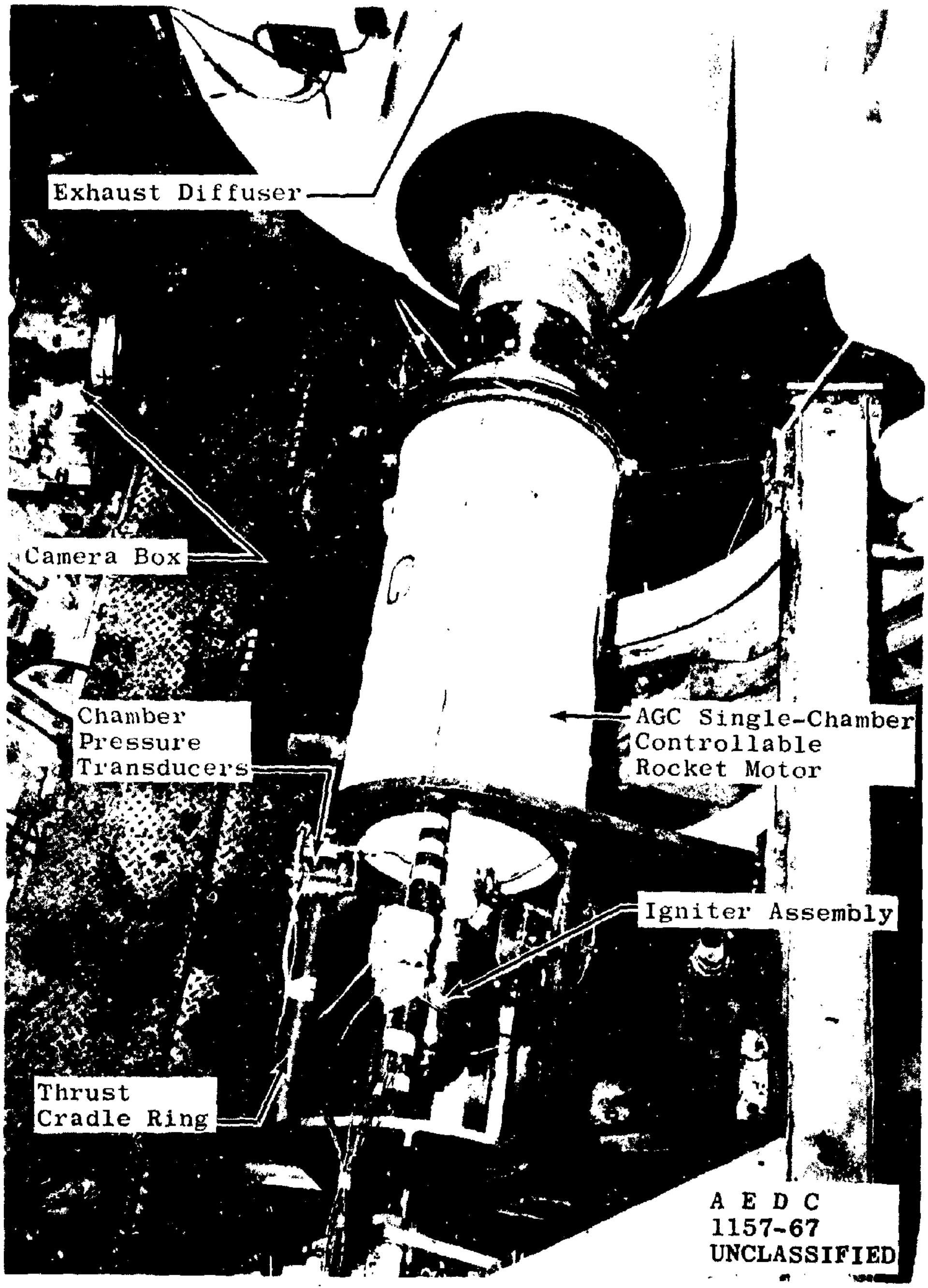

Installation of the AGC Single-Chamber Controllable Solid-Propellant Rocket Motor in the T-3 Test Cell - Photograph

Figure III-186B

a. Instrumentation

(U) Instrumentation was provided to measure axial thrust, igniter and motor chamber pressures, test cell pressure, servovalve hydraulic fluid inlet and outlet pressures, control and feedback signals to and from the servovalve, and motor assembly temperatures. Table II presents instrument ranges, recording methods, and system accuracies for all reported parameters.

(U) The axial thrust measuring system consisted of two double-bridge, strain-gage-type load cells mounted in the axial double-flexure column on the motor centerline.

(U) Bonded strain-gage-type transducers were used to measure chamber pressures and hydraulic pressures, and unbonded strain-gage-type transducers were used to measure test cell pressure. Chromel®-Alumel® (CA) thermocouples were bonded to the igniter assembly, motor case, and nozzle to measure temperatures during and after the motor firing (Figure III-187).

(U) The output signal of each measuring device was recorded on independent instrumentation channels. Primary data were obtained from four axial thrust channels, four test cell pressure channels, and two motor chamber pressure channels. These data were recorded as follows: Each instrument output signal was indicated in totalized digital form on a visual readout of a millivolt-to-frequency converter. A magnetic tape system, recording in frequency form, stored the signal from the converter for reduction at a later time by an electronic digital computer. The computer provided a tabulation of average absolute values for each 0.10-sec time increment and total integrals over the cumulative time increments.

(U) A photographically recording, galvanometer-type oscillograph, recording at a paper speed of 25 in./sec provided an independent backup of all operating instrumentation channels except the thermocouples. The millivolt outputs of these thermocouples were recorded on magnetic tape from a multi-input, high-speed, analog-to-digital converter at a scan rate for each thermocouple of 300 times per second.

(U) Selected channels of thrust, pressure, and temperatures were recorded on null-balance potentiometer-type strip charts for analysis immediately following the motor firing. Visual observation of the firing was provided by a closed-circuit television monitor. High-speed, motion-picture cameras provided a permanent visual record of the firing.

TABLE II
INSTRUMENTATION DESCRIPTION

Parameter	Estimated Measurement Uncertainty*		Measuring Device	Range of Measuring Device	Recording Device	Method of System Calibration
	Steady-State at Operating Level	Integral, percent				
Axial Force, lb_f	±0.31 percent	---	Bonded Strain-Gage-Type Load Cells (2 used)	0 to 25,000 lb_f	Millivolt-to-Frequency or Digital Converter onto Magnetic Tape	Deadweight
Total Impulse, lb_f-sec	---	±0.30				
Motor Chamber Pressure, psia	±0.54 percent	---	Bonded Strain-Gage-Type Transducers (2 used)	0 to 1000 psia		Electrical
Chamber Pressure Integral, psia-sec	---	±0.53				
Test Cell Pressure, psia	±1.10 percent	---	Unbonded Strain-Gage-Type Transducers (4 used)	0 to 1.0 psia		
Test Cell Pressure Integral, psia-sec	---	±0.86				
Time Interval, msec	±2 msec	---	Synchronous Timing Line Generator	---	Photographically Recording Galvanometer-Type Oscillograph	Compare with 60 cps
Temperature, °F	±10°F	---	Chromel-Alumel Thermocouples	0 to 1000°F	Digital Millivoltmeter onto Magnetic Tape	Known Millivolt Source and NBS Temperature Tables
Weight, lb_m	±0.03 lb_m	---	Beam Balance Scales	0 to 3000 lb_m	Visual Readout	Periodic Deadweight Calibration

*All uncertainties are stated at an estimated two-standard-deviation level.

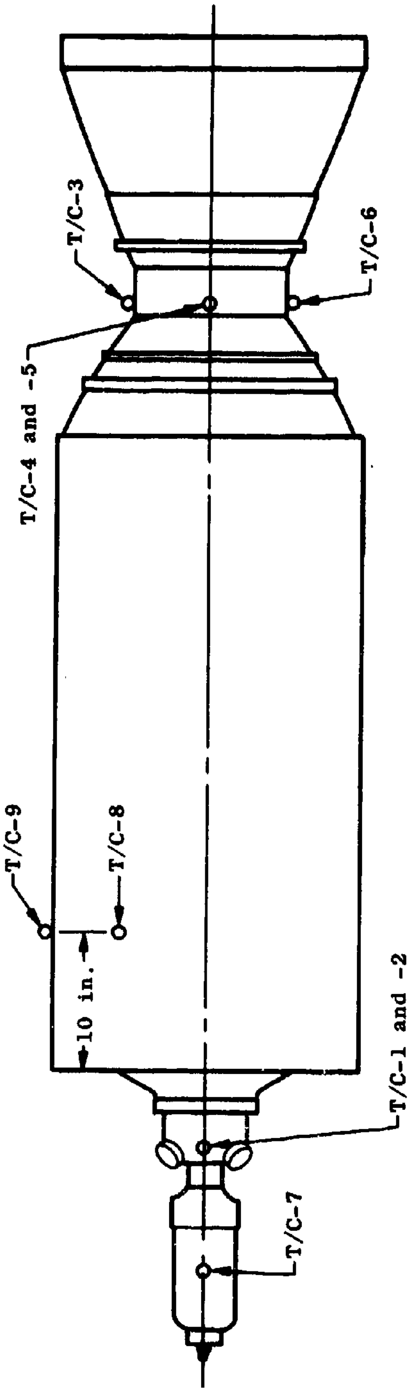

Note: T/C-2 and -5 are located 180 deg from location shown.

UNCLASSIFIED

Thermocouple Locations

Figure III-187

b. Calibration

(U) The thrust calibration weights, thrust load cells, and pressure transducers were laboratory calibrated prior to usage in this program. After installation of the measuring devices in the test cell, the thrust load cells and pressure recording systems were calibrated at sea-level ambient conditions and again at simulated altitude conditions just before the motor firing.

(U) The pressure recording systems were calibrated by an electrical, four-step calibration, using resistances in the transducer circuits to simulate selected pressure levels. The axial thrust instrumentation systems were calibrated by applying to the thrust cradle known forces, which were produced by deadweights acting through a bell crank. The calibrator is hydraulically actuated and remotely operated from the control room. Thermocouple recording instruments were calibrated by using known millivolt levels to simulate thermocouple outputs.

(U) After each motor firing, with the test cell still at simulated altitude pressure, the recording systems were recalibrated to determine any shift.

c. Procedure

(U) The AGC Single-Chamber Controllable Solid-Propellant Rocket Motor arrived at AEDC on 19 January 1967. The motor was visually inspected for possible shipping damage and radiographically inspected for grain cracks, voids, or separation and found to meet criteria provided by the manufacturer. During storage in an area temperature conditioned at 75 $\pm$ 5°F, the motor was checked to ensure correct fit of mating hardware, and the nozzle exit diameters were measured. The entire motor assembly was then weighed and photographed, and the motor thermocouples were installed. The nozzle pintle hydraulic system was flushed with clean oil, and the actuator was checked. The nozzle extension cone was removed, and a pressure check plate was installed. The igniter manifold, the first igniter, and power cartridge were installed on the motor case. The motor assembly was attached to the forward thrust cradle ring, and the transducers were installed. A pressure leak check of the motor assembly was accomplished using gaseous nitrogen at 40-psig pressure. The pressure leak check plate was removed, and the nozzle extension cone was reinstalled.

(U) After installation of the motor in the test cell, instrumentation and hydraulic connections were made, and a continuity check of all electrical systems and a functional check of the pintle control complex was performed. Pre-fire, sea-level calibrations were accomplished, the test cell pressure was reduced to the desired simulated altitude condition, and the

altitude calibrations were completed. During a functional check of the pintle control complex at 2 sec before the scheduled motor ignition, a faulty servovalve operation was discovered, which limited control of the pintle. The firing countdown was stopped and the test was aborted. Overheating of the valve due to insufficient hydraulic cooling and low heat transfer was determined to be the cause of the faulty operation.

(U) The problem was solved by changing the servovalve, adding additional cooling capability to the hydraulic power unit, blowing cold gaseous nitrogen over the servovalve, and limiting the operation time. A functional check of the pintle control system was performed, and the countdown was resumed.

(U) Pre-fire, sea-level calibrations were completed, the test cell pressure was reduced to the desired simulated altitude condition, and the altitude calibrations were completed. The final operation prior to firing was to check the firing circuit. The entire instrumentation measuring-recording complex was activated, and the motor was fired. Motor operation was controlled by the AGC-furnished process control analog computer.

(U) With the test cell pressure still at altitude, post-fire calibrations were accomplished. The test cell pressure when then returned to ambient conditions, a final set of calibrations was taken, and the motor was inspected, photographed, and removed to the storage area. Post-fire inspections at the storage area consisted of measuring the nozzle exit diameters, weighing the motor, and photographically recording the post-fire condition of the motor.

d. Results and Discussion

(U) An Aerojet-General Corporation Single-Chamber Controllable Solid-Propellant Rocket Motor was fired at an average pressure altitude of 108,000 ft as part of the feasibility demonstration. The primary objectives of the test program were to demonstrate the thrust modulation and stop-restart capabilities of the motor and to determine motor ballistic performance. Secondary objectives were to evaluate motor case and nozzle structural integrity and to measure motor case and nozzle temperatures. The resulting data are presented in both tabular and graphic form.

(C) Thrust modulation and termination capabilities, altitude ignition characteristics, ballistic performance, structural integrity, and motor assembly temperatures are discussed. Thrust modulation data are presented and discussed in terms of percent force parameter where the actual force parameter is the product of the instantaneous values of chamber pressure and throat area. The maximum (100%) force parameter is defined as the maximum design chamber pressure (1000 psia) times the maximum throat area (27.25 $in.^2$).

III, F, AEDC Demonstration Test Series (cont.)

Maximum force parameter, as defined, cannot be realized during the test since chamber pressure decreases as throat area increases; it is, however, a convenient reference for comparison of actual performance with programmed performance.

(U) Post-fire inspection of the nozzle revealed that the pintle cap insulator and throat pintle washer had failed during motor burning. Thus the minimum throat area corresponding to the full aft pintle position was too large for the motor to develop the chamber pressure called for by the input program.

(U) With pintle positioned at 86% pintle position to give a throat area of 6.27 in.^{2}, successful motor ignition was accomplished at a pressure altitude of 125,000 ft. An analog trace of the ignition event is shown in Figure III-188. Ignition lag time, defined as the time interval from the time at which firing voltage is applied to the igniter circuit to the time of increase in chamber pressure, was 0.009 sec.

(U) After ignition with the pintle at the 86% linear position, the pintle control system was pre-programmed to follow step-inputs to three increasing levels of thrust, with a motor termination signal at 8.6 sec after ignition. The programmed sequence called for movement of the pintle to the 95% position (A_t = 4.9 in.^{2}) 2 sec after the termination signal to allow the pintle body to cool. Two additional thrust step-inputs were to follow which would provide data in the event that termination of the propellant burning was not successful.

(U) The motor ignited satisfactorily, the pintle stepped through the pre-programmed sequence, the termination signal occurred at 8.6 sec after ignition, and burning terminated at approximately 9.1 sec. Approximately 1.9 sec after the thrust termination, the pintle began movement to the 95% position. However, approximately 2.0 sec after pintle movement, motor reignition occurred, and burning continued until all propellant was consumed, approximately 41.7 sec after the ignition command signal. Figure III-189 presents the programmed force parameter input and the various control system signals as a function of time. The control system signals are presented as a percent of their respective maximum values.

(U) The programmed force parameter input signal is compared with the test results in Figure III-190. The observed force parameter outputs were obtained by multiplying the instantaneous chamber pressure by the nozzle throat area as determined from the instantaneous pintle position potentiometer signal. During the first burn period, the observed force parameter output appeared to respond better to low level programmed force parameter inputs than to the higher level inputs. The observed force parameter output responded very readily to the thrust termination signal to the failsafe manifold.

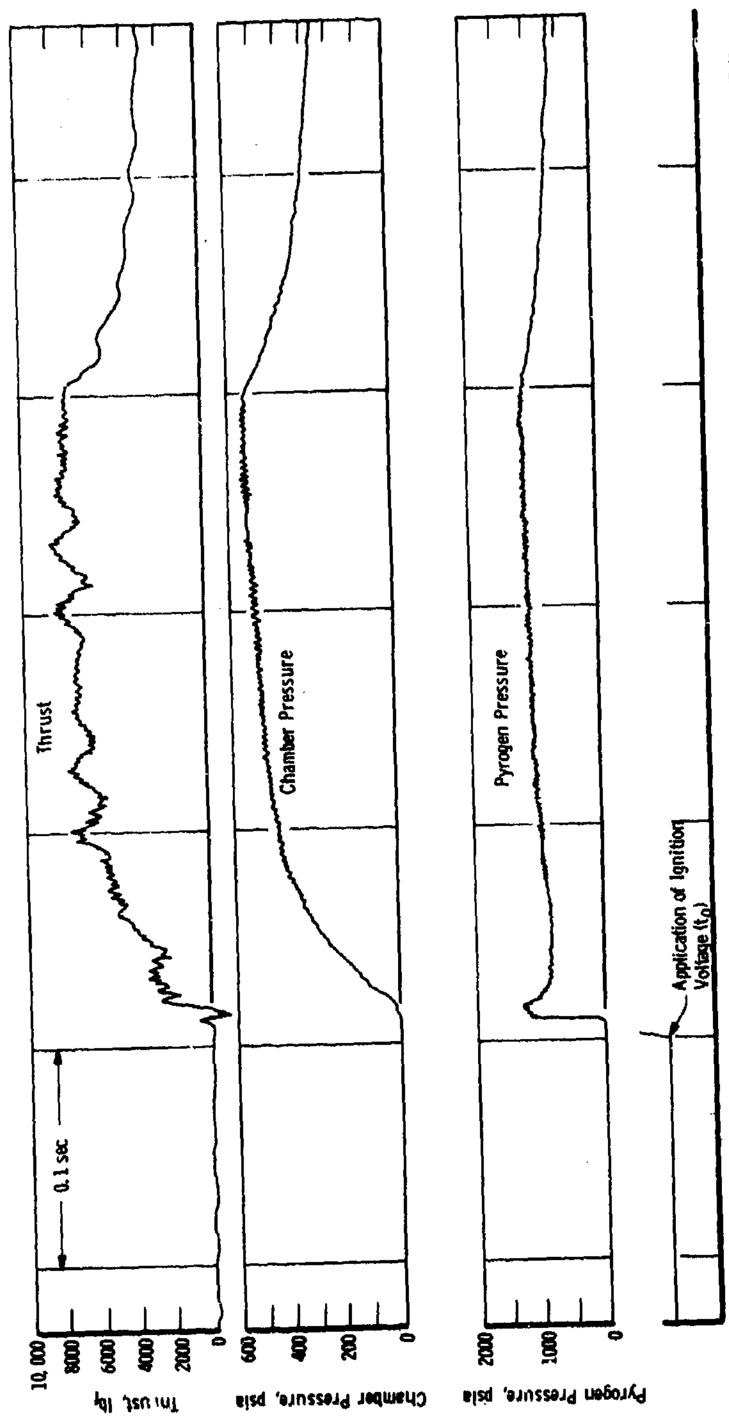

CONFIDENTIAL

Analog Trace of the Ignition Transient

Figure III-188

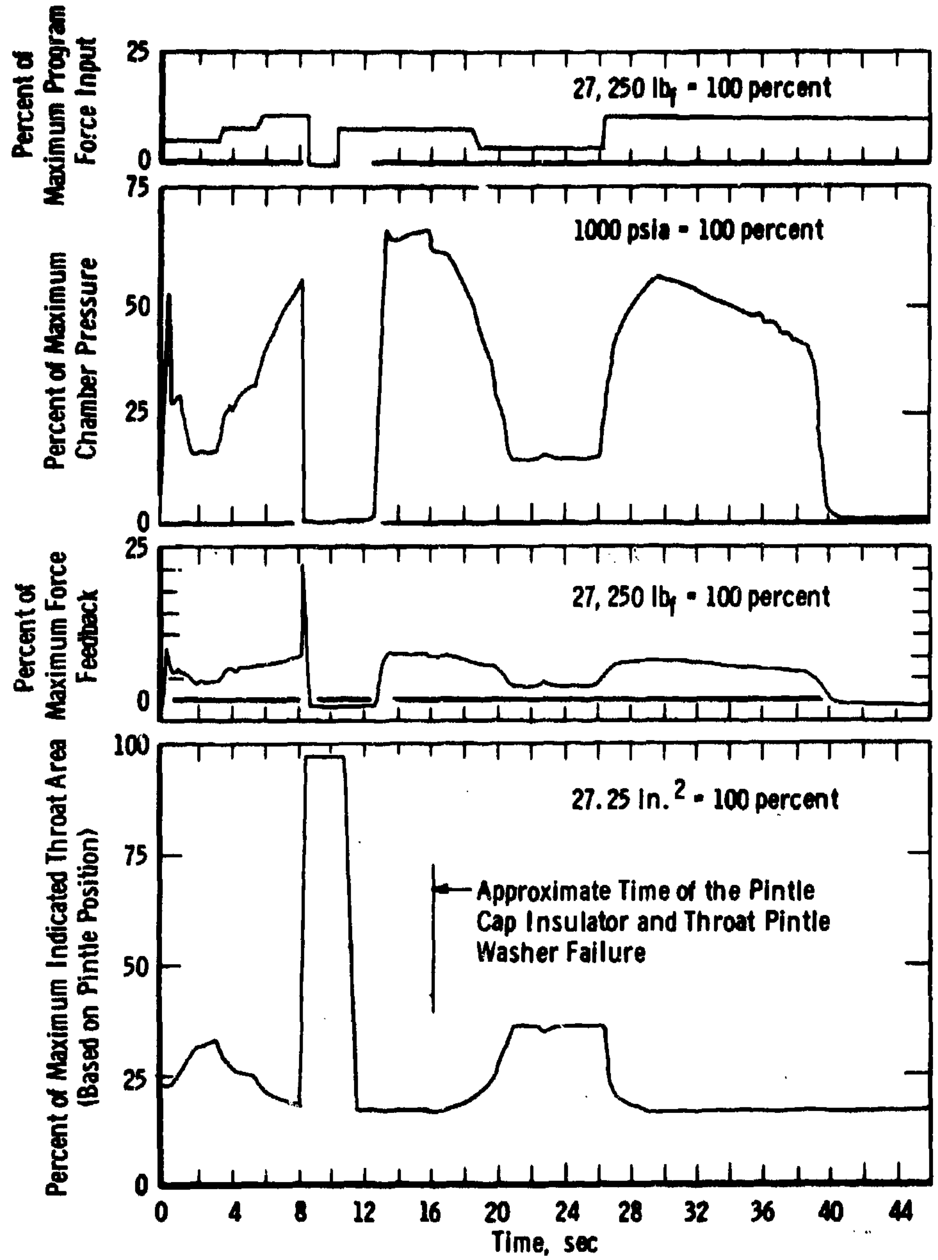

Nozzle Pintle Control and Feedback Parameters (u)

Figure III-189A

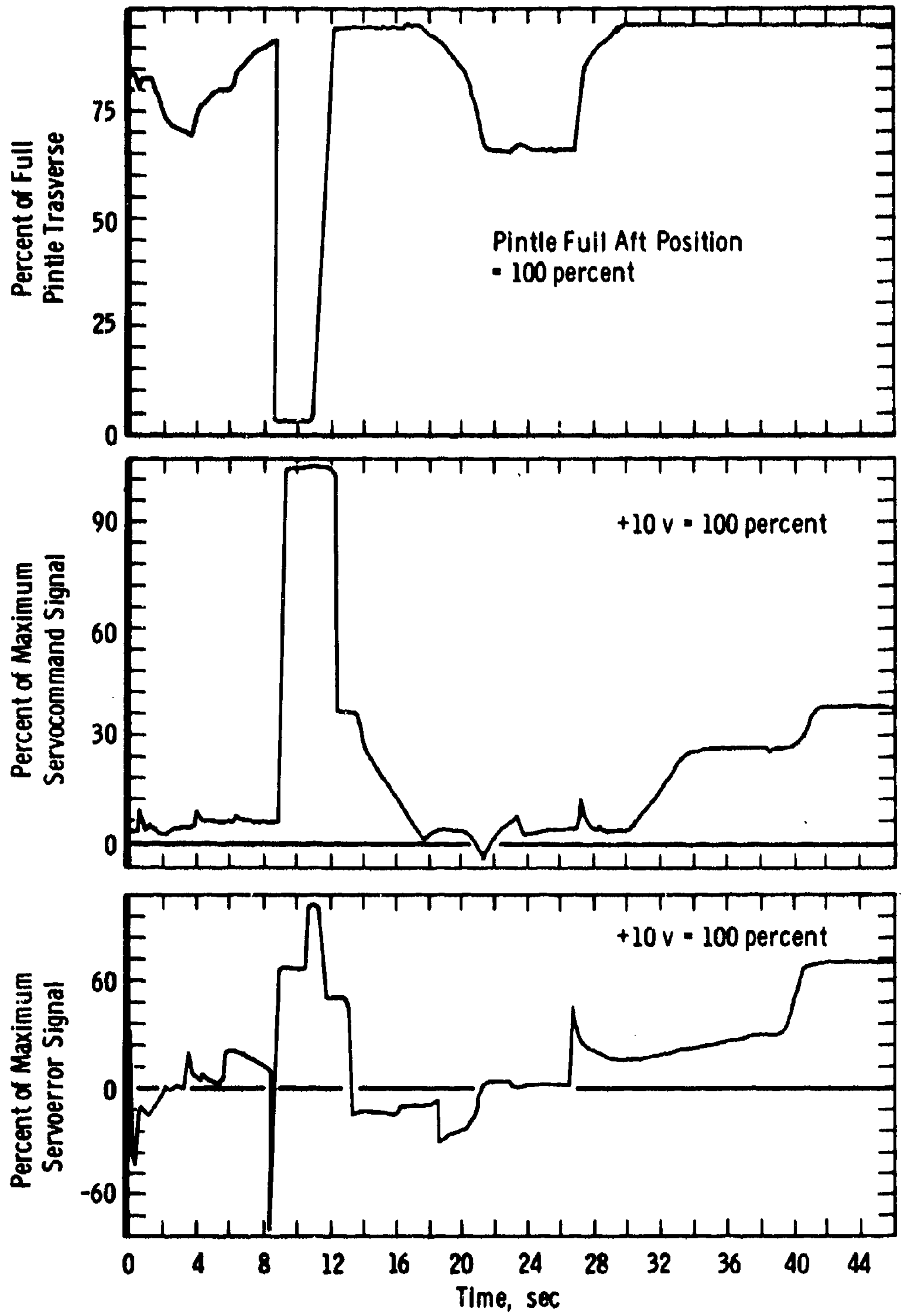

Nozzle Pintle Control and Feedback Parameters(u)

Figure III-189B

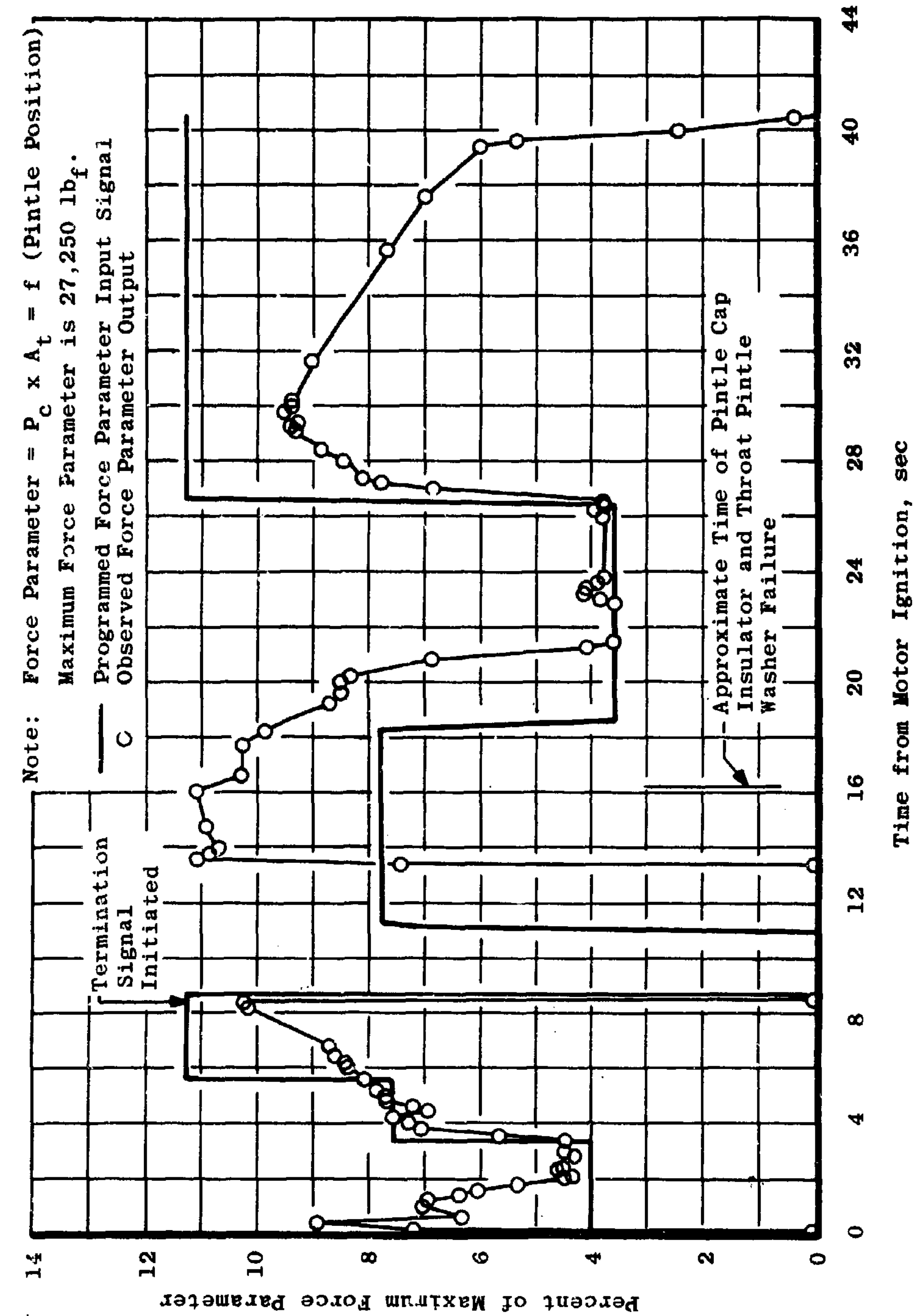

Programmed Force Parameter Input Compared with
Force Parameter Output (u)

Figure III-190

III, F, AEDC Demonstration Test Series (cont.)

(U) Post-fire inspection of the nozzle pintle revealed that the carbon phenolic pintle cap insulator had broken away from the pintle assembly during the firing. In an effort to determine the time of failure, instantaneous vacuum thrust coefficient (C_f) was calculated and plotted as a function of burn time (Figure III-191). Indicated throat area as determined from the pintle position potentiometer signal was used in this calculation. Calculated data presented in Figure III-191 are for indicated throat areas between 4.5 and 5.15 in.^{2}. Indicated instantaneous C_f before motor thrust termination was approximately 1.89. During a 2.6-sec period following motor reignition (13.6 to 16.2 sec from time of initial motor ignition), indicated C_f increased from 1.89 to 1.935. At approximately 16.2 sec, indicated C_f increased to approximately 2.05. The gradual increase in indicated C_f from 13.6 to 16.2 sec may have resulted from severe pintle insulator erosion. The sudden failure of the pintle insulator washer and break away from the pintle may have caused the sudden increase in indicated C_f at 16.2 sec. Motion-pictures taken during the firing verified the ejection of material from the nozzle at approximately 16.2 sec.

(U) As a result of the insulator failure, the minimum throat area corresponding to the full aft pintle position was too large for the motor to develop the chamber pressure called for by the input program. In addition, the pintle position-throat area relationship is in error; therefore, the observed force parameter was lower than the true value.

(U) Motor ballistic performance data based on total burn time (t_b) are summarized in Table III. The averaged measured total impulse was corrected to vacuum conditions by adding to it the product of the cell pressure integral and the average of the pre- and post-fire nozzle exit area. The average vacuum correction was approximately 0.91% of the average measured total impulse. Specific impulse values are presented using both the manufacturer's stated propellant weight and the motor expended mass determined from AEDC pre- and post-fire weights. When multiple channels of equally accurate instrumentation were used to measure the same parameter, the average value was used to calculate the data presented.

(C) Variations of thrust, chamber pressure, and cell pressure during the motor firing are shown in Figure III-192. Total burn time, defined as the sum of the interval from the time of increase in chamber pressure during ignition until chamber pressure has decreased to cell pressure at tailoff for each cycle, was 37.8 sec. Vacuum specific impulse, based on the manufacturer's stated propellant weight, was 274.24 lbf-sec/lbm. Vacuum specific impulse, based on the expended mass, was 268.58 lbf-sec/lbm.

(C) The variations of chamber pressure with throat area during the first 8 sec of motor operation is compared in Figure III-193 with the predicted values supplied by AGC. Actual chamber pressure was approximately 33% lower than predicted, over the range of throat area from 17 to 33% of maximum area.

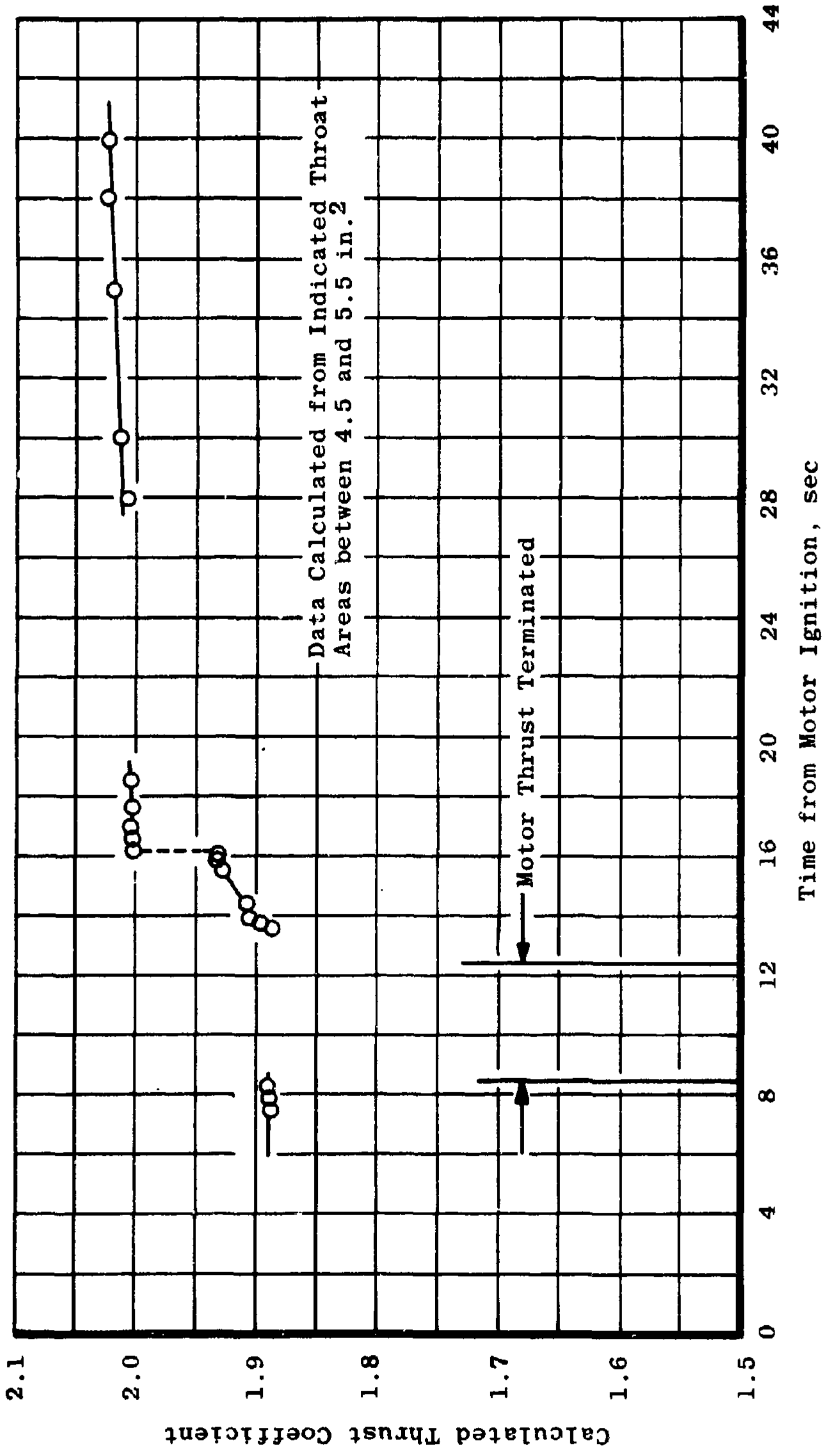

Instantaneous Vacuum Thrust Coefficient versus Burn Time (u)

Figure III-191

Table III

Summary of Motor Performance (u)

Motor Serial Number	LW-5
Conditioning Temperature, °F	80
Test Date (1967)	1/31
Ignition Altitude	125,000
Ignition Lag Time (t_ℓ), sec	0.009
Total Burn Time (t_b), sec	37.8
Measured Total Impulse (average of four channels, based on t_b), lb_f-sec	153,401
Maximum Deviation from Average, percent	-0.022
Chamber Pressure Integral (average of two channels), based on t_b), psia-sec	14,277.0
Maximum Deviation from Average, percent	0.054
Cell Pressure Integral (average of four channels), based on t_b), psia-sec	4.7271
Maximum Deviation from Average, percent	-0.93
Average Simulated Altitude (based on t_b), ft	108,000
Vacuum Total Impulse (based on t_b)	154,669
Vacuum Specific Impulse, lb_f-sec/lb_m	
(based on manufacturer's stated propellant weight)	274.24
(based on expended mass)	268.58

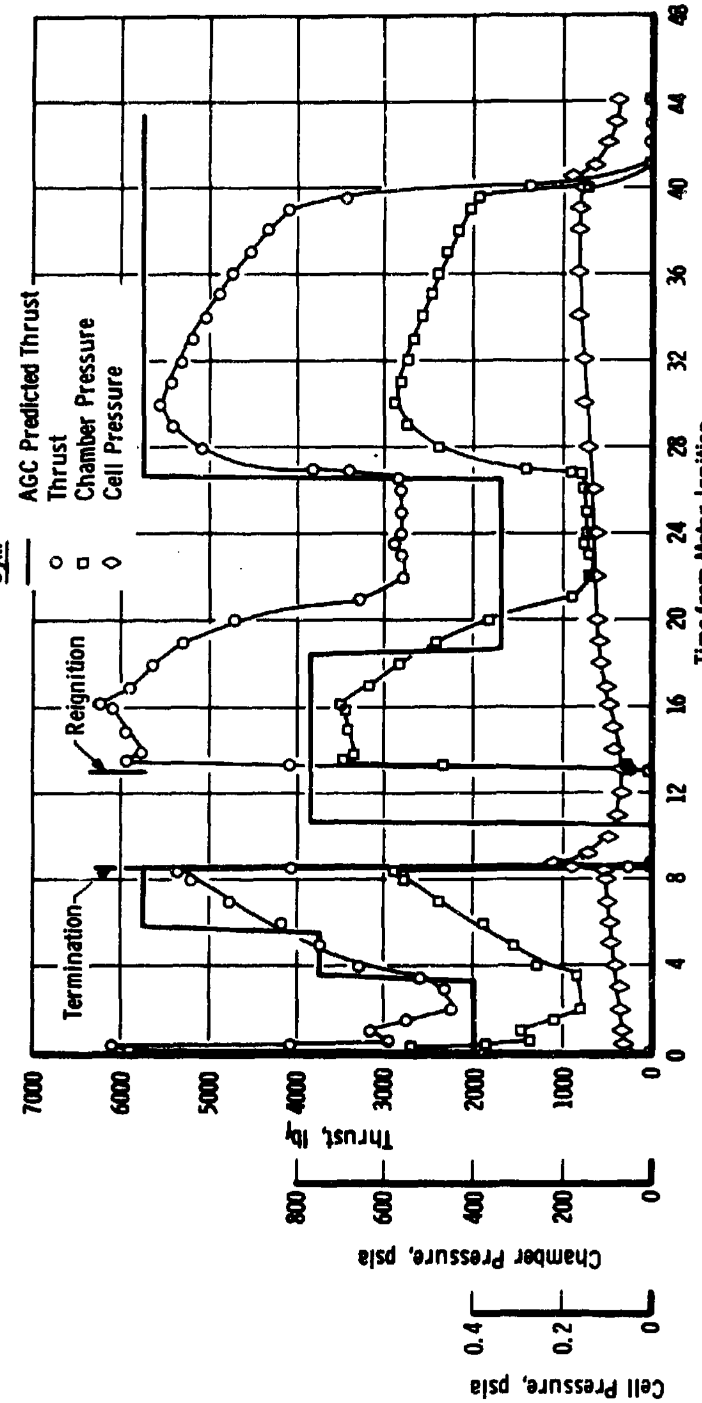

Motor Ballistic Performance Parameters versus Burn Time (u)

Figure III-192

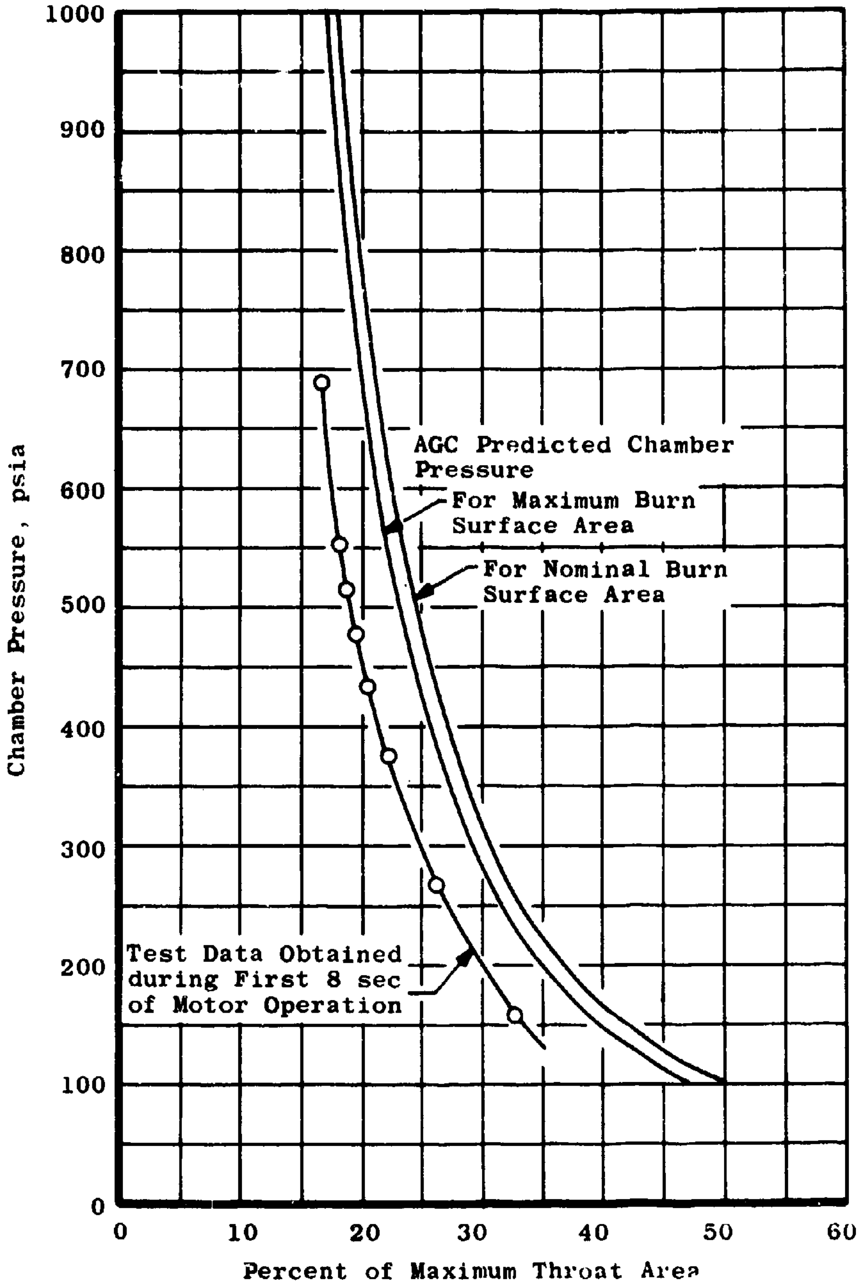

Chamber Pressure versus Throat Area (u)

Figure III-193

III, F, AEDC Demonstration Test Series (cont.)

(U) Post-fire photographs of the motor case, nozzle exit cone, nozzle throat pintle, and nozzle assembly are presented in Figure III-194. Post-fire inspection of the nozzle revealed that the silica-phenolic pintle cap insulator and the pyrolytic graphite pintle throat washer had failed during motor firing. Inspection of the pintle entrance cap, after removal of the nozzle from the motor case, indicated that the silica-phenolic cap had become unbonded.

(U) Post-fire measurements of the nozzle exit area indicated a decrease of approximately 0.46% from the pre-fire area (the post-fire measurement was made without removal of exhaust products deposited on the nozzle flow surface).

(U) Thermocouples were bonded to the igniter assembly, motor case, and nozzle assembly to measure temperatures during and after the firing. Temperature-time histories for all thermocouples are presented in Figure III-195.

(U) The maximum temperature recorded on the igniter assembly was 164°F and occurred 25 min after motor ignition. Maximum temperatures recorded on the motor case and nozzle assembly were 172 and 528°F, respectively, and occurred at 12 and 13 min after ignition.

e. Summary

(U) One Aerojet-General Corporation Single-Chamber Controllable Solid Rocket Motor was fired at an average pressure altitude of 108,000 ft to demonstrate thrust modulation and stop-restart capabilities of the motor and to determine motor ballistic performance. The results are summarized as follows:

(U) (1) The motor ignited satisfactorily, the pintle was stepped through the pre-programmed sequence, and burning terminated at approximately 9.1 sec after ignition. Approximately 1.9 sec after the thrust termination, the pintle moved to the 95% position as programmed. However, approximately 2.0 sec after pintle movement, motor reignition occurred, and burning continued until all propellant was consumed, approximately 41.7 sec after the ignition command signal.

(U) (2) A portion of the nozzle pintle throat washer and cap insulator failed approximately 16.2 sec after the ignition command signal. As a result, minimum throat area (corresponding to full aft pintle position) was too large for the motor to develop the chamber pressure called for by the input program.

(C) (3) Motor chamber pressure before the pintle insulator failure was approximately 33% lower than the predicted values for the nominal burn surface area.

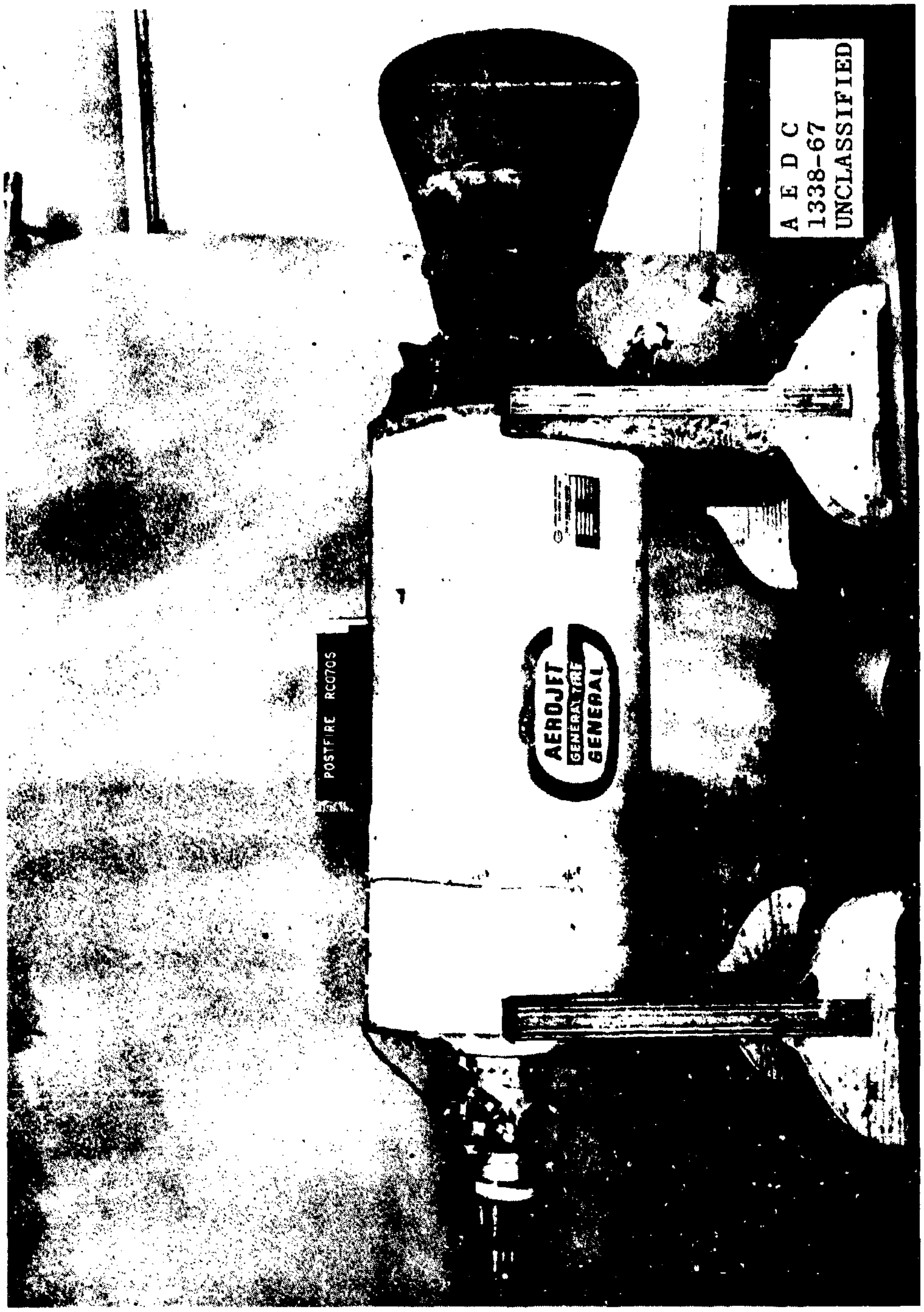

Post-Fire Photographs of the CSR - Motor Case and Nozzle Exit Cone

Figure III-194A

Post-Fire Photographs of the CSR - Nozzle Throat Pintle
(Looking Upstream)

Figure III-194B

Post-Fire Photographs of the CSR - Nozzle Assembly

Figure III-194C

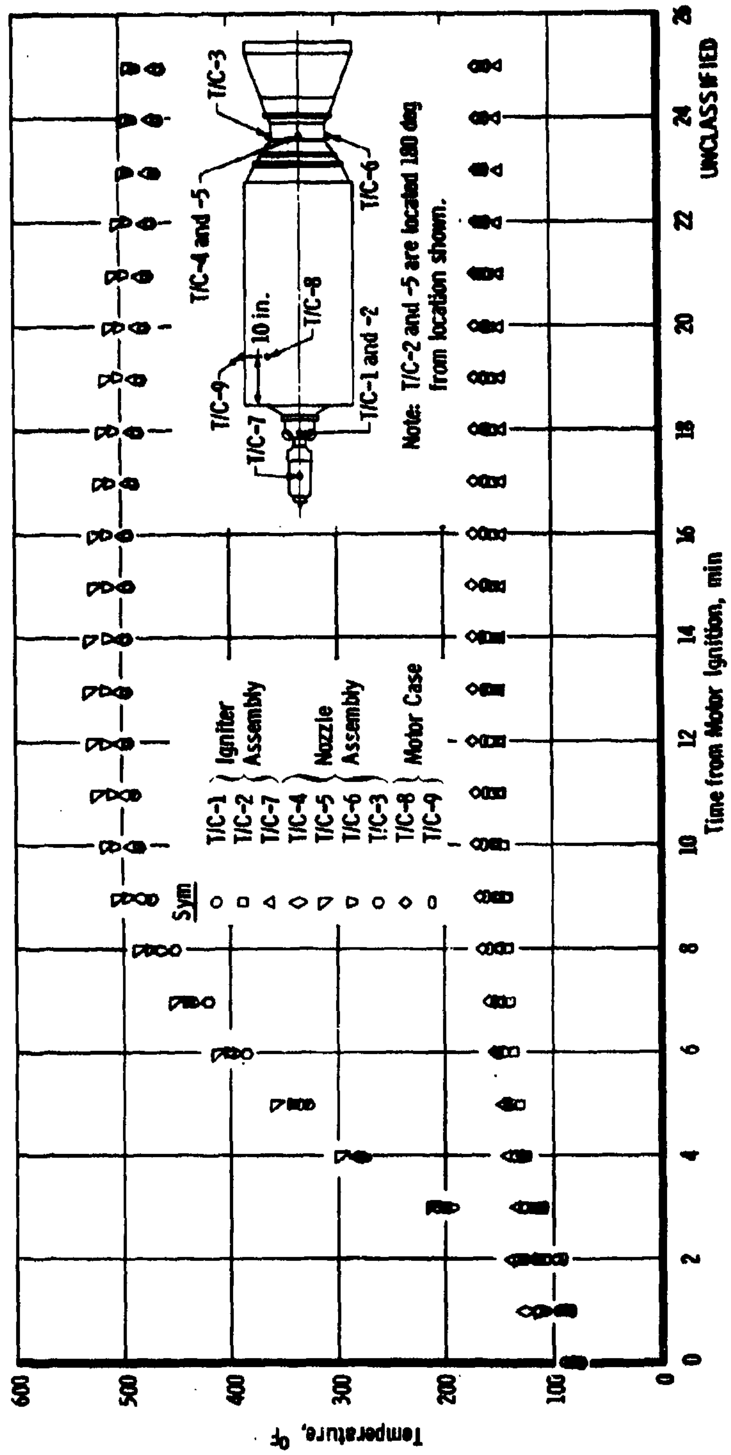

Temperature-Time Histories on the Motor Assembly

Figure III-195

(C) (4) Vacuum specific impulse based on total burn time and the manufacturer's stated propellant weight was 274.24 lbf-sec/lbm. Vacuum specific impulse based on expended mass was 268.58 lbf-sec/lbm.

(U) (5) The time interval from the time at which firing voltage was applied to the ignition circuit to the first indication of a rise in chamber pressure was 0.009 sec.

(U) (6) The maximum temperatures recorded on the igniter, motor case, and nozzle assembly were 164, 172, and 528°F, respectively, and occurred at 25, 12, and 13 min after ignition.

3. Demonstration Motor Design Modification (LW-9)

(U) On the basis of the results of LW-5 test firing, specifically the reignition of this motor after apparent extinction had occurred, it was determined to assure permanent extinction of the remaining three demonstration motors major changes to the configuration would be implemented. Analysis of motor LW-5 and the test results of series RC-0705 indicated that there were three probable areas responsible for the reignition of this motor. These areas were (1) the exposed aft face of the propellant grain, (2) the high temperature char that was formed on the entrance cap of the nozzle, and (3) the rapid closing of the pintle after initial extinction has occurred.

(U) The two factors necessary for ignition of a solid propellant grain, heat and pressure, were both present in LW-5 after initial depressurization extinction. The heat source in this motor was the exposed motor case and nozzle insulation. The pressure was supplied by the combination of the propellant and insulation outgassing and the resetting of the pintle to the minimum nozzle throat area condition. Since the majority of the heat transfer from the 'heat sources' to the propellant grain must be radiant due to the extremely low motor pressures, two approaches to limiting this transfer were applied. These were the limitation of the source temperature and the reduction of the view factor. The source temperature was limited by the removal of some of the silica-phenolic-elastomeric insulation material on the entrance cap and the replacement of this material with V-44, asbestos-filled-nitrile-insulation. This change lowered the entrance cap temperature from an initial char temperature of approximately 4000°F to a char temperature of approximately 1500°F and drastically lowered the total amount of heat that could be stored in this component for eventual feed-back to the propellant grain surface. The view factor was lowered by restricting the aft face of the propellant grain with a corresponding increase in the depth and length of the six forward fins to maintain a constant propellant surface area-web relationship.

(U) To minimize the maximum chamber pressure attainable due to propellant outgassing, the duty cycle of each of the last three motors was set to avoid closing the pintle after shutdown had occurred. Five seconds after command extinguishment, the pintle was moved to a 29% stroke position, the minimum amount necessary to clear the pyrolytic graphite from the steel seal surface. At this position the nozzle area was 22.5 square inches, considerably larger than the 4.8 square inches attained at 100% stroke as was the case during the test of LW-5.

(U) Also during the test of LW-5 the last pyrolytic graphite washer on the pintle assembly was failed and ejected in part of the arc only. This type of failure was not typical of an interlaminar shear failure in that only a portion of the circumferential washer carrying the ejection load had broken off and ejected. This type of failure appeared to be a local thermal expansion restriction failure. Investigation of the pintle design to locate the probable source of this restriction yielded the possibility that the wavy spring could have shifted radially, inducing a non-symmetrical spring load and causing a cocking of the pintle insulator with the corresponding binding and restriction of expansion.

(U) To avoid this problem on the final three demonstration motors a minor redesign was initiated. This redesign simply added a small graphite washer to the stackup of the pintle flame liner and insulator components to pilot the wavy spring thus holding radial position of the spring throughout the test duration.

(U) In summary, there were three changes to the motor assemblies for the final three test motors, and one change in test procedure from that used during the test of LW-5. The motor changes consisted of restriction of the end of the grain which 'sees' the nozzle, a change in the nozzle entrance cap insulation from silica-phenolic to rubber, and the addition of a pilot for the pintle wavy spring. The change in procedure consisted of holding the pintle open for an extended duration after extinguishment had occurred to limit the maximum pressure attainable during propellant and insulation outgassing.

4. Summary of Test Series RC-0730

(C) Between 14 July and 27 July 1967, three single-chamber controllable solid rocket motors designed and fabricated by Aerojet-General Corporation under Contract AF 04(611)-10820 to AFRPL successfully demonstrated both variable thrust and stop-restart operation. This demonstration was conducted at the Arnold Engineering Development Center, Tullahoma, Tennessee in test cell T-3 at a pressure altitude of about 112,000 feet. The first motor tested, LW-9, was fired and successfully extinguished six times for a total running time of about 26 seconds. This motor demonstrated controlled thrust

levels of 1050, 2500, 4200, 4600, 5500, and 6500 pounds. The motor was cooled to ambient temperature between each pulse and a new igniter was installed for each refiring. Two different nozzles were used on this test due to the loss of the pintle end cap after the second pulse. Nozzle LW-9 was removed after the second pulse for repair and nozzle LW-10 was substituted for it for the remaining four pulses. Motor LW-10 was fired six times and successfully extinguished six times with nozzle LW-11 installed for all six pulses. This motor had a total running time of approximately 27 seconds and demonstrated thrust levels of 4000, 4500, 4750, 5500, 5800, 6000, and 6200 pounds. The motor was cooled to ambient temperature between each pulse. The final motor, LW-11, was fired a total of five times using the nozzle that had been previously fired two times on motor LW-9. The first pulse on motor LW-11 was hand throttled by the test conductor using the hand throttle provided on the pressure feedback control console. This pulse had a duration of 15 seconds and demonstrated thrust levels of 5000 and 6200 lb. After cooling to ambient, the motor was fitted with two igniters and two separate firing circuits. The second and third pulses were fired with a total shutdown time of only 2 minutes between them to demonstrate hot restart. After cooling to ambient, the motor was fired twice more, with a cooldown period to ambient between. The total running time of this motor was approximately 28.5 seconds and thrust levels of 3500, 4000, 4200, 4800, 5000, and 6200 were demonstrated.

(C) This test series successfully demonstrated the required thrust variation at altitude of 3:1 about a nominal thrust of 4000 pounds, multiple cycle firing of 6 pulses with 6 extinguishments, both hot refire and refire after cooldown, and in addition, manual thrust control was demonstrated. As can be seen from the levels of thrust demonstrated, the majority of the thrust levels were above 3500 pounds. This was not a motor limitation since the motor could easily operate at a thrust level of 1000 pounds, but rather was a limitation of the type of altitude facility used. To avoid detaching the exhaust plume from the diffuser it was necessary to always step up in pressure since the exhaust ducts have a tendency to 'load-up' with gas and back flow if the pressure in the motor case is drastically reduced causing plume separation and breakdown of the diffusion capability of the cell. Since the propellant in these motors was by nature difficult to ignite at low pressures (a typical characteristic of extinguishable propellants) the limitation on minimum thrust that could be demonstrated was the minimum pressure at which the propellant could be ignited; i.e., the minimum pressure at which the propellant could sustain combustion after igniter burnout and the corresponding drop in pressure associated with the loss of mass addition. The one test in which 1050 pounds of thrust was demonstrated resulted in a spontaneous extinguishment due to a combination of the L* effect and an instantaneous loss of signal during input program relay switching. Previous attempts demonstrate low thrust on motor LW-9 resulted in inadvertent extinction; however, this was traced to a problem in instrumentation. The input signal instrumentation pickup coil resistance (2000 ohms) was far too low for the computer resistance and resulted in a 45% decrease in effective signal to the computer resulting

in an unrealistically low thrust command to the motor immediately after ignition. This problem was located and corrected after the fourth pulse of motor LW-9; however not before three of the four pulses had resulted in this inadvertent extinction.

(C) The only problem of any significance that was encountered during this test series was the loss of some of the pyrolytic graphite from the pintle nozzles. All of the nozzles tested lost the insulative end cap from the pintle, closely followed by a loss of some of the pyrolytic graphite. Although this loss changed the relationship between pintle stroke and nozzle area, it did not result in a major malfunction of the system. The nozzles were refired continuously after the loss of this end cap and some of the pyrolytic graphite without serious damage. Since the loss of the pyrolytic graphite limited the minimum nozzle area attainable, the thrust levels resulting from input commands necessarily were higher after the loss than before the loss; the computer, being unaware of the loss, was calculating nozzle areas from pintle position and arriving at a lower force feedback signal than was actually in effect. This problem did not effect the stability of the system, but merely changed the thrust levels for a given input signal.

(C) For each of the motors, the prefire and postfire weights were taken of the entire hardware including the multiple igniters used. Motor LW-9 had a total expended weight of 410.38 pounds, LW-10 had expended 512.41 pounds, and LW-11 had expended 531.75 pounds. The portion of this expended mass attributable to the igniters for the three motors was 15.54, 15.60, and 12.44 pounds for LW-9, LW-10, and LW-11, respectively. Some of this expended mass was in the form of inert end restriction material (between 10-19 pounds/motor) and some was in the form of nozzle pintle ad cap and pyrolytic graphite washer material; however, this later was less than 0.5 pounds/motor. Considering the total expended mass, the delivered specific impulse of these motors, corrected to vacuum conditions was between 261-262 seconds. All three motors were returned to Aerojet with live propellant remaining; LW-10 had about 75 pounds, and LW-11 had about 35 pounds.

(U) Some of the prefire and postfire photographs taken by ARO, Inc. of these three motors are presented as Figures III-196 through III-206, inclusively. Figure III-196 depicts the aft restrictor on the face of the grain on motor LW-9 with the nozzle removed for clarity. This restriction material was hand trowelled onto the grain, accounting for the slight roughness at the slope break on the face of the restriction material. Figure III-197 shows a view of the symmetrical fins in the forward end of the motor grain, viewing through the igniter boss. An overall motor photo with the nozzle and igniter removed is shown on Figure III-198. With the nozzle, igniter, thrust pentapod, and pressure transducers installed the motor appears as shown on Figure III-199. Figure III-200 depicts a quarter-aft view of the motor as installed in Cell T-3 with hydraulic lines attached. An overhead postfire view of this motor in the

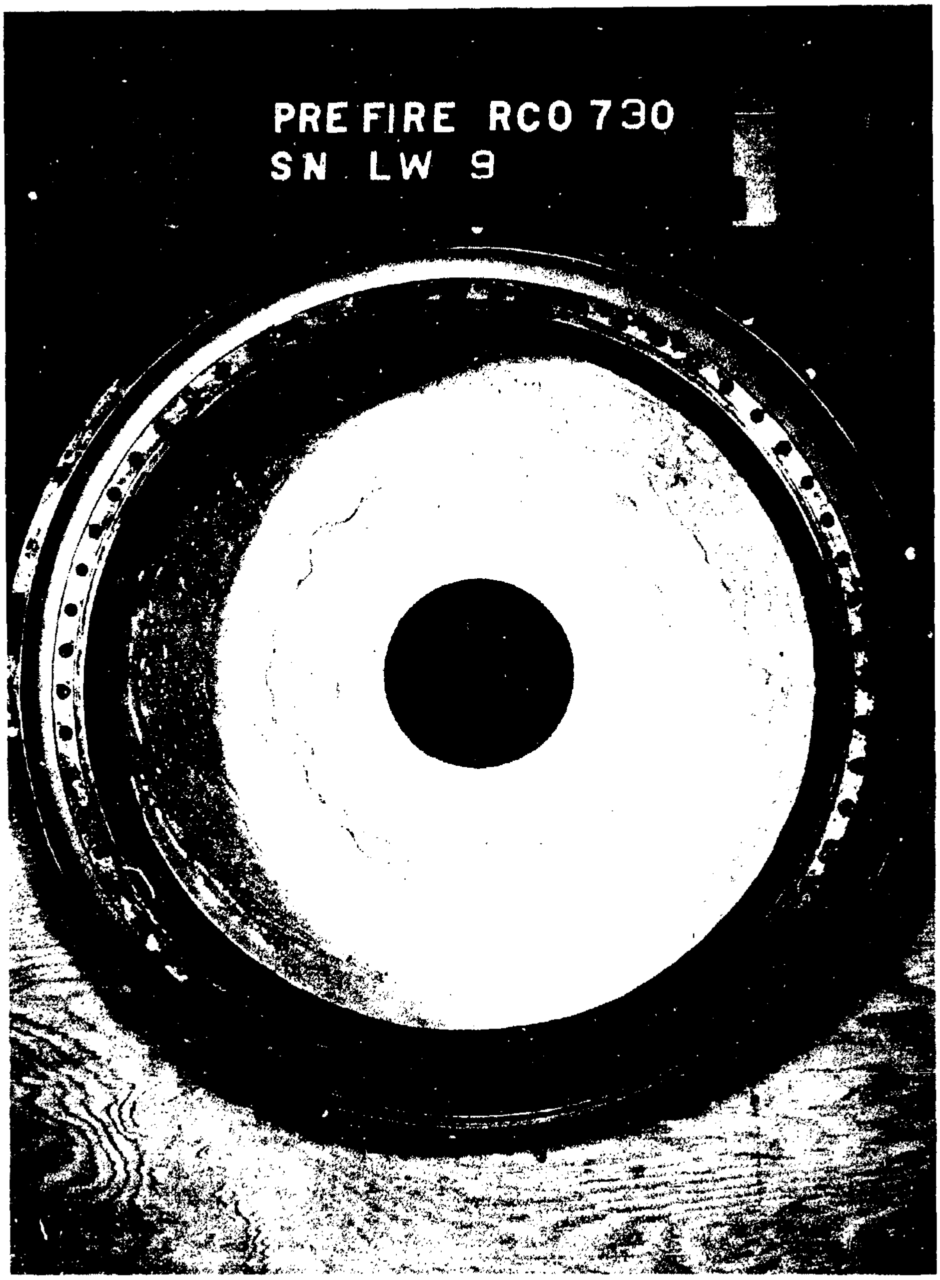

Prefire Grain Aft

Figure III-196

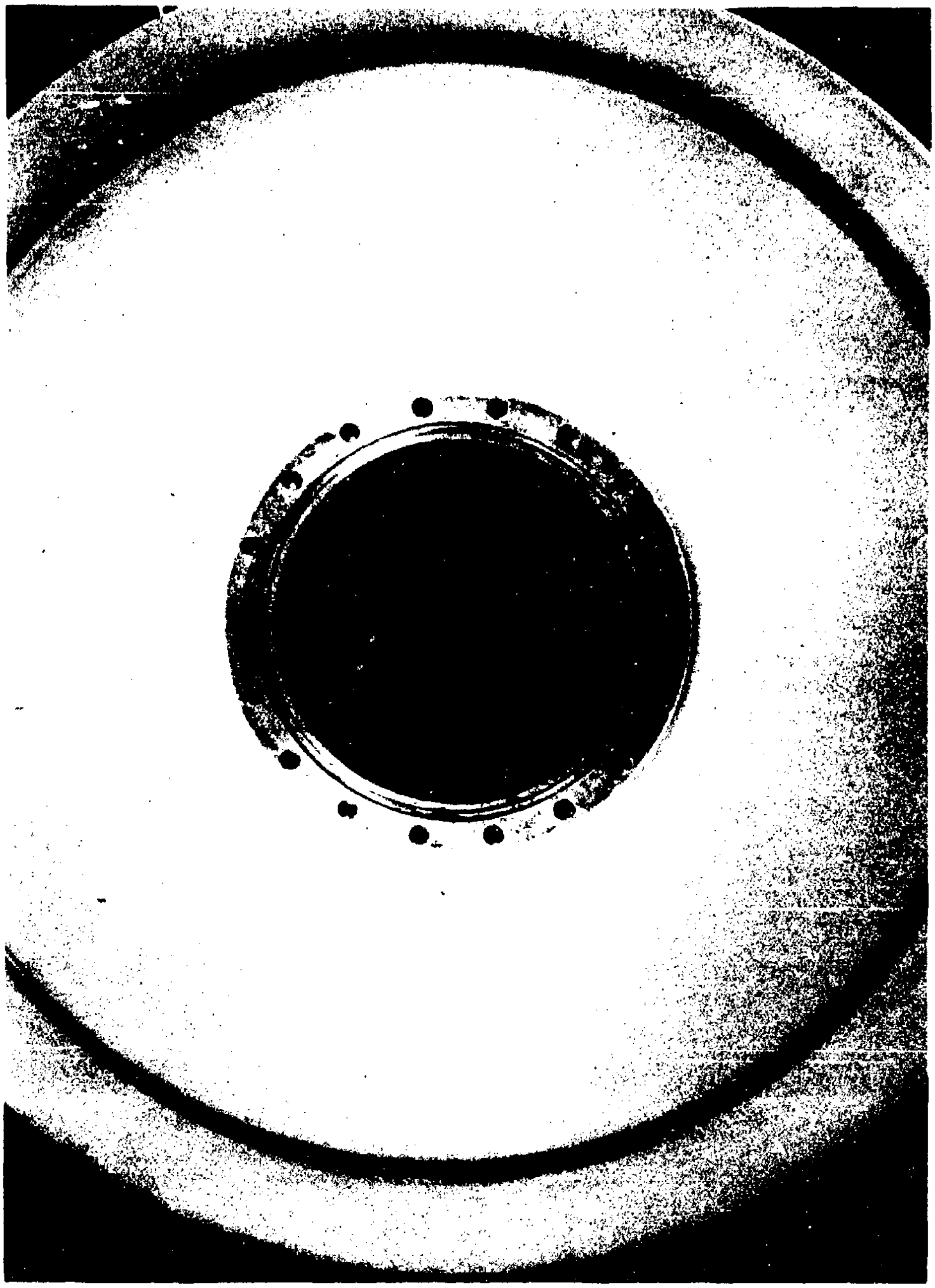

Prefire Grain Forward

Figure III-197

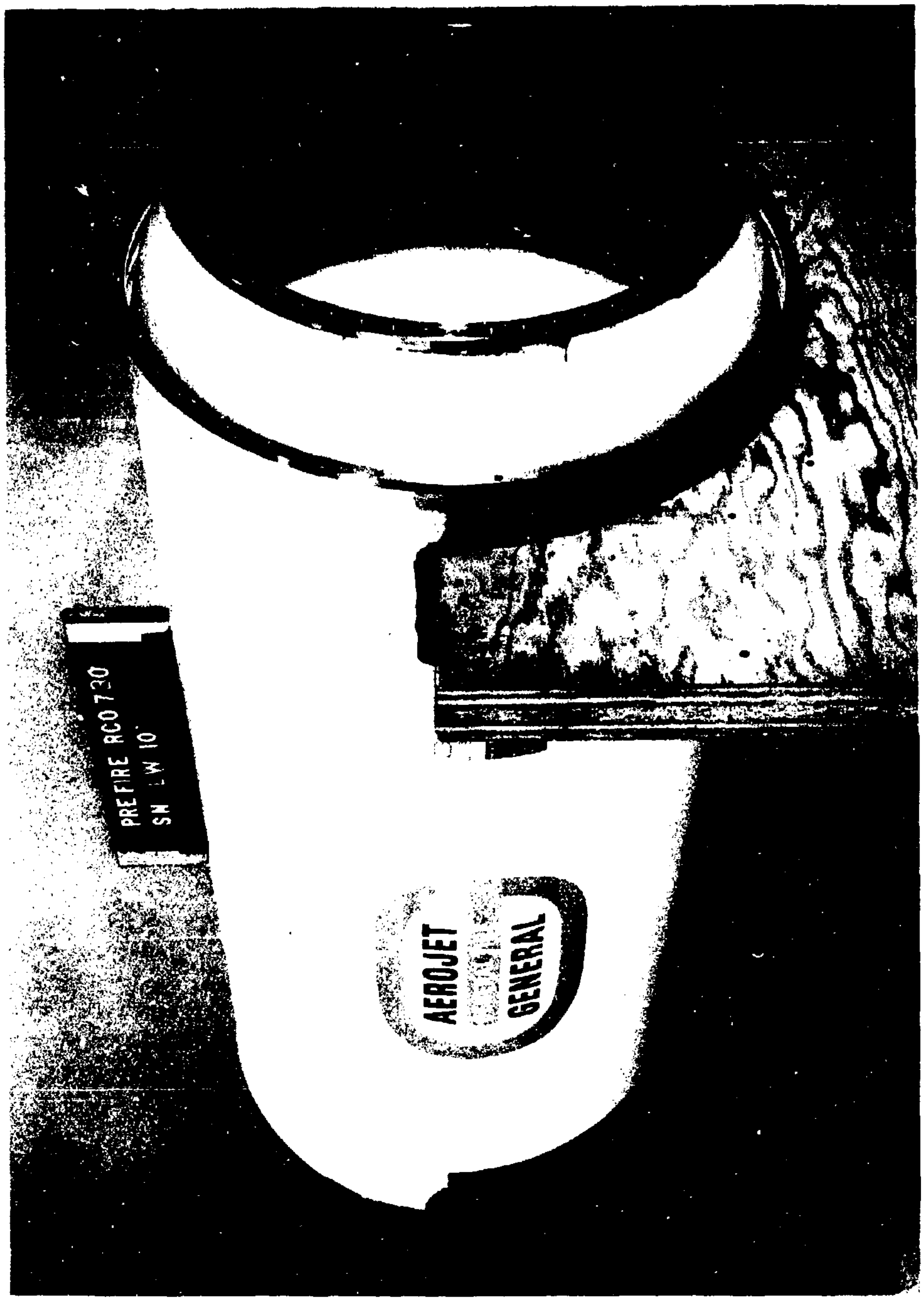

Prefire Motor Case

Figure III-198

Prefire Motor Assembly

Figure III-199

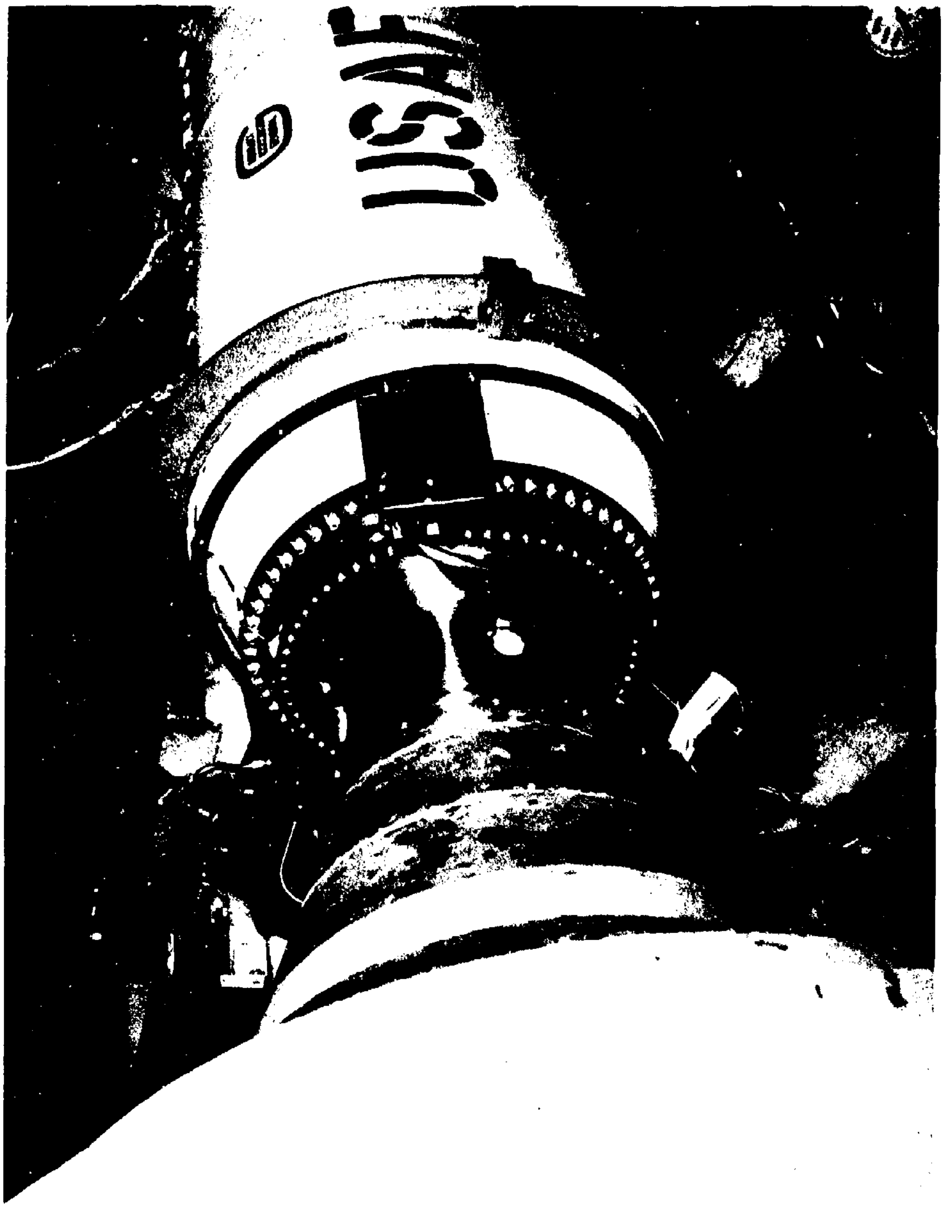

Prefire Motor in Cell

Figure III-200

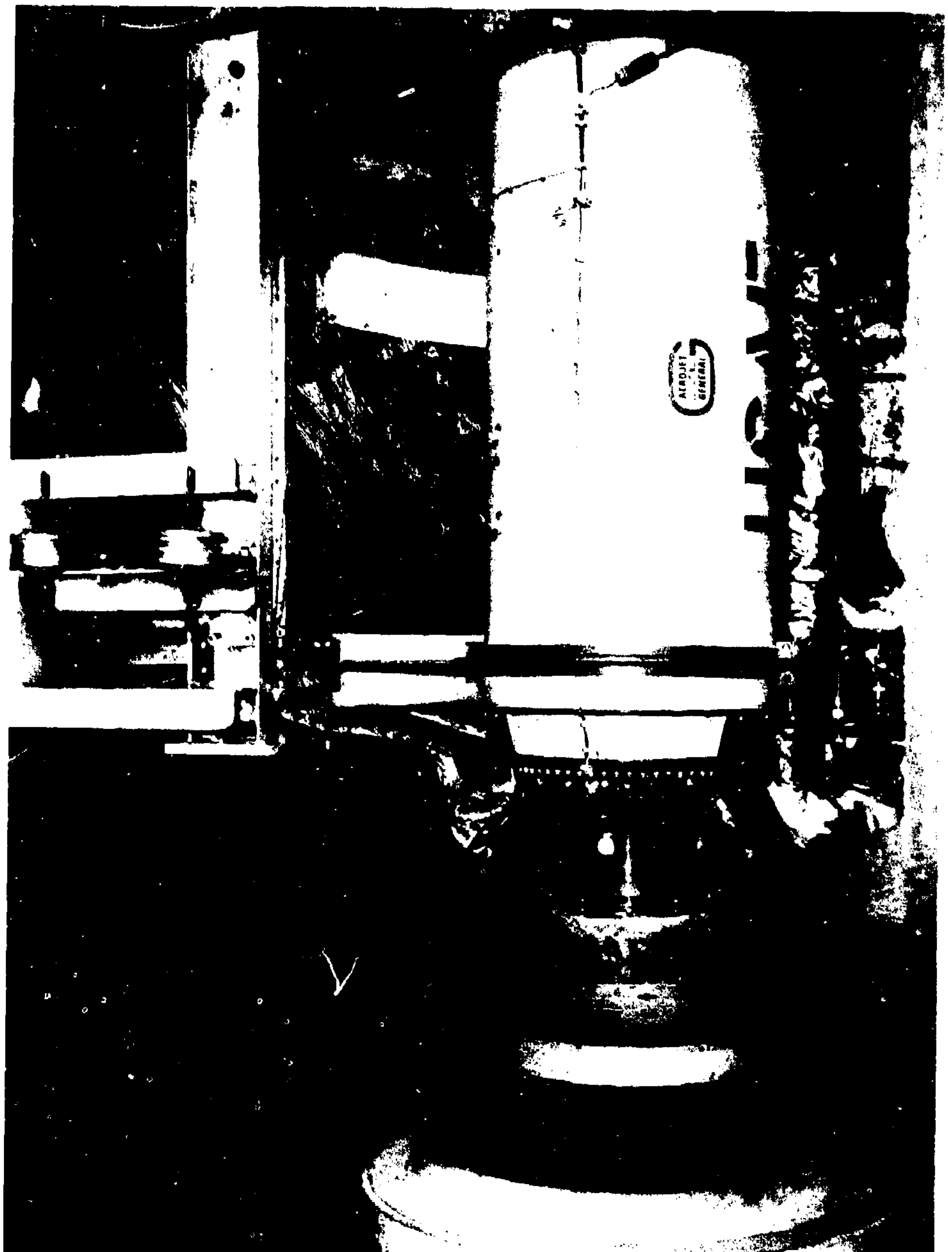

Postfire Motor in Cell

Figure III-201

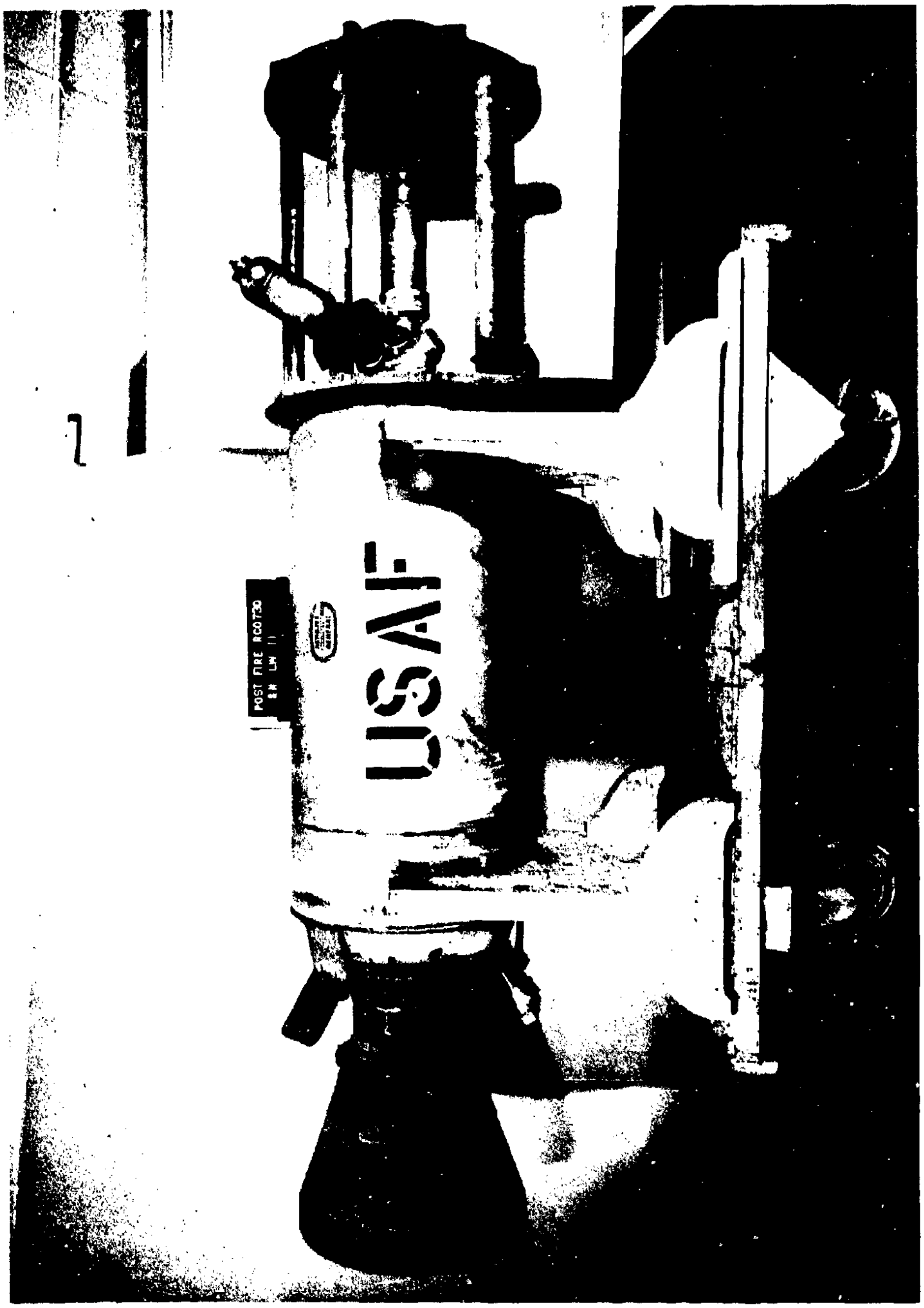

Postfire Motor Assembly

Figure III-202

Grain After 2-Cycles (Aft)

Figure III-203

Grain After 6-Cycles (Aft) LW-9

Figure III-204

Grain After 6-Cycles (Aft) LW-10

Figure III-205

Grain After 6-Cycles (Aft) LW-11

Figure III-206

cell is shown on Figure III-201. After completing the full test series, the motor is shown on Figure III-202 as removed from the cell. The motor shown, LW-11, was the one which had been manually controlled and had demonstrated the hot restart. The two igniters are shown still installed on this unit. The nozzle on this unit had been exposed to a total of 7 firing cycles, 2 on the motor LW-9 and 5 on the unit shown. Figure III-203 shows the aft face of the grain and restriction material after two cycles on motor LW-9. This shot was taken when the nozzle was removed for replacement of the pintle end insulator. At this point in the test series of LW-9, approximately 1.5 inches of web had been consumed. Figure III-204 shows the same motor grain after completion of the 6 cycles. It should be noted that the end restriction material had apparently burned through during the test series as the aft face of the grain in the upper right-hand quadrant appears to be burned back. Figures III-205 and III-206 show the grain on motors LW-10 and LW-11, respectively, after completing the full test series. As can be seen from Figure III-206, only one-inch of web remained in LW-11 after the five firing cycles.

(U) Plots of the thrust, chamber pressure, pintle position, and nozzle throat area deviation from expected for motors LW-9 through LW-11 are shown on Figures III-207, III-208, and III-209. These plots are grouped by nozzle rather than by motor since the only problem encountered in this test series was in the nozzle area; thus, the analysis and discussion of this problem will be facilitated by this grouping. Figure III-207 depicts these parameters for nozzle LW-9 which was fired twice on motors LW-9 and five times on motor LW-11. Figure III-208 covers the data from the firing of nozzle LW-11 on motor LW-10. Figure III-209 covers the data from the firing of nozzle LW-10 on the last four pulses of motor LW-9. These data will be discussed in more detail in the following section.

5. Analysis of Test Series RC-0730

(U) As previously mentioned, the only problem encountered in test series RC-0730 was in the area of the pyrolytic graphite insert of the pintle on the pintle nozzles tested. This analysis thus has been directed toward establishing the cause of the problems and the most feasible remedy for the problem.

(U) Figures III-210 through III-213, inclusive, depict a typical nozzle tested in this test series. The change to the nozzle entrance cap material from the silica-phenolic-elastomeric to V-44 rubber can be seen clearly on Figures III-210 and III-211. This V-44 insulation was molded over approximately 3/8-inches of silica-phenolic-elastomeric as a safeguard since the V-44 was not expected to withstand the environment of the entrance cap for the full duration of the test series and some insulation was an absolute necessity on this cap since it protects an aluminum actuator. Figure III-212 shows the inside of the nozzle exit cone and the end of the pintle. The light ring

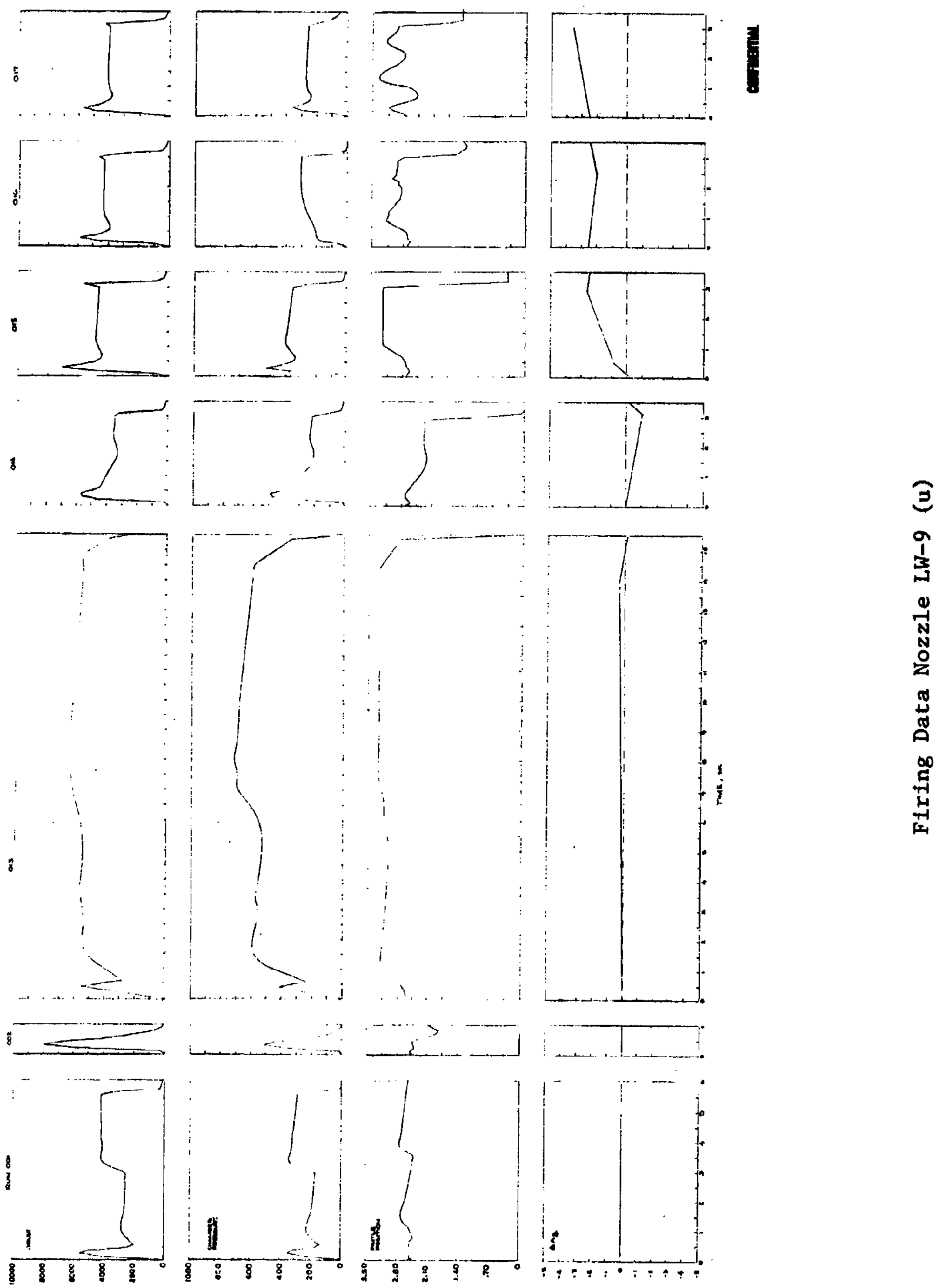

Figure III-207

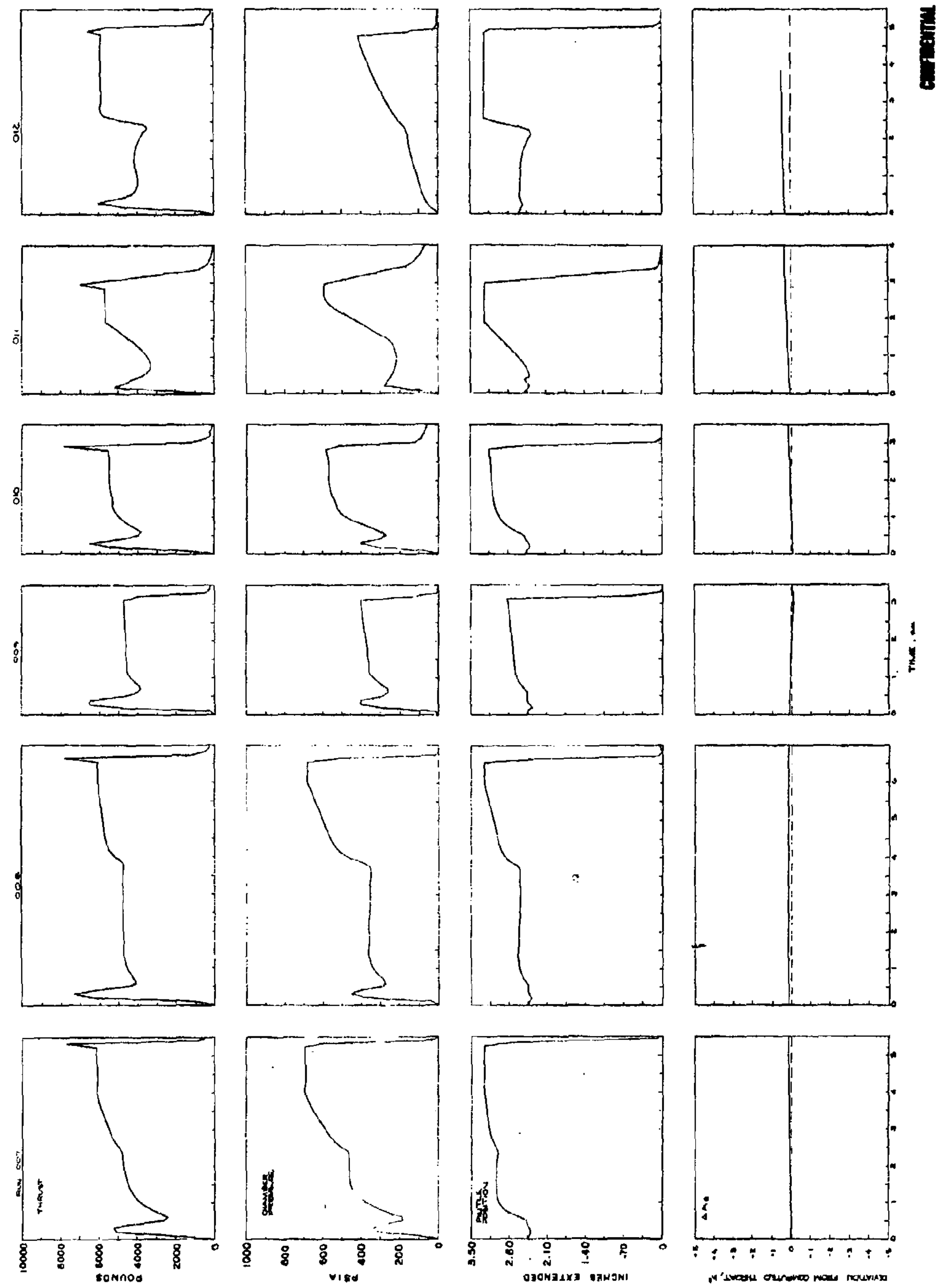

Firing Data Nozzle LW-11 (u)

Figure III-208

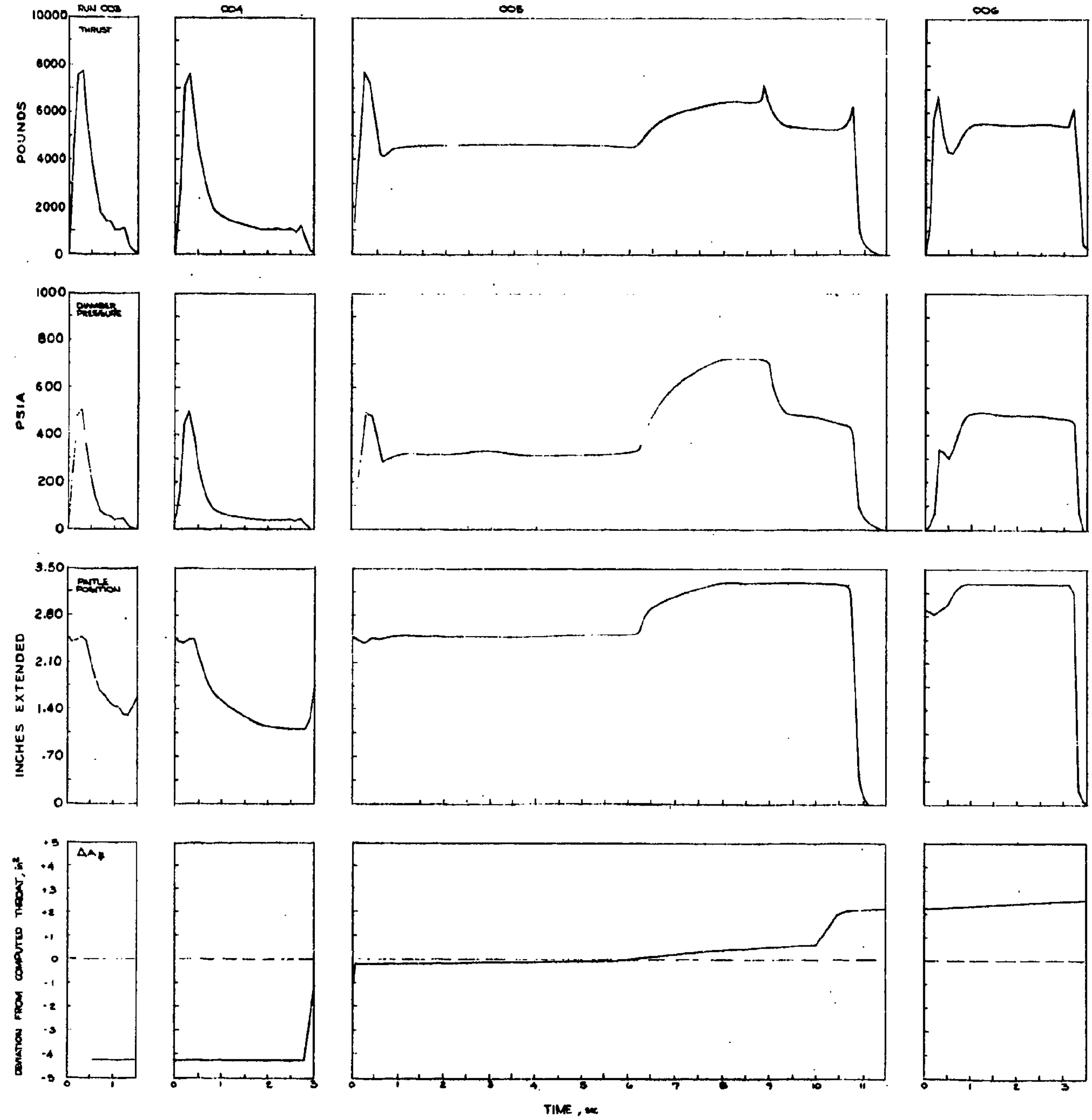

CONFIDENTIAL

Firing Data Nozzle LW-10 (u)

Figure III-209

Prefire Nozzle Assembly

Figure III-210

Prefire Nozzle Assembly Without Exit Cone

Figure III-211

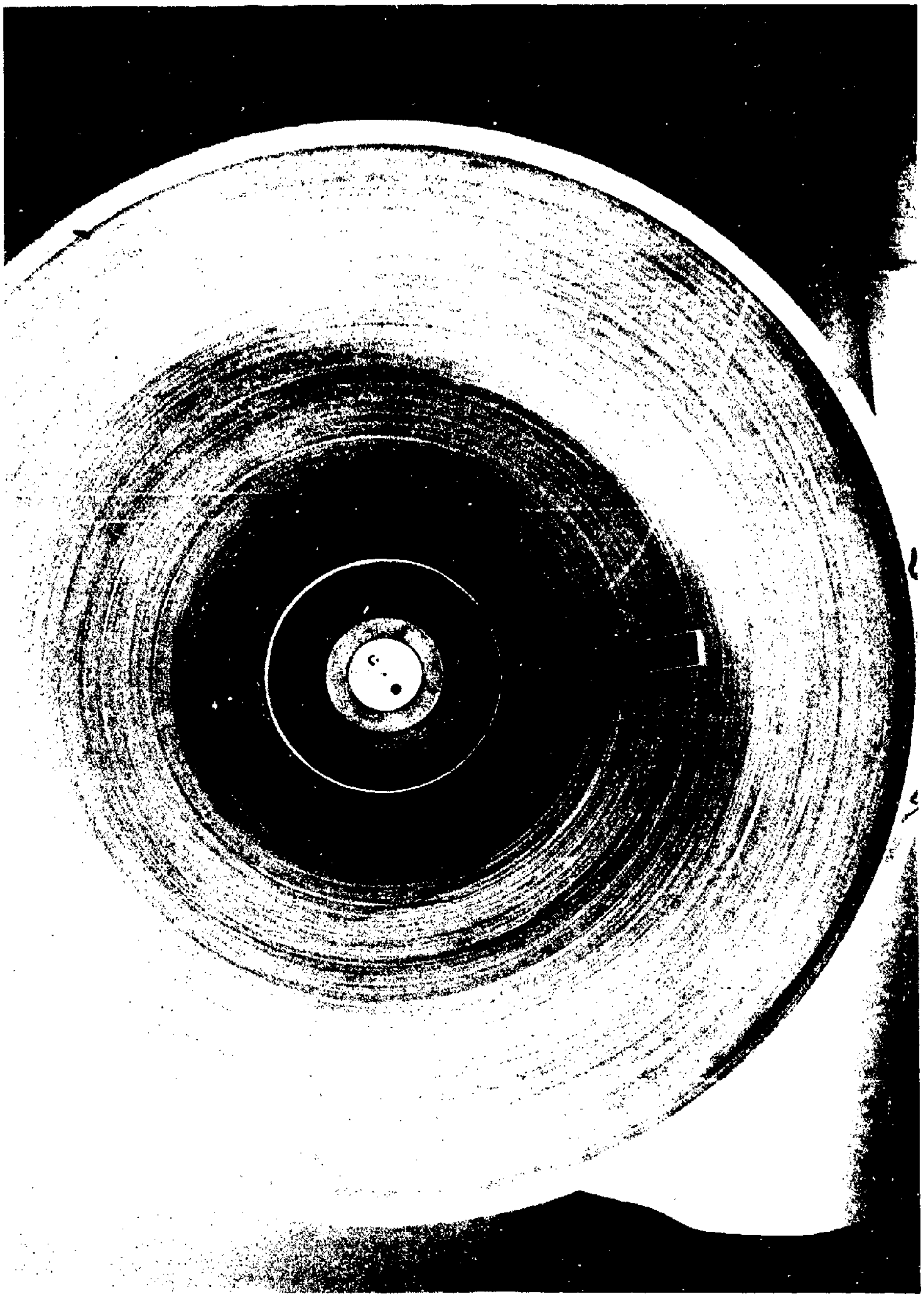

Prefire Nozzle

Figure III-212

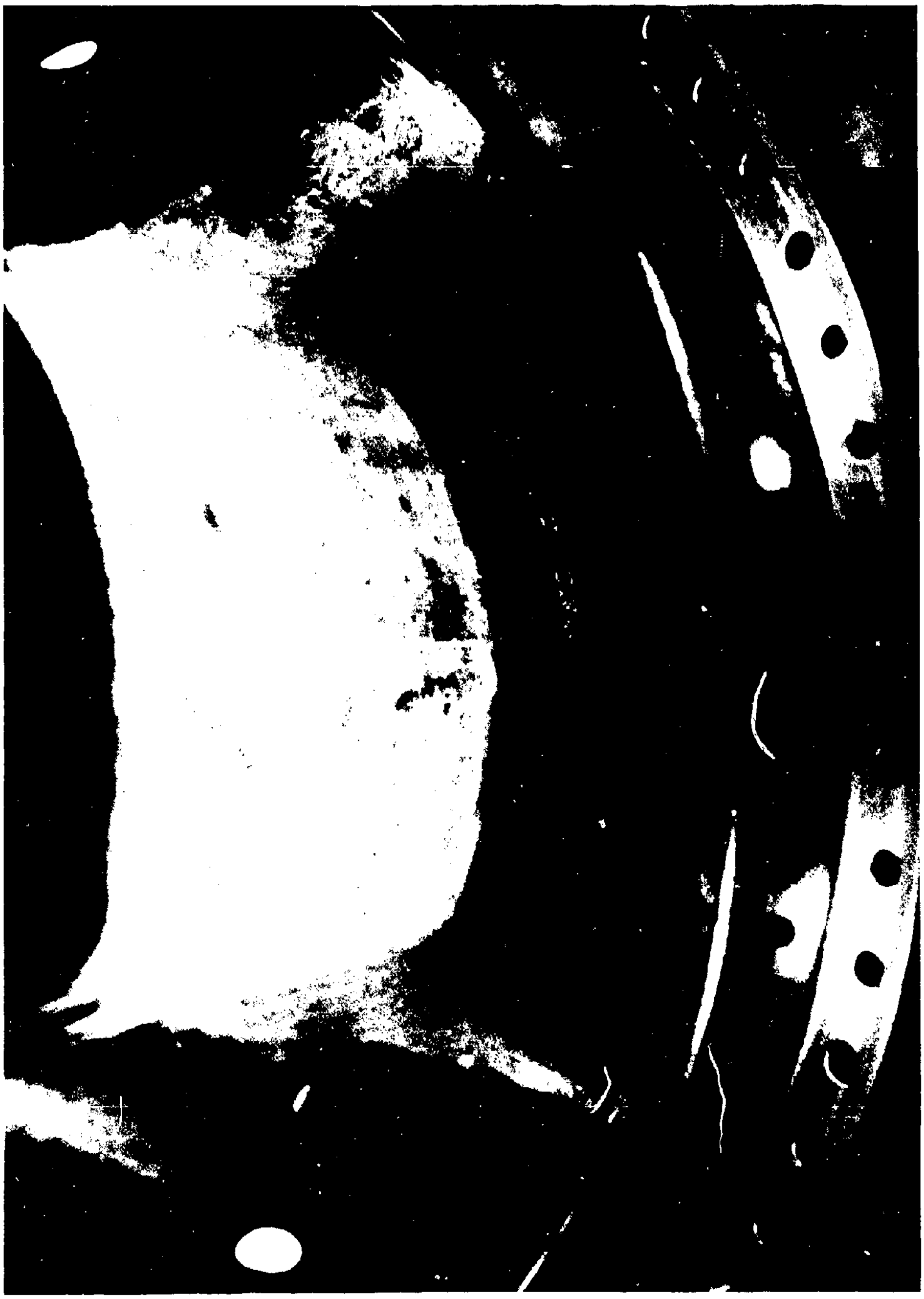

Prefire Nozzle

Figure III-213

on the outer throat is uncured rubber used as an expansion gap filler. This filler is only 0.060-inches thick. Figure III-213 shows the interior of the nozzle from the motor side looking through the struts at the aft housing insulation and the pintle in a retracted (maximum nozzle throat area) position.

(C) A typical nozzle after full exposure to multiple firings is shown on Figure III-214. As can be seen from this figure, most of the V-44 rubber has been consumed from the entrance cap leaving only a thin charred layer of rubber over the MXSE-79 insulation. In comparison, the strutted housing insulation (MXSE-79) is only slightly surface charred and is covered with globules of silicon. The steel nozzle housing shows the effect of extended soak times at temperature as permanent discoloration had occurred. This discoloration took place immediately after the initial soak period after a test of 6 seconds as can be seen from Figure III-215. This figure shows the nozzle assembly after it had only seen two pulses, one of 6 seconds and one of less than 1 second. The advanced deterioration of the rubber on the entrance cap can be seen clearly on this photograph; however, considerable rubber still remained over the MXSE-79. The washing effect of the gas flow through the propellant bore and over the entrance cap is evidenced by the 'bald' appearance of the dome where the char had been washed off.

(C) A typical nozzle interior after repeated cycling can be seen on Figure III-216. There was almost no material loss in the exit cone or the throat support, no erosion of the outer throat pyrolytic graphite, and no deposition of oxide on any of the surfaces. The pintle end cap is missing, and on this specific nozzle, parts of two pyrolytic graphite washers are missing. The specific nozzle had been only fired four times, the last four pulses of motor LW-9. The loss of these washers occurred on the third pulse of this nozzle, Run 005, shown on Figure III-209. Approximately 9 seconds into this pulse at a pressure of approximately 740 psia, both a thrust spike and a pressure drop indicate that this is the point where the nozzle pintle insert was broken and pieces ejected. This particular nozzle was refired with the pyrolytic graphite washers broken and the end gap gone on Run 006. As can be seen from this figure, the missing washers did not effect the capability of the system to maintain constant thrust.

(C) Review of Figure III-208, the firing traces of motor LW-10 and nozzle LW-11, indicates that this nozzle apparently withstood the entire six firing cycles without much damage since the deviation between the actual nozzle area and that calculated by the control computer remained fairly constant until into the fifth pulse, Run 011. At that time the area deviation appeared to occur and diverge from the computer value. That is probably the time at which one-half of the last pyrolytic graphite washer was ejected. On this same figure, the pressure traces for Runs 011 and 012 are shown as recorded and as the computer used them for control. The motor chamber pressure did not appear as shown; however, it was similar to that shown on the preceding traces. These two runs had partially plugged transducer ports on

Postfire Nozzle

Figure III-214

Postfire Nozzle

Figure III-215

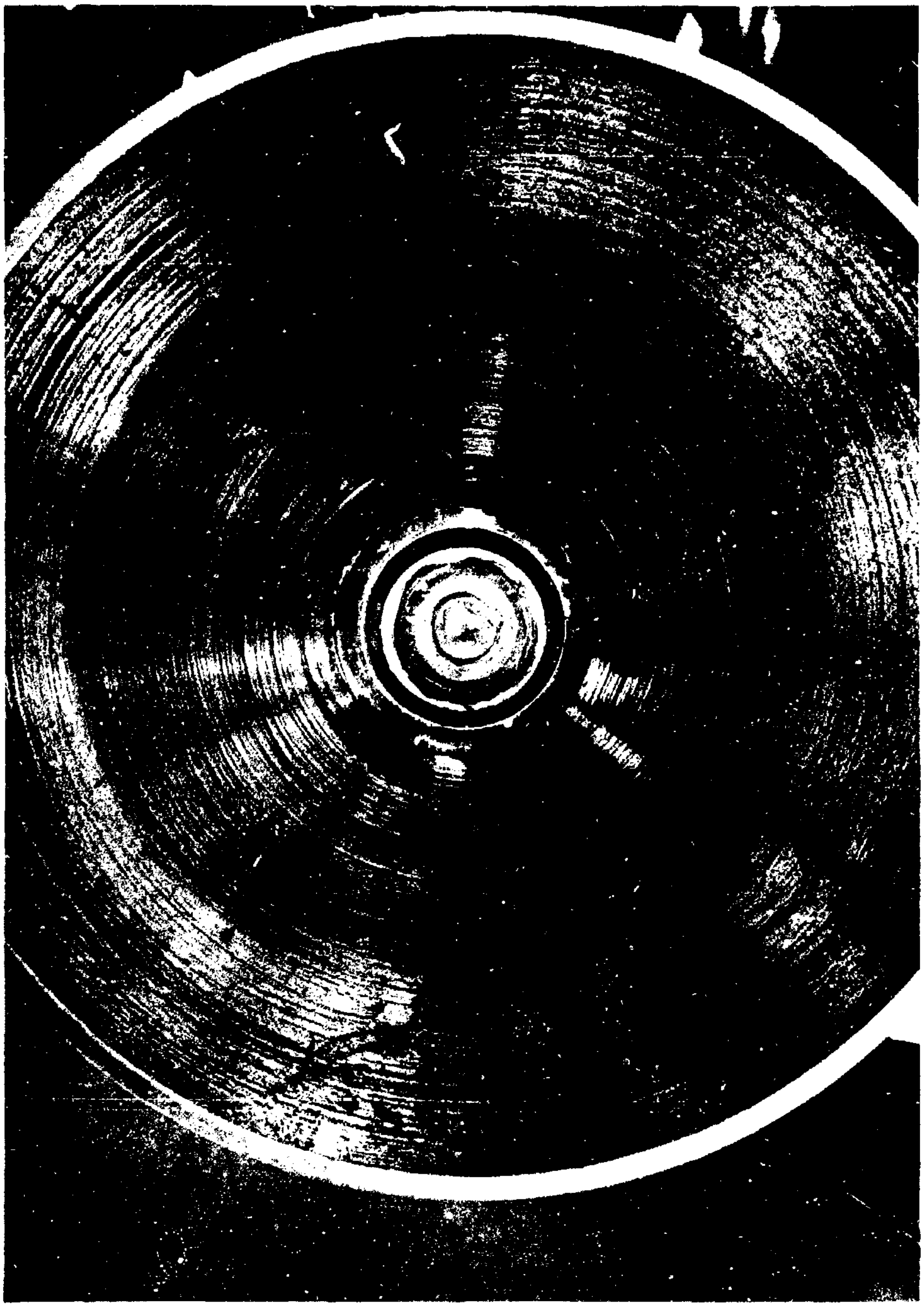

Postfire Nozzle

Figure III-216

both the chamber pressure transducers; however, the actual chamber pressure was correctly recorded by the igniter transducer since the port to that unit is protected from plugging by being in the igniter udder rather than in the main chamber. The somewhat erratic control on Runs 011 and 012 can be attributed to these plugged transducers.

(C) Since nozzle LW-9 received the most firing (seven pulses) and consequently sustained the most damage, the majority of the analytical effort was directed to the investigation of this unit. This nozzle was fired two times on motor LW-9 and five times on motor LW-11. It was also the unit that was manually controlled, Run 013, and hot refired Runs 014 and 015. These runs are shown on Figure III-207. The severity of the environment can be seen from Figure III-217, which shows nozzle LW-9 after the completion of the entire test series. All of the rubber insulation on the entrance cap and most of the MXSE-79 is missing: the char depth of the strutted housing insulation is through to the metal parts; however no bare metal is exposed and only little of the insulation material is missing. Figure III-218 shows the inside of the exit cone and the nozzle pintle of the nozzle. As can be seen, there is almost no material missing from the outer throat and exit cone. The pintle end cap is missing and in fact this nozzle was fired four times without this end cap. What can not be clearly seen from this picture is that all of the pyrolytic graphite is missing from the pintle. The throat is composed of the snap cured carbon phenolic insert which backs up the pyrolytic graphite washer stack in the assembly. This component apparently slipped aft when the pyro was ejected and became an ablative throat. Review of the films indicated that this occurred at ignition of pulse 014, the first of the hot restart series. This nozzle was then fired four times with an ablative throat. The final contour of the pintle was very similiar to the original contour of the pyrolytic graphite as can be seen from Figure III-219, only the material has changed.

(C) As can be seen from the traces of Runs 015, 016, and 017, Figure III-207, thrust control was good, pressure control was fair, pintle hunting occurred but did not affect thrust, and a considerable change in nozzle area from original area occurred. One other point that should be considered is the pintle did not drive to the fully open position at command extinguishment of these runs. It only opened 50% on the last two runs; however the motor still extinguished and maintained permanent extinction. There is evidence that the ablative throat became wedged in the aft housing insulator during Run 015 and remained in such a position to preclude fully opening the nozzle throat. This was not visible from the outside of the motor between Runs 015, 016, and 017; therefore the motor was fired the last two times (016 and 017).

UNCLASSIFIED

Postfire Nozzle

Figure III-217

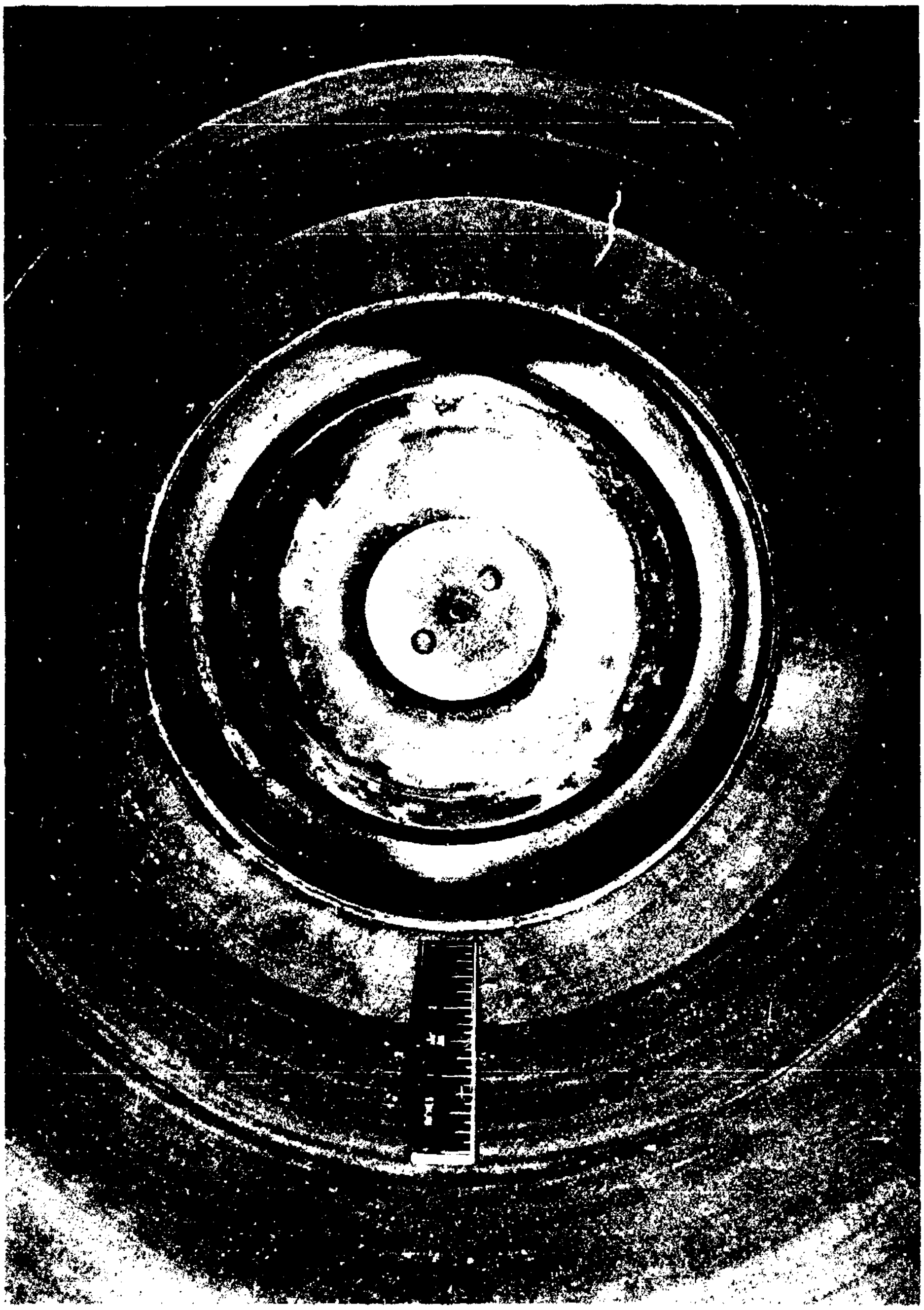

Postfire Nozzle

Figure III-218

Postfire Nozzle

Figure III-219

SECTION IV

PROGRAM CONCLUSIONS

(U) On the basis of the results of the technical effort under Contract AF 04(611)-10820 a number of problem areas in the development of a single chamber controllable solid rocket motor were successfully overcome; however, a number of areas not previously considered as potential problems were uncovered. The technical objectives of this program were met with only slight limitations. The feasibility of a single-chamber controllable solid rocket motor has been demonstrated and the areas requiring further investigation have been uncovered. The conclusions of this program are tabulated below:

(U) 1. A single-chamber controllable solid rocket motor which has the capability of both variable thrust and stop-restart is feasible.

(U) 2. A movable pintle nozzle for the control of thrust and impulse of a single-chamber solid rocket motor has been demonstrated as feasible.

(U) 3. A chamber pressure feedback control system for the control of variable thrust, extinguishment, and reignition of a single-chamber controllable solid rocket motor has been demonstrated as within the state-of-the-art.

(C) 4. A propellant with a standard delivered specific impulse of 237 plus seconds, and an exponent in excess of 0.55, has been developed which can be repeatably and reliably extinguished and reignited.

(C) 5. Variations in propellant burning rate, exposed surface area, and in nozzle contour can be compensated by use of the computerized control system developed under this program. Thrust level control between the levels of 1050 and 6600 pounds have been demonstrated on LW-9 at altitude, and between the levels of 1250 and 8600 pounds have been demonstrated on HW-2 at sea level.

(U) 6. A problem in the prediction of propellant burning rates by the use of small motors has been uncovered at low pressures due to heat losses. A potential solution to this problem has been found.

(C) 7. A problem in the recycling of pyrolytic graphite, specifically as a pintle throat insert, has been uncovered. The type of failure is related to internal delamination and bending failure of the washers. A direct solution to this problem with this material has not as yet been found. The only solution that appears obvious is to avoid using pyrolytic graphite in plate-bending on stop-restart motor applications.

(U) 8. Reignition of extinguishable propellants due to radiation feedback to the grain from hot insulation is a definite problem and provision must be made to avoid a severe radiation environment combined with finite motor pressure (1 - 3 psia) as reignition could occur.

(U) 9. Multiple cannister igniters can be made to work as a multiple ignition system; however, this method incurs problems in the area of protection of the unfired igniters during ignition and motor operation.

V. RECOMMENDATIONS

(U) The recommendations resulting from the technical effort conducted by Aerojet-General Corporation under Contract AF 04(611)-10820 to the Rocket Propulsion Laboratory of the Air Force have been categorized into four general groupings: (1) Propellant Efforts Required, (2) Material Development Required, (3) Design Effort Required, and (4) General.

A. PROPELLANT EFFORTS REQUIRED

(C) One of the primary recommendations for continuing effort is the development of a high impulse propellant with a minimum pressure of deflagration above 25 psia even when still hot from a previous firing. This propellant should have a high burning rate exponent and a relatively non-oxidizing exhaust environment. Low flame temperature is critical as designs are difficult to modify to accommodate high temperatures with long durations and soak periods.

(U) More effort should be directed toward the determination of propellant ballistic characteristics and the scalability of these characteristics from one motor size to another. Of specific importance in this investigation should be the prediction of ballistics for use in system sizing and component design. This will require the development of a lab test motor or some other device for the measurement of burning rate, exponent, flow coefficient, and minimum pressure of deflagration.

B. MATERIAL DEVELOPMENT REQUIRED

(U) On the basis of the results of this program deficiencies were found in the area of materials for use as pintle throat inserts and nozzle entrance cap insulation. The use of pyrolytic graphite as the pintle throat insert was apparently successful for a single pulse firing; however, during subsequent cooldown the pyrolytic graphite washers developed internal delaminations which drastically lowered the section modulus of the washer causing subsequent bending failure on recycling of the parts. In order to use pyrolytic graphite washers as pintle throat inserts successfully on recycling firings it is necessary to remove almost all of the bending loading on these washers. This requires a support material which is capable of withstanding the same environment as the pyrolytic graphite. To date, such a material is not available. Size of the washers appears to be a critical factor in this internal delamination since subscale (3.50-inch diameter and less) pintles do not exhibit this phenomenon. The stress levels under which these small pintles operate successfully are equal to or higher than the levels under which the larger (5.75-inch diameter) pintles fail on recycling. It is possible that the inherent curvature of the pyrolytic graphite plates, as deposited, causes this size effect. In any event, more effort is required in the area of material development for pintle nozzle throat inserts.

V, B, Material Development Required (cont.)

(U) Entrance cap insulation for stop-restart pintle nozzles is apparently a contributing factor in the radiation feedback to the propellant grain and subsequent reignition of the propellant due to this feedback. The use of an ablative rubber apparently lessened the radiation environment; however, the rubber material deteriorated too rapidly to use on a long duration or multiple pulsed motor. The silica, carbon, or graphite materials attain too high a surface temperature and store too much heat to be usable in this area without the resultant high radiation environment to the propellant surface. Asbestos is a possible choice since it has the lowest conductivity of any of the insulation materials; however, it also attains a high surface temperature and a high char surface temperature. Therefore, effort is recommended in the development of a material which has a low conductivity, ablates at a relatively low temperature but requires a high energy input to attain this ablation temperature, forms a strong char which has a very low density and low heat storage capability, and will withstand gas flow at Mach numbers in the range of 0.1 to 0.3 without high regression rates.

C. DESIGN EFFORT REQUIRED

(U) In the area of design, it is recommended that effort be expended in the design of lightweight variable area nozzles for both variable thrust and stop-restart operation. The characteristics of these nozzles should stress the use of highly reliable materials (avoid the use of infiltrated refractory materials as not reliable), low cost components using both low cost materials where possible and specifically avoiding complex fabrication operations, adaptability to high production rates, and simplification of assembly of components. The units designed and successfully demonstrated on this contract make use of complex components and relatively high cost materials. For a production design the use of these techniques is definitely not recommended.

(U) Also requiring a directed design effort is a multiple ignition system which meets the following requirements: (1) lightweight, (2) capable of igniting the motor at altitude under any free volume conditions within 0.100 seconds using any igniter with the exception of the first ignition, (3) each igniter protected from the blast effects of any other igniter and from the radiant heat and heat soak caused by the motor operation and down time between pulses, (4) each igniter should have a safety device to avoid inadvertent reignition such as a safe-arm device or an exploding bridgewire squib.

D. GENERAL

(U) Since the combination of both variable thrust and stop-restart under any operating altitude imposes severe limitations to the design of a single-chamber controllable rocket motor by limiting the propellant selection and the nozzle area change required it is recommended that the initial

V, D, General (cont.)

development of the systems be separated to variable thrust motors and stop-restart motors for a specific altitude application until more technology is developed. The technology required to combine all of the requirements stated for Contract AF 04(611)-10820 into a system ready for development for production is lacking in the areas previously discussed. The limitations of thrust variation range, operating pressure range, number of recycles, and minimum impulse per pulse have not been established in this program and should be established as quickly as feasible. These data are needed to adequately assess the potential of a single-chamber controllable solid rocket motor.

LIST OF REFERENCES

1. Landers, L. C., Development of an Extinguishable Solid Propellant, RPL TR 65-147, Final Report, AF 04(611)-9889, 19 July 1965.

2. Sanders, J. W., Theoretical and Experimental Characterization of Technique for Extinguishment of Solid Propellant Rocket Motors (L*), Preliminary Draft, Final Report, AF 04(611)-9662, 16 June - 19 July 1965.

3. Development of an Intermittent Operating Variable Thrust Solid Propellant Rocket Motor, Contract AF 04(611)-8175, QR 2, APR 702, Amcel Propulsion Co., Asheville, N.C., 15 Mar 1963 - 15 June 1963.

4. Development of an Intermittent Operating Variable Thrust Solid Propellant Rocket Motor, Contract AF 04(611)-8175, QR 2, APR 702, Amcel Propulsion Co., Asheville, N.C., July 1962.

5. Development of an Intermittent Operating Variable Thrust Solid Propellant Rocket Motor, QR-3, APR-21-3, Amcel Propulsion Co., Asheville, N.C., 16 Sept - 15 Dec 1963.

6. Controllable Solid Propellant Rocket Motor, Report APR-21-1, QR-1, Contract AF 04(611)-9067, Amcel Propulsion Company, Asheville, N.C., 16 Apr - 15 July 1962.

7. Controllable Solid Propellant Rocket Motor, Report APR-21-1, QR-2, APR 7-2, Amcel Propulsion Company, Asheville, N.C., 16 July - 15 Oct 1962.

8. Controllable Solid Propellant Rocket Motors, Report APR-21-1, QR-3, APR-21-3, Amcel Propulsion Company, Asheville, N.C., 16 Sept - 15 Dec 1963.

9. Controllable Solid Propellant Rocket Motor, Second Annual Report, APR-21-4, (RPL-TDR-64-52), Amcel Propulsion Company, Asheville, N.C., July 1963.

10. Dual-Chamber Controllable Solid Propellant Rocket Motor, APR-21-5, QR-4 Amcel Propulsion Co., Asheville, N.C., May 1964.

11. Dual-Chamber Controllable Solid Propellant Rocket Motor, APR-21-6, QR-5, Contract AF 04(611)-9067, Amcel Propulsion Co., Asheville, N.C., August 1964.

12. Dual-Chamber Controllable Solid Propellant Rocket Motors, APR-21-7, QR-6, Contract AF 04(611)-9067, Amcel Propulsion Co., Asheville, N.C., Nov. 1964.

LIST OF REFERENCES (cont.)

13. Dual-Chamber Controllable Solid Propellant Rocket Motor, APR-21-8, QR-7, Contract AF 04(611)-9067, Amcel Propulsion Co., Asheville, N.C., Feb 1965.

14. Bennett, H. L., Dual-Chamber Controllable Solid Propellant Rocket Motor, NOTS TP 3755 (C), Feb 1965.

15. Bennett, H. L., Dual-Chamber Controllable Solid Propellant Rocket Motor, Quarterly Progress Report, NOTS TP 3789, (C), May 1965.

16. An Investigation and Feasibility Demonstration of Nozzles for Restartable Solid Rocket Motors, First Quarterly Report, RPL TDE 64-112, Philco U-2794, AF 04(611)-9904, Philco Corp., Newport Beach, Calif., 21 Sept 1964.

17. An Investigation and Feasibility Demonstration of Nozzles for Restartable Solid Rocket Motors, Second Quarterly Technical Report, Philco C-2952(C), RPL-TDR 64-163, 20 Dec 1964.

18. An Investigation and Feasibility Demonstration of Nozzles for Restartable Solid Rocket Motors, Third Quarterly Technical Report, Philco C-3023 (C), RPL TDR 65-53, 22 Mar 1965.

19. Overall, R. E., and Sawyer, T. T., Design, Development and Demonstration of On-Off-On Device for Solid Propellant Rocket Motors, NAS 3-2563, TCC R-40-64, Thiokol Chemical Corp., Huntsville, Ala., 4 Dec 1964.

20. Elzufon, E. E., An Applied Research Program to Demonstrate the Feasibility of a Solid-Propellant Pulse Rocket, RPL TDE 64-66 (C), AF 04(611)-8531, Atlantic Research Corp., Alexandria, Va., Jan-Sept 1963.

21. Study, Design, Analysis, Fabrication and Test of a Solid Propellant Pulse Rocket Motor, LPC 654-Q2 (C), AF 04(611)-9716, RPL RDE 64-102, Lockheed Propulsion Co., Redlands, Calif., 23 July 1964.

22. Study, Design, Analysis, Fabrication and Test of a Solid Propellant Pulse Rocket Motor, LPC R-654-Q3 (C), RPL TR 64-153, Lockheed Propulsion Co., Redlands, Calif.

23. Bureau of Naval Weapons, Supporting Research Program, Quarterly Report, ABL QPR-49 (C), Hercules Powder Co., Cumberland, Md., 1 Jan - 31 Mar 1964.

24. ABL Quarterly Progress Report 50, Contract NOw 64-0366-d, NOw-64-0503d, ABL QPR-50 (C), Hercules Powder Co., Cumberland, Md., 1 Apr - 30 June 1964.

LIST OF REFERENCES (cont.)

25. Bureau of Naval Weapons, Supporting Research Program, Quarterly Report, Contracts NOw 64-0366d, NOw 64-0503d, QPR-51 (C), Hercules Powder Co., July - Sept 1964.

26. Bureau of Naval Weapons, Supporting Research Program Quarterly Report, NOw 65-0173d, QPR-52 (C), Hercules Powder Co., Cumberland, Md., 1 Jan - 31 Mar 1965.

27. Allegany Ballistics Lab. Annual RMMP Supporting Research Report, ABL/X-134 (C), NOw 64-0366-d, Hercules Powder Co., Cumberland, Md., Feb 1965.

28. Campbell, P. B., Total Impulse Control in Solid Propellant Rocket Motors, CPIA Pub. 18, Bulletin of the Interagency Solid Propulsion Meeting, Oct 1963.

29. Anderson, F. A., Strand, L. D., and Strehlaw, R. A., An Experimental Investigation of the Low Pressure Combustion Limits of Some Solid Propellants, Bulletin of the Interagency Solid Propulsion Meeting III, p.p. 157-186, July 1963.

30. Ciepluch, C. C., Spontaneous Re-ignition of Previously Extinguished Solid Propellants, NASA Technical Note D-2167, March 1964.

31. Ciepluch, C. C., Effect of Composition on Combustion of Solid Propellant During a Rapid Pressure Decrease, NASA TN D-1559, Dec 1962.

32. Sehgal, R., and Strand, L., Low-Pressure Combustion, JPL Space Programs Summary No. 37-32, Vol. IV, p.p. 109-112.

33. Morris, R. E., Investigation of the Mechanism of Propellant Extinguishment Final Report, AGC R-8702-34F, Final Report, Feb 1964.

34. Mittermaier, N. P., and Morris, R. E., Start-Stop and Variable Thrust Operation of a Solid Propellant Rocket Motor with Variable-Area Nozzle, Final Report FR 63-1, Aerojet-General Corp., Dec 1960 - Nov 1962.

35. Engstrom, George, Stop-Restart and Variable Thrust in Solid-Propellant Rockets, AGC SRO-2 (C), Aerojet-General Corporation, July 1964.

36. Anderson, W. N., Thrust Modulated Solid Rocket Program, Final Report, Doc. 8701-91, Mar 1962 - Sept 1963.

37. Mittermaier, N. P., Variable Thrust Stop-Restart Motor Investigation, AR 19, Aerojet-General Corporation, 1964.

LIST OF REFERENCES (cont.)

38. Mittermaier, N. P., Variable Thrust Toroidal Motor Investigation, Final Report, AGC R-8708-50A, Aerojet-General Corporation, Dec 1964 - May 1965.

39. Ignition and Thrust Termination Study, Boeing D2-20456-1 (C), (AD 354 802), 5 Nov 1964.

40. Todd, M. A., Solid Propellant Rocket Motors in Space Maneuvering Systems, AFRPL, p. 165-182.

41. Alley, C. D., Intermittent Operating Variable Thrust Solid Propellant Rocket Motors, Bulletin of the 20th Interagency Solid Propulsion Meeting, p.p. 43-68, AMCEL, July 1964.

42. Alley, C. D., and Johnson, B. L., Controllable Dual-Chamber Solid Propellant Rocket Motor, p. 295, AMCEL.

43. Morash, R. T., Start-Stop-Restart System for a Large Scale Solid Propellant Motor, Bulletin of the 21st Interagency Solid Propulsion Meeting, p. 485-501, Hercules Powder Company, June 1965.

44. Bennett, Harold L., Development of High Slope Propellants for Use in Controllable Solid Rocket Motors, Interagency Chemical Rocket Propulsion Group-Solid Propellant Rocket Static Test Working Group, Addendum to the Second Meeting, NOTS, Oct 21-23, 1964.

45. Henisch, M. J., and Kennedy, W. S., Design and Testing of a Thrust Reversal System for a 120-inch Motor, Pt. I, Fundamental Analytic Aspects of Thrust Termination, p. 19, UTC.

Karrer, H. E., Thrust Termination Measurement Techniques, Pt. II, p. 31, UTC.

46. Morash, R. T., Reduction to Practice of a Start-Stop-Restart System for a Solid Propellant Rocket Motor, ABL/R-59 (C), NOw 64-0366, Hercules Powder Company, Nov 1964.

47. Morash, R. T., Start-Stop-Restart Capability in a Solid Propellant Motor, ABL/Z-81 (C), NOw 64-0366, Hercules Powder Company, Feb 1965.

48. Study of Solid Propellant Systems for Space Propulsion, Final Report, NAS 7-123, LPC R-590-F (C), 14 Feb 1963.

49. Nathews, S. F., and St. John, A. D., Unsteady-State Solid Propellant Burning, Final Report, RTD TDR 63-1028 (C), AF 04(611)-5171, Midwest Research Institute, Kansas City, Mo., Apr 1963.

LIST OF REFERENCES (cont.)

50. Fletcher, Edward, Study of Reignitable Solid Propellant Grains Leading to Extinguishable and Restartable Solid Propellant Rocket Motors, Second Quarterly Progress Report, NAS 3-2554, Minnesota U., Minneapolis, Minn., 22 Apr - 22 July 1963.

51. Advanced Technology for Propulsion Systems, Second Quarterly Progress Report, NOw 60-0445, (AD 322 586), North American Aviation - Rocketdyne, Canoga Park, Calif., 15 Dec 1960.

52. Advanced Technology for Propulsion Systems, Third Quarterly Progress Report, NAA-R R-2836-1 (C), North American Aviation - Rocketdyne, Canoga Park, Calif., 16 Dec 1960 - 15 Mar 1961.

53. Jessen, F. C., Further Experiments with Thrust Cut-Off Devices for Solid Propellant Motors, RPE TN 228 (C), Rocket Propulsion Establ., Wescott, U. K., March 1964.

54. Todd, M. A., Applications of Controllable Solid Rocket Motors, RTD TDR 63-1026 Secret (3S9009), SA 63-02668(9993)-7, Rocket Propulsion Lab., Edwards AFB, Calif., Apr 1963.

55. Niessen, W. R., Solid Propellant Rocket Ignition Test and Evaluation (SPRITE) Program, RPL TR 65-23, Rocket Propulsion Laboratory, Edwards AFB, Calif., Jan 1965.

56. Thompson, R. J., and Phen, R. L., Study of Solid Propellant Propulsion Systems for Ballistic and Space Missions, Final Report AF 04(611)-9902, AGC 707FR-1, v. 1, (AFRPL TR-65-59) Secret (5S5034 - SA 65-01869 (8050), Space General Corp., El Monte, Calif., 1 May 1964 - 1 Feb 1965.

57. Grenning, E. M., Design and Demonstration of Unique Methods of Non-Hazardous Thrust Termination of Large Solid Boosters in a Launch Environment, Phase I Final Report, TCC-U-TW 22-10-63 (C) RTD TDE 63-1103 Thiokol Chemical Corp., Wasatch Div., Brigham City, Utah, 30 Dec 1963.

Unclassified
Security Classification

DOCUMENT CONTROL DATA - R & D

(Security classification of title, body of abstract and indexing annotation must be entered when the overall report is classified)

1. ORIGINATING ACTIVITY (Corporate author) Aerojet-General Corporation P. O. Box 15847 Sacramento, California 95813	2a. REPORT SECURITY CLASSIFICATION Confidential 2b. GROUP 4

3. REPORT TITLE
(Unclassified Title)
Feasibility Demonstration of a Single-Chamber Controllable Solid Rocket Motor

4. DESCRIPTIVE NOTES (Type of report and inclusive dates)
Final Report 1 July 1965 through 1 August 1967

5. AUTHOR(S) (First name, middle initial, last name)
Charles T. Levinsky
Gerald F. Kobalter

6. REPORT DATE December 1967	7a. TOTAL NO. OF PAGES 370	7b. NO. OF REFS
8a. CONTRACT OR GRANT NO. AF 04(611)-10820 b. PROJECT NO. c. d.	9a. ORIGINATOR'S REPORT NUMBER(S) None 9b. OTHER REPORT NO(S) (Any other numbers that may be assigned this report)	

10. DISTRIBUTION STATEMENT In addition to security requirements which must be met, this document is subject to special export controls and each transmittal to foreign governments or foreign nationals may be made only with prior approval of AFRPL(RPPR/STINFO), Edwards, California 93523.

11. SUPPLEMENTARY NOTES	12. SPONSORING MILITARY ACTIVITY Air Force Rocket Propulsion Laboratory Edwards, California

13. ABSTRACT

This report deals with the technical effort conducted during the 24 month period covered by Contract AF 04(611)-10820, "Exploratory Development of a Single-Chamber Controllable Solid Rocket Motor."

A preliminary design phase, a propellant development phase, a lightweight motor development phase, and a lightweight motor demonstration phase were conducted. In the preliminary design phase, a trade-off study was conducted to size the system and a preliminary lightweight motor design was prepared and analyzed. In the propellant development phase, a family of extinguishable propellants was investigated. In the subscale design and development phase, the basic material selections were test fired in a motor which was designed to simulate the full-scale CSRM. In the heavyweight motor development phase, a full-scale CSR motor was designed and fabricated, three units were processed, and four tests conducted. In the lightweight motor development phase, the propellant was changed and the nozzle design was modified, four tests were conducted. In the demonstration phase, four motors were tested at Arnold Engineering Development Center, Tullahoma, Tennessee.